

ADDENDUM aux Comptes Rendus N° 11
page 311 : ajouter à la fin du Rapport
National du Japon la signature :

Hirosi Kawasumi
Earthquake Research Institute
Tokyo University

CONSEIL INTERNATIONAL DES UNIONS SCIENTIFIQUES

UNION GÉODESIQUE ET GÉOPHYSIQUE INTERNATIONALE

ASSOCIATION DE SÉISMOLOGIE
ET DE
PHYSIQUE DE L'INTÉRIEUR DE LA TERRE

PUBLICATIONS DU BUREAU CENTRAL SÉISMOLOGIQUE INTERNATIONAL

Sous la direction de J. P. ROTHÉ

SECRETAIRE DE L'ASSOCIATION DE SÉISMOLOGIE ET DE PHYSIQUE DE L'INTÉRIEUR DE LA TERRE

SÉRIE A
TRAVAUX SCIENTIFIQUES

Fascicule 19

Publié avec le concours financier de l'U. N. E. S. C. O.



TOULOUSE
ÉDOUARD PRIVAT & C^e Libraire-Éditeur
14, RUE DES ARTS, 14

1956

AVERTISSEMENT

Le présent fascicule contient, dans l'ordre où elles ont été présentées, le texte de quelques-unes des communications scientifiques discutées au cours des séances de la conférence de Rome.

Les autres communications destinées à être publiées dans différents périodiques scientifiques n'ont pas été réimprimées. On en trouvera les références bibliographiques dans les Comptes Rendus, n° 11, Association de Séismologie et de Physique de l'Intérieur de la Terre, comptes rendus des séances de la X^e conférence réunie à Rome du 14 au 25 septembre 1954, Strasbourg, 1955, pp. 17-169.

J.-P. ROTHE

*Secrétaire de l'Association Internationale
de Séismologie et de Physique
de l'Intérieur de la Terre.*

Strasbourg
Septembre 1955.

TABLE DES AUTEURS

	Pages		Page
Akima (T. S.).....	223	Kirnos (D. P.).....	357
Asada (T.).....	95	Labrouste (Y.) ...	325, 327, 331, 335
Aswathanarayana (U.)	137, 151	Lehmann (I.)	115
Bath (M.)	5	Lynch (J. J.)	177
Beaufils (Y.)	325, 327, 335, 339	Maxwell (A. E.)	395
Belousov (V. V.).....	129	Menzel (H.)	125
Bernard (P.)	325	Molodensky (M. S.)	217
Coulomb (J.)	325, 327	Nagamune (T.)	223
Debrach (J.)	307	Nanda (J. N.)	193
Dilgan (H.)	287	Nishimura (E.)	277
Duclaux (F.)	325	Parijsky (N. N.)	217
Gamburzev (G. A.).....	373	Peterschmitt (E.)	325, 327
Geneslay (R.)	327, 331	Pinar (N.)	297
Gilmore (M. H.)	203	Ram (G.)	345
Giorgi (M.)	197	Rao (G. V.)	345
Goguel (J.)	165	Revelle (R.)	395
Gorshkov (G. P.)	257	Research Group (Japan)	229
Guha (S. K.)	345	Richard (H.)	325
Hagiwara (T.)	287	Rosini (E.)	197
Iwai (Y.)	261	Rothé (J. P.)	325, 327, 331
Iyer (H. M.)	193	Sassa (K.)	277
Jacobs (J. A.)	155	Savarensky (E. F.)	249
Jobert (G.)	327	Shalem (N.)	267
Jung (K.)	315	Suzuki (Z.)	95
Keilis-Borok (V. I.)	383	Tomoda (Y.)	95
Karnik (V.)	319	Tsuboi (Ch.)	243
Kawasumi (H.)	99	Utzmann (R.)	325
Kharin (D. A.)	357	Wadati (K.)	261
		Zatopek (A.)	183



INDEX ALPHABÉTIQUE DES MATIÈRES

	Pages
Agitation microsismique.	
M. H. GILMORE : Microseisms used in Hurricane Forecasting.....	203-215
M. GIORGI et E. ROSINI : Les microsismes d'origine tyrrhénienne....	197-202
H. M. IYER and J. N. NANDA : Microseisms at Cochin.....	193-196
Rev. J. Joseph LYNCH, S. J. : The Great Lakes, A Source of Two-Second Frontal Microseisms. . ..	177-182
A. ZATOPEK : Sur les microsismes de Praha.....	183-191
Constitution de la Terre.	
H. MENZEL : On the Stress-Strain Relation in a not perfectly elastic solid Body. . ..	125-127
Croûte terrestre (Interprétations séismiques et gravimétriques).	
T. S. AKIMA and T. NAGAMUNE : Dispersion of Seismic Surface Waves and the Structure of Continents and Oceans.....	223-228
Y. BEAUFILS, P. BERNARD, J. COULOMB, F. DUCLAUX, Y. LABROUSTE, H. RICHARD, E. PETERSCHMITT, J. P. ROTHÉ et R. UTZMANN : Enregistrement des ondes séismiques provoquées par de grosses explosions. I. — Camargue, 1949.....	325-326
Y. BEAUFILS, J. COULOMB, R. GENESLAY, G. JOBERT, Y. LABROUSTE, E. PETERSCHMITT et J. P. ROTHÉ : Enregistrement des ondes séismiques provoquées par de grosses explosions. II. — Champagne, octobre 1952. . ..	327-329
G. A. GAMBURZEV : On some new Methods of Seismological Research..	373-381
R. GENESLAY, Y. LABROUSTE et J. P. ROTHÉ : Réflexions à grande profondeur dans les grosses explosions (Champagne, octobre 1952). . ..	331-334
V. KÁRNÍK : Les vitesses des ondes séismiques excitées par les explosions industrielles en Bohême.....	319-324
Y. LABROUSTE et Y. BEAUFILS : Réfractions multiples dans les enregistrements sismographiques des explosions de Champagne, octobre 1952. . ..	335-338
RESEARCH GROUP FOR EXPLOSION SEISMOLOGY : Crustal Structure in North-East Japan by Explosion-Seismic Observations.....	229-242
Ch. TSUBOI : Earthquake Epicentres, Volcanoes and Gravity Anomalies in and near Japan.....	243-247

Géographie séismologique.

Pages

J. DEBRACH : Sur quelques alignements séismiques remarquables du Maroc. Essai d'interprétation tectonique.....	307-313
H. DILGAN et T. HAGIWARA : Le Tremblement de terre de Yenice (18 mars 1953).....	287-295
G. P. GORSHKOV : General Survey of Seismicity of the Territory of the U.S.S.R.	257-259
S. K. GUHA, Gurdas RAM and G. V. RAO : Trigger causes in Earth Movements.	345-355
N. PINAR : Le séisme du 18 mars 1953 de Yenice-Gönen (Anatolie NW) en relation avec les éléments tectoniques.....	297-306
K. SASSA and E. NISHIMURA : On Phenomena Forerunning Earthquakes.	277-285
E. F. SAVAREN SKY : Development of Seismic Research and Analysis of Seismic Observations in the U.S.S.R.	249-256
N. SHALEM : Seismicity and Erythrean Disturbances in the Levant....	267-275
K. WADATI and Y. IWAI : The Minute Investigation of Seismicity in Japan (2nd paper).....	261-265

Géothermie.

J. GOGUEL : Le mécanisme des explosions phréatiques.....	165-175
J. A. JACOBS : The Thermal History of the Earth with Particular Reference to a Number of Radioactive Earth Models.....	155-164
A. E. MAXWELL et R. REVELLE : Heat Flow through the Pacific Ocean Basin.	395-405

Isostasie.

K. JUNG : Remarks on the Foundation of the Conception of Isostasy..	315-318
---	---------

Magnitude.

T. ASADA, Z. SUZUKI and Y. TOMODA : On Frequency Distribution of Seismic Magnitude.....	95-98
M. BATH : The Problem of Earthquake Magnitude Determination....	5-93
H. KAWASUMI : Intensity and Magnitude of Shallow Earthquakes....	99-114

Marées terrestres.

M. S. MOLODENSKY and N. N. PARIJSKY : Elastic Tides and Irregularities of the Earth's Rotation in connection with its Structure.....	217-222
--	---------

Méthodes de recherche.

G. A. GAMBURZEV : On some new Methods of Seismological Research.	373-381
V. I. KEILIS-BOROK : Methods and Results of the Investigations of Earthquake Mechanism (a brief information).....	383-394
E. F. SAVAREN SKY : Development of Seismic Research and Analysis of Seismic Observations in the U.S.S.R.	249-256

Microséismes.

Pages

voir agitation microsismique.

Ondes Séismiques.

- | | |
|---|---------|
| T. S. AKIMA and T. NAGAMUNE : Dispersion of Seismic Surface Waves and the Structure of Continents and Oceans..... | 223-228 |
| Y. BEAUFILS : Etude des ondes superficielles dans les enregistrements séismographiques des explosions de Champagne, octobre 1952. | 339-343 |
| I. LEHMANN : The Velocity of P and S Waves in the upper Part of the Earth's Mantle. | 115-123 |

Radioactivité.

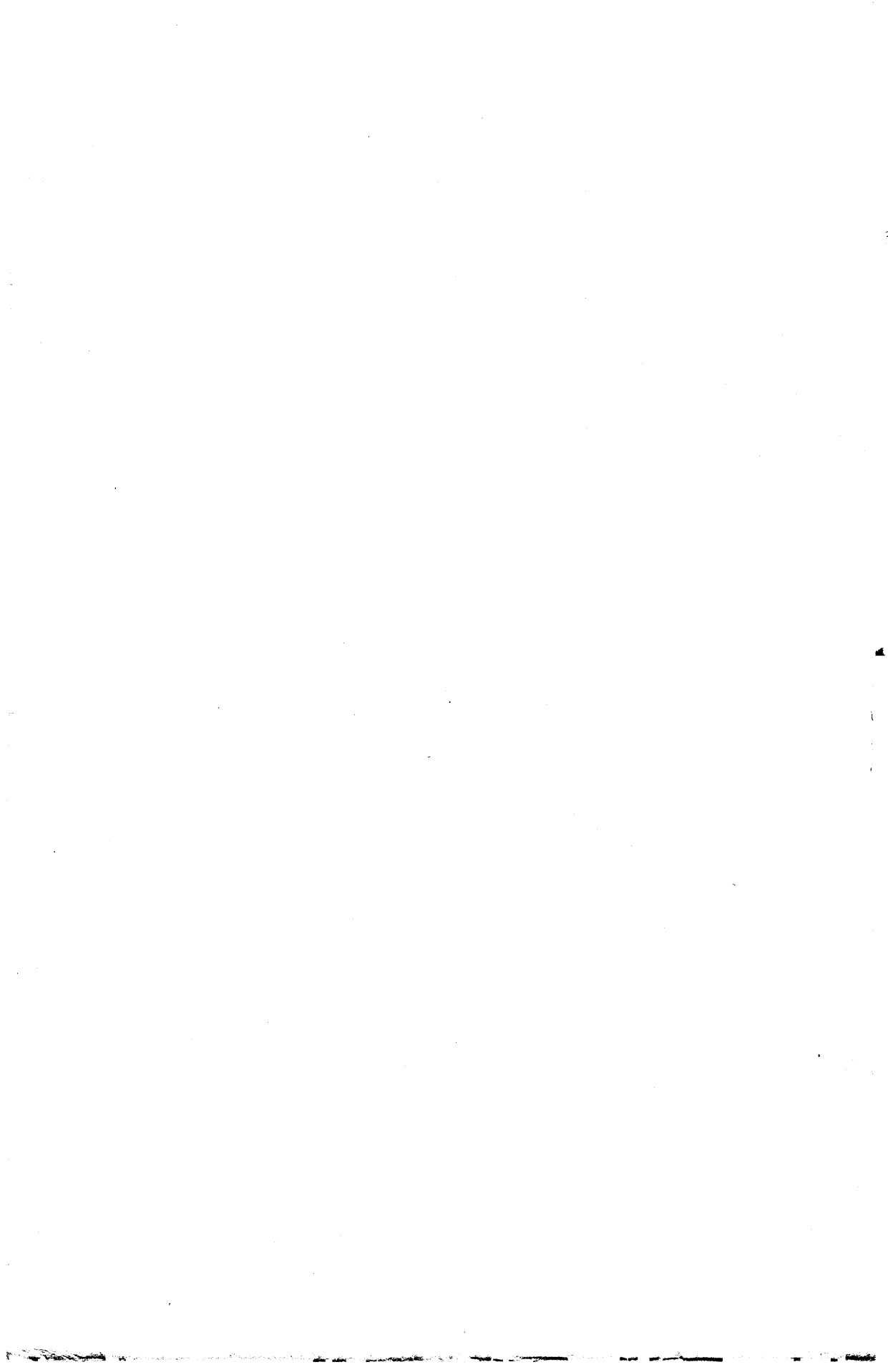
- | | |
|---|---------|
| U. ASWATHANARAYANA : Transfer of Radioactive Matter through Rocks by Diffusion. | 137-149 |
| U. ASWATHANARAYANA : Some Statistical Aspects of the Distribution of Radioactivity in the Salem Gneisses of Madras State..... | 151-154 |

Séismographes.

- | | |
|---|---------|
| D. P. KIRNOS and D. A. KHARIN : Basic Equipment of Seismological Stations in the U.S.S.R..... | 357-371 |
|---|---------|

Tectonophysique.

- | | |
|--|---------|
| V. V. BELOUSsov : La structure interne et l'évolution de la Terre à la lumière des données géotectoniques..... | 129-135 |
|--|---------|
-



THE PROBLEM OF EARTHQUAKE MAGNITUDE DETERMINATION

by MARKUS BATH (Uppsala).

I. INTRODUCTION.

The magnitude scale of earthquakes was first defined by Richter (1935). Its applications were then extended in papers by Gutenberg and Richter (1936, 1942) and especially in three papers by Gutenberg (1945 a, 1945 b, 1945 c). The papers mentioned are of fundamental importance for the theory and the practical applications of the magnitude scale. The three last-mentioned papers by Gutenberg have made it possible to determine the magnitude both for shallow and deep earthquakes. The determinations can be made by means of amplitude and period measurements of P (horizontal or vertical), PP (horizontal or vertical), S (horizontal), or the surface waves (horizontal component) on the records of any station seismograph, provided its constants are known.

In addition to the papers mentioned quite a number of papers have been written by various authors on earthquake magnitudes, mainly being applications of the general methods to particular stations. Equations have been developed by the method of least squares for particular stations, permitting the calculation of the magnitude M from the horizontal amplitude A of surface waves of around 20 sec period. Such formulae known to date are summarized here (A expressed in microns and the epicentral distance Δ in degrees).

Pasadena : $M = \log A + 1.656 \log \Delta + 1.818 + 0.05$ (1)
valid for $15^\circ < \Delta < 130^\circ$ (Gutenberg, 1945 a.)

Rome : $M = \log A + 1.526 \log \Delta + 2.439$ (2)
(Di Filippo and Marcelli, 1949.)

Strasbourg : $M = \log A + 1.62 \log \Delta + 1.97$ (3)
(Peterschmitt, 1950.)

Praha : $M = \log A + 1.66 \log \Delta + 2.15$ (4)
(Zátopek and Vaněk, 1950.)

Hurbanovo : $M = \log A + 1.66 \log \Delta + 2.04$ (5)
(Vaněk, 1953.)

Skalnaté Pleso : $M = \log A + 1.66 \log \Delta + 1.99$ (6)
(Vaněk, 1953.)

Toledo : $M = \log A + 1.916 \log \Delta + 1.357$ (7)
(Bonelli Rubio and Carrasco, 1954.)

Wien : $M = \log A + 1.64 \log \Delta + 1.99$ (8)
(Trapp, 1954.)

Graz : $M = \log A + 1.60 \log \Delta + 2.07$ (9)
(Trapp, 1954.)

On the right-hand side of these formulae the regional correction (D) should be added. We notice a general agreement in the factor of $\log \Delta$. In fact, I have found from the present study that it is not necessary to develop such an equation for every station to be used. It is equally accurate to use the general methods developed by Gutenberg (1945 a) and to determine only the constant term and the regional corrections for every station used. It must also be remarked that the formulae given above are only of limited value. They can only be used for shallow shocks, and in cases of foci slightly deeper than normal (which is often not easy to decide immediately from the records) such formulae will give too low values of the magnitude. In addition to the fundamental studies of Richter (1935) magnitude formulae for smaller distances have been derived by several other authors (Hayes, 1941; Jones, 1944; Di Filippo and Marcelli, 1950; Tsuboi, 1951; Bath, 1953, pp. 196-197). A valuable survey of the general magnitude problem was given by Richter (1950). A number of Japanese writers in addition to Tsuboi have also made notable contributions to various aspects of the magnitude problem (see e.g. Kawasumi, 1944; Wadati et al., 1954). Bath (1952) developed a formula for Pasadena for determination of magnitude from the vertical component of surface waves of 20 sec period. The latest contribution to the magnitude problem by Gutenberg and Richter (1955) contains a revision of their 1942-paper with new important results. The present author is indebted to Professors Gutenberg and Richter for the privilege of reading their paper in manuscript.

It is the merit of Gutenberg and Richter to have developed the practical determination of magnitude to such a simple procedure that it can very easily be applied in the routine bulletin work for any station. At present therefore several stations regularly report magnitudes (see Table 17 at the end of this paper). However, it is the experience of the present author and probably everybody who has dealt with magnitude determinations, that large discrepancies (sometimes amounting to one magnitude unit or even more) may occur between determinations at different stations as well as between the different waves at one and the same station, even between the different waves on the same record. Examples of large discrepancies (\geq one magnitude unit) are to be found in Table 17 for earthquakes No. 22, 32, 64-66, 68, 71, 86, 96, 104, 108, 136, 139, 141, 142, 151, 170, 218, 228, 240, 254, 299 for Uppsala, and No. 32,

58, 71, 87, 88, 99, 196, 200, 206, 208, 213, 251, 259, 270 for Kiruna. For earthquakes especially in Central America but also in other parts of America our stations at Uppsala and Kiruna usually give magnitudes considerably lower than those determined at American stations (Pasadena, Berkeley), and this is valid both for body waves and surface waves (see earthquakes No. 12, 44, 87, 181, 208). Deep-seated faults in the Caribbean area are a probable reason for the weakness at our stations of both body waves and surface waves for Central American and Caribbean earthquakes. For the surface waves also the effect of an oceanic path contributes. For the California earthquake of July 21, 1952 (No. 76), the surface waves at our stations gave magnitudes considerably higher than the body waves. Unsymmetrical radiation of energy in the surface waves is known to have occurred in this case. For earthquakes within approximately 30° distance of our stations, as e.g. for Greek earthquakes, the S wave gives much lower magnitudes than other waves.

The main purpose of this investigation has been to study such discrepancies, their various properties, and the reasons for their existence. Also methods have been developed by means of which their influence will be eliminated. As a by-product methods for magnitude determinations by means of all our records at Uppsala and Kiruna have been obtained.

Gutenberg (1945 b, p. 66) divided the earthquakes into a number of magnitude classes. For instance class *c*, $M = 6-7$, are shocks for which P in general is reported only up to $\Delta = 90^{\circ}$; class *d*, $M = 5.3-6$, includes shocks with P recorded only up to about 45° . This is a statement based mostly on older-type instruments with lower magnification. With high-magnification, short-period electromagnetic instruments the distance limits are considerably increased. For instance, at Uppsala and Kiruna it has happened repeatedly that PKP is recorded for New Zealand shocks (epicentral distance about 150°) of class *d*.

II. METHODS AND MATERIALS USED.

To study the magnitude discrepancies I have used as examples our own records at Uppsala and Kiruna for the years 1952-1953. In all, 309 earthquakes are included in this study. Determinations have been made from the Uppsala Wiechert horizontal records (horizontal P = PH; horizontal PP = PPH; horizontal S = SH; and the horizontal component of surface waves around 20 sec period = LH) and from the Uppsala short-period vertical Grenet-

Coulomb electromagnetic seismograph (short-period vertical $P=PZ'$, short-period vertical $PP = PPZ'$). For Kiruna determinations were made from Galitzin horizontal (PH, PPH, SH, and LH), from Galitzin vertical (PZ , PPZ), and from Grenet-Coulomb short-period vertical (PZ' , PPZ'). Note that SH in this paper means the total horizontal component of S. Determinations were made in all cases where amplitudes and periods could be reliably measured. The periods of PZ' , PPZ' are generally around 1 sec, for PH, PPH, PZ , PPZ approx. 5 sec, and for SH approx. 10 sec. The seismograph constants are well known due to rather frequent determinations (see our yearly bulletins). The ground consists of granite at Uppsala and of porphyry at Kiruna.

The magnitude determinations are all given in Table 17 at the end of this paper, where M = the magnitude. The amplitudes and periods used in the determinations will be found in the seismic bulletins for Uppsala and Kiruna. The table also contains determinations by other stations, and the most likely value of M of each earthquake in case such a value could be given. The data on location (φ , λ) and origin time (θ) have been obtained from BCIS and USCGS. The depth values h are based on both these authorities and our own determinations (n = normal depth; (n) = slightly deeper than normal; both these indications based only on our own records; see chapter III.B.3).

Magnitudes from the surface waves of period around 20 sec have been determined by means of the methods given by Gutenberg (1945 a) with the aid of a special nomogram applicable to any instrument and designed by Mr. Nordquist (in somewhat different form, for the standard Wood-Anderson torsion seismometer, given by Gutenberg and Richter, 1942).

When amplitudes A of surface waves with periods T different from 20 sec have been used, some authors have first computed an amplitude A_{20} corresponding to 20 sec period from the formula

$$\frac{A_{20}}{20} = \frac{A}{T} \quad (10)$$

or

$$\log A_{20} = \log A + \log \frac{20}{T} \quad (11)$$

The underlying idea should be to define A_{20} such that the corresponding energy is the same as for A , rather than to put the velocities equal. However, then equation (10) is not the correct expression, as we have to take account not only of the period

difference but also of the difference in extinction k for different periods. Equation (10) should therefore be replaced by the following expression equating the two energies in a given time interval

$$\frac{A^*_{20}}{20} e^{-k(20)\Delta} = \frac{A^*}{T} e^{-k(T)\Delta} \quad (12)$$

or

$$\log A_{20} = \log A + \frac{1}{2} \log \frac{20}{T} + 24.13 \Delta [k(T) - k(20)] \quad (13)$$

where Δ is to be expressed in degrees and k is the extinction coefficient per km (Båth, 1955). Some values for the extinction for different periods have been given by Giorgi and Valle (1948). Their coefficients refer to the amplitude, whereas our k refers to the energy. Values of k can be obtained from their table 6 by doubling their coefficients. The following abstract (Table 1) is sufficient for the present purpose.

TABLE 1.

T sec	k km^{-1}
10	0.0043
12	0.0020
15	0.0008
20	0.0003

Suppose now $\Delta = 60^\circ$ and $T = 15$ sec. Equation (11) gives
 $\log A_{20} = \log A + 0.12$

and equation (13) gives

$$\log A_{20} = \log A + 0.06 + 0.72 = \log A + 0.78$$

It is evident that in using a period different from 20 sec the difference in the extinction is by far much more important than the period difference itself. Gutenberg's (1945 a) value of $k = 0.0003 \text{ km}^{-1}$ is a mean value for 20 sec period. Due to the rapid variation of k with period it is advisable to use only waves of periods close to 20 sec, when no correction is made. A more accurate knowledge of k for different paths and for different periods is very desirable. When we have that knowledge it would be a simple task to extend the magnitude formula for surface waves also to other periods than 20 sec. In comparison with the uncertainty of k the multiplication with a factor of 1.4 which is made in case only one horizontal component is given, is of practically no importance. This factor introduces an error in the magnitude of

at most 0.1. The same remark applies to the case when the amplitudes AN and AE are not exactly simultaneous.

In Table 17 M(LH) has been given without correction in some cases, where the period is outside the limits 17-23 sec. These magnitudes are given in parenthesis and are not used in any computations in this paper. Most of these cases have low periods, usually around 12-15 sec; periods > 23 sec are used only for earthquakes No. 176, 178, 277 for Uppsala, and No. 6, 118, 179, 299 for Kiruna. In several cases there is good agreement between these magnitudes and those determined from the other waves, but in several other cases these magnitudes are definitely too low (for the lower periods). The reason for agreement in several cases is probably the continental paths with lower extinction. There is also no geographical partition of earthquakes giving good or poor agreement for these M(LH). The conclusion is therefore that no M(LH) can be relied upon if waves of periods < 17 sec or > 23 sec have been used.

Magnitudes from P, PP, S have been computed with Gutenberg's formula (1945 b, 1945 c)

$$M = A + 0.1(M - 7) + \log \frac{u}{T} \quad (14)$$

where A is a function of distance and depth, u is the observed ground amplitude in microns (total horizontal or vertical), and T is the corresponding period in sec. The function A, which is different for horizontal and vertical components, has been given by Gutenberg (1945 b, 1945 c) in tables and graphs. The different significance of A in the formulae for body waves and surface waves will not cause any confusion; the formulae have got here the same appearance as given by their inventors. Equation (14) is valid with a tentative correction of +0.1 (M - 7) for longitudinal waves (P and PP) in shocks below magnitude 6 1/2 or over 7 1/2 according to Gutenberg (1945 b, 1945 c). Equation (14) may be written as follows, putting $M = M_1$

$$M_1 = 1.1 \left[(A - 0.7) + \log \frac{u}{T} \right] \quad (15)$$

If the magnitudes, determined from equation (15), are corrected with the additional term +0.1 ($M_1 - 7$) we get another magnitude value M_2

$$M_2 = M_1 + 0.1(M_1 - 7) = 1.1 M_1 - 0.7 \quad (16)$$

Corresponding numerical values are given in Table 2.

TABLE 2.

M ₁	M ₂	M ₂ — M ₁
6	5.9	-0.1
7	7.0	±0.0
8	8.1	+0.1
9	9.2	+0.2

It is to be observed that the way in which Gutenberg (1945 b) has determined the additional correction +0.1 (M — 7) is identical with the interpretation given in equation (16) above. But it is incorrect on the basis of this to write the magnitude formula as

$$M = A + 0.2(M - 7) + \log \frac{u}{T}$$

For further discussion of this point in the light of our new data, see chapter III.B.3. The magnitude formula for body waves derived by Gutenberg (1945 b) was based on the following relation between energy E and magnitude M,

$$\log E = 11.3 + 1.8 M \quad (17)$$

Revision of the magnitude formula and the possible corrections should be made with regard to more recent results concerning the variation of log E with M.

In view of the tentative nature and the small values of the additional correction +0.1 (M — 7) I considered it preferable in this investigation to use the uncorrected formula (15) in all cases for body waves and to determine any possible correction by means of various comparisons with other determinations. In view of the results presented in chapter III.B.3 future revision of the magnitude scale will be necessary. No regional corrections, corrections for path, or local corrections for the stations used were made in the determinations given in Table 17. These corrections were not known from the start of this investigation, but they have all been determined in the course of the work.

III. COMPARISON OF MAGNITUDES DETERMINED IN DIFFERENT WAYS.

A. Comparison of the same wave at two different stations.

Table 3 gives the results of the computations of the magnitude differences Uppsala-Kiruna for all the waves measured. Both the standard error of the mean and the standard deviation of a single observation are of interest here and therefore both have been given, provided N is large enough to justify such computations.

TABLE 3. — Magnitude differences Uppsala-Kiruna.

Magnitude	<i>h</i>	N	Mean difference	S. E.	S. D.
M (PZ')	<i>n</i> , (<i>n</i>)	134	+0.1*	±0.03	±0.3
	> <i>n</i>	16	-0.2		
M (PH)	<i>n</i> , (<i>n</i>)	37	±0.0	±0.04	±0.3
	> <i>n</i>	5	-0.1		
M (PPZ')	<i>n</i> , (<i>n</i>)	21	-0.1	±0.1	±0.3
	> <i>n</i>	5	-0.1		
M (PPH)	<i>n</i> , (<i>n</i>), > <i>n</i>	19	-0.3*	±0.06	±0.3
M (SH)	<i>n</i> , (<i>n</i>)	110	-0.1*	±0.04	±0.4
	> <i>n</i>	18	-0.2	±0.09	±0.4
M (LH)	<i>n</i> , (<i>n</i>)	157	-0.1*	±0.02	±0.2
	> <i>n</i>	23	-0.1*	±0.04	±0.2

h = depth of foci of earthquakes used (*n* = normal, (*n*) = slightly below normal, > *n* = deep);

N = number of earthquakes used;

* = difference is significantly different from zero (indicated only in case an error computation is made);

S.E. = standard error of the mean;

S.D. = standard deviation of a single observation.

We note that the standard deviations are in all cases around ±1/4 magnitude unit. The significance of the mean differences has been investigated by Fischer's *t*-test (1950, pp. 119, 174) in all cases where error computations were made.

The significant mean difference of +0.1 for M(PZ') is to be observed, as in this case the determinations at the two stations are made on records from exactly the same type of instrument (Grenet) mounted in the same way and with nearly the same constants.

Percentage frequency distributions of the various magnitude differences are shown in Fig. 1. The most remarkable result is that the scatter of the observations is much less for the surface waves than for any of the body waves.

The possible dependence of the individual differences on magnitude, depth, distance, and location has been investigated.

The individual differences between Uppsala and Kiruna have been plotted against magnitude M. It results that there is no variation with M for PZ'; for PH and SH there seems to be some indication of a decrease of the differences with increasing M but probably not significant; for PPH the tendency of a decrease with M is more obvious; finally the differences for LH are independent of M. The possible decrease of certain differences would mean that for increas-

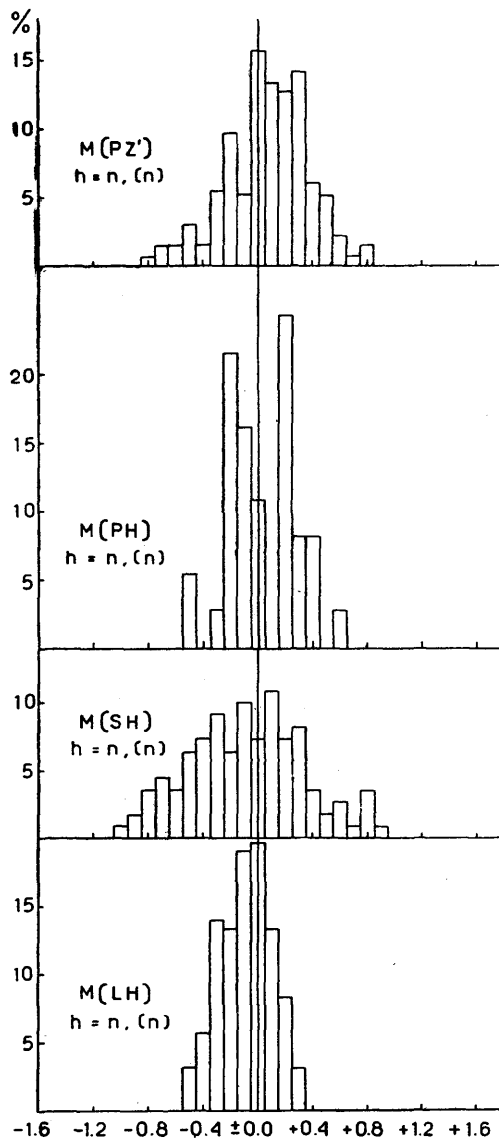


FIG. 1. — Frequency distributions of magnitude differences Uppsala-Kiruna for given waves.

ing M with ensuing increasing amplitudes at both stations, the amplitude increase would be less at Uppsala than at Kiruna. Instrumental effects are not excluded.

From Table 3 we see a clear tendency for all differences to become more negative for $h > n$ compared with $h = n$. This tendency

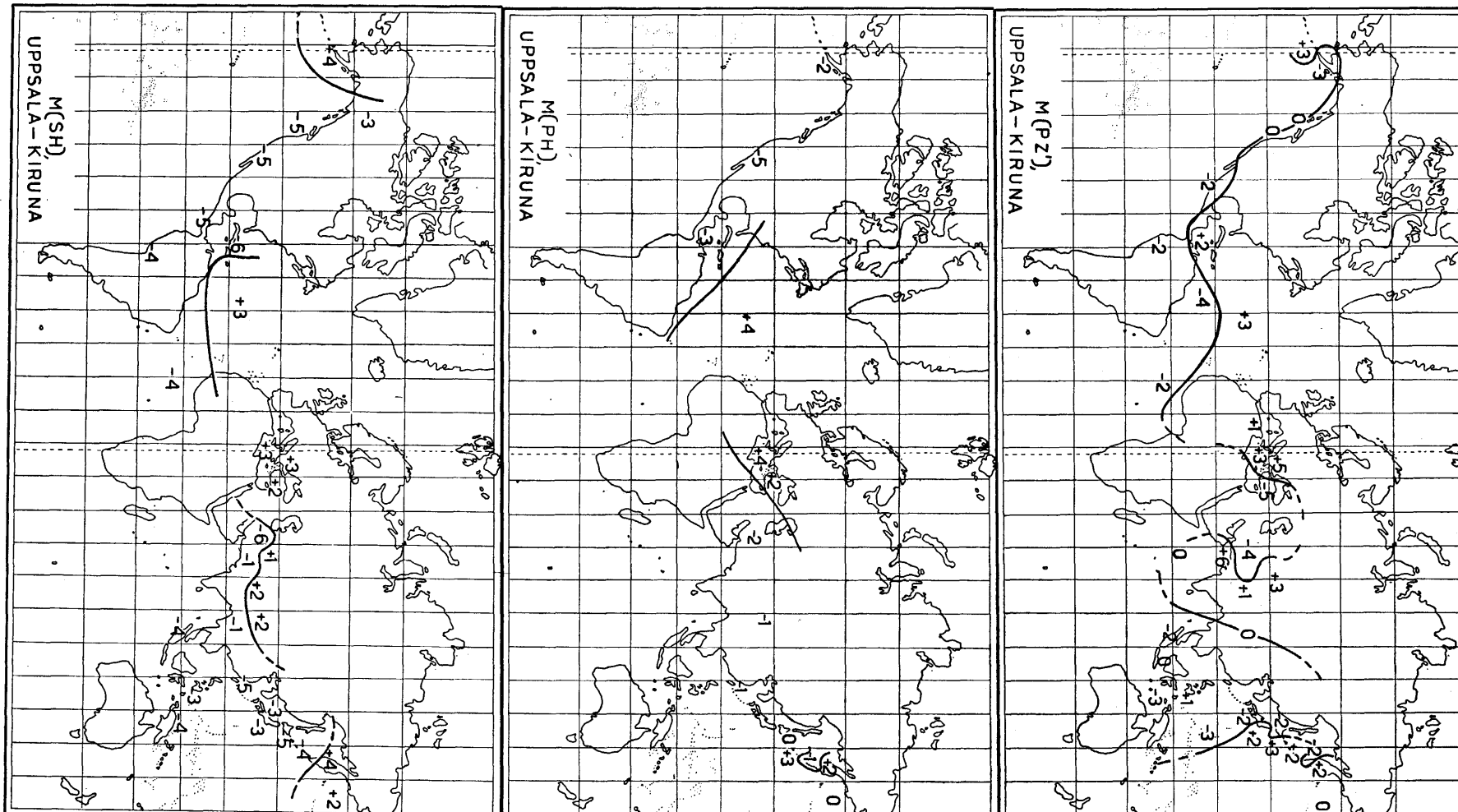


FIG. 2 a. — Regional distribution of magnitude differences between Uppsala and Kiruna. See « Explanation of the maps » at the end of chapter III.

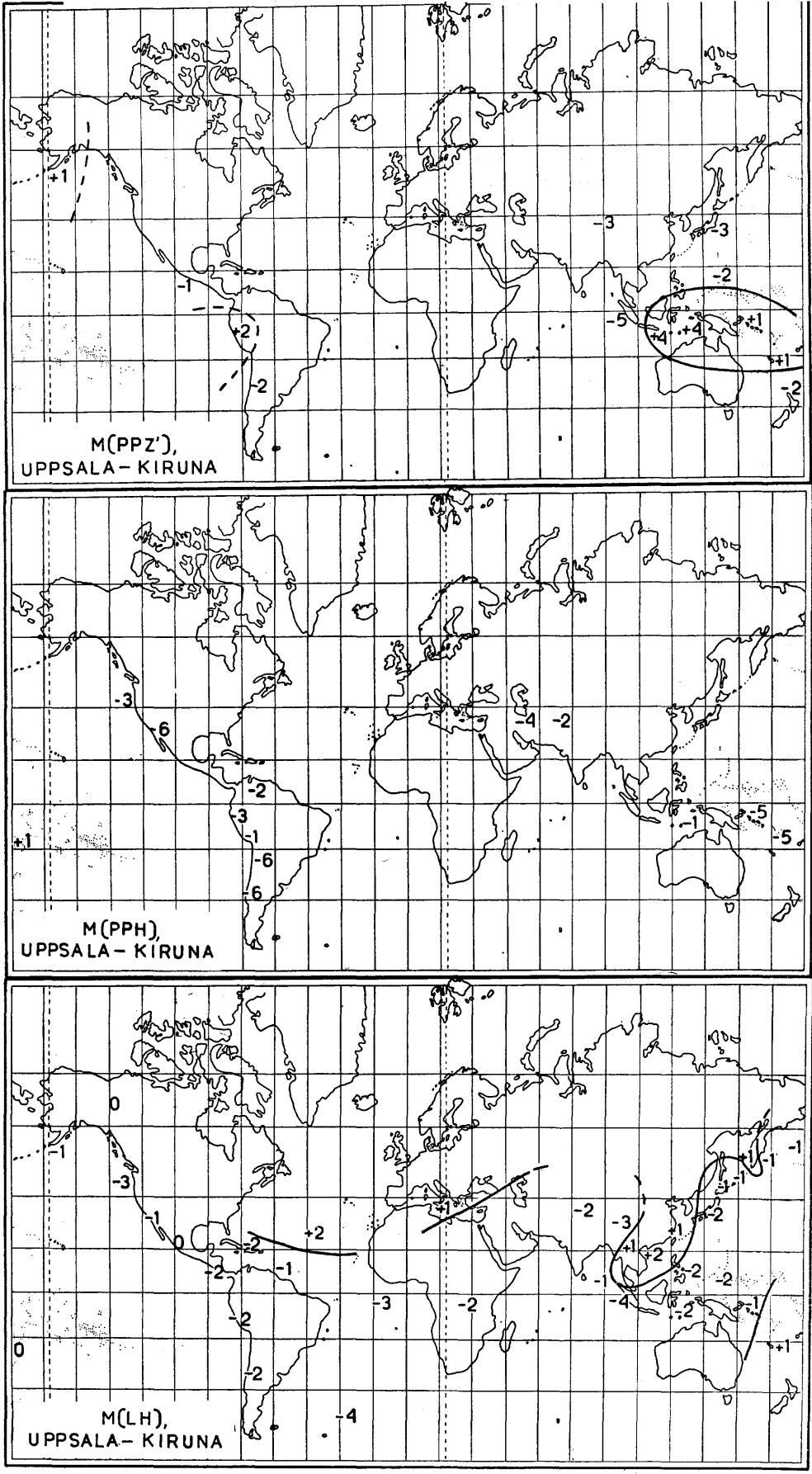


FIG. 2 b. — Regional distribution of magnitude differences between Uppsala and Kiruna.

exists also for LH where the mean for $h = n$ is —0.09 and for $h > n$ it is —0.14; the same applies also to PPZ' where the mean for $h = n$ is —0.08 and for $h > n$ it is —0.14. The reasons cannot be instrumental as the Grenet seismograph has the same characteristics at both stations. The explanation is given below in connection with the regional distribution.

The individual differences have also been plotted against the mean epicentral distance Δ of the two stations and also on maps (Fig. 2 a and 2 b; see « Explanation of the maps » at the end of chapter III). Some of the differences show quite marked variation with distance. However, this is in no case due to any functional relation to Δ , but is altogether explained by the regional distribution of the differences. For a given distance interval often one earthquake region dominates, for another distance another region dominates, and therefore the regional values of the differences explain the spurious variation with distance. There is also no functional relation to azimuth from our stations. The regional distribution of the magnitude differences is the only significant regularity which they follow. Differences between $h = n$ and $h > n$ could be expected from differences in mechanisms (orientation of fault plane, etc.) with focal depth, but they are in general not borne out here. Therefore at least provisionally the same regional corrections can be used for all depths (concerns all maps; see further « Explanation of the maps »). The fact mentioned above that all differences between Uppsala and Kiruna tend to be more negative for $h > n$ than for $h = n$ is explained by the regional distribution : the deeper shocks are usually located in the negative regions. However, this in turn requires a special explanation.

The main properties of the regional distributions of the magnitude differences between Uppsala and Kiruna are as follows. M(SH) shows the most remarkable and regular distribution, with positive differences at Kamchatka and negative in Japan and to the south of it. The very regular distribution especially in this area has been given in more detail in a special map, Fig. 3, where individual earthquakes are given instead of mean values. There is an obvious transition zone in the Kurile Islands. The most likely explanation is the different location of our two stations in relation to the faults (compare the schematic Fig. 9 in a paper by Nelson, 1954). The directions from Uppsala and Kiruna to this area are not very different, but when they form small angles with the faults, as probably in Kamchatka, even a small difference in direction may cause considerable difference in the energy radiated. The gradual change in the fault orientation as we pass from Kamchatka to Japan may

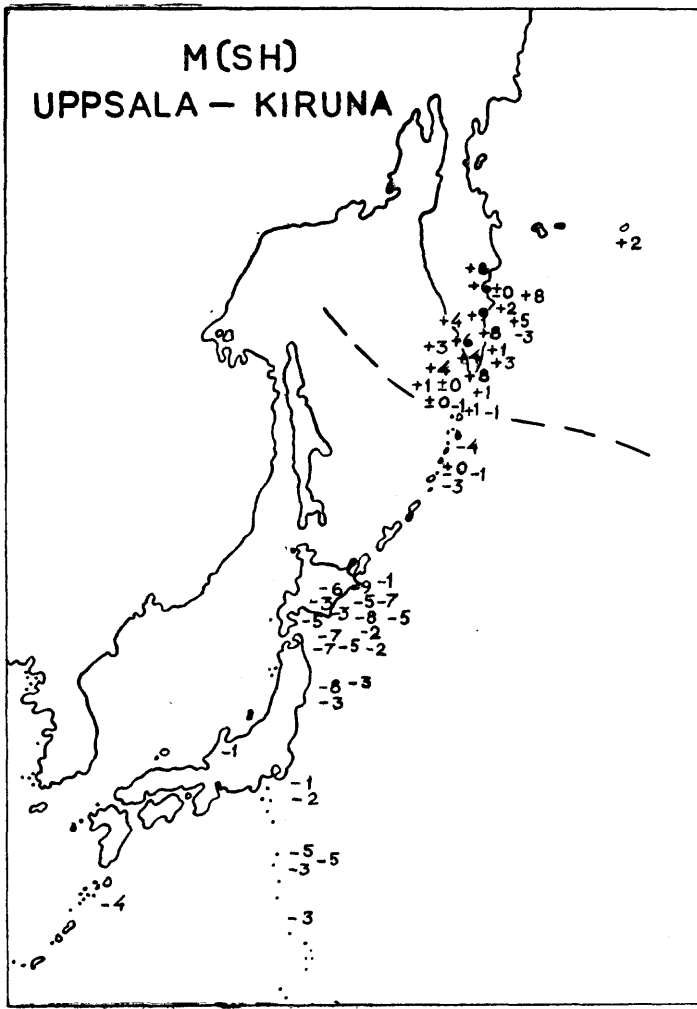


FIG. 3. — Magnitude differences for SH between Uppsala and Kiruna in the Kamchatka-Japan region.

explain the gradual, but very clear change in the M (SH) - difference between Uppsala and Kiruna. A quantitative check requires more accurate knowledge of the fault orientations. The idea, however, gets further confirmation from the corresponding differences between Uppsala and Kiruna for M (PZ') and M (PH). The negative tongue-like area for these two differences just south of Kamchatka coincides with the transition zone for M (SH). This agrees with the explanation given above, as in this area the directions to Uppsala and Kiruna are nearly perpendicular to the fault strike. In the

Kurile Islands south of this area there are positive differences for $M(PZ')$ and $M(PH)$, but negative for $M(SH)$, which also agrees with our explanation (Uppsala and Kiruna are now in the SW quadrant at the focus).

It is a remarkable fact that the tongue-like area at Kamchatka exists also for $M(LH)$, and that the signs of this difference are everywhere opposite to $M(PZ')$ and $M(PH)$ from Kamchatka to Japan. It is also clear that the differences are largest for $M(SH)$, smaller for $M(PZ')$ and $M(PH)$, and smallest for $M(LH)$ in this region. It appears as if amplitude studies like this would be very helpful in earthquake mechanism investigations in addition to the first motion studies, now generally used.

In Burma-Tibet there is a transition zone of $M(SH)$ and all nearer earthquakes (Turkey, Greece) have positive differences. In south Alaska the differences are positive (probably continuation of the positive area in Kamchatka), but along the west coast of America as well as in the Caribbean area the differences are negative.

$M(PH)$ also shows a regular distribution but not to the same degree as $M(SH)$. It is remarkable that there are very clear similarities in the distributions for $M(PH)$ and $M(SH)$. Thus $M(PH)$ shows positive differences for Kamchatka, zero differences beginning around $157^{\circ}E$, $50^{\circ}N$, zero differences for Japan, positive differences for Turkey and Greece, negative differences from Alaska to Central America. One earthquake at about $40^{\circ}W$, $30^{\circ}N$ gave positive differences both for $M(P)$ and $M(S)$. $M(PZ')$ has also a very clear distribution in general agreeing well with that for $M(PH)$. For instance, the «tongue» of negative signs in Kamchatka, negative in inner Asia, positive in Turkey-Greece, positive in the Atlantic, negative south of Alaska are all common features of $M(PZ')$ and $M(PH)$.

Comparing $M(PPH)$ and $M(PPZ')$ we find a remarkable dissimilarity in the region of New Guinea, where the $M(PPH)$ - differences are negative but the $M(PPZ')$ - differences positive; in South America the former are negative, the latter around zero. Comparing $M(PPZ')$ and $M(PZ')$ we note that the $M(PPZ')$ - differences are negative around Japan, but the $M(PZ')$ - differences are positive in the same region. The differences for $M(LH)$ also show a clear regional distribution though not so pronounced as for $M(SH)$. The distribution for $M(LH)$ is not the same as for $M(P)$ and $M(S)$. This concerns e.g. Kamchatka-Kurile Islands where $M(LH)$ has both positive and negative differences; Japan has in the mean a negative $M(LH)$ - difference, but all differences are small; differ-

ences are positive in an area of SE Asia; along the west coast of America, including South America, the $M(LH)$ - differences are predominantly negative; in SW Pacific they centre around zero.

The regional distribution of the magnitude differences between two stations is very striking, and it is certainly not accidental. The mean differences in Table 3 naturally depend on the number of shocks from each region; these numbers used in computing Table 3 correspond fairly well to the seismicity of the earth, and the mean values are therefore representative. The many repeated occasions of the same difference (at least with regard to sign) in a given epicentral region show that the same energy distribution from the focus repeats itself again and again. Also the signs of the differences are the same within relatively large areas, indicating similar energy distribution within these areas. This may have connection with the fact that at a given station the direction of first motion of P is the same within relatively large areas (see e.g. Bath, 1952). In spite of the relatively small distance of 8° between Uppsala and Kiruna considerable differences have been found. Larger differences are to be expected for stations far apart from each other. Our observations demonstrate clearly that the energy distribution from an earthquake is a complicated phenomenon. Any mathematical and therefore necessarily simple expression for the energy distribution is only a very rough approximation to the truth. These circumstances make an exact magnitude and energy determination of an earthquake very difficult.

In addition to the earthquake mechanism also other reasons may contribute to the differences found. The mean differences in Table 3 may at least partly have instrumental reasons (in case different instrument types have been compared), but the regional distributions cannot be explained in this way. This is obvious from a number of facts, as e.g. the similar distribution for $M(P)$ and $M(S)$, the similar distribution for $M(PZ')$ and $M(PH)$ etc. The fact that similar distributions are obtained for $M(P)$ and $M(S)$ indicates that other factors than earthquake mechanism are operative, probably local effects at the stations. For further discussion of this point, see B. 2 below.

B. *Comparison of different waves at a given station.*

1. $M(PZ')$, $M(PZ)$, $M(PH)$, $M(PPZ')$, $M(PPZ)$, $M(PPH)$. *Spectral energy distribution.*

In this section we are comparing magnitudes determined from different waves (P and PP) recorded at a given station. Table 4 summarizes the results of the comparisons.

TABLE 4. — Magnitude differences for P and PP.

Magnitude difference δ	Uppsala					Kiruna				
	h	N	$\bar{\delta}$	S. E.	S. D.	h	N	$\bar{\delta}$	S. E.	S. D.
M (PZ') — M (PZ)	1	1				$n, (n)$	66	+0.2*	± 0.04	± 0.3
M (PZ') — M (PH)	$n, (n)$	61	+0.2*	± 0.03	± 0.2	$> n$	11	+0.6	± 0.05	± 0.4
M (PZ) — M (PH)	$> n$	8	+0.3			$n, (n)$	58	± 0.0		
M (PPZ') — M (PPZ)		1				$> n$	8	+0.4		
M (PPZ') — M (PPH)	$n, (n), > n$	14	± 0.0			$n, (n)$	54	-0.2*	± 0.02	± 0.2
M (PZ') — M (PPZ')	$n, (n), > n$	41	+0.3*	± 0.06	± 0.4	$n, (n), > n$	10	-0.2		
M (PH) — M (PPH)	$n, (n), > n$	9	+0.3			$n, (n), > n$	12	+0.1		
						$n, (n), > n$	14	-0.2		
						$n, (n), > n$	38	+0.2*	± 0.06	± 0.4
						$n, (n), > n$	22	+0.1	± 0.05	± 0.2

For explanation see note of Table 3.

Percentage frequency distributions are shown in Fig. 4 for those differences of which we have most observations, i.e. $N \geq 40$. We observe that the frequency distributions of a given difference, e.g. $M(PZ') - M(PH)$, $M(PZ') - M(PPZ')$, are very similar at the two stations. The general shape of a frequency distribution is

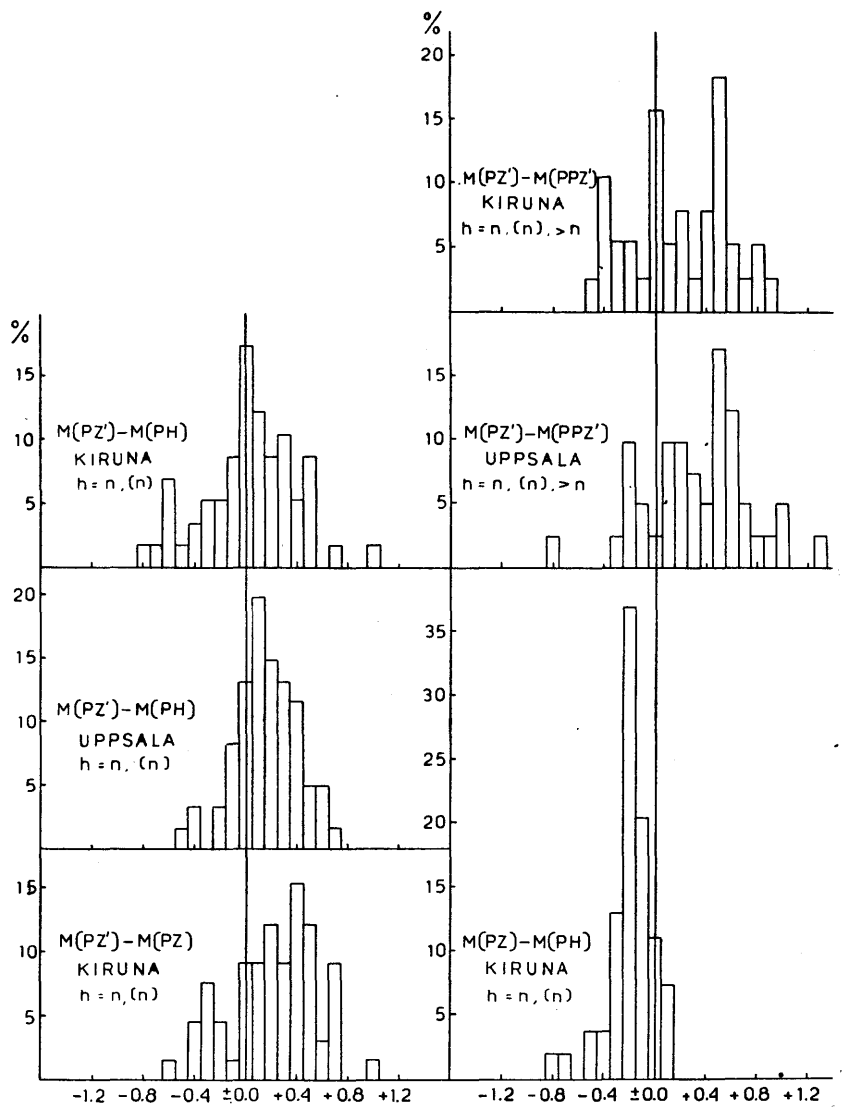


FIG. 4. — Frequency distributions for magnitude differences for various longitudinal waves.

much more dependent on the particular difference involved than on the station to which it applies. This is a general rule concerning all our frequency distributions. By graphical methods we have found the various individual differences to be independent of magnitude as well as of epicentral distance. The only regularity which the differences follow is the regional distribution (Fig. 5 a and 5 b).

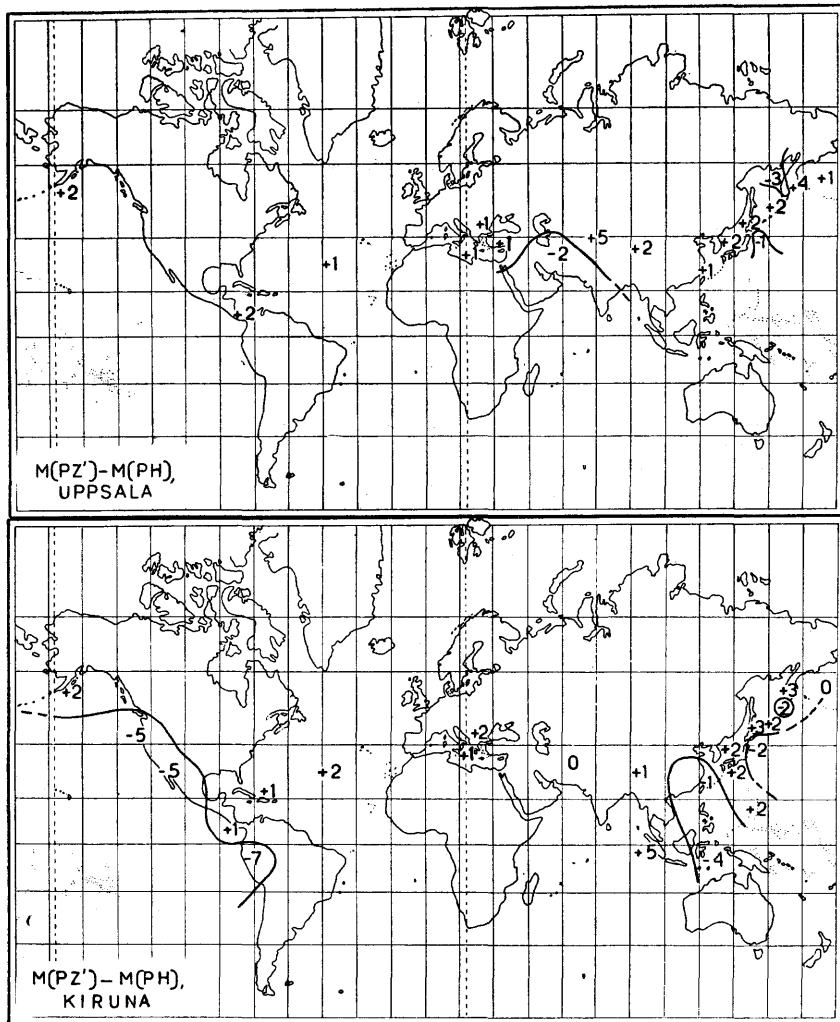


FIG. 5 a. — Regional distribution for magnitude differences for longitudinal waves.

The regional distribution of the differences $M(PZ') - M(PZ)$ for Kiruna is obvious. Positive differences dominate; negative areas are to be found along the west coast of America and within the Kamchatka region. The last-mentioned region is remarkable as this exceptional area inside the surrounding area of opposite sign appears to exist for most magnitude differences investigated in this paper. The regional distribution of $M(PZ') - M(PH)$ for Kiruna is very

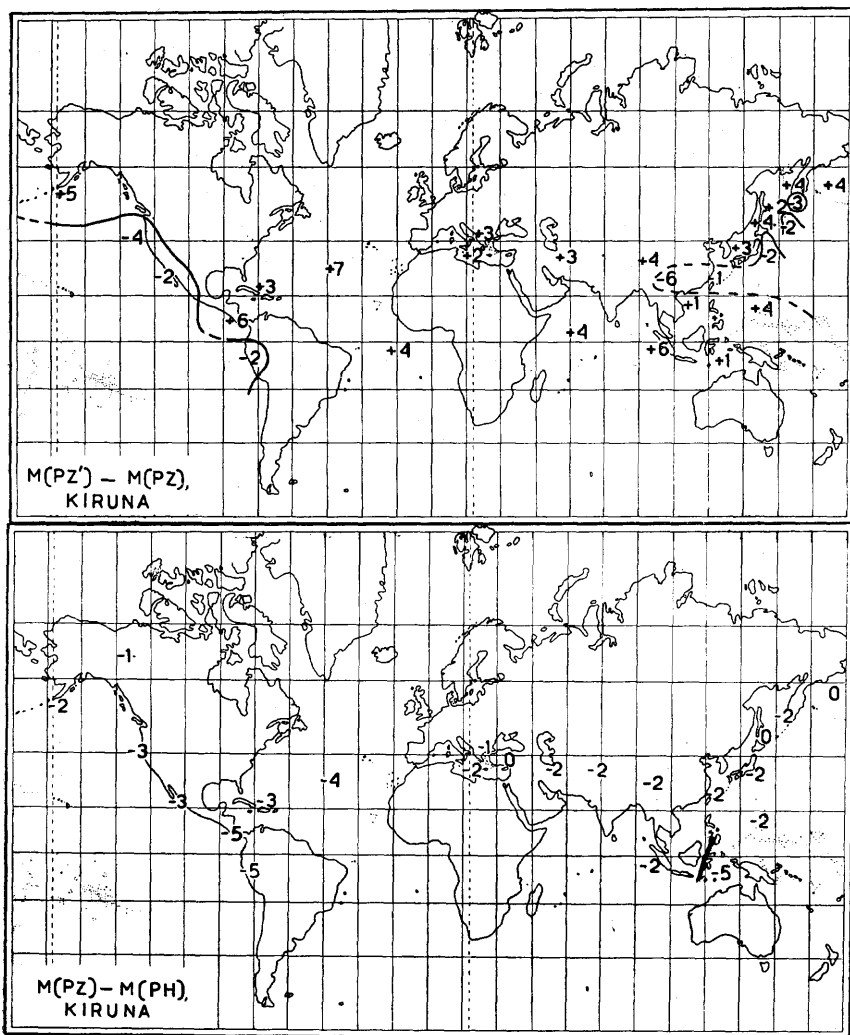


FIG. 5 b. — Regional distribution for magnitude differences for longitudinal waves.

similar to that of $M(PZ') - M(PZ)$; this simply means that $M(PZ)$ and $M(PH)$ run parallel to each other. In general $M(PZ) < M(PH)$, therefore $M(PZ') - M(PZ) > M(PZ') - M(PH)$. There is general agreement of the regional distributions of $M(PZ') - M(PH)$ for Uppsala and Kiruna. The reason for this is most probably the earthquake mechanism and not the local

structures around the stations and not instrumental effects. Practically all the differences $M(PZ) - M(PH)$ for Kiruna are negative (see the frequency distribution in Fig. 4) with only very little regional variation.

The comparison of short-and long-period components (Z' with Z and Z' with H) of the same wave made here (Table 4) is of special interest in view of the question of the energy spectrum. The quantities A (see equations [14] and [15]) are given by Gutenberg as being the same for a given wave regardless of its frequency. At least for P the differences in question are generally positive. However, as the values are based upon different instruments, we need to investigate the possible influence of instrumental differences.

Assuming that u_1, T_1 are amplitude and period as measured and M_1 the corresponding magnitude, whereas u_2, T_2 are the actual amplitude and period of the same wave, corresponding to a magnitude M_2 , we have from equation (15)

$$M_1 = 1.1 \left\{ [A(\Delta, h) - 0.7] + \log \frac{u_1}{T_1} \right\} \quad (18)$$

$$M_2 = 1.1 \left\{ [A(\Delta, h) - 0.7] + \log \frac{u_2}{T_2} \right\} \quad (19)$$

which gives

$$M_1 - M_2 = 1.1 \log \frac{u_1 / T_1}{u_2 / T_2} = 1.1 \log \frac{u_1}{u_2} \quad (20)$$

as $T_1 = T_2$. $u_1/u_2 \neq 1$ or $M_1 - M_2 \neq 0$ depends only on instrumental effects. Table 5 gives numerical values.

TABLE 5.

u_1/u_2	$M_1 - M_2$
1	0
1.2	0.1
1.4	0.2
1.6	0.2
1.8	0.3
2.0	0.3
2.5	0.4
3.0	0.6

A value of $M_1 - M_2 = 0.2$ would therefore correspond to an error of about 50 % in u_1/u_2 , probably much in excess of our instrumental errors. An error of the instrumental magnification curve of 30 % gives $M_1 - M_2 = 0.1$. Incidentally, we note that the claim on instrumental accuracy is not very great in case of magnitude determinations. It is obvious from the comparisons of the instruments at Uppsala and Kiruna that instrumental differences are in no case more than a minor contribution to the magnitude differences.

The conclusion for shallow shocks is that magnitudes determined from short-period P are generally larger than those determined from long-period P. The difference may at least partly be due to instrumental differences. We cannot therefore state with absolute certainty that for shallow shocks the short-period P carries more energy than the long-period P, even if there is an indication in that direction. However, comparing the differences $M(PZ') - M(PZ)$ and $M(PZ') - M(PH)$ both for Uppsala and Kiruna we find that in every case these differences are more positive for deeper shocks (Table 4). This behaviour cannot be explained as instrumental effects. We conclude that in earthquakes deeper than normal the energy ratio of short-period to long-period P is much larger than for shallow shocks. The increase of $M(PZ') - M(PZ)$ with depth h is clear from a graphical plot of the individual differences against the corresponding depths. The relation between the total energy E of the seismic waves, expressed in ergs, and the magnitude is according to a recent investigation by Bath (1955), approximately valid between magnitudes 5 and 8

$$\log \frac{E_1}{E_2} = 2.0(M_1 - M_2)$$

This gives the numerical values in Table 6, showing what total energy ratios are obtained for given magnitude differences.

TABLE 6.

$M_1 - M_2$	E_1/E_2
0.1	1.6
0.2	2.5
0.3	4.0
0.4	6.3
0.5	10.0
0.6	15.9

As the limit of accuracy of an individual M - determination is approx. ± 0.3 , it is seen that the corresponding error of the total energy is a factor of 4. The table also gives the energy ratios to be

expected between short-period and long-period P (compare chapter IV).

As the general mechanism is the same for shallow and deeper shocks, it is probable that the original spectral energy distribution is the same for both. But it is known that there is a very rapid dissipation of the high-frequency waves in the crustal layers in the epicentral area. Our observations agree with these findings, as for deeper shocks the crustal layers are avoided at the origin, and therefore much less of the high-frequency motion should be lost than for shocks within the crust itself.

For PP the magnitudes from short-period instruments (Grenet) are either about equal to or less than those from long-period instruments. It is also a well-known fact that PP is usually unimportant or most often absent on the Grenet records. Around $\Delta = 90^\circ - 100^\circ$, however, PP is rather frequent on the Grenet records and then comparable in size to P (notable examples of this are the earthquakes No. 221 and 222). The periods of PP recorded on the Grenet instrument are generally longer than those of P, which is in line with the explanation given above.

The difference $M(PZ) - M(PH) = -0.2$ for Kiruna will now be studied in some detail. This clearly shows what difference can be obtained between two instruments at the same place, even if the constant determinations are both frequent and made with all care. The difference is significantly different from zero and has very little scatter (see Fig. 4). The corresponding magnitude formulae are

$$M(PH) = 1.1 \left\{ [A(PH) - 0.7] + \log \frac{u}{T} \right\} \quad (22)$$

$$M(PZ) = 1.1 \left\{ [A(PZ) - 0.7] + \log \frac{w}{T} \right\} \quad (23)$$

The period T is the same in both cases, as the formulae are applied to one and the same wave in total horizontal (u) and vertical (w) components. We require that

$$M(PH) = M(PZ) \quad (24)$$

This gives

$$A(PH) - A(PZ) = \log \frac{w}{u} \quad (25)$$

In Table 7 are given $A(PH) - A(PZ)$ taken from Gutenberg's tables (1945 b) and corresponding w/u calculated from formula (25). w/u and $\log(w/u)$ have also been calculated by means of Jeffreys'

theory (1926, p. 327), using Jeffreys-Bullen's tables of 1940 and assuming the velocity of P waves next to the surface = 7.2 km/sec.

TABLE 7.

Δ	GUTENBERG		JEFFREYS	
	A (PH) — A (PZ)	w/u	log (w/u)	w/u
30°	+ 0.2	1.6	0.11	1.30
35				
40	+ 0.2	1.6	0.14	1.38
45				
50	+ 0.3	2.0	0.20	1.59
55				
60	+ 0.3	2.0	0.26	1.83
65				
70	+ 0.4	2.5	0.31	2.05
75				
80	+ 0.5	3.2	0.38	2.42
85				
90	+ 0.4	2.5	0.44	2.76
95				
100	+ 0.6	4.0	0.44	2.76
105				

The two sets of values of w/u in Table 7 are plotted against Δ in Fig. 6 together with our observations from Kiruna. We find that Gutenberg's values of w/u are in excess of our theoretical values as obtained from Jeffreys, and furthermore that our observations agree well with the theory with the assumed value of the surface velocity of P. This explains at least part of the difference $M(PZ) - M(PH)$. Instrumental differences between Z and H are probably not of much influence here. For instance, if the whole error lies in Z, an error of 43 % in w is required to explain the observed

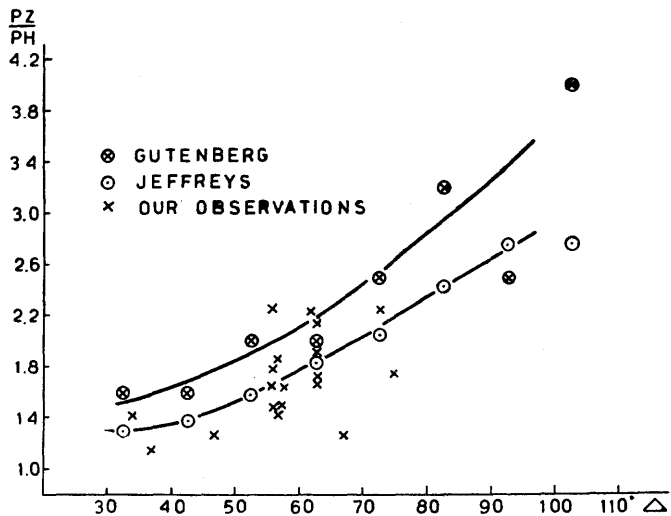


FIG. 6. — PZ/PH or w/u from Gutenberg's data, Jeffreys' theory, and our own observations.

difference. This error is very unlikely to exist. In some cases only one horizontal component was measurable; this component was then multiplied by 1.4 in forming u . The slight overestimate of u due to this procedure can explain a difference in $M(PZ) - M(PH)$ of only 0.04-0.07, not the observed mean difference of 0.2. It is probable that the observed mean difference of $M(PZ) - M(PH)$ is a result of the various cooperating reasons discussed here.

$M(P) - M(PP)$ is clearly positive for all instruments at both stations. The differences seem to be greater at Uppsala than at Kiruna. These differences cannot be due to the instruments, as in all cases only waves recorded by the same instrument have been compared. As already mentioned, PP is generally not well recorded by the Grenet apparatus. It is then interesting to find the same difference $M(P) - M(PP)$ for Wiechert and that a positive difference exists also for Galitzin. The A-values of Gutenberg (1945 b) correspond to mean conditions. For PP at Uppsala and Kiruna they should be increased corresponding to the calculated magnitude differences.

2. $M(PZ')$ and $M(PH)$ compared with $M(SH)$.

Table 8 gives the results of the comparisons of magnitudes determined from P and from S waves. Frequency distributions are given in Fig. 7. These differences are not unrelated to magnitude (for further details, see chapter III.B.3). There is no func-

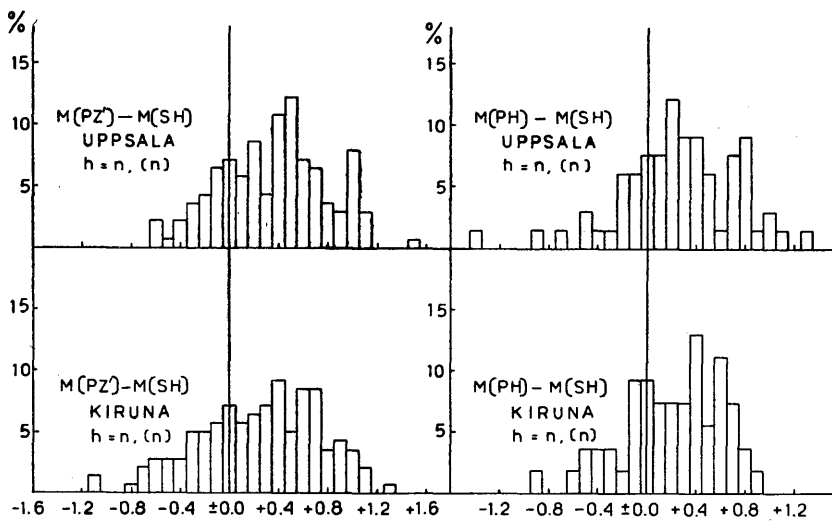


FIG. 7. — Frequency distributions of magnitude differences between longitudinal and transverse waves.

TABLE 8. — Magnitude differences between P and S.

Magnitude difference δ	Uppsala					Kiruna				
	h	N	$\bar{\delta}$	S. E.	S. D.	h	N	$\bar{\delta}$	S. E.	S. D.
M (PZ') — M (SH)	$n, (n)$	139	+0.4*	± 0.04	± 0.4	$n, (n)$	141	+0.2*	± 0.04	± 0.5
M (PH) — M (SH)	$n, (n)$	66	+0.3*	± 0.06	± 0.5	$n, (n)$	54	+0.2*	± 0.05	± 0.4
	$> n$	19	+0.3*	± 0.1	± 0.5	$> n$	19	+0.5*	± 0.1	± 0.5
	$n, (n)$	5	+0.1			$n, (n)$	11	+0.1		
	$> n$					$> n$				

For explanation see note of Table 3.

tional relation to epicentral distance but only regional distributions of the magnitude differences. This fact is especially obvious in the present case. Plotting the differences against distances we find that 60° for Kiruna corresponds to about 67° for Uppsala (Kamchatka and Japan), whereas 30° for Kiruna corresponds to about 22° for Uppsala (Greece). The regional distributions are given in Fig. 8 a and 8 b.

We note from Table 8 that M (SH) is all through less than M (P). This is probably not an instrumental effect, as it is observed when P and S are both measured on the same records (Wiechert or Galitzin). As P and S generally have different periods, an instrumental effect is not completely excluded, but it is remarkable that Wiechert and Galitzin give the same results. Comparing the

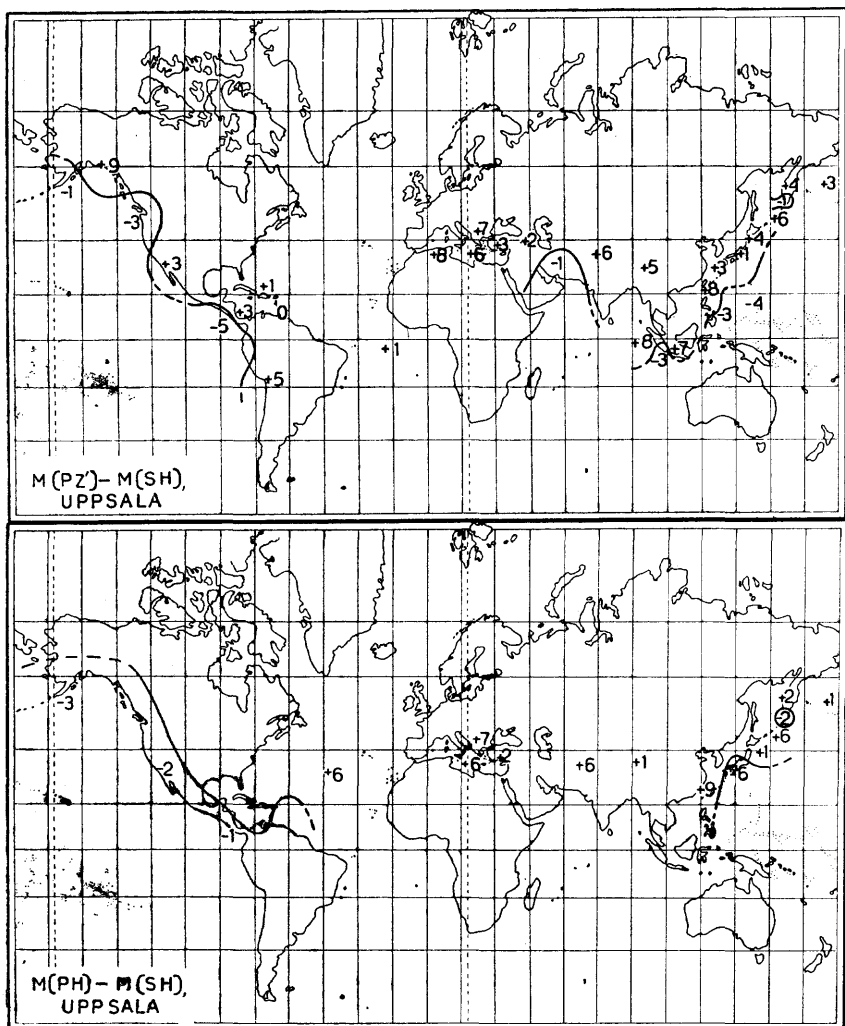


FIG. 8 a. — Regional distribution of magnitude differences between longitudinal and transverse waves (Uppsala).

regional distributions of $M(PZ') - M(SH)$ and of $M(PH) - M(SH)$ for Uppsala and Kiruna we find both clear similarities and clear dissimilarities. Earthquakes deeper than normal have generally differences which agree well with those of the shallow earthquakes in the same region.

Positive differences naturally dominate. $M(PZ') - M(SH)$ for Kiruna has negative values in Japan and an area SE of Asia, in part of Central America, and along the west coast of North America; zero differences occur in Central Atlantic. The positive

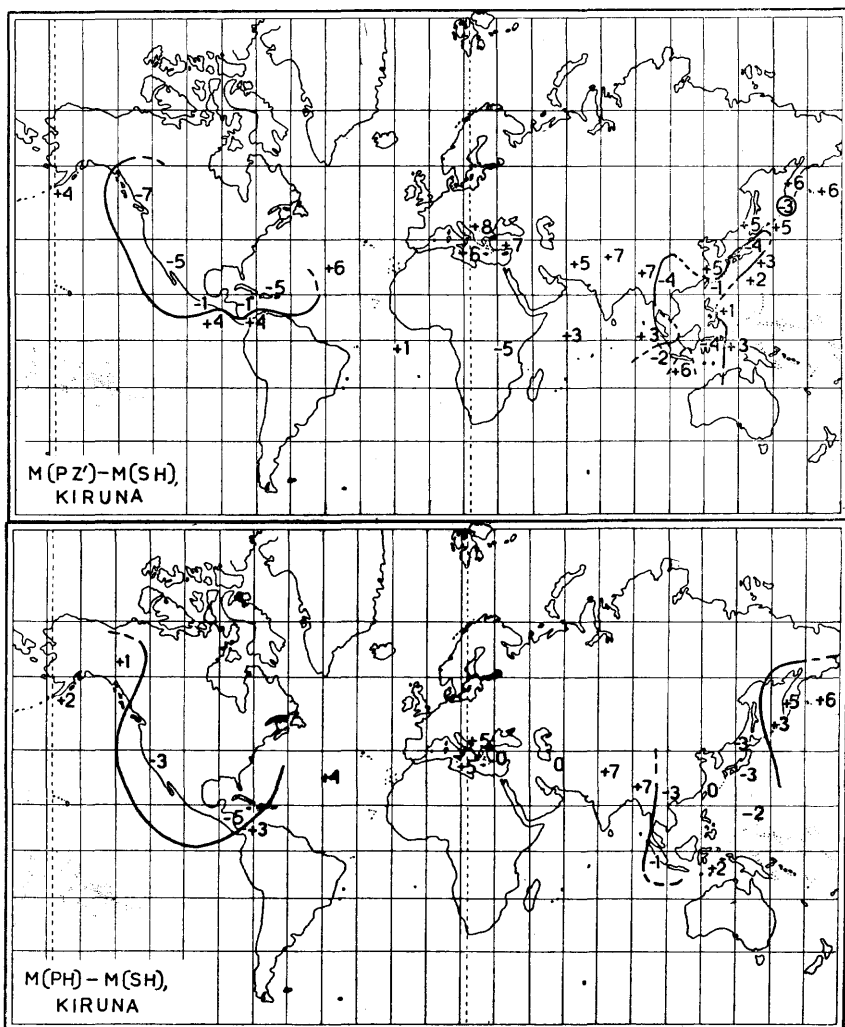


FIG. 8 b. — Regional distribution of magnitude differences between longitudinal and transverse waves (Kiruna).

differences are especially pronounced in Greece, Turkey, and adjacent parts of the Mediterranean, and also in inner Asia. $M(PZ') - M(SH)$ for Uppsala has contrary to Kiruna practically only positive values for Japan; south of Alaska the Uppsala differences are negative, but the Kiruna differences positive. But the very pronounced positive region of Greece, Turkey, and the Mediterranean and also in the inner Asia prevails for both stations. $M(PH) - M(SH)$ has also clear regional distributions with both similarities and dissimilarities between Uppsala and Kiruna. For

a given station $M(PZ') - M(SH)$ and $M(PH) - M(SH)$ have in general the same distributions. All differences have in common the pronounced positive area around Greece, Turkey, and the Mediterranean. The magnitude differences there often approach and in several cases even exceed one magnitude unit. The mean differences for these regions are given in Table 9.

TABLE 9.

Magnitude difference δ	Uppsala			Kiruna		
	Δ	N	$\bar{\delta}$	Δ	N	$\bar{\delta}$
$M(PZ') - M(SH)$	$\leq 30^\circ$	27	+0.6	$\leq 38^\circ$	15	+0.6
$M(PH) - M(SH)$	$\leq 30^\circ$	20	+0.6	$\leq 38^\circ$	8	+0.4

The fact that there are regions where $M(PZ') - M(SH)$ or $M(PH) - M(SH)$ are of opposite sign for two stations so close together as Uppsala and Kiruna is of special importance. Various possible reasons will be discussed.

1. The energy distribution on different seismic waves already at the focus cannot give the explanation. This effect alone would give the same differences at both stations. It results that energy ratios between different seismic waves based on the records at one station cannot be representative for the earthquake.
2. Instrumental effects are unlikely, especially for $M(PH) - M(SH)$.
3. Different position of the two stations in relation to the earthquake faults may contribute. However, in some cases as e.g. for Alaska and the region to the south of it, where opposite signs were observed, Uppsala and Kiruna are in approximately the same direction from the epicentres and the distance differs only by 8° .
4. Local inhomogeneities of the crust around the stations may contribute. Due to these crustal inhomogeneities with irregularly varying velocities for seismic waves the wave-front surfaces are deformed with ensuing convergences or divergences of the ray paths. In its turn this circumstance gives larger or smaller amplitudes resp. than would be observed in a homogeneous crust. A difficulty with this explanation is that a given inhomogeneity in general ought to give an increase (or a decrease) of the energy concentration both for P and S at the same time. However, a change of the velocity for P waves with no change of the velocity

of S waves is possible, if e.g. only λ (Lamé parameter) varies, whereas μ (rigidity) and ρ (density) are constant. If v_p and v_s are the velocities of P and S respectively we have in general that

$$d \left(\frac{v_p}{v_s} \right)^2 = \frac{1}{\mu} d\lambda - \frac{\lambda}{\mu^2} d\mu \quad (26)$$

from which various special cases easily may be deduced.

For more complete discussion of unsymmetrical energy distribution see Nelson (1954). However, his inference of smaller scatter for P than for S observations is not always confirmed by this study (see Table 12). The energy radiation in P, SV, and SH in different directions has been mathematically computed by Heelan (1953) for a particular case. Extensions of such computations to phenomena resembling those occurring in earthquakes and comparison with observations in cases of known earthquake mechanism (orientation of fault plane etc) would be very desirable. Summing up, the most probable explanation for the magnitude differences found and their regional variation is unsymmetrical energy distribution from the hypocentre, modified by the local structure at the source and particularly at the stations.

3. M (PZ'), M (PH), and M (SH) compared with M (LH). Comparison of magnitude scales. Relations to focal depth.

It is well known that the part of the total energy which appears as surface waves decreases rapidly with increasing focal depth. Therefore magnitude determinations based on LH can only be made for $h = n$. For all depths in excess of the normal, LH will give too low magnitudes, unless a special correction depending on h is made.

Magnitude differences $M (PZ') - M (LH)$, $M (PH) - M (LH)$, and $M (SH) - M (LH)$ were computed for Uppsala and Kiruna in the first case only for $h = n$, while $h = (n)$ and $h > n$ were excluded. Table 10 summarizes the mean values and the error computations.

TABLE 10. — Comparison of magnitudes from body waves and from surface waves for $h = n$.

Magnitude difference δ	Uppsala				Kiruna			
	N	$\bar{\delta}$	S. E.	S. D.	N	$\bar{\delta}$	S. E.	S. D.
$M (PZ') - M (LH)$	68	+ 0.0	± 0.06	± 0.5	77	- 0.0	± 0.05	± 0.5
$M (PH) - M (LH)$	24	- 0.2*	± 0.1	± 0.5	30	+ 0.0	± 0.08	± 0.4
$M (SH) - M (LH)$	64	- 0.1*	± 0.05	± 0.4	69	- 0.0	± 0.05	± 0.4

For explanation see note of Table 3.

We find that for $h = n$ most of the differences mentioned are in the mean not significantly different from zero. The range of variation is approximately + 1.0 to - 1.0 for $M(PZ') - M(LH)$ and $M(PH) - M(LH)$ and about + 0.7 to - 0.9 for $M(SH) - M(LH)$.

The various differences have been investigated in relation to magnitude, region, and focal depth.

The magnitude differences between surface waves and body waves vary with magnitude. The following least-square solutions have been obtained for $h = n$ valid for magnitudes from 5.0 to 8.5.

Uppsala :

$$M(LH) - M(PZ') = 0.45 [M(LH) - 7] + 0.33 = 0.45 [M(LH) - 6.3] \quad (27)$$

(N = 76)

$$M(LH) - M(PH) = 0.46 [M(LH) - 7] + 0.27 = 0.46 [M(LH) - 6.4] \quad (28)$$

(N = 24)

$$M(LH) - M(SH) = 0.23 [M(LH) - 7] + 0.32 = 0.23 [M(LH) - 5.6] \quad (29)$$

(N = 71)

Kiruna :

$$M(LH) - M(PZ') = 0.59 [M(LH) - 7] + 0.48 = 0.59 [M(LH) - 6.2] \quad (30)$$

(N = 100)

$$M(LH) - M(PH) = 0.50 [M(LH) - 7] + 0.26 = 0.50 [M(LH) - 6.5] \quad (31)$$

(N = 30)

$$M(LH) - M(SH) = 0.30 [M(LH) - 7] + 0.28 = 0.30 [M(LH) - 6.1] \quad (32)$$

(N = 94)

This means that the magnitude scales based on body waves and on surface waves are inconsistent with each other. This was noted already by Gutenberg (1945 b), but the variation with $M(LH)$ is much larger than inferred at that time and exists not only for P but also for S. We also note that the variations of $M(LH) - M(PZ')$ and of $M(LH) - M(PH)$ with $M(LH)$ are approx. the same, whereas the variation of $M(LH) - M(SH)$ is definitely less. We also find that at our stations equality between magnitudes from surface waves and from body waves exists at a magnitude definitely below 7. A linear relation has been assumed here. This may be questionable, but in view of the relatively large scatter of the observations (due to regional variations) no better approximation can be made. The writer is indebted to Professor Gutenberg and Professor Benioff for recent discussion in letters concerning these problems. In the light of their recent results (1955) it appears that the magnitudes from body waves are the more reliable and that magnitudes from surface waves for the larger shocks are overestimates.

From the relations (27)-(32) we immediately deduce the following relations, valid for $h = n$.

Uppsala :

$$M(PZ') - M(SH) = -0.22 [M(LH) - 7.0] \quad (33)$$

$$M(PH) - M(SH) = -0.23 [M(LH) - 7.2] \quad (34)$$

Kiruna :

$$M(PZ') - M(SH) = -0.29 [M(LH) - 6.3] \quad (35)$$

$$M(PH) - M(SH) = -0.20 [M(LH) - 7.1] \quad (36)$$

The differences given therefore decrease with increasing $M(LH)$, i.e. with increasing M . This means that also the magnitude scales of P and S are not quite consistent with each other.

Summing up, when the real magnitude increases, all magnitudes determined from different waves increase, but the rate of increase is different for different waves in the present definition of magnitude. Similar variations involving M instead of $M(LH)$ are studied in chapter III.C.

The differences studied in this section also show well developed regional distributions (see Fig. 9 a and 9 b). The regional values are not corrected for their magnitude dependence; this was not found necessary. The distributions of $M(PZ') - M(LH)$ agree in general for Uppsala and Kiruna. In the Kamchatka region there is a « tongue » of negative values surrounded by positive values; along the east coast of Asia from Japan to the south it is also very good agreement with both positive and negative areas; the west coast of America has negative differences, but the West Indies positive. Comparing the regional distributions of $M(SH) - M(LH)$ for Uppsala and Kiruna we find both similarities and dissimilarities. For instance, the Kamchatka region is negative for Kiruna, but partly negative and partly positive for Uppsala; Japan is positive for Kiruna, but partly negative, partly positive for Uppsala; differences exist also on the west coast of America. On the whole there is agreement, but it appears as if the boundaries of the different regions are somewhat shifted as we pass from one station to another.

The general agreement of the regional distributions for Uppsala and Kiruna indicates that the reason may lie in the earthquake mechanism and the crustal layering at the source. It is especially important to note that on account of the regional corrections we are not allowed to assume that the focal depth is in excess of the normal depth, as soon as a positive magnitude difference has been obtained between body waves and surface waves. Only in case

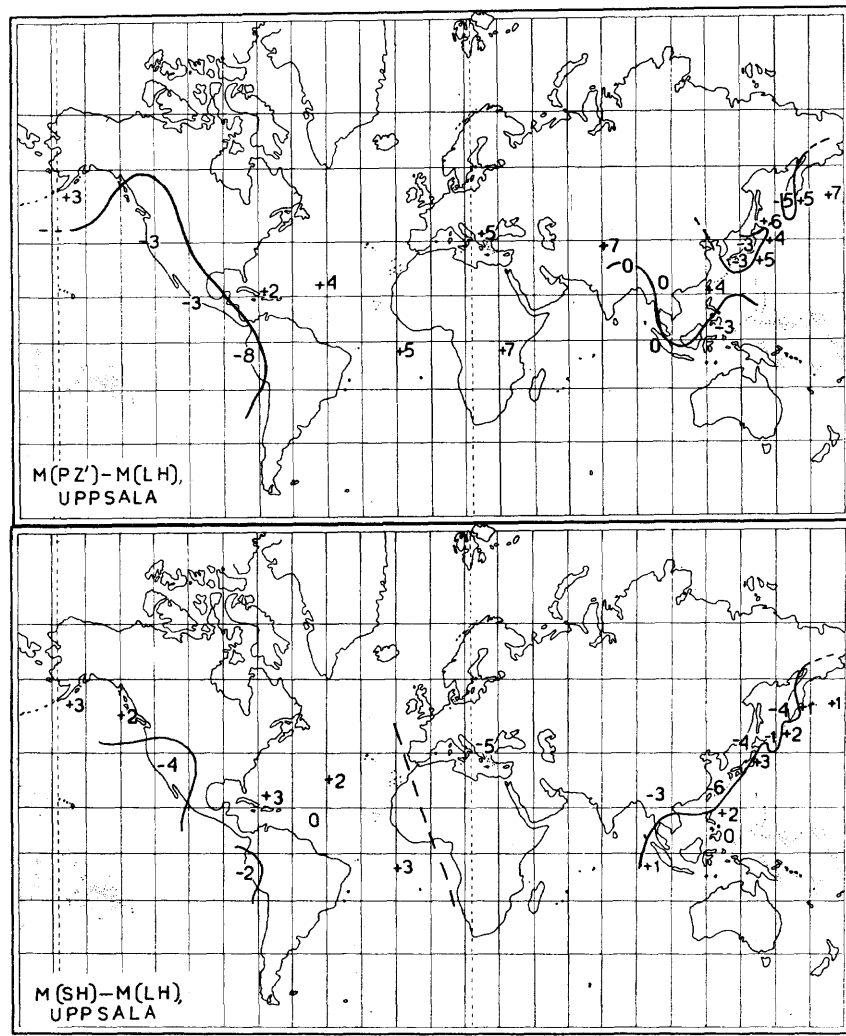


FIG. 9 a. — Regional distribution of magnitude differences between body waves and surface waves for normal depth (Uppsala).

a positive difference exists together with a clear pP phase, a depth greater than normal is likely, but not in other cases. The crustal layering at the epicentre is different in different areas and may cause that a larger or smaller part of the total energy goes into forming surface waves, even if the focal depth is unchanged. Also the different paths may influence the surface waves.

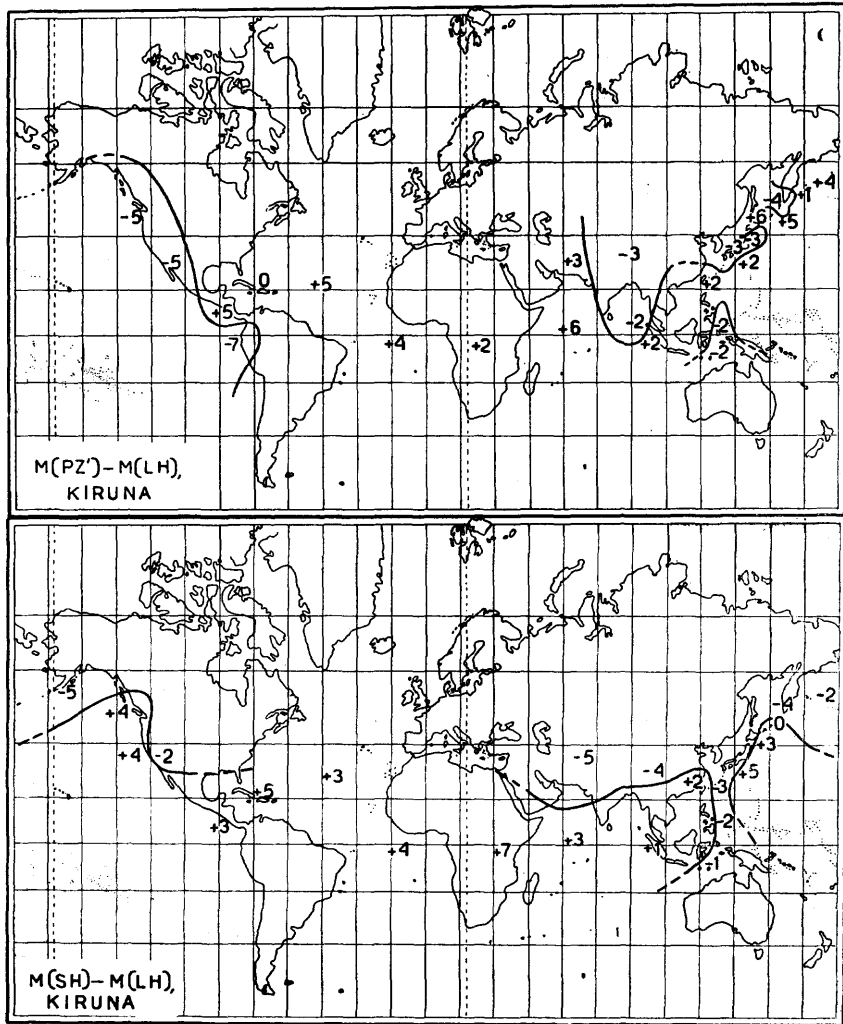


FIG. 9 b. — Regional distribution of magnitude differences between body waves and surface waves for normal depth (Kiruna).

The magnitude differences $M(PZ') - M(LH)$ and $M(SH) - M(LH)$ have been computed also for all earthquakes of greater focal depth in order to find out their relation to focal depth h . As already shown, these differences depend both on region and on depth (and on magnitude). As the regional corrections are comparable to the depth variation, it was found necessary first to eliminate the regional correction. Suppose for a given region we have found

$$\text{for } h = n : M(PZ') - M(LH) = R_1$$

$$\text{for } h > n : M(PZ') - M(LH) = R_2$$

where R_1 is the regional correction only, but R_2 in addition depends on h . We compute

$$[M(PZ') - M(LH)]_{h>n} - [M(PZ') - M(LH)]_{h=n} = R_2 - R_1 \quad (37)$$

where the difference $R_2 - R_1$ depends only upon focal depth, if the regional correction is the same regardless of depth. This has been verified for most of our differences. The calculations show that the corrected differences $R_2 - R_1$ are much better related to depth than the uncorrected differences R_2 . This is obvious from the graphical plots with reduced scatter of the points as well as from many individual cases, as e.g. earthquake No. 275 (Kamchatka) which gave a negative uncorrected difference $M(PZ') - M(LH)$ in spite of depth greater than normal but had a positive corrected difference. The same procedure was applied to SH. The remaining scatter of the differences is largely due to the uncertainty of the regional correction R_1 (variation with magnitude). Within a given region they agree quite well, but nevertheless there are some variations from earthquake to earthquake.

As the exact focal depth h is not known in many cases, especially not for $h = (n)$, i.e. depth slightly in excess of normal, I plotted the corrected magnitude differences against the time difference $pP - P$ instead of against h . This means that only cases with a clear pP recorded on the short-period Grenet instruments were used, i.e. cases where we can rely on the depth (see Table 11 a). There is a very simple relation between $pP - P$, expressed in sec, and h , expressed in km,

$$4(pP - P) = h \quad (38)$$

TABLE 11 a. — Time differences $pP - P$ in sec for earthquakes used
in the study of relations to focal depth.

No.	Uppsala	Kiruna	No.	Uppsala	Kiruna
5		(12)	151		14
12	64		152	(14)	16
18	11	10	156	11	10
21	6	6	158		11
24	9		164	5	10
32	8	(11)	167	12	
37	18	(16)	169		14
44		33	173	26	25
48	6	7	181	53	56
49	(17)	16	186	13	12
50	(11)	11	191	(6)	
58		85	196	13	14
65	10		201		10
66	9	6	205	(19)	15
77	(12)	(12)	207	15	16
83		(17)	209	13	
90		(20)	215	6	6
91		11	217	17	16
96	64		228	60	59
97	28		235		(13)
116	17	(17)	241	12	12
117	11	9	242	49	45
119	(7)		275	10	
124	13		278	28	29
126	9	8	280		(8)
127		11	287	26	25
128		11	290	17	17
129	13		293	(29)	26
130		12	295	15	17
132	9	9	297	8	
133	(14)		298	6	
136	12	12	300	19	17
138	10	10	308	12	11
142	11	11	309	18	(18)
143		15			
144	10	9			

NOTE. — Of the earthquakes tabulated in Table 11 a the following have been given as of normal depth ($h = n$) in Table 17 : No. 119, 130, 133, 138, 143, 169, 201, 309. For No. 169 various statements are contradictory; for the others there are no indications of depth in excess of normal except the probable existence of pP on our records.

valid for $\Delta \geq 60^\circ$, and therefore applicable in our cases. For $pP - P < 45$ sec the error of h obtained from this formula is at most 5 km.

$pP - P = 6$ sec corresponds to $h = 24$ km, i.e. approximately normal depth. The assumption of $pP - P = 6$ sec for normal shocks may be in error by one or two seconds due to the uncertainty of the normal depth and due to the uncertainty of the velocity of P in the crust. Combining the following equations

$$\left. \begin{aligned} M(PZ') - M(LH) &= a(pP - P - 6) \\ 4(pP - P) &= h \end{aligned} \right\} \quad (39)$$

we obtain

$$M(PZ') - M(LH) = \frac{a}{4}(h - 24) \quad (40)$$

and a similar equation for $M(SH)$ with another value of a . The following least-square solutions have been obtained

Uppsala : $M(PZ') - M(LH) = 0.019(h - 24)$ (41)
 $(N = 35)$

Kiruna : $M(PZ') - M(LH) = 0.020(h - 24)$ (42)
 $(N = 36)$

and

Uppsala : $M(SH) - M(LH) = 0.008(h - 24)$ (43)
 $(N = 25)$

Kiruna : $M(SH) - M(LH) = 0.009(h - 24)$ (44)
 $(N = 29)$

These formulae are valid at least up to $pP - P = 20$ sec, i.e. $h = 80$ km, and they can probably be used with confidence up to $pP - P = 25$ sec, i.e. $h = 100$ km.

For both magnitude differences the agreement between Uppsala and Kiruna is extremely good in spite of relatively large scatter of the observations. Depth corrections computed by Zátopek and Vaněk (1950 b) for Praha correspond to a factor of h of only 0.004. On the other hand, there is almost perfect agreement between the variation of $M(SH) - M(LH)$ with h found here and similar relation earlier derived for Pasadena by Báth (1952, equation (5), p. 83). Our formulae also agree well with the findings of Gutenberg (1945 c) as well as with theory (theory requires a factor of about 0.01). This concerns only the difference $M(SH) - M(LH)$ where the reason is only the decrease of the surface waves with increase of focal depth.

The variation of $M(PZ') - M(LH)$ with depth is more than twice as rapid. We have here two depth effects which reinforce each other; one is the relative increase of the short-period P with focal depth (see chapter III.B.1), the other is the decrease of the

surface waves. The variation with h for $M(PZ') - M(LH)$ is at Uppsala $0.019 h = 0.008 h + 0.011 h$, and at Kiruna it is $0.020 h = 0.009 h + 0.011 h$. The first term in h is the decrease of the surface waves, and the second term, $0.011 h$ for both stations, gives the effect of increasing PZ' . The last-mentioned effect is evidently approximately equal to or slightly in excess of the surface wave effect.

Table 11 b gives the mean magnitude difference corresponding to given depths h , calculated from formulae (41) to (44). Due to the more rapid variation with h the difference $M(PZ') - M(LH)$ would be more suitable for depth estimations. However, the magnitude differences must be corrected for the regional value before the formulae or Table 11 b is applied. Even then we may expect individual depths to deviate considerably from the value thus obtained. In fact, the standard deviations of individual depth determinations by means of our formulae are as follows.

	Uppsala	Kiruna
$M(PZ') - M(LH)$	$\pm 17 \text{ km}$	$\pm 21 \text{ km}$
$M(SH) - M(LH)$	$\pm 36 \text{ km}$	$\pm 25 \text{ km}$

TABLE 11 b.

h km	Uppsala		Kiruna	
	$M(PZ') - M(LH)$	$M(SH) - M(LH)$	$M(PZ') - M(LH)$	$M(SH) - M(LH)$
24	± 0.0	± 0.0	± 0.0	± 0.0
30	$+ 0.1$	± 0.0	$+ 0.1$	$+ 0.1$
35	$+ 0.2$	$+ 0.1$	$+ 0.2$	$+ 0.1$
40	$+ 0.3$	$+ 0.1$	$+ 0.3$	$+ 0.1$
45	$+ 0.4$	$+ 0.2$	$+ 0.4$	$+ 0.2$
50	$+ 0.5$	$+ 0.2$	$+ 0.5$	$+ 0.2$
55	$+ 0.6$	$+ 0.2$	$+ 0.6$	$+ 0.3$
60	$+ 0.7$	$+ 0.3$	$+ 0.7$	$+ 0.3$
65	$+ 0.8$	$+ 0.3$	$+ 0.8$	$+ 0.4$
70	$+ 0.9$	$+ 0.4$	$+ 0.9$	$+ 0.4$
75	$+ 1.0$	$+ 0.4$	$+ 1.0$	$+ 0.5$
80	$+ 1.1$	$+ 0.4$	$+ 1.1$	$+ 0.5$
85	$+ 1.2$	$+ 0.5$	$+ 1.2$	$+ 0.5$
90	$+ 1.3$	$+ 0.5$	$+ 1.3$	$+ 0.6$
95	$+ 1.3$	$+ 0.6$	$+ 1.4$	$+ 0.6$
100	$+ 1.4$	$+ 0.6$	$+ 1.5$	$+ 0.7$

The relations to depth h are mean formulae. In any individual region the depth relation may be different due to different crustal layering. This in part explains the scatter of the individual observations. Another reason for the great errors is the fact that in the relations to h the variations with $M(LH)$ were disregarded.

If h were known, as e.g. from pP — P, the formulae (41) to (44) could be used to correct the directly obtained M(LH) for focal depth. Surface waves are in general not very usable for $h > 100$ km. For such depths SS and SSS often have an appearance very similar to surface waves.

The differences $M(PZ') - M(LH)$ and $M(SH) - M(LH)$ were investigated for 163 earthquakes of those listed in Table 17 at the end. I found from our records that of these earthquakes 92 were at normal depth and 71 at depths greater than normal; of these 71 only 7 had $h > 100$ km. If our magnitude differences were the *only* indication of greater depth, no account was taken of this, and such earthquakes were classified as normal. Comparing our results with the data of USCGS or BCIS (in both cases obtained from the international bulletin IUGG from Strasbourg) we find that of our 163 earthquakes 116 are given as normal and only 47 as of greater depth. In 52 cases both our magnitude differences and the existence of very clear pP indicate greater depth. pP probably exists in more cases, but less clear. In 37 of these cases no depth has been given in the international bulletin. For some clear cases of pP belonging to this group, see the reproductions in Fig. 10. On the other hand, of the 47 cases given by the international bulletin as having greater depths than normal, there are 13 cases where there is no confirmation of this from any of our records. However, these 13 cases are limited to a small area in the Kamchatka region, and this result may therefore be regionally influenced. Furthermore, in several of these 13 cases there is no agreement between different authorities. In several of these cases USCGS gives $h = n$. The conclusion is that there are many more earthquakes with depths in excess of the normal than what appears from the international bulletin. This concerns only the range $24 < h < 80$ km. Greater depths are usually given in the bulletin.

The result found is of importance in any attempt to construct frequency distributions of focal depths, especially for $h < 100$ km. Koning (1953) has given such a curve with a minimum at $h = 60 - 80$ km. It is evident from our investigation that no such frequency distribution can be drawn unless a careful investigation of the depths has been made. Koning's frequency minimum for the depth $h = 60 - 80$ km appears very questionable. The same remark applies to a statement by Ritsema (1954). He believes that large shocks have a frequency maximum at a depth of about 70 — 90 km, probably at 80 km, and that smaller shocks have a frequency maximum between 80 and 120 km. But these maxima presuppose

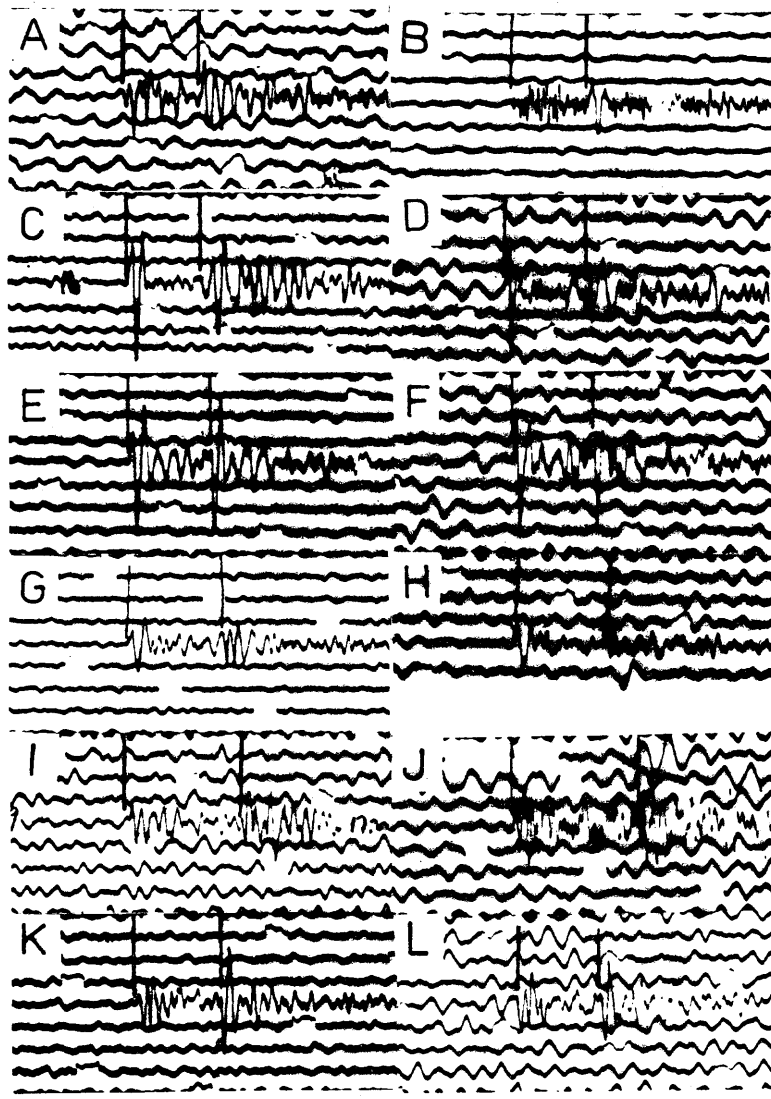


FIG. 10. — Reproductions of Grenet records showing P (first mark) and clear pP (second mark). 1 mm = 1 sec. The notations mean : A No. 18 for Uppsala (= 18 U), B No. 18 for Kiruna (= 18 K), C 142 U, D 142 K, E 156 U, F 156 K, G 186 U, H 186 K, I 295 U, J 295 K, K 308 U, L 308 K.

the existence of a frequency minimum at shallower depth, which, however, is doubtful and requires further detailed investigation.

C. Comparison of our magnitudes with those of other stations.

In this section we shall compare the various magnitude determinations for Uppsala and Kiruna with the most likely magnitude

M of each earthquake. The adopted value of M (see Table 17) is based only on data by other stations than Uppsala and Kiruna and given only in case a reliable estimate could be made. Such a value of M has generally been given only in the following cases :

1. if only one other station has given M, provided that station is Pasadena;

2. if two or more other stations have given consistent values of M. The values of M are evidently based both on surface waves and body waves. The comparisons with our magnitudes are summarized in Table 12. We find significant positive differences for all waves, somewhat less for Grenet (PZ') and generally larger for $h > n$ than for $h = n$. Percentage frequency distributions for the cases with more observations are given in Fig. 11.

The magnitudes determined directly from our records are obviously too low. This concerns all our instruments and both Uppsala and Kiruna. Of decisive importance for the usefulness of a given wave for magnitude determinations is not the numerical value of the mean difference $\bar{\delta}$, but instead the scatter of the individual observations (S. D.). We then find that for Uppsala PZ' is least useful and that SH and LH are best suited for magnitude deter-

TABLE 12. — Comparison of our magnitudes and the most likely magnitude M.

Magnitude difference δ	Uppsala					Kiruna				
	h	N	$\bar{\delta}$	S. E.	S. D.	h	N	$\bar{\delta}$	S. E.	S. D.
M — M (PZ')	$n, (n)$	103	+0.1*	± 0.05	± 0.5	$n, (n)$	105	+0.2*	± 0.04	± 0.4
	$> n$	20	+0.3*	± 0.1	± 0.6	—	16	+0.2	—	—
M — M (PZ)	—	—	—	—	—	$n, (n), > n$	61	+0.4*	± 0.05	± 0.4
M — M (PH)	$n, (n)$	51	+0.2*	± 0.05	± 0.4	$n, (n)$	48	+0.2*	± 0.04	± 0.3
	$> n$	6	+0.5	—	—	$> n$	9	+0.4	—	—
M — M (PPZ')	$n, (n), > n$	44	+0.5*	± 0.07	± 0.4	$n, (n), > n$	29	+0.4*	± 0.08	± 0.4
M — M (PPZ)	—	—	—	—	—	$n, (n), > n$	29	+0.5*	± 0.06	± 0.3
M — M (PPH)	$n, (n), > n$	18	+0.6*	± 0.1	± 0.4	$n, (n), > n$	39	+0.3*	± 0.06	± 0.4
M — M (SH)	$n, (n)$	91	+0.4*	± 0.03	± 0.3	$n, (n)$	88	+0.3*	± 0.04	± 0.4
	$> n$	18	+0.4*	± 0.09	± 0.4	$> n$	19	+0.4*	± 0.1	± 0.4
M — M (LH)	n	91	+0.3*	± 0.03	± 0.3	n	87	+0.3*	± 0.03	± 0.3

For explanation see note of Table 3.

minations; for Kiruna PH and LH are the best. Concerning LH we add that it is useful only for shallow shocks; in other cases LH is less useful (see chapter III. B. 3, also concerning additional

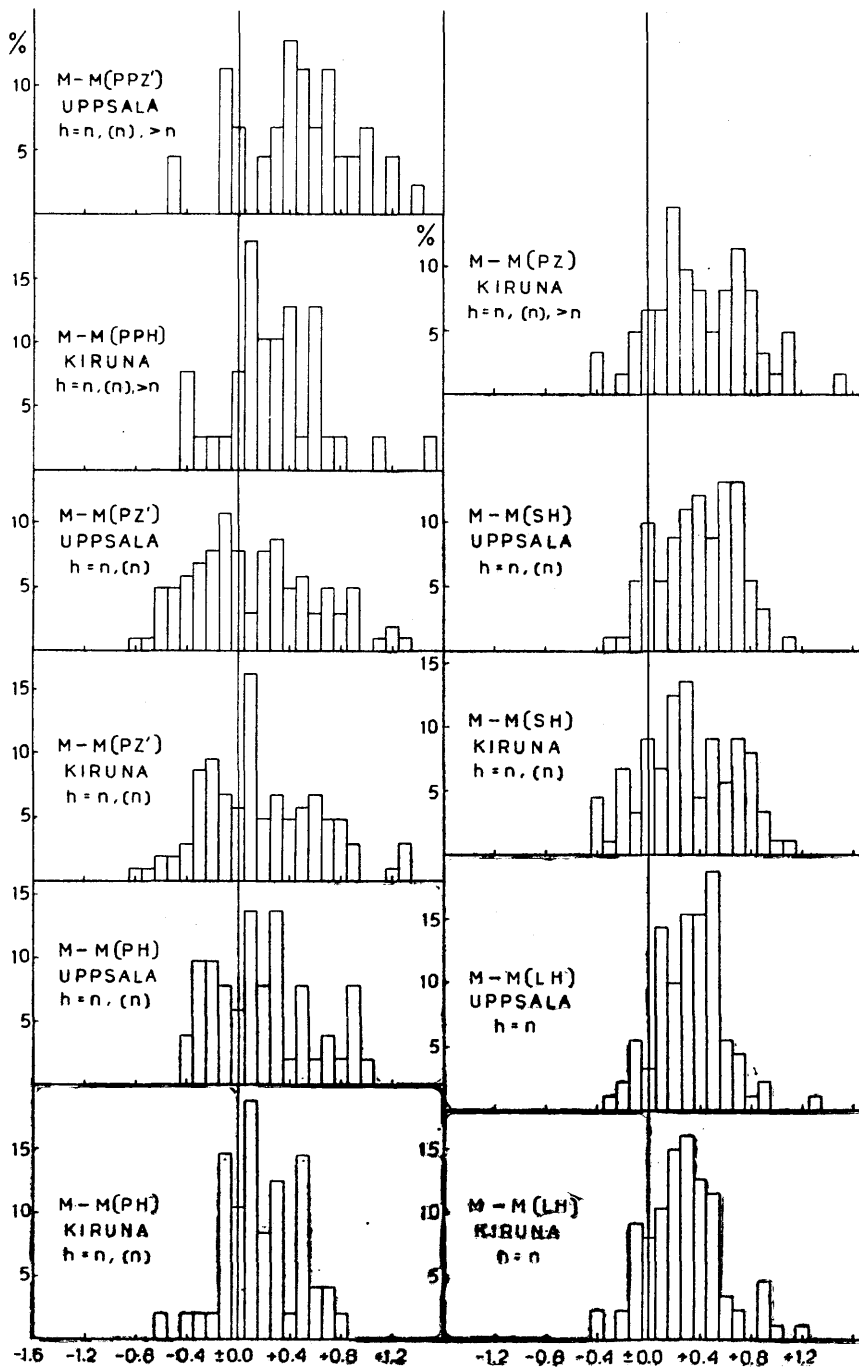


FIG. 11. — Frequency distributions of differences between adopted M and our magnitudes.

limitations in the use of LH, especially for large shocks). Even for the best waves there is a standard deviation of a single observation of ± 0.3 magnitude units. This agrees with my earlier results for Pasadena (Bath, 1952) that in a single magnitude determination we can never guarantee an error less than about $\pm 1/4$ of a magnitude unit. If the regional correction is well known, this error may be decreased somewhat. But also the regional correction has some range of variation, varying somewhat from earthquake to earthquake even in the same location. Even earthquakes occurring in the same point of the earth are not exactly repetitions of the same event over and over again, but they are links in a successive development over geological periods. These circumstances put a definite limit to the accuracy of any magnitude determination.

The magnitude differences studied in this section also show clear regional distributions. As all mean differences $\bar{\delta}$ are positive, I have preferred to give here the regional distributions of « reduced corrections » $\delta - \bar{\delta}$, i.e. the individual values have first been corrected by their respective mean value. In this way the distribution is made clearer, as there will be both positive and negative areas (see the maps in Fig. 12 a and 12 b).

The distribution for $M - M(PZ')$ is very similar for Uppsala and Kiruna. Kamchatka is a striking example of close similarity also with regard to the numerical values of the reduced corrections. Most of America is positive with exception for the Alaska region. In fact, America is the largest positive area for this difference, corresponding to the circumstance that our Grenet instruments are apparently much less sensitive to earthquakes in this part of the world than to those occurring in most other parts. A transition to negative values occurs in the Atlantic, and the Mediterranean region is clearly negative. The next positive area is in SE Asia. Japan is a mixed area for both stations.

The distributions of the reduced values of $M - M(SH)$ show some notable differences for the two stations. For instance, Kamchatka is partly positive, partly negative for Uppsala, but only positive for Kiruna; Japan is mainly positive for Uppsala but negative for Kiruna; there are differences also on the west coast of America but general agreement in the Mediterranean and the Near and Middle East. The distributions for PZ' and SH for a given station are not the same. For instance, Kiruna gives for Japan much more regular corrections for SH than for PZ' . This means that at

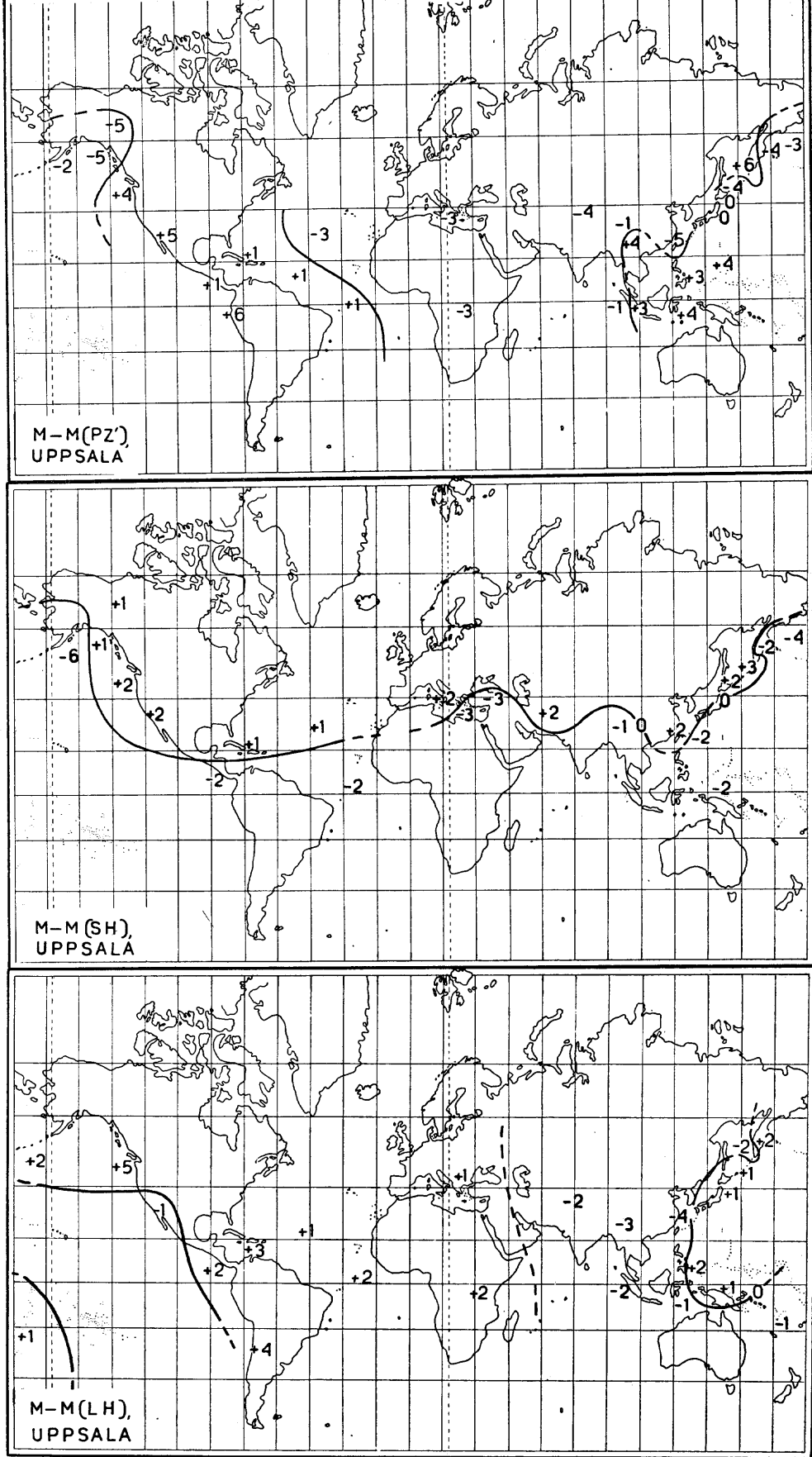


FIG. 12 a. — Regional distributions of differences between adopted M and our magnitudes (Uppsala).

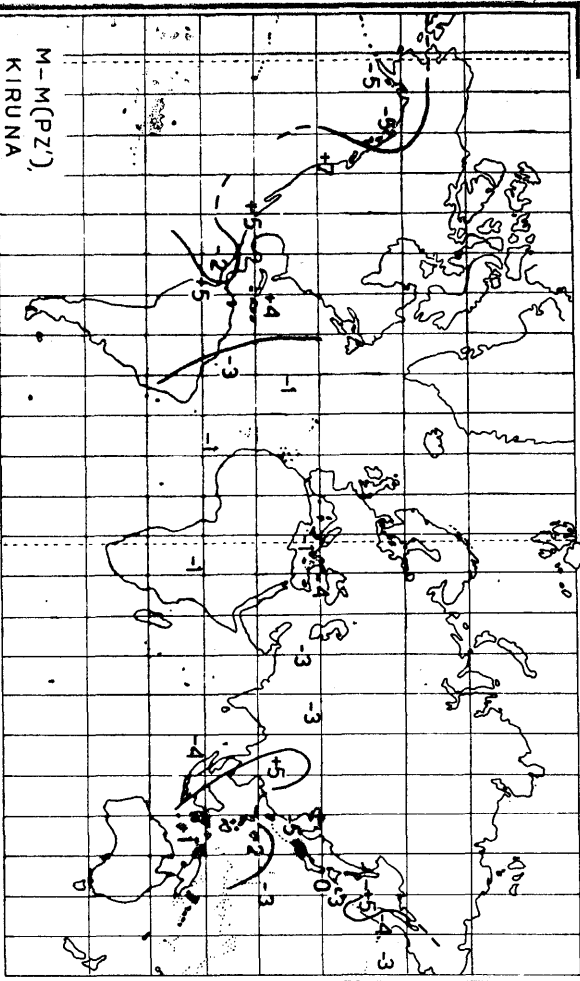
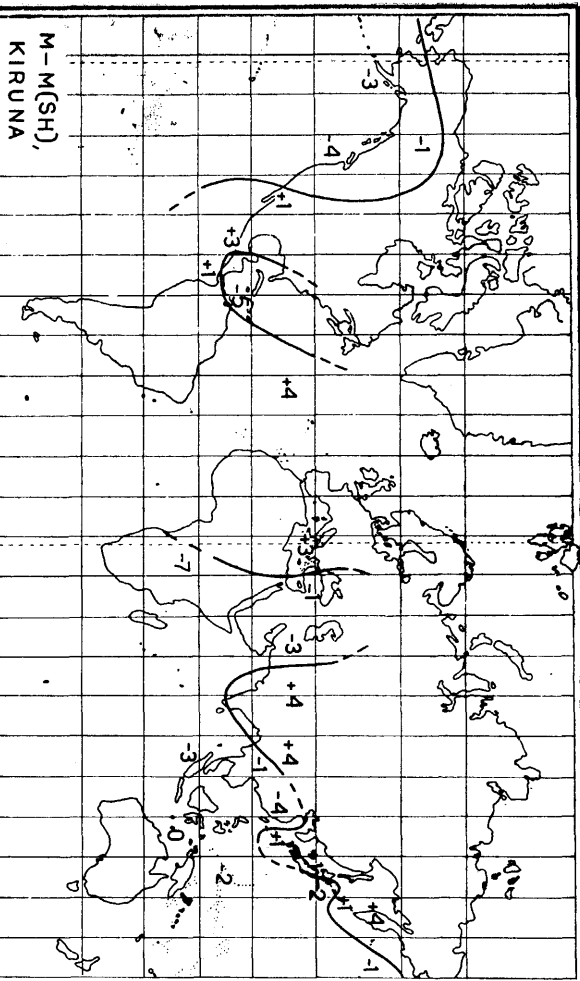
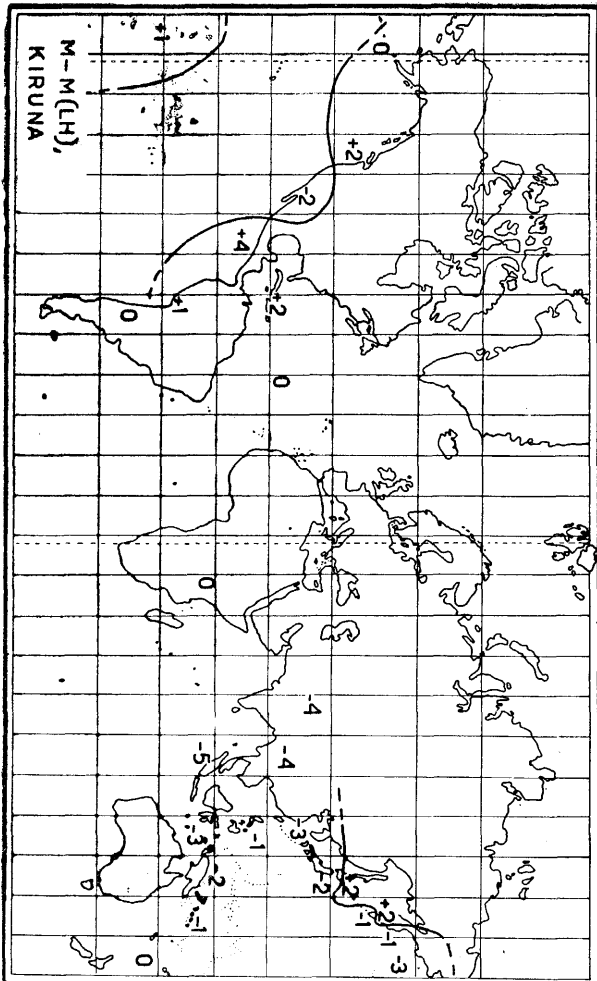


FIG. 12 b. — Regional distributions of differences between adopted M and our magnitudes (Kiruna).

least for this area and for Kiruna, SH is more suited to magnitude determination than PZ'.

There is generally good agreement between the distributions of the reduced values of $M - M(LH)$ for Uppsala and Kiruna. The largest positive values are to be found in Central America. In the determination of $M(LH)$ the extinction coefficient k was assumed to be 0.0003 km^{-1} in all cases (Gutenberg, 1945 a). This coefficient is, however, different for different paths (Gutenberg, 1945 a). From the M - formula for surface waves we deduce that

$$dM = 24.13 \cdot \Delta \cdot dk \quad (45)$$

with Δ expressed in degrees and other variables kept constant. The term $-24.13 \cdot 90^\circ \cdot k$ is cancelled by a corresponding term included in the constant term 5.04, and it shall therefore not be included in formula (45). Table 13 gives numerical values of dM .

TABLE 13. — dM corresponding to given values of dk .

Δ	$dk = 0.0001$	$dk = 0.0002$
30°	0.07	0.14
60	0.14	0.29
90	0.22	0.43
120	0.29	0.58

As differences of dk as assumed here may very well exist between continental and oceanic paths, it is clear that this effect may have considerable influence on the determination of M . This effect alone would give larger values of $M - M(LH)$ for oceanic paths than for continental paths. This is a contributing reason for the positive reduced corrections in Central America and the negative reduced corrections in Central and SE Asia. In case of strong extinction $M(LH)$ may be considerably less than M determined from the body waves. This can give an incorrect impression of greater focal depth. However, we also observe that for other parts of the world there is no clear-cut division between areas of positive and negative signs according to path. This means that also other factors are operative, as e.g. unequal radiation of energy in different azimuths. The regional distribution of $M - M(LH)$ has been investigated by a few other authors for their respective stations (Peterschmitt, 1948 and 1950; Zátopek and Vaněk, 1950 a and 1950 b; Bonelli Rubio and Carrasco, 1950). There is some general agreement between our observations and those of Praha and Toledo but not of Strasbourg with regard to differences between continental and oceanic paths, but there are many cases of disagreement in detail between the

various stations. Similar studies have been made for Pasadena (Gutenberg, 1945 a; Båth, 1952).

A limit to the accuracy is the variability of the regional corrections even within the same region. In order possibly to increase the accuracy it was investigated if the regional corrections within a limited area followed some general rule. By graphical methods it was then found for Japan and Kamchatka both for Uppsala and Kiruna that

1. $M - M(PZ')$, $M - M(PH)$, $M - (SH)$ increase with increasing M ;
2. $M - M(LH)$ decreases with increasing M .

A few examples for $h = n$, (n) are given in Fig. 13. This means also that the difference between our body-wave magnitude and surface-wave magnitude decreases with increasing M . In spite of the scatter of the points these tendencies are very clear in every single diagram. This fact cannot be explained as an instrumental effect, as we observe it for all instruments and at both stations. It means that the body waves increase slower and the surface waves more rapidly than the corresponding increase of M . This could be due to some variation with magnitude of the partition of the total energy on body waves and surface waves; here it would mean that the larger the earthquake is (normal depth only considered), the larger is the percentage of the total energy that goes to the surface waves.

It follows that $M(SH) - M(LH)$ decreases with increasing M for Japan and Kamchatka. We have

$$M(LH) = \log \frac{a_{LH}}{T_{LH}} - \log B + \text{constant} \quad (46)$$

Compare Gutenberg (1945 a). I have included the period $T_{LH} \approx 20$ sec in the formula. The distance Δ is given, i.e. B is given, also the depth $h = n$, the instrument, and the station. The scale for $M(LH)$ is then determined by $\log(a_{LH}/T_{LH})$. Similarly

$$M(SH) = 1.1 \left[(A - 0.7) + \log \frac{a_{SH}}{T_{SH}} \right] \quad (47)$$

where A is given. The scale for $M(SH)$ is determined by $\log(a_{SH}/T_{SH})$. We have from (46) and (47)

$$\begin{aligned} M(SH) - M(LH) &= 1.1 \log \frac{a_{SH}}{T_{SH}} - \log \frac{a_{LH}}{T_{LH}} + \text{constant} \\ &= 0.1 \log \frac{a_{SH}}{T_{SH}} + \frac{1}{2} \log \frac{\left(\frac{a_{SH}}{T_{SH}}\right)^2}{\left(\frac{a_{LH}}{T_{LH}}\right)} + \text{constant} \end{aligned} \quad (48)$$

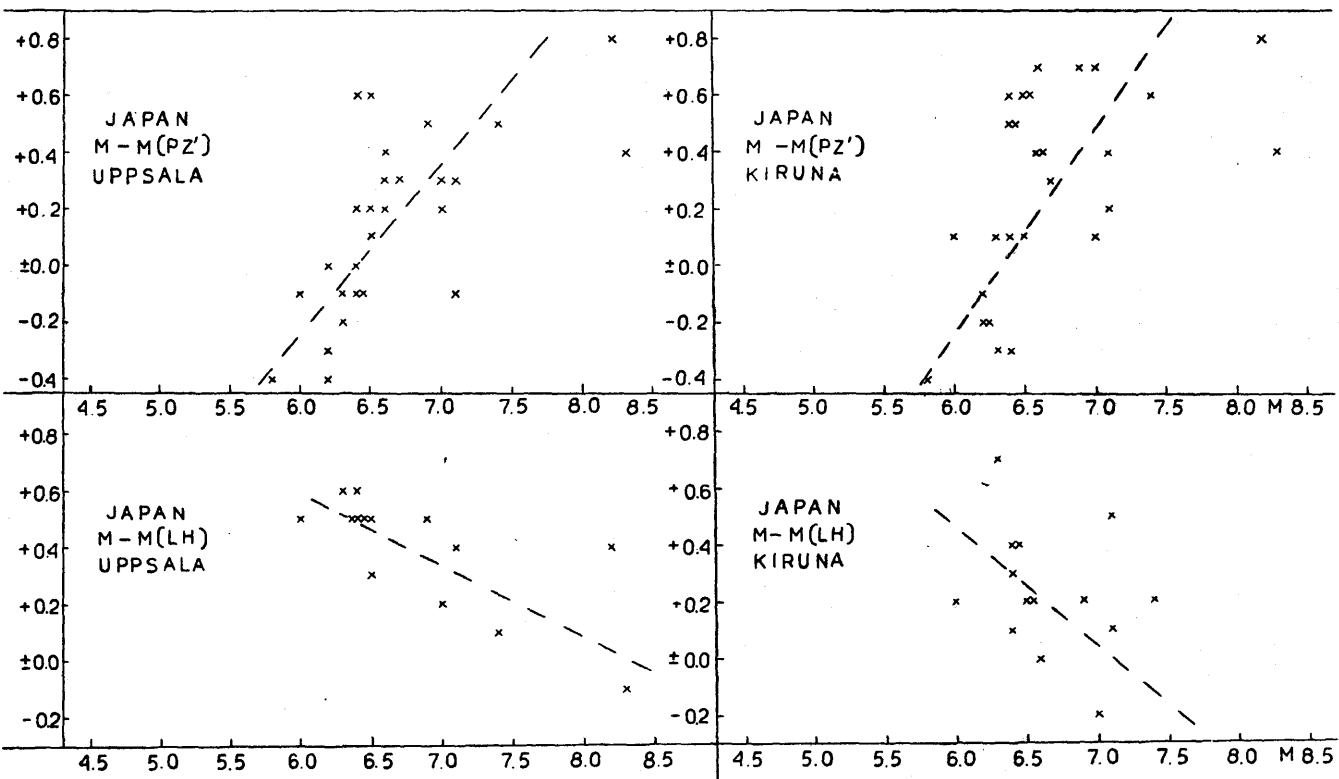


FIG. 13.— Variations with M of certain magnitude differences for earthquakes in Japan.

This decreases with increasing M in Japan and Kamchatka. As the first term increases with M and the third term is constant, it results that the second term must decrease with increasing M . According to Gutenberg (1945 b) the factor 0.1 in the first term could be replaced by 0.2 or 0.3, but only for longitudinal waves. But such a change of this factor even in this case (S waves) is by no means sufficient to explain the observed variation with M . We call for a moment the factor of the first term in (48) x instead of 0.1. Then x can be determined in such a way that $M - M(LH)$ is independent of M . We then find the following expression for x

$$x = \frac{d \log \frac{a_{LH}}{T_{LH}}}{d \log \frac{a_{SH}}{T_{SH}}} - 1 \quad (49)$$

It is obvious that for certain regions more reliable regional corrections can be obtained by taking account of their magnitude dependence. For a given region we may therefore write for instance

$$M - M(SH) = c M + d \quad (50)$$

instead of putting the left-hand side equal to a constant, the regional correction. This formula gives the following expression for the magnitude M to be determined.

$$M = \frac{M(SH)}{1-c} + \frac{d}{1-c} = C M(SH) + D \quad (51)$$

where

$$C = \frac{1}{1-c} \quad \text{and} \quad D = \frac{d}{1-c}.$$

Instead of giving only one regional correction, it may improve the accuracy to give two quantities, C and D , for each region. They can, however, be reliably determined only in regions of many observations.

The results above concern Japan and Kamchatka. For America, taking all observations from Alaska to Central America together, I found no variation of $M - M(PZ')$, $M - M(SH)$, or $M - M(LH)$ with magnitude. If all observations are taken together regardless of region, there is no variation of $M - M(LH)$ with M , but there is some tendency for increasing $M - M(PH)$ with M , even if the observations of Japan and Kamchatka are excluded. The M -variations found for Japan and Kamchatka are not general properties. That they are so well developed may be due to particular conditions in those regions.

In conclusion, we state that the rate of variation of the magnitude differences between body waves and surface waves studied in chapter III. B. 3 depends upon the region. The relations given there are mean relations for all regions. The differences studied in this section have shown very pronounced variations with M in Japan and Kamchatka; and these variations are much in excess of those given in equations (27)-(32) above. Approximate computations have shown that for the Kamchatka-region $M(LH) - M(PH)$ varies with $M(LH)$ with a factor of 0.69 for Kiruna instead of 0.50 in the mean; for Uppsala the corresponding figures are 0.73 and 0.46. Similarly for the Kamchatka-region $M(LH) - M(SH)$ varies with $M(LH)$ with a factor of approx. 0.78 for Kiruna instead of 0.30 in the mean, and for Uppsala the corresponding figures are 0.88 and 0.23. At the same time there are other regions with practically no similar variations.

The relations of $M - M(LH)$ to focal depth h have been determined by the same method as in chapter III. B. 3. The least-square solutions are

$$\text{Uppsala : } M - M(LH) = 0.009 (h - 24) \quad (52)$$

$(N = 27)$

$$\text{Kiruna : } M - M(LH) = 0.006 (h - 24) \quad (53)$$

$(N = 15)$

This determination is less reliable than the one in chapter III. B. 3 based on $M(SH) - M(LH)$; $M(SH)$ has namely been obtained from the same instrument as $M(LH)$, whereas M is based upon determinations at other stations.

Besides the general results of this section also the practical means have been developed for computing magnitudes from our records at Uppsala and Kiruna giving the smallest possible deviations from the most likely values of M . The directly determined magnitudes (using Gutenberg's standard methods) must be corrected for

1. the mean corrections δ in Table 12, and
2. the regional corrections in Fig. 12 a and 12 b.

This procedure is simple in practice, and it is equally reliable as to use a special magnitude formula for our stations.

The regional correction can naturally be applied only if the region is known. Due to the very regular distribution of the magnitude differences it is possible to make an accurate determination of M even when only the data of a single station are at hand. Suppose that for a shallow earthquake at a distance Δ we have determined $M(PZ')$, $M(PH)$, $M(SH)$, and $M(LH)$ from the records

at a single station. The mean corrections are applied, giving resp. $M'(PZ')$, $M'(PH)$, $M'(SH)$, and $M'(LH)$. When correct regional corrections R are applied, the same value of M is obtained in all cases, i.e.

$$\begin{aligned} M'(PZ') + R(PZ') &= M'(PH) + R(PH) = M'(SH) + R(SH) \\ &= M'(LH) + R(LH) \end{aligned} \quad (54)$$

The un-corrected differences $M(PZ') - M(PH)$, $M(PZ') - M(SH)$, $M(PZ') - M(LH)$ etc have been mapped. At the given distance we then look for a region satisfying the various magnitude differences determined. If only one such region is found, it is the probable epicentral region. The regional corrections R are then known for all waves, and a more accurate M -determination is possible.

Explanation of the maps.

The following explanations are applicable to all the maps, Fig. 2, 3, 5, 8, 9, 12. The differences are given in units of one tenth of a magnitude. Most values given are mean values for several earthquakes in the same area except in Fig. 3; the number of earthquakes used in forming the mean values naturally varies in various parts of the world, being most in Japan and Kamchatka. The values given are therefore representative of their respective areas. The curves only serve the purpose of limiting positive from negative areas. No other iso-lines can be drawn as there is no obvious regular distribution within the different regions. Earthquakes on the lines have zero difference. Maps have been given only in case the number of earthquakes is well over 50. The maps are strictly valid only for $h = n, (n)$, and in case $M(LH)$ enters into a difference only for $h = n$. The cases with $h > n$ used are too few in order to give special maps. The differences for $h > n$ often agree well with those for $h = n, (n)$. Plotting individual differences against h , we find in general no clear variation with h . As a general rule, for $h > n$ we may take the same regional correction as for $h = n, (n)$ and correct this by means of the values given in Table 14. For the differences between magnitudes determined at other stations and the various determinations at our stations (Fig. 12) it is the reduced correction that is mapped, i.e. the correction which remains when the mean correction (Table 12) has been applied. In all other maps the directly determined differences are mapped.

TABLE 14. — Corrections in tenths of magnitude to be applied to earthquakes with $h = n$, (n) to obtain the corresponding values for $h > n$.

Magnitude difference	Japan		Kamchatka		Hindu Kush		S of Alaska		Central America		South America	
	Upp	Kir	Upp	Kir	Upp	Kir	Upp	Kir	Upp	Kir	Upp	Kir
M (PZ') — M (PZ)	-	+ 2	-	0	-	+ 10	-	+ 4	-	0	-	1 1 1 1 9
M (PZ') — M (PH)	+ 3	+ 1	-	+ 4	-	+ 8	-	-	-	0	-	(0) 0
M (PZ) — M (PH)	-	- 3	-	0	-	- 2	-	+ 1	-	3	-	(4)
M (PZ') — M (SH)	0	+ 4	0	0	+ 7	+ 7	0	-	+ 3	0	-	0 0 0 0
M (PH) — M (SH)	0	+ 8	0	0	+ 3	-	1	-	+ 6	0	-	0 0 0 0
M — M (PZ')	0	- 4	0	0	-	-	-	-	-	2	-	2 1 1 0
M — M (SH)	0	- 3 ⁽²⁾	+ 2	0	-	0	-	-	-	5	-	0
Upp — Kir												
M (PZ')		0		0		0		0		3		
M (PH)		0		0		0		0		0		
M (SH)		0		0		0		0		0		
M (LH)		0		0		0		0		0		

1) The limit on the map gives in this case for South America rather the limit between shallow and deeper earthquakes.

- 2) Concerns W Japan.
- 3) South of 20°S the correction is — 3 for deeper earthquakes to be applied together with the mean correction.
- 4) The following corrections are valid together with the mean correction : +3 north of 20°S; — 6 south of 20°S.

IV. NEW METHODS OF MAGNITUDE DETERMINATION.

In case the location of an earthquake has not been determined only the mean corrections $\bar{\delta}$ (Table 12) can be applied to the directly determined magnitudes, but naturally no regional corrections. Such magnitude determinations are only preliminary. When the location is known, also the regional correction is applied. The uncertainty of the regional correction then limits the accuracy of the magnitude determination. As pointed out in the Introduction, it is desirable to increase the accuracy of magnitude determinations. Every effort in that direction must be towards increasing the accuracy of the regional corrections. In the previous chapter (III. C) one way was outlined. In this chapter two other methods will be described. Both methods are based on combinations of magnitude determinations from P, S, and L. So far, these new methods are only to be considered as suggestions. Future work may give still better methods.

The first method, here called the ε - method, is based on energy considerations. The relation between the total energy E of the seismic waves and the correct value M of the magnitude (to be determined) is in general form assumed to be

$$\log E = f [M] \quad (55)$$

The magnitudes determined directly from P, S, and L, i.e. M(P), M(S), and M(L) resp., generally deviate from M and also from each other. The energy computed by means of (55) from any one of these magnitudes does therefore not agree with E. Instead we get

$$\left. \begin{array}{l} \log \left(\frac{p}{p_i} E \right) = f[M(P)] \\ \log \left(\frac{s}{s_i} E \right) = f[M(S)] \\ \log \left(\frac{l}{l_i} E \right) = f[M(L)] \end{array} \right\} \quad (56)$$

where the factors $p = p_i$ only if $M(P) = M$, $s = s_i$ only if $M(S) = M$, and $l = l_i$ only if $M(L) = M$. p_i, s_i, l_i are the values of p, s, l

corresponding to the mean conditions assumed in the magnitude determinations. Generally, p , s , and l have not the same numerical values as p_1 , s_1 , l_1 resp. Combining equations (56) and (55) we get

$$\left. \begin{aligned} \log \frac{p}{p_1} &= f[M(P)] - f[M] \\ \log \frac{s}{s_1} &= f[M(S)] - f[M] \\ \log \frac{l}{l_1} &= f[M(L)] - f[M] \end{aligned} \right\} \quad (57)$$

from which we obtain, solving p , s , l

$$\left. \begin{aligned} p &= 10^{f[M(P)] - f[M] + \log p_1} \\ s &= 10^{f[M(S)] - f[M] + \log s_1} \\ l &= 10^{f[M(L)] - f[M] + \log l_1} \end{aligned} \right\} \quad (58)$$

We have

$$p_1 + s_1 + l_1 = 1 \quad (59)$$

corresponding to the partition of the total energy E on P , S , L which must be assumed in mean conditions. In the actual conditions we have

$$p + s + l = e = 10^{-\varepsilon} \quad (60)$$

which defines the quantity ε . It is not correct in actual conditions to assume the sum in (60) to be equal to one. If, for instance, there is something in the wave path that partly prevents the transmission (as between Central America and our stations), the total energy computed from P , S , L on our records does not correspond to the total energy but is smaller. Generally $e \leq 1$, but cases with $e > 1$ are not excluded due to local effects (local convergence of ray paths at the station). Combining equations (60) and (58) we then get

$$\begin{aligned} 10^{-f[M]} [10^{f[M(P)] + \log p_1} + 10^{f[M(S)] + \log s_1} + 10^{f[M(L)] + \log l_1}] \\ = 10^{-f[M]} 10^m = 10^{-\varepsilon} \end{aligned} \quad (61)$$

which defines the quantity m

$$10^m = 10^{f[M(P)] + \log p_1} + 10^{f[M(S)] + \log s_1} + 10^{f[M(L)] + \log l_1}$$

Equation (61) gives

$$f[M] = m + \varepsilon \quad (62)$$

which is the solution, from which the wanted quantity M is calculated. In this formula m is determined from $M(P)$, $M(S)$, and $M(L)$ once the numerical values of p_1 , s_1 , and l_1 are agreed upon. m depends on the energy partition on different waves. ε is a combined regional correction. M is calculable once $f[M]$ is known. In this method the energy partition on different waves is taken into

account for each individual earthquake. The method ought to be applicable also to deep earthquakes.

In the numerical tests of the ϵ - method I assumed $p_1 = 1/4$, $s_1 = 1/4$, and $l_1 = 1/2$, furthermore $\log E = a + b M$ with $b = 1.8$. In this case it is easily shown by similar calculations that equation (62) simplifies to

$$M = \frac{m + \epsilon}{b} \quad (62)$$

The computations are summarized in Table 15.

TABLE 15. — Numerical application of the ϵ - method and the R - method for $h = n, (n)$.

Earthquake region	Station	N	ϵ - method		R - method
			$\epsilon \pm S. D.$	dM	
Japan	Uppsala	19	+ 0.6 ± 0.3	± 0.17	+ 0.4 ± 0.16
	Kiruna	19	+ 0.2 ± 0.3	± 0.17	+ 0.2 ± 0.15
Kamchatka	Uppsala	19	+ 0.1 ± 0.5	± 0.25	+ 0.3 ± 0.24
	Kiruna	16	+ 0.5 ± 0.3	± 0.18	+ 0.4 ± 0.19

The mean errors of the resulting M are about ± 0.2 . Comparing this result with determinations by means of each of the waves PZ' , SH , LH separately (Table 16), we see that the ϵ - method is superior to PZ' and SH but of about the same accuracy as LH .

TABLE 16. — Tests of accuracy of magnitudes determined from PZ' , SH , and LH ; shallow earthquakes.

Earthquake region	Station	M — M (PZ')		M — M (SH)		M — M (LH)	
		N	Mean ± S.D.	N	Mean ± S.D.	N	Mean ± S.D.
Japan	Uppsala	27	+ 0.1 ± 0.3	20	+ 0.1 ± 0.3	14	+ 0.1 ± 0.2
	Kiruna	27	+ 0.1 ± 0.4	20	- 0.2 ± 0.2	14	- 0.1 ± 0.2
Kamchatka	Uppsala	24	- 0.1 ± 0.6	25	± 0.0 ± 0.3	16	± 0.0 ± 0.2
	Kiruna	25	- 0.1 ± 0.5	19	+ 0.4 ± 0.2	15	+ 0.1 ± 0.2

But this is valid only for shallow-focus earthquakes. For deeper shocks, however, the ϵ - method is superior also to LH . The more lengthy calculations in the ϵ - method can be considerably reduced by using special graphs or tables. There is some tendency for a certain regional distribution of ϵ within the areas investigated. If account is taken of that, some further increase of the accuracy is possible. Another advantage of this method is that we need only

one regional correction (ε) instead of one correction for each wave used. In several of the numerical examples studied $M(P)$, $M(S)$, $M(L)$ deviated considerably from each other, so much that it would be hardly possible to give a magnitude by guess from these three values; however, application of the ε -method yielded also in such cases results in good agreement with the most likely magnitude (based on determinations at Pasadena and other stations).

The other method I am suggesting, the R - method, is also based on a combination of P, S, and L. It is not so well physically based as the ε -method but is simpler in practice. The correct magnitude M equals the directly determined magnitude (with a mean correction applied) plus the regional correction R, thus

$$\left. \begin{array}{l} M = M(P) + R(P) \\ M = M(S) + R(S) \\ M = M(L) + R(L) \end{array} \right\} \quad (63)$$

The regional corrections R should be added terms as in (63) and not factors. This is evident from the logarithmic definition of M. Equations (63) give

$$\begin{aligned} 3M &= M(P) + M(S) + M(L) + R(P) + R(S) + R(L) = \\ &= M(P) + M(S) + M(L) + 3R \end{aligned} \quad (64)$$

which defines the combined regional correction R

$$R = \frac{1}{3} [R(P) + R(S) + R(L)] \quad (64')$$

The desired value of M is then given by

$$M = \frac{1}{3} [M(P) + M(S) + M(L)] + R \quad (64'')$$

The R - method has been tested numerically on the same cases as the ε - method (Table 15). The standard deviation of M is in this case equal to the standard deviation of R. It is evident that the errors of M are just as small in this simple method as in the more elaborate ε - method. This is interesting because the ε - method is better physically based than the R - method, but still it does not give higher accuracy. The R - method has also the advantage of simple calculus. The mean correction of $M(PZ')$, $M(SH)$, and $M(LH)$ taken together is $+0.3$ both for Uppsala and Kiruna (Table 12). It would be sufficiently accurate in most cases to apply this correction to the mean of the directly determined magnitudes, $M(PZ')$, $M(SH)$, and $M(LH)$. In the same way, any waves may be combined, i.e. the magnitude is given as the mean value of the directly determined magnitudes after application of the corrections in Table 12.

Further developments of the magnitude scale for other waves are desirable, especially for deep earthquakes for $\Delta > 105^\circ$. In these cases we can determine the magnitude only from PP at present. It is evident that if we rely only upon one wave large discrepancies may occur. For distant earthquakes it would be valuable to use also PKP, SKS, PKS, SKP as well as other core waves. Notable efforts in this direction have been made especially at the Seismological Laboratory in Pasadena (Gutenberg, 1951; Nelson, 1954).

The general methods are not applicable to distances $< 18^\circ$. For earthquakes within this distance it is necessary to develop special formulae, which may be different in different regions.

SUMMARY OF RESULTS.

The magnitudes have been determined using all waves possible from the records at Uppsala and Kiruna for 309 earthquakes from the years 1952-1953. The determinations have been compared in various ways with each other and with determinations at other stations. The main results are summarized below.

1. Large discrepancies (sometimes amounting to one magnitude unit or even more) may occur between determinations at different stations as well as between the different waves at one and the same station (see I).
2. It is shown that due to the rapid variation of the extinction coefficient with the period of the surface waves, it is necessary in magnitude determinations from the surface waves to use only waves with periods close to 20 sec (II).
3. Comparing the same wave at Uppsala and Kiruna we find much less scatter of the differences for surface waves than for any of the body waves (III. A and Fig. 1).
4. All differences investigated, both for the same wave at two stations and for the different waves at the same station, are in every case independent of epicentral distance, but they all show a distinct regional distribution. These distributions have been studied in detail (see the maps Fig. 2, 3, 5, 8, 9, 12) and the reasons discussed (unsymmetrical energy distribution from the focus, effects of path, and local structure near the station; III. B. 2). The study of the regional distributions may be of value in combination with first-motion studies in investigations of earthquake mechanisms.
5. The energy ratios between different waves determined at a single station are not representative for the earthquake (III. B.). The energy radiation from the focus is a very complicated process.
6. The energy ratio of short-period to long-period P increases with increasing focal depth (III. B. 1).

7. The magnitude differences between body waves and surface waves have been put into relation with focal depth. The difference between short-period P and surface waves varies about twice as rapid with depth as the difference between S and surface waves, and furthermore short-period P gives better accuracy (III. B. 3). In individual cases it is impossible to rely only upon these magnitude differences in inferring greater focal depth.

8. There are many more shocks at depths slightly below normal, i.e. 30-80 km, than is obvious from the bulletins (III. B. 3).

9. Comparing our magnitudes with those of other stations we find positive corrections for both stations and all waves used. The standard deviation of a single determination is about $\pm 1/4$ of a magnitude unit, due to uncertainty of the regional correction (III. C.).

10. The regional corrections show for both of our stations for earthquakes in Kamchatka and Japan striking variations with magnitude, implying that the body waves increase slower and the surface waves more rapidly than the corresponding increase of magnitude (III. C.). It is shown that also in the mean the magnitude scales based on surface waves and on body waves are inconsistent with each other (III. B. 3).

11. Two new methods for obtaining greater accuracy in magnitude determinations have been outlined, the ϵ - method and the R - method, both based on a combination of several waves (IV). The R - method is preferable .

12. Suggestions for further work include the following items :

a. Revised definitions of magnitude so that the scales based on different waves are consistent. This includes studies of the energy partition on different waves and its variation with magnitude.

b. Extension of the methods for magnitude determination from surface waves to periods deviating considerably from 20 sec. This includes detailed studies of the extinction coefficient for different periods and also for different paths.

c. Extension of the magnitude scale to other waves, especially the various core waves.

ACKNOWLEDGMENT.

Miss E. Wilson, Uppsala, has assisted me in drawing the figures and maps.

REFERENCES.

- BATH (M.) : Earthquake magnitude determination from the vertical component of surface waves, *Trans. Amer. Geophys. Un.*, Vol. 33, No. 1, pp. 81-90, 1952.
- BATH (M.) : Initial motion of the first longitudinal earthquake wave recorded at Pasadena and Huancayo, *Bull. Seism. Soc. Amer.*, Vol. 42, No. 2, pp. 175-195, 1952.
- BATH (M.) : Seismicity of Fennoscandia and related problems, *Gerl. Beitr. z. Geophysik*, Bd 63, Heft 3, pp. 173-208, 1953.
- BATH (M.) : The relation between magnitude and energy of earthquakes, *Trans. Amer. Geophys. Un.*, Vol. 36, No. 5, pp. 861-865, 1955.
- BONELLI RUBIO (J.) y CARRASCO (L. E.) : La magnitud de los sismos en Toledo, *Inst. Geograf. y Catastral*, 14 pp., Madrid, 1954.
- DI FILIPPO (D.) e MARCELLI (L.) : La « magnitudo » dei terremoti e la sua determinazione nella stazione sismica di Roma, *Ann. di Geofisica*, Vol. 2, No. 4, pp. 486-492, 1949.
- DI FILIPPO (D.) e MARCELLI (L.) : Magnitudo ed energia dei terremoti in Italia, *Ann. di Geofisica*, Vol. 3, No. 3, pp. 337-348, 1950.
- FISHER (R. A.) : *Statistical Methods for Research Workers*, 11th ed., 354 pp., Edinburgh and London, 1950.
- GIORGI (M.) e VALLE (P. E.) : Contributo allo studio delle onde « M », *Ann. di Geofisica*, Vol. 1, No. 1, pp. 87-102, 1948.
- GUTENBERG (B.) : Amplitudes of surface waves and magnitudes of shallow earthquakes, *Bull. Seism. Soc. Amer.*, Vol. 35, No. 1, pp. 3-12, 1945 a.
- GUTENBERG (B.) : Amplitudes of P, PP, and S and magnitude of shallow earthquakes, *Bull. Seism. Soc. Amer.*, Vol. 35, No. 2, pp. 57-69, 1945 b.
- GUTENBERG (B.) : Magnitude determination for deep-focus earthquakes, *Bull. Seism. Soc. Amer.*, Vol. 35, No. 3, pp. 117-130, 1945 c.
- GUTENBERG (B.) : PKKP, P'P', and the earth's core, *Trans. Amer. Geophys. Union*, Vol. 32, No. 3, pp. 373-390, 1951.
- GUTENBERG (B.) and RICHTER (C. F.) : On seismic waves, Third paper, *Gerl. Beitr. z. Geophysik*, Bd 47, pp. 73-131, 1936.
- GUTENBERG (B.) and RICHTER (C. F.) : Earthquake magnitude, intensity, energy, and acceleration, *Bull. Seism. Soc. Amer.*, Vol. 32, No. 3, pp. 163-191, 1942.
- GUTENBERG (B.) and RICHTER (C. F.) : Earthquake magnitude, intensity, energy, and acceleration, in press, 1955.
- HAYES (R. C.) : Measurement of earthquake intensity, *New Zealand Journ. of Sci. and Tech.*, B., Vol. 22, No. 4 B, pp. 202-204, 1941.
- HEELAN (P. A.) : Radiation from a cylindrical source of finite length, *Geophysics*, Vol. 18, No. 3, pp. 685-696, 1953.
- JEFFREYS (H.) : The reflexion and refraction of elastic waves, *Monthl. Not. Roy. Astr. Soc., Geophys. Suppl.*, Vol. 1, No. 7, pp. 321-334, 1926.
- JONES (A. E.) : Earthquake magnitudes, efficiency of stations, and perceptibility of local earthquakes in the Lake Mead area, *Bull. Seism. Soc. Amer.*, Vol. 34, No. 3, pp. 161-173, 1944.
- KAWASUMI (H.) : Intensities and magnitudes of shallow earthquakes, *Assoc. Séism. et Phys. l'Int. Terre, Ass. de Rome*, Rés. 6, 1954.
- KONING (L. P. G.) : Preliminary note on the frequency-depth relation of earthquakes, *Proc. Koninkl. Nederl. Akad. v. Wet.*, Ser. B., 56, No. 3, pp. 301-302, 1953.

- NELSON (R. L.) : A study of the seismic waves SKS and SKKS, *Bull. Seism. Soc. Amer.*, Vol. 44, No. 1, pp. 39-55, 1954.
- PETERSCHMITT (E.) : La magnitude des séismes, *Comptes rendus des séances de la conférence réunie à Strasbourg du 4 au 8 juillet 1947*, Un. Géod. et Géophys. Int., Ass. de Séism., pp. 86-88, Strasbourg, 1948.
- PETERSCHMITT (E.) : Étude de la magnitude des séismes, *Ann. Inst. Phys. du Globe de Strasbourg*, N. S., T. VI, 3^{me} partie, pp. 51-58, 1950.
- RICHTER (C. F.) : An instrumental earthquake magnitude scale, *Bull. Seism. Soc. Amer.*, Vol. 25, No. 1, pp. 1-32, 1935.
- RICHTER (C. F.) : History and applications of the magnitude scale, *Bur. Centr. Séism. Int.*, Sér. A, Trav. Sci., Fasc. 17, pp. 217-224, 1950.
- RITSEMA (A. R.) : Discontinuities and the distribution of earthquake foci in depth, *Met. and Geophys. Service, Djakarta, Verhand.*, No. 46, pp. 10-26, 1954.
- TRAPP (E.) : Ableitung der Magnitudengleichung für die Erdbebenstationen Wien und Graz und allgemeine Bemerkungen zur Magnitudenberechnung, *Archiv für Met., Geophysik und Bioklimatologie*, Ser. A, Bd 6, Heft 3-4, pp. 440-450, 1954.
- TSUBOI (C.) : Determination of the Richter-Gutenberg's instrumental magnitudes of earthquakes occurring in and near Japan, *Geophysical Notes*, Geophys. Inst., Tokyo, Vol. 4, No. 5, pp. 1-10, 1951.
- WADATI (K.) et al. : Sur la magnitude des séismes, surtout des séismes à foyer profond à courte distance, *Assoc. Séism. et Phys. l'Int. Terre, Ass. de Rome, Rés.* 7, 1954.
- VANEK (J.) : Determination of earthquake magnitude from surface waves for the stations Hurbanovo and Skalnaté Pleso, *Trav. Inst. Géophys. Acad. Tchécoslovaque Sci.*, No. 6, pp. 83-89, 1953.
- ZÁTOPEK (A.) : On the magnitude scale as objective numerical characteristic of seismic activity, *Sborník Čs. spol. zem.* (Journ. Czechoslovak Geograph. Soc.), Vol. 55, pp. 14-19, 1950.
- ZÁTOPEK (A.) and VANEK (J.) : On the regional repartition of magnitude differences between Pasadena and Praha, *Kartografický Prehled* (Cartographical Review), IV, 41-55, 123-128, pp. 1-24, 1950 a.
- ZÁTOPEK (A.) et VANEK (J.) : Les magnitudes de Praha et leur relation avec les « revised values » de Pasadena, *Bur. Centr. Séism. Int.*, Sér. A, Trav. Sci., Fasc. 18, pp. 137-152, 1950 b.

APPENDIX

TABLE 17.

This table contains all the data upon which the present investigation is based.

Abbreviations used for seismic stations :

U = Uppsala, K = Kiruna, A = Athens, B = Berkeley, C = Christchurch, D = De Bilt, H = Hurbanovo, L = Lisbon,
 Ma = Manila, M = M'Bour, Pa = Pasadena, Pr = Praha, R = Rome, Sk = Skalnaté Pleso, St = Strasbourg, T = Tacubaya,
 W = Wellington.

In the column headed « Remarks » are given magnitude determinations by other stations than our own (U and K).

No.	θ	φ, λ	h	M	Station Δ	Magnitude determined from								Remarks
	GMT		km			PZ'	PZ	PH	PPZ'	PPZ	PPH	SH	LH	
1	1952 Jan 3 060348	40.0 N 41.6 E	n	5.6	U 25° K 30	5.7						5.5 5.4	(5.4)	Pr 5 1/2, R 5.6
2	Jan 3 100517	17.2 N 98.3 W	n	6.5	U 87 K 84	5.6						5.7	5.6	Pa 6 1/2, T 6 1/4
3	Jan 12 201138	53.8 N 167.2 W	n	6.4	U 67 K 59	6.4 6.9								Pa 6 1/2, Pr 6 1/4 R 6.25
4	Jan 13 040337	22 N 124 1/2 E	n	7.1	U 79 K 75	6.6	6.9					6.6 6.7	7.2 7.1	Pa 6.9, Pr 7.3 R 6.9, St 7 1/4
5	Jan 21 034304	53 N 166 1/2 W	60	6.4	U 68 K 59	6.1	5.9	6.1				5.7	5.7	B 6.3, Pa 6 3/4, Pr 6 1/4, R 6 1/4
6	Jan 31 201643	15 1/2 N 93 1/2 W	60	--	U 87 K 84	6.5 7.2						6.7	(5.9)	Pa 5 3/4, Pr 6 T 6 3/4
7	Jan 31 205512	4 S 30 1/2 E	n	6.2	U 64 K 72	6.4 6.1					6.6	6.6	5.7 5.9	Pa 6 1/4, Pr 6
8	Feb 11 070105	5.5 S 109.8 E	660	6.9	U 96 K 95	7.2 7.0			6.7			6.5 6.4		Pa 6.9
9	Feb 14	7.7 S	n	7.3	U 107	c.c.	c.c.	7.2	6.7	6.8	7.2	7.0	7.1 7.4	H 7, Pa 7 1/4, Pr 7.4 Sk 7 1/4, R 7 + St 7 1/4

TABLE 17 (cont.).

No.	θ GMT	φ, λ	h km	M	Station Δ	Magnitude determined from								Remarks
						PZ'	PZ	PH	PPZ'	PPZ	PPH	SH	LH	
10	1952 Feb 14 210235	7 1/2 N 76 1/2 W	n	6.8	U 86 K 85	5.6 6.2						6.2	5.6	Pa 6 3/4
11	Feb 25 011702	18 1 S 172.8 W	n	6.9	U 137 K 129				7.0	6.7	6.9	6.2 6.5	H 7, Pa 6.9, Pr 6.9 R 6.92, Sk 6 3/4, St 6 3/4, W 7	
12	Feb 26 113104	14.1 S 69.9 W	250	7.1	U 101 K 103	6.4			6.4 5.9	6.4 6.5	5.8 6.4	6.1 6.1	B 7 1/4, Pa 7	
13	Mar 4 012256	42.5 N 143.6 E	n	8.3	U 69 K 63	7.9 7.9		8.0 8.0				8.5	8.4	B 8, Pa 8.3, Pr 8.7, St 8.5
14	Mar 4 163100	43 N 146 E	n	6.4	U 69 K 63	6.5 6.7						5.8 6.7	5.9 6.0	Pr 6.4, R 6.2, St 6 1/2
15	Mar 4 195610	42.0 N 145.0 E	n	7.1	U 70 K 63	6.8 6.7		6.6				6.3 6.8	6.7 6.6	H 7, Pr 7.1, R 7.1, Sk 7, St 7 1/4
16	Mar 5 034903	42.0 N 145.0 E	n	6.5	U 70 K 63	6.3 6.4	6.1					5.9 6.7	6.2 (6.1)	Pr 6.4, R 6.3, St 6 3/4
17	Mar 5 091703	42.0 N 145.0 E	n	6.4	U 70 K 63	5.8 5.9						5.8 6.5	5.9 6.1	Pr 6 1/4, St 6 1/2
18	Mar 5 155413	42.0 N 145.0 E	(n)	6.7	U 70 K 63	6.4 6.4						6.3 6.6	6.1 6.2	Pr 6 7, R 6.5, Sk 6 3/4, St 6 3/4
19	Mar 7 073237	36.2 N 136.1 E	n	--	U 72 K 66	6.5 6.4	6.1	6.2				6.5 6.6	(6.6) 6.7	Pa 6 1/2, Pr 7 1/4, R 7.1, St 7
20	Mar 9 170343	42 N 143 1/2 E	n	7.4	U 70 K 63	6.9 6.8	6.8	6.8 6.9		6.5		6.7 7.4	7.3 7.2	Pa 7.1, Pr 7 1/2, R 7.3, Sk 7 1/2, St 7 1/2

TABLE 17 (cont.).

No.	θ GMT	φ, λ	h km	M	Station Δ	Magnitude determined from								Remarks
						PZ'	PZ	PH	PPZ'	PPZ	PPH	SH	LH	
	1952													
21	Mar 9 200017	59 1/2 N 136 W	(n)	6.0	U 59 K 52	6.4 6.3			5.5			5.5 5.6	5.6 5.6	Pa 6, Pr 6
22	Mar 14 205512	42.0 N 145.0 E	n	--	U 70 K 63	6.6 6.5						5.6 5.7	(5.4) 5.8	Pr 6
23	Mar 15 111546	5 1/2 S 100 1/2 E	n	6.3	U 92 K 91	5.9 6.5						6.3 6.5	6.2 6.7	Pr 6 1/4, R 6 1/4
24	Mar 16 220921	42.5 N 143.6 E	(n)	5.8	U 69 K 63	6.2 6.2						5.6	5.2 5.4	Pr 5 3/4, R 5.85
25	Mar 19 012724	40.0 N 28.8 E	n	--	U 21 K 28	6.1 5.9						5.4 5.0	(5.4)	Pr 5
26	Mar 19 090414	40 N 125 E	n	--	U 67 K 59	5.9						5.3	(5.6) 5.9	Pr 6 3/4
27	Mar 19 105709	9 1/2 N 127 E	n	7.9	U 91 K 88	7.0 7.4		6.9		7.5 7.8	7.7	7.5 7.7	H 7 3/4-8, Pa 7 3/4, Pr 7.9, R 8, Sk 8, St 7 3/4	
28	Mar 23 152150	11 N 125 E	n	--	U 89 K 86	5.5 6.2						5.8	5.8 6.2	Pr 6 1/4
29	Mar 25 033511	34.3 N 23.4 E	n	--	U 26 K 33	5.7 6.1								
30	Mar 27 160950	6.8 S 11.5 W	n	--	U 70 K 77	5.6 5.6						5.6	5.2	
31	Apr 2 183450	16 1/2 N 99 1/2 W	n	6.3	U -- K 85		5.6			5.9		5.7	5.4	Pa 6 1/4-6 1/2, T 6 1/4

TABLE 17 (CONT.).

No.	θ GMT	φ, λ	h km	M	Station Δ	Magnitude determined from								Remarks
						PZ'	PZ	PH	PPZ'	PPZ	PPH	SH	LH	
1952														
32	Apr 4 025255	52 N 159 1/2 E	(n)	6.3	U 64 K 56	6.7 6.6	6.1	6.5 6.2				5.7 5.6	5.7 6.0	Pa 6 1/4, Pr 6 1/4, R 6.3
33	Apr 8 100006	8.5 N 122.7 E	n	—	U 90 K 87	5.6 5.8						6.1 6.5	6.1 6.2	Ma 5 1/2
34	Apr 10 055720	25 N 126 E	n	—	U 77 K 72	6.8 6.6						6.1 6.1	6.4 6.3	Pr 6 1/4, R 6.3
35	Apr 12 012709	14 1/4 S 66 3/4 E	n	—	U 84 K 88	5.6						5.7	5.6	
36	Apr 14 234945	3 1/2 N 126 1/2 E	n	—	U 97 K 93	6.1 6.2						6.3 6.4	6.3 6.6	Pr 6 1/2
37	Apr 15 055950	42.1 N 142.4 E	(n)	—	U 69 K 62	6.5 6.3						5.8 5.8	5.7 5.7	R 6.12
38	Apr 19 095853	7 N 71 1/2 W	60	6.8	U 83 K 84	6.5		6.7 6.9			6.3 6.5	6.7 7.2	6.1 6.3	Pa 6.8, Pr 6 1/4, R 6.3
39	Apr 28 105418	42 1/2 N 143 E	n	6.3	U 68 K 62	6.5 6.6						5.6 6.2	5.7 5.6	Pa 6 1/2, Pr 6-6 1/4, R 6.2, W 6 1/4-6 1/2
40	May 4 141516	24 1/2 S 177 1/2 W	n	6.4	U 144 K 136								6.1 6.0	Pr 6 1/4, W 6 1/2
41	May 8 005840	35 1/2 N 140 E	60	6.2	U 74 K 68	6.1 6.2						5.8 6.1	5.4 5.8	Pa 6 1/4, Pr 6-6 1/4, R 6
42	May 8 211040	20 1/2 N 127 E	n	6.5	U 97 K 94	6.2 6.2		5.5			6.3	6.3	6.1 6.1	Pa 6 1/2-6 3/4, Pr 6 1/4, R 6.5

TABLE 17 (cont.).

No.	θ GMT	φ, λ	h km	M	Station Δ	Magnitude determined from								Remarks	
						PZ'	PZ	PH	PPZ'	PPZ	PPH	SH	LH		
	1952														
43	May 9 174743	6 3/4 S 155 E	60	7.0	U 118 K 112				5 8	6.5	6.4 6.6	6.6 7.1	H 7, Pa 7, Pr 7, R 6 3/4, Sk 7		
44	May 13 193148	10 1/2 N 84 1/2 W	120	6.6	U 87 K 86		5.7	6.1		5.9	6.2	5.8 6.6	5.8 6.4	Pa 6 3/4, Pr 6 1/2, R 6.5	
45	May 14 003655	42.1 N 145.2 E	n	6.4	U 70 K 63	6.2 5.9	6.2	6.2				6.3 6.5	5.8 6.0	Pa 6 1/2, Pr 6.4, R 6 1/4	
46	May 14 211136	16 1/2 N 86 1/2 W	n	—	U 82 K 81						6.5	5.6	5.2	B 5.9	
47	May 16 054211	14 1/2 N 91 3/4 W	n	5.8	U — K 84			5.5				5.5	5.3	Pa 5 3/4, T 5 3/4	
48	May 16 100823	19 N 112 3/4 E	(n)	—	U 81 K 77	5.7 5.6	5.5					5.6	5.4 5.2		
49	May 16 204541	6.5 N 79.0 W	(n)	6.6	U 88 K 87	6.5 7.2	6.6	6.4 6.9		6.5	6.7	5.9 6.8	5.9 6.2	B 6 1/2, Pa 6 3/4, Pr 6.5, Sk 6 1/2	
50	May 17 094814	42 1/4 N 143 1/2 E	(n)	6.6	U 69 K 63	6.2 6.2	6.1	6.3 6.1				5.8 6.3	6.0 6.4	H 6 1/2, Pa 6 1/2-6 3/4, Pr 6.6, Sk 6 1/2	
51	May 19 183221	42 1/4 N 143 1/2 E	n	7.0	U 69 K 63	6.7 6.9	6.5	6.3 6.4				6.3 6.8	6.8 7.2	Pr 7.3, Sk 7 1/4, H 7 1/4, Pa 6 3/4, St 6 3/4-7, W 6 3/4-7	
52	May 22 230821	29 1/2 N 131 1/2 E	n	—	U 76 K 71	5.8 5.8						5.5 5.9	5.8 6.2	Pr 6 1/2, Sk 6 1/2	
53	May 23 042052	33 N 136 E	60	6.0	U 74 K 69	{ 6.2 6.7 6.2							5.5 5.7	Pa 6, Pr 6	

No.	θ GMT	φ, λ	h km	M	Station Δ	Magnitude determined from								Remarks	
						PZ'	PZ	PH	PPZ'	PPZ	PPH	SH	LH		
1952															
54	May 24 015905	21 1/2 S 71 W	n	6.8	U — K 111									5.8	Pa 6 3/4
55	May 24 160553	1.0 S 98.8 E	n	6.5	U 87 K 87	6.5 6.8	6.1	6.3		6.3	6.4	5.8 6.4	6.3 6.6	Pa 6 1/2-6 3/4, Pr 6.1, Sk 6 1/2	
56	May 26 024631	28 1/2 N 95 E	n	—	U 59 K 58	6.4 6.2	5.9	6.1				5.5 (5.3)	(5.5)	Pr 5 3/4	
57	May 28 074740	36.5 N 70.5 E	240	—	U 41 K 42	5.8 6.7			5.6		5.9				
58	May 28 075909	35 1/2 N 136 E	400	6.8	U 72 K 66	6.3 7.3		5.9 6.5				6.4 6.5	5.6 5.5	Pa 6.8	
59	Jun 5 055635	6 N 77 1/2 W	(n)	—	U 88 K —	{ 5.6 (6.3)						5.9	5.4	Pa 6 1/4, R 5 1/4	
60	Jun 10 095827	15 1/2 S 178 1/2 W	n	6.7	U 134 K 126				5.8					6.4 6.3	B 6 3/4, Pa 6 1/2-6 3/4, Pr 6.7, R 6.7, W 6 1/2
61	Jun 11 003136	32.1 S 67.9 W	n	6.8	U 115 K 118				6.4		6.4			6.1 6.5	Pa 7, Pr 6.4, R 6 1/2, W 6 3/4
62	Jun 13 010723	37.5 N 22.1 E	n	—	U 23 K 30	5.5 5.4						4.6			
63	Jun 19 121256	22.6 N 100.0 E	n	6.7	U 67 K 65	5.9 6.3					6.2	6.4 6.5	6.9 6.8	Pa 6 1/2, Pr 7.1, R 6.5	
64	Jun 20 054617	24.3 N 121.8 E	n	6.6	U 76 K 72	6.7 6.6	6.5	6.7			6.3	5.7 6.7	6.6 6.5	B 6 1/2, Pa 6 1/2, Pr 6.7, R 6.75	

TABLE 17 (cont.).

No.	θ GMT	φ, λ	h km	M	Station Δ	Magnitude determined from								Remarks
						PZ'	PZ	PH	PPZ'	PPZ	PPH	SH	LH	
1952														
65	Jun 21 062857	46 N 153 1/2 E	(n)	6.2	U 68 K 60	6.7 6.4		6.3 5.9				5.6 5.6	5.5 5.6	Pa 6 1/4, Pr 6.1
66	Jun 22 100814	46 N 153 1/2 E	(n)	6.2	U 68 K 60	6.4 6.4		6.4 6.1				5.4 5.7	5.4 5.5	Pa 6 1/4, Pr 6.2
67	Jun 22 214153	46 N 153 1/2 E	n	7.0	U 68 K 60	6.8	7.0	6.7 6.9	6.5		6.1	6.6 6.7	6.7 6.8	B 6 1/2, Pa 7, Pr 7.3, R 7, St 6 3/4, W 7 1/4
68	Jun 23 120310	24.3 N 121.8 E	n	6.0	U 76 K 72	6.7 6.8			6.1			5.7 6.2	6.1 6.1	Pa 5 3/4-6, Pr 6, R 6
69	Jun 24 162903	46 N 153 1/2 E	n	5.9	U 68 K 60	6.2 5.9		5.9				5.6 5.6	5.4 5.5	Pr 6, R 5 3/4
70	Jun 25 231956	31.0 N 101.5 E	n	6.1	U 61 K 58	6.1			5.8 5.8			5.7 5.4	5.7 6.2	Pr 6-6 1/4, R 6
71	Jul 5 171950	36.5 N 70.5 E	220	—	U 41 K 42	6.8 6.9	5.8	6.3 6.1	5.8		5.9 6.1	5.5 5.5		
72	Jul 6 061047	0.0 16.5 W	n	—	U 65 K 72	5.5 5.7						5.7 5.7	5.2 5.2	
73	Jul 9 181518	7 1/2 N 82 W	n	6.4	U 88 K 87	6.1						5.8 5.8	5.8 5.5	Pa 6 1/2, Pr 6-6 1/4, R 6-6 1/4
74	Jul 13 173426	3 S 128 E	n	6.9	U 103 K 100	6.2 6.8						6.2 (6.0)	6.3 (6.2)	Pa 6 3/4-7, Pr 6 1/2, R 6 3/4-7, W 6 3/4
75	Jul 17 160952	34 1/2 N 136 E	80	7.0	U 73 K 68	6.6 6.6	5.9	5.9				6.4 6.8	(6.0) (6.2)	H 7, Ma 7 1/4, Pa 6 3/4, Pr 6 3/4, R 7 1/4, W 6 3/4

No.	θ GMT	φ, λ	h km	M	Station Δ	Magnitude determined from								Remarks	
						PZ'	PZ	PH	PPZ'	PPZ	PPH	SH	LH		
1952															
76	Jul 21 115214	35.0 N 119.0 W	n	7.6	U 79 K 73	6.8	6.8	6.7 7.2		6.9	6.4 7.0	6.9 7.3	7.8 7.5	H 8 1/4, Pa 7.6, Pr 8.2, R 7 3/4, Sk 8	
77	Jul 24 220920	42 1/2 N 145 1/2 E	(n)	—	U 70 K 63	6.5	5.9	6.1				5.7 6.2	5.7 6.0	Pr 6 1/4	
78	Jul 25 190942	35 N 119 W	n	5.7	U 79 K 73	5.5						5.3 5.5	5.6 5.6	B 5 1/2-5 3/4, Pa 5 3/4	
79	Jul 26 142635	20 N 95 E	80	—	U 67 K 66	6.1					5.8		4.9		
80	Jul 27 082322	20 1/2 S 179 W	500	—	U 139 K 131					6.1	6.4 6.3		5.5	W 6 3/4-7	
81	Jul 29 070345	35 N 119 W	n	6.3	U 79 K 73	5.2					5.4 5.8	6.0 6.0		B 6 1/4-6 1/2, Pa 6 1/4, Pr 6 1/4, T 6 1/2	
82	Aug 4 014939	31.5 N 49.3 E	n		U 35 K 40	5.8 6.1					5.5		(<5)		
83	Aug 7 215322	41 1/2 N 144 E	(n)	—	U 70 K 63	6.3 5.6					5.8	5.5 5.3	Pr 6		
84	Aug 13 143035	33 3/4 N 47 3/4 E	n	—	U 33 K 38	5.4 5.7			5.6 5.6						
85	Aug 14 231642	6 S 155 E	n	6.4	U 117 K 111							5.9		R 6 1/4, St 6-6 1/4, W 6 1/2-6 3/4	
86	Aug 17 160205	30 1/2 N 91 1/2 E	n	7.6	U 56 K —		6.8			6.6	7.3	7.9		D 7 1/2, H 7 3/4, Pa 7 1/4-7 1/2, Pr 8.0, R 7.5, Sk 7.9, St 7 1/4	

TABLE 17 (cont.).

No.	θ GMT	φ, λ	h km	M	Station Δ	Magnitude determined from							Remarks	
						PZ'	PZ	PH	PPZ'	PPZ	PPH	SH	LH	
	1952													
87	Aug 20 152500	43.0 N 126.7 W	n	7.0	U 74 K 67	5.8 5.8		6.2 6.3			6.1 6.4	6.2 6.9	6.1 6.5	D 6 3/4, Pa 7-7 1/4, Pr 6 1/2, R 7.3, Sk 6 3/4
88	Aug 25 014440	27 1/4 N 95 3/4 E	n	—	U 61 K 60	6.3 6.6						5.5	(5.0) 5.6	
89	Aug 29 052817	6 N 95 3/4 E	n	—	U 79 K 79	5.6						5.9	5.7 5.8	R 5.5
90	Aug 31 160933	42 N 142 1/2 E	(n)	6.2	U 69 K 63	6.2 6.3						5.8 6.1	5.7 5.5	Pr 6, R 6.4
91	Sep 9 125444	8 1/2 N 84 1/2 W	(n)	6.8	U 88 K 88	6.8 6.7		6.5 6.7	6.3			6.6 6.8	6.6 6.6	B 6 3/4-7, Pa 6 3/4-7, Pr 6.8, R 6.7
92	Sep 11 222641	29 S 177 W	n	6.5	U 147 K 140		6.1						6.0 6.2	B 6 1/2-7, Pr 6 1/2, R 6 1/2, W 6.4
93	Sep 14 093410	34 N 93 1/2 E	n	—	U 54 K 53	{ 6.5 6.2						5.4 5.3	(5.9) 5.8	Pr 6
94	Sep 15 112806	30 3/4 N 72 E	n	—	U 46 K 48	5.6 5.8		5.7					(5.1) (5.6)	Pr 5 1/2
95	Sep 20 125744	56.1 S 145.1 E	n	—	U — K 152								6.0	R 6.1, W 6 1/2-6 3/4
96	Sep 21 023030	22 1/2 S 65 W	250	7.2	U 105 K 108	7.9	7.4		6.6 6.9	6.8	6.6 7.2	7.0 7.4	6.2 6.6	M 7, Pa 7 1/4, R 7.3, T 7, W 7
97	Sep 24 202930	56 1/2 N 157 W	100	—	U 65 K 57	5.8 6.4						5.9 6.3	5.3	

No.	θ GMT	φ, λ	h km	M	Station Δ	Magnitude determined from								Remarks	
						PZ'	PZ	PH	PPZ'	PPZ	PPH	SH	LH		
1952															
98	Sep 27 190546	50 1/2 N 157 E	100	6.4	U 66 K 58	5.9 6.3						5.8 5.8	B 6 1/2, Pr 6 1/2, R 6.2		
99	Sep 30 125200	28 1/2 N 102 E	n	6.9	U 63 K 61	6.4 5.6	6.2	6.4		6.1	6.3	6.5 (6.4) 6.7 7.0	Ma 6 1/2-6 3/4, Pa 6 1/2, Pr 7 1/4, R 6.9, Sk 7-7 1/4		
100	Oct 1 074903	2 1/2 N 65 1/2 E	n	—	U 68 K 73	6.1 6.1	5.7					5.8 5.5			
101	Oct 1 132102	36 1/2 N 94 E	n	—	U 53 K 51	5.6 5.8			5.9 6.2				(5.2)		
102	Oct 3 073645	6 1/2 N 83 W	n	—	U — K 89		6.3	5.6	6.3	6.3		5.6 5.3	B 6 1/2		
103	Oct 5 105456	37 1/2 N 20 1/2 E	n	—	U 23 K 30		5.4		6.1 5.7			5.4 5.3 (5.1) (5.4)	Pr 5 1/2		
104	Oct 5 220423	37 N 93 E	n	—	U 51 K 50	6.5 6.5		6.3 6.4	5.6 6.1	5.7	6.2	5.5 5.5 (5.2) (5.9)	Pr 6		
105	Oct 6 222935	53 1/2 N 161 E	n	5.8	U 64 K 56	5.9 6.2 5.8						5.7 5.5 (5.2) 5.3	Pr 5 3/4-6, R 5 3/4		
106	Oct 10 155530	15 1/4 S 174 3/4 W	n	6.4	U 136 K 127							6.1 6.2	Pa 6 1/4-6 1/2, Pr 6 1/4-6 1/2, R 6.5		
107	Oct 10 184737	30 1/2 N 69 E	n	6.2	U 45 K 47	5.6 (6.4) 6.1		6.3	5.5	5.8	6.2	5.6 5.5 (6.3)	Pr 6, R 6 1/4-6 1/2		
108	Oct 13 164224	38.9 N 23.7 E	n	—	U 22 K 29	6.2 5.1		5.8				4.7 (<5) 5.0	Pr 5		

TABLE 17 (cont.).

No.	θ GMT	φ, λ	h km	M	Station Δ	Magnitude determined from							Remarks	
						PZ'	PZ	PH	PPZ'	PPZ	PPH	SH	LH	
	1952													
109	Oct 18 052232	16 S 168 E	n	6.5	U 131 K 126					5.9	6.4	6.3 6.3	Pa 6 1/2-6 3/4, Pr 6 1/4, R 6 1/2	
110	Oct 18 115736	13 N 46 W	n	5.6	U 65 K 68	5.4 5.7						5.1 5.7 5.8	Pr 5 1/2, R 5 3/4	
111	Oct 22 041452	36.7 N 27.9 E	n	—	U 24 K 32	5.3 5.1	5.4				4.6 (4.9)			
112	Oct 22 170039	37.1 N 35.7 E	n	—	U 26 K 32	5.7 6.4					5.4 5.1 (4.8) (5.0)	Pr 5, R 5		
113	Oct 26 084103	34 1/2 N 137 E	280	6.0	U 74 K 68	6.3 6.6					6.2 (5.2)	Pa 5 3/4-6, R 6, W 6 1/4		
114	Oct 26 155303	39 N 143 E	n	6.5	U 71 K 64	5.9 5.9					(6.0) 6.3	D 6 1/2, Pa 6 1/2, Pr 6.5, R 6 1/4		
115	Oct 26 180200	39 N 143 E	n	6.6	U 71 K 64	6.3 5.9					5.8 6.6 (6.0) 6.6	D 6 1/2-6 3/4, H 6 3/4, Pa 6 1/2, Pr 6.8, R 6 1/2, St 6.6		
116	Oct 26 191912	38 1/2 N 143 1/2 E	(n)	6.2	U 72 K 65	6.6 6.4		6.3			5.9 6.2	H 6 1/2, Pa 6, Pr 6 1/2, R 6		
117	Oct 27 031712	39 N 143 E	(n)	6.6	U 71 K 64	6.4 6.2		6.3 5.9 6.4			6.2 6.5 6.1 6.4	H 6 1/2, Pa 6 1/2, Pr 6.6, R 6 1/2, St 6 3/4		
118	Oct 28 042952	18.3 N 73.3 W	n	6.0	U 75 K 74	6.1	6.4	6.6			5.6 6.4 (5.8)	Pa 6, Pr 6, T 6		
119	Oct 28	40 N	n	6.4	U 71	6.5					5.9	Pr 6.5, R 6 1/4		

No.	θ GMT	φ, λ	h km	M	Station Δ	Magnitude determined from							Remarks	
						PZ'	PZ	PH	PPZ'	PPZ	PPH	SH	LH	
1952														
120	Oct 28 164521	39 N 143 E	n	—	U 71 K 64	5.9 5.6							5.6 5.7	
121	Oct 31 163714	39 N 143 E	n	6.5	U 71 K 64	6.4 5.9			6.2			6.2 6.5	6.0 6.3	D 6 1/2, Pr 6.6, R 6 1/2
122	Oct 31 235136	34 1/2 N 100 3/4 E	n	—	U 58 K 56	5.9 5.9			5.8			5.8 5.6	5.9 6.0	Pr 6 1/4
123	Nov 4 165823	52.9 N 160.1 E	n	8.4	U 64 K —			8.1				8.2	8.4	B 8 1/2, D 8, L 8 1/4, H 8 3/4, Ma 8 1/4, Pa 8 1/4, Pr 8 1/2, R 8 1/2-8 3/4, Sk 8 1/2, St 8 1/4-8 1/2
124	Nov 4 221254	52 N 161 E	(n)	—	U 64 K 56	7.0 6.6		6.4				6.3	6.3	
125	Nov 5 021958	50 1/2 N 157 E	n	—	U 65 K 58	5.5 5.9						5.8	6.2 6.0	Sk 6 1/4
126	Nov 5 032944	51 N 159 E	(n)	—	U 65 K 58	6.7 6.5		6.4				6.2 5.9	5.7 5.9	Sk 6 1/4
127	Nov 5 130624	52 N 159 1/2 E	(n)	6.9	U 64 K 56	7.4 7.0	6.6	6.9 6.7				6.9 6.1	6.5 6.6	H 7, Pr 7.0, R 6.8, Sk 6 3/4
128	Nov 5 190826	53 1/2 N 161 1/2 E	(n)	6.2	U 64 K 56	6.6 6.2 6.3						6.2 5.7	5.8 6.0	Pr 6.1, R 6.4, Sk 6
129	Nov 5 224610	53 1/2 N 160 E	(n)	—	U 63 K 55	6.4 6.4						6.3 6.0	5.8 6.0	Pr 6.4

TABLE 17 (cont.)

No.	θ GMT	φ, λ	h km	M	Station Δ	Magnitude determined from							Remarks	
						PZ'	PZ	PH	PPZ'	PPZ	PPH	SH	LH	
	1952													
130	Nov 6 194557	51 1/2 N 159 1/2 E	n	6.7	U 65 K 57	6.8 6.6	6.7					6.3 5.9	6.3 6.4	Pr 7.0, R 6.6, Sk 6 1/2
131	Nov 6 194720	5 S 145 1/2 E	n	7.0	U 112 K 108				6.4				6.5 (7.0)	Pr 6 3/4, W 7 1/4-7 1/2
132	Nov 7 120909	52 N 161 E	(n)	—	U 64 K 57	6.7 6.6						6.3 5.5	5.5	Pr 5 3/4
133	Nov 7 220519	47 N 155 E	n	—	U 68 K 61	6.4 6.1						6.2 6.6	6.0 6.3	Pr 6 1/4
134	Nov 7 231204	31 S 177 W	n	—	U 149 K 141				5.9 6.1				6.4 6.3	W 7.0
135	Nov 8 193318	48 1/2 N 156 E	n	6.6	U 67 K 60	6.2						5.9 6.4	6.5 6.4	H 6 1/2, Pr 6.6, R 6.7
136	Nov 10 005500	50 N 158 1/2 E	(n)	—	U 66 K 59	6.8 6.5		6.5				5.8 5.7	5.7 5.7	Pr 6 1/4
137	Nov 13 075845	50 1/2 N 157 E	n	—	U 65 K 58	5.9						5.6 5.7	6.4 6.4	Pr 6 3/4
138	Nov 13 222534	50 N 158 E	n	—	U 66 K 59	6.3 5.5	5.9	6.1				5.4 5.4	5.5 5.6	Pr 6
139	Nov 22 074637	35.8 N 121.1 W	n	6.0	U 79 K 72	6.6						5.6 6.4	5.5 6.0	B 6.1, Pa 6, Pr 6
140	Nov 26 132518	53 N 160 E	n	—	U 64 K 56	6.7 6.2						6.2 5.3	(5.4) 5.4	

TABLE 17 (CONT.).

No.	θ GMT	φ, λ	h km	M	Station Δ	Magnitude determined from								Remarks	
						PZ'	PZ	PH	PPZ'	PPZ	PPH	SH	LH		
1952															
141	Nov 27 072034	36.5 N 70.5 E	220	—	U 41 K 42	6.5 6.1		6.1			5.7	5.4			
142	Nov 28 080530	52 N 160 E	(n)	—	U 64 K 57	6.9 6.7		6.3	6.1		5.8	6.4	5.6 5.8	Pr 6	
143	Nov 29 082234	53 N 160 E	n	7.3	U 64 K 56	6.5 7.0 6.4		6.3				7.2	7.0	B 7 1/4, D 7 1/4	
144	Nov 29 234625	56 N 155 W	(n)	6.8	U 64 K 56	6.8 7.0		6.7	6.4			6.9	6.4	B 7-7 1/4, D 7, H 6 3/4, Pa 6 3/4, Pr 6.8, R 6 3/4, St 6.5, T 7	
145	Nov 30 192844	52 1/2 N 159 W	n	—	U 64 K 56	6.2 5.9						6.2	5.9	Pr 6 1/4	
146	Dec 4 035125	52 N 178 E	100	5.9	U 68 K 60	6.4						5.9	5.7	B 6, R 5.8	
147	Dec 6 104114	8 S 157 E	n	7.3	U 120 K 114				6.3		6.8	7.6	7.0 7.3	B 7 1/4-7 1/2, D 7 1/2, H 7 1/4, Ma 7 1/2, M 7, Pa 7, Pr 7.5, R 7.5, Sk 7 1/4, St 7 1/4, W 6 1/2-6 3/4	
148	Dec 7 005012	53 N 172 1/2 E	n	6.4	U 66 K 58	7.0 6.8	6.8	6.8	6.4			6.4	6.3	D 6 1/4, Pa 6 1/4, Pr 6.5, R 6.4, St 6.5	
149	Dec 7 163310	51 1/2 N 159 E	n	—	U 65 K 57	6.1 6.4						6.2 (5.4) 5.6	5.5	Pr 6	

TABLE 17 (cont.).

No.	θ GMT	ϕ, λ	h km	M	Station Δ	Magnitude determined from							Remarks		
						PZ'	PZ	PH	PPZ'	PPZ	PPH	SH	LH		
	1952														
150	Dec 11 085818	49 N 155 E	n	—	U 66 K 59	5.9 5.6						5.9 6.2 6.3		Pa 6, Pr 6 3/4, R 6.5	
151	Dec 17 230355	34 3/4 N 24 3/4 E	(n)	—	U 26 K 33	7.3 6.8	6.6	7.0 6.7				6.2 5.9 6.5 6.4		M 6, Pa 6 3/4, Pr 6 3/4, St 6-6 1/4	
152	Dec 18 092028	53 1/2 N 162 E	(n)	—	U 63 K 56	5.9						5.9 6.2 5.6 5.8		Pr 6 1/4	
153	Dec 22 222442	54 N 160 1/2 E	n	—	U 63 K 55	6.4 6.1			5.9			5.9 5.9 6.0 5.9		Pa 6 3/4, Pr 6 1/4	
154	Dec 24 183936	5.9 S 151.2 E	n	7.1	U 116 K 109								7.0 7.1	Pa 7, Pr 7.2, St 7-7 1/4, W 7-7 1/4	
155	Dec 25 222242	29 N 69 1/2 E	n	—	U 48 K 48	5.6 5.8			5.7			5.5 5.6 (5.8) (5.9)		Pr 6	
156	Dec 27 012554	53 N 160 E	(n)	—	U 64 K 56	6.8 6.8		6.7				6.4 6.3 5.6 5.7		Pr 6.1	
157	Dec 28 150120	6.5 N 127.0 E	n	—	U 94 K 89	6.1 5.5 6.3	6.3					6.2 6.6 6.3		Pr 6.6	
158	Dec 29 020913	49 N 158 E	(n)	—	U 67 K 59	6.5 6.4 6.5		6.1	6.3			6.2 6.3 5.6		Pr 6.4	
159	Dec 31 144839	35 1/2 N 25 3/4 E	n	—	U 25 K 32	5.0 5.2 5.9								A 6, Pr 4 1/2	
160	Dec 31	35 1/2 N	n	—	U 25	5.3								(4.9) (5.4)	A 6, Pr 5

No.	θ GMT	φ, λ	h km	M	Station Δ	Magnitude determined from								Remarks	
						PZ'	PZ	PH	PPZ'	PPZ	PPH	SH	LH		
161	1953 Jan 5 074817	54 N 170 E	n	7.1	U 65 K 57	6.8 6.9		6.8				7.1	(7.1)	D 7 1/4, Pa 6 3/4-7, Pr 7 3/4, R 7, St 7 1/4-7 1/2	
162	Jan 5 100625	49 N 156 E	n	—	U 67 K 59	6.7 6.7		6.5				6.7	7.1	D 7 1/4, Pa 6 3/4, Pr 7 1/3, R 7.25, St 6-6 1/4	
163	Jan 7 140820	5 1/2 S 150 1/2 E	n	6.3	U 115 K 110									6.2 (6.6)	Pr 6 1/4, R 6.3
164	Jan 11 225330	65 3/4 N 133 1/2 W	(n)	6.4	U 53 K 46	{ 6.6 6.9		6.2	6.3		5.9	6.2	6.2	5.8	D 6 1/2, B 6, Pa 6 1/2, Pr 6 1/3, R 6.38, St 6
165	Jan 12 172339	49 1/2 N 156 E	60	7.0	U 65 K 57	5.5 5.9								6.9 (6.8)	B 6 1/4, D 7, Pa 6 3/4-7, Pr 7, R 7.1
166	Jan 20 173306	1 1/2 N 126 E	n	6.5	U 98 K 95	6.4 6.2								6.1	Pa 6 1/2, R 6 1/4-6 1/2
167	Jan 27 031255	52 N 159 1/2 E	(n)	—	U 64 K 57	6.9 6.7								6.5 6.1	6.0 6.0
168	Feb 5 224205	35 3/4 N 22 3/4 E	n	—	U 25 K 32	5.8 6.1			5.6					5.1 (<5) (4.8)	
169	Feb 6 131259	42 1/2 N 143 1/2 E	n	6.9	U 69 K 62	6.4 6.2	6.5	6.2	6.4	5.9				5.8 6.5	6.4 6.7
170	Feb 7 223105	35.0 N 24 1/2 E	n	—	U 26 K 33	6.3 6.3		5.8	5.6					5.3 (<5) (5.5)	Pr 5 1/4, R 5 1/2
171	Feb 12 081532	35.8 N 55.0 E	n	6.5	U 34 K 37	5.8 6.6	6.3	6.3	6.5			6.5	5.9 (6.2)	H 6 1/4, Pa 7, Pr 6 1/2, R 6 1/2-6 3/4, Sk 6 1/4, St 6 1/4	

TABLE 17 (cont.).

No.	θ GMT	ϕ, λ	h km	M	Station Δ	Magnitude determined from								Remarks
						PZ'	PZ	PH	PPZ'	PPZ	PPH	SH	LH	
	1953													
172	Feb 14 084313	35 1/2 N 26 1/2 E	(n)	—	U 25 K 31	5.9 6.2		5.9		6.3		5.7	4.9 4.9	
173	Feb 14 214812	18 1/2 N 146 E	(n)	6.8	U 91 K 85	6.3 6.9						6.5	5.7 6.0	Pa 6 3/4
174	Feb 19 151743	0.0 17.9 W	n	6.7	U 65 K 72	6.5 6.6						6.4	6.2	H 6 3/4, Pr 6 3/4, Sk 6 1/2-6 3/4, St 6 1/2
175	Feb 23 004608	29 1/2 N 81 E	n	—	U 52 K 52	6.3 6.2			5.8		5.7	5.5	(5.2) 5.7	
176	Feb 25 211618	56 N 156 1/2 W	60	6.8	U 65 K 57	6.6 6.9						6.8	(5.8) 6.6 5.5	Pa 6 3/4
177	Feb 26 114230	11.0 S 164 1/4 E	n	7.2	U 125 K 118							7.0 6.8		B 7 1/4, H 7 1/4, Pa 7 1/4, Sk 7-7 1/4, W 7
178	Mar 5 210120	52.0 N 157 E	(n)	6.7	U 64 K 56	6.4 5.9	6.3	6.5				6.2 5.8	(6.3) 6.2	B 6 3/4, D 6 1/4, Pa 6 3/4, R 6 1/2
179	Mar 17 130433	50 1/2 N 156 1/2 E	n	—	U 65 K 57	5.9 5.9						5.7	5.7 (5.8)	R 5.8
180	Mar 18 190613	40.1 N 27.3 E	n	7.7	U 21 K 28	6.8 6.4		6.8				6.8	7.3	B 8, D 7, H 7.5, Pa 7 3/4, R 7.4, St 7 3/4, T 7 3/4
181	Mar 19 082757	14 N 61 W	225	7.7	U 73 K 74	6.5 6.2	6.2	5.9			6.2	7.3 6.7	6.4 6.5	B 7 3/4, D 7-7 1/4, Pa 7 3/4, R 7.6, T 7 1/2
182	Apr 4	36.0 N	n	6.3	U 74	6.4							(5.8)	Pa 6 1/4, Pr 6 1/4, D 6 1/4

No.	θ GMT	φ, λ	h km	M	Station Δ	Magnitude determined from								Remarks	
						PZ'	PZ	PH	PPZ'	PPZ	PPH	SH	LH		
1953															
183	Apr 5 101530	22 N 123 E	n	--	U 78 K —	5.6								5.9	
184	Apr 6 003616	7.3 S 131.0 E	n	--	U 108 K 104	6.7			6.5 6.2			(6.1) 6.4	6.0 6.1	R 6.1, W 7 1/2	
185	Apr 6 034932	9 3/4 N 123 3/4 E	n	--	U 90 K 87	6.3 6.2						5.8	5.6 5.6		
186	Apr 6 121445	52 1/2 N 160 E	(n)	6.0	U 64 K 56	6.6 6.3	6.1						5.4 5.7	Pr 6, R 6	
187	Apr 14 132926	7 1/2 S 71 1/2 W	600	7.0	U 96 K 97	6.4 6.7			6.2 6.2	6.5	6.7	6.3		Pa 7, T 6 3/4	
188	Apr 23 162417	4 S 154 E	n	7.7	U 115 K 109				6.5 6.4	6.5	6.6		7.5 7.8	D 7 3/4-8, Pa 7 1/2-7 3/4, Pr 7 3/4, R 7 3/4, St 7 1/2-7 3/4, W 7 1/2	
189	Apr 25 162338	43 1/2 N 86 E	n	—	U 43 K 42	6.1 6.1			5.3 5.6				(5.0) (5.1)	R 5.1	
190	Apr 29 033120	10.0 S 159.5 E	n	—	U 122 K 116								6.0 6.1	R 6.25	
191	Apr 29 202100	43 N 143 E	(n)	—	U 68 K 62	5.8 6.1						5.7	5.2	R 5.3	
192	Apr 30 062640	20 1/2 S 170 E	(n)	6.8	U 136 K 129				6.6	6.4	6.2 6.4		6.6 6.7	Pa 6 3/4, Pr 6.9, R 6.85	
193	Apr 30 154524	41 1/2 N 47 3/4 E	n	—	U 26 K 30	5.2 5.7			5.5				(<5) (4.8)		

TABLE 17 (cont.).

No.	θ GMT	φ, λ	h km	M	Station Δ	Magnitude determined from							Remarks	
						PZ'	PZ	PH	PPZ'	PPZ	PPH	SH	LH	
	1953													
194	May 1 211815	34 N 72 3/4 E	n	—	U 44 K 45	5.5 5.5			5.7					
195	May 2 183811	52 1/2 N 159 E	(n)	—	U 64 K 56	5.8 5.8						5.7 (5.5) 5.6		
196	May 4 112908	53 1/2 N 161 E	(n)	—	U 63 K 56	6.7 6.6	5.9	6.4 6.2				5.6 5.4 5.6	Pr 6, R 6	
197	May 4 152630	28 S 62 1/2 W	600	6.5	U 111 K 115				6.1 6.1					Pa 6 1/2, T 6 1/4
198	May 6 171648	36 1/2 S 73 W	(n)	7.6	U 121 K 124				7.2 7.5	7.3	6.9 7.5	7.5 7.6		Pa 7 1/2-7 3/4, Pr 7 3/4-8, R 7 1/2, St 7 1/2-7 3/4, T 7 1/4
199	May 11 101643	21 3/4 S 168 1/2 E	n	6.6	U 137 K 130				6.4 6.3	6.3	6.3	6.2 6.1		B 7, Pa 6 3/4, Pr 6 1/2, R 6 1/4, W 6
200	May 13 041628	52 N 174 E	100	—	U 67 K 59	6.1 6.2	5.3					4.9 5.0		
201	May 18 081528	4 3/4 S 103.0 E	n	—	U 88 K 91	5.9						5.5 6.3	5.2 5.7	
202	May 19 031106	51 N 159 E	n	6.5	U 65 K 58	6.8 6.7		6.4				6.2	6.0	B 6 1/2, D 6-6 1/4, Pa 6 1/2, Pr 6 3/4, R 6 1/4, Sk 6 1/2
203	May 20 074526	53 S 134 W	n	7.3	U 164 K —								6.0	Pa 7 1/4

No.	θ GMT	φ, λ	h km	M	Station Δ	Magnitude determined from								Remarks
						PZ'	PZ	PH	PPZ'	PPZ	PPH	SH	LH	
	1953													
204	May 24 011955	51 S 28 W	n	—	U 116 K 123								5.8 6.2	Pr 6
205	May 25 123813	3 1/2 S 101 E	(n)	—	U 90 K 90	5.6 6.6	5.9					5.8 5.9	5.4	
206	May 25 174030	51 N 159 1/2 E	(n)	—	U 66 K 58	6.5 6.4	6.2					6.2 5.4	(5.1) (5.4)	R 5 1/2
207	May 26 014311	42 N 142 1/2 E	(n)	—	U 69 K 62	6.4 6.5	6.1				6.3	5.6 5.8	5.8 6.0	Pr 5 3/4, R 6 1/2
208	May 31 195835	20 N 70 1/2 W	r	7.0	U 71 K 71	6.5 6.4	5.9	6.3	6.2			6.5 7.2	6.2 6.5	B 7 1/2, D 6 3/4-7, Pa 7, Pr 7 1/4, R 6 3/4, T 7, St 6 3/4
209	Jun 2 175013	30 N 142 E	(n)	—	U 80 K 74	5.9 6.1			6.1 6.1			5.7	5.1	
210	Jun 3 160523	40.1 N 28.8 E	n	—	U 21 K 28	5.4		5.7	5.9			5.0 (<5) (5.4)	A 6, Pr 5	
211	Jun 7 122356	20 N 70 W	n	—	U 72 K 72	5.6 5.6	5.6					5.9 5.9	5.5 5.5	Pr 5 3/4
212	Jun 8 114034	53.3 N 159.1 E	60	6.5	U 64 K 56	6.3 6.3	6.4 6.3	5.6				6.1 5.5	5.8 6.0	Pa 6 1/2, Pr 6 1/2
213	Jun 9 013904	53.8 N 160.0 E	(n)	6.5	U 63 K 56	6.8 6.7	6.4 6.2					6.2 5.6	5.7 (5.9)	H 6 1/4, Pr 6 1/4-6 1/2, St 6 3/4

TABLE 17 (cont.).

No.	θ GMT	φ, λ	h km	M	Station Δ	Magnitude determined from								Remarks
						PZ'	PZ	PH	PPZ'	PPZ	PPH	SH	LH	
1953														
214	Jun 10 182343	4 S 128 E	n	—	U 104 K 100	6.1 6.6			6.1	6.2	6.1 6.3	5.9	5.7	
215	Jun 15 174714	56 1/2 N 154 W	(n)	6.5	U 64 K 56	6.7 6.7 6.9	6.4	6.6	6.1		6.3	6.8 6.5	5.9 6.0	B 6.7, D 6 1/2, H 6 1/4, Pa 6 1/2, Pr 6 1/4, St 6-6 1/4
216	Jun 16 095306	31 N 141 E	n	6.0	U 78 K 73	6.1 5.9	5.9	5.9		5.6	5.9	6.1 6.4	5.5 5.8	Pr 6, St 5 3/4-6
217	Jun 16 194825	55 1/2 N 160 W	60	6.4	U 64 K 56	6.2 6.6	5.7	6.2				5.4	5.5 5.2	Pa 6 1/4-6 1/2
218	Jun 18 054406	41.7 N 26.5 E	n	—	U 19 K 26	5.9 5.3	5.0	6.1 5.1				4.8 4.6	(4.9)	Pr 4 3/4
219	Jun 18 100448	6 1/2 S 155 E	n	—	U — K 112				5.7	5.7	6.2		5.9	Pr 6 1/4
220	Jun 23 135330	52 1/4 N 157 E	n	6.4	U 64 K 57	5.5	5.8	5.9 6.1				5.7	5.8	Pa 6 1/2, Pr 6 1/4, R 6 1/2, St 6
221	Jun 25 104457	8 1/2 S 123 1/2 E	n	6.9	U 106 K 103	6.6	6.6	6.9	7.4 7.0	6.9	7.0 7.3		6.8 7.0	Pa 6 3/4-7, Pr 6.9, R 6 3/4, H 6 3/4, C 7.9, W 7.7
222	Jun 26 054250	8 S 124 E	n	6.8	U 105 K 103	6.5 6.7			7.3 6.9		6.9 6.7		6.6 6.8	B 7, C 6.8, H 6 1/2-6 3/4, Pa 6 3/4, Pr 6 3/4
223	Jun 28 053705	31 N 141 1/2 E	n	—	U 79 K 72	6.1 5.8						5.7 (5.2)	6.2 5.3	

No.	θ GMT	φ, λ	h km	M	Station Δ	Magnitude determined from								Remarks	
						PZ'	PZ	PH	PPZ'	PPZ	PPH	SH	LH		
		1953													
224	Jul 1 025934	51 3/4 N 157.0 E	n	6.7	U 65 K 57	6.4	5.9	6.3 6.1				5.7	6.3 6.2	Pa 6 3/4, Pr 6 1/2, R 6.8	
225	Jul 2 065655	19.0 S 168 1/4 E	200	—	U 135 K 127				6.4	6.6	6.2 6.7		6.6 6.7	Pa 7 3/4, W 6 3/4-7	
226	Jul 3 053100	30 N 137 1/4 E	n	—	U 78 K 73	5.3 5.6						5.6	5.5 5.2		
227	Jul 6 215537	6.4 S 147.3 E	n	—	U — K 110								5.8	W 6 1/4	
228	Jul 7 040748	1 N 100 E	250	—	U 85 K 85	6.6 6.6				5.7		5.5 6.3	5.6 5.6	W 6 1/2-6 3/4	
229	Jul 7 134403	47 1/2 N 156 E	n	—	U 68 K 60	6.4 6.2	5.7	5.9					5.1		
230	Jul 7 172825	31 N 141 1/2 E	n	—	U 79 K 72	5.9 6.1	5.9					5.6 6.1	(5.3) 5.6	R 6.2	
231	Jul 9 190206	40 1/4 N 78 1/2 E	n	5.9	U 42 K 42	6.5 6.1		5.9	5.9		5.3	5.7	5.4 6.3	Pr 6, R 5.8	
232	Jul 9 212348	30 N 42 1/2 W	n	6.4	U 50 K 53	6.6 6.3	5.6	6.5 6.1					5.9 5.7	5.5 5.5	Pa 6 1/2-6 3/4, Pr 6 1/4, R 6.2
233	Jul 12 064305	2 S 139 1/2 E	n	6.4	U 107 K —				6.1					6.1	Pa 6 1/2, Pr 6 1/4, R 6.3
234	Jul 20 080820	21 S 177 W	100	6.5	U 137 K 132									6.1 6.1	C 6 1/2, Pa 6 1/2, Pr 6 3/4, W 6 1/2

TABLE 17 (cont.).

No.	θ GMT	φ, λ	h km	M	Station Δ	Magnitude determined from								Remarks
						PZ'	PZ	PH	PPZ'	PPZ	PPH	SH	LH	
	1953													
235	Jul 21 172235	26 3/4 N 128.0 E	(n)	6.0	U 77 K 72	6.3				5.5		5.7	5.5	Pr 6, R 6
236	Jul 22 051115	51 N 157 E	n	6.8	U 65 K 58	6.3 5.9	6.2	6.3				6.1 6.1	6.3 6.4	B 6 3/4, Pa 6 3/4-7, Pr 6 3/4, R 6 1/2-6 3/4, St 6 1/2
237	Jul 22 125212	42.0 N 143 1/2 E	n	—	U 70 K 63	5.9 5.8						5.4	5.4	Pr 5 1/2
238	Jul 22 150932	39.0 N 28.4 E	n	—	U 22 K 29	5.1						4.7	5.2 (5.2)	A 5 3/4, Pr 4 3/4
239	Jul 22 180430	26 1/2 N 44 1/2 W	n	—	U 54 K 56		5.5	5.7			5.6	5.2 5.2	5.2 4.9	Pr 5 1/4
240	Jul 23 010544	26 1/4 N 65.0 E	n	—	U 47 K 50	6.2 5.6			5.2	5.4	5.6	5.2	5.3	
241	Jul 23 182416	52 N 160 E	(n)	—	U 65 K 57	6.1 5.6	5.5	5.7				5.3	5.3	
242	Jul 26 165318	17.8 N 145.2 E	200	7.0	U 92 K 85	6.1 6.3	5.9	6.1	5.6 5.8			6.5 6.3	5.7 5.9	Pa 7, R 7
243	Jul 29 133236	2 3/4 S 12 1/4 W	n	—	U — K 74	6.1						5.6	5.3	Pr 5 1/4
244	Jul 29 181534	13 N 90 1/2 W	n	6.0	U 88 K 85		5.6		5.9			5.7	5.7	Pa 6, Pr 6, R 5 3/4-6
245	Jul 29 231802	16 S 173 W	n	6.3	U — K 128								5.7	Pa 6 1/2, Pr 6 1/4, R 6-6 1/4

No.	θ GMT	φ, λ	h km	M	Station Δ	Magnitude determined from								Remarks
						PZ'	PZ	PH	PPZ'	PPZ	PPH	SH	LH	
1953														
246	Aug 6 185542	45 N 86 E	n	5.4	U 42 K 41	6.2 5.7 5.8			5.3			(5.1) (4.9)	Pr 5 1/2, R 5.3	
247	Aug 9 074106	38.1 N 20.8 E	n	6.5	U 22 K 29	6.5	6.3 5.7				5.9 5.4	(6.0) (6.0)	D 6 1/4, II 6 1/2, Pa 6 3/4, Pr 6.3, St 6-6 1/4	
248	Aug 11 033220	38.1 N 20.8 E	n	6.8	U 22 K 29	7.0 6.7	6.5 6.7	6.7			6.5 6.3	(6.5) (6.5)	D 6 3/4, H 6.9, Pa 6 3/4, Pr 6.7, R 6.8, St 6 3/4-7	
249	Aug 12 092349	38.1 N 20.8 E	n	7.2	U 22 K —	7.3		7.5			7.2	(6.8)	B 7 1/4, D 7 1/4, H 7 1/4, Pa 7 1/4, Pr 7.1, R 7.2, St 7 1/4	
250	Aug 12 113342	38.1 N 20.8 E	n	—	U 22 K —	5.7					5.1	(4.8)	Pr 5 3/4	
251	Aug 12 120520	38.1 N 20.8 E	n	6.1	U 22 K 29	6.6 6.6		6.5			6.2 5.5	(6.0)	D 6, H 6.2, Pa 6, Pr 6.1, R 6.7, Sk 6.1	
252	Aug 12 140838	38.1 N 20.8 E	n	6.1	U 22 K 29	6.2 5.9		6.3	5.9		5.6 5.3	(5.5)	Pa 6, Pr 6, R 6.4	
253	Aug 13 092323	21 1/2 S 170 E	150	6.9	U 137 K 130							(6.4) 6.4	B 6 3/4-7 1/4, Pa 6 3/4-7, Pr 6 3/4, R 7, W 6 1/2	
254	Aug 13 101650	38.1 N 20.8 E	n	—	U 22 K 29	5.7 5.4		5.7			4.7	(5.1)	Pr 5	

TABLE 17 (cont.).

No.	θ GMT	φ, λ	h km	M	Station Δ	Magnitude determined from								Remarks	
						PZ'	PZ	PH	PPZ'	PPZ	PPH	SH	LH		
	1953														
255	Aug 17 031433	7 1/2 S 115 E	n	—	U 100 K 99	6.4 6.4			6.2 5.8				5.7		
256	Aug 23 071805	1 1/4 S 13 3/4 W	n	—	U 67 K 73	5.7 5.9	5.5					5.5 5.9	5.2 5.5		
257	Aug 25 020416	4 1/4 S 152 3/4 E	n	6.7	U 115 K 108				6.2				6.2 6.4	B 7, Pa 6 1/2-6 3/4, Pr 6 1/4-6 1/2, R 6 1/2-6 3/4	
258	Aug 27 204610	2.4 N 97.5 E	n	—	U 83 K 83	5.9	5.5		5.9 6.2			6.1 5.8	5.5 5.5		
259	Aug 27 221630	44 N 142 1/2 E	100	—	U 66 K 61	6.4 6.5	5.8	6.2				5.4		Pa 6	
260	Aug 29 015826	28 N 82 E	n	—	U 54 K 54	6.3 6.2						5.6 5.4	(5.2) (5.2)		
261	Aug 29 140850	35.8 N 5.0 E	n	—	U 25 K 33	5.6 5.5						4.8	(5.0)		
262	Aug 31 075246	53 1/2 N 160 E	(n)	6.0	U 63 K 55	6.6	5.9	6.3 6.1				5.8	5.4 5.4	Pa 6 1/4, Pr 5 3/4, R 6	
263	Sep 2 003558	41 1/4 N 47 1/4 E	n	—	U 27 K 30	5.0 5.2			5.6			4.8 4.8	(4.8)		
264	Sep 4 072305	51.0 N 156 1/4 E	n	7.0	U 65 K 58	6.1 6.5	6.4	6.5 6.5				6.3 6.2	6.9 6.7	D 7, H 7.2, Pa 6 3/4-7, Pr 7.1, R 6 1/2-6 3/4, Sk 7, St 6 3/4-7	
265	Sep 4	32 S	(n)	—	U 117							6.0		Pa 6 3/4-7, Pr 6 1/4,	

TABLE II (CONT.)

No.	θ GMT	φ, λ	h km	M	Station Δ	Magnitude determined from								Remarks
						PZ'	PZ	PH	PPZ'	PPZ	PPH	SH	LH	
	1953													
266	Sep 5 141841	37.8 N 23.0 E	n	5.7	U 22 K 30	5.9 5.7		5.8 5.9	5.7		5.9	5.4 (5.2) 5.2 (5.6)		A 6, D 5 1/2, H 5 3/4-6, Pr 5.6, Sk 5 1/2
267	Sep 5 185809	51 N 157 E	n	6.4	U 65 K 58		5.6					5.7 5.6 5.7		Pa 6 1/2, Pr 6 1/4, R 6 1/4-6 1/2
268	Sep 7 035857	41 1/4 N 32 3/4 E	n	6.0	U 21 K 27	6.2		5.9		6.3		5.9 5.8 (6.1)		A 7, D 5 3/4-6, H 6, Pa 6 1/4, Pr 5.9, Sk 5 3/4, St 5 3/4
269	Sep 9 155110	2.0 N 100.0 E	n	—	U 84 K 84	6.1 5.9						5.7 5.7		
270	Sep 10 040603	35.0 N 32 1/4 E	n	6.2	U 26 K 34	6.3 6.9	5.9	6.1 5.9	6.1			6.2 5.9 (6.5)		D 6 1/4-6 1/2, H 6 1/4, Pa 6 1/2, A 6 1/4 Pr 5 3/4-6, Sk 5 3/4-6, St 6
271	Sep 14 002636	18 1/2 S 178 1/2 E	(n)	6.6	U 136 K 128				6.2		6.5 6.2	6.3 6.2		H 6 1/2, Pa 6 3/4, Pr 6 1/2, R 6 1/2, Sk 6 1/2, St 6 1/2
272	Sep 14 145610	38.3 N 21.0 E	n	5.6	U 22 K 30	5.9 5.5		5.9				5.1 (4.8)		A 5 3/4, Pr 5 1/2
273	Sep 23 021436	50 1/2 N 156 E	n	7.0	U 65 K 57	6.2 6.4	6.3	6.1 6.4		5.9 6.2		6.3 6.8		B 6 3/4, H 6 3/4-7, Pa 7, Pr 7.2, Sk 7, St 6 3/4
274	Sep 25 134107	28 1/4 N 140 1/4 E	n	—	U 81 K 75	6.1 6.1	5.7	5.9		5.5		5.6 5.9 (5.4) (5.5)		Pr 6

TABLE 17 (cont.).

No.	θ GMT	φ, λ	h km	M	Station Δ	Magnitude determined from							Remarks	
						PZ'	PZ	PH	PPZ'	PPZ	PPH	SH	LH	
1953														
275	Sep 26 010230	51 1/4 N 156 3/4 E	60	6.2	U 65 K 57	5.5 5.6	5.5	5.8				5.3 5.4	5.8 5.8	H 6-6 1/4, Pr 6-6 1/4
276	Sep 27 060527	14 N 58 W	n	—	U 70 K 73	5.8 6.3						5.4	5.5 5.6	Pr 6
277	Sep 29 013645	36 1/2 S 177 E	300	7.2	U 153 K 146				7.2		6.5		(6.8)	B 7, Pa 7 1/4
278	Sep 30 045421	4.0 S 102 1/4 E	(n)	—	U 91 K 91	5.9			5.6 6.2			6.2	5.4	
279	Sep 30 230408	22 N 107 1/2 W	n	6.7	U 88 K 83	6.1 6.2	6.5	6.8				6.4 6.4	6.4 6.4	B 6.5, Pa 6 3/4-7, Pr 6 3/4, T 6.5
280	Oct 5 043140	53 1/2 N 160 1/2 E	(n)	—	U 63 K 55	7.0 6.7	6.5	6.7				6.4 5.8	6.0 5.8	B 6 1/2, H 6 1/4-6 1/2, Pa 6 3/4-7, Pr 6, Sk 6-6 1/4
281	Oct 6 213816	3 1/2 S 151 E	n	6.9	U 113 K 108				6.5				6.5 6.5	H 6 3/4, Pa 6 3/4-7, Pr 6 3/4-7, R 6 1/2, Sk 6 3/4-7
282	Oct 11 130834	50 N 155 1/2 E	n	6.9	U 65 K 58	5.6 5.6						6.7 6.4	Pa 6 3/4, Pr 7, R 6 3/4-7, Sk 6 3/4-7	
283	Oct 11 170800	31 1/2 N 83 E	n	6.5	U 51 K 50	6.3 6.2						6.3 6.3	6.3 6.3	H 6-6 1/4, Pr 6 3/4, R 6 1/2, St 6 1/2
284	Oct 13 085345	30 N 113 1/2 W	n	6.1	U 82 K 78	5.4						5.7	5.8 6.0	Pa 6-6 1/4, T 6
285	Oct 14	43 N	110	6.8	U 69	7.4		6.8				6.6		B 6 3/4, Pa 6 3/4

No.	θ GMT	φ, λ	h km	M	Station Δ	Magnitude determined from								Remarks	
						PZ'	PZ	PH	PPZ'	PPZ	PPH	SH	LH		
		1953													
286	Oct 16 214440	38 1/4 N 20 3/4 E	n	—	U 22 K 30	5.6						4.8		(5.0)	A 5 1/2, Pr 4 3/4-5
287	Oct 17 210722	52 N 159 E	(n)	6.4	U 64 K 57	7.0 6.9	6.4	6.7				6.4	6.1 6.0		H 6 1/4, Pr 6 1/4-6 1/2, Sk 6 1/4-6 1/2
288	Oct 21 183951	38.3 N 20.8 E	n	6.4	U 22 K 30	6.6 6.3		6.6				5.8 5.7	(5.8) (6.4)		H 6-6 1/4, Pa 6 1/2, A 5 3/4-6, Pr 6 1/2, Sk 6-6 1/4
289	Oct 24 231940	35 1/2 S 179 1/2 W	n	6.2	U 153 K 145								5.9 5.7		B 6 1/4, R 6.2
290	Oct 27 034045	43 N 145 E	(n)	6.2	U 69 K 62	6.5 6.4							5.6 5.5		Pr 6, R 6.3
291	Nov 4 034904	12 1/2 S 166 1/2 E	n	—	U 126 K 121					6.4	6.6				B 7, H 7 3/4, D 7 3/4, Pa 7.3, Pr 7 3/4, R 7 3/4, Sk 8, St 7 1/2, W 6 1/2
292	Nov 4 122741	12 1/4 S 166 1/4 E	n	6.6	U 126 K 121					5.7			6.3 6.4		B 6 3/4, Pa 6 1/2, Pr 6 3/4, R 6 1/2
293	Nov 9 172542	52 1/2 N 159 E	(n)	6.5	U 64 K 56	6.8 6.5	6.3	6.4 6.5				6.3	6.3 6.2		H 6 1/2-6 3/4, Pa 6 1/2, Pr 6 1/2, R 6 1/2, Sk 6 1/4-6 1/2
294	Nov 10 234020	50 1/2 N 157 E	n	7.0	U 65 K 58	6.3 6.2						6.4 6.3	6.9 6.7		B 6 1/2-6 3/4, D 7, H 6 3/4-7, Pa 7-7 1/4, Pr 7, R 7 1/4
295	Nov 13 161705	3.5 N 96.0 E	(n)	—	U 81 K 81	6.2 6.4			6.1			5.9	5.7 5.7		

TABLE 17 (cont.).

No.	θ GMT	φ, λ	h km	M ,	Station Δ	Magnitude determined from								Remarks
						PZ'	PZ	PH	PPZ'	PPZ	PPH	SH	LH	
1953														
296	Nov 13 191537	13 S 166 E	n	6.8	U 127 K 121								6.7 6.5	H 6 3/4-7, Pa 6 3/4, Pr 6 3/4, R 6 3/4, St 6 3/4
297	Nov 14 200330	52 3/4 N 160 1/4 E	(n)	6.3	U 64 K 57	6.8 6.6		6.6	6.4			6.4	5.9 5.9	H 6 1/4, Pr 6 1/4, Sk 6 1/4-6 1/2
298	Nov 17 132950	13.3 N 92.0 W	(n)	7.2	U 88 K 86	6.8 7.0			6.7 6.8			7.2	6.7 7.1	B 7-7 1/4, H 7, Pa 7 1/4-7 1/2, Pr 7, R 7 1/4, Sk 6 3/4-7, St 7, T 7
299	Nov 25 174850	34.1 N 141.0 E	n	8.2	U 76 K 69	7.4 7.4		7.3		7.0		6.9	8.0 (7.7)	B 8 1/4-8 1/2, H 8 1/4, Pa 8 1/4, Pr 8.2, R 7.7, Sk 8-8 1/4, W 8.3
300	Nov 26 000328	34 N 141 E	(n)	7.0	U 76 K 69	6.8 6.3			6.3 6.7			6.4	6.5 6.7	B 7, H 6 1/2-6 3/4, Pa 6 3/4, Pr 7, R 7.1, W 7.4
301	Nov 26 081412	34 N 141 E	n	7.1	U 76 K 69	7.2 6.9	6.4		6.6 6.9	6.4		6.5 6.7	(6.6) 7.0	B 7, H 7 1/4-7 1/2, Pa 6 3/4-7, Pr 7 1/4, R 7.2, St 7, W 7
302	Nov 28 201731	37 3/4 N 20 1/4 E	n	—	U 22 K 30	5.6 5.4						4.7	(5.1)	A 5 1/2-5 3/4
303	Dec 2 042451	2 3/4 S 141 1/2 E	n	6.7	U 109 K 104							6.5 6.9	6.3 6.6	B 6 3/4, Pa 6 3/4, Pr 6 1/2, R 6 1/2, W 6.8
304	Dec 3 145403	31 N 85 1/2 E	n	6.5	U 53 K 52	6.5 6.4						5.7	(6.1) (6.3)	H 6 1/4-6 1/2, Pr 6 3/4, R 6 1/2, St 6 1/4

TABLE 17 (cont.).

No.	θ GMT	φ, λ	h km	M	Station Δ	Magnitude determined from							Remarks	
						PZ'	PZ	PH	PPZ'	PPZ	PPH	SH	LH	
1953														
305	Dec 4 145446	49 1/2 N 129 W	n	6.5	U 68 K 61	5.8 5.8						6.1 6.5	5.8 6.1	B 6, H 6 1/4-6 1/2, Pa 6 1/2, Pr 6 1/2, R 6 1/2, St 6 1/4-6 1/2, T 6 1/2
306	Dec 7 020537	22 S 68 1/2 W	100	7.1	U 107 K 110				6.6 6.8			7.2 7.3	6.4 6.5	B 7, Pa 7 1/4, Pr 6 3/4, R 7, T 7 1/4
307	Dec 12 173123	3.7 S 80.7 W	n	7.5	U 97 K 98	6.6 6.7	6.9	7.4	6.8 6.5	6.8 6.9	6.6	7.2 7.4	7.4 7.4	B 7.4, H 7 1/4, Pa 7 3/4, Pr 7.6, R 7 1/4-7 1/2, St 7 1/4, T 7 1/4
308	Dec 20 212014	34 1/2 N 140 1/2 E	(n)	6.4	U 75 K 68	6.4 6.3			6.5				5.9 6.1	H 6 1/4-6 1/2, Pr 6 1/4, R 6 1/2, St 6 1/4
309	Dec 25 015129	53.0 N 159 3/4 E	n	7.0	U 64 K 56	7.3 7.0	6.7	7.0				6.8 6.5	6.7 6.9	H 7, Pa 6 3/4, Pr 7.2, R 7, St 7



ON FREQUENCY DISTRIBUTION OF SEISMIC MAGNITUDE

by Toshi ASADA, Ziro SUZUKI and Yoshibumi TOMODA.

§ 1. In Japan and her neighbourhood, we have several hundreds of shallow earthquakes every month whose magnitude are bigger than 4. Several hundreds of « conspicuous » earthquakes with the magnitude of 6.5 are also registered during the period of every ten years. The number of these earthquakes are sufficient as materials for the statistical research of the occurrence of shallow earthquakes. The frequency distribution of magnitude is one of the important problems in statistical seismology. (Asada, 1953, 1954 a; Asada and Den, 1954.) If we know little about this distribution, it will be difficult for us to make detailed studies of space and time distribution of earthquakes. (Asada, 1954 b; Utsu, 1953.)

§ 2. Gutenberg and Richter (1949) have studied the magnitude frequency distribution of the earthquakes ($M > 6$) occurring during the period of 1904 and 1946. Kawasumi (1952 a) and Tsuboi (1951, 1952) have determined the magnitude of earthquakes occurring in and near Japan, and obtained the frequency distribution of their magnitude. Kawasumi has defined M_k as the logarithm of maximum acceleration, and Tsuboi has determined the magnitude of an earthquake according to its maximum displacement. Their formulas representing the magnitude frequency distribution are as follows;

Gutenberg and Richter,

$$\begin{aligned} \log N &= a + b(8 - M), \\ b &= 0.90, \text{ shallow earthquakes, } M > 6, \\ b &= 0.88, \text{ } 6 > M > 4 \text{ (South Calif.)} \end{aligned} \quad (1)$$

Kawasumi,

$$N(M_k) dM_k = \text{const } 10^{-0.5M_k} dM_k \quad (2)$$

Tsuboi,

$$\begin{aligned} \log N &= a + b(8 - M) \\ b &= 1.01 \end{aligned} \quad (3)$$

§ 3. Generally it is impossible to determine the magnitude of minor shocks with smaller magnitude than 4, because they are seldom registered simultaneously at several seismological stations. In order to study the magnitude frequency distribution of minor earthquakes having magnitudes of zero or less, what are available are only the seismograms recorded at a certain station.

It is possible to obtain the frequency distribution of maximum trace amplitude, A, recorded by a displacement-seismograph at a

certain station, and the frequency distribution of A_0 (amplitude at hypocenter) can be obtained from this trace-amplitude frequency distribution. The distribution of « A » may be directly regarded as the distribution of A_0 itself under a few assumptions (Matuzawa, 1941; Suzuki, 1954). According to our studies, the following distribution holds good in case of shocks whose magnitudes are between 4 and —1;

$$N(A) dA = \text{const } A^{-1.8} dA \quad (4)$$

§ 4. In the above mentioned formulas representing the frequency distribution curve of M , the value of $N(M)$ becomes infinite, when the value of M becomes infinitely small. This is, of course, physically irrational. However, it might be permitted, in practical viewpoint, to express the empirical frequency distribution of magnitudes by those formulas, although their applicability is somewhat limited.

As already mentioned in a previous paper (Asada, Suzuki and Tomoda, 1951; Asada, 1954 b), the relation between M , M_k and A_0 are known, we can study the relation between the formulas, (1), (2) and (3), through the transformation of the variables.

As M is defined as, $M = \text{const.} + \log A_0$, we can compare the formula, $N(A_0) dA_0 = \text{const. } A_0^{-1.8} dA_0$, (a) with the result obtained by Gutenberg and Richter. Transforming A_0 in formula (a) into M , we have,

$$N(M) dM = \text{const } 10^{-0.8M} dM \quad (b)$$

As the relation between M and M_k is expressed by the formula,

$$M_k = \text{const.} + 2M,$$

we can transform the variable M_k in formula (2) into M , and we get,

$$N(M) dM = \text{const } 10^{-1.0M} dM. \quad (c)$$

Comparing the formulas (1), (b) and (c) with each other, we can reasonably say that they agree with each other within the range of statistical fluctuations. This result leads to the conclusion that a similar magnitude frequency curve can be applied both to earthquakes with magnitude bigger than 6 and to minor earthquakes as aftershocks, the minimum of which is less than zero in its magnitude. In other words, a similar statistical law holds good both in the occurrence of major earthquakes and of minor earthquakes.

The minimum of earthquakes which have been observed by us is —1 in its magnitude and 10^{10} ergs in its energy (Asada, Suzuki, 1951).

§ 5. As already mentioned in previous papers the energy

frequency distribution of earthquakes occurring in a certain area during a certain period, and whose magnitudes are within a certain range, can be expressed by the formula,

$$N(E) dE = K E^{-m} dE. \quad (5)$$

And the value of the coefficient « m » was the same in every case. Is the value of the constant K the same in all cases? It is doubtful that the frequency of all earthquakes whose energy are from 10^{10} ergs to 10^{26} ergs can be expressed by one frequency curve as given by the formula (5). According to the recent study of shallow earthquakes occurring in Kanto District in Japan (Asada, T., 1954), it is shown that the applicability of the formula (5) is restricted within certain limits concerning the area of the « seismic zone » and the range of the magnitude. Concretely speaking, the formula (5) may be applied to the earthquakes with the M from 6 to 4, if the statistics are made on the shocks occurring in a seismic zone with the dimensions of approximately $50 \times 50 \text{ km}^2$.

§ 6. We can study the partition of the energy released in seismic waves by calculating the values of $(N \times E)$, as Gutenberg and Richter did. Their result is,

$$\log N(M) E = k + 0.9 M \quad (6)$$

Now, we adopt E as the variable, and transforming M into E (Asada, T., Suzuki, Z., & Tomoda, Y., 1951) in the formula (6), we get,

$$N(E) \times E dE = \text{const } E^{-0.5} dE \quad (7)$$

It appears that, in the formula (6), $(N E)$ becomes bigger with the increase in M , and on the contrary, in the formula (7), $(N E)$ decreases with increasing E .

In case the variable is A_0 , we have,

$$N(A_0) \cdot E dA_0 = \text{const } dA_0 \quad (8)$$

This means that the energy, $(N E)$, is equally partitioned among A_0 (Matuzawa, T., 1953; Kawasumi, H., 1952 b). The apparent difference between the three formulas is, of course, wholly dependent on the nature of variables.

§ 7. If one wants to estimate the total energy released in seismic waves in a certain area during a certain period, he may get the value through estimating the energy of the maximum earthquake which has occurred there during that period; it is roughly equal to the total energy.

If the approximation is too rough, he may estimate the energy of the second biggest earthquake and sum up the value of energy

of the biggest and the second biggest earthquake. Thus he will get the value of the total energy with better approximation.

REFERENCE CITED.

- ASADA (T.). 1953 : On the Relation between the Predominant Period and the Maximum Amplitude of Earthquake-Motions. Zisin, Ser. II, 6, p. 69.
— 1954 a : The Frequency Distribution of the Magnitude of minor Earthquakes. Zisin, Ser. II, 8, p. 30.
— 1954 b : The Magnitude defined as the Logarithm of the maximum Acceleration. Zisin, Ser. II, 8, p. 45.
ASADA (T.), DEN (N.). 1954 : On the Frequency Distribution of the P-S Intervals of the Earthquakes Recorded at a Certain Station. Zisin, Ser. II, 8, p. 37.
ASADA (T.), SUZUKI (Z.), TOMODA (Y.). 1951 : Notes on the Energy and Frequency of Earthquakes. B. E. R. I., 29, p. 289.
ASADA (T.), SUZUKI (Z.). 1951 : On Micro-earthquakes observed after the Imaichi Earthquake, Dec. 26, 1949. B. E. R. I., 28, p. 415.
UTSU (T.). 1953 : On Energy and Frequency of Aftershocks. Kensin-zoho, 18, p. 66.
GUTENBERG (B.), RICHTER (C.-F.). 1949 : Seismicity of the Earth.
KAWASUMI (H.). 1952 a : On the Energy Law of Occurrence of Japanese Earthquakes. B. E. R. I., 30, p. 319.
— b : Energy Law of Earthquake occurrence in Vicinity of Tokyo. B. E. R. I., 30, p. 325.
TSUBOI (C.). 1951 : Determination of the Richter-Gutenberg's Instrumental Magnitudes of Earthquakes occurring in and near Japan. Geophys. Notes, 4 No. 5.
— 1952 : Magnitude-Frequency Relation for Earthquakes in and near Japan. Journ. of Phys. Earth., 1, p. 47.
MATUZAWA (T.). 1941 : Über die empirische Formel von Ishimoto und Iida zwischen der Bebenhäufigkeit n und der Amplitude a . B. E. R. I., 19, s. 411.
SUZUKI (Z.). 1954 : A statistical study on the Occurrence of small Earthquakes (I). Sci. Rep. Tohoku Univ. Ser. 5, vol. 5, No 3, p. 177.
-

INTENSITY AND MAGNITUDE OF SHALLOW EARTHQUAKES

by Hirosi KAWASUMI.

It is well-known that the intensity of an earthquake is the degree of the human feeling due to the stimulus of an earthquake motion at a point, while the magnitude of an earthquake is the measure of the whole energy transmitted by seismic waves. Historically these definitions were not necessarily accepted by all from the beginning. As early as 1783, D. Pignataro first made an intensity scale of an earthquake and used the earthquake force as the measure of earthquake intensity. But Mallet identified the maximum velocity of an earthquake motion with the seismic intensity, while Milne assented to Pignataro's view, and identified the earthquake force to the acceleration of ground motions. Testimony of this lies in the Newton's second law of dynamics. M. Ishimoto later found that the Weber-Fechner's law also holds in human feeling of seismic intensity and the maximum acceleration as observed by means of his acceleration seismographs. The law revised by the present writer with ampler materials is

$$z = 0.8 \times 10^{0.5(I-\alpha)} \quad (1)$$

where α stands for maximum acceleration in gals and I the intensity in Japanese scale [Fig. 1].

We are now in a position to use the observations of seismic intensity with our unaided senses as data for our quantitative studies. Hitherto the comparison of severities of earthquakes and determination of an epicentre have been made by the use of an intensity scale. But as far as such relative comparisons are concerned, it matters little whether we know the quantitative relation as (1) or not, but it is very important to know it for the study of the so-called foundation coefficient for the enhancement of earthquake motion at respective geological formations. This foundation coefficient to which great importance is attached by engineers may now be obtained from the anomaly of seismic intensity as determined by our unaided senses.

More valuable seismological application of (1) follows from the fact that the distribution of an earthquake intensity is in itself connected directly with the earthquake magnitude. There are no needs to say that the intensity of an earthquake depends not only

on the magnitude, but also on the epicentral distance and the depth of the hypocentre as well as on the subsoil conditions and the mechanism of the earthquake occurrence.

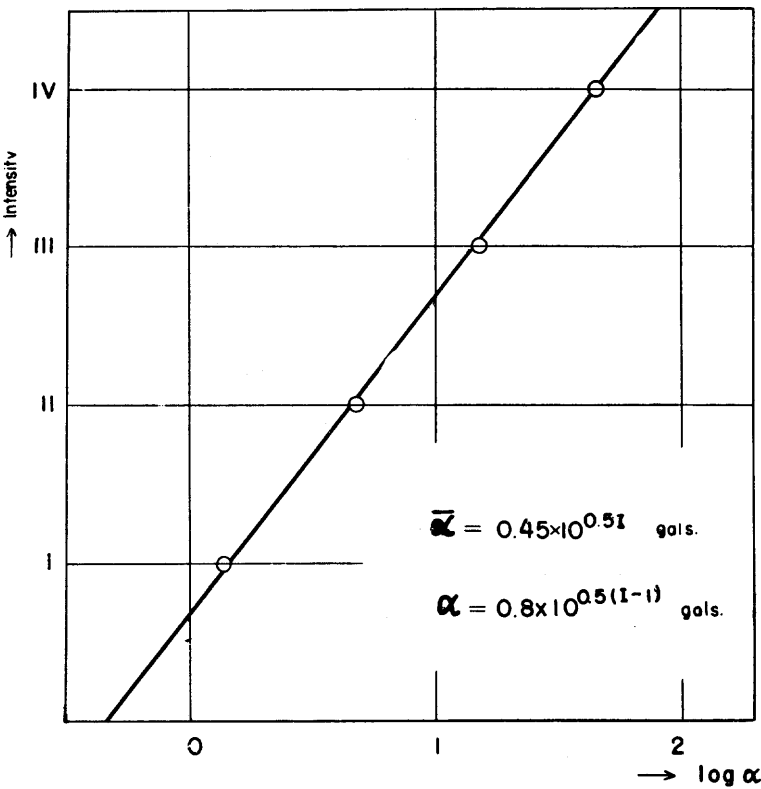


FIG. 1. — Relation between earthquake intensity and maximum acceleration.

Moreover deep focus earthquakes in Japan almost invariably display anomalous distributions of seismic intensity. Such anomalously high intensity areas are usually confined to the same districts, and this fact has been explained by crustal structures or subsoil conditions in those districts. But recently the writer found an interesting reciprocal relation between the intensity distribution and epicentral region of shallow earthquakes. The earthquakes which originated off the SE coast of Hokkaido are felt along the Pacific coast as far south as the Kwanto district more strongly than in the northern part of Hokkaido, while the earthquakes originated off the S or SE coast of the Kwanto district are more strongly felt at the SE coast of Hokkaido than in the nearer place on the Japan Sea side of the Tyûbu district [Fig. 2 and 3]. This fact may probably show the existence of some kind of channel

such as a low velocity layer between these regions and it conveys better earthquake vibrations of short period with larger accelerations. Interesting as it is, we must at present leave this out of our problem, and confine ourselves to the study of normal shallow earthquakes.

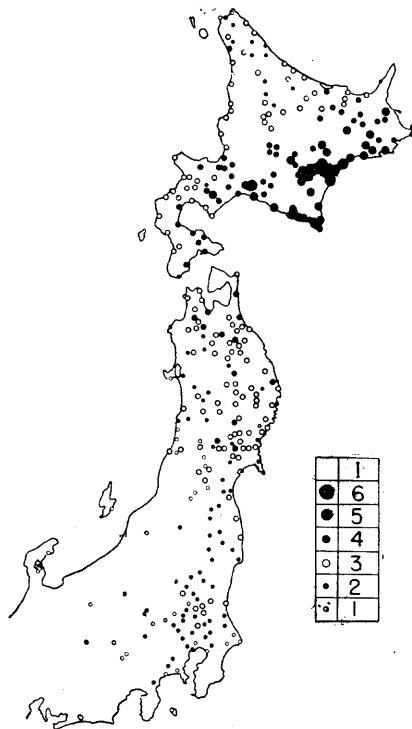


FIG. 2. — Intensity distribution of the Tokai-oki Earthquake of March 4, 1952.

If we plot the observed intensity I versus epicentral distance and take the mean of I in all azimuths, then we can nearly eliminate the effects of the mechanism of the earthquake occurrence and subsoil conditions, so that an approximate mean $I-\Delta$ curve may thus be obtained. Observing that these $I-\Delta$ curves for normal earthquakes are almost similar in shape and differ only in their ordinates by a constant amount depending on the magnitudes of these earthquakes, the writer read off the inclinations of these curves of 95 earthquakes at every 50 km of epicentral distance and calculated their means for respective distance. The $\frac{dI}{d\Delta}$ curve thus obtained from the mean inclinations was integrated to obtain a mean $I-\Delta$ curve for normal earthquakes.

nations was integrated to obtain a mean I- Δ curve for normal earthquakes.

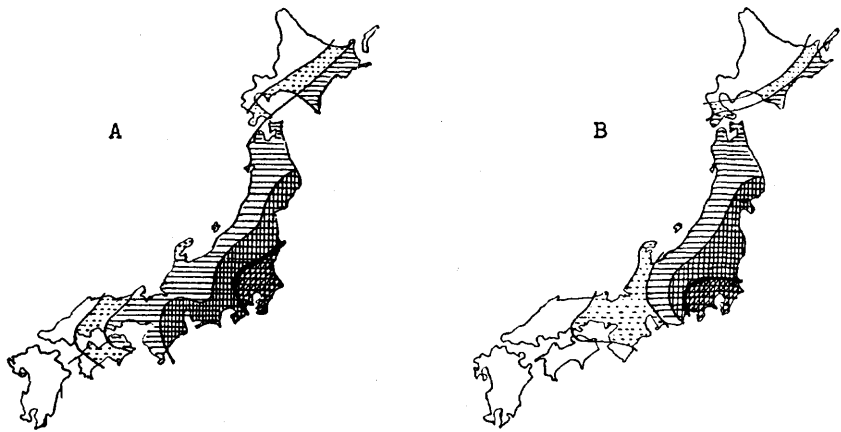


FIG. 3. — Intensity distribution of the earthquakes originated in the south and east parts of the Kwanto district.

A : Earthquake of Jan. 21, 1906.

B : Earthquake of Feb. 24, 1906.

Mean station anomalies from this mean I- Δ curve were then calculated and this correction was applied to each observation to eliminate the effect of subsoil conditions. The above process was once more repeated using these corrected values of I, and I- Δ curve of the second approximation was thus obtained. This empirical formula was then compared with 120 earthquakes with ampler observations which took place in 20 years from 1924 to 1943, and the mean deviations of the observed intensities of all the earthquakes from the above curve in every 100 km of epicentral distance were calculated. Subtracting these mean deviations from the values of I for corresponding mean distances, the I- Δ curve for the third approximation was determined, with the result

$$e^I = \left(\frac{100}{\Delta} \right)^* e^{M_k - 0.00166 (\Delta - 100)} \quad (2)$$

where Δ is the epicentral distance in km, while I and M_k are the intensities in Japanese scale. This M_k which is the intensity at $\Delta = 100$ km may be deemed as an index of the earthquake magnitude.

Similar analysis was applied to the logarithms of maximum amplitudes, and empirical formulae for the third approximation thus obtained were

$$\left. \begin{aligned} A &= \left(\frac{100}{\Delta} \right)^{\frac{1}{2}} e^{m-0.00307(\Delta-100)} \quad \text{for } 100 \text{ km} \leq \Delta \leq 750 \text{ km} \\ A &= \left(\frac{100}{\Delta} \right)^{\frac{1}{2}} e^{m-0.90-0.00183(\Delta-100)} \quad \text{for } 750 \text{ km} \leq \Delta \leq 2000 \text{ km} \end{aligned} \right\} \quad (3)$$

The value of $\log A$ as given by these formulae does not differ from the previous curve of the second approximation more than 0.02, which is almost negligible from practical point of view. It is also to be remarked that the curve (3) is nearly equal to that for the strong motion instruments used in Pasadena as given by Gutenberg and Richter (See curves E and B in Fig. 4). This may be nothing

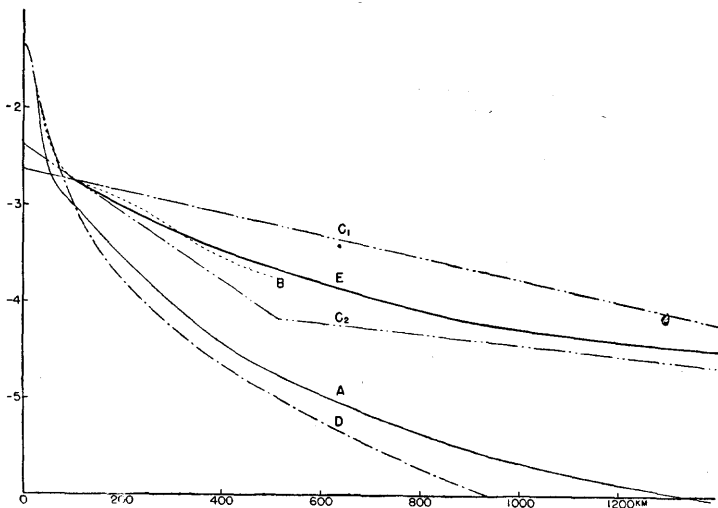


FIG. 4. — Comparison of the amplitude factors $f(\Delta)$ after various investigations. (The amplitude at the distance 1 km from the hypocentre is assumed to be unity.) A : from equation (2); E : from (3); B : Pasadena (strong motion seismograph); D : Pasadena (Wood-Anderson seismograph); C : Tsuboi.

but the $A-\Delta$ curve for true amplitude of ground does not much differ in Japanese and American earthquakes.

Now these empirical formulae were applied for the determination of M , and A_{100} of conspicuous earthquakes in Japan during the

20 year period above mentioned. Plotting the $\log A_{100}$ versus M_k of the same earthquake (*Fig. 5*), we find a very good linear rela-

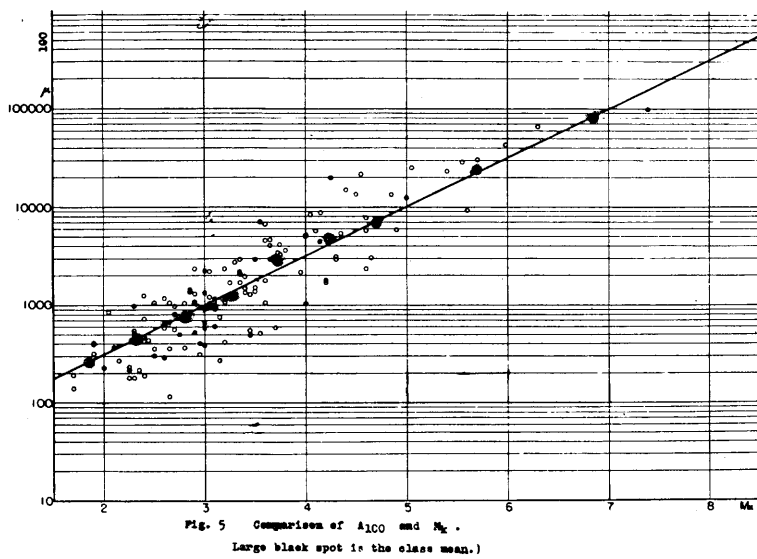


FIG. 5. — Comparison of A_{100} and M_k . (Large black spot is the class mean.)

tion which is represented by

$$\log A_{100} = 1.5 + 0.5 M_k \quad (4)$$

In the « Seismicity of the Earth and Assosiated Phenomena » Gutenberg and Richter list the magnitude of world earthquakes. 92 Japanese earthquakes in this list were also analysed by the writer, and the M_k as determined from I or A or both with the aid of (4) are compared in *Fig. 6*. The straight line in the figure represents

$$M = 4.85 + 0.5 M_k \quad (5)$$

The large deviation of the spot on *Fig. 6* from the straight line (5) may partly be explained by the variance of the observed amplitude due to the mechanism of earthquake occurrence and other causes.

In fact our statistics show that the mean error of single observation is ± 0.43 in $\log A$ and ± 0.56 in I. These large errors remind us of the importance of using many observations in different azimuths for the determination of earthquake magnitude. The

above variance include also the effect of subsoil conditions.

We, therefore, took statistics of station anomalies of I and $\log A$

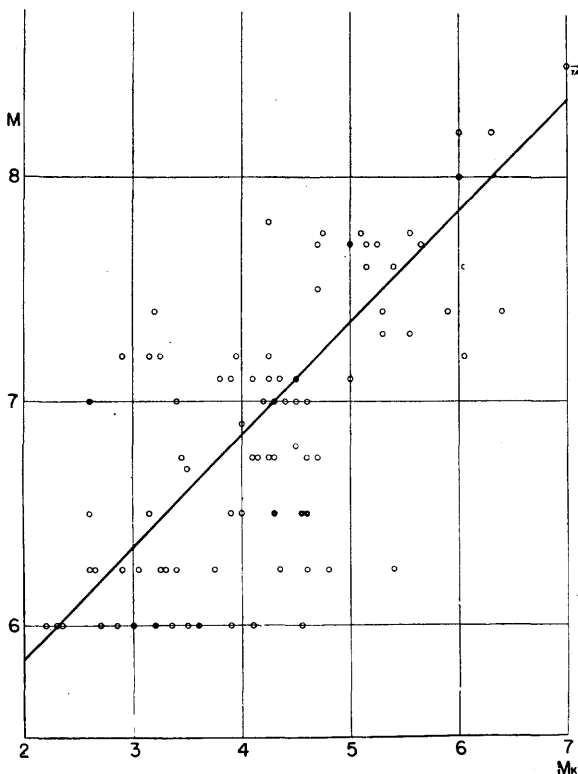
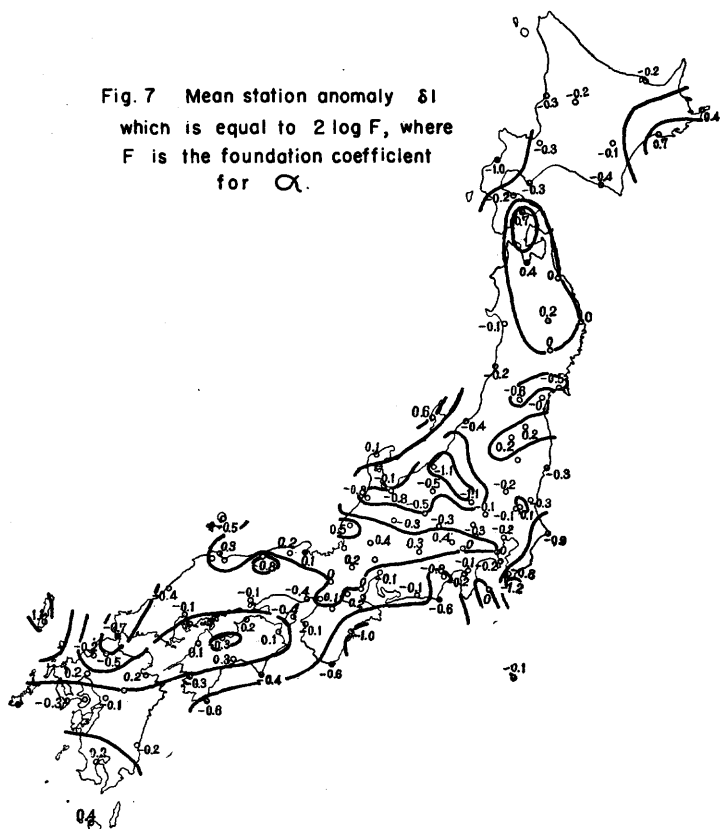


FIG. 6. — Comparison of the Pasadena Magnitude M and M_k .

from the data of 226 and 150 earthquakes respectively. The mean station anomalies are plotted on geographical maps (*Fig. 7 and 8*). Theoretically speaking, we have no reason to believe the existence of a systematic geographic distribution of foundation coefficients, but we perceive some systematic tendencies that negative station anomalies in $\log A$ (and less clearly in I) cluster along the coastal zones and some special regions. Verification and interpretation of this fact will be made in future with more materials.

The theories of elastic waves over homogeneous semi-infinite body as worked out by H. Nakano and others suggest that the amplitudes of bodily and surface waves diminish with inverse squares and square roots of the epicentral distances respectively as in the formulae (2) and (3). But as the actual structure of the earth's crust is far from the assumption made in the theory, the writer does not claim that the extinction coefficients in (2) and (3)

represent the absorption of the wave energy in the crustal layers. Theoretically, absorption coefficient must increase with the fre-



quency of earthquake waves. R. Yoshiyama suggested this possibility, but as far as the data treated in the present paper are concerned, we cannot testify the fact in the variations of $I-\Delta$ and $A-\Delta$ curves. The mean residues from the $I-\Delta$ curve of the second approximation of the observed intensities for respective magnitude groups shown in Fig. 9 do not show the required tendencies. We must therefore examine the relation of M_k and periods of T_n of maximum motions. In Japan, where Wiechert seismographs have acquired currency, no marked difference of T_n is observed in earthquakes of different magnitudes and with epicentral distances up to 1000 km. In view of the law of equipartition of energy in spectra of earthquake waves as suggested by the analyses of strong motion

earthquake records in California and other data, the proper periods of seismograph used must play important roles on the observed

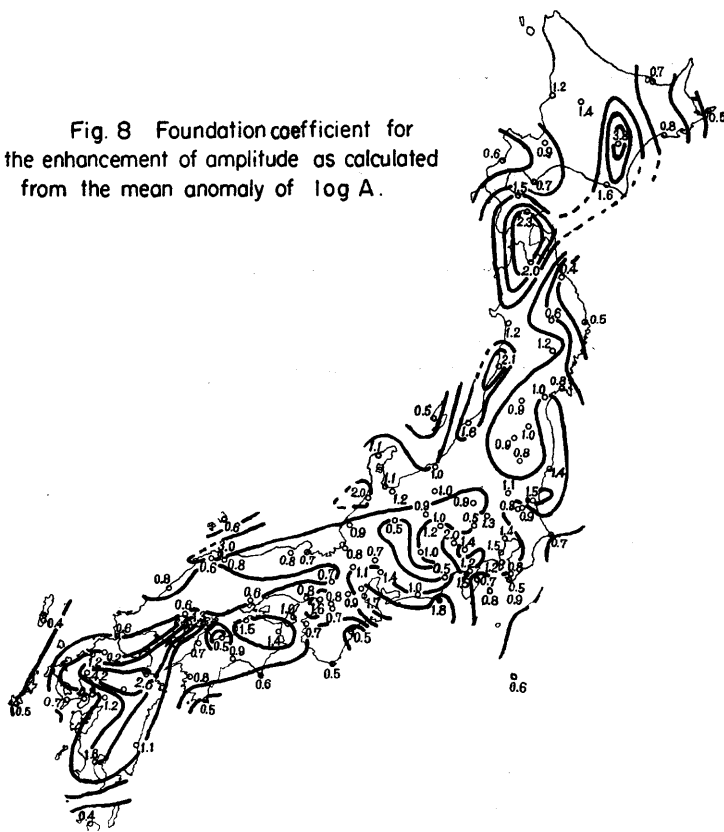


Fig. 8 Foundation coefficient for the enhancement of amplitude as calculated from the mean anomaly of $\log A$.

maximum amplitude. The writer is not certain whether the long periods as reported in larger earthquakes are observed or not by means of lower magnification instruments with longer proper periods than those of Wiechert seismographs. It is to be stated here that from 635 felt earthquakes in Tokyo in 30 years from 1911 to 1940, the relation of the maximum amplitude with its period was obtained as follows :

$$A = 0.46 \times T_m^{1.03} \quad \text{in mm and sec. (6)}$$

This does not in itself indicate the increase of period with the magnitude, but it does not contradict with the same relation. Further analysis in this respect must be made in future. Anyhow, the study in this respect at other places is to be desired.

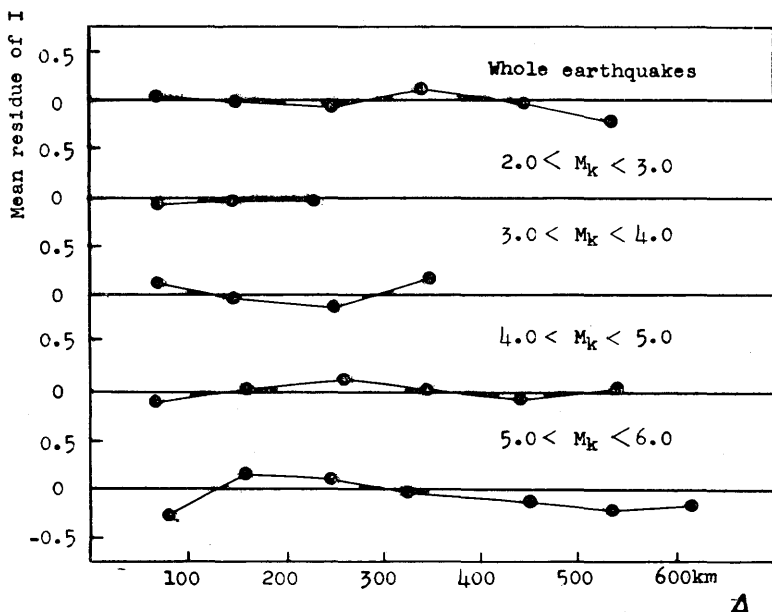


FIG. 9. — Mean residues from the I- Δ curve for respective magnitude groups.

There are many other data which show very close correlation with the earthquake magnitude of shallow earthquakes. Gutenberg and Richter have suggested the duration of principal portion of earthquake motion and the highest intensity at the epicentre. The writer examined the total durations D of an earthquake at different stations on Wiechert seismograms and found that there is no systematic variation of D with Δ , less than 2,000 km but logarithm of geometrical mean D of total durations at all the stations is seen to have a positive correlation with M_k as we see in *Fig. 10*. The average relation is

$$D = 1.3 \times 10^{0.3} M_k = 1.5 \times 10^{0.6(M-5)} \quad \text{in min} \quad (7)$$

In major earthquakes the amount of damage wrought by them show remarkable dependence on the magnitudes of these earthquakes. The *Fig. 11-14* are the correlation diagrams between the magnitude and the logarithms of the amount of damage such as the number of collapsed houses, loss of lives etc. in historical Japanese earthquakes since the 15th century. These relations are represented approximately by the following formulae.

$$N = 10^{(M_k-1)} = 0.2 \times 10^{2(M-5)} \quad (8)$$

$$n = 10^{1.25(M_k-2)} = 2.4 \times 10^{2.5(M-6)} \quad (9)$$

$$B = 10^{-5} \times N^* \quad (10)$$

$$n = 10^{-2} \times N^{1.3} \quad (11)$$

In these formulae N, n and B represent the numbers of collapsed houses, the loss of lives and burned houses respectively.

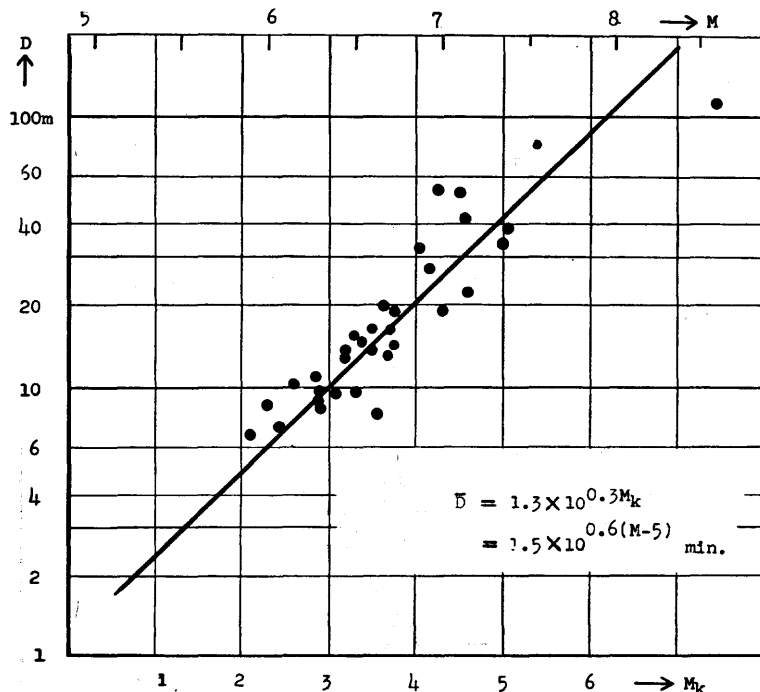


FIG. 10. — Relation between total duration and magnitude.

But we know that the amount of damage is much subjected to the density of population and the traditional manners of constructions. In a given country, where no marked change in these circumstances is expected, the formulae given above have in themselves bearing in political and economical undertakings. In Japan these formulae are now used in the enterprise of earthquake insurance. On the other hand, if similar analyses are made by the amount of damage with proper correction for the density of population in the devastated area, the parameters of these formulae will show the average strength of man-made structures provided the general subsoil conditions are equal. In view of the promotion of the earthquake proof constructions such study in various countries will be worth doing.

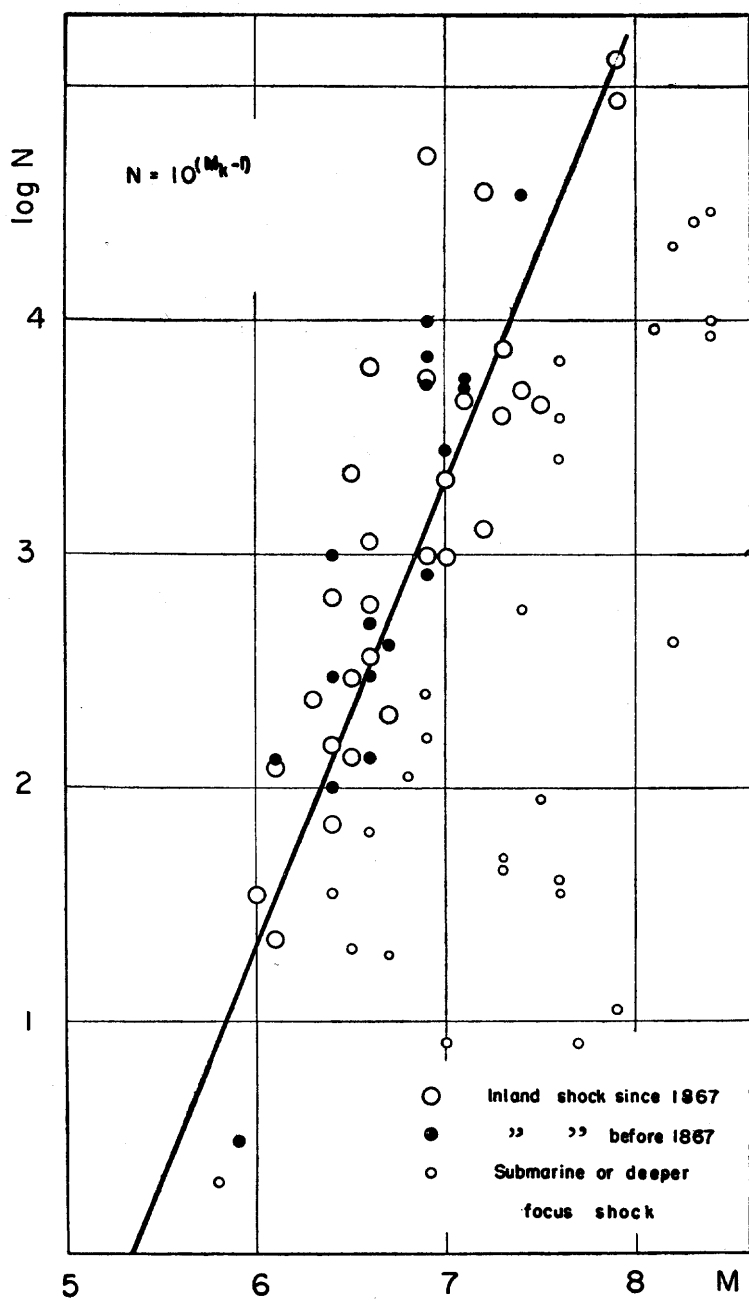


Fig. II Relation between the number of collapsed houses N and the magnitude M

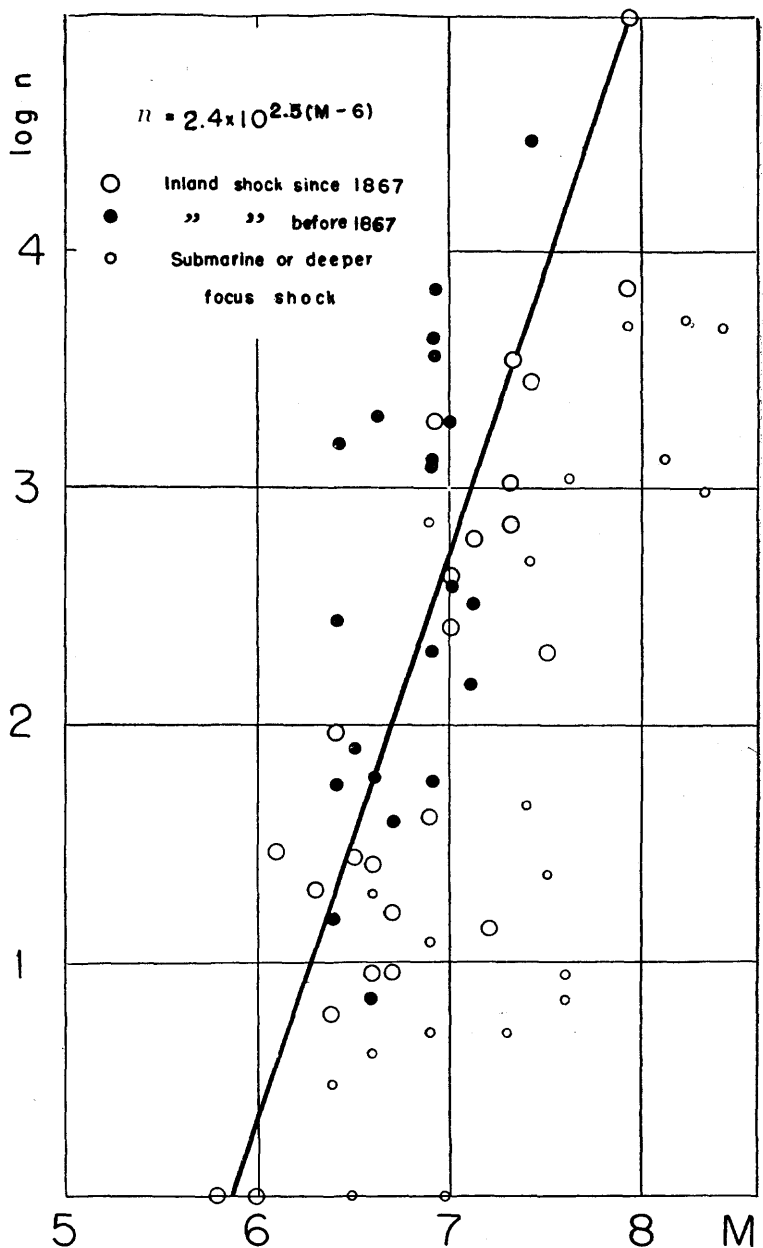


Fig. 12 Relation between the loss of lives n
and the magnitude M

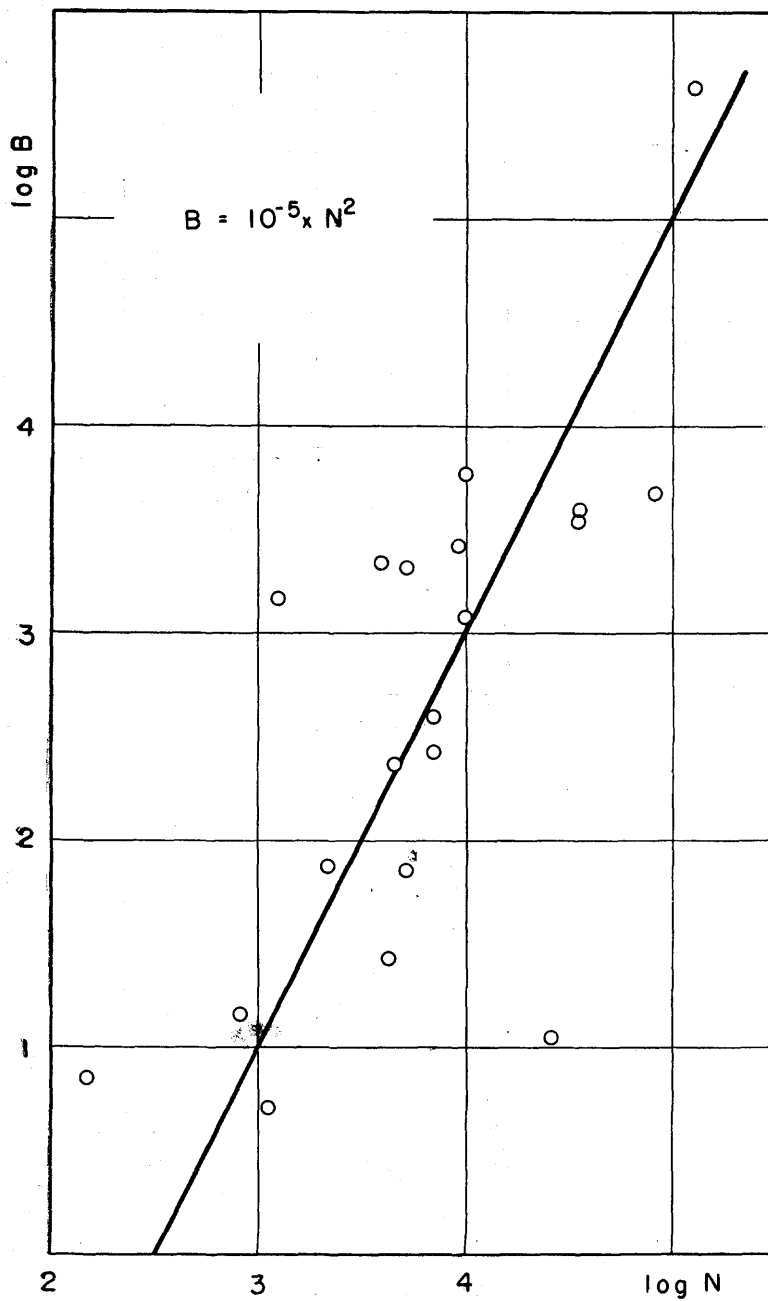


FIG. 13. — Relation between the number of burned houses B and the number of collapsed houses N .

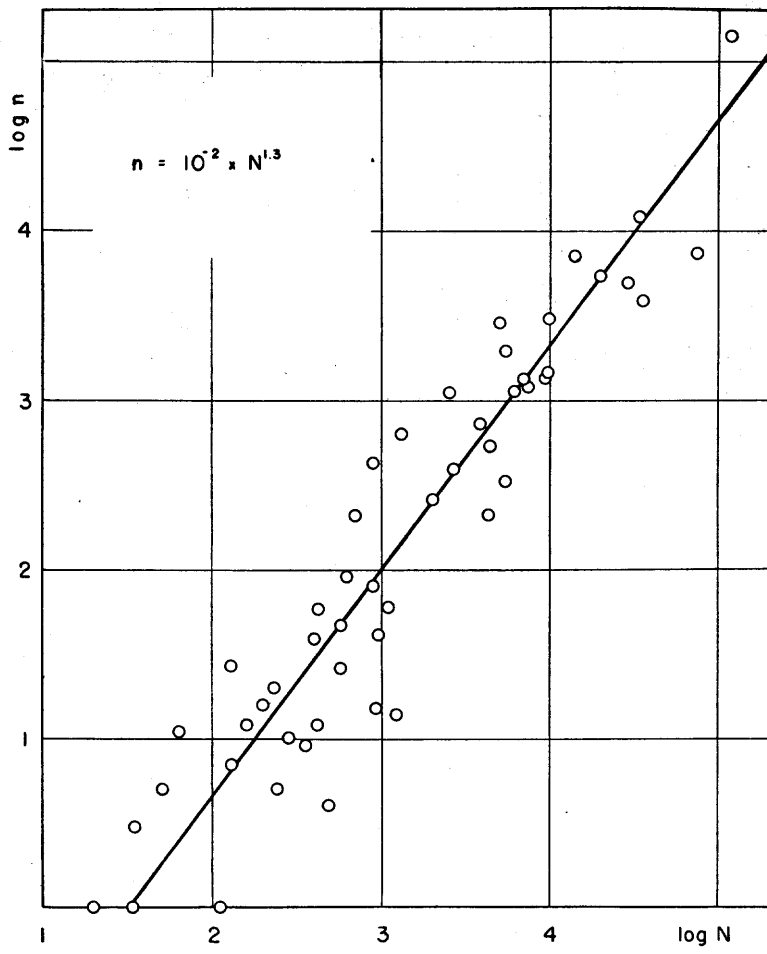


FIG. 14. — Relation between the loss of lives n and the number of collapsed houses N .

SUMMARY.

In this paper the writer determined quantitative relation between the earthquake intensity and the maximum acceleration of the motion of the ground. He applied this quantitative relation to the determination of the magnitude of shallow earthquakes.

He obtained the intensity-distance and the amplitude-distance curves for the third approximation. He derived parameters related to the magnitude in these curves, and compared them with the magnitudes as determined by Richter and Gutenberg for Japanese earthquakes.

He then endeavoured to reveal the accuracies of his curves, and examined also some effects on these curves of possible factors such as the magnitude, the period and others, but no crucial evidence to necessitate the alteration of these curves could yet be found. so far as shallow earthquakes are concerned.

He then found other factors than the intensity and the amplitude which may be applied to the determination of magnitudes of shallow earthquakes. Total durations of the earthquake motions observed with similar seismographs and amounts of various damages were revealed to be promising.

Earthquake Research Institute, Tokyo University, Japan.

THE VELOCITY OF P AND S WAVES IN THE UPPER PART OF THE EARTH'S MANTLE

by I. LEHMANN.

It has in later years been possible to record explosions and rockbursts at distances great enough for the P wave through the upper part of the Earth's mantle to be observed. The results obtained for the velocity just below the Mohorovicic discontinuity is about 8.15 km/sec, not differing too much at the various places where it has been determined. This is a higher value than usually found in earthquake work.

The P velocity as determined from the Jeffreys-Bullen tables (1940) is only 7.8 km/sec. corresponding to the slope 14.3 sec/degree of the first part of the time-curve. The finding of the higher velocity from explosions caused Jeffreys to revise his results and, on a somewhat different interpretation, his data could be brought into agreement with those obtained from explosions. Using more recent I.S.S. data he has found lately that for Europe the P time-curve is practically a straight line up to 15° (Jeffreys 1952). Its slope is close to 13.7 sec/degree which corresponds to the velocity 8.1 km/sec. below the Mohorovicic discontinuity. From 15° onwards the time-curve bends.

The J-B curve has a uniform curvature all the way up to 19°. The travel-times were indeed smoothed on a 3. order polynomial. At about 19° there is a change of slope and thereafter a stronger curvature which later decreases with distance.

The shape of this time-curve did not seem to be consistent with amplitude observations. Gutenberg a good many years ago observed that European P amplitudes were relatively very small from about 5° to 15° (Gutenberg 1926) and the same was found to be true in California (Gutenberg and Richter 1931, 1939. Gutenberg 1944, 1945). This indicates that the curvature of the time-curve should be very small for this range of distance. From about 15° epicentral distance amplitudes increased and became large at distances around 18°-19° indicating that an increase of curvature began already at about 15° in agreement with Jeffreys' latest results (1952).

It was possible to calculate the increase of velocity with depth from the J-B time-curve by the usual methods. There was found to be a steady increase of velocity with depth down to about 400 km

where an abrupt increase of velocity or velocity gradient took place. Below this so-called 20° discontinuity the velocity increased more strongly with depth than it did above.

The velocity-depth function cannot be calculated from a straight time-curve. If it were a straight line in the mathematical sense it could correspond only to a constant surface velocity. But it is straight only to the degree of accuracy with which we observe and there is quite a variety of velocity functions that will produce such a straight line. Some trials suffice to show that a velocity increasing slightly with depth will produce a straight time-curve and so will a constant velocity or a velocity decreasing with depth — provided of course the decrease is not strong enough to prevent the rays from emerging at the surface.

Gutenberg (1948) published various trial solutions for the velocity function. He is now of the opinion that not only is P small in a range of distance, but the first direct wave is missing and a later one is recorded instead. He concludes, as we know, that there is a low velocity layer producing a shadow for P. In the Kern County shocks so well recorded by the excellent net of California stations all equipped with short period Benioff seismographs it was found that beyond 4° epicentral distance P was delayed (Gutenberg 1954). The P points did not fit the line of slope 13.6 sec/degree to which the points for smaller distances had a very close fit.

A similar delay of P has not, to my knowledge, been found in

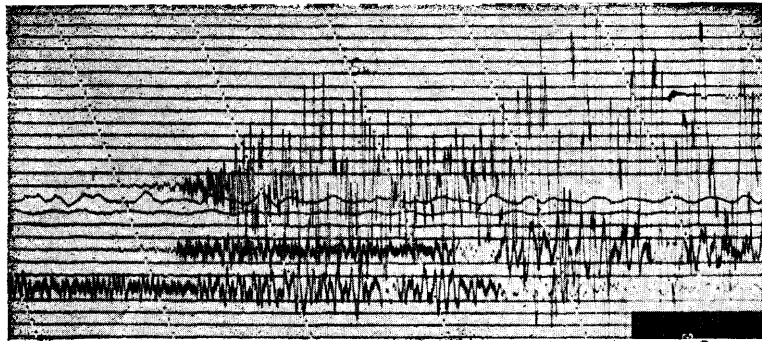


FIG. 1.

Europe. The Heligoland explosion was recorded out to a distance of 9° and the P points were all very close to a line of slope 13.6 sec/degree (Willmore, 1949). And, as mentioned, Jeffreys could fit a line of this slope to I.S.S. observations out to 15° . I have made some collective studies of European earthquakes recorded at many

stations at the distances in question. P was always found to be relatively small but quite clear and well recorded. The older European observations, however, are all from long-period instruments, the response of which is not comparable to that of the short period Benioff seismograph. Fig. 1 shows, as an example, how relatively weak the first P wave often is in California at small distances, even on the Benioff records. The strongest record is from a distance of 5°. Obviously the small beginnings shown here may be missed or not well recorded on a long-period seismograph.

However, there is at the moment nothing to show that in Europe there is at any distance a shadow for P and I shall take it that the P curve is a straight line out to 15°. As already pointed out, the velocity-depth function cannot be calculated from such a time-curve.

Amplitude observations tell us that the variation of velocity with depth is small, but many unknown factors affect the amplitudes as recorded and the actual variation of velocity with depth cannot be obtained from them. However, since P usually is observable in all except quite small earthquakes it seems as if the P velocity is likely to increase with depth. A decrease, even a slight decrease, would spread the energy carried by the rays a great deal and probably too much for clear records to be obtainable.

For a trial solution I therefore took the velocity of P below the Mohorovicic discontinuity to increase slightly — from 8.1 km/sec to 8.2 km/sec according to the Wiechert law $v = a - br^2$ — down to a depth of about 200 km. There resulted a time-curve which to the degree of accuracy with which we measure was indistinguishable from a straight line up to 15°. I could now have stripped the earth of this 200 km layer and calculated the velocity function below, but the result would have been a rather peculiar velocity variation. I preferred to let the velocity deeper down also vary according to Wiechert's law but to increase more strongly so as to produce a bending time-curve. I took the velocity gradient to change abruptly at the 200 km level. This, however, caused the time-curve to run backwards and form a loop the progressive branch of which cut the straight line time-curve at about 10°. So it was necessary to let the slow velocity increase continue to a greater depth, about 250 km. Then a nearly straight time-curve out to 21° was obtained. After various attempts I succeeded in finding a velocity function for the deeper layer which would make the progressive part of the loop intersect the first branch at about 17° and follow approximately the J-B curve from that distance up beyond 20°.

Slichter (1932) has shown that if we have at first a small velocity variation and then, deeper down, a stronger increase, a loop in the time-curve is very likely to form. So, in this case, a loop may be expected as a natural result of the strong velocity increase indicated by the bend in the time-curve. It may be objected that observations have not indicated the existence of it. This is true for its lower part, but in the example, I calculated, the branches were so close together, only about 2 sec. apart at the lowest point, that the second phases would not be distinguishable. And at the distances of the upper end second phases have occasionally been observed, but they have been explained as belonging to a first branch somewhat different from the one here considered (Lehmann 1934). They would probably fit this one as well or better. It will be objected that no focal point has been found to exist and this is true. But I found when I calculated this example that actually no focal point is formed if the increase of gradient is abrupt. The curve just turns and goes backwards without hesitation, so to speak. There is no concentration of energy at the turning point. Focal point or no focal point seems always to have been taken to distinguish between gradual or abrupt increase of velocity. But actually a gradual increase of velocity combined with an abrupt increase of velocity gradient gives no focal point.

The solution I made is just a trial solution and one out of a great many possible ones. The details of it are not of interest, but I believe this type of solution has something to be said for it.

One thing we should very much like to know is at what depth the strong velocity increase sets in, i.e. to what depth we have to shift the 20° discontinuity. Approximate limits could be found for it if the straight time-curve ended at 15° . We could let the velocity increase as strongly as possible or decrease as strongly as possible while the straight segment of the time-curve was preserved and find the depths of the deepest rays. But realizing that a loop is likely to be formed we can not use this method. Continuing the nearly straight time-curve beyond 15° we can arrive at values for the depth of the discontinuity which are quite unreasonable. So the depth just cannot be found from the time-curve and we have to look for other ways of doing it.

Gutenberg recently made use of the fact that the velocity at the depth of an earthquake focus is determined by the slope of the tangent at the inflection point of the time-curve (Gutenberg 1953). He applied the method to a great number of deep focus earthquakes and thus determined the velocity as a function of depth. There is considerable spreading of the values, and revision is obviously

needed since in calculating the depths of the earthquakes the velocities are taken to be known. Better results will be obtainable by successive approximations. The result of interest in the present context is that the velocity increase is found to set in at a depth of 200 km or slightly below. Revision is perhaps unlikely to alter this result very greatly.

Recent very interesting work done by Dr. Benioff (1954) also points to the existence of a discontinuity but at a somewhat greater depth. He finds that the earthquakes connected with the structural arcs around the Pacific ocean occur on very long and deep faults (see *fig. 2*). They intersect the surface on the steep slopes of the

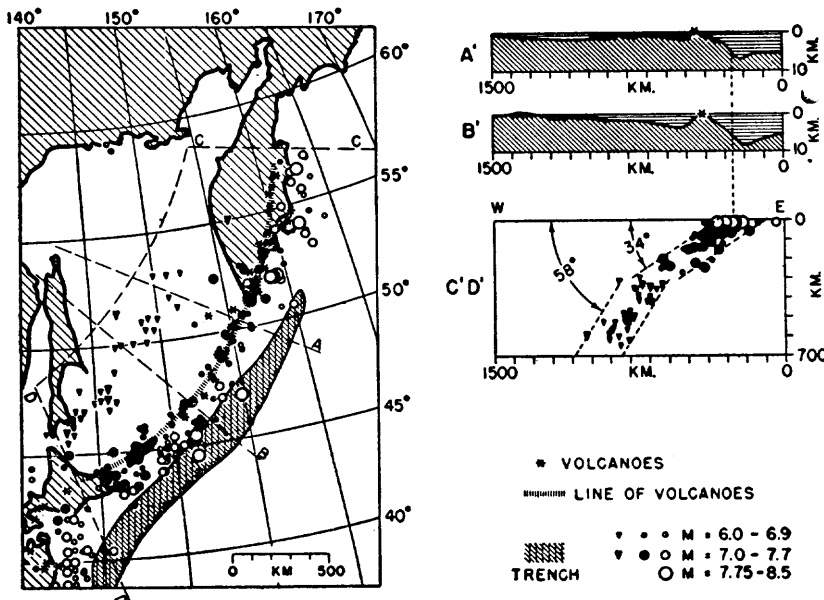


FIGURE 2.—MAP AND COMPOSITE PROFILE, KURILE-KAMCHATKA EARTHQUAKE SEQUENCES
(from BENIOFF, 1954, p. 388).

oceanic trenches where in a layer about 60 km deep the shallow earthquakes occur. The faults extend downwards to a depth of 200-300 km with an average dip of about 30°. Some of them extend to far greater depth, 600-700 km, but the deepest components of the faults have dips distinctly different from those of the intermediate components. The average dip is 60°. The elastic strain-rebound characteristics of these marginal faults indicate that the components of the structures move as separate units. The 200-300 km level thus represents a tectonic discontinuity which is apparently the lower boundary of the continents. It is absent in the ocean; the

intermediate and deep parts of the oceanic faults have one and the same dip, about 60° . It is probable that the discontinuity surface thus revealed is the one at which the wave velocity increases. The depth found for it is somewhat varying. This may be due to its not being exactly the same everywhere; but, at the moment, the results obtained are not very definite.

It is P I have been considering so far, but we have also S to consider, and it behaves differently. It is known that in Europe the so-called normal S often is absent at distances between about 5° and 15° and that instead a later phase is recorded. It may be up to 20° late. This indicates that S rays are spread and the waves delayed in the corresponding layer.

For my trial solution I, therefore, took the S velocity to decrease slightly in the *same* layer in which the P velocity increased slightly. I took it to decrease from 4.6 to 4.5 km/sec according to the Wiechert law. It is easily seen that this will cause the deepest S ray to emerge at a much greater distance than the deepest P ray. In my example it emerged at an epicentral distance of 63° . We know the P transmitted by this layer to be weak but obviously S will be relatively very much weaker, because the rays are far more widely spread. If actually the S rays are spread like this they are not very likely to be recorded except perhaps in very strong earthquakes. So a shadow may be produced even though the decrease is not so strong as to prevent the rays from reaching the surface.

Below the discontinuity at 250 km depth I took the S velocity to increase in the same ratio as the P velocity. This caused a long loop to be formed, and a very much more open loop than the P loop since the S waves were much more delayed in the layer. By a lucky chance its lowest point was 21 sec. above the first progressive branch of the curve, and this is approximately the delay of the late S phases as observed.

Now in earlier investigations I found most of the late S points from about 12° to 25° to be close to straight lines of slopes 20 to 21 sec/degree, and I suggested that they formed parts of loops in the S curve. However, this slope is too small for the lines to form part of a loop as the one now calculated, at least in its upper part. It seems as if it would be necessary to assume that the decrease in the S velocity did not continue until the base of the layer. A small increase of velocity may cause the time-curve to bend gradually, or to form a small loop before the long loop which is caused by the strong velocity increase. The later S phases beyond 20° sometimes

have very large amplitudes that may indicate the presence of a cusp.

I have here taken the S velocity to decrease in a layer in which the P velocity increased. We have

$$v_p = \sqrt{\frac{k + \frac{4}{3}\mu}{\rho}} \quad v_s = \sqrt{\frac{\mu}{\rho}} \quad \frac{v_p}{v_s} = \sqrt{\frac{k}{\mu} + \frac{4}{3}}$$

so we see that with k and μ varying always in the same ratio, the P and S velocities vary in the same ratio. But if μ does not increase in the same ratio as k , and not in the same ratio as ρ either, then we have v_s decreasing while v_p may go on increasing. Then Poisson's ratio increases. In my example it increased from .27 to .29 which latter value according to Gutenberg is retained all through the lower mantle. Thus it seems as if the whole of the increase in Poisson's ratio may take place in this thin layer close to the upper boundary of the mantle. I have on an earlier occasion spoken of the layer as being soft, but the word soft is, perhaps, not very well chosen, since μ is not likely actually to decrease and become small. Dr. Benioff suggests that we should say that the compliance of the material increases. — The relative smallness of μ affects the evaluation of the strength of the material as considered by Bullen and others.

I took the P velocity in the layer to increase on the supposition that there was no delay in P. Should there prove to be a slight delay it could be explained in the same way as the delay in S has been explained. But we know that, if there is a delay, it is smaller than that of S, and therefore the corresponding velocity decrease would be smaller.

As mentioned previously Gutenberg has found a considerable delay in the Californian P and therefore expects the rate of decrease of the velocity to exceed the critical value. He finds that in California S is also more strongly delayed than is P, so here again we have the compliance increasing in the uppermost part of the mantle.

Northeastern American S up to about 14° have been found to differ markedly from European and Californian S in that they are clearly recorded and arrive at the time at which the normal S is expected. I observed this first in a study of the Temiskaming earthquake of November 1, 1935. I then searched for other Northeastern American earthquakes strong enough to give good records of S at these distances and from 1925 onwards I found 7 I could use (Lehmann 1955). In all of these earthquakes S was clearly recorded though not very large and the travel time points fitted a straight line of slope 24.0

sec/degree corresponding to the line of slope 13.6 sec/degree on which the P points here, as in other regions, lie. This showed that in Northeastern America S was not delayed as it is in the other regions considered.

However, when S beyond 14° was considered, it turned out that the travel time points could be fitted to a J-B curve for a surface focus, but this curve did not join on to the straight line. The continuation of the line intersected the J-B curve at about 21° epicentral distance, so there was no way of joining the two except possibly by a loop. This would be produced if there were a gradual decrease of velocity downwards from the depth reached by the ray emerging at 14° and then at some greater depth an increasing velocity. But the break in the time-curve could also be explained on the superposition that at the depth reached by the ray emerging at 14° there is a sudden decrease of the S velocity followed by a rapid gradual increase. There being no break in the P curve there is no corresponding decrease of velocity and we have again at some depth a relatively small rigidity or an increase of compliance of the material. The difference observed between the North-American S on the one side and the Californian and European S on the other is very marked so although there is at present no way of determining the velocities with any degree of certainty yet the conclusion that there are regional differences in the velocity in the upper mantle is definite.

ACKNOWLEDGMENT.

The work here reported on was done during a four months stay at the California Institute of Technology as a visiting research fellow. I am greatly indebted to Dr. Beno Gutenberg, Director of the Seismological Laboratory, for bringing about my visit and for the interesting and pleasant time I had. My thanks are due also to Dr. Hugo Benioff, Dr. Hewitt Dix, Dr. C. F. Richter and all the personnel of the Laboratory.

The paper was written during a stay at the Dominion Observatory, Ottawa. I wish to express my best thanks to Dr. C. S. Beals, Dominion Astronomer, for the facilities afforded me and, likewise, to Dr. J. H. Hodgson and Dr. P. L. Willmore.

LITERATURE REFERENCES

- BENIOFF (H.) : Orogenesis and deep crustal structure. — Additional information from seismology. — Bull. Geol. Soc. Amer., vol. 65, pp. 385-400. 1954.
GUTENBERG (B.) : Untersuchungen zur Frage zu welcher Tiefe die Erde kristallin ist. — Zeitschr. Geoph., II. 1926.

- GUTENBERG (B.) : Travel times of principal P and S phases over small distances in Southern California. — Bull. Seism. Soc. Amer., vol. 34, pp. 13-32. 1944.
- GUTENBERG (B.) : Variation in physical properties within the Earth's crustal layers. — Amer. Journ. Science, vol. 243-A. Daly vol. pp. 285-312. 1945.
- GUTENBERG (B.) : On the layer of relatively low wave velocity at a depth of about 80 kilometers. — Bull. Seism. Soc. Amer., vol. 38, pp. 121-148. 1948.
- GUTENBERG (B.) : Wave velocities at depths between 50 and 600 kilometers. — Bull. Seism. Soc. Amer., vol. 43, pp. 223-232. 1953
- GUTENBERG (B.) : Low velocity layers in the Earth's mantle. — Bull. Geol. Soc. Amer., vol. 65, pp. 337-348. 1954.
- GUTENBERG (B.) and RICHTER (C. F.) : On supposed discontinuities in the mantle of the Earth. — Bull. Seism. Soc. Amer., vol. 21, pp. 216-222. 1931.
- GUTENBERG (B.) and RICHTER (C. F.) : New evidence for a change in physical conditions at depths near 100 kilometers. — Bull. Seism. Soc. Amer., vol. 29, pp. 531-537. 1939.
- JEFFREYS (H.) : The times of P up to 30° . — Monthly Not. R. Astron. Soc. Geoph. Suppl., vol. 6, pp. 348-364. 1952.
- JEFFREYS (H.) and BULLEN (K. E.) : Seismological tables. London 1940.
- LEHMANN (I.) : Transmission times for seismic waves for epicentral distances around 20° . — Geod. Institut, København. Medd. no. 5, pp. 1-45. 1934.
- LEHMANN (I.) : P and S at distances smaller than 25° . — Transact. Amer. Geoph. Union, vol. 34, pp. 477-483. 1953.
- LEHMANN (I.) : The times of P and S in Northeastern America. — Annali di Geofisica, vol. VIII, pp. 351-370. 1955.
- SLICHTER (L. B.) : The theory of the interpretation of seismic travel — time curves in horizontal structures. — Physics, vol. 3, pp. 273-295. 1932.
- WILLMORE (P. L.) : Seismic experiments on the North German explosions, 1946 to 1947, — Phil. Transact. R. Soc. London, Ser. A, no. 843, vol. 242, pp. 123-151. 1949.

ON THE STRESS-STRAIN RELATION IN A NOT PERFECTLY ELASTIC SOLID BODY

by H. MENZEL (Hamburg).

It is a well known fact, that the material of the Earth is not perfectly elastic. There are some differential equations proposed by various seismologists representing the relation between stress and strain in imperfect elastic solids. These equations have been suggested from the viewpoint of physics, but have not been deduced exactly from the general principles of physics. This deduction is meeting with great mathematical difficulties and is successful only for adiabatic and isothermal processes. In both cases the medium behaves like a perfectly elastic one, the corresponding differential equations differing only in the values of bulk modulus. The latter equations may be used as a test for each stress-strain relation, because such a relation must transform itself into the equation of adiabatic processes for very fast changing ones and into the equation of isothermal processes for very slowly changing ones.

The stress-strain relation suggested 1949 by Nakamura⁽¹⁾ fulfills these conditions. Using the distortional stress tensor and distortional strain tensor introduced by Bullen⁽²⁾ the relation of Nakamura is as follows :

$$\begin{aligned} \left(a + \frac{\partial}{\partial t} \right) P_{ij} &= 2 \left(a \zeta + \zeta' \frac{\partial}{\partial t} \right) E_{ij} \\ \left(a + \frac{\partial}{\partial t} \right) p_{kk} &= 3 \left(a k + k' \frac{\partial}{\partial t} \right) e_{kk} \end{aligned} \quad (1)$$

In this formula P_{ij} and E_{ij} means the distortional stress and the distortional strain tensor respectively, p_{kk} and e_{kk} the contraction of the ordinary stress and strain tensor respectively and a , ζ , ζ' , k and k' are constants. From (1) we find in the case of adiabatic processes :

$$P_{ij} = 2 \zeta' E_{ij} \quad (2)$$

$$p_{kk} = 3 K' e_{kk}$$

and in the case of isothermal processes :

$$P_{ij} = 2 \zeta E_{ij}$$

(1) Nakamura, S. T., Sci. Rep. Tohoku Un., V. 1, Nr. 2, 1949.

(2) Bullen, K. E., An introduction to the theory of seismology. 1. Ed. 1947, p. 31 (Cambridge).

$$p_{kk} = 3 K e_{kk} \quad (3)$$

Hence, following Jeffreys⁽³⁾ we have :

$$\mathcal{G}' = \mathcal{G} \quad , \quad k' = k + \frac{9 k^2 \alpha^2 T}{\rho c} \quad (4)$$

In equation (4) is T the temperature in Kelvin degrees, ρ the density, c the specific heat, α the coefficient of cubical expansions, \mathcal{G}' and \mathcal{G} the rigidity, k' and k the bulk modulus in adiabatic and isothermal processes respectively.

In sedimentary layers of Earth-crust the values of α , T , c and ρ may be estimated. Thus it will be found that there is only a very small difference between k and k' . Consequently the velocity of propagation of compressional waves depends only very little on the frequency.

The most significant departure from perfectly elastic behaviour is the attenuation of amplitudes of waves. The decrease of amplitudes depends of course on the period of the waves. In order to get an idea about this selective absorption we consider a periodic changing strain and calculate the energy dissipated per unit volume during one period. This energy will be found by

$$W = \Phi \left(P_{ij} d E_{ij} + \frac{1}{3} p_{kk} d e_{kk} \right) \quad (5)$$

From (1) we get

$$p_{kk} = 3 k' e_{kk} - 3 \alpha (k' - k) \int_{-\infty}^t e^{-\alpha(t-t')} e_{kk}(t') dt' \quad (6)$$

and with respect to (4)

$$P_{ij} = 2 \mathcal{G}' E_{ij} \quad (7)$$

Now we assume a periodic compression without shear. It may be expressed by

$$e_{kk} = \sin \omega t, e_{ij} = 0 \text{ for } i \neq j \quad (8)$$

From (5) and (6) follows

$$W = \pi \frac{\alpha (k' - k)}{\alpha^2 + \omega^2} \quad (9)$$

This dissipation energy has a maximum value $W_m = \frac{\pi}{2} (k' - k)$ at

$$\omega = \alpha \quad (10)$$

Now we consider the wave propagation. From (10) follows that the amplitude of compressional waves with frequencies near $\omega = \alpha$

(3) Jeffreys H., Cartesian Tensors. Cambridge, 1952, p. 81.

will decrease more than in other parts of the spectrum, *i.e.* this frequency is absorbed.

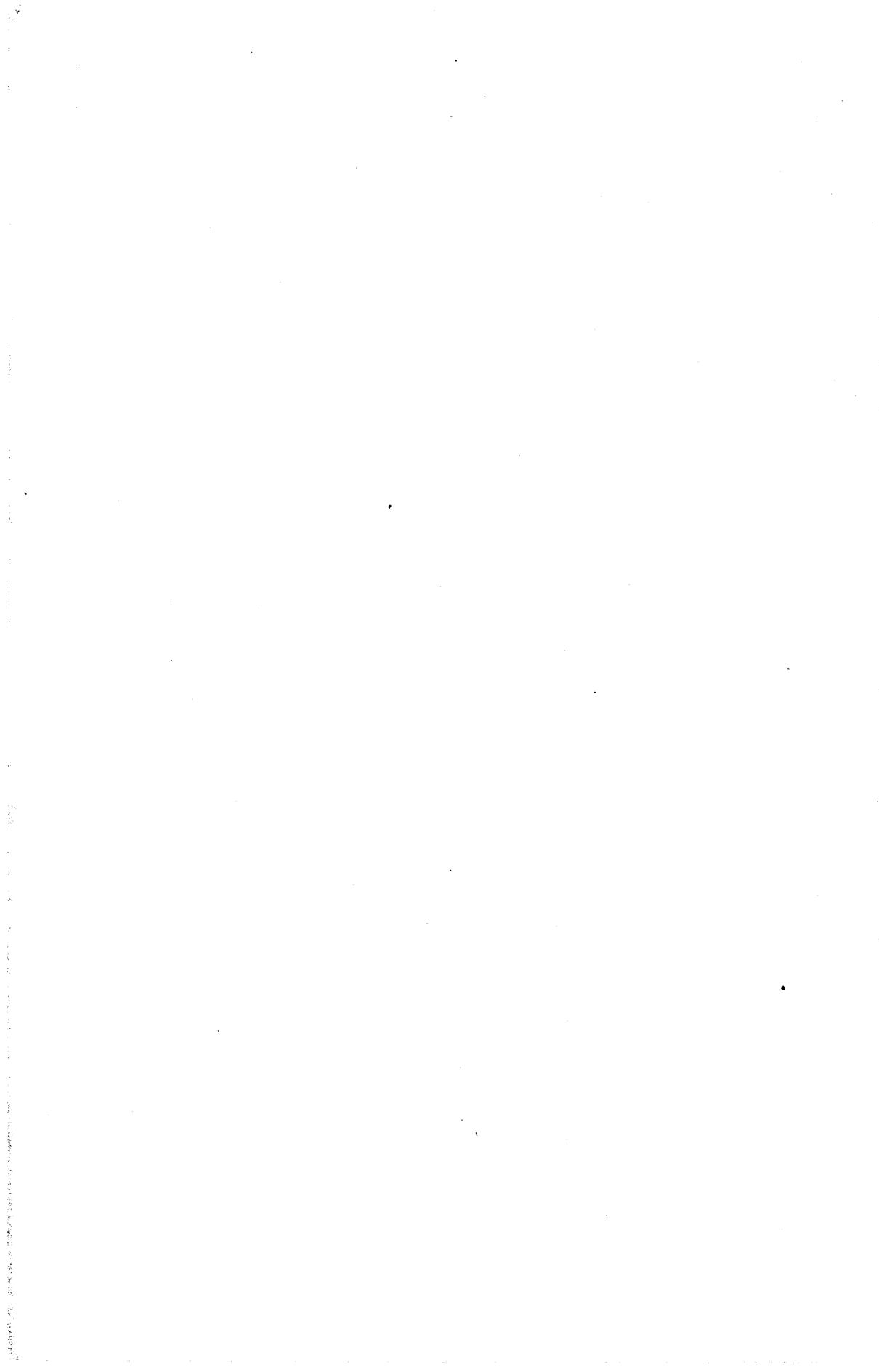
But this is only valid for compressional waves. If we deal with shear waves it is easy to derive that there is no departure from perfect elasticity. This is not in agreement with observation. According to our present knowledge there is none or only a very small departure from perfect elastic behaviour for strain changing due to hydrostatic pressures; whereas in shear experiments larger departures occur.

Therefore the stress-strain relation of Nakamura cannot be accepted. It can be generalised by adding terms on both sides of equation (1). So we may get equations of the form

$$\sum_{n=0}^N a_n \frac{d^n}{dt^n} p = \sum_{n=0}^N b_n \frac{d^n}{dt^n} e \quad (11)$$

If $N = 2$ two frequencies within the spectrum are absorbed which are separated by a frequency for which the dissipation energy has a minimum value.

At present it is impossible to estimate the values of the constants occurring in these equations, for our knowledge of absorption of seismic waves is far too poor. It is very important to establish the absorption-frequencies. If this could be done, it would be possible to find out the general form of stress-strain relation due to (11) *i.e.* the number N and we could hope to estimate the values of constants involved.



LA STRUCTURE INTERNE ET L'ÉVOLUTION DE LA TERRE A LA LUMIÈRE DES DONNÉES GÉOTECTONIQUES

par V. V. BELOUSSOV (Moscou).

Les données sur la structure, sur les mouvements et sur les déformations de l'écorce terrestre, ainsi que sur les phénomènes magmatiques dont la géotectonique dispose jettent la lumière sur la structure profonde et l'évolution du Globe entier.

Les données de la géologie permettent de considérer comme réelle la division de l'écorce terrestre en couches granitique et basaltique.

L'étude de l'histoire géologique montre que l'écorce terrestre est soumise à un ensemble très complexe de mouvements et de déformations de différents types et de différents ordres qui se superposent mutuellement. On est en droit de parler de mouvements primaires et secondaires de l'écorce terrestre. Les premiers sont des mouvements verticaux, soulèvements ou subsidences. Parmi les processus primaires se classent également les phénomènes magmatiques. Les plissements de l'écorce terrestre ainsi que les failles constituent les phénomènes secondaires. Les mouvements verticaux de l'écorce terrestre se sont manifestés partout et continuellement durant toute l'histoire géologique. On peut distinguer au moins trois différents types de mouvements : 1° les oscillations générales ou les pulsations de vastes régions de l'écorce terrestre; 2° les mouvements ondulatoires et lents de l'écorce, et 3° les mouvements qui forment les continents et les océans.

Les oscillations générales ou les pulsations de l'écorce terrestre se fixent dans l'histoire géologique d'après les transgressions ou les régressions des mers. Elles apparaissent simultanément sur d'importantes superficies et englobent tant les zones géosynclinales que les plates-formes.

On observe la superposition mutuelle de pulsations d'ordres différents. Les plus importantes définissent les « cycles tectoniques » — alternance périodique et régulière sur de vastes territoires de soulèvements et de subsidences de l'écorce terrestre avec une période de l'ordre de 150 millions d'années.

La distribution des pulsations de divers ordres à la surface du Globe n'a presque pas été étudiée. Il est cependant hors de doute que d'importantes pulsations de même direction se manifestent simultanément sur de vastes territoires permettant ainsi aux géolo-

gues de parler du « pouls général de la Terre ». Cette notion demande cependant à être limitée. C'est ainsi par exemple qu'à l'époque datant au moins de la fin du Paléozoïque on observe un écart extrêmement important dans l'évolution des pulsations de l'écorce terrestre entre les zones qui entourent l'Atlantique d'une part et les domaines adjacents au Pacifique de l'autre.

En ce qui concerne la nature des pulsations, ces dernières ne peuvent être dues qu'aux soulèvements et aux subsidences des continents ou de leurs parties importantes relativement au fond de l'Océan.

Les mouvements ondulatoires de l'écorce terrestre se manifestent par la division de la surface de la Terre en zones de soulèvements et zones de subsidence conservant longtemps leur position ou se déplaçant lentement par un mouvement ondulatoire. Ces mouvements se traduisent dans la structure de l'écorce terrestre par un développement de zones d'accumulation d'assises sédimentaires d'une part, et de zones d'érosion de l'autre. La disposition de ces zones peut changer au cours du temps.

Le contraste relatif des soulèvements et des subsidences permet de distinguer dans l'écorce terrestre des régions de mobilité différente : les géosynclinaux et les plates-formes. Les premiers sont caractérisés par une plus grande amplitude de mouvements ondulatoires, et par le rapprochement étroit des zones de soulèvement et de subsidences intenses. L'amplitude des mouvements y atteint de 12 à 15 kilomètres.

Les secondes se distinguent par l'intensité réduite de leurs mouvements ondulatoires, par de vastes régions de subsidence ou de soulèvements de faible amplitude, qui sont généralement des contours flous et arrondis. L'amplitude des mouvements n'y dépasse pas deux à trois kilomètres.

On a observé généralement l'extension des plates-formes aux dépens des géosynclinaux au cours des temps géologiques. Cependant, dès le milieu de la période tertiaire, on peut observer au Tian-Chan, en Sibérie méridionale et orientale ainsi qu'en Afrique orientale où le régime de plate-forme était déjà établi vers la fin de l'ère Paléozoïque, un renouvellement de mouvements ondulatoires très intenses. Ces plates-formes « activées », par exemple celle du Tian-Chan, se rapprochent par le régime de leurs mouvements des géosynclinaux. Il est plus probable cependant que nous avons affaire ici à quelques formes nouvelles de l'évolution de l'écorce terrestre qui suivent au point de vue historique celle de la formation des plates-formes.

Il est extrêmement intéressant de noter que les mouvements ondulatoires à faibles contrastes des plates-formes viennent s'étendre jusque dans les géosynclinaux. Ils y transparaissent pour ainsi dire à travers les mouvements à grands contrastes qui caractérisent les géosynclinaux.

On a ainsi l'impression que les mouvements calmes des plates-formes ne sont que le reflet à la surface du Globe de quelques processus qui interviennent dans les régions de la Terre plus profondes que celles où les mouvements ondulatoires des géosynclinaux ont lieu.

A ce point de vue le passage des conditions qui président à la formation des géosynclinaux à celles qui conduisent à la création des plates-formes s'explique par l'extinction des mouvements à l'« étage » supérieur et la persistance de ces mouvements dans les zones plus profondes.

A en juger d'après des données encore incomplètes, on peut observer au cours du temps des époques d'intensification des mouvements ondulatoires de l'écorce terrestre, qui sont suivis par des époques d'affaiblissement de ces mouvements sur de grandes superficies.

Les mouvements ondulatoires de l'écorce terrestre sont étroitement liés à des phénomènes magmatiques tant intrusifs qu'effusifs. Le magmatisme se manifeste principalement dans les géosynclinaux. Aux endroits (et au cours) des soulèvements de l'écorce terrestre on observe de préférence des manifestations de magma acide se traduisant surtout par des intrusions granitoïdes.

Quant aux emplacements des subsidences on y constate au cours de l'évolution de celles-ci une prédominance marquée d'un magmatisme basique représenté principalement par des effusions basaltiques.

Le problème le plus compliqué de la géologie moderne est celui des *continents* et des *océans*.

A la lumière des données récentes, il devient de plus en plus évident que les dépressions océaniques d'aspect actuel sont des formations relativement jeunes. Des forages exécutés dans les atolls du Pacifique ont prouvé que les édifices coralliens y atteignaient 1.300 mètres. Ils sont d'âges tertiaire et quaternaire. C'est ainsi qu'au cours du Coenozoïque le fond de la partie centrale de l'océan Pacifique s'est abaissé de plus d'un kilomètre sous le niveau des eaux. Les subsidences notables des bassins océaniques sont indiquées par l'aplatissement des hauteurs sous-marines usées par l'abrasion, par les terrasses abrasées sur les versants de ces hauteurs ainsi que par le pendage vers l'océan des formations mésozoïques et coenozoïques sur les shelves et les côtes.

Bien qu'on puisse douter de l'existence à une époque quelconque du continent grandiose de Gondwana, la diffusion des faunes et des flores paléozoïques et mésozoïques permet d'affirmer qu'au cours du Paléozoïque et du Mésozoïque inférieur les terres fermes avaient sur le Globe une extension plus considérable qu'à présent et que les continents étaient réunis par des chaînes insulaires et des mers de faible profondeur. Il existe des données prouvant l'existence aux temps reculés, à la place des océans actuels, de régions d'érosion élevée : au Dévonien — à l'est de l'Amérique du Sud, au Paléozoïque supérieur — à l'est et à l'ouest de l'Afrique du Sud, au Jurassique — à l'ouest des Cordillères des Andes ainsi qu'à l'ouest de l'Afrique Équatoriale, etc... A l'emplacement des océans actuels il y avait aussi certains centres de glaciation du Paléozoïque supérieur (notamment à l'ouest de la Tasmanie, à l'est de l'Afrique du Sud, au sud des îles Falkland).

De telles données laissent supposer qu'au Paléozoïque il n'y avait aucun (ou presque aucun) océan profond sur la Terre. Cette hypothèse nous oblige à poser le problème de la variation au cours des temps de la quantité d'eau sur le Globe.

Les données géologiques laissent supposer que parmi les processus des régions profondes, le rôle essentiel appartient à la différentiation de la matière en première approximation d'après la densité. L'histoire géologique montre clairement que la couche granitique s'est formée graduellement, par accumulation dans les parties supérieures de l'écorce terrestre de matériaux d'intrusions granitiques multiples. Nous sommes en droit de voir dans ce phénomène la manifestation la plus éclatante de la différentiation de la matière terrestre. Il n'y a aucune raison de nier la possibilité de ce même processus aux grandes profondeurs.

Les mouvements ondulatoires de l'écorce terrestre pourraient être directement reliés à ce phénomène de différentiation de la matière. Du soulèvement localisé des matières acides formant pour ainsi dire une grosse « goutte » devrait résulter à la surface du Globe une excroissance de l'écorce terrestre. Cette hypothèse se confirme par la correspondance, déjà notée auparavant, des manifestations de magma acide avec les soulèvements de l'écorce terrestre et du magma basique avec les subsidences de celle-ci. Ce mécanisme hypothétique des mouvements ondulatoires permet de concevoir le caractère conjugué des soulèvements et des subsidences : le mouvement ascensionnel des masses localement concentrées de matières acides plus légères doit être accompagné par l'abaissement des matières plus lourdes provoquant ainsi la com-

pensation des soulèvements de terrains par la naissance de subsidences voisines.

Les conditions qui président à la différentiation doivent varier avec la profondeur. Cela s'explique tout d'abord par l'augmentation de la viscosité de la matière en profondeur et d'autre part par la décroissance de la pesanteur à partir de la profondeur de 1.000 mètres. Ces deux facteurs doivent inhiber la différentiation aux grandes profondeurs. Il est donc probable que le noyau de la Terre n'est soumis à aucune différentiation, mais que cette dernière intervient dans toute l'enveloppe terrestre en s'affaiblissant graduellement à mesure qu'on s'approche de la base de celle-ci.

La différence entre les conditions de différentiation aux divers niveaux ainsi que la différence fort probable entre les propriétés et l'état de la matière dans les diverses couches du Globe laissent supposer une certaine autonomie des différents « étages ».

En coordonnant ces hypothèses avec ce qui a été dit plus haut sur les rapports entre les mouvements ondulatoires des géosynclinaux et des plates-formes, nous pouvons conclure à titre d'hypothèse que les uns et les autres sont dus aux progrès de la différentiation de la matière aux divers étages; les mouvements ondulatoires des géosynclinaux se rattachent à ce point de vue à une différentiation relativement active et rapide intervenant de préférence dans une couche plus proche de la surface. D'autre part les mouvements plus calmes et plus lents des plates-formes sont régis par une différentiation beaucoup plus lente qui intervient à un étage inférieur aux grandes profondeurs. Dans ce cas, le passage des conditions de formation de géosynclinaux à celles de la formation des plates-formes pourra s'expliquer par l'extinction de la différentiation à l'« étage » supérieur et sa persistance à l'« étage » inférieur. La puissance de l'étage supérieur est en tous cas d'au moins 100 kilomètres. A ce point de vue, le passage du géosynclinal à la plate-forme se présente comme un phénomène régulier tendant à établir un équilibre dans la distribution de la matière à l'intérieur du Globe.

Cependant le phénomène d'« activation » des plates-formes montre, qu'au moins dans certains cas, il peut y avoir des conditions capables de compromettre cet équilibre et de provoquer le renouvellement d'une différentiation intense en profondeur. La nature de ces conditions est inconnue. On peut supposer toutefois que le phénomène de la différentiation « multiétagée » peut provoquer dans des conditions propices des inversions de densité entre les étages amenant au toit de l'étage inférieur des matières plus

légères que celles du fond de l'étage supérieur. Un tel état de choses serait bien entendu instable et devrait tôt ou tard se terminer par une percée de la matière légère vers le haut et une poussée de la matière lourde vers le bas. Cela équivaudrait à un renouvellement de la différentiation et des courants de matière.

La différentiation de la matière du Globe est compliquée par la migration des éléments radioactifs. Ces derniers, en vertu de leurs propriétés géochimiques, se concentrent dans les lieux d'accumulation des produits acides de la différentiation. Comme les éléments radioactifs émettent de la chaleur, leur redistribution doit entraîner des différences de température. L'échauffement et le refroidissement relatifs de certaines régions du Globe peuvent avoir pour conséquence la dilatation et la compression de la matière, ce qui activerait à son tour davantage les soulèvements et les subsidences de l'écorce terrestre tout en provoquant des déviations de la compensation isostatique.

Au total, la formation de la couche granitique de l'écorce est accompagnée d'une migration des éléments radioactifs vers la périphérie de la Terre. Cette migration centrifuge des éléments radioactifs peut provoquer un certain refroidissement des régions subcorticales de la Terre.

Un autre problème complexe est celui des pulsations de l'écorce terrestre. On peut supposer que ces pulsations sont provoquées par des variations périodiques de la température à l'intérieur de certaines régions du Globe. La cause de ces variations hypothétiques de la température reste cependant inconnue.

Certaines questions inattendues sont liées à l'origine des continents et des océans. Les données des observations prouvent l'approfondissement graduel des océans et leur extension progressive aux dépens des continents.

Si cependant jadis à la place des océans il y avait des terres fermes et des mers peu profondes, il n'y a aucune raison de supposer qu'à cette époque la structure dans ces régions de l'écorce terrestre se distinguait sensiblement de sa structure sous les continents actuels. Or les recherches géophysiques récentes, y compris les sondages séismiques effectués en de nombreux points des océans, montrent que presque partout la couche granitique de l'écorce est absente dans ces régions.

Il nous reste à conclure ainsi que la formation des dépressions océaniques a été liée à la modification de la structure de l'écorce terrestre qui s'est manifestée par la destruction de la couche granitique. A l'heure actuelle il serait difficile de supposer ce qui

a provoqué ces changements. Il faut cependant noter que d'après les données récentes les océans, au cours de leur formation, ont été le champ d'une activité volcanique grandiose, leurs fonds étant parsemés d'énormes cônes volcaniques éteints et submergés. Dans l'océan Pacifique, ces cônes tant submergés qu'émergents se groupent, comme on l'a déjà noté depuis longtemps, en des chaînes linéaires s'étendant de préférence au nord-ouest, dénotant ainsi nettement la présence dans les régions abyssales d'énormes failles qui ont laissé échapper des matières magmatiques. On voit ainsi que les régions océaniques sont caractérisées par une fragmentation extrême de l'écorce terrestre.

Nous sommes donc là en présence d'un processus encore inexpliqué.

Quant aux origines de l'eau venue remplir les dépressions océaniques formées à la surface de la Terre, on admet de plus en plus souvent qu'au cours des périodes géologiques la quantité de l'eau sur la Terre a dû augmenter aux dépens de la vapeur d'eau qui se dégage du magma. Si la structure stratifiée du Globe et sa division en géosphères est une conséquence de la différentiation de la matière terrestre, on se demande pourquoi il faudrait en exclure les couches aqueuse et gazeuse qui sont, elles aussi, des géosphères? De même que les autres géosphères (solides), l'hydroosphère et l'atmosphère devraient se constituer lentement et graduellement au cours de la différentiation de la matière terrestre tout en accroissant leur volume.

Il faut constater qu'à mesure que nous apprenons à connaître les aspects nouveaux du phénomène géotectonique, il nous paraît de plus en plus complexe. Cependant les difficultés nouvelles ne doivent pas nous décourager, elles doivent bien au contraire stimuler des recherches nouvelles.

Ces recherches devraient éclairer les questions suivantes :

- a) L'histoire des mouvements verticaux de l'écorce terrestre; les lois qui régissent leur évolution;
- b) Les rapports du magmatisme avec les différents types de mouvements tectoniques;
- c) Les particularités des mouvements tectoniques et du magmatisme de l'ère archéenne;
- d) La structure de l'écorce terrestre dans la région des bassins océaniques;
- e) L'histoire de l'hydroosphère et de l'atmosphère.

V. V. BELOUSSOV.

TRANSFER OF RADIOACTIVE MATTER THROUGH ROCKS BY DIFFUSION

by U. ASWATHANARAYANA.

(Department of Geology, Andhra University, Waltair, India.)

ABSTRACT.

An attempt is made in the course of this paper to apply the physical principles of diffusion in spherical shells to investigate the influence of a batholithic intrusion on the radioactivity distribution patterns in the intruded country rocks. Starting with fundamental laws of diffusion, a mathematical analysis is developed to work out the quantity of radioactive matter added to any unit area of cross-section in the spherical shell. The importance of diffusion processes in the transfer of matter through rocks is outlined and attention is drawn to the inadequacy of the data on the subject. The economic implications of the work on diffusional transfer of matter are mentioned and its limitations are pointed out.

INTRODUCTION.

Though the importance of the processes of diffusion in the transfer of matter through rocks has long been recognised, their role, efficacy and mode of operation in effecting metamorphic and metasomatic changes have continued to be controversial. While Bowen (1948) representing the magmatist school visualises diffusion as being of negligible import in metamorphism and metasomatism, Eskola (1934), Bugge (1945), D. L. Reynolds (1946), Perrin and Roubault (1949) and others seek to explain their concepts of granitisation by taking recourse to large scale diffusion of matter through rocks. Ramberg (1944, 1945 a, b, 1946) discussed diffusion on the basis of the forces which govern the movement of ions in a rock, which, according to him, is comparable to osmotic phenomena. Bugge (1945) thought that a better approach was the application of chemical potentials in all diffusion processes. Rosenquist (1947) pointed out that the work of Ramberg and Bugge was largely of theoretical interest as they did not pertain to conditions actually existing in upper lithosphere.

In the field, the role and efficacy of diffusion in the transfer of matter through rocks can be best studied in the case of radioactive

elements, as the modern emanation techniques (Evans, 1935) permit a very precise determination of radium in quantities as low as 10^{-12} gm/gm of rock. An attempt is made in the course of this paper to apply the physical principles of diffusion in spherical shells (Barrer, 1944, 1951) to investigate the influence of a batholithic intrusion on the radioactivity distribution patterns in the intruded country rocks.

GENERAL CONSIDERATIONS.

Principles of Diffusion :

Diffusion is usually defined as the process by which, under the influence of a concentration gradient and/or chemical potential gradient, atoms and ions move from one position to another within a solvent phase, which may be a gas, liquid or solid (Jensen, 1952). Diffusion in ideal gaseous, liquid or crystalline mixtures is governed by Fick's first and second laws for stationary and non-stationary currents respectively :

$$\frac{\partial m}{\partial t} = - A \cdot D \cdot \frac{\partial c}{\partial x}$$

$$\frac{\partial c}{\partial t} = D \cdot \frac{\partial^2 c}{\partial x^2}$$

where $\frac{\partial m}{\partial t}$ is the quantity of matter transferred in a unit time through cross-section A when the concentration gradient is $\frac{\partial c}{\partial x}$ and D is the diffusion constant. Fick's second law expresses the relation pertaining to the rate of change of concentration with time.

Diffusion is a statistic process. The macrobodies of matter are visualised as being composed of large number of discrete particles, among which a certain amount of kinetic energy is distributed at a given temperature. « Under certain circumstances, the probability for the motion of a particle is greater in one direction than in the other and hence a nett diffusional transfer of matter extends in that direction » (Ramberg, 1952).

Diffusion through rock bodies :

An excellent résumé on this subject appeared recently (Ramberg, 1952). Studies on diffusion through complex systems of rocks met with in nature have to take cognisance of numerous environmental factors affecting diffusion. The free energies of several constituents are appreciably affected by types of mineral lattices, pressure, température, position in the gravitational field, chemical

milieu and the size of the phases and thus tend to complicate diffusion studies. Further, each type of individual particle, (ion, atom or molecule) within a rock has its own characteristic potential, which results in widely diverging diffusion directions in the same rock, the diffusion paths being controlled by the mineralogical character of the rock, the pressure, temperature, structure, presence of catalysts in the intergranular network and above all the nature of the diffusing particle. « The power of diffusion through unit cross-section is controlled by the diffusion coefficient, the magnitude of the driving free-energy gradient and the concentration of the diffusing particle » (Ramberg, 1952).

Increasing temperatures enhance the mobility of the particle and the diffusion coefficient increases exponentially with temperature, according to the equation

$$D_T = D_0 \cdot e^{-Q/R\cdot T}$$

where D_T is the diffusion constant at T° K, D_0 is the diffusion constant at T_0° K and Q is the molal activation energy of diffusion. Buerger (1948) emphasized the decisive role of temperature in diffusion. According to him, whenever temperature is high enough to cause spontaneous growth of crystals, it is already maintaining a very high level of diffusion, permitting smaller atoms and ions to migrate freely.

Increase in pressure produces a decrease in intergranular dimensions and consequently increases the rate of intergranular diffusion. It also tends to produce more closely packed structures with concomitant reduction of free space between atoms and ions in the structures and the consequent lowering of the rate of internal diffusion (Rankama and Sahama, 1950).

The rate of ionic diffusion depends on the size of the ion. The investigations of Backlund (1936) on the rate of diffusion of K, Na, Al and Si between granite and limestone and the studies of Bugge (1945) and Lapadu-Hargues (1945) on granitisation problems can be cited in favour of such a surmise.

The diffusion processes are not efficacious in the solid rocks in the outermost parts of the crust because of low temperatures and relative rarity and restricted scope of shearing and plastic deformation movements, which are capable of accelerating chemical migration. The transfer of matter in these zones is largely effected by circulating fluid solutions through open channels and porous rocks. The situation is markedly different in deeper portions of the crust where the rocks are too compact to permit such a process of transfer. « In the deeper portions of the folded mountain zones,

where temperature is high and mechanical deformation takes place continuously and evenly over large volumes of rocks, the resistance against diffusion appears to be low enough to permit considerable rearrangement of matter by this mechanism » (Ramberg, 1952).

TREATMENT OF THE DIFFUSION PROBLEM.

Formulation of the problem :

The problem pertains to the consequences of a batholithic intrusion on the radioactivity distribution patterns in the intruded country rocks. A hemi-spherical body of a batholith (of radius b) of granitic to intermediate nature is visualised to have intruded in the form of molten fluid into a mass of country rock of enormously large dimensions (hemi-spherical body of radius a), when compared with the former. The radioactive matter of the batholithic material migrates from the batholith into the surrounding country rocks through processes of diffusion which, by the addition of radioactive elements, influences the pre-existing radioactivity distribution patterns. (Vide figure I.)

Mathematical Treatment :

Starting with Fick's laws of diffusion and the simple equations of Barrer (1944, 1951), a mathematical analysis is made to work out expressions for the quantity of matter (m) added to any unit area of cross-section in the spherical shell. An assumption is made in this treatment that diffusion of radioactive elements into rocks is governed by the same laws as the conduction of heat in solids.

The simplest case is the diffusion in uniform medium. It may be mentioned in this connection that diffusion in a sphere is a special case of diffusion in a spherical shell.

Radius of inner sphere = b

Radius of outer sphere = a $0 < b < a$

Concentration at any point = C

$$C = C_1 \text{ at } r = b, \text{ at all } t$$

$$C = C_2 \text{ at } r = a, \text{ at all } t$$

The equation for C is

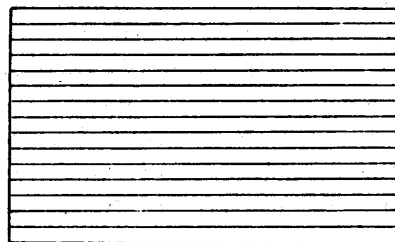
$$\frac{\partial C}{\partial t} = D \left(\frac{\partial^2 C}{\partial r^2} + \frac{2}{r} \cdot \frac{\partial C}{\partial r} \right) \dots \dots \dots \quad (i)$$

where D is the diffusion constant.

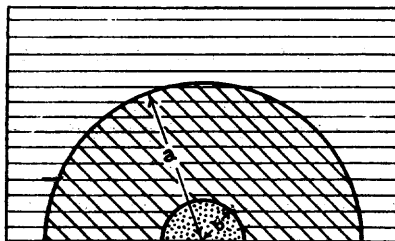
Using the substitution $\mu = Cr$, we have

$$\frac{\partial u}{\partial t} = D \cdot \frac{\partial^2 u}{\partial r^2} \quad (2) \quad (6)$$

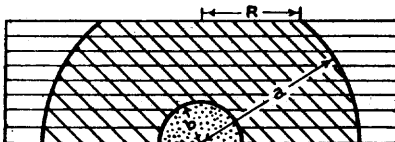
DIFFUSION IN SPHERICAL SHELLS.
IDEALISED GEOLOGICAL SECTIONS.
(NOT TO SCALE)



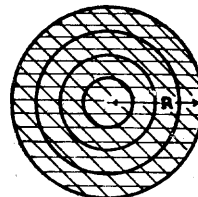
**VERTICAL CROSS-SECTION OF THE COUNTRY ROCK.
 (INITIAL CONDITION)**



**VERTICAL CROSS-SECTION OF THE ROCKS/
 AFTER INTRUSION.**



**VERTICAL CROSS-SECTION OF THE ROCKS
 AFTER EROSION.**



**HORIZONTAL CROSS-SECTION OF THE AFFECTED COUNTRY ROCK
 (AS SEEN FROM ABOVE)**

- Country rock.*
- Country rock affected by batholithic intrusion.*
- Batholithic intrusion.*

FIG. I

Case I.

The first case considers a batholithic intrusion which is capable of providing continuous supply of radioactive elements to be diffused into the surrounding rocks. It visualises a situation wherein in a unit area of cross-section in the spherical shell, the nett outflow of radioactive matter is constant. For simplicity's sake, the country rock is supposed to contain initially a uniform distribution of radioactive matter. This case corresponds to steady state of flow in the terminology of the diffusion studies.

Steady state of flow :

$$c = \frac{c_1 b}{v} + \frac{c_2 a - c_1 b}{a - b} \cdot \frac{v - b}{v}$$

The concentration gradient at any point v is

$$\frac{\partial c}{\partial v} = - \frac{c_1 b}{v^2} + \frac{c_2 a - c_1 b}{a - b} \cdot \frac{b}{v^2}$$

The quantity of the matter transferred in unit time per unit area is given by

$$\begin{aligned} \frac{\partial m}{\partial t} &= - D \cdot \frac{\partial c}{\partial v} \\ &= D \left\{ \frac{c_1 b}{v^2} - \frac{c_2 a - c_1 b}{a - b} \cdot \frac{b}{v^2} \right\} \end{aligned}$$

The total amount of matter transferred is

$$m = \frac{A \cdot D \cdot (c_1 - c_2) ab \cdot t}{v^2 (a - b)}$$

where A is the area of cross-section.

Case II.

The second case takes into cognisance the diffusional history of radioactive ions. As the process of diffusion proceeds, some amount of radioactive matter is continuously deposited along the diffusion paths and the concentration gradient steadily decreases with time. In this case also, a uniform distribution of radioactive matter in the country rocks is assumed.

Now let us consider the non-steady state of flow, initial concentration within the shell being constant.

$$\text{i.e. } C = C_0 \text{ for } b < v < a \text{ and } t = 0$$

In this case, C may be written as

$$\begin{aligned}
 c &= \frac{c_1 b}{v} + \frac{c_2 a - c_1 b}{a - b} \cdot \frac{v - b}{v} \\
 &+ \frac{2}{\pi v} \sum_{n=1}^{\infty} \frac{c_2 a \cos n\pi - c_1 b}{n} \sin \frac{n\pi(v-b)}{(a-b)} \cdot \text{Exp} \left(-\frac{Dn^2 \pi^2 t}{(a-b)^2} \right) \\
 &- \frac{2c_1}{\pi v} \sum_{n=1}^{\infty} \sin \frac{n\pi(v-b)}{a-b} \cdot \frac{a \cos n\pi - b}{n} \cdot \text{Exp} \left(-\frac{Dn^2 \pi^2 t}{(a-b)^2} \right) \\
 \frac{\partial c}{\partial v} &= -\frac{c_1 b}{v^2} + \frac{c_2 a - c_1 b}{a - b} \cdot \frac{b}{v^2} \\
 &+ \frac{2}{\pi} \sum_{n=1}^{\infty} \frac{c_2 a \cos n\pi - c_1 b}{n} \left[\frac{n\pi}{a-b} \cdot \frac{1}{v} \cos \frac{n\pi(v-b)}{(a-b)} \right. \\
 &\quad \left. - \frac{1}{v^2} \sin \frac{n\pi(v-b)}{(a-b)} \right] \cdot \text{Exp} \left(-\frac{Dn^2 \pi^2 t}{(a-b)^2} \right) \\
 &- \frac{2c_1}{\pi} \sum_{n=1}^{\infty} \frac{a \cos n\pi - b}{n} \left[\frac{n\pi}{(a-b)} \cdot \frac{1}{v} \cos \frac{n\pi(v-b)}{(a-b)} \right. \\
 &\quad \left. - \frac{1}{v^2} \sin \frac{n\pi(v-b)}{(a-b)} \right] \cdot \text{Exp} \left(-\frac{Dn^2 \pi^2 t}{(a-b)^2} \right)
 \end{aligned}$$

And therefore we have

$$\begin{aligned}
 m &= A. D. t \left\{ \frac{c_1 b}{v^2} - \frac{c_2 a - c_1 b}{(a-b)} \cdot \frac{b}{v^2} \right\} \\
 &+ \frac{2 A (a-b)^2}{\pi^3} \sum_{n=1}^{\infty} \frac{c_2 a \cos n\pi - c_1 b}{n^3} \left\{ \frac{n\pi}{a-b} \cdot \frac{1}{v} \cos \frac{n\pi(v-b)}{(a-b)} \right. \\
 &\quad \left. - \frac{1}{v^2} \sin \frac{n\pi(v-b)}{(a-b)} \right\} \\
 &- \frac{2 A c_1 (a-b)^2}{\pi^3} \sum_{n=1}^{\infty} \frac{a \cos n\pi - b}{n^3} \left\{ \frac{n\pi}{a-b} \cdot \frac{1}{v} \cos \frac{n\pi(v-b)}{(a-b)} \right. \\
 &\quad \left. - \frac{1}{v^2} \sin \frac{n\pi(v-b)}{(a-b)} \right\}
 \end{aligned}$$

+ terms which tend to zero in infinite time.

$$\begin{aligned}
 &= \frac{AD(c_i - c_o) ab \cdot t}{v^2(a-b)} + \frac{2A \cdot a(a-b)}{\pi^2} \cdot \frac{c_2 - c_o}{v} \sum \frac{\cos n\pi \cos \frac{n\pi(v-b)}{(a-b)}}{n^2} \\
 &- \frac{2A(a-b)(c_i - c_o)b}{\pi^2 v} \sum \frac{\cos \frac{n\pi(v-b)}{(a-b)}}{n^2} \\
 &- \frac{2A(a-b)^2(c_i - c_o)a}{\pi^3 v^2} \sum \frac{\cos n\pi \sin \frac{n\pi(v-b)}{(a-b)}}{n^3} \\
 &+ \frac{2A(a-b)^2(c_i - c_o)b}{\pi^3 v^2} \sum \frac{\sin \frac{n\pi(v-b)}{(a-b)}}{n^3}
 \end{aligned}$$

+ terms which tend to zero at infinite time.

$$\begin{aligned}
 &= \frac{AD(c_i - c_o) ab \cdot t}{v^2(a-b)} + \frac{2A \cdot a \cdot c_2 - c_o)(a-b)}{\pi^2 v} \times \\
 &\quad \left\{ \frac{\pi^2}{12} - \frac{\pi^2(v-b)^2}{4(a-b)^2} \right\} \\
 &- \frac{2A(c_i - c_o)(a-b)b}{\pi^2 v} \left\{ \frac{\pi^2}{6} - \frac{\pi^2(v-b)}{2(a-b)} + \frac{\pi^2(v-b)^2}{4(a-b)^2} \right\} \\
 &- \frac{2A(c_2 - c_o)a(a-b)^2}{\pi^3 v^2} \left\{ \frac{\pi^2}{12} \cdot \frac{\pi(v-b)}{(a-b)} - \frac{\pi^3(v-b)^3}{12(a-b)^3} \right\} \\
 &+ \frac{2A(c_i - c_o)b(a-b)^2}{\pi^3 v^2} \left\{ \frac{\pi^3(v-b)}{6(a-b)} - \frac{\pi^3(v-b)^3}{4(a-b)^2} + \frac{\pi^3(v-b)^3}{12(a-b)^3} \right\} \\
 &= \frac{AD(c_i - c_o) ab \cdot t}{v^2(a-b)} \\
 &+ \frac{A(c_2 - c_o)a(a-b)}{6v} \left\{ \frac{b}{v} - \frac{2(v-b)^2}{(a-b)^2} - \frac{b(v-b)^2}{v(a-b)^2} \right\} \\
 &+ \frac{A(c_i - c_o)b(a-b)}{3v} \left\{ \frac{b}{v} - \frac{3(v-b)}{(a-b)} + \frac{(v-b)^3}{v(a-b)^2} + \frac{3a(v-b)^2}{2v(a-b)^2} \right\} \\
 &+ \text{terms which become zero in infinite time.}
 \end{aligned}$$

Case III.

In this case, unlike in the two cases dealt with above, an initially variable distribution of radioactive matter is assumed.

Let us consider the non-steady state of flow, initial concentration within the shell decreasing with r

$$i.e. \text{ at } t = 0, c = \frac{c_o}{v} \text{ for } b < v < a$$

Then

$$c = \frac{c_1 b}{v} + \frac{c_2 a - c_1 b}{a - b} \cdot \frac{v - b}{v}$$

$$+ \frac{2}{\pi v} \sum_{n=1}^{\infty} \frac{c_2 a \cos n\pi - c_1 b}{n} \sin \frac{n\pi(v-b)}{(a-b)} \cdot \text{Exp} \left(- \frac{D n^2 \pi^2 t}{(a-b)^2} \right)$$

$$+ \frac{4 c_2}{\pi v} \sum_{m=0}^{\infty} \sin \frac{(2m+1)\pi(v-b)}{(a-b)} \cdot \frac{1}{2m+1} \cdot \text{Exp} \left(- \frac{D \overline{2m+1}^2 \pi^2 t}{(a-b)^2} \right)$$

$$\frac{\partial c}{\partial v} = - \frac{c_1 b}{v^2} + \frac{c_2 a - c_1 b}{a - b} \cdot \frac{b}{v^2}$$

$$+ \frac{2}{\pi} \sum_{n=1}^{\infty} \frac{c_2 a \cos n\pi - c_1 b}{n} \left[\frac{n\pi}{a-b} \cdot \frac{1}{v} \cos \frac{n\pi(v-b)}{(a-b)} \right.$$

$$\left. - \frac{1}{v^2} \sin \frac{n\pi(v-b)}{(a-b)} \right] \cdot \text{Exp} \left(- \frac{D n^2 \pi^2 t}{(a-b)^2} \right)$$

$$+ \frac{4 c_2}{\pi} \sum_{m=0}^{\infty} \frac{1}{2m+1} \left[\frac{(2m+1)\pi}{(a-b)v} \cdot \cos \frac{(2m+1)\pi(v-b)}{(a-b)} \right.$$

$$\left. - \frac{1}{v^2} \sin \frac{(2m+1)\pi(v-b)}{(a-b)} \right] \cdot \text{Exp} \left(- \frac{D \overline{2m+1}^2 \pi^2 t}{(a-b)^2} \right)$$

$$m = \frac{AD(c_1 - c_2)ab \cdot t}{v^2(a-b)}$$

$$- \frac{2A}{\pi} \sum_{n=1}^{\infty} \frac{(a-b)^2}{n^2 \pi^2} \cdot \frac{c_2 a \cos n\pi - c_1 b}{n} \left[\frac{n\pi}{a-b} \cdot \frac{1}{v} \cos \frac{n\pi(v-b)}{(a-b)} \right.$$

$$\left. - \frac{1}{v^2} \sin \frac{n\pi(v-b)}{(a-b)} \right]$$

$$- \frac{4 c_2 A}{\pi} \sum_{m=0}^{\infty} \frac{(a-b)^2}{(2m+1)^2 \pi^2} \left[\frac{(2m+1)\pi}{(a-b)v} \cdot \cos \frac{\overline{2m+1} \cdot \pi(v-b)}{(a-b)} \right.$$

$$\left. - \frac{1}{v^2} \sin \frac{\overline{2m+1} \cdot \pi(v-b)}{(a-b)} \right]$$

+ terms which tend to zero at infinite time

$$= \frac{A \cdot D - (c_1 - c_2) ab \cdot t}{(a-b)}$$

$$- \frac{2A}{\pi} \left[\frac{a-b}{v} \cdot c_2 a \sum_{n=1}^{\infty} (-)^n \cos \frac{n\pi(v-b)}{(a-b)} - \frac{(a-b)^2}{\pi^2 v^2} \right].$$

$$\begin{aligned}
 & \times c_1 b \left[\sum \frac{\sin \frac{n\pi(v-b)}{(a-b)}}{n^4} \right] \\
 & - \frac{4c_0 A}{\pi} \left[\frac{(a-b)}{v} \sum_{m=0}^{\infty} \frac{\cos \frac{2m+1}{(a-b)} \pi(v-b)}{(2m+1)^4} - \frac{(a-b)^3}{\pi^4 v^4} \times \right. \\
 & \quad \left. \sum \frac{\sin \frac{2m+1}{(a-b)} \pi(v-b)}{(2m+1)^4} \right] \\
 & = \frac{AD(c_1 - c_2) ab \cdot t}{v^4 (a-b)} \\
 & - \frac{2A}{\pi} \left[\frac{(a-b)c_2 a}{\pi v} \left\{ \frac{\pi^4}{12} - \frac{\pi^4(v-b)^4}{4(a-b)^4} \right\} - \frac{(a-b)^3 \cdot c_1 b}{\pi^4 v^4} \times \right. \\
 & \quad \left. \left\{ \frac{\pi^4(v-b)}{6(a-b)} - \frac{\pi^4(v-b)^5}{4(a-b)^5} + \frac{\pi^4(v-b)^3}{12(a-b)^3} \right\} \right] \\
 & - \frac{4c_0 A}{\pi} \left[\frac{(a-b)}{\pi v} \left\{ \frac{\pi^4}{8} - \frac{\pi^4(v-b)}{4(a-b)} \right\} \right. \\
 & \quad \left. - \frac{(a-b)^3}{\pi^4 v^2} \left\{ \frac{\pi^4(v-b)}{8(a-b)} - \frac{\pi^4(v-b)^4}{8(a-b)^4} \right\} \right] + 0 \dots (i) \\
 & = \frac{AD(c_1 - c_2) ab \cdot t}{v^4 (a-b)} \\
 & - \frac{2A(a-b)}{\pi v} \left[c_2 a \left\{ \frac{1}{12} - \frac{(v-b)^4}{4(a-b)^4} \right\} - \right. \\
 & \quad \left. \frac{c_1 b}{v} \left\{ \frac{(v-b)}{6} - \frac{(v-b)^3}{4(a-b)} + \frac{(v-b)^5}{12(a-b)^5} \right\} \right] \\
 & - \frac{4c_0 A(a-b)}{\pi v} \left[\left\{ \frac{1}{8} - \frac{(v-b)}{4(a-b)} - \frac{1}{v} \left\{ \frac{(v-b)}{8} - \frac{(v-b)^4}{8(a-b)} \right\} \right\} \right] \\
 & + 0 \dots (2)
 \end{aligned}$$

DISCUSSION.

Though the third case treated above roughly corresponds to what occurs in nature under conditions of metasomatic hypometamorphism, it must be said that at best it is an approximation, in view of the natural heterogeneity of the constitution of the batholith as well as the surrounding country rocks. Further the diffusion through rock systems is an enormously complicated physical process, which, as has been mentioned earlier, has got to take into account several factors on which we virtually do not have any data.

Professor R. M. Barrer of Aberdeen University, in a personal communication, kindly suggested that two more aspects also must be considered — namely, the existence of thermal gradients in the batholithic material and the decay of radioactive elements that goes on simultaneously with diffusion.

It therefore becomes obvious that any systematic work on this subject requires adequate data on

- (i) The consolidational history of a batholith, as can be adduced from evidences of geological thermometry.
- (ii) Diffusion constants of radioactive elements through various rock types.
- (iii) The radioactive content of batholithic material.
- (iv) The dimensional relationship between the batholith and the intruded rocks and
- (v) The temperature gradient set up in the intruded rocks by heat radiated into them from the batholithic material and its influence on the diffusion constants.

In view of the recognised relationship between batholiths, mineralisation patterns and radioactivity distribution patterns (Gross, 1952), most of the advanced countries of the West include in their geophysical exploration programmes, air-borne scintillometric surveys and other types of radiometric investigations (Pringle et al, 1953), (Stead et al, 1953). It can be seen from the work detailed above that the expressions derived are likely to be helpful in locating the locii of high radioactive mineral concentrations, particularly when the latter are present as impregnations introduced by batholithic action under conditions comparable to metasomatic hypo-metamorphism which allows considerable play for diffusion processes.

A case of the following type may be cited as an example (vide Figure 1). A certain type of radioactivity distribution pattern has been brought into existence in an extensive rock body by the diffusion of radioactive emanations from a batholith. As it normally happens, the impregnated rock body is eroded to some extent by geological agents, thus exhibiting a semi-plane surface. It is now possible, by an extension of this method, to locate roughly the locus of radioactivity concentration around which are located semi-concentric shells of uniform radioactivity. It must be mentioned, however, that this method takes into consideration only diffusion as an agent of mineralisation, which, in nature, is poly-genetic in its aspect. The analysis is hence valid only to the interpretation of mineralisation patterns which have come into existence under hypo-metamorphic conditions.

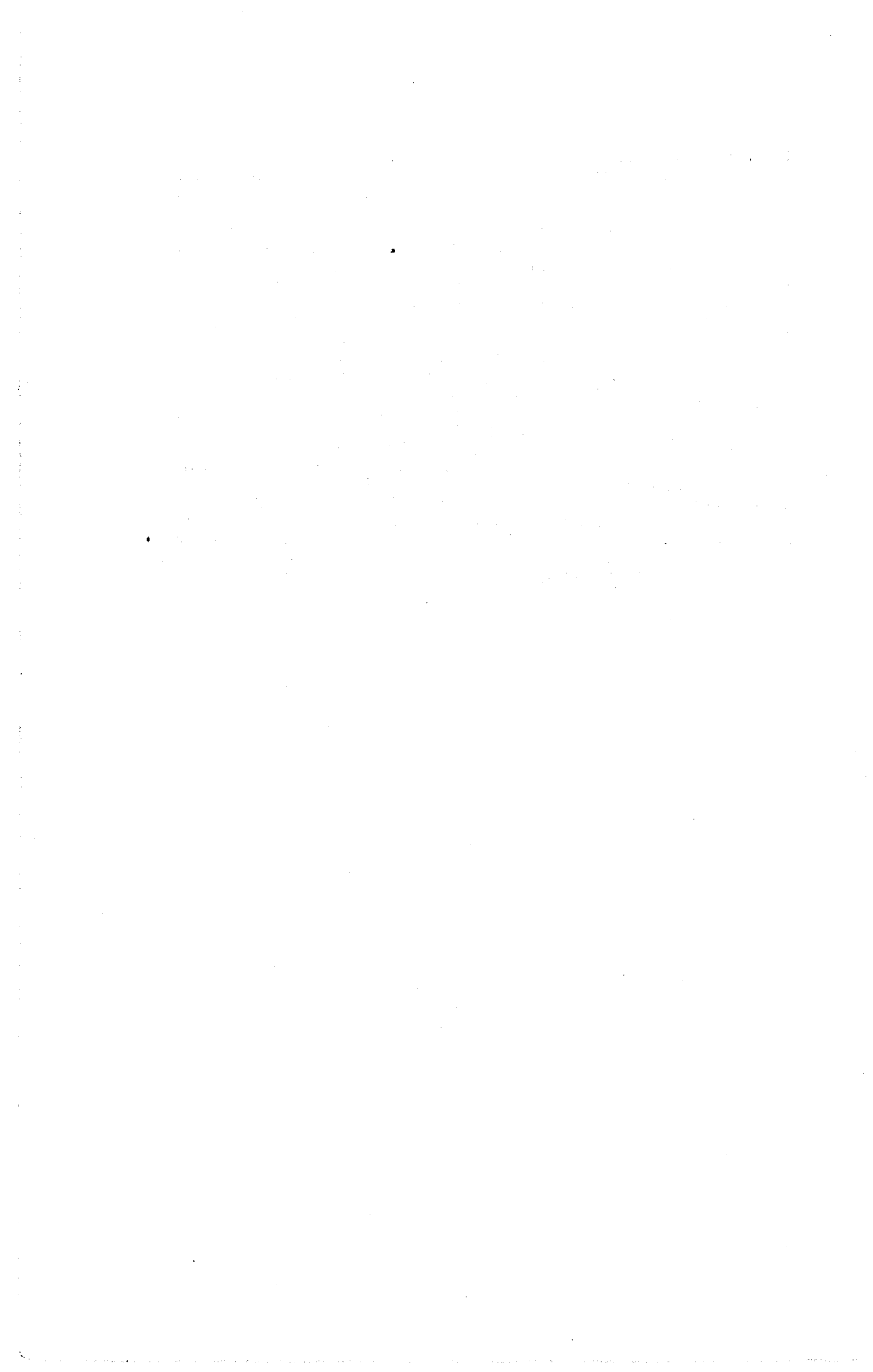
ACKNOWLEDGMENTS.

The author is grateful to Professor C. Mahadevan for his kind encouragement and interest in the work. It is a great pleasure to place on record my deep sense of gratitude to Professor S. Minakshisundaram and Mr. S. Ramamoorthy of the Mathematical Physics Department of the Andhra University for their kind help in working out the mathematical theory. The kind suggestions of Professor R. M. Barer of Aberdeen University and Professor Swami Jnanananda of the Andhra University are thankfully acknowledged. The work has been sponsored by the Council of Scientific and Industrial Research.

REFERENCES.

1. BACKLUND (H. G.) (1936) - Der « Magmataufsteig » in Faltengebirgen. Compt. rend. Soc. geol. Finlante 9; Bull. Comm. geol. Finlante 115, p. 293.
2. BARRER (R. M.) (1944) - Diffusion in spherical shells and a new method of measuring thermal diffusivity constant. Phil. Mag. 35, 802-811.
3. BARRER (R. M.) (1951) - « Diffusion in and through solids » Cambridge University Press. pp. 28-31.
4. BOWEN (N. L.) (1948) - Method of multiple prejudices : Origin of granite. Geol. Soc. Am. Memoir, 28, p. 54.
5. BUERGER (M. J.) (1948) - The role of temperature in mineralogy. Am. Mineral. 33, 101.
6. BUGGE (J. A. W.) (1945) - The geological importance of diffusion in solid state. Avhandl. Norske Videnskaps — Akad. Oslo I. Mat. naturv. Klasse No. 13.
7. ESKOLA (P.) (1934) - A note on diffusion and reaction in solids. Compt. rend. Soc. Geol. Finlante 8; Bull. Comm. geol. Finlante 104, 144.
8. EVANS (R. D.) (1935) - Apparatus for the determination of radium, radon and thoron in solids, liquids and gases. Rev. Sci. Inst. 6, 99.
9. GROSS (W. H.) (1952) - Radioactivity as a guide to ore. Econ. Geol. 47, 722-743.
10. JENSEN (M. L.) (1952) - Solid diffusion of radioactive sodium in perthite. Amer. Jour. Sci. 250, 808-821.
11. LAPADU-HARGUES (P.) (1945) - Sur l'existence et la nature de l'apport chimique dans certaines séries cristallophylliennes. Bull. Soc. Geol. France. 15, 255.
12. PERRIN (R.) et ROUBAULT (M.) (1949) - On the granite problem. Jour. Geol. 57, 357-359.
13. PRINGLE (R. W.) ROULSTON (K. I.) BROWNE (G. W.) and LUNDBERG (H. T. F.) (1953) - The scintillation counter in the search for oil. Trans. Amer. Inst. Min. Met. Engineers, 196, 1255-1261.

14. RAMBERG (H.) (1944) - Relation between external pressure and vapor tension of compounds and some geological implications. *Avgandl. Norske Videnskaps — Akad. Oslo I. Mat. Naturv. Klasse No. 3.*
15. RAMBERG (H.) (1945 a) - The thermodynamics of the Earth's crust : I. Preliminary survey of the principal forces and reactions in the solid crust. *Norsk. Geol. Tids.* 24, 98, 1944.
16. RAMBERG (H.) (1945 b) - Note on the metamorphic differentiation of solid rocks. *Norsk. Geol. Tids.* 115, 1944.
17. RAMBERG (H.) (1946) - Litt om diffusjon; de faste begarter og dens betydning for metamorfose — og metasomatosefenomenene — *Geol. Foren. Stockholm. Forh.* 68, 56.
18. RAMBERG (H.) (1952) - « The origin of metamorphic and metasomatic rocks ». *Univ. Chicago Press.* p. 201-211.
19. RANKAMA (K.) and SAHAMA (Th. G.) (1950) - « Geochemistry », *Chicago Univ. Press.* p. 255.
20. REYNOLDS (D. L.) (1946) - The sequence of geochemical changes leading to granitisation. *Quart. Jour. Geol. Soc. Lond.* 102, 389-446.
21. ROSENQUIST (I. T.) (1947) - On the relation between external pressure and recrystallisation of minerals. *Norsk. Geol. Tids.* 26, 206.
22. STEAD (F. W.) MOXHAM (R. M.) and DAVIS (F. J.) (1953) - Progress in air-borne radio-activity surveying. *Bull. Geol. Soc. Am.* 64, No. 12, 1477.



SOME STATISTICAL ASPECTS OF THE DISTRIBUTION OF RADIOACTIVITY IN THE SALEM GNEISSES OF MADRAS STATE

by U. ASWATHANARAYANA

(Department of Geology, Andhra University, Waltair, India).

ABSTRACT.

The diopsidic-hornblende gneisses of the Salem area of Madras State have been examined for their radioactivity, which has been computed from the β -radiation impulses of a sample. The data which is obtained in the form of counts is then grouped into classes and the frequency distribution curve is drawn. It is found that the data indicate a unimodal distribution and hence attempts are made to examine the nature of the distribution. Statistical computations indicate that grouping into classes of size 30 counts gives data which is satisfactorily explained by the Poisson law as tested by the χ^2 test of goodness of fit. It is suggested that this result constitutes additional evidence in favour of the surmise that some natural processes favour a Poisson distribution. Attention is drawn to the lack of pre-designed pattern in sampling and the consequent difficulty in computing the goodness of the estimate of the parameter of Poisson distribution.

The diopsidic-hornblende gneisses of the Salem area of Madras State have been examined for their radioactivity, which has been computed from the β -radiation impulses of each sample. The impulses due to cosmic and terrestrial radiations (background), which add up to the radioactivity of the specimen, are deducted from the total number of impulses recorded for each sample.

The data which is obtained in the form of counts is then grouped into classes and the frequency distribution curve is drawn. It is found that the data indicate a unimodal distribution and hence attempts are made to examine the nature of such a distribution. In view of the wide applicability of Poisson law to a variety of radioactive processes, it is considered that the present data may be most appropriately graduated by the same law.

The data is initially grouped into class intervals ranging from 10 to 60. In each case, $\hat{\lambda}$ (an estimate of the parameter of the Poisson

distribution) is calculated and the distribution is graduated according to that Poisson law. The extent of discrepancy between the observed frequency (f) and the computed frequency (f_c) is then examined by applying the χ^2 test and in order to conform to the requirements of such a test, the computed and observed frequencies are grouped such that no cell contains less than 10 individuals. It is found that grouping into classes of size 30 counts and more gives data which is satisfactorily explained by Poisson law, as tested by χ^2 test of goodness of fit, in each case. As it is felt that there is no need to group the counts by intervals of more than 30, this interval is finally adopted and in this particular case, the estimated value of the parameter λ of the Poisson distribution is obtained as $\hat{\lambda} = 4.38$.

In the Table I are presented the details of grouping. Table II deals with the χ^2 test of goodness of fit.

TABLE I.

Serial No.	Class interval (in number of counts).	Observed frequency (f)	Computed frequency (f_c)
1.	0 - 29	7	0.89
2.	30 - 59	1	3.90
3.	60 - 89	8	8.54
4.	90 - 119	7	12.47
5.	120 - 149	14	13.65
6.	150 - 179	11	11.96
7.	180 - 209	7	8.73
8.	210 - 239	10	5.86
9.	240 - 269	4	2.98
10.	270 - 299	2	1.46
11.	300 and above.	-	0.56*
		71	71.00

* This figure is computed as residual.

TABLE II.

Serial No.	Class interval (in number of counts).	f	f_c	$f - f_c$	$(f - f_c)^2$	$\frac{(f - f_c)^2}{f_c}$
1.	0-119	23	25.80	-2.80	7.84	0.30
2.	120-149	14	13.65	+0.35	0.13	0.01
3.	150-179	11	11.96	-0.96	0.92	0.08
4.	180-300 and over.	23	19.59	+3.41	11.63	0.59
		71	71.00			0.98

From the χ^2 table (Croxton, 1953), it appears that the probability of obtaining a value of χ^2 of 0.98 or more when $n = 3$, is 0.80 to 0.90. Since a discrepancy between f and f_c of magnitude evident for this data may occur this often because of variations due to random sampling, it can be concluded that the fit is satisfactory. It may be mentioned in this connection that this result constitutes additional evidence in favour of the surmise that some Natural processes favour a Poisson distribution. It is learnt that in a recent meeting of the Geological Society of America, W. C. Krumbein and H. A. Slack have presented a paper on the « Areal variation in the low level radioactivity of some Pennsylvanian Black Shales » in which they have postulated a Poisson law for the distribution of radioactivity in the Black Shales. (Personal communication from Prof. R. L. Miller).

It must, however, be mentioned in this connection that initially samples were not collected according to a pre-designed pattern and this factor should be taken cognisance of in estimating the goodness of the value of λ . Besides, Professor Miller, in a personal communication, pointed out that the small size of the present data on Salem gneisses requires the choice of a higher level of significance though, he agrees, that it is arbitrary. Thus while the result obtained is of deep interest, it is of tentative nature which should be confirmed by more extensive work.

The author is grateful to Professor C. Mahadevan for his kind interest and encouragement in the course of the work. It is a great pleasure to place on record my deep sense of gratitude to Professor K. Nagabhushanam and Mr. V. K. Murty of the Statistics Department of the Andhra University and Professor R. L. Miller of Chicago University for their kind suggestions. The work has been sponsored by the Council of Scientific and Industrial Research (India).

REFERENCES.

CROXTON (F.E.) (1953) : « Elementary Statistics with applications in medicine ». Prentice Hall, New York.

**THE THERMAL HISTORY OF THE EARTH WITH
PARTICULAR
REFERENCE TO A NUMBER OF RADIOACTIVE
EARTH MODELS**

by J. A. JACOBS (Toronto, Canada).

INTRODUCTION.

Of all the problems connected with the constitution of the Earth's interior, its thermal properties are the least well understood, and a more complete understanding of them would go a long way towards solving many of the outstanding problems in geophysics. In any investigation of the thermal properties of the Earth, sooner or later the question of the initial temperature of the Earth and the mode in which it has cooled (or heated) since then, is bound to arise. This in its turn leads to the question of the origin of the Earth and to other deeper and more far reaching astrophysical problems. Since such questions are in their very nature bound to be extremely controversial, they will be avoided as far as possible, although some discussion of them is inevitable. Most theories of the origin of the Earth agree that at some stage in its history, the Earth passed through a molten stage before finally separating into different layers. It is the subsequent history of the Earth from the molten stage that will be considered in this paper.

In the past most investigators have considered the initial, the present, and, in some cases, the final equilibrium state of the Earth — few writers have investigated the thermal history of the Earth. In a discussion of the thermal properties within the Earth, it has been the custom to assume that a steady equilibrium state has been reached. In practice this is likely to be far from the truth. Temperatures at the core boundary, for example, probably fluctuate, not only in space, but also in time — especially if convection currents are present. In examining the significance of radioactivity in geophysical problems, most investigators have assumed (for simplicity) a constant rate of heat generation, yet the decrease in heat generation during the Earth's lifetime is approximately 50 %. One of the difficulties of the problem is of course; the unknown distributions and concentrations of radioactive substances in rocks. Present knowledge is expanding rapidly, but even by 1940 most results were unreliable and have since been shown to be too high.

STATEMENT OF THE PROBLEM.

The equation of heat conduction for a radioactive Earth is :

$$\rho c \frac{\partial T}{\partial t} = \frac{1}{r^2} \frac{\partial}{\partial r} \left(K r^2 \frac{\partial T}{\partial r} \right) + H(r, t)$$

where $H(r, t)$ is the rate of production of heat by radioactivity per unit time and volume, ρ the density, c the specific heat and K the thermal conductivity.

Its solution presents considerable mathematical difficulties and the assumptions made in obtaining a solution will now be discussed. It was found that the practice of using the solution for a semi-infinite plane as an approximation can lead to considerable errors. Only two types of radioactive distributions are of practical importance. The first is one in which the concentration of radioactivity falls off exponentially with depth, and the other is one in which the radioactive substances are distributed in spherical shells in each of which their concentrations are constant. The second type of distribution is preferred since it can be made to fit any given distribution fairly well by taking a sufficient number of shells. It also gives rise to a solution well suited to calculation with different sets of values of the radioactive concentrations in the various shells. Moreover, the first type of exponential distribution leads to an extremely slowly convergent series.

The Earth is considered radially symmetric as regards all physical properties and taken as solid throughout. The effect of the liquid part of the core will be to equalize the temperature in the liquid, causing the temperature gradient to become approximately the adiabatic and the error produced by treating the entire Earth as solid will be negligible in the greater part of the mantle. The temperature at the surface of the Earth is determined, not by the amount of heat arriving from the interior, but by equilibrium between heat received from the sun and that radiated back into space. The effect of diurnal and annual variation in surface temperature dies out in a few tens of feet, and the effect of climatic changes such as the ice ages is also negligible when considered over time intervals of billions of years. Provided that there has been no great change in the amount of heat radiated by the sun — a fact which is substantiated on astronomical grounds — it is safe to assume that the surface temperature of the Earth has remained practically constant throughout the whole of geologic time and an average value of $0^\circ C$ has been chosen. It should be noted that even under the most extreme hypotheses as to the extent of vulcanism in the past, the transport of heat to the surface by volcanic

processes is an order of magnitude less than loss of conduction for the whole Earth and will be neglected. Finally there is the question of the variation of the thermal conductivity K and the thermal diffusivity k . For reasons given later, both K and k are treated as constant. K varies fairly widely for common rocks, and Uffen (1) using seismic data and the theory of solids finds a considerable increase in K with depth. However Urry (2), using experimental results of Birch together with thermodynamical theory, has constructed a semi-empirical theory of conductivity of rocks. His results show that the diffusivity is remarkably constant down to a depth of 600 km at least and that a value of $0.007 \text{ cm}^2/\text{sec}$ should be reasonably accurate for the mantle.

SOLUTION OF THE PROBLEM.

The solution of the equation of heat conduction for a radioactive Earth is exceedingly complex and details will be published elsewhere (3). One or two points, however, may be noted. The rate of production of heat due to radioactivity $H(r, t)$ may be written :

$$H(r, t) = \sum h_i(r) e^{-\lambda_i t}$$

where $h_i(r)$ is the heat production per unit volume and λ_i the decay constant of the i^{th} radioactive substance. The time t is measured from the time of solidification t_0 years ago. It is not difficult to show that the solution for a radioactive Earth with a given initial temperature distribution is the sum of the solutions for a non-radioactive Earth cooling from the given initial tempe-

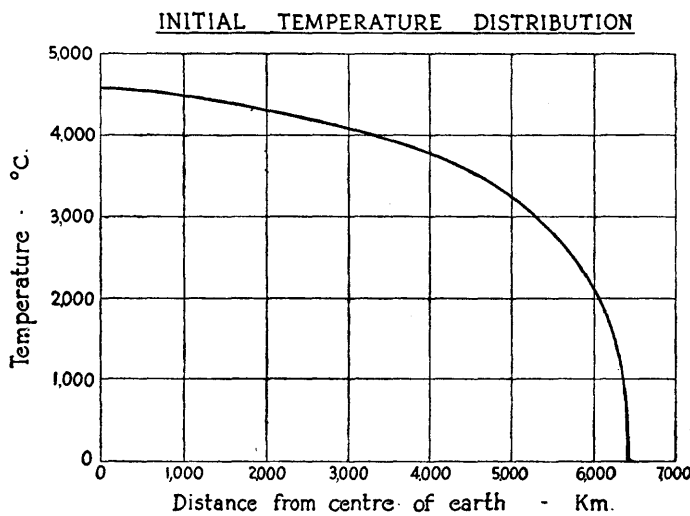


FIG. 1. $T = f(r)$.

ature distribution and for a radioactive Earth heating up from zero temperature. The solution to the first problem, i.e. the cooling of a non-radioactive Earth, is well known, having first been given by Fourier (4). The numerical results will depend of course upon the values adopted for the initial temperature distribution, which has been assumed to be everywhere the melting point of the substance concerned — with a slight correction near the surface where the temperature is assumed to be zero. A smooth curve (see Fig. 1) was drawn using the melting point values of Daly (5) for the mantle and Simon's (6) values of the melting point of iron at high pressures in the core. The solution involves carrying out a harmonic analysis of the function $rf(r)$. For the present calculations a sine series for $rf(r)$ was evaluated to 44 terms. Values were obtained both for the heat flow and the temperature at six depths in the Earth and at six times in the past. Some of the results are shown graphically in Fig 2, which serves to

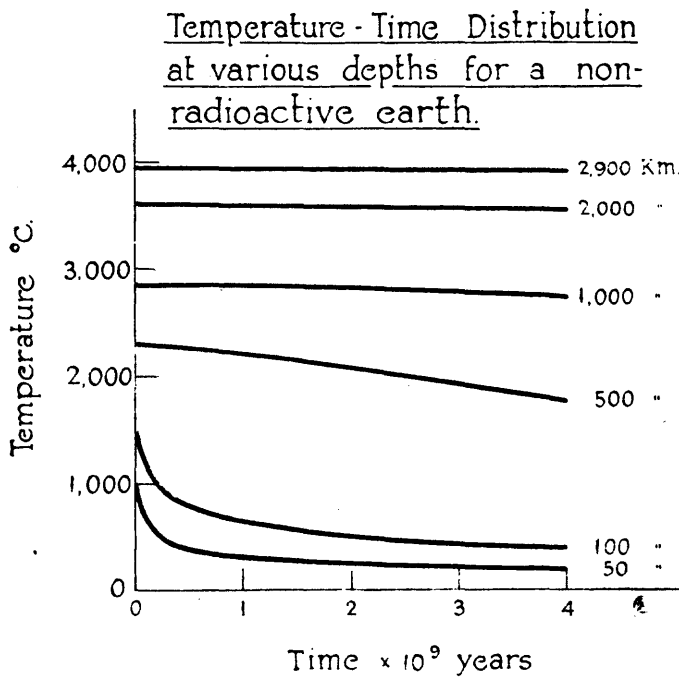


FIG. 2.

demonstrate how slowly temperatures change at great depths. At these depths thermal conditions are not greatly different from their initial values, and a correction can be made for the increase of

conductivity with depth in the calculation of the heat flows. Near the surface, on the other hand, cooling is considerable, and the surface heat flow for 4×10^9 years is but little affected by the values taken for the initial temperature distribution in the first few tens of kms. Finally, the labour involved in obtaining the solution for the cooling of a non-radioactive Earth is not great, and the solution with any initial temperature distribution may be readily obtained. Thus the solution of the complete problem given in this paper may easily be modified to fit any theory of the origin of the Earth with its attendant initial temperature distribution.

The solution for a radioactive Earth is more complex. It is easy to show that the effect of each radioactive substance may be evaluated separately and that their sum will give the total effect. Again, provided that the thermal conductivity is constant, the temperature at any point can be regarded as due to the sum effect of the radioactive concentrations in the different shells of the Earth model i.e. the general solution can be built up from a number of solutions of one type. Unfortunately the general solution cannot be found by the superposition of a number of simple solutions unless K is treated as a constant. An analytical solution of the differential equation has been obtained involving an infinite series. Computations of the temperature and heat flow were carried out on Ferut, the electronic computer at the University of Toronto. The actual concentration and distribution of radioactivity does not appear in the series solution (although the decay constant λ does), so that once these series are summed and tabulated, the results may be used for any desired distribution of radioactivity. The naturally radioactive substances of long period, which occur in sufficiently high concentrations in rocks to have a decided thermal effect are U^{238} , U^{235} , Th^{232} , and K^{40} . Tables have thus been drawn up allowing for any desired concentration of these four radioactive substances in nine different shells. These tables enable the temperature and heat flow at six depths within the Earth and at six times in the Earth's history to be readily evaluated for any Earth model. The construction of these tables involved summing over 2500 series, many of them to more than 100 terms. Such an undertaking would have been impossible by hand computation.

RESULTS FOR PARTICULAR EARTH MODELS.

It remains now to discuss some of the results obtained for different Earth models. The most important feature of any Earth

model is that it should be capable of portraying as faithfully as possible the physical properties it is desired to investigate. Thus in a discussion of the properties of the mantle it is legitimate to neglect the detailed complex structure of the crust and to represent it by a thin shell of uniform thickness and composition. This does not imply that such a crude representation of the crust is considered actually to exist, but such a representation is perfectly adequate for the investigation in hand. If a model can satisfy the geological and chemical facts as well, it is of course to be preferred, but there is no harm in constructing an abstract model to investigate specific physical phenomena so long as it is realized that there will be no attempt to treat the structure in detail and identify each shell with a specific rock type.

Three models have so far been considered. The first is a simplified one which does not attempt to fit the details of crustal structure. This simplified model consists of three shells, — a thin crustal layer 20 km thick of granite-granodiorite composition, a uniform mantle of dunite, and a dense core of the composition of iron meteorites. Apart from the simplified crustal layer, this model is identical with one proposed by Bullen (7). The second model, originally due to Adams and Williamson (8), is considerably more detailed. A structure of four 15 km. layers is taken for the crust, with the top layer of granite-granodiorite composition, and the remaining three layers of composition changing from acidic to basic. From 60 to 1600 km. the material of the mantle is identified as dunite, and from 1600 to 3000 km. it is taken as of the same composition as pallasitic meteorites. The core is again identified with iron meteorites. The presence of relatively high amounts of radioactivity to a depth of 60 km. in this model should give an indication of what thermal conditions may be like under the oceans, since recent measurements of the heat flow through the ocean floors by Bullard (9) (in the Atlantic) and Revelle and Maxwell (10) (in the N. Pacific) suggest that there may be the same total amount of radioactivity beneath both continents and oceans, but extending in high concentrations to greater depths in the case of the latter. The temperatures at different depths in the Earth at different times in the past for the second model are shown in Fig. 3. This figure shows only the heating up of the Earth from zero temperature due to radioactivity. To get the complete picture, the results of Fig. 2, i.e. the cooling of the Earth from its initial temperature, must be added. This is shown in Fig. 4 which gives the total temperature due to both cooling and radioactive heating. A number of interesting features are imme-

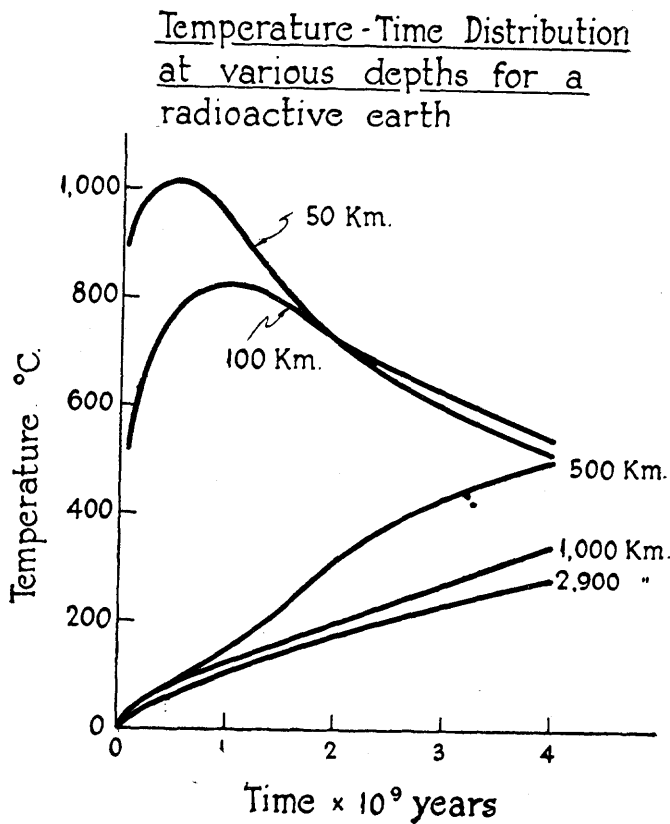


FIG. 3.

diately evident. In spite of the extremely low concentrations of radioactivity in the deep mantle and core, there is still a heating up there of two or three hundred degrees. Near surface conditions appear to have been greatly different in the far past from those existing at present — in fact there may even have been remelting of the material at depths of 50 to 100 km. during the first billion years or so. However this brief temperature rise at the very beginning soon ceases and cooling commences. The rate of cooling, for both these models, was greater in the past than it is now, and this suggests that orogenetic activity may have decreased with time, and perhaps have been caused by different processes in the far past. The present temperatures at depths of 50-100 km. differ by as much as 200° C for the two models, and this suggests that similar differences may hold beneath the oceans and continents. The present surface heat flow obtained for the first model agrees well with observed values, although that for the second

model is somewhat higher, which suggests that too much radioactivity has been included in the surface layers of this model.

The third model is a modification of the second in which too much radioactivity had been included in the surface layers. A structure of two fifteen km. layers is taken for the crust, instead of the four of Model II. Thus the layer of dunite extends from

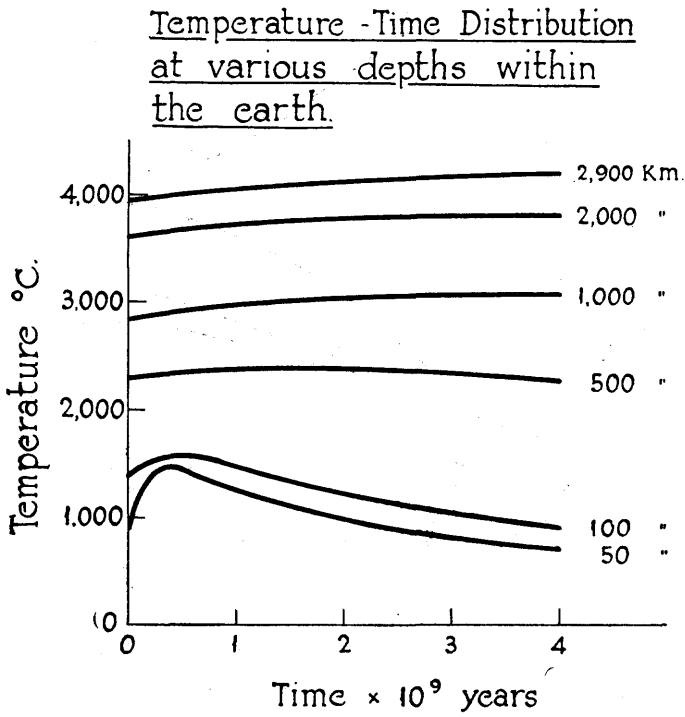


FIG. 4.

30-1600 km. instead of from 60-1600 km. Both the temperatures and heat flows for this model are given in Fig. 5 which presents the results in tabular form. The general trends of Model II are unchanged, although the present surface heat flow for this third model viz. 40 cal./cm yr. agrees with the observed average value of 38 cal./cm yr. It is not implied of course, that the temperatures and heat flows are known to the accuracy given in Fig. 5. The extra figures have been retained in the computations in order to facilitate comparison of the results at different depths and times in the Earth's history.

Temperature (°C)		50	100	500	1000	2000	2900
Time (10 ⁹ yr.)	Depth (km.)						
0		665	1220	2310	2856	3615	3958
.25		991	1255	2330	2885	3643	3985
.5		945	1204	2346	2910	3667	4010
1		828	1101	2353	2960	3705	4052
2		654	914	2316	3017	3763	4117
3		552	800	2239	3051	3808	4168
4		484	721	2183	3072	3841	4209

Heat Flow (cal./cm ² yr.)		50	100	500	1000	2000	2900
Time (10 ⁹ yr.)	Depth (km.)						
.25		13.0	12.8	5.3	5.8	4.8	3.7
.5		13.4	12.9	5.6	5.8	4.9	3.7
1		13.2	12.8	6.9	5.9	4.9	3.8
2		12.4	12.3	9.1	6.1	5.0	3.9
3		11.7	11.7	10.2	6.7	5.0	4.0
4		11.0	11.2	10.9	7.3	5.1	4.2

FIG. 5. Temperatures and Heat Flows for Model III.

CONCLUSIONS.

The numerical evaluation of the solutions just discussed requires a knowledge of the decay constant λ of each of the four radioactive substances, together with their rates of heat production H and their concentrations in the shells of whatever Earth model is selected. The values used in the preceding examples were obtained by an exhaustive study at Toronto of all the existing literature on the subject. In conclusion it should be emphasized that the value of the work just described lies not so much in the particular results of any Earth model, as in the fact that a general solution has been set up which will give the thermal properties of an Earth model with any desired distribution and concentration of radioactivity.

REFERENCES.

1. UFFEN (R. J.) (1952) - A Study of the Thermal State of the Earth's Interior, Ph. D. Thesis, Univ. of Western Ontario.
2. URRY (W. D.) and COMENETZ (G.) (1947) - Thermal History of the Earth (Private communication).

3. JACOBS (J. A.) (1955) - The Earth's Interior, Handbuch der Physik v. 47, Chapter 12, J. Springer, Berlin (new edition).
4. FOURIER (J.) (1822) - Théorie Analytique de la Chaleur, Paris.
5. DALY (R. A.) (1943) - Geol. Soc. Am. Bull. v. 54, p. 401.
6. SIMON (F. E.) (1953) - Nature, v. 172, p. 746.
7. BULLEN (K. E.) (1953) - Introduction to the Theory of Seismology, Cambridge.
8. ADAMS (L. H.) and WILLIAMSON (E. D.) (1925) - Smithsonian Report for 1923, p. 241.
9. BULLARD (E. C.) (1954) - Proc. Roy. Soc. A, v. 222, p. 408.
10. REVELLE (R.) and MAXWELL (A. E.) (1952) - Nature, v. 170, p. 199.

J. A. JACOBS.

LE MÉCANISME DES EXPLOSIONS PHRÉATIQUES

par Jean GOGUEL (Paris).

On sait que certains phénomènes volcaniques, à caractère explosif, présentent cette particularité de remettre en mouvement un matériel inerte anciennement refroidi, sans adjonction de magma neuf; la phase gazeuse est constituée essentiellement de vapeur d'eau. A ce type appartient l'éruption du Bandaï San, au Japon, le 15 juillet 1888, celle du Azuna San cinq ans plus tard, celles de l'Ararat en 1840, du Galung Gung (Java) en 1822. De l'explosion de l'Usu San (Yeso, Japon) en juin et juillet 1944, une description particulièrement précise a été publiée au Bulletin Volcanologique⁽¹⁾.

De telles éruptions, que l'on désigne d'ordinaire comme « explosions phréatiques » (ou semi-volcaniques, Dana, ultra-volcaniques, Mercalli, indirectes, Wolff), paraissent dues à la vaporisation de l'eau souterraine; elles paraissent se produire au début d'une phase d'activité, après une phase de repos suffisamment longue pour que les terrains superficiels se soient refroidis et aient été envahis par l'eau.

On sait d'ailleurs que la présence de vapeur d'eau dans les véritables éruptions volcaniques n'implique aucune analogie avec les explosions phréatiques, et qu'elle doit provenir du magma lui-même.

Nous nous proposons d'analyser ici le mécanisme des explosions phréatiques, à la lumière des propriétés thermodynamiques de l'eau.

Les lois qui gouvernent l'équilibre ou le mouvement de l'eau souterraine sont bien connues. On sait qu'une roche peut être caractérisée par sa porosité, c'est-à-dire le volume offert à l'eau par unité de volume, et par sa perméabilité, ou éventuellement, ses perméabilités horizontale et verticale, qui peuvent être différentes. Comme on le verra par la suite, l'explosion phréatique est surtout vraisemblable dans une roche à forte porosité (cendres volcaniques, etc...) qui possède généralement une perméabilité notable.

(1) Takeshi Minakami, Toshio Ishikava et Kenzo Yagi. The 1944 eruption of Volcano Usu in Hokkaido, Japan. *Bulletin Volcanologique*, sér. II, t. XI, pp. 45-157, 25 planches; Naples, 1951.

Si l'eau est immobile, sa pression propre dépend de la profondeur du point considéré sous le niveau phréatique, limite de la zone où le terrain est saturé d'eau. Si l'eau est en mouvement, la hauteur phréatique décroît de l'amont vers l'aval; en particulier, si l'eau s'élève de bas en haut, la pression sera plus élevée en profondeur que si l'équilibre régnait; toutefois, elle ne peut surpasser la pression supportée par la charpente de la roche, et due au poids des couches surincombantes; s'il en était autrement, la roche se souleverait ou se gonflerait.

Les considérations qui précèdent ne supposent rien quant à la température de l'eau. Sauf peut-être dans le cas de cavités de grandes dimensions, parcourues par un courant rapide (que nous laisserons de côté), il est évident que l'eau est à la même température que le terrain qu'elle imprègne.

La température en dessous de laquelle l'eau peut rester liquide dans les pores de la roche dépend de la pression propre de cette eau : elle augmente donc assez rapidement avec la profondeur sous le niveau piézométrique, atteignant 200° à 170 m, et 140° à 38 m.

Avant de rechercher quelles hypothèses on peut faire sur la répartition des températures avant l'explosion, il nous faut examiner le mécanisme de celle-ci.

Considérons un certain volume de la roche imprégnée d'eau, à une température supérieure à 100°, qui se trouvait dans un équilibre stable, pour la pression supportée par le fluide dans le terrain, la pression transmise au solide étant d'ailleurs plus élevée. Supposons que ces pressions s'abaissent brusquement; l'eau va se vaporiser dans chacun des pores de la roche, son volume augmentera beaucoup, la roche sera pulvérisée, et l'ensemble de l'eau et de la roche, transformé en un nuage de poussière, subira une forte détente. Si l'eau était seule, cette détente la refroidirait beaucoup, et une partie seulement serait transformée en vapeur (la température s'abaissant jusqu'à 100° C si la détente se produit jusqu'à la pression atmosphérique). Mais, ici, la vapeur, et l'eau qui subsistent, se réchauffent au contact des particules solides (dont la masse est beaucoup plus élevée) et il peut arriver que ceci permette la vaporisation totale de l'eau, qui pourra même se trouver surchauffée. Comme il arrive souvent en thermodynamique, le calcul ne permet d'aborder qu'un cas limite, celui où la détente envisagée ci-dessus, adiabatique, puisque nous supposons nuls les échanges de chaleur avec l'extérieur pendant la détente, se produirait d'une manière réversible.

On peut alors utiliser pour représenter la transformation le diagramme entropique de l'eau. Soit ω la porosité, c la capacité calorifique de la partie solide de 1 cm³ de roche, l'entropie de 1 cm³ du système est :

$$S = \omega S_e + c \log T$$

où S_e est l'entropie de 1 gr d'eau, et T la température absolue. Dans la détente adiabatique du système constitué par la roche et son eau d'imprégnation, S reste constant, et donc

$$S_e = -\frac{c}{\omega} \log T + \text{constante}$$

équation de la courbe que décrit le point représentatif sur le diagramme entropique de l'eau : la détente s'arrêtera lorsque la pression est tombée à 1 atm., mais deux cas sont possibles, suivant qu'à ce moment le point représentatif est dans le domaine de la vapeur humide, caractérisé par un titre x à la température de 373° K, ou de la vapeur surchauffée, à une température plus élevée T_1 .

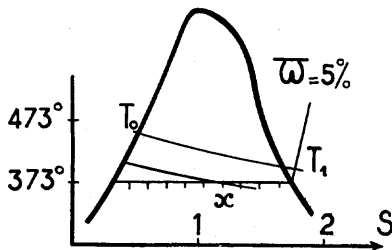


FIG. 1. — Représentation, sur le diagramme entropique de l'eau, de la détente de la roche humide surchauffée.

On peut, sans erreur sensible, considérer comme constantes la chaleur spécifique de l'eau (prise égale à 1) et celle de la vapeur à pression constante (0,49 au voisinage de 100°) et négliger les variations de volume de l'eau liquide. Il est alors possible de calculer l'état final, de la manière suivante : au point initial, à la température T_0 , l'entropie est

$$S_e = (c + \omega) \log \frac{T_0}{273}$$

Pour la vapeur surchauffée, à la température T_1 , l'entropie est :

$$S_e = (c + \omega) \log \frac{373}{273} + \omega \frac{L}{373} + (c + 0,49 \omega) \log \frac{T_1}{373}$$

et pour la vapeur humide, à 373°, de titre x

$$S_2 = (c + \varpi) \log \frac{373}{273} + x \varpi \frac{L}{373}$$

(L , chaleur de vaporisation à 100°, est égal à 539 cal)

En égalant à S_0 l'une ou l'autre de ces deux expressions, on trouve, suivant les cas, la valeur de x (< 1) ou celle de T_1 ($> 373^\circ$).

Il est facile de calculer le travail \mathcal{T} disponible dans cette détente, qui est effectuée contre la pression atmosphérique. On a donc

$$\mathcal{T} = \int (P - P_A) dV$$

Pour calculer \mathcal{T} , imaginons que les produits de la détente soient, sous la pression de 1 atm., refroidis jusqu'à 373° K, puis condensés, et qu'enfin, le système eau + roche soit ramené à la température initiale T_0 , par un échauffement, à volume sensiblement constant. Nous avons décrit un cycle fermé, qui fournit le travail \mathcal{T} . Le principe de la conservation de l'énergie nous permet donc d'écrire, selon le cas, l'une ou l'autre des équations :

$$\mathcal{T}/J = (c + \varpi)(T_0 - 373) - \varpi L - (c + 0,49 \varpi)(T_1 - 373)$$

$$\text{ou } \mathcal{T}/J = (c + \varpi)(T_0 - 373) - x \varpi L$$

La figure 2 donne le résultat de ce calcul et indique, en fonction de la porosité ϖ et de la température initiale T_0 , en posant $c = 0,5$ le titre en eau de la vapeur formée, si la température s'abaisse jusqu'à 100°, ou la température finale, ainsi que l'énergie mécanique que fournirait la détente, effectuée contre la pression atmosphérique.

Pour rendre plus concrètes les valeurs ainsi trouvées, on peut calculer la vitesse que cette énergie pourrait communiquer à la masse qui s'est détendue, et la hauteur à laquelle elle pourrait être soulevée :

\mathcal{T} :	10	100	500	$\times 10^6$	$\frac{\text{erg}}{\text{cm}^3}$
vitesse :	27,2	86	193		m/sec
hauteur :	37,6	376	1880		m

Les énergies ainsi dégagées sont considérables, et on se rend compte immédiatement qu'il doit exister des répartitions initiales de la température telles que le système soit en équilibre (tension de vapeur partout inférieure à la pression hydrostatique) et pour

lesquelles cependant, si la détente se produit, toute la masse du terrain peut être projetée bien au-dessus de la surface du sol : on est donc bien dans les conditions où une explosion est possible.

L'inspection de la figure 2 montre que l'énergie ne devient notable que pour les températures initiales de 150° ou plus, qui ne peuvent se rencontrer qu'à quelques dizaines de mètres de profondeur. La couche superficielle se comporte donc comme une couverture inerte, dont la destruction absorbera de l'énergie venant des couches plus profondes : l'explosion ne peut donc pas se produire à partir de la surface; on peut imaginer une crevasse pro-

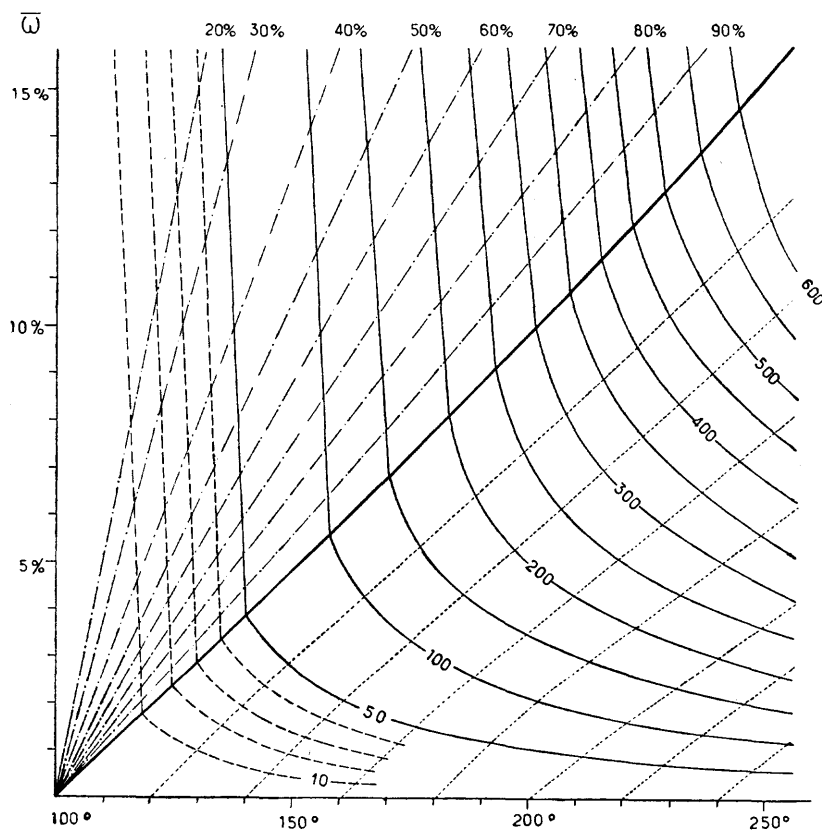


FIG. 2. — Énergie disponible (en 10^6 erg/cm³) dans la détente adiabatique réversible, en fonction de la température initiale et de la porosité \bar{W} . Le diagramme donne, de plus, en haut, le titre final de la vapeur (trait mixte), en bas, la température finale après détente (pointillé).

fonde, accidentellement vidée d'eau : les couches profondes se détendront vers cette crevasse, et le nuage de poussière et de vapeur

sera projeté vers le haut, érodant au passage les parois de la crevasse, qui donnera naissance à une sorte de cratère. En profondeur, au niveau des couches dont la détente fournit le plus d'énergie, l'explosion se propagera latéralement tandis que le cratère superficiel ne s'élargira peut-être que plus lentement.

A l'instant même de l'explosion, l'eau qui remplissait un pore doit se transformer en vapeur humide, puis se dessécher à mesure que la chaleur est transmise par conduction de l'intérieur des grains jusqu'à leur surface : si on assimile les grains à des sphères de rayon a cm, la moitié de la chaleur des grains sera dégagée en $0,297 a^2$ sec, les $9/10^{\circ}$ en $1,85 a^2$ sec et les $99/100^{\circ}$ en $4,18 a^2$ sec. Ce n'est donc que dans une roche de grain très grossier, ou dans laquelle l'eau n'occuperait que des fissures espacées, que ceci peut ralentir l'explosion d'une manière appréciable.

Revenons sur les approximations consenties pour estimer l'énergie mise en jeu.

L'hypothèse d'une détente adiabatique paraît satisfaisante, étant donné les volumes considérables mis en jeu, et la rapidité du phénomène. Le refroidissement du nuage de poussière et de vapeur peut être considéré comme pratiquement négligeable pendant la durée de l'explosion. Tout au plus peut-il se produire des mélanges entre des parties du nuage d'origines différentes : une partie surchauffée peut vaporiser partiellement de la vapeur humide provenant d'une assise superficielle, d'où une énergie disponible supérieure à la somme des énergies calculées pour les différentes parties.

Mais inversement, la détente n'est certainement pas réversible. Les grains de la roche cèdent leur chaleur à la vapeur, à la température de leur surface, qui est inférieure à celle qui règne encore dans leur cœur, et il existe certainement bien d'autres causes d'irréversibilité. Par conséquent, la détente produit moins de travail que ne l'indique le calcul ci-dessus. La différence doit se retrouver sous forme de chaleur : de la vapeur surchauffée se retrouvera à température plus élevée, et de la vapeur humide, à un titre en vapeur plus élevé que nous ne l'avons calculé. La perte de travail sera vraisemblablement moindre dans le second cas que dans le premier. L'énergie mécanique fournie par la détente prend la forme d'énergie cinétique, mais, s'il y a des mouvements turbulents, elle se transformera en chaleur, sans contribuer au phénomène éruptif proprement dit. Toute analyse précise est évidemment impossible, mais il est vraisemblable que l'ordre de grandeur au moins de l'énergie calculée reste valable.

La manière dont se produira l'explosion dépend, évidemment, de la répartition des températures qui se sera établie auparavant. Nous allons examiner, pour nous rendre compte de son influence, un certain nombre de cas schématiques.

Supposons d'abord — c'est évidemment un cas limite — que la température soit en chaque point la plus élevée compatible avec la présence d'eau liquide, c'est-à-dire telle que la tension de vapeur soit égale à la pression hydrostatique. La figure 3 donne la tempé-

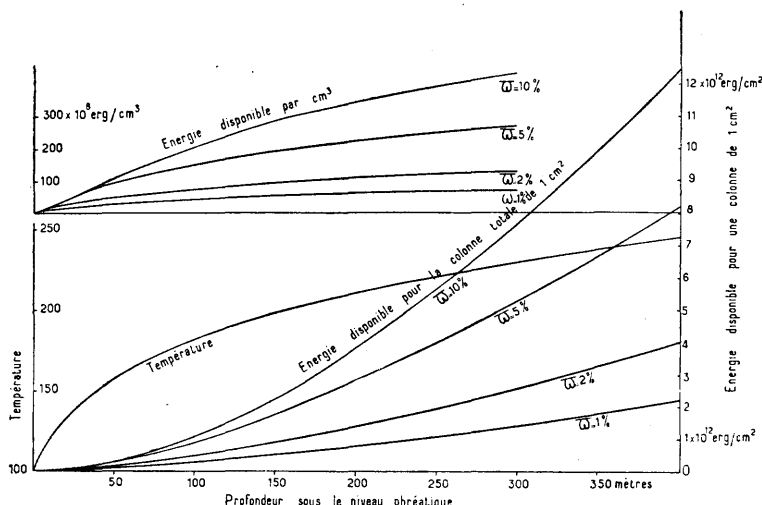


FIG. 3. — Répartition limite des températures, pour une pression hydrostatique égale à la tension de vapeur, et valeurs correspondantes de l'énergie disponible dans la détente adiabatique réversible, par cm^3 (en haut) et pour une colonne de 1 cm^2 descendant jusqu'à la profondeur considérée (en bas).

rature ainsi calculée (compte tenu de la densité vraie de l'eau), en fonction de la profondeur sous le niveau phréatique.

Théoriquement, s'il y avait un flux d'eau de bas en haut (par exemple, d'eau juvénile provenant d'un magma) à travers des assises peu perméables, la pression de l'eau pourrait être un peu plus forte, et donc la température plus élevée, mais ceci ne doit guère jouer que très localement. Pour différentes valeurs de la porosité, on a calculé l'énergie disponible dans une détente adiabatique réversible, contre la pression atmosphérique, par centimètre cube, et pour une colonne s'étendant jusqu'au jour, d'un cm^2 de section.

Si l'on suppose 10 m de terrain sec au-dessus du niveau phréatique, et que l'on considère une épaisseur de 210 m, on voit qu'une explosion devient théoriquement possible (énergie suffisante pour éléver toute la masse à 500 m de haut) pour une porosité de 0,3 % seulement.

Mais il s'agit là d'une répartition très particulière de la température.

On a refait un calcul analogue en supposant le gradiant de température uniforme, la température superficielle de 10° , et le niveau phréatique à la surface et en prenant pour la possibilité d'une explosion un critère moins sévère (énergie dans la détente adiabatique réversible suffisante pour soulever la colonne de terrain de sa hauteur). La hauteur du terrain que l'on peut supposer saturée d'eau est d'ailleurs limitée par la nécessité que la tension de saturation ne dépasse pas la pression statique. En dessous, il pourrait y avoir une roche non poreuse ou anhydre.

Pour une porosité de $\varpi = 2\%$, l'explosion paraît n'être possible pour aucun gradiant uniforme.

Pour $\varpi = 5\%$, elle est possible pour un gradiant compris entre 1° par mètre (couche épaisse de 200 m) et 2° par mètre (couche épaisse de 85 m).

Pour $\varpi = 10\%$, on peut aller d'un gradiant de $0,5^\circ$ par mètre (épaisseur 470 m), à 2° par mètre (épaisseur 75 m).

Si le gradiant est plus faible que les valeurs indiquées l'énergie fournie par la détente est insuffisante pour soulever toute la colonne de terrain, si il est plus fort, les conditions correspondant à la vaporisation de l'eau sont atteintes à une profondeur faible, et, dans la couche que nous pouvons envisager, les parties superficielles, qui fournissent peu ou pas d'énergie, jouent un rôle trop considérable pour qu'une explosion soit possible.

On notera que les gradiants envisagés sont d'un tout autre ordre de grandeur que ceux que l'on observe ordinairement (1° pour 30 m, pouvant s'élever par place à 1° pour 8 m), constatation rassurante, sinon inattendue. Il convient donc d'examiner comment a pu se faire le réchauffement, et si il y avait quelques chances pour qu'il conduise à un gradiant uniforme.

La première idée qui peut venir à l'esprit est que les gradiants très élevés dont nous avons besoin pourraient avoir la même origine que le gradiant normal, et résulter simplement d'une augmentation considérable du flux de chaleur transmis par conduction. Mais cette hypothèse soulève de grosses difficultés; de tels gradiants se traduiraient par la fusion de toutes les roches à très faible

profondeur — de l'ordre de 1000 à 2000 m — et même dans ces conditions, le gradiant au voisinage de la surface n'approcherait de sa valeur moyenne par simple conduction qu'au bout d'un temps très long, se chiffrant par dizaines de milliers d'années.

D'autre part, comme nous l'avons montré dans une autre publication (2), l'existence d'eau imprégnant le terrain modifie sensiblement le régime thermique : si l'on suppose un réchauffement progressif, des complications surviennent lorsque le gradient atteint 1° pour 7 m 50. A ce moment, en effet, le point critique se trouve atteint vers 2700 m de profondeur. Sauf dans le cas où les roches régnant à ce niveau seraient tout à fait compactes et dépourvues d'eau, il apparaîtra une coupure entre le domaine de l'eau et celui de la vapeur. Mais celle-ci, plus légère, ne peut rester au-dessous, et elle tendra à s'élever en formant une série de courants ascendants, dans l'intervalle desquels l'eau du terrain tendra au contraire à descendre : la vapeur s'élèvera de plus en plus haut, jusqu'à atteindre éventuellement la surface et transportera la chaleur venant de la profondeur, sous forme de chaleur latente ; la stratification thermique régulière ne peut donc subsister.

Sauf le long des colonnes ascendantes de vapeur, le gradient restera voisin de 1° pour 8 m. Si l'échauffement se poursuit, les zones de vapeur s'étendront jusqu'à ce que tout le terrain soit progressivement desséché.

Au total, l'hypothèse selon laquelle la répartition des températures susceptible de conduire à une explosion phréatique résulterait d'un réchauffement général de l'écorce apparaît donc comme très peu vraisemblable.

On est donc conduit à chercher un mode d'échauffement beaucoup plus local, et en quelque sorte, accidentel. Imaginons par exemple une intrusion de roche fondu, se produisant à une profondeur relativement faible, au milieu de terrains humides. L'eau sera inévitablement vaporisée à son contact, la pression de la vapeur peut très facilement dépasser la pression supportée par la roche solide, et donc repousser ou soulever celle-ci. Ce peut être l'origine de secousses ou de grondements souterrains. Mais en même temps, la superficie de la roche intrusive se refroidit rapidement, constituant une pellicule peu conductrice. La vapeur s'infiltre dans le terrain ; et sa pression baissera, sans que la roche soulevée reprenne immédiatement sa place, et ceci peut faciliter la pénétration de la roche intrusive.

(2) Jean Goguel. Le régime thermique de l'eau souterraine. *Annales des Mines*, X, 1953, p. 3 à 32, Paris.

La vapeur qui s'infiltre dans le terrain poreux rencontre bientôt une roche beaucoup plus froide, qu'elle échauffera en se condensant. Ce mode d'échauffement, pour peu que la roche ait une certaine perméabilité, peut être beaucoup plus actif que la simple conduction : la chaleur apportée par la condensation de la vapeur s'accumule dans chaque couche jusqu'au moment où la température de saturation est atteinte : à partir de cet instant, la vapeur peut progresser plus loin, et contribuer à l'échauffement des assises plus élevées. La répartition des températures peut donc, semble-t-il, tendre à se rapprocher de celle que nous avions envisagée en premier lieu (température telle que la tension de vapeur soit égale à la pression hydrostatique) ; nous avons vu qu'une telle répartition était si favorable à une explosion, que celle-ci est possible, même pour une porosité très faible. Par contre, pour que le transfert de chaleur puisse se faire par le mécanisme envisagé — dégagement et condensation de vapeur — il faut que la roche soit suffisamment perméable.

Ce mode de transfert peut également expliquer le déclenchement de l'explosion : si, au lieu de progresser régulièrement de couche en couche, la vapeur atteint une fissure, elle peut déboucher au jour, ce qui entraîne une baisse brutale de pression dans la fissure. Cela peut suffire pour provoquer l'explosion des roches avoisinantes, et la projection violente de leurs débris, explosion qui se propagera dans toute la masse échauffée.

Si, comme nous venons de le supposer, c'est une masse intrusive laccolithique qui constitue la source de chaleur, il est vraisemblable que les couches situées immédiatement à son contact auront leurs pores occupés plutôt par de la vapeur, que par de l'eau. Leur détente fournira donc beaucoup moins d'énergie, et il est vraisemblable qu'elles ne participeront guère à l'explosion ; même sans tenir compte des débris qui peuvent retomber dans le cratère, on doit donc s'attendre à ce que l'explosion ne dégage pas la masse intrusive qui l'a provoquée.

Les accumulations de cendres volcaniques, qui ont des porosités élevées, sont évidemment le matériel de choix, dans lequel on doit s'attendre à des explosions phréatiques, si des intrusions de magma frais s'y produisent à une ou quelques centaines de mètres de profondeur. Mais il n'est pas exclu que d'autres types de roches ne puissent être le siège d'explosions phréatiques. La communication

de M. l'abbé Bordet³ pose la question pour les roches du socle cristallin. D'après ce qui précède, une fissuration assez marquée suffisait peut-être à y permettre des explosions; on peut même se demander si la première intrusion du magma n'aurait pas contribué à déterminer, ou tout au moins à accentuer, cette fissuration.

Jean GOGUEL.

(3) P. Bordet. Les cratères d'explosion de l'Ahaggar (Sahara Central). *Bull. volcanologique*, Série II, t. XVII, Napoli, 1955, pp. 127-134.



THE GREAT LAKES, A SOURCE OF TWO-SECOND FRONTAL MICROSEISMS

by Rev. J. LYNCH, S. J. (Fordham University).

The problem presented here has taken some five years of preparation. Parts of it have already appeared in print. These will only be mentioned in passing. For purposes of continuity however it has been deemed practical to give a brief resumé of the whole problem leading up to the present stage. Since July 1947 (1) the records of 2 second microseisms have been studied intensively at Fordham University. It had been suggested by several and confirmed by the writer that these were associated with the passage of cold fronts. It was presumed that these micros were generated when the cold front passed on to the Atlantic. To investigate the precise source of these microseisms, a tripartite station was set up first at Fordham University (2) then at the New York State Maritime Academy (3). The predominant source of these micros was off the coast, but the occasional appearance of a source of these microseisms to the west of New York and hence possibly on land suggested our setting up a tripartite station upstate away from New York traffic. This was set up (4) near Poughkeepsie, New York, some three miles north of the town on the grounds of our college there, adjoining the Roosevelt estate. Records from this station clearly confirmed a source of the microseisms almost due west of Poughkeepsie. Moreover, two of the instruments happened to be just in line with the source, giving us a reliable value for the velocity of the microseisms as 1/2 mile per second. On March 2 and March 5, 1951, when the tripartite group indicated a source to the west, weather map indicated a cold front moving southeastward from the Great Lakes. Since the Hudson River is a sizable body of water west of Poughkeepsie, it was thought advisable to set up a tripartite group on the other side of the river to eliminate the Hudson as a possible source. This was done at West Park (5). Results obtained here indicated a persistent source to the West, thus eliminating the Hudson River. Moreover two predominant sources were observed over a period of a month — one from due west and one from N. W. Lake Erie is 350 miles due west while Lake Ontario is 175 miles N. W. This suggested to

us for the first time that the Great Lakes were probably the source of our 2 second microseisms. We felt it advisable now to set up a tripartite station to the South of the Great Lakes. We selected Hot Springs, North Carolina, as our site since we had a mission there (6) near the Tennessee border. This station indicated a persistent source du North of Hot Springs. Lake Erie is due North of Hot Springs and due West of Poughkeepsie and West Park and we now felt reasonably sure that the origin of our 2 second microseisms lay in the Great Lakes. Longuet-Higgins had advanced the theory that microseisms can be caused by standing waves in large bodies of water. On the basis of this theory it seemed reasonable to suppose that a cold front moving down from Polar regions and meeting warm air over the lakes would disturb the lake surface and generate sizable waves. These waves on reaching the shore would be reflected and would give rise to standing waves on interfering with the approaching direct waves. These standing waves pounding on the lake bed would give rise to the ground microseisms which travel over the continent with a velocity of half a mile per second. Thus the passage of a cold front over the lakes is announced by seismographs in New York in a matter of minutes. When the cold front itself arrives over New York a day or so later, it gives rise to microseismic waves caused by standing waves produced in the Atlantic. This plausible view suggested that we now turn our attention to the Great Lakes themselves which brings us to



FIG. 1. — The under water Seismometer, housed in watertight case.

our present stage in the problem. Prior to going to the Great Lakes themselves we experimented in the Sound off Fort Slocum near New Rochelle (7). Our experiments here enabled us to design a horizontal instrument which could be suspended several feet below the surface of the water and leveled by means of turnbuckles from the

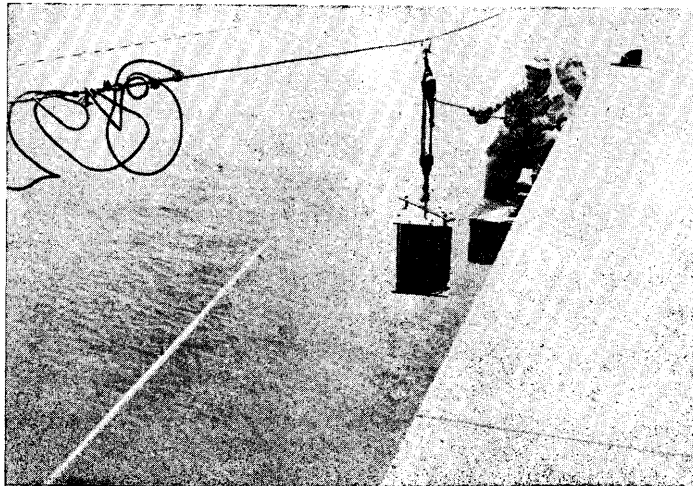


FIG. 2. — The Seismometer being lowered into Lake.

surface. A description of this instrument was presented at the last meeting of the Geophysical Union and will not be repeated here. A companion vertical instrument of sufficiently long period was not so easy to design. Since it has not been described elsewhere a brief description seems advisable. Since the ground microseisms are of two seconds period, Longuet-Higgins' theory postulates progressive water waves of 4 seconds to give rise to the necessary standing waves of 2 seconds period. We needed therefore a pendulum of 4 seconds free period coupled to a rugged Galvanometer of about the same period. We wound a coil to match the General Electric 232G9 Galvanometer with a critical damping period of 900 ohms, period 3.6 seconds and sensitivity .006 microamperes per mm. scale division. The long period is obtained by introducing buoyancy to counteract the effective pull of the coil on the vertical spring. The moving mass consists of the coil attached rigidly to a heavy rectangular brass plate. Four hollow copper spheres attached to this plate counteract its weight by buoyancy when the whole is immersed in kerosene.

The mass is suspended by a brass spring from the center of the cross piece of a gallows. Two very fine beryllium copper springs attach two edges of the suspended brass plate to these two uprights to prevent swaying motion of the mass. Damping is electromagnetic by means of copper plates attached to the flat faces of the coil. The diagram sufficiently explains the details of the pendulum. Kerosene was chosen for buoyancy purposes simply to prevent rust of the magnet. The instrument is housed in a heavy copper cylinder 18" high \times 12" diameter, — the whole weighing some 200 lbs. At first the instrument was suspended by steel cable five feet below the surface of Lake Michigan from an arm projecting six feet out from the pier. The depth of the water here is about 10 feet. The swaying motion of the instrument as so suspended proved to be too great. We then drove two 20 ft. 2" steel pipes one each side of the instrument into the bed of the lake at an angle from the dock — anchoring them at the top to the dock. Two corners of the bottom of the instrument were then wired to these pipes. This effectively stopped the swaying of the instrument and allowed free access of wave motion to it on all sides. We allowed the instrument to operate in this position for two days and obtained good records of the wave movement, one of which is reproduced here. The period of the waves varies somewhat but averages about 3.5 seconds. This confirmed what we had previously observed while sitting on the Lake shore. Timing the waves as they rolled by a 20 ft. dock we found the predominant period to be 3.5 secs.

Moreover, as these waves rolled into the dock at roughly a 45 degree angle, you could watch the reflected wave move out from the dock. Sometimes the reflected wave was quite conspicuous as a single wave — at other times complicated interference patterns would result. After running the instrument for two days, to make sure that it faithfully recorded water waves we left for New York and were one day's drive from Chicago when an unusual seiche rolled along the Michigan shore line. The water washed some 8 feet over the dock on which we had been working. Unfortunately it tore the electrical lead wires from the instrument and broke the latter loose from its moorings, leaving it suspended by the steel cable but swaying violently. A new type of mooring is being designed which we hope will withstand any wave action. The instrument will then be kept running and the daily Lake records compared with the land records in New York. If our two second microseisms are caused by standing waves in the lakes then increased activity

on our instruments in New York should be preceded some 25 minutes earlier by increased activity on the Lake instruments.



FIG. 3. — First record of water waves — dots indicate minute marks.



FIG. 4. — Wave action on Lake while above record was being made.

Our reason for choosing Lake Michigan for our first trial was because Loyola University, whose property borders the Southern end of the Lake offered to cooperate and house and run the recorder for us. We are greatly indebted to Father Donald Roll, S. J. and his assistants for their very generous help in this regard. Lakes Erie and Ontario are of course much nearer and it would probably be wise to install similar instruments both in Erie and Ontario. For the present however, we plan to run the Lake Michigan instrument alone and find out the extent of the correlation between progressive wave activity on the Lake and two second microseismic activity in New York. Owing to the difficulty of levelling the horizontal instrument, we plan to operate the vertical instrument only for the present. We should like to stress the following two facts :

- 1) We have observed and recorded progressive waves in Lake Michigan of the right period to produce two second ground oscillations.
- 2) We have succeeded in installing an underwater seismograph capable of recording progressive waves in the lakes.

We are fully aware of many difficulties still to be ironed out, but felt that this attempt to track down the origin of one group of frontal microseisms should be given the light of day — as we have now done — with some timidity.

BIBLIOGRAPHY :

- (1) LYNCH (J. Joseph), S.J. : *Earthquake Notes*, Eastern Section Seismological Society of America, Vol. XX, no. 2, December, 1948, p. 15.
- (2) LYNCH (J. Joseph), S.J. : *Earthquake Notes*, Eastern Section Seismological Society of America, Vol. XX, no. 4, June, 1949, p. 35.
- (3) LYNCH (J. Joseph), S.J. : « An Investigation of Two Second Microseisms Associated with Cold Fronts and a New Method for Tracking the Cold Front Center », reprinted in U.S.A. from *Transactions of American Geophys. Union*, Vol. 31, 1950, pp. 525-528.
- (4) LYNCH (J. Joseph), S.J. : *Earthquake Notes*, Eastern Section Seismological Society of America, Vol. XXII, No 1, March, 1951, p. 6.
- (5) « The Great Lakes, a Source of Two-Second Frontal Microseisms », *Trans. American Geophys. Union*, Vol. 33, pp. 432-34, 1952.
- (6) LYNCH (J. Joseph), S.J. : *Earthquake Notes*, Eastern Section Seismological Society of America, Vol. XXIV., Number 2, June 1953, p. 17.
- (7) LYNCH (J. Joseph), S.J. : *Earthquake Notes*, Eastern Section Seismological Society of America, Vol. XXIV., Number 3-4, September-December, 1953, p. 29.

SUR LES MICROSEISMES DE PRAHA

par A. ZATOPEK (Université Charles, Praha).

En considérant le fait que les microséismes montrent une relation étroite avec les éléments météorologiques, surtout ceux situés sur les océans, il paraît particulièrement intéressant de les étudier dans une station continentale comme celle de Praha⁽¹⁾, située au centre de l'Europe. Ici, on peut attendre a priori des effets des phénomènes se produisant dans la zone frontale entre l'Amérique du Nord et le continent européen aussi bien que ceux appartenant au régime méditerranéen.

La présente étude s'étend principalement sur la période du 1^{er} janvier 1948 au 31 mai 1954. Elle est basée sur les inscriptions d'un pendule horizontal Wiechert⁽²⁾ et partiellement aussi de deux séismomètres à torsion⁽³⁾. Une représentation graphique des périodes et amplitudes⁽⁴⁾ déterminées pour les termes principaux météorologiques à 0^h, 6^h, 12^h et 18^h T. M. G. respectivement, dans un système de coordonnées à quatre axes parallèles de temps (voir p. ex. fig. 1, 2, 3) permet de suivre facilement d'une manière continue les variations des microséismes avec le temps et de les confronter avec les cartes synoptiques correspondantes⁽⁵⁾. Cette méthode est utile de même pour comparer l'allure des microséismes de différentes stations. Les microséismes étant très faibles en été, on n'a représenté que les intervalles allant de septembre à mai pendant les années étudiées. La méthode fournit une vue d'ensemble des valeurs représentées et en même temps chacune de celles-ci peut être examinée immédiatement, soit comme individu, soit par rapport à des valeurs voisines. Les graphiques sont bien utilisables aussi pour des déductions du caractère statistique.

Partant de l'image générale, nous avons choisi la plupart des cas, caractérisés par un accroissement rapide des amplitudes, pour une étude plus détaillée. Celle-ci a été complétée par l'analyse d'un nombre de situations, traitées déjà dans les mémoires publiés antérieurement sur les microséismes européens — voir Bibliogra-

1. $\phi = 50^{\circ}04,2' N$, $\lambda = 14^{\circ}26,0' E$, $h = 225$ m, sous-sol : Ordovicien.

2. Masse 1000 kg. comp. N et E; constantes moyennes : $T_0 = 10$ sec, $V_0 = 220$, $\epsilon = 5 : 1$, $r/T_0^2 = 0,003$ mm/sec².

3. Comp. N et E, $T_0 = 2 - 5$ sec, $V_0 = 1500$, $\epsilon = 5 : 1 - 15 : 1$.

4. Valeurs moyennes d'une série de mesures faites dans les intervalles respectifs de $0^h \pm 30^m$, $6^h \pm 30^m$ etc.

5. Cartes de l'Institut Hydrométéorologiques de Praha; Bulletin Quotidien d'Etudes de l'Etablissement Central de la Météorologie, Paris.

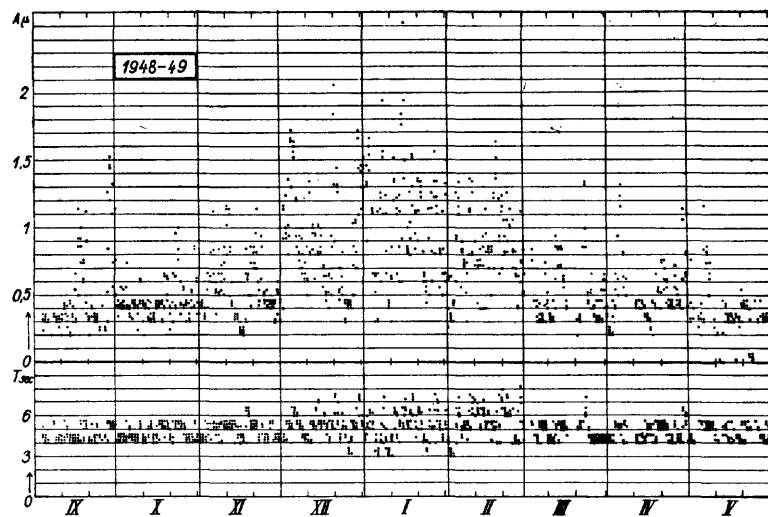


FIG. 1. — Les amplitudes horizontales $A = \sqrt{A_x^2 + A_y^2}$ et les périodes moyennes $T = \frac{1}{2}(T_N + T_E)$ des microséismes à Prague pour 0^h, 6^h, 12^h et 18^h T.M.G. pendant l'époque du 1^{er} septembre 1948 au 31 mai 1949. Les bases respectives pour 6^h, 12^h et 18^h sont graduellement déplacées vers le haut.

phie (1)-(10). Pendant l'analyse, il a été considéré la position, la profondeur, l'étendue et le mouvement des dépressions (quelque-

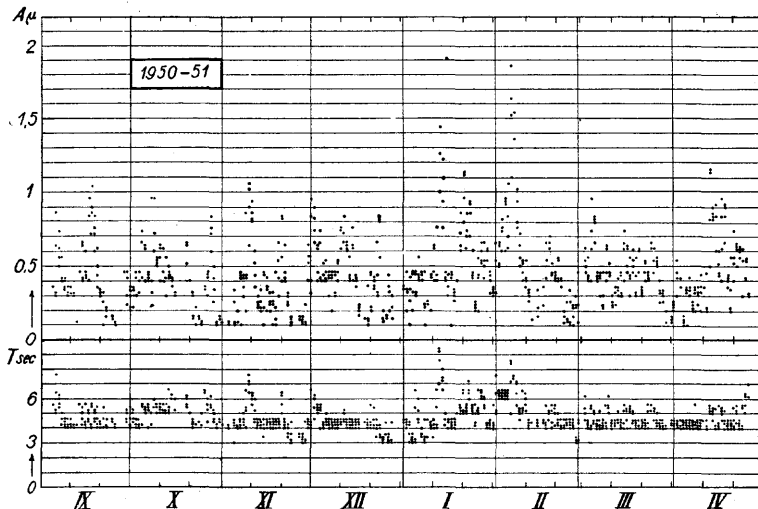


FIG. 2. — Les amplitudes A et les périodes T des microséismes à Prague pour 0^h, 6^h, 12^h et 18^h T.M.G. pendant l'époque du 1^{er} septembre 1950 au 30 avril 1951.

fois aussi des hauteurs) barométriques, le caractère et la marche des fronts, la force et la direction du vent, la profondeur de la

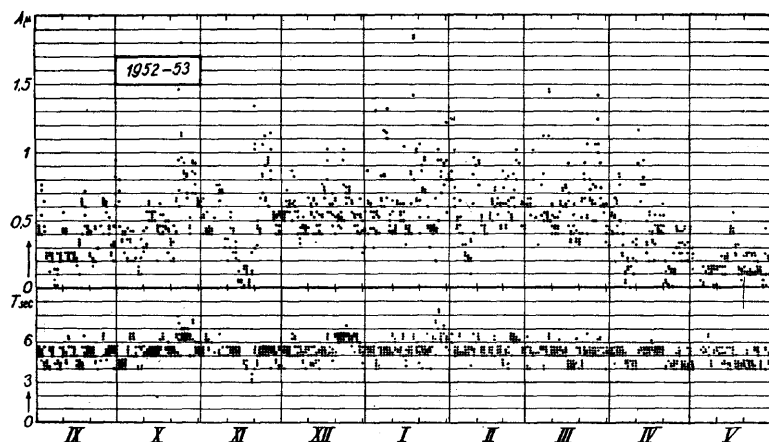


FIG. 3. — Les amplitudes A et les périodes T des microséismes à Prague pour 0^h, 6^h, 12^h et 18^h T.M.G. pendant l'époque du 1^{er} septembre 1952 au 31 mai 1953.

mer, etc... Une attention particulière a été concentrée à des cas où, malgré la présence de dépressions profondes, on n'a observé aucune influence sur les amplitudes des microséismes. Un phénomène perturbateur, c'est-à-dire l'agitation causée par le vent passant au-dessus de la station, a été soumis à une étude individuelle.

Passons maintenant en revue les résultats :

1° Les microséismes sont inscrits à Praha le plus fréquemment en forme de groupes des oscillations sinusoïdales dont les périodes se trouvent entre 3 et 9 secondes, la fréquence maximum étant voisine de 4,5 secondes. Les amplitudes qui généralement sont plus grandes à la composante N ne dépassent jamais 3 microns. Elles sont donc considérablement inférieures à celles de Strasbourg, de De Bilt et d'Uppsala, et sont de l'ordre de celles de Iéna. On pourrait penser ici à des causes géologiques qui, en effet, entrent en jeu pendant la propagation des ondes séismiques à travers la masse de Bohême. Dans les inscriptions des instruments à torsion on a trouvé aussi des périodes de 2 secondes qui sont probablement de l'origine locale, car elles ne sont jamais observées sur les séismogrammes du Wiechert horizontal, éloigné 240 m vers l'est et reposant sur une autre formation géologique. Cette interprétation a reçu un appui par un cas bien étudié (11) des microséismes locaux observés à Praha en 1940.

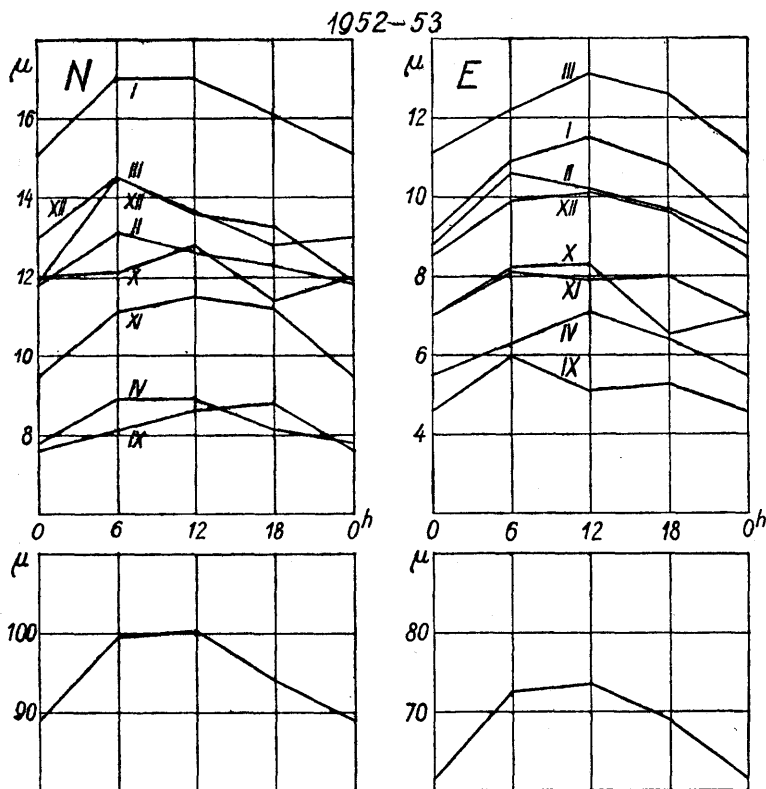


FIG. 4.a. — Variation diurne des amplitudes mensuelle et annuelle: a) 1952-1953.

On peut dire en général que les situations météorologiques plus compliquées se manifestent dans les microséismes par des interférences qui indiquent une action simultanée de plusieurs sources, mais il est difficile de présenter des corrélations satisfaisantes. Par contre, l'influence des vents d'ouest qui passent au-dessus de la station avec une vitesse parfois supérieure à 90 km/h et produisent des perturbations des microséismes, a pu être interprétée comme une réaction des appareils à des oscillations et inclinaisons du sol, causées par de brusques changements de la pression du vent sur les parties exposées des bâtiments.

2° Le caractère général des variations des microséismes de Praha en fonction du temps montre une ressemblance, qui est quelquefois surprenante, avec l'allure des microséismes à De Bilt, Iéna, Strasbourg⁽⁶⁾ et Uppsala. Les différences individuelles ont pu être bien souvent expliquées par des effets de la distance entre la source

6. L'auteur est très obligé à M. le Professeur J.-P. Rothé, Directeur de l'Institut de Physique du Globe à Strasbourg, qui lui a fait parvenir les données de Strasbourg en manuscrit avant leur publication.

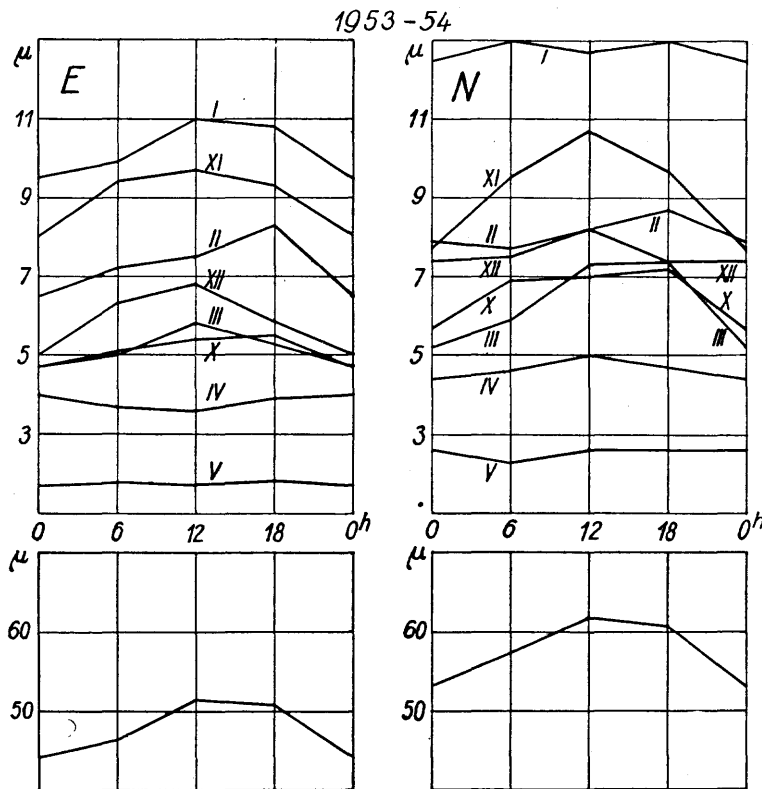


FIG. 4 b. — Variation diurne des amplitudes mensuelle et annuelle : b) 1953-1954

et la station, par l'influence différente des fronts et d'autres agents météorologiques ou par des conditions géologiques. D'autre part, une comparaison analogue avec des données de Rome ou de Trieste indique — contrairement à ce qu'on pourrait expecter — que les effets du régime méditerranéen ou adriatique ne sont pas observables dans nos microséismes.

3° Les microséismes de Praha sont alors dominés exclusivement par le régime de la zone frontale entre le Labrador, le Groenland et la Scandinavie. En effet, les changements synoptiques dans cette zone ont une influence décisive sur la génération et sur l'évolution des microséismes de Praha. L'augmentation des amplitudes la plus intense a été observée quand une dépression profonde, avec le centre situé à l'est de 30° environ de longitude d'ouest et au nord de 50° de latitude du nord, procède rapidement vers l'est ou vers le nord-est. A mon avis, on peut parler pour Praha de l'existence des positions critiques des centres cycloniques accentués. Elles se

trouvent dans une région située vers le sud et sud-ouest de l'Islande et sur la mer entre l'Islande, l'Écosse et la Scandinavie. On observe aussi des microséismes puissants lorsque les centres des cyclones traversent la partie septentrionale de la Mer Baltique.

A l'extérieur des régions critiques mentionnées, l'effet des cyclones sur les microséismes a été trouvé insignifiant, excepté la partie extrême du nord de la Norvège.

Il a été observé plusieurs fois qu'au cours de l'époque étudiée une dépression bien accentuée et possédant le minimum dans la zone critique n'a causé, contre toute attente, aucune augmentation des amplitudes microsismiques. Il s'agissait dans ces cas-là des cyclones stationnaires dont les centres se déplaçaient relativement très lentement.

Il est difficile à préciser l'influence des fronts sur les microséismes étudiées. Si elle existe, elle est généralement peu marquée. Les fronts froids procédant vers la côte norvégienne semblent causer une variation des amplitudes, légère et de caractère irrégulier. Il n'a pas été possible de constater avec sûreté un effet du passage du front lui-même de la mer au continent. Un résultat plus sûr a été obtenu en corrélant les microséismes avec les passages des fronts à travers la Mer Baltique. Là, le passage d'un front vers l'est a été accompagné, dans un nombre de cas, d'un accroissement considérable des périodes et amplitudes. L'explication par des ondes stationnaires dans la Mer Baltique me semble la plus probable.. On n'a pas réussi à prouver un effet des vents, excepté pour la partie centrale (et peut-être aussi septentrionale) de la côte de Norvège. D'après la coïncidence avec les forts vents d'ouest ou du nord-ouest dans cette partie de la côte tenant compte des résultats de M. Bath (1), il semble justifié d'attribuer une part des microséismes à période de 4-5 secondes au « surf effect ».

Quant aux périodes observées, le résultat connu que les périodes de microséismes augmentent généralement avec les amplitudes a été statistiquement confirmé aussi par notre étude. Néanmoins, en cas individuels, on trouve des exceptions. Nos observations conduisent à la conclusion que les dépressions étendues et bien accentuées, qui se forment au voisinage de l'Islande, donnent la naissance aux microséismes à période supérieure à 5 secondes, tandis que les périodes plus courtes sont plutôt caractéristiques pour les microséismes qui se forment sous des circonstances régulières dans le voisinage de la côte norvégienne. Les longues périodes qui coïncident avec les phénomènes sur la Mer Baltique ont été déjà mentionnées.

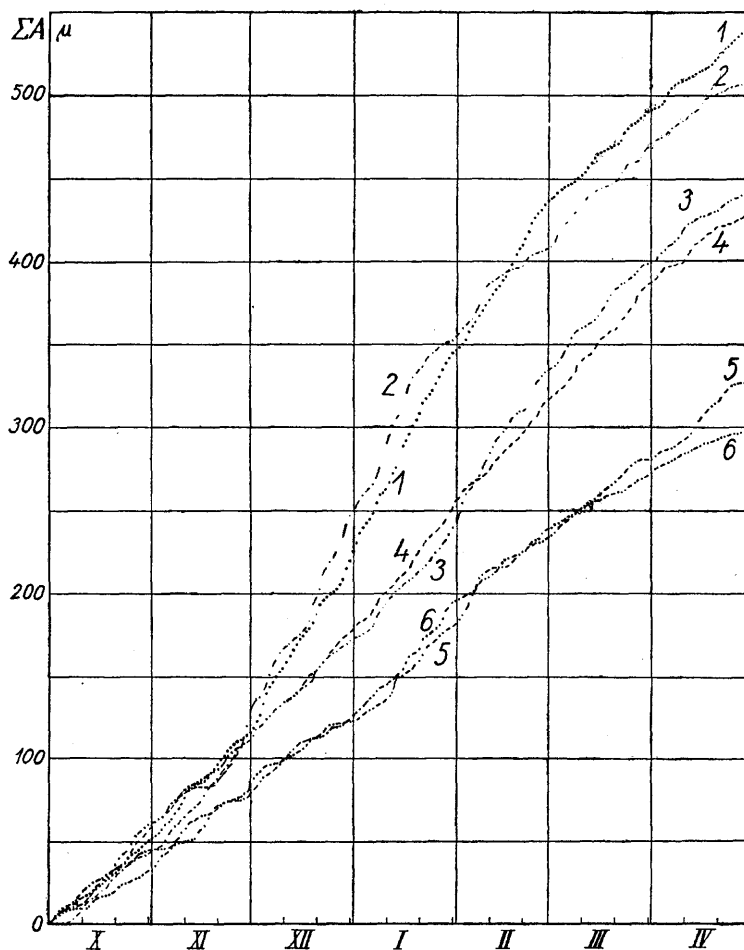


FIG. 5. — Courbes des sommes des amplitudes en fonction du temps : 1) 1948-1949, amplitude moyenne $A^* = 0,64 \mu$; 2) 1951-1952, $A^* = 0,60 \mu$; 3) 1949-1950, $A^* = 0,52 \mu$; 4) 1952-1953, $A^* = 0,51 \mu$; 5) 1950-1951, $A^* = 0,38 \mu$; 6) 1953-1954, $A^* = 0,35 \mu$. Là, où les microséismes ont été perturbés par des coups de vent ou par des tremblements de terre, on a introduit des valeurs interpolées. A cause de l'uniformité on n'a pas considéré le 29 février 1952.

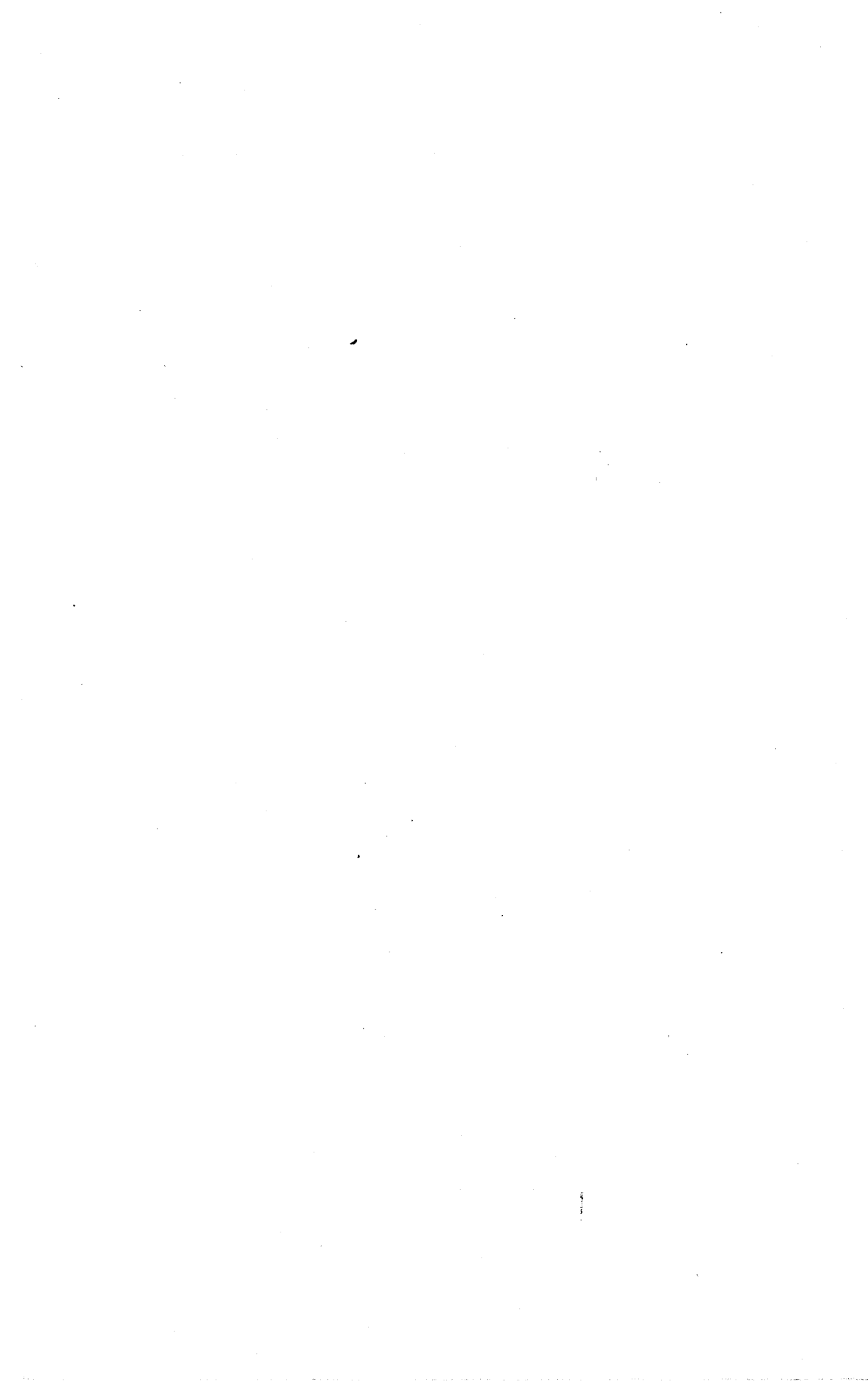
4° Une statistique des valeurs d'amplitudes représentatives indique pour Praha l'existence d'une variation diurne des microséismes (*fig. 4 a, b*) avec un minimum vers minuit et un maximum entre 12^h et 18^h T. M. G. Pour Uppsala une telle variation n'a pas été prouvée (1). On ne peut donc dire si notre résultat a une valeur plus générale.

5° Pendant la recherche de corrélations entre les microséismes et les agents météorologiques ce sont les méthodes de la statistique graphique qui offrent de nombreux avantages. La figure 5 en présente un exemple. On y a représenté en fonction du temps la croissance des sommes des amplitudes pour les « périodes d'activité » tombant dans l'intervalle étudié. Les courbes 1-6 ne sont que des courbes intégrales déduites de la représentation fondamentale (voir fig. 1-3). On pourrait les approximer par des courbes nettes et sans à coup si l'on voulait donner une analyse complète, mais ce n'est pas nécessaire dans le cas considéré. On voit p. ex. immédiatement que pendant la saison de 1948-49 et celle de 1951-52 l'activité microsismique à Praha, mesurée par les amplitudes, a été à peu près deux fois plus forte que pendant la saison de 1950-51 ou celle de 1953-54. On voit plus loin que les courbes 1 et 2 admettent facilement une approximation par des courbes possédant un point d'inflexion; il est beaucoup plus difficile de trouver un tel point sur les courbes 4 et 5. L'existence d'un ou de plusieurs points d'inflexion sur une courbe des sommes indique qu'il existe une qualité typique de l'ensemble considéré. Dans les cas représentés par les courbes 1 et 2, cette qualité typique est le renforcement considérable des microséismes pendant la période de décembre à février qui n'a pas lieu sur les courbes 4, 5 et 6 respectivement. L'analyse des causes de tels phénomènes pourrait contribuer à l'étude de la circulation générale.

BIBLIOGRAPHIE.

- (1) BATH (M.), An Investigation of the Uppsala Microseisms, Medd. Met. Inst. Uppsala No. 14, Uppsala 1949.
- (2) BATH (M.), The microseismic importance of cold fronts in Scandinavia, Arkiv för Geofysik, 1, 267-358, 1951, Stockholm.
- (3) BATH (M.), The distribution of microseismic energy with special reference to Scandinavia, Arkiv för Geofysik, 1, 359-393, 1951, Stockholm.
- (4) BATH (M.), The Problem of Microseismic Barriers with Special Reference to Scandinavia, Geol. Foren. Forhandl., 74, 427-449, 1952, Stockholm.
- (5) BATH (M.), Comparison of Microseisms in Greenland, Iceland and Scandinavia, Tellus, 5, 109-134, 1953.
- (6) BERNARD (P.), Étude sur l'agitation microsismique et ses variations, pp. 1-77, Annales de l'Inst. de Phys. du Globe, Université de Paris, tome XIX, 1941, Paris.
- (7) BONCHKOVSKY (V. F.), Microseisms and their causes (en russe, résumé en anglais), Publ. de l'Inst. Séismol. de l'Ac. des Sc. de l'U. R. S. S., n° 120, 1946, Moscou-Leningrad.
- (8) CALOI (P.), Sull' origine di microsismi con particolare riguardo all' alto Adriatico, Annali di Geofisica, 4, 525-577, 1951, Roma.

- (9) D'HENRY (G.), MORELLI (C.), Sulle cause dei microsismi, Annali di Geofisica, 2, 281-290, 1949, Roma.
 - (10) D'HENRY (G.), Sulla natura fisica dei microsismi, Annali di Geofisica, 3, 87-94, 1950, Roma.
 - (11) ZATOPEK (A.), Microséismes et le mouvement des dépressions barométriques (en tchèque), Bulletin Météorologique (Meteorologické zprávy), 1, 129-131, 1947, Praha.
 - (12) ZATOPEK (A.), On the Relation between the Gustiness and the Structure of the Wind-unrest of Seismographs, Geofysikální Sborník, année 1953, 65-82, 1954, Praha (en tchèque, résumés en russe et en anglais).
-



MICROSEISMS AT COCHIN

by H. M. IYER and J. N. NANDA.

ABSTRACT.

Recently a microseism pendulum of 3 sec. period obtained by the courtesy of Carnegie Institution, Washington has been set up at I.N. Physical Laboratory, Cochin. The records are taken on a commercial tape recorder run at a very low speed. The analysis is made when the tape is running at a high speed, thus bringing the microseismic frequency into the sonic region. Preliminary analysis shows the preponderence of four to six second periods in the microseisms. A « Microseismic Counter » has also been developed for quick study of the intensity from the tape. Work is in progress for finding direction of microseisms using Derbyshire's correlation method. Additional stations are planned for Trivandrum and Mangalore and from intensity observations also direction of microseisms will be obtained.

1. INTRODUCTION.

Usually the microseisms are recorded by the photographic method or by a pen and ink recorder. In both the methods harmonic analysis is a difficult job. Most of the workers have used a photo-electric type of curve following machine and then analysing the electrical output. The method adopted in I.N. Physical Laboratory enables quick study of intensity and harmonic contents of the microseisms. The amplified pendulum output is recorded on a commercial sound recorder when the tape is run at a very low speed (1/3 m.m. per sec). After the recording is over the tape is run at a high speed (190 m.m./sec) thus converting the microseismic low frequency into the sonic range, the multiplication factor being known.

The reliability of the tape recorder as a frequency multiplying instrument was first verified by feeding a known frequency and analysing the output both when the tape was run at the recording speed or at a faster speed.

2. INSTRUMENTATION.

A horizontal pendulum of the electromagnetic type of 3 second period, supplied by the Carnegie Institution, Washington was used for the study, with a high gain wide band R.C. amplifier with a cathode follower output fed to the exciting coil of the tape recorder which is run at a very slow speed from a geared motor unit. (*fig. 1*).

The recorded signal is analysed when the tape is running at the normal fast speed. A frequency analyser and level recorder of the Brüel & Kjaer type was used to do the analysis. For example results are given for microseisms recorded for a period of 18 hrs from

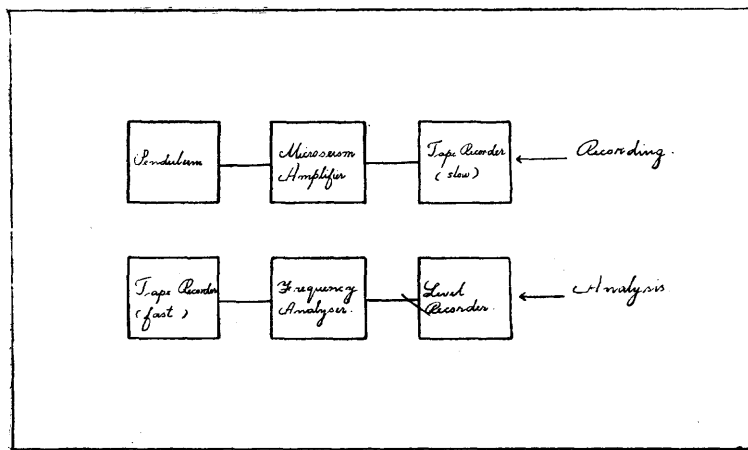


FIG. 1. — Block diagram of the instruments used for the recording and analysis of microseisms.

1535 on 22nd Dec. to 0935 next morning. The whole record took only 1 min. 54 sec for playing back. From the analysis the microseismic spectra for the period was drawn (fig. 2). A predominance

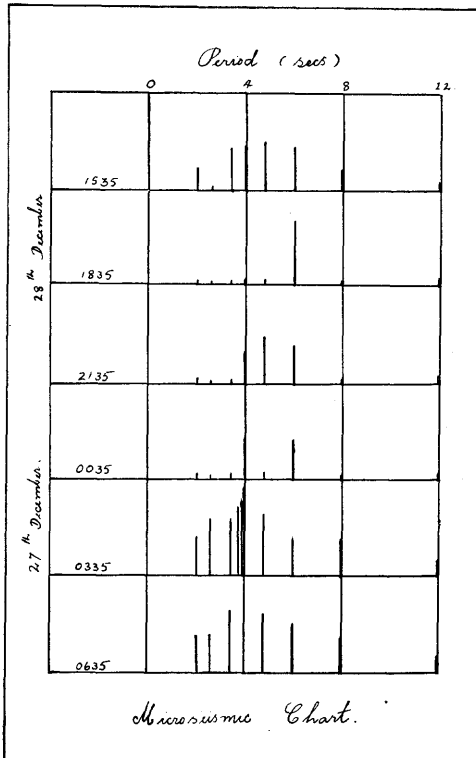


FIG. 2. — Frequency Analysis of microseisms using three hour records from the tape recorder.

of microseisms of 3 to 6 seconds period is noticed.

3. INTENSITY MEASUREMENTS.

A unit was developed to measure the average relative intensity of the recorded waves. Even though the level recorded can be used for this purpose, yet a simpler device would be enough for this measurement. The electrical circuit of the counting unit is given in (fig. 3). The output of the tape recorder is rectified by the valve V_1

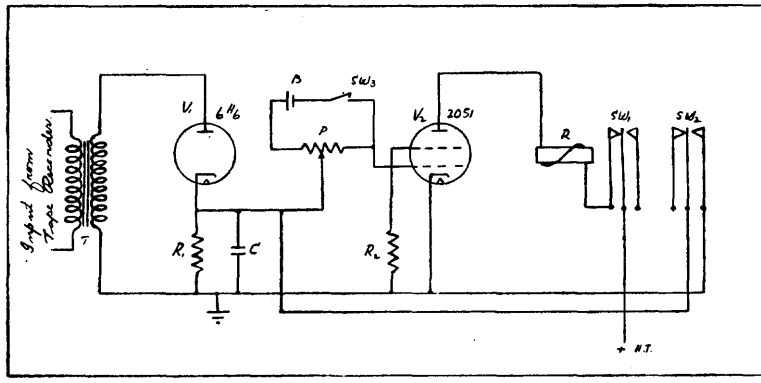


FIG. 3. — The microseismic counter.

R_1 : 0.5 Megohm; R_2 : 1.0 Megohm; C : 2 Mf; T : 1.3 Interstage transformer;
R : D.P.D.T. Relay with contacts SW_1 and SW_2 ; B.P.S. W_3 : Circuit for
biasing the thyratron very near to the firing point.

and the cathode condenser gets steadily charged. When the voltage across it exceeds a certain value, the thyratron V_2 discharges, operating the relay R in its plate circuit. This relay immediately shorts the condenser and thus brings it to the normal position. The process repeats itself. The rate of counting of the relay is a measure of the recorded intensity of microseisms. The counts are recorded on a paper recorder or counted mechanically. Intensity variations studied by this method are given in (fig. 4).

4. PROGRAMME OF FURTHER WORK :

Two horizontal pendulums and one vertical pendulum are available in the laboratory, and it is proposed to study the direction of approach of microseisms by the correlation method outlined by J. Darbyshire. Also two more stations along the West Coast are to be set up, one at Trivandrum where the relation between sea waves and microseisms will be studied, and another at Mangalore. The

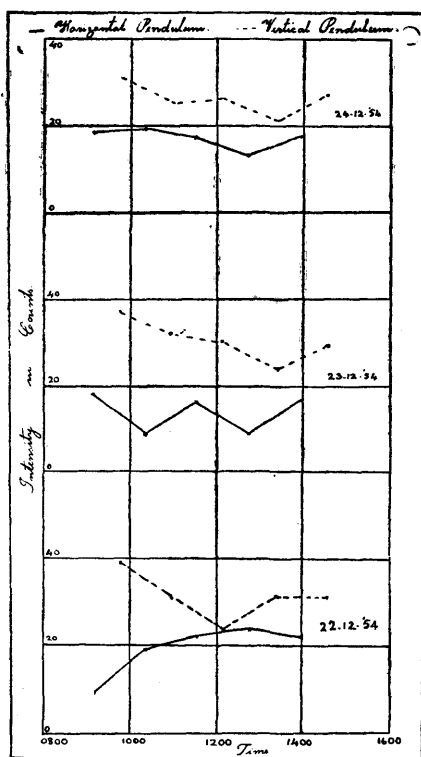


FIG. 4. — Variation in intensity of microseisms as measured by the micro-seismic counter.

three stations will be used to study storm bearing from comparison of average intensities.

LES MICROSEISMES D'ORIGINE TYRRHENIENNE

par M. GIORGI et E. ROSINI (Roma).

Nous avons déjà fait des publications sur ce sujet; nous nous sommes proposés d'étudier systématiquement les relations entre tempêtes microsismiques et perturbations atmosphériques, pour déterminer l'agent spécifique qui établit le rapport entre les deux séries de phénomènes.

Un des principes fondamentaux sur lequel nous avons basé nos recherches est le suivant : on ne peut pas faire un choix unilatéral et fragmentaire de la situation à étudier, en considérant seulement les quelques cas spéciaux où la perturbation microsismique est plus évidente, si l'on veut examiner l'allure de quelques éléments météorologiques; il faut, au contraire, établir une comparaison systématique et continue entre l'activité microsismique et l'évolution du temps, pour obtenir un tableau complet des concordances et éventuellement des différences. Le deuxième principe fondamental est le suivant : l'étude météorologique ne peut pas se limiter à la considération de quelques éléments choisis « *a priori* », mais il faut considérer l'évolution météorologique dans son ensemble, sans négliger aucune des données et des éléments que les météorologues élaborent au cours de leurs analyses. Seulement en partant de cette base et examinant une longue période de temps, on peut arriver à des conclusions qui seront objectives, parce que ce sera la recherche même qui les aura suggérées, et qui seront sûres, parce qu'elles se fonderont sur la réalité des situations.

Le matériel d'élaboration est le suivant : pour ce qui concerne les microsismes, on a étudié les enregistrements obtenus dans les Observatoires Séismiques de l'Istituto Nazionale di Geofisica et en particulier les enregistrements des séismographes électromagnétiques Galitzin et Galitzin-Wilip ayant respectivement les périodes 25^s et 10^s fonctionnant à l'Observatoire de Rome et des séismographes des Observatoires de Padoue, Bologne, Messina et Catania. Pour ce qui concerne les situations météorologiques, on a utilisé toute la documentation graphique du Centre National des Prévisions du Service Météorologique de l'Aviation Militaire italienne, ainsi que les archives générales d'observation et d'enregistrement du même Service.

L'analyse ainsi effectuée pendant bien des années nous a permis d'arriver à des résultats que nous considérons sûrs et définitifs. Dans cette courte exposition récapitulative nous donnons un exemple de

la documentation recueillie, afin d'éclaircir les conclusions auxquelles nous sommes parvenus.

En premier lieu, grâce à la richesse du matériel à notre disposition, il a été facile de constater la concordance entre les caractères morphologiques des tempêtes microséismiques et surtout leur période et les points géographiques des perturbations météorologiques qui les produisent. Ceci nous a permis d'établir un rapport quantitatif entre la période des microséismes et la distance des zones dérangées. On a pu concentrer ainsi l'attention sur les rapports entre les enregistrements microséismiques de courte période, limitée à 4-5 secondes au plus, et les perturbations voisines, qui frappent la Mer Tyrrhénienne et les zones environnantes. Cela a permis d'utiliser complètement les observations météorologiques des stations italiennes, et pourtant d'examiner tous les aspects de la question; en outre, la proximité de la zone d'origine contribuait à rendre le rapport entre les microséismes et l'agent capable de les produire plus étroit et par conséquent plus facile à identifier. A ce point de vue la comparaison entre les enregistrements obtenus dans les Observatoires Séismiques situés dans différentes régions d'Italie a été particulièrement significative.

Les résultats déduits de l'examen comparé de l'activité microséismique enregistrée dans les différents Observatoires et l'évolution simultanée des perturbations atmosphériques, — examen effectué, désormais, comme nous l'avons dit, pendant plusieurs années — peuvent être résumés de la manière suivante :

- a) le retard que l'on observe toujours entre le passage d'un centre de dépression, quand il existe, et le point d'origine d'une activité microséismique confirme que celle-ci ne dépend pas du centre dépressionnaire;
- b) il n'y a pas dépendance directe entre le passage de fronts à caractère froid et l'activité microséismique;
- c) il n'y a aucun rapport entre l'activité microséismique et les fronts à caractère chaud;
- d) il n'y a aucune corrélation constante entre la force du vent, la direction du vent et la condition de la mer d'un côté, et l'activité microséismique de l'autre;
- e) la quasi-totalité des cas examinés a démontré, au contraire, d'une manière absolument évidente que l'activité microséismique dépend directement de la présence, de l'extension et de l'intensité des noyaux de tendance barométrique positive en pleine mer; les quelques cas où cette théorie ne s'est pas révélée absolument certaine, ne peuvent pas être considérés comme une preuve contraire; il est

important, en effet, de considérer que même dans les cas douteux, cet élément — voire le noyau de tendance barométrique positive, a toujours existé, même s'il ne présentait pas une prévalence nette et évidente vis-à-vis des autres éléments. Bref, cet élément était toujours présent, et seulement dans quelques cas les observations n'ont pas permis de déterminer une cause plus précise et définie.

Le résultat fondamental de cette recherche est donc le suivant : *les microséismes d'origine méditerranéenne sont produits dans des zones en pleine mer touchées par des noyaux de tendance barométrique positive, stationnaires ou en mouvement.*

Ce résultat permet de passer à la phase successive de la recherche : ayant déterminé la cause spécifique, il faudra déterminer la cause de son aptitude à produire les microséismes, ainsi que le mécanisme de son action.

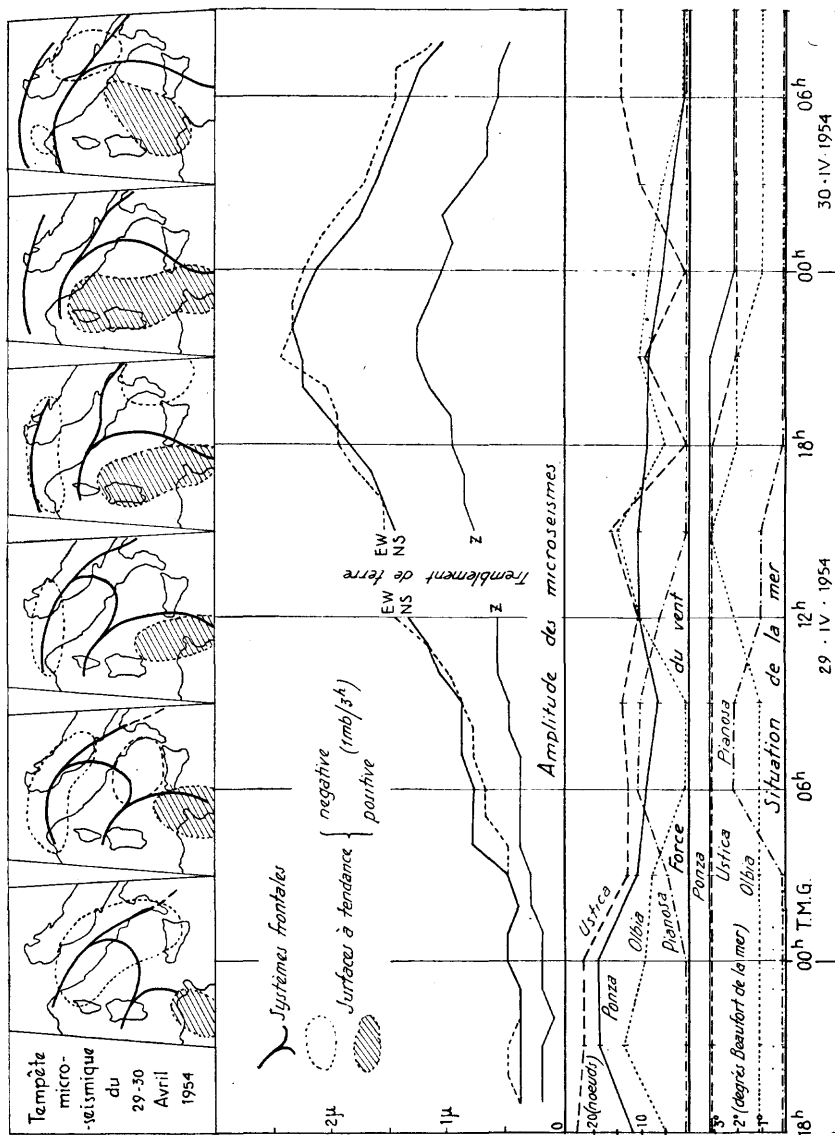
Quant à la cause même, elle peut être probablement localisée dans la turbulence de la masse froide et surtout dans les ondulations qui se forment à la surface de discontinuité avec la masse d'air chaud au-dessus; il est raisonnable en effet de supposer que la zone, à une certaine altitude où la substitution des masses produit les effets bariques plus évidents (c'est-à-dire en correspondance des noyaux de tendance positive) soit la même zone où la turbulence est plus active, et les ondulations de la surface frontale sont plus profondes. Quant au mécanisme de l'action, il peut être construit de la manière suivante : le dérangement, la turbulence en altitude et les ondulations de la surface frontale transmettent de l'énergie, à travers les couches atmosphériques, à la surface de la mer sous forme de nombreuses poussées de pression; sous l'action de ces poussées, la mer, selon sa profondeur et son extension, entre en résonance avec des périodes déterminées, et peut ainsi transmettre l'énergie de ses vibrations à la croûte solide de la Terre.

TEMPÊTE MICROSÉISMIQUE DU 29-30 AVRIL 1954.

A titre d'exemple nous donnons l'examen d'une tempête microsismique signalée pendant deux jours (29-30 avril 1954) par les trois composantes des séismographes Galitzin-Wilip de l'Observatoire Séismique de Rome (Istituto Nazionale di Geofisica).

Sur un graphique nous avons rapporté d'une manière synthétique tous les principaux éléments de l'examen : l'allure de l'amplitude effective (en microns) des microséismes pour les trois composantes depuis 21 h. (T. M. G.) le 28 avril jusqu'à 09 h. (T. M. G.) le 30, les allures de la force du vent (en noeuds) et des conditions de la mer (en degrés Beaufort) relatives à quelques Stations Météorologiques

significatives de l'Aéronautique Italienne; une série de cartes du temps chaque six heures; les cartes montrent la position des discon-



tinuités frontales et les noyaux de tendances barométriques positives et négatives (avec la seule indication des aires relatives aux tendances supérieures en valeur absolue à 1 mb/3h).

Les Stations météorologiques que nous avons choisies comme indicatives de la situation du vent et de la mer Tyrrhénienne sont les suivantes : l'Ile de Ustica au large de la Sicile nord-occidentale, l'Ile de Ponza au nord-ouest de Naples, l'Ile de Pianosa entre la côte Toscane et la Corse, Olbia dans la côte nord-orientale de la Sardaigne.

Comme l'on peut déduire des cartes du temps, à 00 h. (T. M. G.) le 29 avril un ensemble de deux perturbations frontales, déjà dans une phase d'occlusion, intéresse l'Italie avec la mer Tyrrhénienne et la Tunisie. La première des deux perturbations est déjà passée sur la mer Tyrrhénienne sans produire une évaluable agitation micro-séismique bien que le vent ait été fort ou modéré et la mer agitée au moins jusqu'à l'Ile de Ponza.

La carte à 00 h. (T. M. G.) le 29 avril montre que cette première perturbation n'est pas accompagnée ni suivie d'un accroissement bien organisé de la pression; au contraire on peut vérifier un large noyau de tendances négatives.

La deuxième perturbation ne cause que des vents faibles ou très faibles, exception faite pour quelques renforcements locaux mais temporaires et modérés entre 12 h. et 15 h. le 29 avril (brises); la mer aussi ne réagit pas à son passage; au contraire l'agitation devient partout plus petite jusqu'à s'annuler en diverses zones.

La série des cartes prouve toutefois qu'un noyau de tendances positives bien caractérisé suivit de loin le front froid qui partant de la Tunisie se dirige vers le Nord-Est.

Lorsque le noyau, le 29 après 06 h., entre dans la mer Tyrrhénienne, l'agitation microséismique qui auparavant était très faible, devient bien distincte; ensuite elle se renforce graduellement et atteint son maximum d'intensité à 21 h. le même jour, pendant que le noyau s'approche à la côte latiale.

Afin d'individualiser l'élément météorologique directement responsable de la tempête microséismique il faut souligner que lorsque l'agitation atteint sa plus grande valeur le front froid a quitté depuis longtemps la mer et est désormais passé au-dessus de Rome.

En conclusion, les trois éléments météorologiques plus fréquemment cités, à savoir la force du vent, les conditions de la mer et le passage sur la mer (ou sur la Station séismique) du front froid, sont dans cet exemple absents ou en discordance de phase avec l'agitation microséismique, tandis que le noyau de tendances positives en marche sur la mer Tyrrhénienne explique l'allure avec une précision chronologique exacte.

L'exemple que nous avons donné ci-dessus n'est pas unique ni le plus éclatant : il représente la règle générale et nous l'avons choisi seulement à cause de sa particularité de correspondre à une perturbation typiquement méditerranéenne provenant du Sud-Ouest, tandis que le plus grand nombre des perturbations associées à des tempêtes microsismiques proviennent du Nord-Ouest.

MICROSEISMS USED IN HURRICANE FORECASTING

Prepared by Mr. Marion H. GILMORE, Geophysicist.
U. S. Navy Microseismic Research Project,
U. S. Fleet Weather Central,
Miami, Florida.)

The Microseismic Research Project, initiated by the U. S. Naval Aerological Service, has recorded storm microseisms on one or more seismographs since June 1944. This project, together with several independent microseismic research studies conducted in the United States, shows that group microseisms and microseismic storms are generated by various types of meteorological disturbances. A review of these studies shows some items of interest to the forecaster of tropical storms. Microseisms are now used to give an indication of the existence of severe tropical storms and to supplement other information concerning their movement and intensity when they pass in range of one or more seismograph stations. Upon strictly empirical evidence several relationships between severe tropical storms and the amplitude of microseisms have been formulated. The fundamental relationship may be stated as follows : A tropical disturbance generates recordable microseisms, and when it is within range of a microseismic station, the amplitude of the microseisms recorded at that station will increase or decrease in proportion to the changing intensities of the disturbance and / or changing distances from the station. This is based on empirical evidence that similar storms passing over the same area generate microseisms of the same order of amplitude, and that the magnitude of the microseisms is closely related to storm intensity. This relationship has been found valid in most, if not all, observed cases in the last ten years.

There are many examples that show this relationship between microseisms and tropical storms. The hurricane of September 1945, Figure 1, is a good example to show that a tropical storm generates microseisms that increase and decrease in amplitude according to changing distances of the storm. This hurricane developed east of Puerto Rico on 12 September and passed north of Roosevelt Roads, Guantanamo Bay and directly over the station at Richmond, Florida. The seismograph at Roosevelt Roads recorded storm microseisms late on 12 September and reached a maximum of 20 mm by noon the next day when the hurricane passed 100 miles north of the station. The microseisms increased, Figure 1, as

the storm approached each station and then decreased after it passed the nearest point to that station. The microseisms conti-

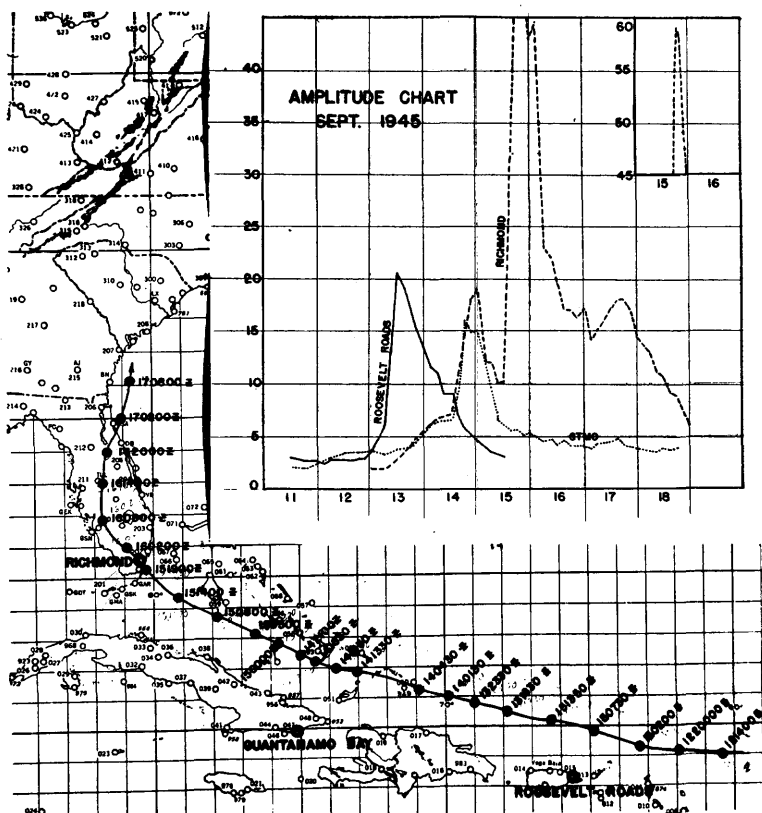


FIG. 1.

nued to increase until the storm passed a station, over land or over shallow water. After the hurricane passed Guantanamo Bay the microseisms fell at that station. They also fell at Richmond, a station the storm was approaching. It is believed that this drop in amplitude was caused by the shallow water in the Bahamas. After the storm passed over the Bahamas the microseisms again increased sharply and reached a peak of 59 mm. As the storm crossed Florida the microseisms fell to 14 mm and then increased to 18 mm as it briefly passed into the Atlantic. The microseisms decreased to normal when the storm went inland again and filled.

Another example that supports the relationship mentioned above was the hurricane of June 1945, in which the amplitude of the microseisms increased and decreased in close relation to the changing intensities of the storm and its distance from the station.

This hurricane was indicated by a slight rise in microseisms at Richmond on 21 June, Figure 2. Special weather reconnaissance

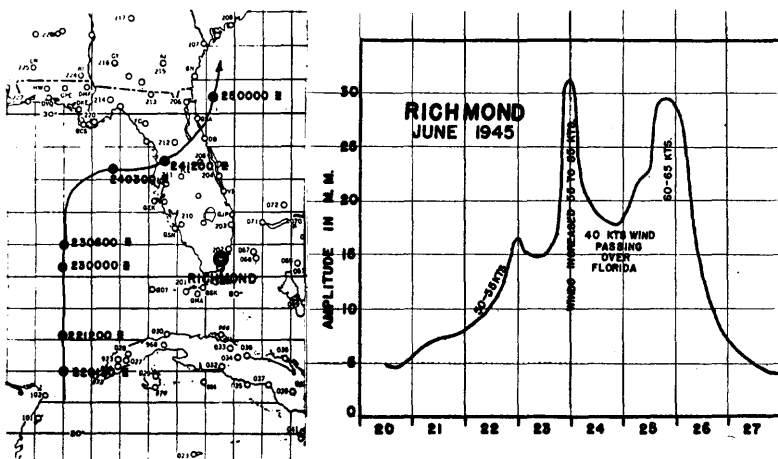


FIG. 2.

aircraft scouted the area during daylight hours and reported the storm moving due north from the western end of Cuba with winds estimated at 55 knots. The microseisms at Richmond increased slowly to a maximum of 17 mm by the time the storm passed 250 miles west of the station. In the next 18 hours the microseisms decreased to 14 mm and then increased to 17 mm again while the storm moved away from the station. During this time Army and Navy planes continued to report a northward movement with no indication of intensification. A reconnaissance plane reported early on 23 June that the storm was veering to the west, still with 55 knots. A plane in early afternoon also reported the northwestward movement and reported the storm one degree west of its old track with no intensification. The microseisms rose slightly that day, Figure 2, when they normally would have decreased if the storm were actually moving further away, and the winds remaining constant. The mid-afternoon forecast was for a continued north-northwest movement with no intensification anticipated. In the afternoon another plane made a last check on the storm and found it over 100 miles east of its last reported position with maximum winds estimated at 85 knots. The sharp increase in hurricane winds from 55 to 85 knots coincided with the increase in microseisms from 17 to 32 mm in the same three-hour period preceding

2100 GCT. This fact, and its probable interpretation, were reported to forecasting agencies in Miami before the plane report was available.

It is also significant that, during the night, the microseisms dropped from 32 to 18 mm by the time the hurricane reached the Florida Coast. The storm then had decreased to 40 knots. However, as soon as it reached the Atlantic its intensity increased to 65 knots and the microseisms increased to 30 mm, Figure 2, which is similar in most respects to the storm of September 1945 in the same area (see Figure 1). These data show that each change in intensity of the hurricane was significantly registered on the seismograph at Richmond in the form of a change in the amplitude of the microseisms which was simultaneous with the change in intensity.

The empirical data which supported the main premise also suggested the following basic working hypotheses that apply to all storms within range of one or more properly located microseismic stations :

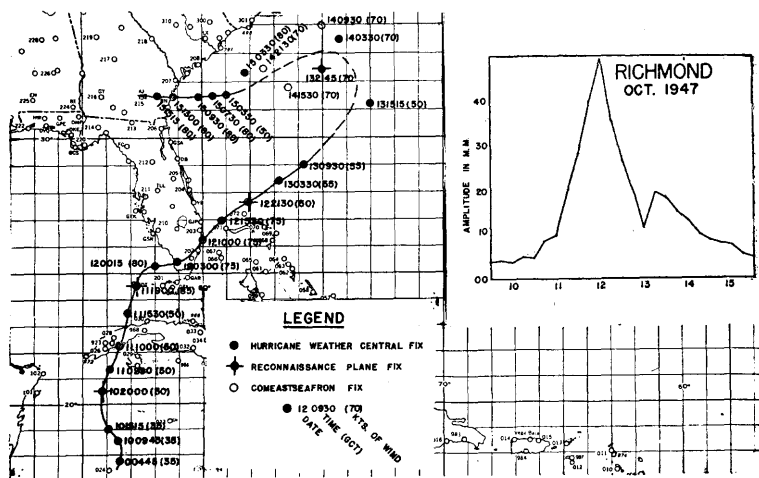
1. When a hurricane of *constant* intensity approaches a microseismic station the amplitude recorded at that station will increase; the converse of this statement is also true.
2. When a storm intensifies within range of a station, the amplitude of the recorded microseisms will increase; when such a storm fills the amplitude will decrease.
3. When a hurricane of constant intensity is between two stations the amplitude of the microseisms recorded at the one it is approaching will increase, and at the other decrease.
4. When a hurricane undergoes a change in position and intensity at the same time, the microseismic trend at a single station is more difficult to analyze. A storm could be moving away from a station as in the converse of hypothesis 1, and undergo sufficient intensification to cause an increase in amplitude where a decrease would normally be expected. This possible confusion can be resolved in most cases when the storm is in range of three or more properly located stations.

The following are two exemplary hypothetical illustrations of the above hypotheses :

- a) When a hurricane moves away from Station A and toward station B while it is increasing sharply in intensity, the amplitude recorded at both stations *will increase* but a *much more rapid rise* will occur at station B.

b) When a storm is located in range of three stations, A, B and C, its intensity and movement can be determined with a fair degree of accuracy. In the case where the amplitude at station A is falling, at B remaining constant, while rising at station C the storm is receding from A, remaining a constant distance from B and approaching C.

The hurricane of October 1947 is an example that supports hypothesis number 1. It approached the Richmond seismograph station with almost constant winds. This hurricane was indicated on the seismograph when it was still south of Cuba, Figure 3.



After it crossed that island the microseisms started to increase rapidly and reached an amplitude of 20 mm at 1900 GCT of the 11th when a weather reconnaissance plane located the storm west of Key West accompanied by winds of 85 knots. The continued northward movement indicated that it would reach the Florida coast near Fort Myers about midnight. However, since there were no weather stations in Southwest Florida it was impossible to keep track of the storm at night. Also, since no increased winds were reported at Fort Myers, it was reasonable to assume that the 85 knot storm was rapidly filling as it approached. Figure 3 shows, instead, that the storm made an abrupt eastward turn and then moved in a direct line toward Miami. However, storm warnings were continued at the same level because of the constant

rise in the microseisms at Richmond which continued until the storm passed over the station. The hurricane passed into the Atlantic and its winds decreased slightly along with a rapid decrease in microseismic amplitude. At 1800 GCT on 17 October the storm intensified from 50 to 70 knots and the microseisms increased in amplitude from 14 to 18 mm even when the storm was moving away from the station. These changes in amplitude fully agree with the fundamental relationship given above and specifically with hypothesis number 1.

An outstanding example of the converse of hypothesis number 1 is shown in the behavior of microseisms during the hurricane of October 1946. The microseisms at Richmond station increased from 10 to 23 mm while the storm was still south of Cuba. However, they decreased when it passed over Cuba, Figure 4, and

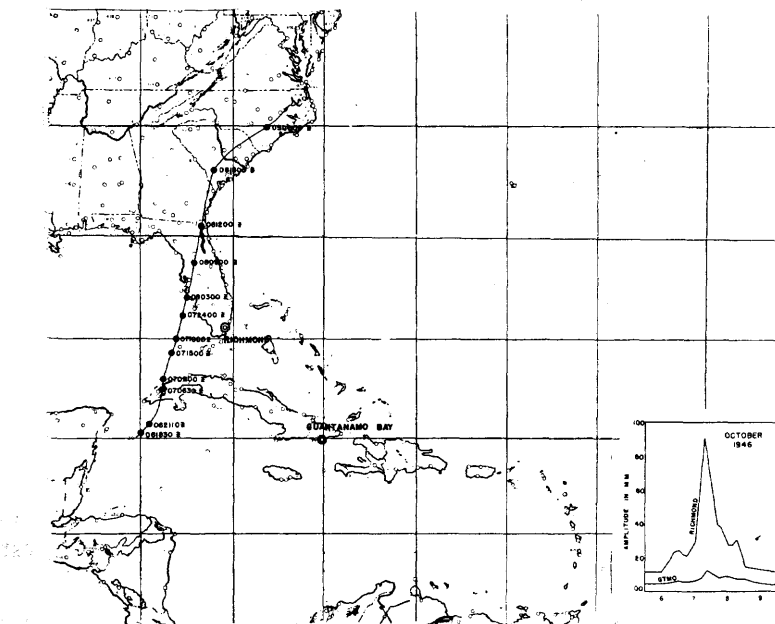


FIG. 4.

then rapidly increased to a maximum of 90 mm by the time the storm reached a point just west of Key West. The hurricane was moving northward, with winds estimated at over 100 knots, according to a plane report at 1800 GCT on October 7. Since there were no night reports from that area the storm was projected on a

northward track and was expected to reach the coast near Tampa before morning with the same intensity. However, the microseisms at Richmond told a far different story, in that their amplitude started a rapid decrease at the time of the last plane report. Before the storm reached the coast the amplitude dropped from 90 to less than 40 mm. This indicated that the hurricane was rapidly filling, and was verified when a 40-knot storm reached the coast at 0300 GCT, Figure 4. This agrees with the converse of hypothesis number 1 which states that a storm of decreasing intensity will generate smaller microseisms. This storm also passed near Jacksonville and intensified slightly so that a small increase in microseisms was again noted, Figure 4 (see Figures 1 and 2).

Hypothesis number 2 is well illustrated by the microseisms recorded during the October hurricane of 1944. It was indicated by increased microseisms on the seismograph at Guantanamo Bay two days before it appeared on official weather maps. The microseisms, Figure 5, increased from 3 to 8 mm on 11 October and then

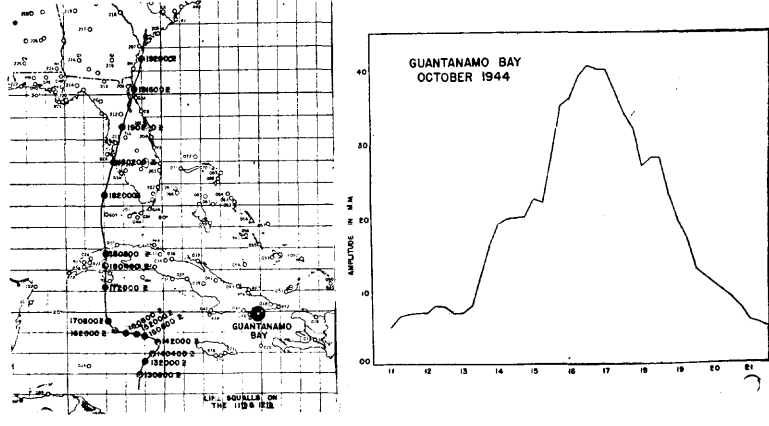


FIG. 5.

remained nearly constant for two days while the hurricane slowly developed and moved westward away from the station. At 1600 GCT on 13 October the microseisms started a rapid increase and leveled off at 20 mm by the end of 24 hours. During this time the storm increased to hurricane intensity as it approached the station. This increase in microseisms when the distance from the storm to station was increasing indicated intensification of the hurricane, and

was later verified when it passed over Grand Cayman Island. When the hurricane turned northward the microseisms decreased sharply, especially when it passed over Cuba. However, the hurricane intensified again after it crossed Cuba and the microseisms also increased slightly even though the storm was still moving away from the station. Later, as it passed over Florida and filled, the microseisms returned to normal.

Hypothesis number 3 is well illustrated by the microseisms recorded during the hurricane of September 1945, Figure 1. This shows that the microseisms at one station increase as the storm of constant intensity approaches, while the microseisms decrease at the station the storm is leaving. The microseismic data presented above are intended to show how the new micro techniques are used in detecting and tracking tropical storms. These data show that each typhoon and hurricane generates vibrations in the earth's crust, called storm microseisms, that will be recorded on properly tuned seismographs when within range of the instrument. Their correct interpretation, according to the hypotheses given above, will produce valuable information concerning the movement and intensity of tropical storms. This indicates that microseisms may be used by the forecaster of tropical storms in four specific ways :

- A. To aid in early detection of storm;
- B. To indicate storm's intensity;
- C. To indicate changes in intensity;
- D. To aid in the location of the storm.

Each separate function listed above is at present dependent on the requirement that the microseisms recorded at a station *must* be generated *only* by the storm being tracked. The four items that make complete microseismic storm detection are discussed below.

A. EARLY DETECTION OF STORM.

From a study of the data submitted above there is good evidence that a seismograph will record large storm microseisms each time a severe tropical storm is within range of a microseismic station. This prior detection of a storm will normally occur in advance of other methods except direct plane or ship observation, and occasionally in advance of these, since so many tropical storms have their genesis in areas of sparse reports. In 1953 the Guam seismograph recorded typhoons Hester and Irma at least 18 hours before they were located by plane. During the same year in the Caribbean, the development of hurricanes Florence and Dolly, and the reintensification of tropical storm Hazel, after it crossed Florida, were

detected by the seismograph at night in advance of aircraft. In 1952 hurricane Fox was indicated by the Swan Island seismograph about 48 hours before a plane located it.

There are many other examples of detecting a storm development prior to reports from aircraft and/or ship. It is believed that if a sufficient number of seismographs were properly located in specific areas, they would always detect the early development of a hurricane. Figure 6 shows a small storm starting to intensify

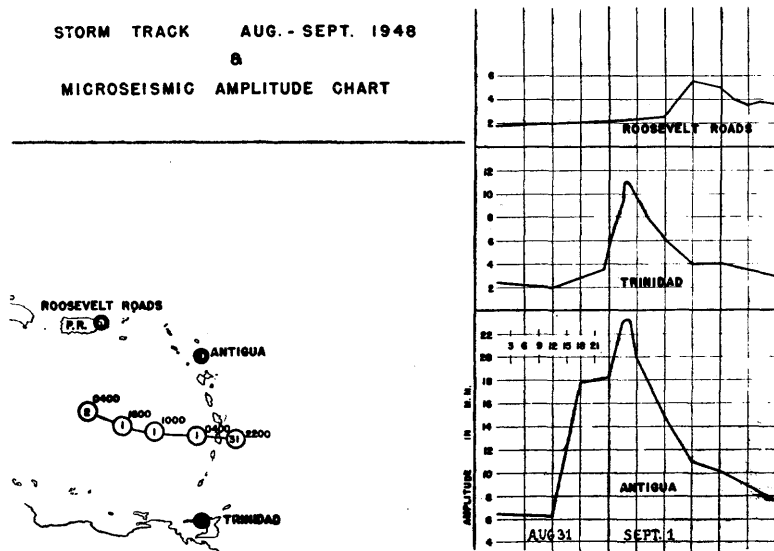


FIG. 6.

in the Leeward Islands. This was apparent on the microseisms recorded at Antigua and Trinidad. This would also be true of any suspicious area east or north of Barbados. It does not seem probable that a storm could develop hurricane winds without sending a message in the form of microseisms to each micro station in the area.

B. TO INDICATE STORM'S INTENSITY.

The working hypotheses show that it is possible to determine the intensity of a storm by the size of the vibrations it transmits. Amplitude grids, such as shown in Figure 7, have been constructed around microseismic stations in order to estimate more exactly the

amount of vibrations or amplitude of microseisms that may be expected from hurricanes in the same area. Micro grids are made

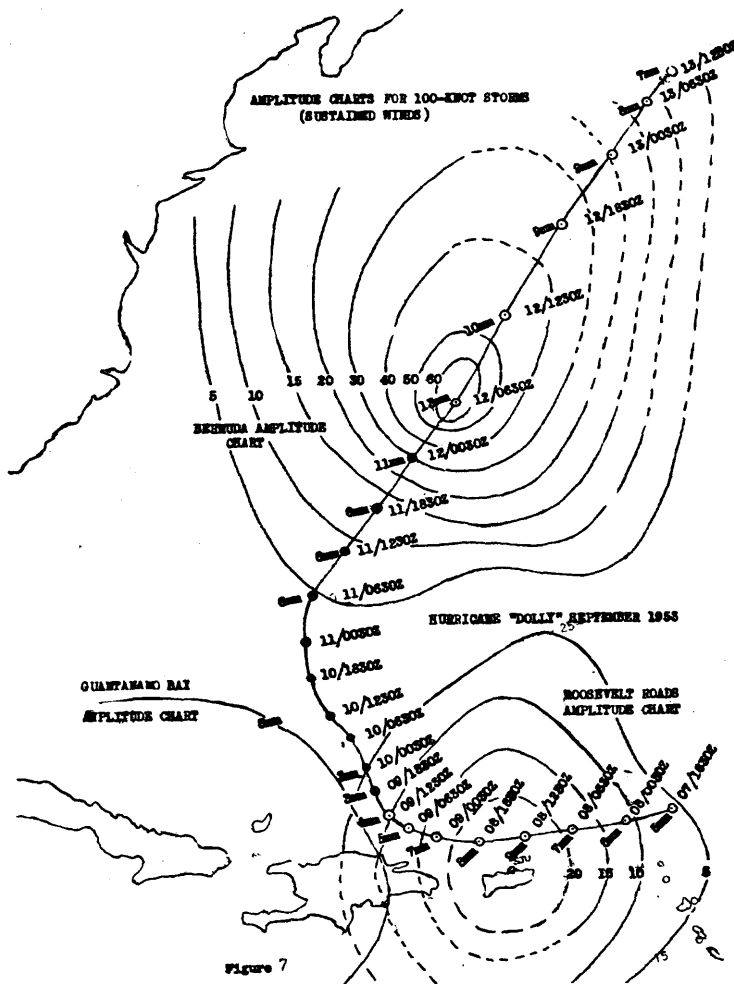


FIG. 7.

entirely from empirical data, which in most cases are insufficient to make perfect grids. However, grids now being used around some of the stations produce good information on the intensity of storms. The aircraft or radar position of the storm is plotted on the grid and the microseisms recorded at that time are compared with the amplitude line on the grid nearest the storm's position. The ratio of the two numbers multiplied by the storm intensity for which the

grid was constructed will give a fairly accurate estimate of winds in the new storm.

These grids have been used during the past two years at Miami with acceptable results. They often indicate when to lower or raise estimates of wind and such information is valuable during the night when storms can be located by radar, but wind cannot be observed. A storm within range of one or more micro stations transmits continuous messages via the microseisms. When this information is recorded on only one seismograph it may be subject to several interpretations. It could be going away from the station and intensifying so that it would retain a constant amplitude. Or it could be coming toward the station and filling and still have the same amplitude. However, if its position is fairly well known by radar or by other means, then a more correct interpretation can be made.

A good example in 1953 was given by the Swan Island and Guantanamo Bay stations when they indicated the hour that Hurricane Florence started developing. At a time when the « low » was going away from both stations the amplitude started increasing between 0900 GCT and 1200 GCT on 24 September 1953. A reconnaissance plane located the storm shortly thereafter and estimated the winds at 65 knots.

The seismographs at Whiting, Jacksonville and Miami gave strong evidence that tropical storm Hazel of 1953 intensified during the first nine hours after it crossed Florida. This information helped the forecast officer to keep the advisory winds up to the proper velocity.

Another good example may be found in hurricane Carol of 1953 when it passed west of Bermuda. The microseisms indicated constant winds but several radar fixes placed the storm about 100 miles nearer Bermuda than it was thought to be. Had it been in that position with the same winds the microseisms would have been higher.

A Tropical Depression Warning was issued at Guam at 0000 GCT 17 September 1953 when a small circulation was located 500 miles southeast of the station with only 20 knots. Twenty-four hours later the storm had increased to typhoon intensity as the microseisms were decreasing. According to the fundamental micro *hypotheses* it would be impossible for a 20 knot storm to approach a station and reach typhoon intensity while the microseisms were decreasing. Warning on Typhoon Tess were reduced to tropical storm within 12 hours. However, by this time the microseisms

indicated that the storm was developing rapidly into a typhoon. When warnings were again raised to typhoon, with 80 knots, the microseisms of 24 mm indicated the same. At 21/1200 GCT when the storm was reported at 85 knots the microseisms had reached 87 mm and thus indicated a storm of 120 knots or higher. The next two six-hourly post analysis position reports indicated typhoon intensification from 100 to 150 knots which then agreed with the micro report. It does not appear safe to neglect the messages that storms transmit through the earth's crust because they contain important data on intensity.

C. TO INDICATE CHANGES IN INTENSITY.

This phase is very similar to the section above because both deal with intensity. Storms do not maintain a constant intensity throughout their lives so it is necessary to find a method to detect these changes when they occur. This is especially needed at night when conventional methods are not too precise. The seismograph, as explained above, should detect these changes when and as they occur. Since 1944 there have been many examples that show a rapid increase or decrease in hurricane winds in a short period of time, which were reflected immediately in the recorded microseisms.

Typhoon Kit passed about 350 miles southwest of Guam on 28 June with winds estimated at 100 knots. The microseisms of 45 mm agreed with this estimate. During the next 24 hours the microseisms increased to 68 mm when the storm was 485 miles from Guam. This indicated winds of at least 150 knots at 29/1200 GCT. The post analysis chart shows only 120 knots. However, 12 hours later it shows 170 knots but the microseisms were then down to 48 mm. It is probable that Kit had a gradual change in intensity. The intensities at six hourly positions, starting at 28/1200 Z, were 100-110-120-120-120-170-150-150-150-120-140 knots.

A more striking example of detecting intensity change was in Hurricane Dolly, Figure 7, as it approached Bermuda. When the hurricane was in range of the station aircraft reported 100 knot winds. The storm then continued on a straight line toward Bermuda according to radar fixes, but the microseisms remained a constant 6 mm for 18 hours. The logical interpretation was that the storm was filling. This proved an accurate estimate because the storm passed Bermuda with only 41 knots sustained wind.

D. TO AID IN THE LOCATION OF THE STORM.

Hurricanes and typhoons can be located by the new micro-grid technique, but they must be recorded simultaneously on three or more microseismic stations from which sufficient data on past storms have been obtained to construct accurate amplitude grids such as shown in Figure 7. There are very few such examples because there are insufficient microseismic stations that make up units of three or more. Even when Miami, Jacksonville and Cherry Point record the same storm, one of them is usually under the influence of a front or a low pressure system. It is possible, according to the micro grid hypothesis, to obtain a storm's position at any time that readings are taken simultaneously at three or more stations. This is accomplished by drawing an extra grid line in each grid, such as shown in Figure 7, to represent the microseismic amplitude at the respective stations. The storm is then located at the intersection of the three grid lines which theoretically intersect at one point. In practice it is found that the storm is located in the area bounded by the overlap of these grid lines.

Therefore, in summation, it would appear that the data submitted above presents substantial evidence in favor of the hypotheses and theories outlined. One micro station can be of great utility in discovering tropical storm genesis. Such a station can furnish considerable additional data to supplement aircraft reconnaissance, estimates of wind intensity and, to some extent, storm movement. When a single tropical storm is within range of three or more microseismic stations the following independent conclusions can be made : (1) Existence of the storm can be verified. (2) The storm's movement can be followed 24 hours a day by comparing the data from any one station with those from the other stations.

ELASTIC TIDES AND IRREGULARITIES OF THE EARTH'S ROTATION IN CONNECTION WITH ITS STRUCTURE

by M. S. MOLODENSKY and N. N. PARIJSKY

Many scientists have availed themselves of the results of the studies of elastic tides occurring during the luni-solar tides and of free nutation of the Earth to estimate the average value of the rigidity of the Earth, or of its general characters of variation in relationship to depth. At present, these estimates are of no interest. As the relationship between the rigidity and bulk modulus of the elasticity to density are determined, for all depths of the Earth's shell, by means of seismological observations, it is obvious that to each density hypothesis corresponds a definite distribution of these moduli within the shell. In spite of the uncertainty connected with the choice of the hypothesis of density distribution, such a method of hypothesis gives better and more accurate results, as far as the shell is concerned, than those obtained by a study of elastic tides.

The case is altogether different in respect to the Earth's core. As far as the core is concerned, only the velocities of the longitudinal seismic waves are known to us. Transverse waves either do not pass through the core, or lose so much of their original energy, that it has not been up till now possible to detect them. Therefore, studies of seismic waves have not yet permitted to obtain definite estimates of the rigidity of the core.

For these estimates, observations of free nutation and of elastic tides are required. A series of models has been studied with this aim.

In all the models treated by us the velocities with which longitudinal and transverse seismic waves are spreading in the shell correspond to the observed phenomena in nature (they are, however, slightly smoothed). The values of the rigidity (μ) and of the density distribution law vary from model to model. In the first model the density in the shell and core is constant, increasing discontinuously from the shell to the core. In the second model the densities are close to those of Bullen and in the third they are accepted in accordance with Legendre's model. For all the three models the actual value of the mass of the Earth and its moment of inertia are accepted. The rigidity of the core varies from zero to infinite. In the cases of models with a « liquid » core, the heterogeneous

density of it was always taken into account. In other models the core was considered homogeneous. In one of the variants the compressibility of an elastic core was taken into account, and the influence of this compressibility proved to be imperceptible. Hence, in all the other cases, the core was considered to be incompressible. The deformations were considered to be purely elastic because during semi-diurnal and even annual perturbations the relaxations of the strains and the elastic consecutive effect could be neglected. Calculations were carried out with utmost accuracy because the variations of the theoretical value of the limits of free nutation (with reasonable variations of the rigidity of the core and the density hypothesis) are extremely narrow. An approximate theory for the study of such comparatively difficult questions is not, of course, acceptable.

In determining the deformations of the shell we applied precise equations of the theory of elasticity taking into account the compressibility of the Earth and the heterogeneity of its elastic properties and density in dependence on depth. Our problem was, in all cases, reduced to the sixth order non-homogeneous boundary problem (we received a system of three ordinary second order linear differential equations with varying coefficients depending on the elasticity coefficients and on density (both of which varying with depth). Out of the six boundary conditions, three concern the surface of the model (absence at the surface of normal and tangential strains and continuity of the radial derivative of the potential). The remaining three conditions, the same as the first three, were taken at the boundary of the core.

An analytical solution of the boundary problem under examination is hardly possible. We have arrived at a solution of differential equations by means of numerical integration. For each of the variants of the density distribution, four partial solutions were computed. Taking into account the linearity of the boundary conditions and that of the differential equations, we received the required solution of our boundary problem as a linear combination of these partial integrals.

The chief result of the above mentioned calculations can be expressed with a sufficient accuracy by the following empiric formula :

$$K = K_{\infty} + \frac{K_0 - K_{\infty}}{1 + 0,65 \cdot 10^{-12} \mu} \quad (1)$$

$$h = 2 K$$

Here K_0 is the value of Love's number K when the rigidity in the core is $\mu = 0$.

K_∞ is the same when $\mu = \infty$

K is the same for any intermediate value of μ .

μ is expressed in dynes per cm^2 .

h is the value of the Love's number h with the same value of μ .

The parameter K_0 and K_∞ have the following values :

1)	density variant	$K_0 = 0.327$	$K_\infty = 0.069$
2)	»	»	0.310
3)	»	»	0.287

From the above table we see that a considerable variation of the density distribution (the moment of inertia and the mass of the Earth being unvaried), influences the Love's numbers h and K to a very small extent. A further improvement of the density law will hardly alter K more than by 0.01.

We have also studied the influence of the ellipticity of the Earth on the constants h and K . It was shown that a 1 % variation of the ellipticity changes the number K by 0.004. A variation of the radius of the core by 0.01 of the Earth's radius changes this number by 0.015. Changes in the density of the Earth's crust also influence h and K to a very small extent. Thus, the theoretical value of Love's numbers K and h depends mainly on the value of the rigidity of the core. To compare the results of our observations with theoretical data we must take into account an essential difference between our models and the Earth. There are oceans at the Earth's surface the waters of which are freely moving during elastic tides and give rise to additional deformations by means of their pressure on the Earth's surface and by means of gravitation of the additionally deformed inner masses of the Earth. These effects were taken into account by numerically integrating the equations of the equilibrium of the elastic sphere, using the method briefly described above. Thus, we established that in the case of a static tide (free nutation) the theoretical value of the number K formerly obtained, should be increased by 0.038.

Passing from Love's number K to Chandler's period and adopting our density distribution (which is close to that of Bullen) we obtain the following expression for :

$$T_c = 350 + \frac{113}{1 + 0.65 \cdot 10^{-12} \mu}$$

where T_c is expressed in days.

Here we used the Euler's period for the whole Earth, i.e. we assumed that the rigidity in the core was $\mu = 0$.

Taking Chandler's period equal to 433 days we obtain from the last expression the value of the rigidity in the core :

$$\mu = 0.6 \cdot 10^{12} \text{ dynes per cm}^2.$$

Now only one peculiar case remains to be examined and that is the case when the rigidity of the core is zero (liquid core). In this case, the shell is in a state of free nutation independently on the core, while Chandler's period depends upon the Euler's period of the shell alone (and not of the Earth as a whole). For the same value of Chandler's period (433 days) Euler's period for the shell equals 275 days. Hence we can easily conclude that the moment of inertia of the core represents about 10 % of the general moment of the inertia of the Earth. (The fact of taking into account the viscosity leads inevitably to a small increase of the moment of inertia of the core.)

Thus, from the observed value of the period of free nutation follows one of the two possibilities :

- 1) the rigidity of the core is close to 0.6×10^{12} dynes per cm^2 ;
- 2) the core is liquid and its moment of inertia, is not less than 10 % of the Earth's moment of inertia.

The choice between these two possibilities must be based on the study of amplitudes of short period terms of the forced nutation, and of the elastic luni-solar tides. As far as the latter case is concerned, it is difficult to estimate the effect of tides in oceans. It can be excluded, however, by the formula (2) (using for this purpose the observed variations of the tilts as well as of gravity). It is rather difficult to estimate whether this method will prove reliable, if we take into account the small amount and the insufficient precision of observations at our disposal.

Molodensky's method for the solution of the problem of the elastic deformations of the Earth, described above, enabled us to examine quantitatively one of the hypotheses about the sources of discontinuities of the angular speed of the Earth. As it is known, with the annual and secular changes in the velocity of the Earth's rotation, irregular discontinuities and abrupt changes in the speed of its rotation must also be taken into consideration. These reach the value :

$$\frac{\delta\omega}{\omega} = -\frac{\delta I}{I} \approx 4 \cdot 10^{-8}$$

where ω denotes the angular velocity of the Earth, I — its moment of inertia. These discontinuities have been studied in detail by

de Sitter, Spencer Jones, Brouwer and the others. The discontinuities take place either during a period of 1-3 years or, according to Brower's theory, they occur as a result of an accumulation of a great number of slight variations of occasional character. Independently on the details of this process, changes of the above mentioned value of angular velocity are observed in the course of one or two decades.

We have studied a great deal of processes which occur at the Earth's surface, and which generally can cause a variation in the angular velocity of the Earth. As well as other authors we have also come to the conclusion that the influence of these processes is imperceptibly small. The greatest effect can be caused by a redistribution of waters between the Ocean and the Antarctica, and by the degree of its glaciation.

The resulting change of the moment of inertia of the Earth leads to a corresponding change of its angular velocity, as the result $I\omega = \text{const}$. A change in the glaciation of the Antarctic must reach as much as 10 m. and the corresponding change in the oceans level — 0,5 m. But no changes of that amount have ever been observed (see for instance Munck and Revelle). They must, besides, cause a displacement of the pole which will be at any rate ten times greater than it has been observed. At present we are perfectly entitled to consider that the source of discontinuity of the Earth's rotation lies in the interior of the Earth.

N. N. Parijsky has investigated the possible variations in the interior of the Earth which provoke the above mentioned changes in the Earth's rotation and calculated the changes of gravity that must be expected at the Earth's surface in this case.

A study of models in which recrystallization has taken place in a thin layer at different depths from the Earth's centre r_0 was carried out (as for instance according to Burnel's hypothesis). The recrystallization leads to changes in the density of this layer and to a difference h_0 of elastic displacements on its lower and upper boundaries.

Equations of elastic balance for small deformations following spherical functions of any order, were used. These equations can be applied to the Earth with unhomogeneous density ρ and elastic properties μ, λ . The solution of the equations has been obtained by means of a numerical method for a great number of the models of the Earth. The density distribution was evaluated according to Molodensky's law (close to that obtained by Bullen) with the only correction : for some models the second inner

homogeneous core with $r = 0.2$ has been introduced. Numerical characteristics of the density are as follows :

At the surface ($r = 1.00$) $\rho = 3.34$; at the boundary of the core ($r = 0.55$) $\rho_e = 5.66$ $\rho_i = 9.95$; at the boundary of the inner core ($r = 0.20$) $\rho = 12.27$; inside the inner core $\rho = 12.50$. Variations of the elastic constants with distance were taken according to Jeffreys. But inside the core the following values were accepted : $\mu = 0.16 \times \bar{\mu} = 0.6 \times 10^{12}$ dynes per cm^2 .

Homogeneous models were also discussed.

In the case of spherical symmetrical deformations ($n = 0$) (when the distances of the varying layers change from 0.99 to 0.55 of the Earth's radius, a displacement of the Earth's surface from 0.41 to 0.12 m is required in order to provide the observed change of the moment of inertia. The thickness of the recrystallized layer for a density change of 0.1 gr per cm^3 must equal but 8.9 and 6.6 respectively. Variations of gravity at the surface are equal to 0.13 to 0.04 mgals, respectively. Far greater changes are required for the distribution of deformations in accordance with the second order ($n = 2$) spherical functions. When $r_o = 0.94$ the amplitude of the displacement at the surface equal to 0.80 m is required, the thickness of the layer being of 27 m and the variation of gravity — 0.25 mgal. Thus, only slight changes within the Earth are required to explain the discontinuities of the Earth's rotation. These changes cause such small variation of height and gravity at the Earth's surface that they could easily remain undetected if the observations were approximate. However, it is far more probable that the inner changes do not embrace the whole Earth as it is represented by the zero and second order spherical functions but by higher order functions. Greater changes in gravity and vertical displacements which can at present be observed by means of the existing methods are to be expected in that case. On the initiative of Prof. A. A. Mihailov, investigations have been undertaken at the Geophysical Institute of the Academy of Sciences of the URSS concerning gravity variation with time. J. D. Boullanger developed a method for the relative gravity measurements with an accuracy of about 0.1 and 0.2 mgal for a difference of several gals. This method does not require any standardization by means of the pendulum observations. Investigations of the gravity variations with time are being carried out. Observations of the initial epochs for a number of points in various regions of the Soviet Union have been obtained.

DISPERSION OF SEISMIC SURFACE WAVES AND THE STRUCTURE OF CONTINENTS AND OCEANS

by T. S. AKIMA (Tokyo) and T. NAGAMUNE (Matusiro Observatory).

INTRODUCTION.

Many authors have studied the crustal structures of various regions by observation of the dispersions of Love or Rayleigh waves. But, nearly none has ever made the estimation of crustal structures by observation of Rayleigh wave as well as Love wave dispersions.

In 1952, Y. Sato gave a quite important remark to the problem of crustal structure and the dispersion of seismic surface waves. By the examples he showed in his paper, there exists an equivalent double layered structure which gives quite the same dispersion curve of Love waves as in a single layered one. This means that crustal structure cannot be uniquely determined only from dispersion curve of Love waves.

His remark given above somewhat weakened the trust on all conclusions for crustal structures which have been interpreted by the observations of dispersion of Love or Rayleigh waves. One method to obtain more reliable results, for this reason, must be to make estimations by using the dispersions of *both* Love and Rayleigh waves.

We now put forward the discussions on the structure of continents and oceans along this line in the following.

PART I.

The dispersion curves of Love and Rayleigh waves due to the Great Assam Earthquake of August 15, 1950, and the estimations of crustal structure.

The observational stations at which the seismograms were obtained and the epicenter of the Earthquake are shown in *Fig. 1*. As these stations are all located east of the epicenter, Love and Rayleigh waves must be recorded separately on NS and EW or UD components of all seismograms respectively. The original seismograms, recorded by Wiechert Seismographs ($T = 4.5$ sec), however, contain many short period waves which made difficult to recognize clearly the long period surface waves. This undistinctness was removed by using a torsion pendulum low-pass filter which was constructed

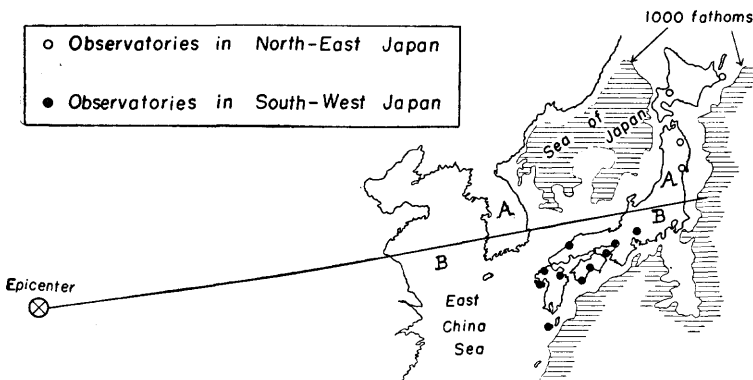


FIG. 1. — Epicenter of the Great Assam Earthquake of August 15, 1950. The distribution of the observatories at which the seismograms used were obtained.

for that purpose by one of the writers. An example of the filtered wave form is shown in *Fig. 2*.

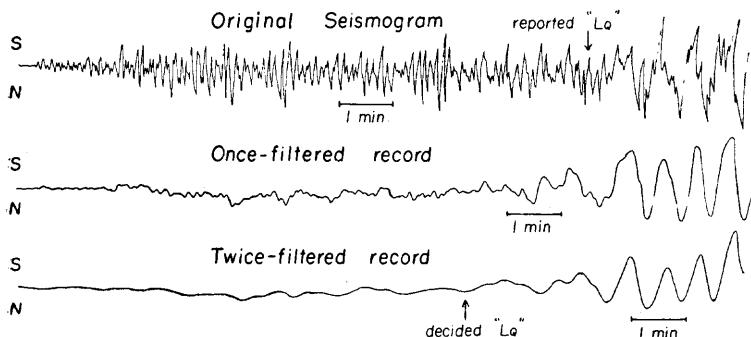


FIG. 2. — An example of filtration of a seismogram of Assam Earthquake. First filtration was performed with cut off period of approximately 50 sec. Second one was done with 60 sec. The short period waves clearly disappeared successively.

The dispersion data obtained from the filtered records are shown in *Fig. 3* concerning Love and Rayleigh waves separately. This figure shows an interesting evidence that the dispersion obtained at the observational stations of northeastern part of Japan (A) differs from that at southwestern part of Japan (B). Judging from the paths of wave propagations from the epicenter to the stations which belong to (A) and (B) groups given above (See *fig. 1*), the difference of dispersions above mentioned may be considered to be due to the « oceanic » crustal structure beneath Sea of Japan. The details of the process to determine the averaged crustal structure

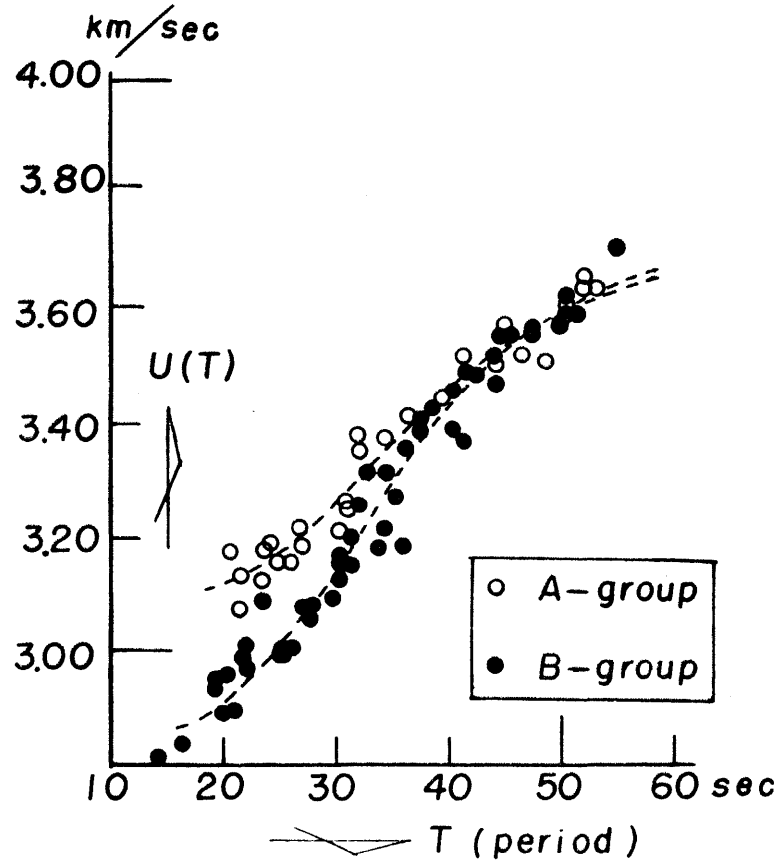
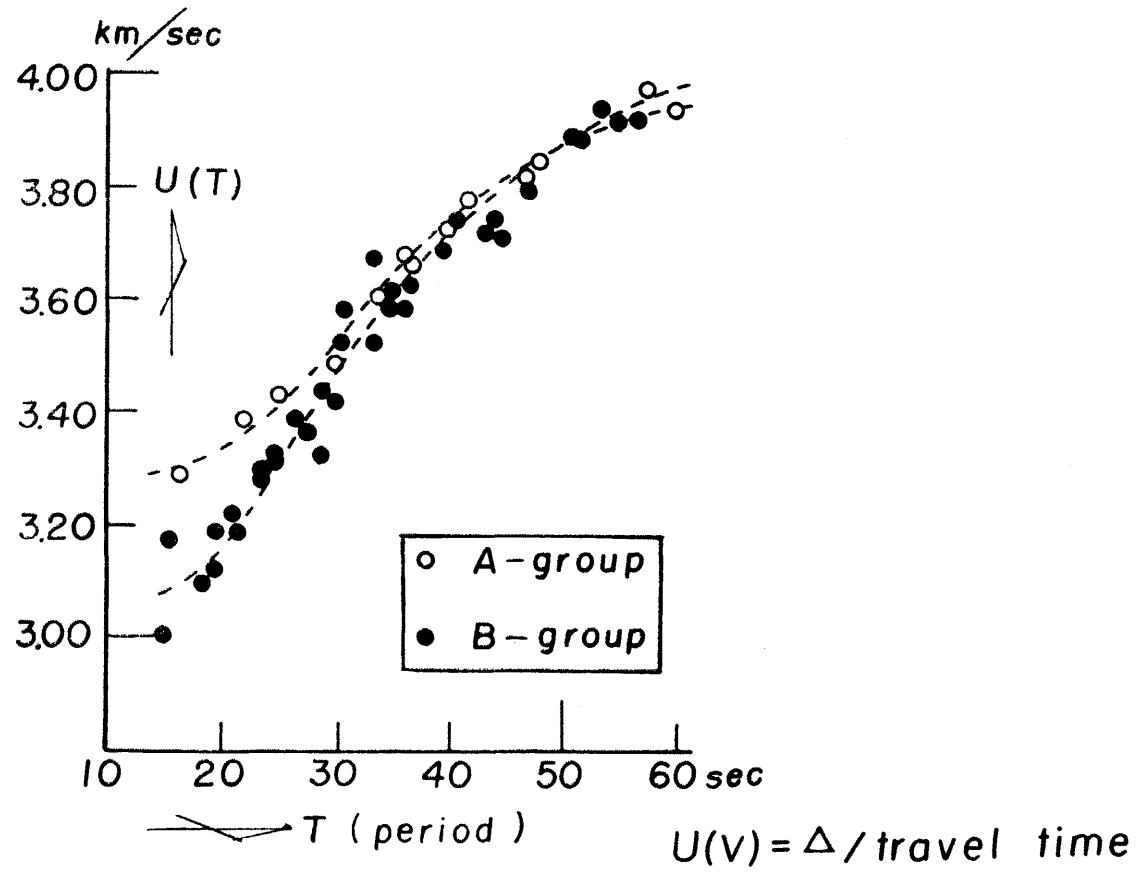


FIG. 3. --- The dispersion data concerning the group velocities of Love (left) and Rayleigh (right) waves.

They are classified into two groups (A) and (B). The latter corresponds to the data obtained at the observatories in North-eastern Japan and the former belongs to those in South-western Japan.

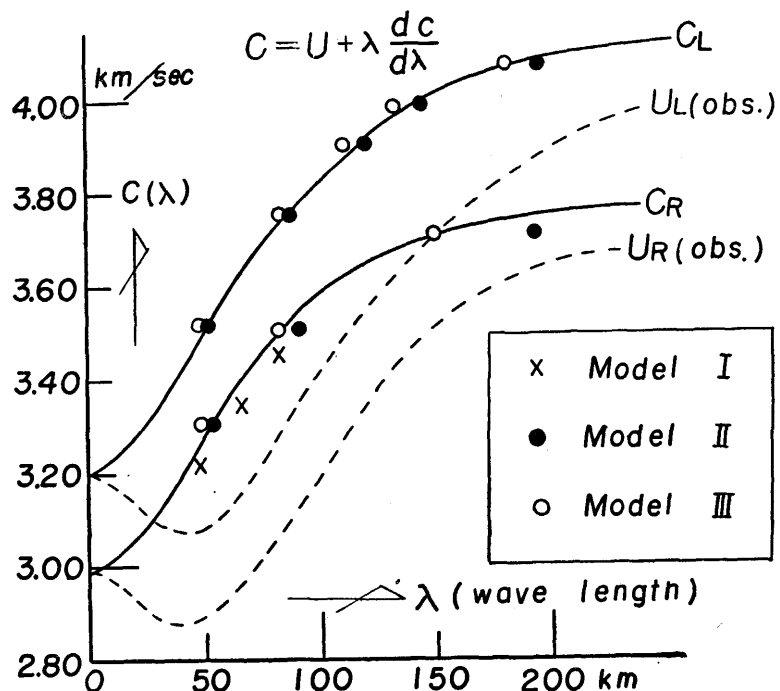


FIG. 4. — Crustal structure for (B) region.

Dispersions of Love waves calculated from models I and II agree with C_L determined by observations. But they do not agree with C_R determined by observations. The model III seems to agree with both of them.

Model I

V	ρ	H
3.2	2.6	22
4.2	3.30	∞

Model II

V	ρ	H
3.2	2.6	12
3.4	2.7	14
4.2	3.35	∞

Model III

V	ρ	H
3.2	2.6	11
3.4	2.7	13
4.2	3.35	∞

for (A) region have been reported in another paper. Among the models I, II, III which are all suitable for the observational dispersion curve of Love waves, the model III only could be adopted as a suitable one as well for that of Rayleigh waves (See *fig. 4*). Therefore, the model III was accepted as the averaged crustal structure for (B) region.

In the course of this study, however, we had to take much labour to perform quite tedious numerical calculations for the dispersion curve of Rayleigh waves under the assumption of double layered crustal structure. The method of these calculations were referred to the recent study by N. A. Haskell.

In the course of procedures to determine a crustal structure suitable for the observed dispersion curve of Rayleigh waves as well as that of Love waves, it was also noticed that calculated points move rather largely by changing the thicknesses of assumed two crustal layers by only 1 km respectively. (See *fig. 4*). From this fact we may say that dispersion curve of seismic surface waves, especially that of Rayleigh waves, depends much upon the thickness of underground crustal structure.

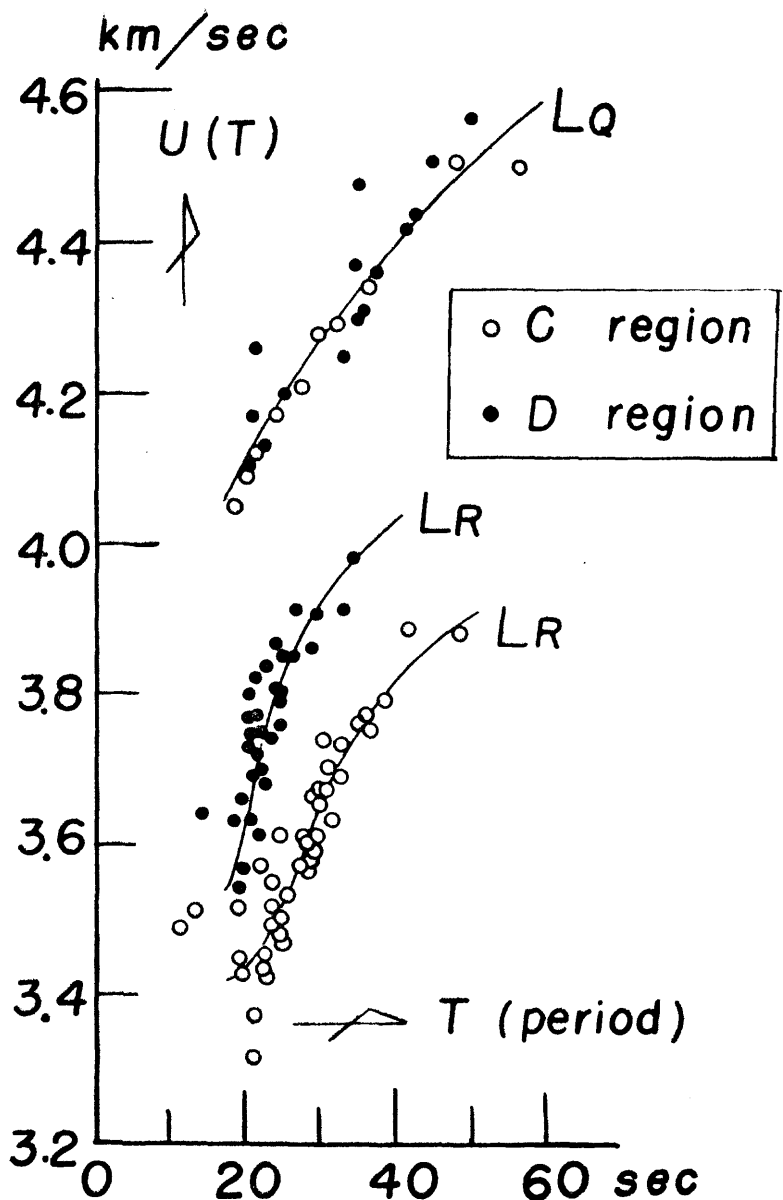
PART II.

The dispersion curves of Love and Rayleigh waves due to several continental and oceanic earthquakes observed at one station, and some discussions for the continental and oceanic structures.

Seismograms analysed in this Part were all recorded at Matusiro Seismological Observatory by a long period seismograph ($T = 35$ sec., $V = 150$). Nine oceanic earthquakes were selected as suitable ones for the separate examination of Love and Rayleigh waves. (See the map at right hand of *fig. 5*).

FIG. 5, showing the dispersion data due to these oceanic earthquakes indicates quite noticeable evidence that the difference of the path (C) and (D) gives a remarkable influence only upon Rayleigh waves dispersion but gives nearly none upon that of Love waves. Estimations of the structures for these two regions considering the water layer have not yet been completed.

Epicenters of selected seven continental earthquakes are shown in *fig. 6*. The same figure, showing the dispersion data due to these earthquakes observed at Matusiro, also indicates a remarkable difference in the dispersions of Love waves. It is regrettable that we could not study Rayleigh wave dispersion curves in southern path (E) on account of very few data. The determined crustal structure of (F) region, after the same procedures as described in Part 1 for



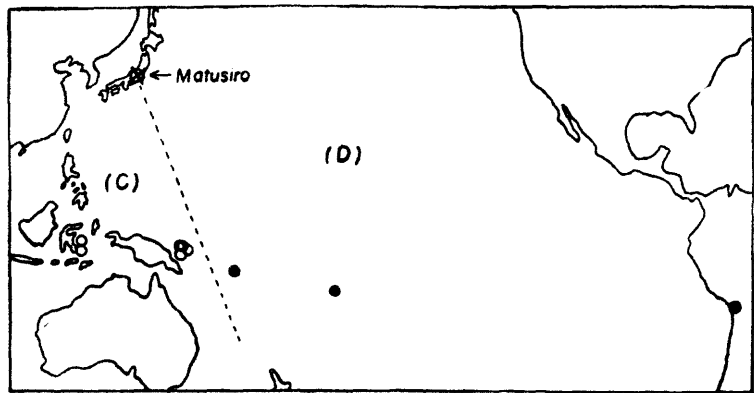
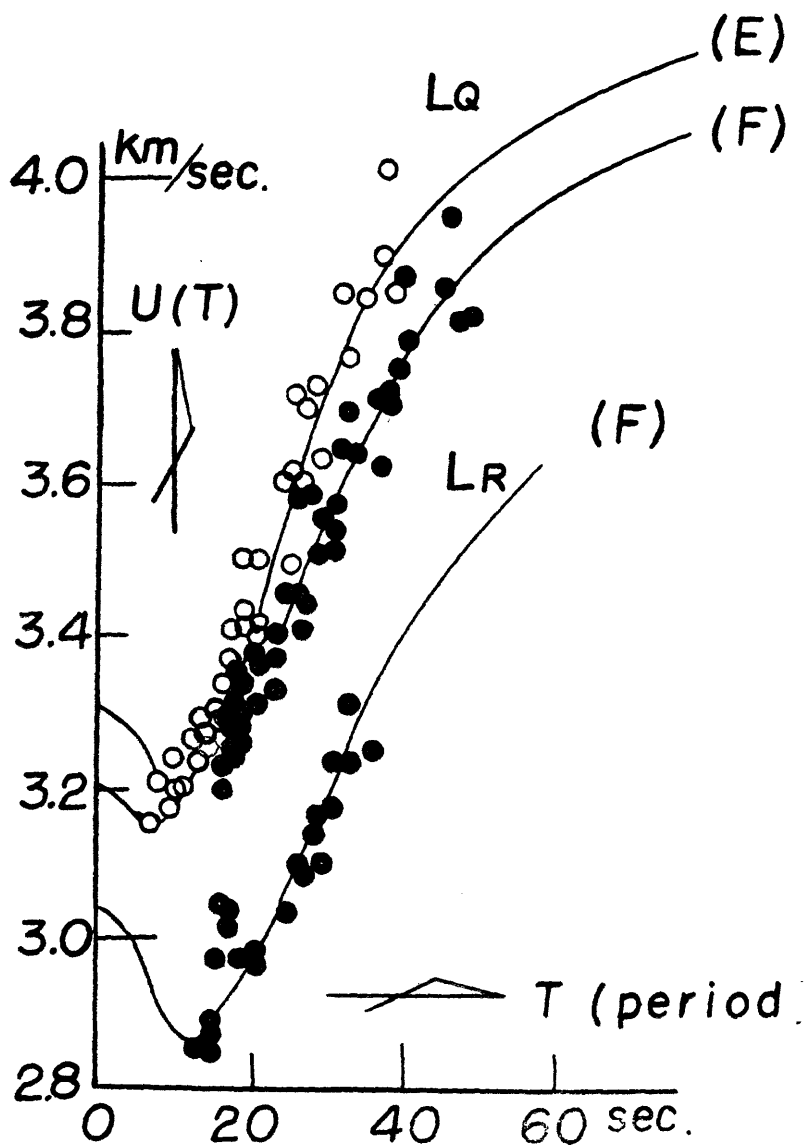


FIG. 5. — Epicenters of oceanic earthquakes and the dispersion data for Love and Rayleigh waves observed at Matusiro.
Differences of Rayleigh waves dispersion for (C) and (D) regions are very conspicuous.



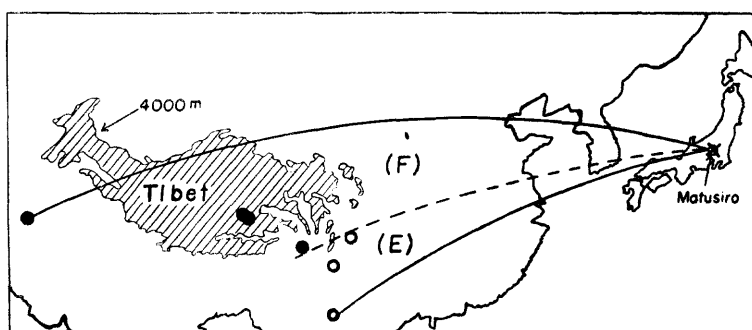


FIG. 6. — Observed dispersion data for two continental paths. Dispersion data of L_{so} for northern paths (F) and southern paths (E) differ clearly, and it seems to be due to the existence of Tibet, Tsinghai or Sikang plateau in the northern path.

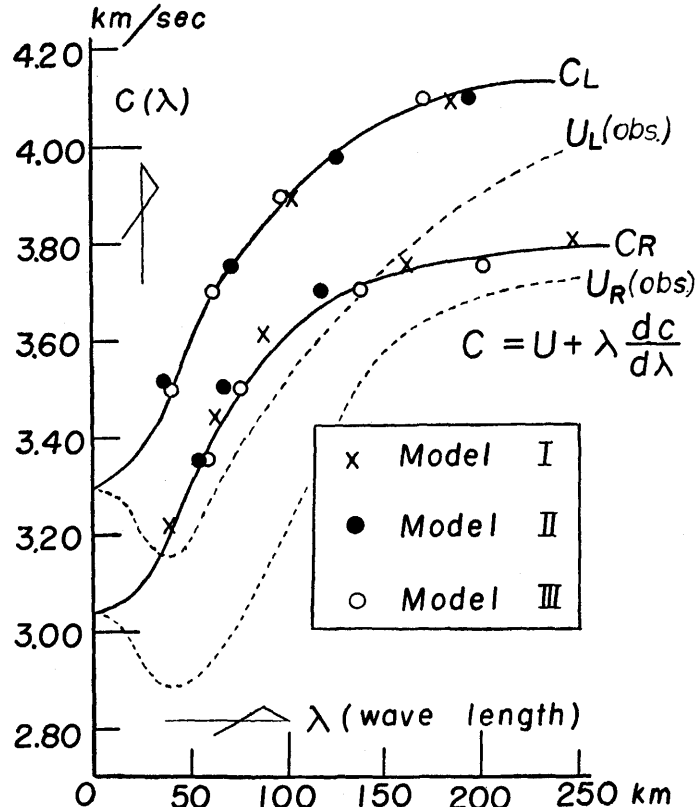


FIG. 7. — Crustal structure of (F) region.

Dispersions of Love waves calculated from models I and II agree with C_L determined by observations. But they do not agree with C_R determined by observations. The model III seems to agree with both of them.

	V	ρ	H
Model I	3.3	2.7	22
	4.2	3.4	∞
Model II	3.3	2.7	16
	3.8	3.0	14
Model III	4.2	3.3	∞
	3.3	2.7	16
	3.8	3.0	15
	4.2	3.3	∞

(A) and (B) regions, is like the model III in *Fig. 7*. In this case, the velocity of shear waves adopted for middle layer, which we cannot get from the observation of surface wave dispersions, was referred to the data by C. Rozava, the only data for the crustal structure of Central Asia.

From *Fig. 6*, we may be able to consider the existence of Tibet, Tsinghai and Sikang plateau as a cause which makes the dispersion curve of surface waves in the region (F) different from that in (E) region. The sensitivity of the dispersions of surface waves for the underground crustal layers can also be recognized by *Fig. 7*.

CONCLUSIONS.

The essentials we want to emphasize in this paper will be concluded as follows;

1. Many examples were practically indicated which show that the crustal structure estimated from the observed dispersion of Love waves only cannot satisfy the dispersion of Rayleigh waves.
2. A torsion pendulum low-pass filter is quite powerful for the observational study of seismic surface waves especially when a seismogram to be analysed contains many short period waves in the portion of surface waves.
3. The dispersion of surface waves, especially that of Rayleigh waves is quite sensitive to the underground crustal structures.
4. The difference of wave paths to Japan through the central and the western Pacific region has much influence upon the dispersion of Rayleigh waves but has nearly none upon that of Love waves.
5. The specialities of crustal structure beneath Sea of Japan and Tibet plateau regions against other places were clearly indicated on dispersions of surface waves in spite of the small proportions of their path length to the total wave path length.

REFERENCES.

1. SATO (Y.) - Study of Surface Waves 4. Equivalent Single Layer to Double Superficial Layer.
Bull. earthq. Res. Inst., Tokyo. Vol. 29 (1951).
2. AKIMA (T.) - A New Mechanical Low-pass Filter for Seismogram Analyses.
Bull. Earthq. Res. Inst., Vol. 30 (1952).
3. AKIMA (T.) - On Dispersion Curves of Surface Waves from the Great Assam Earthquake of August 15, 1950.
Bull. Earthq. Res. Inst., Vol. 30 (1952).
4. HASKELL (N. A.) - The Dispersion of Surface Waves on Multilayered Media.
Bull. Seis. Soc. Amer., Vol. 43 (1953).

CRUSTAL STRUCTURE IN NORTH-EAST JAPAN BY EXPLOSION-SEISMIC OBSERVATIONS

by Research Group for Explosion Seismology (Japan).

I. PREFACE.

Since the big blast of Oct. 25, 1950 in Isibuti, Iwate Pref. our research group for explosion seismology has made several observations of similar blast in Northeast Japan. Reports have been published separately in each time, in which analysis was made independently from each other. However, when these reports are looked over, some contradictions in velocity, depth of layer, etc. are found.

In taking the observation accuracy into consideration, these contradictions cannot come from the observational errors, but can be clues for closer analysis of the crustal structure of the earth. Most of the contradictions found among the interpretations in each observation are resulted from an assumption of horizontal structure which was employed as the first approximation. In this paper material is taken from all our past observations, and most probable interpretation will be made. We hope, our new way of analysis will open a new phase in the interpretation of significantly scattered travel times.

II. MATERIAL AND ACCURACY.

*1. Material.

A series of blasts of which we made observations are listed below.

Notation	Explosion Point	Charge	Shot Time	Obs. line
I 1	Isibuti, Iwate Pref.	57 tons	12 h 06 m, Oct. 25, 1950	IE and IS
I 2	"	7.8	12 h 06 m, Dec. 27, 1951	IO, IE and IS
I 3	"	5.5	12 h 05 m, July 25, 1952	IO, IS and IW
K 1	Kamaisi, Iwate Pref.	29.7	03 h 35 m, Dec. 7, 1952	KO, KW and KS
K 2	"	42	03 h 35 m, Sep. 13, 1953	KS

Table I.

Table of explosions

- IE : Eastern line of Isibuti Explosion
IW : Western line of Isibuti Explosion
IS : Southern line of Isibuti Explosion
KW : Western line of Kamaisi Explosion
KS : Southern line of Kamaisi Explosion
IQ : Vicinity of Isibuti Explosion
KO : Vicinity of Kamaisi Explosion

Detailed description of observation point, blast, instrument, observer, etc. are reported in the following publications.

Blast	Publication
I : 1	Bull. of Earthq. Res. Inst. Vol. XXIX (1951) p. 97
I : 2	Bull. of Earthq. Res. Inst. Vol. XXX (1952) p. 279
I : 3	Bull. of Earthq. Res. Inst. Vol. XXXI (1953) p. 281
K : 1	Journal of Seismological Soc. of Japan (in Japanese) Series 2, Vol. 6 Part 3 (1953) p. 122
K : 2	Journal of Res. Group for Explosion Seismology, Vol. 8 (1953)

The area where the structure was studied is shown in *Fig. 1* by a hatched part and covers approximately 20,000 square kilometers. *Fig. 2* shows blast and observation points which amounted to 10 and about 140 in total respectively.

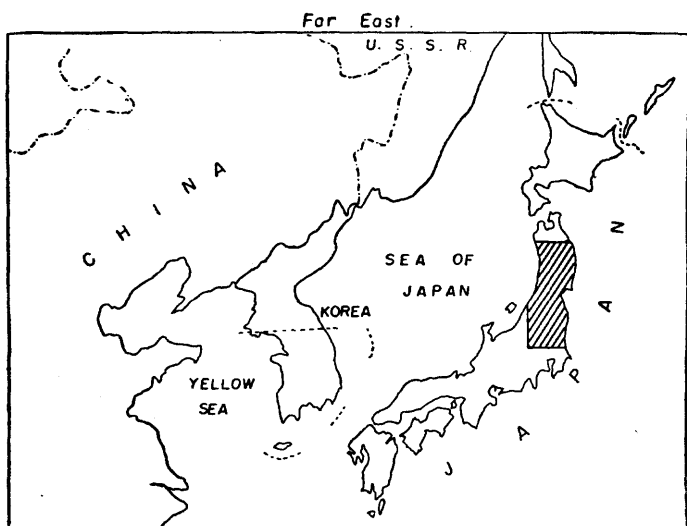


FIG. 1.

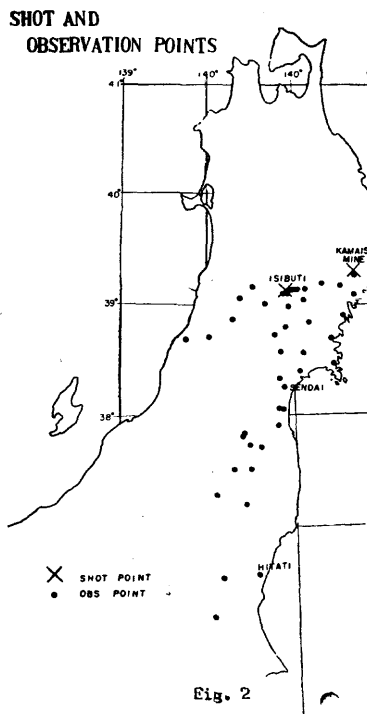


Fig. 2

*2. Estimation of shot time.

In the blasts I : 3, K : 1 and K : 2 shot times were directly registered on the oscillosograph, but in the blasts, I : 1 and I : 2 no shot time could be directly registered. Estimation of shot time in the

first two blasts must be made. Otherwise, the data in these blasts could not be used with others in the same level.

Since the surface structure near Isibuti is known from the third blast when the shot time was directly registered, the shot times in I : 1 and I : 2 were reduced by least squares from the travel times of near-by points.

In Table 2, whole data, travel time, epicentral distance and azimuth (clockwise from the north) are given.

ISIBUTI SOUTH.

Number of observation	Station	Δ_{km}	H. _o	T sec	$T - \frac{\Delta}{6}$ sec
(azimuth)					
3	C	2.70	182	0.95	0.50
2	Hondera	15.3	166	2.96	0.41
3	Hondera	15.3	166	3.02	0.47
2	Kurikoma	22.5	175	4.17	0.42
3	Hosokura	32.2	180	5.83	0.46
1	Hanaizumi	38.5	141	6.83	0.43
2	Kawatabi	41.9	196	7.61	0.63
3	Kawatabi	41.9	196	7.59	0.61
* 1	Matsushima	81.4	169	14.59	1.02
* 2	Matsushima	81.6	169	14.68	1.08
3	Nenoshiroishi	87.8	185	15.24	0.61
1	Sendai	98.2	182	16.86	0.43
* 1	Watari	119.4	180	20.03	0.14
3	Daiyama	148.8	197	25.07	0.27
2	Shinobu	159.9	194	26.75	0.10
3	Hatori	216.4	199	34.6	— 1.47
* 3	Motegi	290.7	193	44.50	— 3.95
3	Tsukuba	327.1	192	50.2	— 4.32

ISIBUTI WEST.

3	Katsurazawa	22.20	241	4.41	0.71
3	Yuzawa	33.77	280	6.31	0.68
3	Innai	45.98	262	8.56	0.90
* 3	Mamurogawa	58.72	243	10.74	0.95
3	Shinasawa	89.99	238	16.04	1.04

ISIBUTI EAST.

2	Umadome I	4.31	69	1.36	0.64
2	Umadome II	4.40	69	1.39	0.66
2	Atago	8.65	78	2.38	0.94
2	Dobashi	12.09	83	3.08	1.07
2	Wakayanagi	14.62	80	3.21	0.77
1	Wakayanagi	15.06	80	3.16	0.65
2	Mizusawa	21.10	83	4.11	0.59
1	Maesawa	21.24	110	4.40	0.87
2	Setamae	55.90	86	9.97	0.65
* 2	Kamaishi	87.54	80	14.84	0.25

KAMAISI SOUTH.

2	Nakasone	11.1	203	2.03	0.18
1	Setamae	20.6	222	3.60	0.17
2	Sakari	23.8	182	4.08	0.11
1	Kesennuma	45.8	194	7.72	0.09
2	Kesennuma	45.6	194	7.58	— 0.02
2	Shizugawa	72.2	197	11.96	— 0.07
* 1	Onagawa	97.6	193	15.92	— 0.25
2	Onagawa	97.4	193	16.03	— 0.20
2	Mukaiyama	137.3	211	22.93	0.05
2	Funaoka	159.6	209	26.00	— 0.60
* 1	Kanayama	173.9	207	28.28	— 0.70
2	Kanayama	173.6	207	28.13	— 0.84
1	Kawamata	202.5	209	31.84	— 1.94
2	Kawamata	202.4	209	31.82	— 1.91
1	Shiraiwa	226.0	208	35.35	— 2.32
2	Shiraiwa	225.9	208	35.31	— 2.34
1	Nogisawa	261.2	206	39.09	— 4.44
2	Nogisawa	260.9	206	40.0	— 3.48
2	Motegi	331.5	201	49.0	— 6.25

KAMAISI WEST.

2	Umanokiuchi	4.82	263	0.90	0.10
1	Ide	37.1	248	6.39	0.21
1	Mizusawa	51.6	250	9.09	0.49
* 1	Yuzawa	103.5	262	18.13	0.88
1	Mamurogawa	130.7	248	22.66	0.88

*3. Accuracy.

It is of importance to pay attention to the accuracy of data in deriving out an interpretation from the above data. In the present study the accuracy depends on the following factors.

- (1) Identification of commencement,
- (2) Time reading, and
- (3) Delay of travel time due to surface weathering layer.

As to (1), the identification was made by several persons independently, and readings were accepted only when satisfactory agreement was found.

As to (2), the highest accuracy is assured among three factors. The reasons are : in most of the observation points, the running speed of recording paper is 2-3 cm per second or more, and second marks are placed directly from JJY Radio Time Signal. As far as this factor is concerned, the accuracy is higher than one hundredth of a second in the absolute time.

As to (3), this is not due to observations. However, it is very local, and in this paper it is considered as a sort of errors. A layer of 2.51 km/sec is accepted as the surface layer, and any local weathering layer comes under the present category. However, most observation points were selected in such a way that instrument could be installed on the bed rock. From the geologic viewpoint and some trial computations, it was found that the error due to this factor cannot be more than 0.1 second.

In considering these factors, the total amount of the error is estimated to be less than 0.1 second. In other words, if a fluctuation in travel times is more than one tenth of a second, the amount must be significant. It may be due to complication of the crust or due to random fluctuation of velocity itself in layers.

III. STRUCTURE NEAR THE SHOT POINTS AND VELOCITY IN THE SURFACE LAYER.

*1. Near Isibuti Shot Point.

Near Isibuti shot point a layer of 2.51 km/sec covers the surface. For its intercept time is zero.

*2. Near Kamaisi Shot Point.

In the blasts K 1 and K 2 observations were also made near the shot point. As a velocity in the surface layer, 6.0 km/sec was obtained approximately. Time accuracy is very high in these observations. However, determination of epicentral distances could not follow the time accuracy because the blast was not a single point. Therefore, with the present data a value, 6.0 ± 0.2 km/sec is accepted. However, it is certain that near K shot point a higher velocity layer lies on the very surface.

IV. TRAVEL TIME CURVE.

*1. General Consideration.

Fig. 3 gives travel times, in which all data except near-by points are equally plotted. Because of a high time accuracy $T - \Delta/6$ (T : travel time in second; Δ : epicentral distance in kilometer) is plotted in the ordinate to visualize all significant deviations.

TRAVEL TIME CURVE IN GENERAL

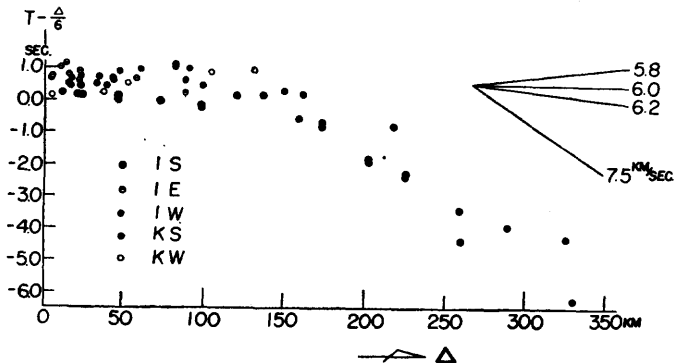


FIG. 3.

Points do not fall on a straight line, and fluctuations are much larger than the observational accuracy.

It is liable to think that these deviations are at random and to draw the « so-called » travel time curve by least squares.

However, if the general travel times are separated according to the directions of observation points from shot point as shown in *Fig. 4* to *Fig. 8* and closer examination is made on these materials, the following important features can be found among them.

- (1) Apparent velocities vary in different profiles.
- (2) Intercept time of a curve corresponding to 6.2 km/sec layer varies in different blasts.
- (3) Time deviation and azimuth have a definite relation.

These features indicate that deviations are not at random, but systematic, and an assumption of horizontal structure is no longer adequate. In order to meet the above features, three dimensional inclination of layers must be taken into consideration. Then, in this paper, the analysis is made on the following points.

- (1) Interpretation of the crustal structure is made only from the seismological data. Geologic or gravitational data will be taken into consideration only to check whether the seismological interpretation is adequate or not.
- (2) Simpler model will be proposed. Only when discrepancy exceeds the accuracy, modification of model will be considered.
- (3) Velocity is constant in a layer. Velocity change in the horizontal direction will not be considered.

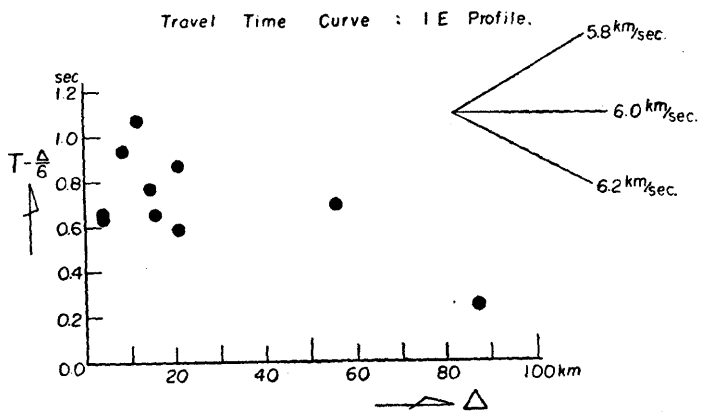


FIG. 4.

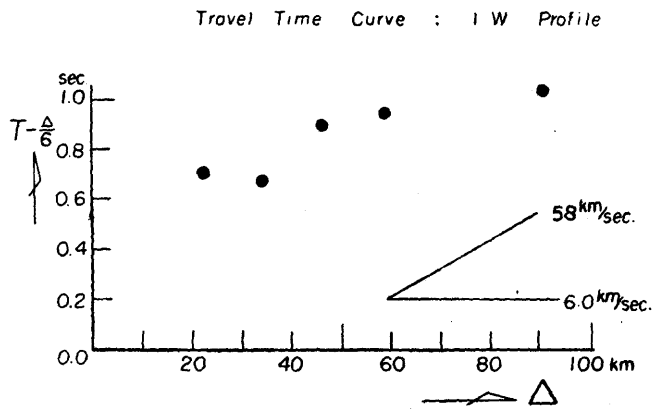


FIG. 5.

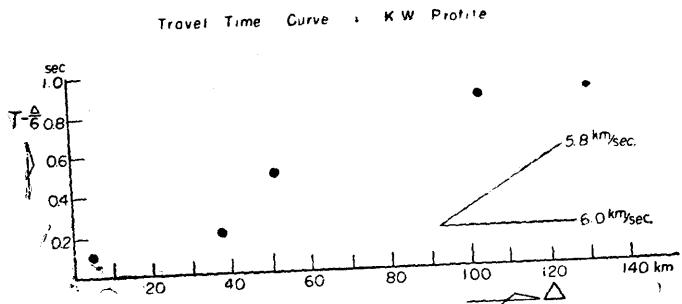


FIG. 6.

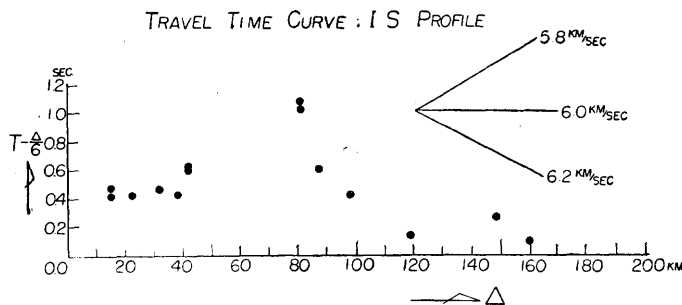


FIG. 7.

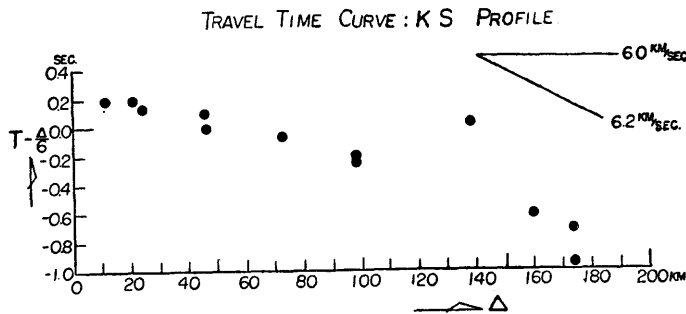


FIG. 8.

In proceeding the analysis on the above stand points, in the first place number of layers, approximate velocities of these layers, etc. must be estimated from the general view of travel time curves drawn in each observational profile.

*2. General View in each Profile.

From the inspection of travel times (fig. 4 - fig. 8) the following quantitative outlines are derived.

- (1) Only in IE profile a layer of 4.4 km/sec is seen under the surface layer of 2.5 km/sec. The travel time curve in this layer is discontinuous to the curve which corresponds to the next layer.
- (2) Near the Kamaisi shot point no extension of 2.5 km/sec layer is found.
- (3) Under the surface layer, a layer of 5.7-6.0 km/sec is found.
- (4) Further below, a layer of 7.5-8.0 km/sec (probably P_n) is found.
- (5) Velocity changes by layers.
- (6) Even in travel times of a single profile deviations from a straight line exceed the observational accuracy. This can be seen particularly in southern profile.

Since an assumption of horizontal structure is not adequate, velocities mentioned above are merely apparent ones. In deriving out a quantitative interpretation from the above general view, no definite formula is available as in case of horizontal structure or two dimensional problem in seismic prospecting. The only way to make a qualitative analysis on travel times is to take approximate values in velocity, strike, dip and depth of layers and employ trial and error method so that observation can be adequately interpreted within the accuracy.

The detail of the computations and considerations made in the course of the study amounts to a large volume and will not be presented in this paper. Only a few examples in the analysis will be given.

V. DETERMINATION OF P 2 LAYER.

In the travel times in IE profile, a velocity of 4.4 km/sec is seen.

Two Proposed Models in IE Profile

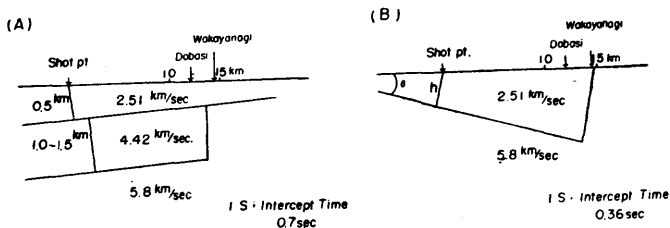


FIG. 9.

Accordingly, two models were proposed to explain this velocity (See fig. 9). In A, a layer of 4.42 km/sec is actually considered, but in B this velocity is considered to be apparent due to the inclination of a layer. In order to determine which is more probable, an intercept time of a travel time curve corresponding to the lower layer (5.7-6.0 km/sec) in IS profile was calculated in both cases, A and B. A gives 0.7 sec and B, 0.36 sec. Observation gives 0.3-0.4 sec, and B is accepted.

VI. AZIMUTH AND DEVIATION.

To determine a strike of the boundary between P 2 and P 3 layers, travel time is formulated in the three dimensional case. (See fig. 10).

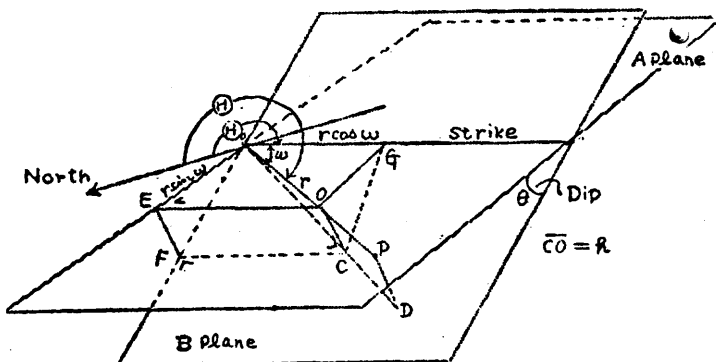


Fig. 10

$$T = \frac{2 h \cos i}{V_2} + \frac{\Delta}{V_3} + a \Delta \sin(H - H_0)$$

where $a = \frac{\theta}{V_3 \tan i}$, H_0 : strike, H : azimuth of obs.

The first term is intercept time, the second term is the real travel time and the third term is due to inclination. If the boundary is inclined $T = \Delta/V_3$ and $\Delta \cdot \sin(H - H_0)$ must be linearly related, and deviations must be systematic as expressed in this equation. In other words, deviations in travel time and quantities which depend only on the location must have a linear relation. The examination was made schematically. In Fig. 11 $T - \Delta/V_3$ and $\Delta \cdot \sin(H - H_0)$ are taken in ordinate against the observation

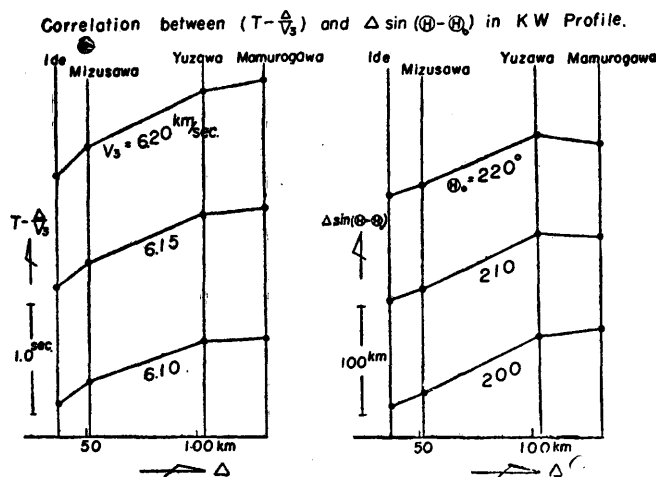


Fig. 11.

points in abscissa, and V_3 and H_0 are taken as parameters. As seen clearly two pictures give a very similar pattern which indicates linear relation in the two quantities. Then, it is certain that deviations are systematic and can be explained by the difference in azimuth in the case of inclined layer.

After many other similar considerations and computations, the following model is derived as the crustal structure in Northeast Japan.

VII. CRUSTAL STRUCTURE OF THE AREA.

Crustal structure of the area consists of the following layers.

- P 1 : 2.51 km/sec
- P 2 : 5.75-5.85 km/sec
- P 3 : 6.1 -6.2 km/sec, and
- P 4 : 7.5 -8.0 km/sec

SCHEMATIC ILLUSTRATION OF CRUSTAL STRUCTURE IN THE AREA.

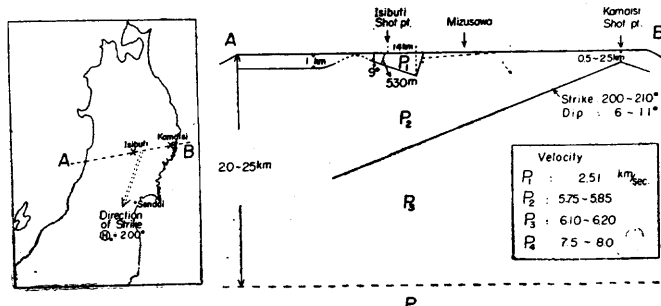


FIG. 12.

Interval gives « absolute allowance », but not « probable error ». True velocity must be in that interval. Fig. 12 shows a schematic representation of our final interpretation. It will be summarized as follows.

- (1) P 1 layer has a depth of 530 meters near Isibuti shot point and inclines eastward with a dip angle of about 9 degrees.
- (2) P 1 layer thins out abruptly in a fault structure at a point 14 kilometers east of Isibuti shot point. However, further eastward near Mizusawa and Umanokiuti a thin surface layer is again found.
- (3) West of Isibuti P 1 layer is very thin or lacking. However, further westward the layer resumes a depth of about one kilometer.
- (4) No P 1 layer is found near Kamaisi shot point.

- (5) South of Isibuti shot point P 1 layer is found, but its shape is unknown.
- (6) A layer which had been considered to be a single one of about 6.0 km/sec is found to be actually two layers, P 2 and P 3.
- (7) The boundary between P 2 and P 3 layers runs in 200-210 degrees from the north with a westward dip of 6-11 degrees. The boundary is considered to be a plane.
- (8) On an assumption that P 4 layer is horizontal, its depth is 20-25 kilometers. (See *fig. 13* which shows travel times in this layer.)

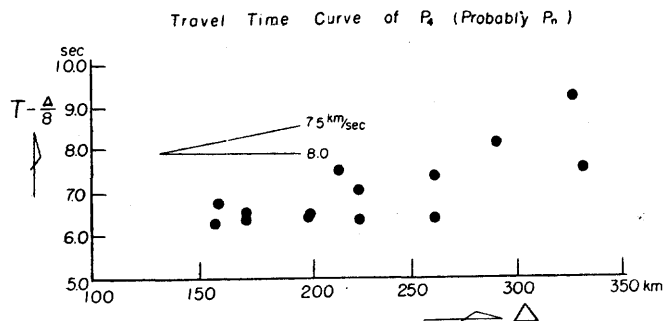


FIG. 13.

VIII. ADDITIONAL BLAST.

Observations of four smaller blasts were made at the east edge of the studied area. *Fig. 14* shows blast and observation points, and *Fig. 15* shows travel times. Analysis was made in the same

Shot and Observation Points in Last Blast

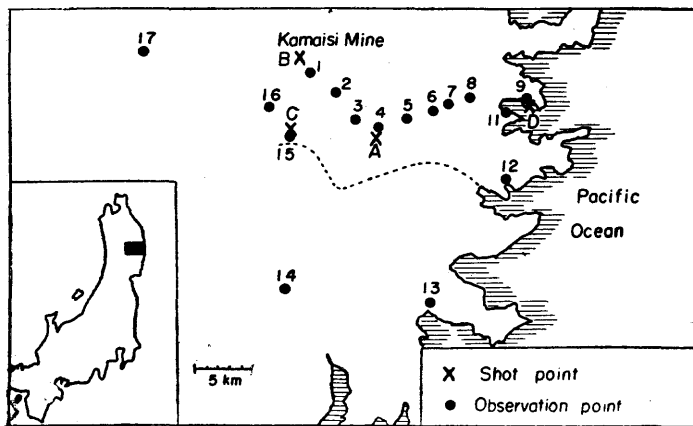


FIG. 14.

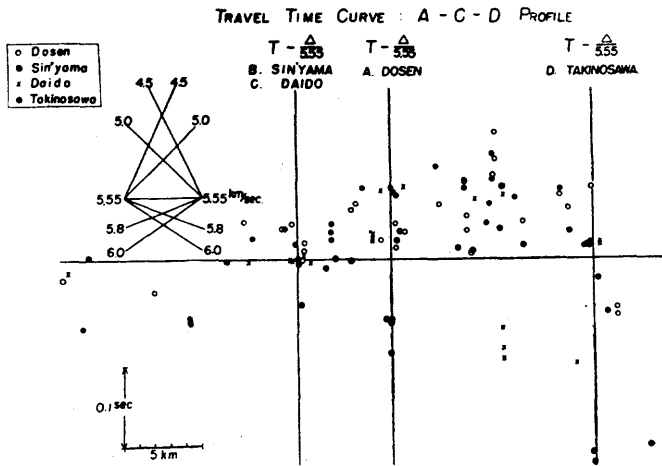


FIG. 15.

Schematic Illustration of Crustal Structure near Kamaishi.

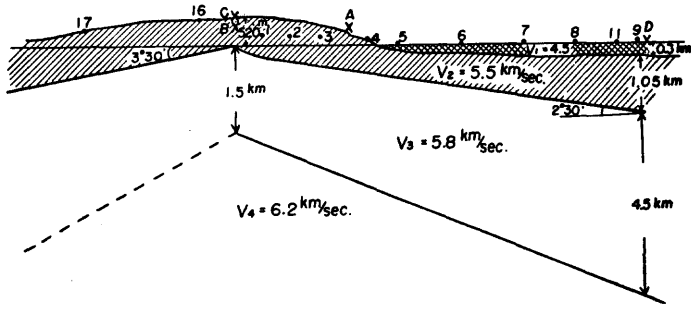


FIG. 16.

way, and the results are shown *Fig. 16*. This cross-section is an eastern part of the A-B section in *Fig. 12*. This additional observation strongly supports our final result.

IX. SOME CONSIDERATIONS FROM OTHER GEOPHYSICAL DATA.

The area is covered by gravity observations made by Tsuboi. Our seismological interpretation of the crustal structure of the area is beautifully supported by Bouguer Anomaly observation. For instance, if density difference between P 2 and P 3 layers is 0.15-0.20 which seems quite possible, even a quantitative agreement can be found.

From the geologic point of view, also, no difficulty is found.

X. CONCLUSION.

If deviations exceed the accuracy, « least squares » is not an adequate method of analysis. Seemingly scattered travel times can be very important for the closer interpretation of crustal structure. The following points will be emphasized.

- (1) All significant deviations can be explained consistently by the analysis based on our stand points. Calculated and observed values agree within the accuracy, 0.1 second.
- (2) Proposition of simpler model and assumption of constant velocity in a layer are possible means to derive self-consistent interpretation of seemingly scattered travel times

EARTHQUAKE EPICENTRES, VOLCANOES AND GRAVITY ANOMALIES IN AND NEAR JAPAN

by Ch. TSUBOI

(Department of Geophysics, Faculty of Science, Tokyo).

With its abundant earthquakes, numerous volcanoes and very characteristic distribution of gravity anomalies, the area comprising Japanese islands and the neighbouring seas forms evidently one of the most interesting fields on the earth from geophysical points of view. Much can be learned if the three phenomena above stated are comparatively investigated.

It has long been known that earthquake epicentres, volcanoes and gravity anomalies in Japan are associated and closely correlated. For such a qualitative statement like this to be drawn, even rough knowledge about the distributions might have been sufficient. If one wishes to get more concrete knowledge, however, the measurements of gravity anomalies, determination of epicentres and the volcanological survey must be enhanced in number as well as in accuracy.

As to the gravity survey throughout the whole country of Japan, the Geodetic Commission of Japan, the Earthquake Research Institute and the Geographic Survey Institute have done much. By the first named institution, 122 pendulum land stations have been occupied up to 1915, while 61 maritime stations in 1934 and 1935 on board of submarines. After the world war II, the Earthquake Research Institute has made an extensive survey by means of a Worden gravimeter establishing about 3,500 points throughout Honshu, Shikoku and Kyushu. On the other hand, the last named Geographic Survey Institute has occupied about 1,000 stations in Hokkaido by means of a North American gravimeter. Thus there are now available altogether 4,500 gravimeter stations throughout the country. These measurements have mostly been made at the sites of bench marks for precise levels. Considering the area of the country which is approximately 38×10^4 km², the density of the gravimeter stations may be said fairly high and there can scarcely be any gravitationally anomalous area of great geophysical interest that could escape our observations. *Fig. 1* shows the distribution of the Bouguer anomalies based on the International Formula. The especially interesting facts to be noted in the figure are :

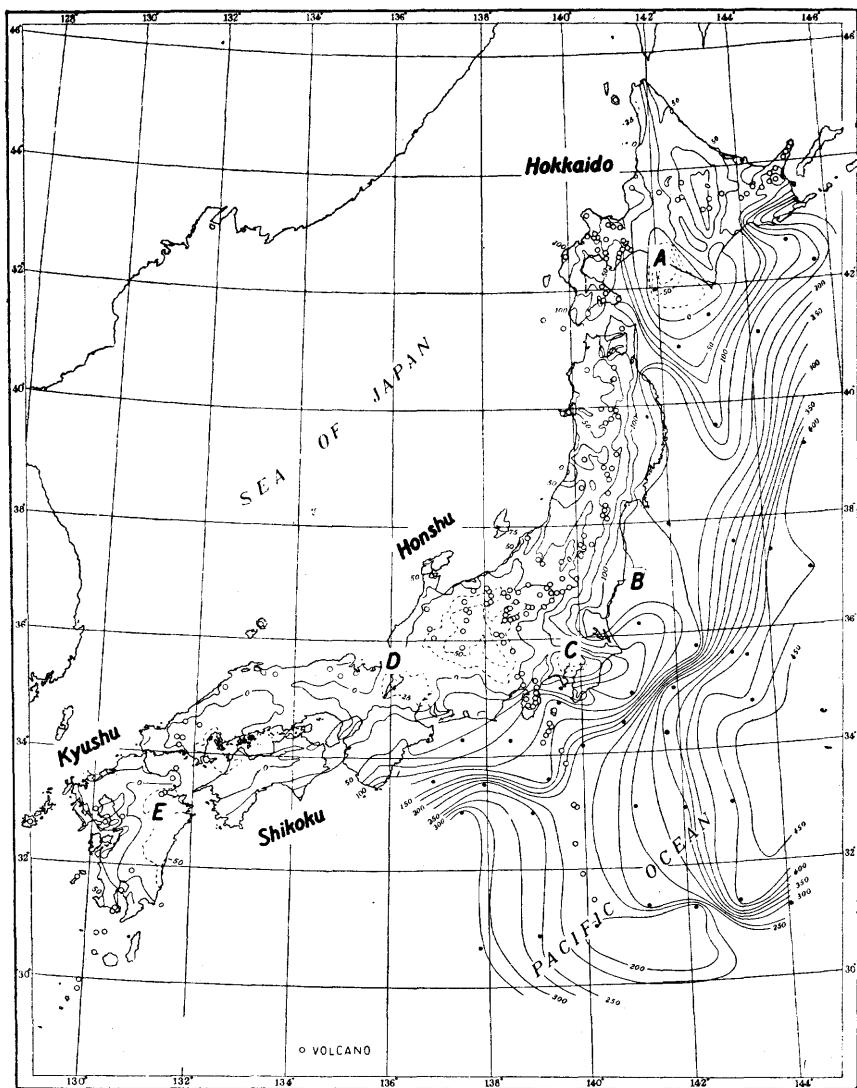


FIG. 1. — Lines of Equal Bouguer Anomalies in and near Japan based on the International Gravity Formula on the Basis of 4,500 Gravimeter Measurements on Land and 61 Maritime Measurements. Interval, 25 mgals. Full Line, Positive Anomaly. Dotted Line, Negative Anomaly. ● Maritime Stations. ○ Volcano.

G 1) In the north eastern half of Japan, the Bouguer anomalies are mostly positive in a contrast with the south western Japan in which there are positive as well as negative anomalies.

G 2) In the south western Japan, the Bouguer anomalies increase systematically towards the Pacific Ocean and the Sea of Japan.

It is interesting to observe that the anomalies do so also towards the west margin of Kyushu, although the sea to the west of Kyushu is about 200 m deep and is therefore too shallow to suggest its « oceanic » nature.

G 3) In the mountainous middle part of Honshu, the main island of Japan, the Bouguer anomalies are negative. The higher the stations, the more negative are the anomalies, indicating that a certain state of isostasy does exist in this area.

G 4) There are several areas which are not high lands yet in which the Bouguer anomalies are negative, such as indicated by A, C, D, and E, in *Fig. 1*. The anomalies suggest local depressions of the earth's crust.

G 5) Along the eastern coast of Honshu, the Bouguer anomalies are remarkably positive, B, which fact suggests that the subcrustal denser material is situated very shallow close to the earth's surface. At the eastern extremity of Hokkaido, the positive anomaly of as much as more than 250 mgal. is observed. This will probably be one of the highest values ever observed on land.

G 6) Southward from the south western extremity of Hokkaido, a remarkable zone of negative or relatively minimum gravity anomaly goes down southwards. (A).

For the location of earthquake epicentres in and near Japan, the Central Meteorological Observatory, Tokyo, is exclusively responsible. To this Observatory belong about 100 local seismological stations and provide material for locating the epicentres. *Fig. 2* shows the epicentres of 3147 « conspicuous » and « rather conspicuous » earthquakes which took place between 1900-1951 in and near Japan. The remarkable facts to be noticed in *Fig. 2* are :

E 1) In the north eastern part of Japan, the epicentres are located chiefly on the Pacific side of the islands. In a striking contrast to this, they are generally located along the islands in south western Japan.

E 2) To say in more detail, in the north eastern part of Japan, the epicentres are clustered in two rather well separated groups A' and B', as indicated in *Fig. 2*.

E 3) There are also several areas in patch where epicentres are anomalously numerous, such as C', D' and E'.

For our knowledge concerning volcanoes in Japan, we owe much to Drs. H. Kuno, T. Minakami and others who investigated their nature, rocks, histories based on their own observations as well as on volcanological literatures. After these investigations, they compiled a map showing the distribution of Quaternary volca-

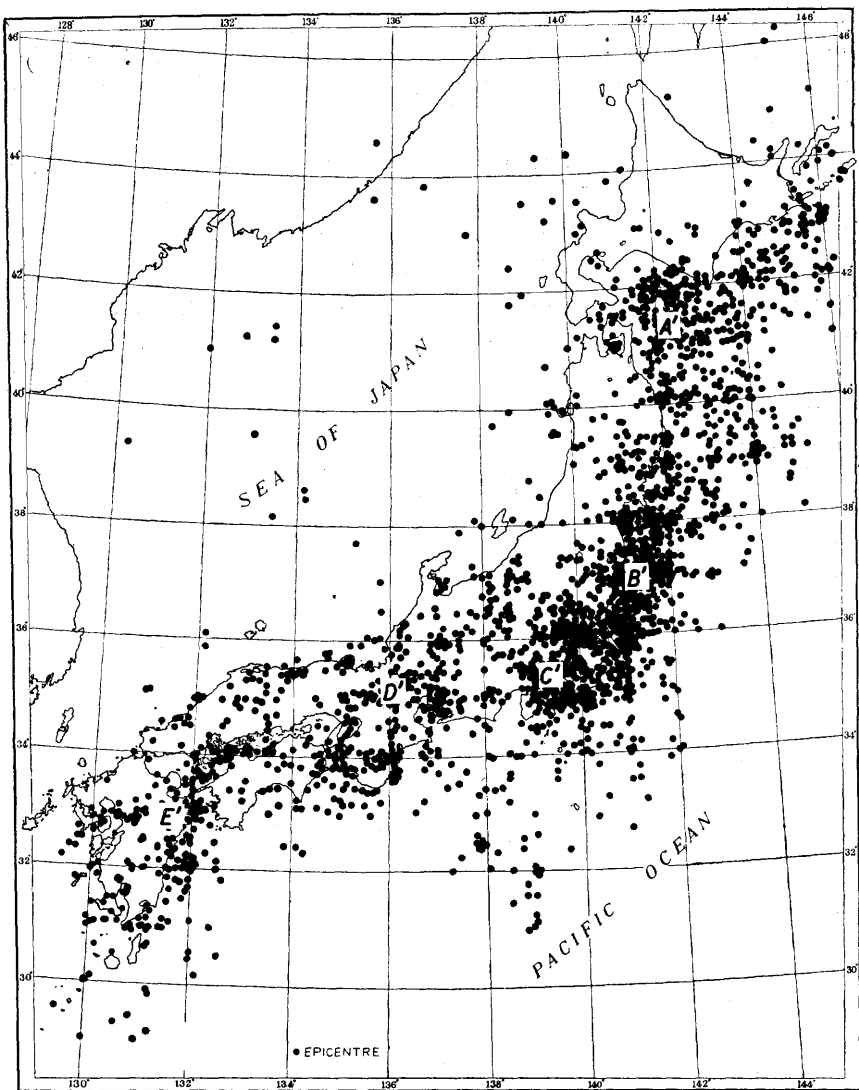


FIG. 2. — Epicentres of 3147 « Conspicuous » and « rather conspicuous » Earthquakes (1900-1951) in and near Japan.

noes in Japan. In *Fig. 1*, the locations of these volcanoes are shown by circles.

We have now prepared maps showing the distributions of the Bouguer anomalies, epicentres of earthquakes and Quaternary volcanoes. Comparing these, we see there is much to be learned. Just a single glimpse on the maps will be sufficient to know that the three phenomena are very closely correlated.

First of all, it was stated that the patterns of distribution of earthquake epicentres are different between north eastern Japan and south western Japan. (E 1). This contrast between the two is also seen in the distribution of Bouguer anomalies. (G 1).

In the central mountainous part of Honshu, the Bouguer anomalies are negative as was stated before (G 3) and here earthquakes occur rarely. This can be reasonably understood as due to the isostatic equilibrium condition prevailing here. Except for this area, earthquakes are seen to occur in those areas where Bouguer anomalies are remarkably positive or negative (G 4, E 3).

Especially notable is the coincidence of the two areas with frequent earthquakes and those of gravity anomalies in north eastern Japan. The one earthquake area corresponds to the abnormally negative Bouguer anomalies, ($A \sim A'$) while the other to the positive anomalies ($B \sim B'$) (G 5, G 6, E 1, E 2). Are there any differences between the seismogram characters of earthquakes coming from the above mentioned two areas? For instance, are there any differences in the mechanism of earthquake occurrence, as indicated by the distribution of the first impulsion of P waves? This problem deserves further investigation.

In the areas corresponding to patches of negative gravity anomalies such as A, C, D, E, earthquakes occur particularly frequently (G 4, E 3).

As to volcanoes, they are situated in narrow zones and it is interesting to observe that these zones run generally parallel to the isoanomaly lines, particularly where they are narrowly spaced. In other words, the volcano rows run parallel to the zones of steep gravity gradients. It is also interesting to observe that volcanoes are always situated along the inner (continental) side of the zones at an average distance of 30 km from them. Areas of earthquake epicentres and of volcanoes are generally not overlapping and more or less distinctly separated.

All that has been stated here is entirely qualitative in nature. More detailed and quantitative studies will be published elsewhere.

DEVELOPMENT OF SEISMIC RESEARCH AND ANALYSIS OF SEISMIC OBSERVATIONS IN THE USSR

by E. F. SAVAREN SKY.

Systematic studies of earthquakes in Russia were initiated in the eighties of last century by I. V. Mushketov and A. P. Orlov. These scientists compiled a catalogue of earthquakes for the Russian Empire.

It contains information on more than one thousand earthquakes that occurred in the country. The information is based on the inspection of destroyed buildings and on geological prospecting. Worthy to be mentioned are some other works analysing geological conditions of occurrence of destructive earthquakes. Among them are the works : by Mushketov on the Verny earthquake in 1887, by K. I. Bogdanovich on the Kebinsk earthquake in 1911, V. N. Weber on the Shemakha earthquake in 1902, etc...

At the end of last century instrumental observations over earthquakes were at their initial stage. Like in other countries they were effected in Russia together with observations over oscillations of the plumb line under the influence of lunar and solar gravitation. First observations of this kind were made in Kharkov, Yuriev (now Tartu) and Nikolayev.

Special systematic seismic instrumental observations were not carried out until 1899 when a seismic committee was founded at the Russian Academy of Sciences. The main effort of the seismic committee was aimed at the creation of seismic stations in Russia and at a systematic study of earthquakes.

Since 1900 Academician B. B. Golitzin, an eminent seismologist, took an active part in the work of the committee. In 1902 he began constructing highly sensitive seismic instruments. He was the first to make galvanometric measuring of the ground displacement by means of a seismograph. The galvanometric method made it possible to separate the seismographs from the recording devices. This represented a very important improvement promoting the design of portable seismographs; observations effected with the aid of portable seismographs are at the base of seismic prospecting.

In 1906 Golitzin constructed a seismograph for recording horizontal movements of the ground and before the end of the year these seismographs were installed for permanent operation in the astronomical observatory of Pulkovo. In 1910 Golitzin created a vertical seismograph.

In 1910-11 the Golitzin seismographs were adopted in Russia, France, Scotland, Belgium and many other countries. Golitzin took great pains to set up in Russia seismic stations of the second class.

First-class stations were mainly intended for studies of general seismicity and of the internal constitution of the Earth, while the main purpose of the second-class stations was to investigate seismicity of the regions in which they were installed. The galvanometric record seismographs were later improved by I. I. Vilip, Golitzin's pupil.

Of great importance for the location of epicentres by means of data obtained by respective stations was B. B. Golitzin's work (1909) on the use of horizontal displacement in determining the direction to the epicentre at the moment of the arrival of the condensation wave.

A very important general appliance for seismologists of that time was another Golitzin's book « Lectures on Seismometry » published in 1912.

After the Great October Revolution the development of industry and growth of towns in the seismically active regions of the Soviet Union stimulated the necessity of a thorough seismic prospecting of these regions and primarily the necessity of dividing the territory of the USSR according to seismicity.

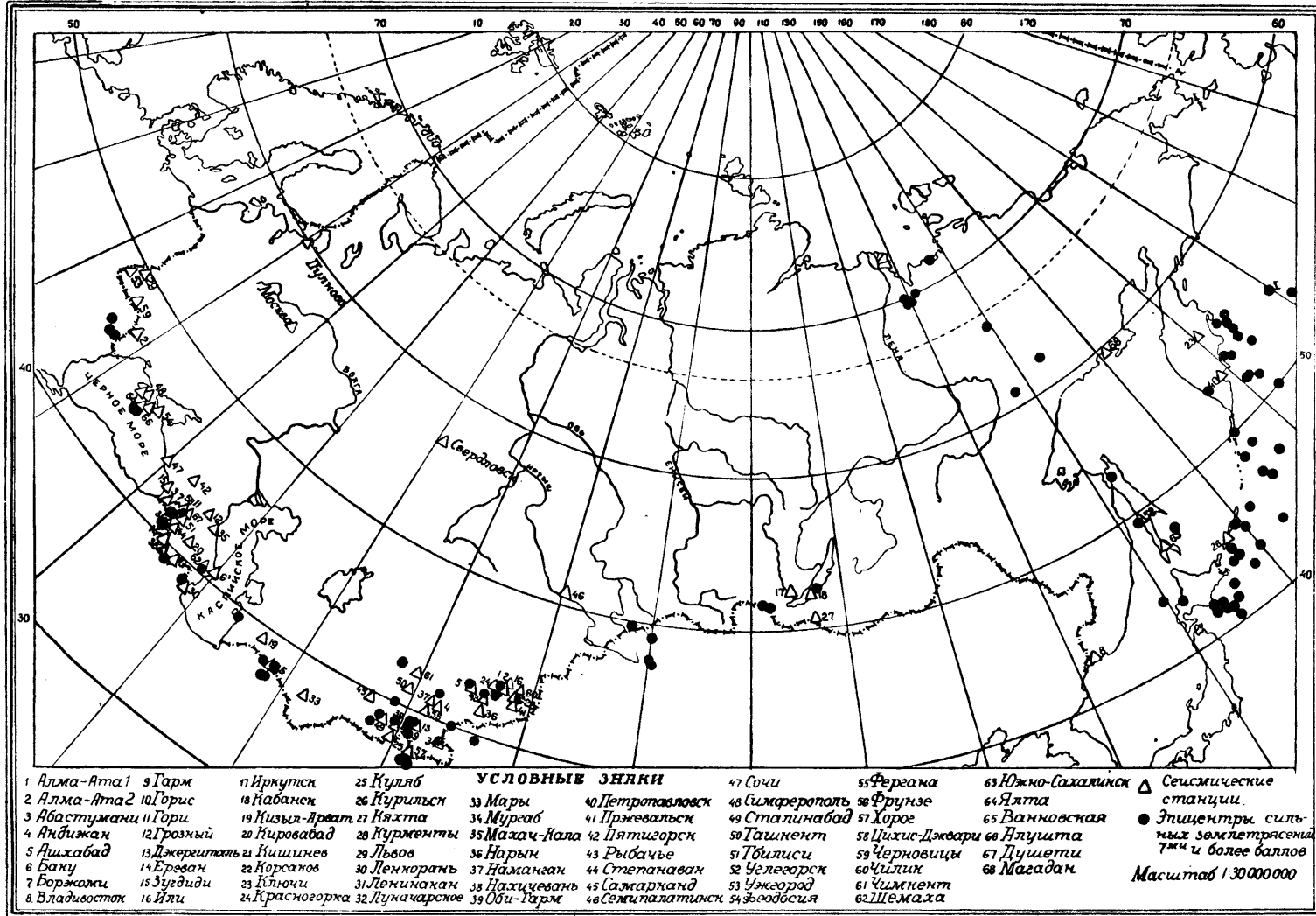
For this purpose, some years ago, a number of special seismic stations to record local and near earthquakes were built in different seismic regions under the supervision of Prof. P. M. Nikiforoff. These regional stations were equipped with special seismographs with optical record (designed by Prof. Nikiforoff).

Within the territory of the USSR the most frequent and the strongest earthquakes are to be found in Central Asia, the Far East, the Caucasus, the Crimea and also in the area adjoining the Carpathians. Therefore first regional seismic stations were set up in 1930 in Central Asia, the Caucasus and in the Crimea.

By their work permanent and temporary seismic stations have rendered essential assistance to the construction of the first big railway of that time — Turksib, which joined the towns of Novosibirsk and Alma-Ata.

The observations of the seismic stations formed a basis for the study of the structure of the Earth's crust in some regions of the USSR and especially on the territory of the Soviet part of Central Asia (E. A. Rozova). It was, for instance, found out that the Earth's crust on the territory of the Soviet Republics in Central

FIG. 1. — Map of seismic stations (Δ) and Epicentres of strong Earthquakes (●).



Asia is thicker than in the European part of the Soviet Union, being approximately 50 km deep. This was later confirmed by the observations of seismic waves during a strong explosion in Korkino (Ural) and by a deep seismic sounding effected recently (G. A. Gamburtzev).

In 1941 we had 32 stations, teleseismic and regional. A general map of seismic regions of the USSR (G. P. Gorshkov) drawn up by this time, played a great part in the construction work in areas liable to be affected by earthquakes.

Each degree in the scale of seismic intensity is matched by definite measures securing stability against earthquakes. Special types of earthquake-proof structures of dwelling and industrial buildings were worked out.

At the same time progress was made in the theory of the elastic wave propagation. A general theory of wave propagation was developed by Academicians S. L. Sobolev and V. I. Smirnov. The basis of the theory is the solution of the wave equation in the form of superposition of waves with complex coefficients having the property of integral invariability. By this method the problem of oscillations of an elastic semi-space, under the momentum of an arbitrarily concentrated force, was completely solved. The problem was formulated by Lamb, but he did not solve it completely having confined his solution to the case where the force is applied to the surface of an elastic semi-space.

Earthquakes do not occur casually, the time of their occurrence being governed by certain laws of nature. These laws are difficult to discover. Nevertheless, they must be detected as many human lives are lost only because of the suddenness of earthquakes.

The research work in the sphere of earthquakes forecasts demanded an increase in the number of seismic stations. Therefore new seismic stations were set up, mainly in Central Asia (23 stations); in the Caucasus (16 stations) and also in the Far East where only one station of the first class operated in Vladivostok.

The map given on *Fig. 1* shows the regions of seismic stations and epicentres of strong earthquakes of last century.

At present 69 seismic stations are in operation in the USSR.

It stands to reason that this extension of the seismic network will make it possible to investigate more thoroughly the location of the seismic sources in different regions of the Soviet Union. With these data being obtained, a better definition of seismic areas can be made.

In order to obtain necessary information for the solution of the problem of earthquake forecasts and other seismological problems, our seismic stations were equipped with two new types of galvanometric record seismographs. Some stations were equipped with D. P. Kirnos seismographs providing a constant magnification (about 1000) within a wide range of seismic wave periods (from 0.5 to 9-10 seconds) so that in the case of near earthquakes these seismographs give records of the ground movements rather exactly. They are also used for the registration of distant earthquakes, thus providing information for the solution of a series of seismological problems. The rest of the stations are equipped with very sensitive D. A. Charin seismographs with periods of 0.5-0.8 seconds. Such seismographs are devised to register the slightest local and near earthquakes.

It is also necessary to create a recording device capable of registering both very weak and strong earthquakes. So far highly sensitive seismographs which register imperceptible ground movements are known to be of no use for strong near earthquakes; however, in the latter case, the knowledge of the character and strength of the movements is of a special practical importance. For this purpose some additional seismographs were set up with a considerably smaller coefficient of magnification. In the Soviet Union special automatic devices are also used to register weak and large earthquakes.

An automatic device consists of a photoelectric relay operated by a galvanometer by means of which the record is taken. When the amplitude of the oscillation increases, the photoelectric device increases the incandescence of the lamps. When the amplitude is so great that the tape is not wide enough to contain the record of oscillations, a special contrivance automatically lowers the sensitivity of the apparatus. In this way it is possible to record both the weak and the strong ground movements. Photoelectrical relays of this type are connected with a device which brings into operation a signal bell in case of a strong earthquake; thus raising considerably the efficiency of the seismic research.

At present we try to obtain complete records of ground movements in destructive earthquakes (amplitude of velocity and acceleration) because only by comparing the obtained information on the character of the ground movements in destructive earthquakes damaging the buildings better methods of earthquake-proof constructions can be worked out. Thus, 15 seismic stations are now

provided with seismographs which record strong oscillations of earthquakes.

The seismic research in the USSR was considerably intensified by the opening of the Seismological and Geophysical Institutes in the Union Republics.

In all the seismic stations of the Soviet Union the same equipment installed, the same method of observations and the same way of treating the obtained data are to be found. Thereby, the drawing of general conclusions from the observations is greatly facilitated. At present the seismic stations of the USSR record over 10,000 earthquakes per year.

The results of the observations are published in the quarterly bulletins which are transmitted to various institutes in the USSR and abroad.

Prof. B. B. Golitzin was the first scientist to measure energy emitted by a hypocentre. His method consisted in measuring the amplitudes and periods on the whole seismogram but this laborious procedure found no practical application.

The method used at present in the measurements of the energy of earthquakes has been worked out by B. Gutenberg and C. Richter. As in Golitzin's method, use is made of the velocity of the oscillation process at the moment when seismic waves cross the point of observation. The measure of energy is the logarythm of the ratio of the amplitude of oscillation to the period of the oscillations, the use being made of parameters of surface waves. This method is expressed in the form of the so-called earthquake intensity scale or M - scale.

The M - scale gives quite good results by recording surface waves when the intensity of distant earthquakes, with hypocentres located within the crust of the Earth, is being estimated. Difficulties arise when the epicentral distance is not long or the hypocentre is deep down under the Earth's crust. It is very important to develop a method for numerous estimates of the energy of earthquakes in order to find out the causes of earthquakes which is at present being effected in the USSR. Among the features essentially characteristic of the liabilities of the different parts of the Earth's crust to earthquakes, is the velocity of shearing stresses resulting from tectonic processes. At a low velocity the stresses relax and there is no accumulation of elastic energy. Under such conditions earthquakes cannot originate. But when

the process is sufficiently rapid an accumulation of considerable elastic stresses is possible with the consequent occurrence of an earthquake.

A map of epicentres with the indication of the intensity of earthquakes shows those parts of the Earth's crust where the emission of energy in the earthquakes was at its maximum, hence where the energy accumulated most quickly.

The degree of accuracy in locating the hypocentre is very important for revealing the cause of earthquakes. This is necessary to be confident in comparing earthquakes with definite tectonic structures of the Earth's crust. In this connection the problem of reducing the possible errors in the location of hypocentres is regarded as most essential.

At present the accuracy in determining the position of hypocentres is indicated in seismic observation bulletins issued in the USSR. Two accuracy types, A and B, have been introduced. Earthquakes for which the location of the hypocentres is determined from near stations (up to 1000 km) and the error in determining the position of the epicentre does not exceed 25 km, belong to A type. Type B comprises earthquakes for which the positions of the epicentres are mainly determined by remote stations (more than 100 km) and the error locating the epicentre is not above 100 km.

The seismic stations of the Soviet Union have been functioning for a long time and now an atlas of seismic maps is being prepared. In compiling the maps account is taken of energy, and accuracy in determining the position of hypocentres for the various seismically active Russian zones.

In the course of the last years, seismologists studying the internal constitution of the Earth on the basis of seismic observations have performed an extensive research work. Prof. A. A. Treskov, head of the Irkutsk station, has created a new method for determining the thickness of the Earth's crust, called a teleseismic method. He has shown that in certain cases the distinct arrival of a wave, reflected from the Earth's surface (perhaps wave P , reflected from the vicinity of the epicentre in the case of a deep earthquake hypocentre, or wave PP , i.e. an ordinary reflected wave) is preceded by a less intense arrival of a wave reflected from the foot of the Earth's crust. The difference between the passage times of the two reflected waves depends on the velocity of the waves within the Earth's crust and on the thickness of the latter. By this means Prof. Treskov has determined the thickness

of the Earth's crust at reflection points in Asia, Europe, the Pacific, Africa, the Indian Ocean, etc... A definite advantage of this method consists in the fact that the thickness of the Earth's crust can be determined in places where no earthquakes occur.

Another important result is the determination of the character of the displacement in the hypocentre from the observed amplitudes at the arrival of condensation and shear waves. This method was first applied by Omori in Japan. However, all the determinations of the directions of displacements in earthquake hypocentres are based on the registration of the displacement at the arrival of condensation waves at the seismic stations. This method, however, fails to give a precise answer concerning the direction of displacements in hypocentres.

Our colleagues, Prof. V. I. Keilis Borok and A. V. Vvedenskaya from the Geophysical Institute of the Academy of Sciences of the USSR have created a new improved method for the determination of forces in the hypocentre during an earthquake. Use was made not only of the signs of the directions of the ground displacement at the arrival of condensation waves, but of the ratio of amplitude of shear and condensation waves at each point of observation. This extends the possibilities of the determination of the character of displacements in the hypocentre.

In investigating the structure of the Earth, Academician B. B. Golitzin was the first to make observations of the direction of the seismic rays and their emergence to the Earth's surface. For this purpose he made use of the amplitudes of the ground movements during the arrival of a condensation wave. In 1912-13 Prof. Golitzin determined the angle of emergence for 85 earthquakes. From these data he was enabled to graphically represent the dependence of the emergence angle on the epicentral distance. From the apparent angle of seismic radiation thus obtained the true angle is derived by calculation. The solution of the problem of the internal velocity distribution can be obtained without the empirical passage time curve differentiation. The application of this method was for long under question because it was supposed that the influence of the upper non-homogeneous layers might be considerable. Prof. E. F. Savarensky, author of this report, was able to investigate this point and to find out that geological non-homogeneities are not likely to exert an appreciable influence on the value of the seismic radiation emergence angle. Only in cases when the length of the observed wave is less than the thickness of layers in the Earth's crust, can the non-homogeneities have an

effect. Emergence angle determinations effected over a long period of time at the seismic stations in Pulkovo, Sverdlovsk and Moscow, have shown that the emergence angle varies to a very little extent under the influence of the conditions of the soil.

The seismic observations of the first-class stations of the USSR made it possible to reveal the arrival of seismic waves reflected from the surface of the internal core — sub-core — and thereby to find its radius rather exactly.

GENERAL SURVEY OF SEISMICITY OF THE TERRITORY OF THE USSR

by G. P. GORSHKOV.

The problem of dividing a territory into seismic regions consists in obtaining information concerning the potential seismic activity at any point located in the region of tectonic activity that is the determination, for a definite point, of the maximum strength of future earthquakes.

Maps of seismological regions (in Russian : « seismicheskogo raionirovania ») represent the graphic expression of this idea.

The solution of the problem of the seismic regions division may be obtained on the basis of a thorough investigation of the seismological regime of the causes of tectonic movements and also by the study of the relationship between earthquakes and the young geological structures.

On the territory of the Soviet Union there are many thousands of earthquakes to be recorded every year; some of them reach a great violence.

The earthquakes in the Carpathians are mainly concentrated in the Eastern wing of the folding system near Ploeshty and so on and they are sometimes characterized by the creation of great quantities of energy in the hypocentre; in this case the violence of earthquakes reaches nine or ten balls, and the perceptible oscillations spread over a vast area reaching Moscow.

The central parts of the depression of the Black Sea are deprived of epicentres, except the peripherical parts of the depression. There is an important concentration of epicentres in the Crimean peninsula, mainly in the Southern area of the main Crimean anticlinarium. The depth of the hypocentres does not exceed here 40 km. These earthquakes rarely have a destructive violence.

In the Caucasus a great many earthquakes occur every year. A great number of them are very strong. They are chiefly concentrated on the territory of the Minor Caucasus. The depth and the spreading area of the hypocentres are generally limited. The perceptible oscillations never go beyond the boundaries of the Caucasus proper.

The territory of Turkmenia is distinguished by an important seismic activity. The hypocentres here are concentrated within the folding mountainous system of Kopet Dag. There are some hypocentres which are linked with the structure of the Kopet Dag front

depression. According to some data, local earthquakes develop as a deformation of the shear in the depth of crystalline and sedimentary rocks.

The eastern regions of Central Asia are among the most active seismic regions of the Soviet Union. Within the northern area, *i. e.* in Tien Shan, there are earthquakes with hypocentres located at a depth of some 100 km. and within the southern one, *i. e.* in the Pamir, neighbouring parts of the Tadjik depression and Afghanistan, at a depth of about 300 km. Within the Tien Shan area earthquakes occur very rarely but sometimes reach the greatest level of intensity which seems to be the result of tectonic peculiarities : Tien Shan is an area consolidated already in the Quaternarian Age. In the southern parts of Central Asia earthquakes occur with a greater frequency but never attain the violence, that is recorded in Tien Shan, which may be also accounted for by a peculiar tectonic development in the plastic deposits of the Mesozoic and Cenozoic Ages of the geosynclinal type.

The mountainous parts of Western Siberia, the Altai, Kuzbass and Sajany are characterized by rare and weak earthquakes.

At present the rate of differentiation and intensity of the tectonic movements is on the increase in the region of the Lake Baikal, neighbouring mountain ranges and in the depressions connected with them. Correspondingly does the rate of seismic activity also increase. Earthquakes, which are to be found in the depressions of the Quaternarian Age, sometimes reach here a very great strength.

The Far East is the most active area from the seismological point of view. Earthquakes occur here mainly in the zone of the Kuril Islands and Kamchatka. The depth of hypocentres increases in the direction of the continent, attaining 600 km. under the bottom of the Sea of Okhotsk and in Primorie. Seaquakes are sometimes accompanied by strong « tsunami ». There are also volcanic earthquakes in the area.

A certain number of earthquakes occur in the area of the Verkhoyansk Range; from this area the epicentres spread as a wide band across the Arctic Ocean from the Lena estuary to Spitzbergen, determining the boundaries of the zone of some tectonic movements within the Arctic area.

Very rare and weak earthquakes are to be recorded in the Urals, on the territory of the Baltic shield and on the Russian Platform. Many of them are probably caused by the fall of the backs of underground cavities.

The survey of the seismic phenomena, connected with the territory of the Soviet Union, shows that the main cause of earthquakes are existing sufficiently differentiated and intensive tectonic movements. Therefore it must be supposed that the chief characteristics of the seismological regime nowadays will be preserved for long without important changes. This is one of the basic principles to be considered in dividing the territory into seismic regions.

A special map shows seismic zones, divided according to the ball system, which indicates to the maximum violence of prospective earthquakes, independently to the fact whether they have been observed in the past or not.

In the Soviet Union such maps are official documents which oblige the building organisations to take into account the danger of possible earthquakes in the seismically active regions and take measures for preventing the houses they build from destruction.



THE MINUTE INVESTIGATION OF SEISMICITY IN JAPAN (2ND PAPER)

by K. WADATI and Y. IWAI (Tokyo).

§ 1. SUMMARY.

We experience frequent earthquakes near Japan, and due to many seismic stations, we can accurately locate the epicenter and determine the focal depth of each earthquake. In the first report (1), authors published « Seismicity Maps » of the Kwanto and Kyushu areas where seismic activities are most vigorous. Recently we made similar investigations in other areas and completed now the seismicity maps of Japan and its vicinity.

This map will serve as a material essential for the study of the structure of earth's crust and for the research in the causes of earthquake occurrences. The especially interesting part lies in the relation between the places of occurrence of intermediate earthquakes ($H = 70 - 200$ km) and active volcanic regions.

§ 2. OBSERVATIONAL MATERIALS.

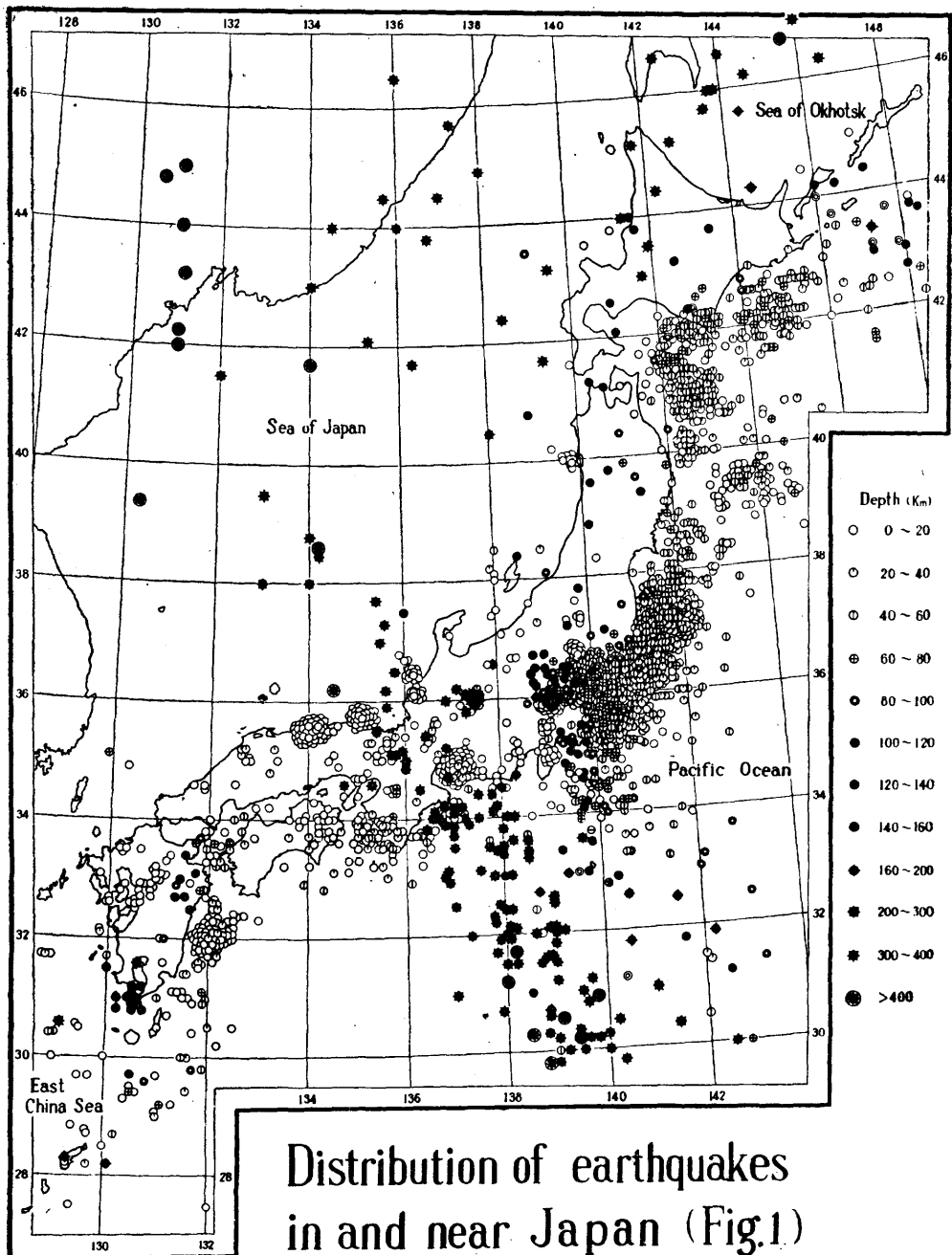
The earthquakes dealt with in this paper are all the earthquakes with magnitude above 5 which occurred near Japan during 28 years' period from 1926 through 1953. As regards the intermediate earthquakes, small ones with magnitude less than 5 are also included. The total number of earthquakes treated in this investigation is 2088. The frequency of earthquakes, classified by focal depths, is shown hereunder.

Focal depth	0-50	60-90	100-130	140-200	210-290	≥ 300 km.
No. of earthquakes	1403	362	115	40	44	124

A table showing the various elements of each of those earthquakes (time of occurrence, location of epicenter, focal depth, etc.) is omitted here. The values of those elements were taken chiefly from the data printed in the « Earthquake Report » (2) published by the Central Meteorological Observatory, Tokyo, after re-examination. The elements not printed in the « Earthquake Report » by reason of comparatively small magnitude, were obtained from the earthquake reports made by each seismological station to the C.M.O., Tokyo.

§ 3. SEISMICITY MAPS OF JAPAN AND ITS NEIGHBORHOOD.

Fig. 1 shows the seismic activities of Japan and its neighborhood obtained by this investigation. A similar map has already been

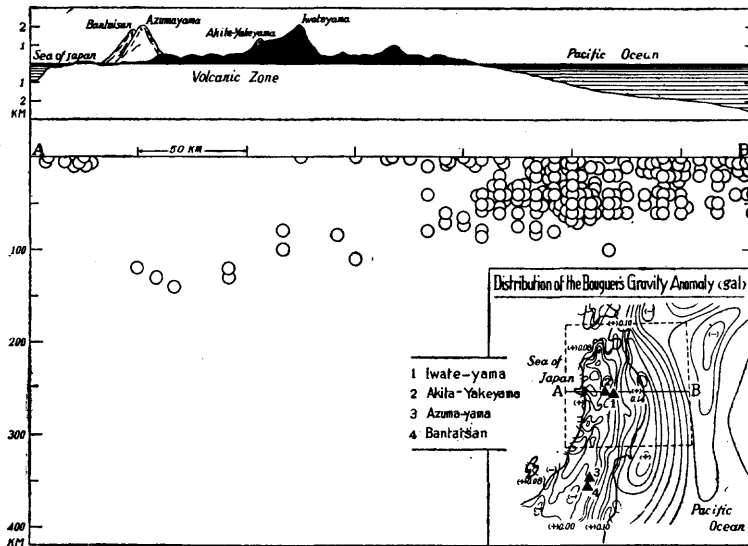


published by Gutenberg (3). Our new map, however, can be said much more detailed than that, since it contains the earthquakes of small magnitude, each of which is closely investigated referring to the data of numerous near-earthquake observations.

As to the regional distribution of hypocenters, we have already explained in the first report, showing the profiles of Kwanto and Kyushu areas. Here we applied the same method to Hokkaido and Tohoku districts. In both districts, major part of shocks are the shallow ones with the focal depth less than 60 km, occurring along the Pacific side. The general tendency indicates that the focal depths of earthquakes which occur at the bottom of the Pacific are shallow-seated, and shifting towards inland, the focal depths tend to become deeper, particularly in Hokkaido, going farther from Tokachi plain to the volcanic region, focal depths increase suddenly and then intermediate earthquakes are observed. Also in Tohoku district, where Nasu volcanic zone traverses from north to south, with several volcanoes in its vicinity, intermediate earthquakes are recorded, while both in the Japan Sea and Soya Strait areas, deep focus earthquakes are observed.

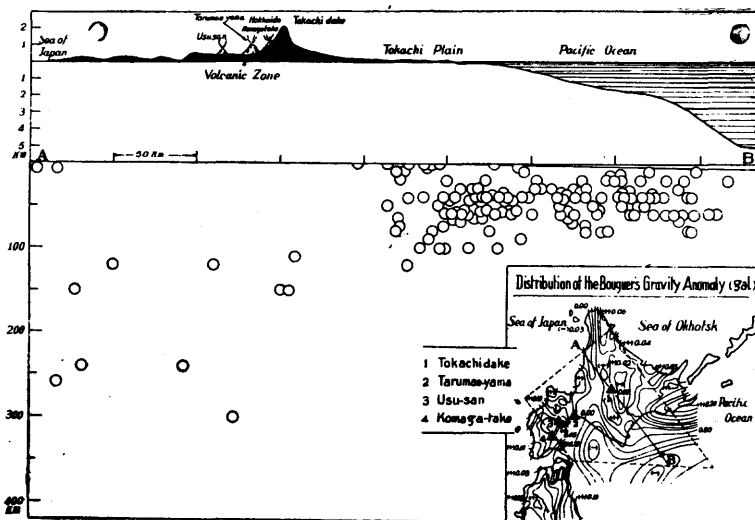
Fig. 2 and 3 are the profiles showing the vertical distribution of hypocenters in those two districts, that is, line A-B cuts the

Fig. 2 Profile showing earthquake hypocenters in the Tohoku District.



earth's crust vertically. On the profile obtained thus, hypocenters of the earthquakes which occurred in the zonal region surrounded

Fig. 3 Profile showing earthquake hypocenters in the Hokkaido District.



by dotted lines are projected. These figures clearly show the above-mentioned spacial distribution of hypocenters. In Fig. 2 and 3, gravity anomalies (4) of those districts are shown for reference.

§ 4. SOME REMARKS.

The purport of this paper is to introduce Fig. 1, but I wish to add some explanations to it. Japan lies in the seismic zone encircling the Pacific Ocean, where frequent earthquakes are recorded. The distribution of hypocenters of these earthquakes has regularities, generally speaking, at any localities of that seismic zone, as is known. According to our latest minute investigation, we can notice regularities of similar nature even in the small areas in and near Japan.

As one (5) of the authors already concluded, almost all deep-focus earthquakes occur in the two zones; one is the transverse deep-focus earthquake zone (from Vladivostok and vicinity extending southward to the Marianas traversing Japan along the west side of Fuji volcanic zone), the other the Soya deep-focus earthquake zone (from Vladivostok and vicinity extending eastward to Kamchatka through Soya Strait). And a vast number of shallow-seated earthquakes are recorded along the coast or the sea-bottom off the east or south of the Kuriles down to the Islands of Japan. Between these two zones intermediate earthquakes occur, but they occur only where the active volcanoes exist and almost none in

the area where active volcanoes do not exist. On the other hand, the distribution of gravity anomalies and the spacial distribution of earthquake hypocenters have close relations. The authors have special interest in the fact (6) that intermediate earthquakes appear only in the active volcanic zone and are intending to make further investigations in this connection.

REFERENCES.

- (1) WADATI (K.) and IWAI (Y.) : The Minute Investigation of Seismicity in Japan. Geophys. Mag., Vol. 25, No. 3-4. Published by C.M.O., Tokyo, Mar. 1954.
 - (2) The Geophysical Review and the Seismological Bulletin. Published by C.M.O., Tokyo.
 - (3) GUTENBERG (B.) and RICHTER (C. F.) : « Seismicity of the Earth », 1949.
 - (4) « Report of the Geodetic Works in Japan for the Period from Jan. 1939 to Dec. 1953 », Section of Geodesy, National Committee for Geodesy and Geophysics of Japan.
 - (5) WADATI (K) : Shallow and Deep Earthquakes (3rd paper). Geophys. Mag., Vol. 4, pp. 231-283.
 - (6) GALANOPoulos (A.) : « On the Intermediate Earthquakes in Greece ». Bull. Seism. Soc. Am., Vol. 43, pp. 159-178.
-



SEISMICITY AND ERYTHREAN DISTURBANCES IN THE LEVANT

by N. SHALEM (Jerusalem).

According to the geographical division of Gutenberg and Richter, based on the magnitude of the tremors, the East of the Mediterranean Sea — Palestine included — does not appear as a seismic region. It figures as a problematic zone which is situated between

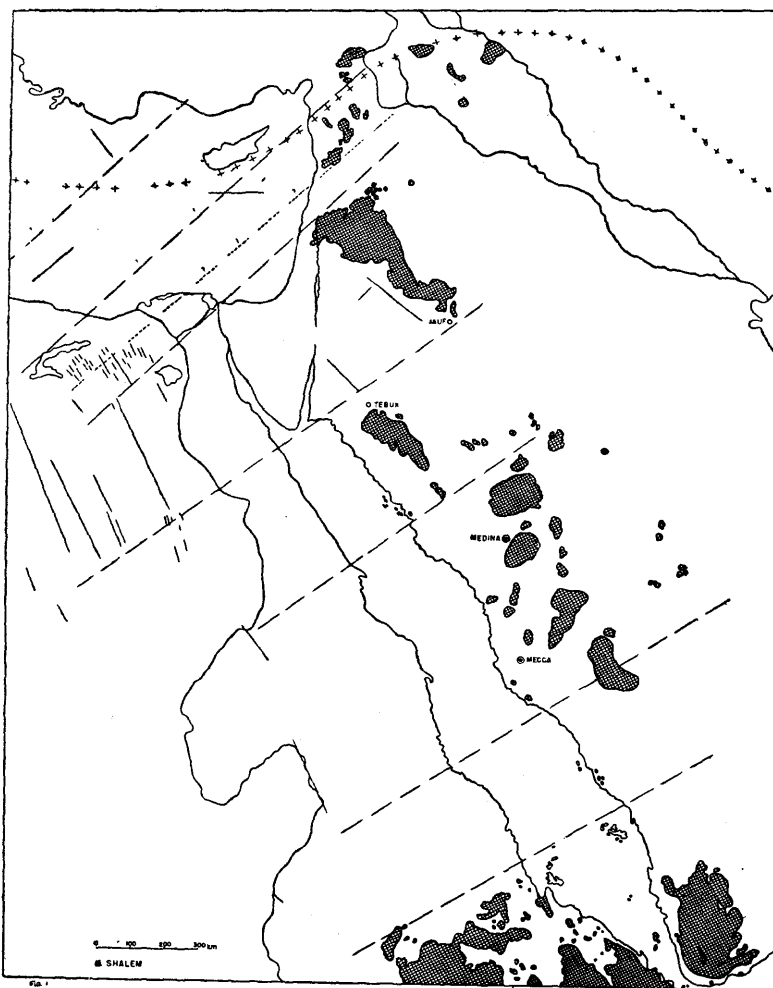


FIG. 1. — *Some tectonic elements of the Red Sea region and the Levant.*
The line of crosses : the Southern limit of the folded region.
The cross-hatched spots : Lav. flows.

the transasiatic band and the African Rifts region. According to the recent geological and seismological research, we can assess the situation of the hinterland of the Jordan Valley and designate it as a region submitted to the prevalent forces of the Alpo-Himalayan orogenic band. These forces act on it in a direction of a series of fractures we call « Erythrean », in allusion to the Red Sea (Erythrea Thalassa) directed NW-SE (see map Fig. 1). These fractures are elsewhere an integral part of the East African Rifts, and therefore the whole system is the result of the strain of the above mentioned orogenic transasiatic band.

Experience shows us that if we receive data from *macro-seismological* surveys allowing us to fix an isoseismic line in an approximate manner only, this is a sign that the study has been insufficient and it would be imprudent therefore, to draw any tectonic conclusions from it.

Palestine abounding in faults, requires a multitude of data furnished by a very close network of observers in order to control rigorously the peculiar behaviour of every point observed. For our purposes the intensity of the tremor is of no importance. In consequence we have established a macro-seismological network of about 400 observers, in a relatively small country, observing even harmless tremors not generally considered in other countries. All tectonic conclusions have been drawn from this practical arrangement.

The 13.9.1954 tremor, solidly confirmed the last macro-seismical survey. Since 1951 there occurred in Palestine four medium shocks of different foci and extent. We dealt systematically with their macro-seismical survey, and this enabled us to come to conclusions based on pure inductive observations, rather than on deductive speculations. To these four tremors we add the disastrous earthquake of 11.7.1927, reliably recorded. Historical tremors also confirm our conclusions, but because of lack of reliable data we shall not state them here.

THE DIRECTION OF THE ACTIVE FAULTS.

The most characteristic feature of the Palestinian seismicity consists in its action along the NW-SE fault system. On a seismological map this is illustrated by NW-SE nuclei in the general shaken area.

The first palestinological observers in the last century noted this surprising phenomenon. They observed that two adjacent places may be shaken differently by the same shock. This empiric

statement includes the seismic typology of Palestine. As far as seismo-direction is concerned, we may speak of two groups :

I. *The N-S direction.* — (The direction of the Jordan Graben). The 1951 tremor brought a N-W strip of land in Northern Hula to a stronger emotion than the surroundings. In the last tremor (1954), the active faults in the Araba Valley were put in seismal relief. This can be seen even by the naked eye. In addition, the 1953 and 1954 tremors detected a small meridional nucleus on the coastal plain near Natania. These are all the meridional shaken strips which have been noted until now.

II. *The NW-SE direction.* — (The « Erythrean » or the Red Sea direction), constitutes the bulk of the seismic belts, on the two sides of the Jordan Basin. In western Palestine one can divide them into two systems lying on both sides of the watershed.

The watershed is in general subject to seismic activity rather than to exogenous dynamics. These shaken strips are situated intermittently on both sides of the Palestinian anticlinoria. They are of great value for the development of the Karst phenomenon and for the problems of subterranean hydrology. Their importance is greater when they are situated on their crests, that is to say, on the *structural watershed*, as for example in the west of Jerusalem. In the vigorous 1927 earthquake 3 independent nuclei were detected on the divide itself in the Nablus, Jerusalem and Tel Arad districts; so that evident erythrean perturbances which can be directly observed, contribute to deduce seismic lines in unsettled areas, where direct observation is very difficult, as in the case of the Negev wilderness. On the other hand the revelation of erythrean seismic bands in a given locality will be a sign of the existence of erythrean fractures, although disguised by recent sediments, as for example in the coastal plain. Many of these faults pass into the sea. A clear indication of this fact is the frequency of historical earthquakes whose pleisto-seismal area was situated entirely or partly in the sea. From this point of view it is worthwhile noting that the 1953 tremor whose focus ⁽¹⁾ was situated SW of Cyprus, did not shake the adjacent Syro-Lebanese coast, but expanded in North Palestine, from Galilee to South Judea (Jaffa-Lydda seismic band). One can assume therefore that the sea

(1) With reference to the foci we can note that the focus of the 11.7.1927 earthquake was situated in Trans-Jordan, between Amman and Es-Salt. The 1951 earthquake in the Mediterranean Sea, ca. 100 kms west of Jaffa; 1952 — in the Carmel; 1953 — in the sea SW of Cyprus, and 1954 — in the neighbourhood of Wadi Sirhan. All these heterofoci earthquakes shook the same system of faults, more or less according to the intensity of the shock.

bottom, even far from the continental shelf, is affected by erythrean faults. Highly interesting also is the fact that the latest tremor (13.9.1954) spread over the South-West areas, which are affected by erythrean disturbances, reaching even as far as Cairo at a distance of ca. 600 kms from the epicenter, whereas in the NW, as we have already pointed out, its limit was in Galilee not touching the Lebanon at all, though situated at a shorter distance. This territory was in no way affected by these disturbances.

From the seismological point of view it is evident that the behaviour of the *Jesreel Valley* is a « separator » between the two Palestinian blocks : the Galilean and the Samaro-Judean. To a certain extent the Jordan Graben behaves in a similar way; it offers no room for foci, and there is no seismo-tectonic unity. Its unceasing sinking is a result of its correlation with volcanic phenomena.

ERYTHREAN FAULTS AND VULCANISM.

Seismological research throws light on the problem of vulcanism in the « erythrean » regions as well. This vulcanism is connected with the erythrean fissures acting as « the spirit of the living creature in the wheel ». Our vulcanism is generally considered extinct, but we must not forget that in the 8th century A.D. volcanoes were still active in the Tebuk area, and even in the 13th century A.D. in the Medina region. It is a pity that seismic records from this affected territory (which is to be reckoned as a seismic one), were not conserved. Here is an example from the last years : in 1951 the Medina district was severely shaken, even the earthquake of the 13th September 1954 caused a serious agitation in the entire area of Medina, Tebuk, Jauf and Wadi Sirhan.

We were to note also that among our earthquakes there are many of sufficiently deep focus, for instance the one felt in 1941, 100 kms, or even more than 130 kms in the 1953 earthquake. It is not unlikely, therefore, that our earthquakes, which mark the sensitive erythrean fissures and faults, may severely shake these half closed fissures, or cause the opening of new fissures, stimulating the volcanic activity appearing as dormant in our days, and consequently renewing the subsidence of the Jordan Graben. In our opinion the endodynamics in this famous Rift Valley are not submitted to the aggressive activity of the earthquakes; it has a passive behaviour, and its subsidence is a result of the emission of the lavas from the interior.

The Alpo-Himalayan activity after its paroxysmal phase in the tertiary, now acts as the fundamental factor for the epeirogenic dynamics in the whole area. From the Seismo-Vulcanological study in Turkey we know that the direction of the disturbances is actually in accordance with the fold axes. It may be assumed that similar conditions are predominating in the Iran territories, but no exact surveys have been carried out there until now.

The situation in the Syro-Arabian block is different, for there the volcano-seismical bands show an « erythrean » trend, as in the case of cis and Trans-Jordan regions. North of the Palmyra-Damascus folds we have a different state of affairs. In this region we find an intermediate position between the steady orogenic region of the North, and the firm erythrean areas of the South. The erythrean element is very rare here, although its traces are to be found in the Urfa district. On the other hand the direction of the epeirogenic elements according to the fold axes is not predominant here, meridional and equatorial faults being very common.

We still have therefore to wait for the macro-seismological studies in order to ascertain which in our case is the real active fault at present.

**

What is the contribution that *instrumental research* can give us?

There is no doubt that it is premature to obtain a sufficiently good idea of the kind of seismicity in this country. A year of seismological registration using the two seismographs installed in Jerusalem and Safad is not sufficient. It is obvious that a directional instrument will have to be employed. Furthermore, experience shows that for *local shocks*, one cannot use the data supplied by Ksara and Helouan (the two nearest observatories to us) in conjunction with our own. Hence the necessity of installing at least one seismograph in Elath (Red Sea), in order to pick up the local shocks as in Jerusalem and Safad.

A general perusal of the list of foci shows us that the overwhelming majority of the 1954 foci are situated in the Mediterranean Sea, in the Dodecanese region, on the S coast of Asia Minor, and the coast line of Cyprus and neighbourhood. This position is in conformance with the agitated state existing now in this part of the Mediterranean, which caused the recent catastrophes.

In addition, shocks have been occasionally registered whose foci are situated in the open sea, between Cyprus and Egypt, or along

the boundary of the Levantine continental shelf. In any case there are many indications that apart from the tremors which occurred on the 13/15th September, 1954, quite a large number of shocks occurred on the continent, in Syria, in Lebanon, in Palestine, in Sinai and on the North coastline of the Red Sea. Our task in the future will be to bring forward evidence of the existence and nature of these shocks.

Moreover, we think that there are sufficient data for 1954, which indicate seismic activity in the East and South East of Palestine, and which point to the existence of a seismic agitation along, both the Erythrean and Adenic (NE-SW) lines of weakness. In our case in Palestine (in the broadest sense of the word), the perturbed lines are essentially erythrean ones. These lines follow exactly the direction of the volcanic fissures, which are dormant at present, and as we pointed out, we note that the volcanic hot springs are still active.

Our macro-seismological observations since 1950, added to the extensive historical records, and proved to us that our land is certainly not aseismic, but that its seismicity is mainly restricted to small dimensions to such an extent that only an insignificant number of shocks are detected by the population. Seeing the overwhelming number of shocks observed instrumentally, illustrates this clearly.

**

In addition to the tremors which were registered in common by the Jerusalem and Safad instruments, other shocks were picked up by Jerusalem alone and Safad alone. The shocks proper to Jerusalem instrument can be divided into 3 groups. They occur regularly from 1 to 3 shocks per month. On 13/15 September, however, 6 successive shocks were registered.

- 1) At a distance of 15 kms (7 shocks);
- 2) At a distance of 40-45 kms (12 times);
- 3) At a distance of 85-90 kms (11 times).

These distances pass through typical lines of weakness, but we have not yet sufficient data for an exact determination of their foci.

Safad as Jerusalem, noted a number of local shocks which can be divided into 6 groups. These shocks, as those of Jerusalem, were spread over the months regularly :

- 1) At a distance of 15 kms (3 times);
- 2) At a distance of 20-25 kms (3 times);
- 3) At a distance of 30-35 kms (5 times);

- 4) At a distance of 40-45 kms (5 times);
- 5) At a distance of 60-65 kms (5 times);
- and finally, 6) At a distance of 85-100 kms (11 times).

The multitude of shocks in the Safad groups is in harmony with the geological structure of Galilee and appears completely fractured vis-à-vis of Judea, the fractures being essentially erythrean. This structure is in concordance with that of North Trans-Jordan, which is entirely covered by volcanic lavas spread out from series of volcanoes arranged in erythrean fissures (*fig. 2*).

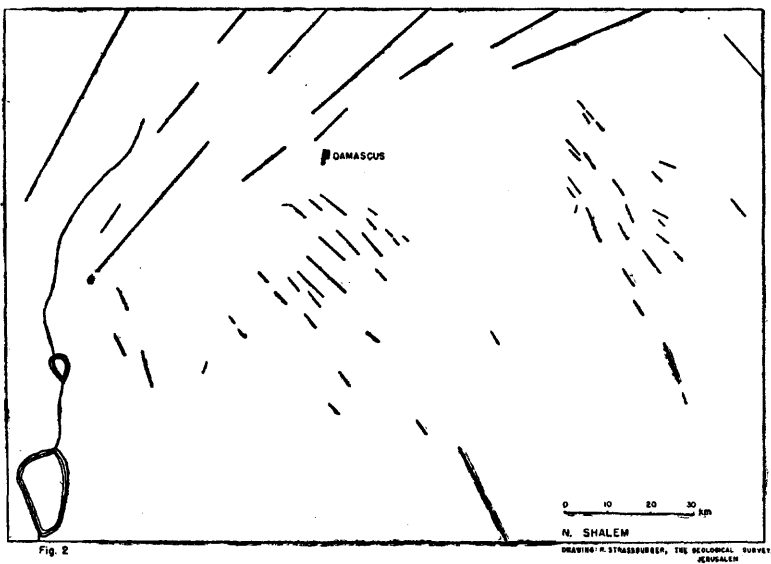


FIG. 2. — *The two systems of tectonic lines in the Damascus zone.*

The trend of the volcanic fissures is NW-SE, while the direction of the Damasco-Palmyra folds is NE-SW. (In the SW of the map — Sea of Galilee).

Apart from the shocks proper to Palestine registered by Jerusalem and registered by Safad separately, as mentioned above, the Jerusalem instrument received approximately 30 shocks, whose foci are situated at distances from 200-1.000 kms.

Similarly the Safad instrument received approximately 50 shocks which are situated at similar distances. One can divide these shocks into groups according to their distances also. This state of affairs points to places of weakness destined to be exposed to shocks. These distances are important for the determination of the tectonic structure of regions neighbouring Palestine. We are noting them here in order to indicate their existence, without going into details as the data received are sporadic.

All these tremors can be classified in various groups, testifying a presence of special lines of weakness which may be shaken from time to time.

These distances are important for an exact determination of the active tectonics of the zone surrounding Palestine. It is a task for

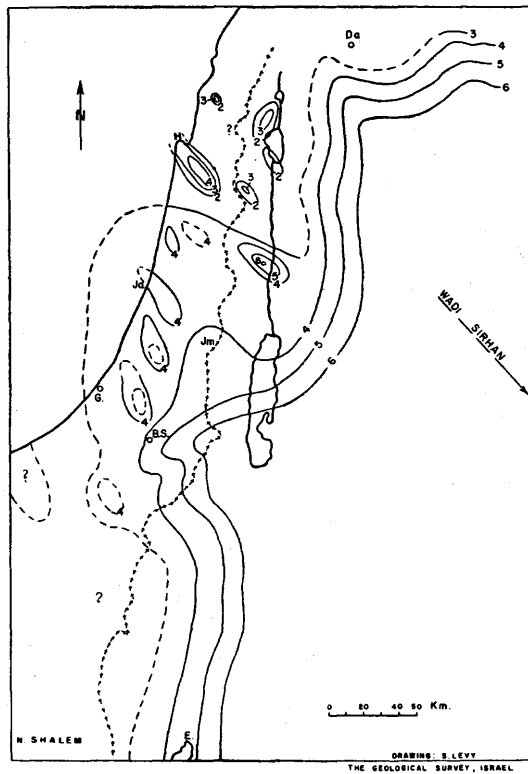


FIG. 3. — *The tremor of 13th September 1954.*
DA — DAMASCUS, H — HAIFA, JA — JAFFA, JM — JERUSALEM,
G — GAZA, B.S. — BEER-SHEBA, E — ELATH.
The line of crosses indicates the principal watershed.

the future (when sufficient data will be available), to support this conception.

*
**

Shocks registered at distances above 1.000 kms are beyond the scope of this paper and are therefore not mentioned. (Our seismographs registered about 100 shocks per month).

Note finale.

Since the summer of 1954 the following earth tremors have occurred :

1. 13.IX.1954 (focus in Wadi Sirhan).
2. 12.IX.1955 (focus in Mediterranean).
3. 12.XI.1955 (focus in Red Sea or Aswan region).
4. 16.III.1956 (focus in Lebanon).

The foci of the first three tremors are located in regions of Erythrean perturbances; whereas the fourth focus is located north of the limit line — Damascus-Palmira — in a region of NE-SW folds (normal to the Erythrean direction). This earthquake spreads along the Lebanese fold axis ; while in Israel, as with the other tremors, the Erythrean faults are the sensitive ones *.

BIBLIOGRAPHY.

- SHALEM (N.) : The Red Sea and the Erythrean Disturbances. Congrès Géologique Intern. C. R. de la XIX^e Session, Alger, 1952. Section XV, La Paleo-vulcanologie et ses rapports avec la tectonique, pp. 223-231.
- SHALEM (N.) : Séismicité, et les cassures érythréennes dans l'hinterland de la Vallée du Jourdain. Assoc. de Séism. et de Physique de l'Intérieur de la terre, Résumé, n° 82, Rome, 1954 et Comptes Rendus, n° 11, pp. 153-154, Strasbourg, 1955.
- SHALEM (N.) : A propos des dernières éruptions en Palestine. Idem, Assoc. Intern. de Vulcanologie, pp. 11-12, Rome, 1954.
- SHALEM (N.) : The tremor of the 10th September 1953. Bull. Res. Coun. of Israel, Vol. III, N° 3, p. 266, Jerusalem, 1953.
- SHALEM (N.) : La Séismicité au Levant. Idem, Vol. II, N° 1, pp. 1-16, Jérusalem, 1952.
- LAHN (E.) : Les zones sismiques de l'Anatolie Orientale. Public. du Bureau Cent. Séism. Intern. Série A. Travaux Scient. Fasc. 18, pp. 15-22 (Mémoires présentés à l'Assemblée de Bruxelles, 1951).
- WIENER (G.) : Geology and Mineral Deposits of Makhtesh Hathira. Bull. Swiss. Assoc. Pet-Geol. and Eng., Vol. 21, N° 61, pp. 41-56, 1955.

* Additional note recorded at the time of proof reading. N. S. (2. V. 1956.)

ON PHENOMENA FORERUNNING EARTHQUAKES

by Kenzô SASSA and Eiichi NISHIMURA (Kyoto, University, Japan).

1. INTRODUCTION.

Among various natural disasters the damage caused by destructive earthquakes is the most horrible and fatal because of their great violence and unforeseen occurrence. Recently developed seismology tells us in great detail of various phenomena observed after an instance of earthquake-occurrence, such as the location of focus, total energy of the earthquake, propagation mode of the seismic wave, safety factors in building and construction against earthquakes, and others. But, much to our regret, we have no definite knowledge concerning the period just before an earthquake-occurrence. The study of the phenomena foretelling the occurrence of destructive earthquakes is considered to be one of important items in both the practical and basic aspects of seismology, because an early warning against a coming destructive earthquake would considerably reduce much disastrous loss, especially that of human life, and furthermore, the knowledge about the phenomena fore-running earthquakes would serve greatly towards the solution as to the real nature of earthquakes, namely the process of the accumulation of earthquake energy, the mode of its release, the triggering action for its release, and others.

Among the various phenomena observed in the epicentral region after the occurrence of destructive earthquakes, the upheaval of the ground is the most conspicuous. And it has also been observed by the repetition of precise levelling that this sort of ground movement in some cases precedes the occurrence of earthquakes. In these cases the continuous observation of the ground movement with suitable instruments would certainly serve the purpose of foretelling earthquake-occurrence.

Along this line some observations with tiltmeters, extensometers and other instruments have been made, since 1937, at several stations in Japan under the management of our Institute. At present forty tiltmeters, twenty extensometers, ten geomagnetic declinometers and five gravimeters are set up at the following fifteen stations [Ref. 1].

	Longitude	Latitude	Rock formation	Room depth below the ground surface
Makimine	131°27' E,	32°37' N	Paleozoic slate	180 ^m , 165 ^m
Hondo	131 05 ,	32 53	Volcanic rock	1
Kōchi	133 32 ,	33 34	Paleozoic	40
Ikuno	134 50 ,	35 10	Liparite	719, 326, 237
Susami	135 30 ,	33 32	Paleozoic	10
Kishyu	135 53 ,	33 52	Tertiary sandstone and shale	60
Yura	135 07 ,	33 57	Mesozoic sandstone and shale	30
Ide	135 49 ,	34 48	Paleozoic	35
Abuyama	135 34 ,	34 52	Paleozoic	20
Osakayama	135 51 ,	34 59	Paleozoic	150
Kamigamo	135 46 ,	35 04	Paleozoic	10, 9
Tsuchikura	136 18 ,	35 36	Paleozoic	170
Ogoya	136 33 ,	36 17	Tertiary tuff	300, 300, 200
Kamioka	137 19 ,	36 21	Gneiss	800
Hosokura	140 54 ,	38 48	Tertiary	160

In the following detailed descriptions will be made of some peculiar changes of ground-tilt and ground-strain intimately related to the recent occurrence of some destructive earthquakes in Japan.

2. CHANGES WITHIN SEVERAL HOURS.

Some examples of a peculiar change of ground-tilt observed within a period of several hours just before the occurrence of destructive earthquakes are described in the following :

On September 10, 1943, a destructive earthquake occurred in the vicinity of Tottori City; there were 7348 casualties and 13,897 buildings were damaged. The position of epicenter was 134° 2 E and 35° 5 N, the depth of focus and seismic magnitude being 10 km and 7.5 in Pasadena Scale respectively. Our nearest observation station to the epicenter ($\Delta = 60$ km) was Ikuno Station, and there a minute but clear and characteristic tilting motion of the ground was observed several hours before the occurrence of the Tottori Earthquake. In Figure 1, this peculiar ground-tilt is schematically expressed, the direction of the arrowed line showing the direction of the downward tilting motion of the ground and its length representing the amount of tilt. The annexed numerals denote the time in hours counted back from the instant of earthquake occurrence. Although the amount of this forerunning tilting motion is minute, its S-type motion is very peculiar and clearly distinguishable from the other usual tilting motions [Ref. 2, Ref. 3].

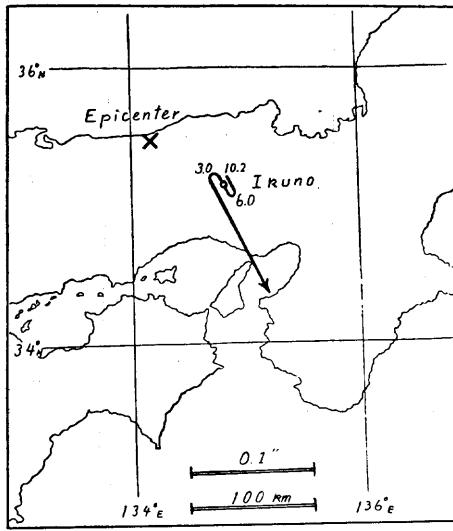


FIG. 1. — Tilting motion of ground observed at Ikuno before the occurrence of the Tottori Earthquake on September 10, 1943.

On December 7, 1944, the great Tōnankai earthquake occurred at a point 20 km offshore in the open sea of Kumano-Nada ; there were 3133 casualties and 76,151 buildings were damaged, mainly by a tsunami reaching several meters in height. The epicenter, focal depth and seismic magnitude were estimated to be $136^{\circ} 2$ E and $33^{\circ} 7$ N, about 20 km and 8.0 in Pasadena Scale respectively. In this case the only observation anywhere near the epicenter was Kamigamo Geophysical Observatory, 160 km distant in the northern part of Kyoto City. In this case also, an extremely minute but clear ground-tilt was observed at Kamigamo, the schematic diagram being expressed in Figure 2 [Ref. 3].

On April 26, 1950, the strong Nanki earthquake occurred in the southern part of Kii Peninsula. The epicenter, focal depth and seismic magnitude were $135^{\circ} 8$ E and $33^{\circ} 9$ N, 40 km, and 6.7 in Pasadena Scale respectively, but the damage was small. In this case, the tiltgrams obtained at Tamamizu Station (at present in suspension), Kamigamo Geophysical Observatory and Kōchi Station showed the peculiar S-type ground-tilt several hours before the occurrence of the Nanki Earthquake. The Tamamizu, Kamigamo

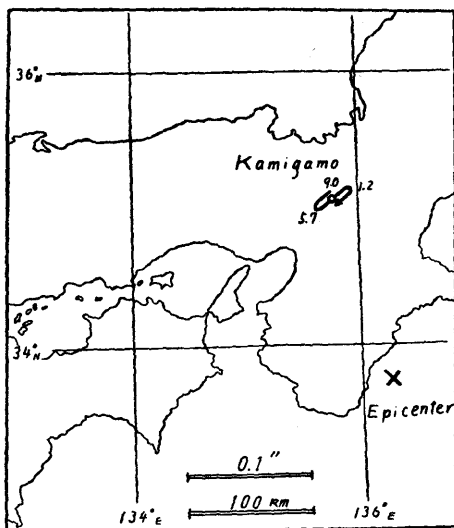


FIG. 2. — Tilting motion of ground observed at Kamigamo before the occurrence of the Tōnankai Earthquake on December 7, 1944.

and Kōchi Stations were respectively 80 km, 120 km and 200 km distant from the epicenter as shown in Fig. 3 [Ref. 3].

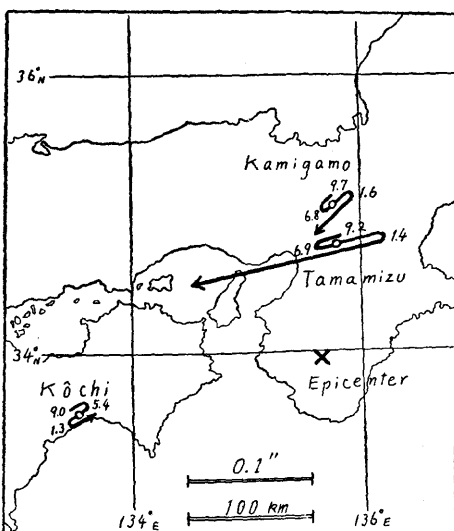


FIG. 3. — Tilting motions of ground observed at Tamamizu, Kamigamo, and Kōchi before the occurrence of the Nanki Earthquake on April 26, 1950.

Comparing Figures 1, 2 and 3 with each other, it is concluded that a great or destructive earthquake is in some cases (at least in the present cases) preceded by a minute and characteristic S-type tilting motion of the ground several hours before its occurrence. Roughly speaking, observed tilts were of the order of magnitude of $0''1$ in angle at a distance of 100 km from the epicenter.

3. CHANGES IN SEVERAL DAYS AND SEVERAL MONTHS.

The above described changes observed several hours before the earthquake-occurrence are considered to be very important and suggestive for the research as to the nature of earthquakes, but it is practically very difficult to make them serviceable for the early warning of earthquake-occurrence because of its imminence in time. For the purpose of warning against the occurrence of a destructive earthquake and reducing disastrous loss, it is desirable to catch any phenomena foretelling the disaster which should appear at a sufficient interval before the earthquake-occurrence. But the accurate observation of secular change in ground-tilt and ground-strain is a considerably difficult task, because of the amount of change sought is generally very minute compared with the irrelevant disturbances caused by ground movements of local character, meteorological effects, instrumental defects and artificial interruptions. [Ref. 4]. In spite of these difficulties two cases were recently observed, in which slow and peculiar ground-tilt and ground-strain appeared several months before earthquake-occurrence, and the rapid and severe change was observed several days before the instant of occurrence. Their circumstances may be reported in some detail.

(a) *The Case of Daishōji-Oki Earthquake.*

The strong Daishōji-Oki Earthquake of March 7, 1952 had its epicenter 40 km distant from Ogoya Station in the NW-direction. Its epicenter, focal depth and seismic magnitude were $136^{\circ} 2$ E and $36^{\circ} 5$ N, 20 km and 6.5 in Pasadena Scale respectively. The secular change of ground-tilt observed is shown in Figure 4 as a vector diagram, in which the direction and amount of change of downward ground-tilt are successively plotted in a vector-representation and the annexed numerals denote the date of observation. As seen in the Figure, the ground at Ogoya, after the commencement of tilt-metric observation on September 23, 1951, had continued its downward tilting in the NW direction until December 5, and since that date turned its tilting direction to NW. And since February 27, 1952 the westward tilting motion became more and more severe

and continued to the day of the catastrophic Daishōji-Oki Earthquake occurrence of March 7. Several days after earthquake-occurrence the tilting motion of the ground turned its direction to NE, orthogonal to the preceding, and the ground has continued its tilting motion in the same direction (NE) up to the present. Namely the ground at Ogoya commenced its downward tilting motion in the direction of the epicenter three months before the earthquake-occurrence, increasing its speed of motion several days before the catastrophe, and then several days after earthquake-occurrence turned its direction for the orthogonal to the preceding [Ref. 4, 5, 6,].

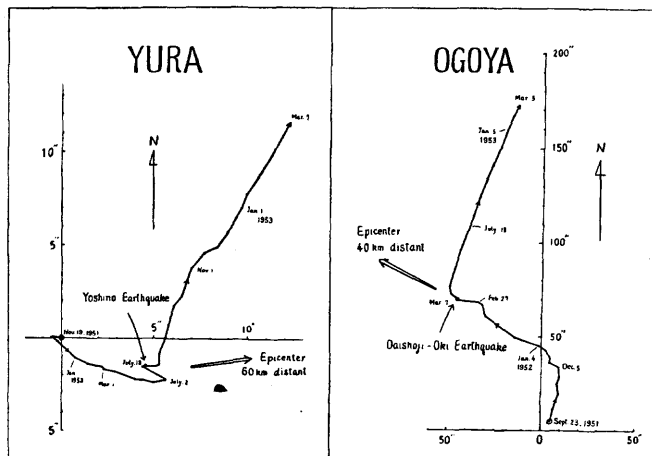


FIG. 4. — Vector diagrams of secular change of ground-tilt observed at Yura and Ogoya. Single arrows show the time of occurrence of earthquake and double arrows the direction of epicenter respectively.

(b) *The Case of the Yoshino-Earthquake.*

The strong Yoshino Earthquake of July 18, 1952 has its epicenter 55 km, 72 km and 94 km distant respectively from the Yura, Ide, and Osakayama Stations as seen in Figure 5. Its epicenter, focal depth and seismic magnitude were $135^{\circ} 40' E$ and $34^{\circ} 10' N$, 70 km deep and 7.0 Pasadena Scale respectively. As to the tiltmetric observation at Yura, the schematic vector diagram of ground-tilt is shown in Figure 6 as in the case of the Daishōji-Oki Earthquake. In this case also the downward tilting motion of the ground at Yura had been towards the ESE direction (the epicenter of the Yoshino Earthquake being in the ENE direction from Yura) until July 2, then turning to the WNW until July 16. And after two days of its reverse motion to E on July 16, the strong Yoshino Earthquake has occurred. After the occurrence the eastward til-

ting motion continued to July 30, and the succeeding ground-tilt in the NE-direction continued to September 1953. Roughly speaking the downward tilting motion of ground at Yura was towards the direction of the epicenter during several months before the earthquake-occurrence, reversing its tilting direction sixteen days before the occurrence, and from twelve days after the occurrence the tilting direction has been nearly orthogonal to that of preceding epoch. Thus the modes of secular tilting motion of the ground related to the occurrence of destructive earthquakes are very similar with one another in both cases of Ogoya and Yura [Ref. 6].

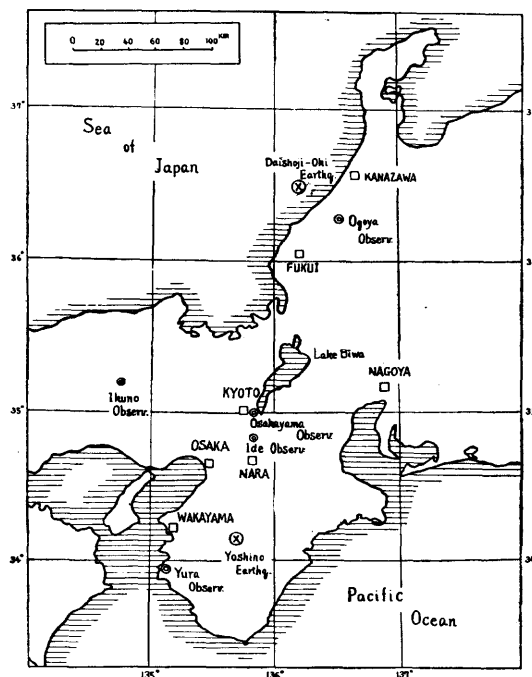


FIG. 5. — Positions of the Observatories, and epicenters of the Daishōji-Oki and Yoshino Earthquakes.

In the case of the Yoshino Earthquake some remarkable changes of ground-strain were observed several months before the earthquake-occurrence in the extensometric observation at the Ide and Osakayama Stations [Ref. 7, Ref 8]. The extensometric observation at Osakayama Station was commenced early in 1949, and several reports on the relation between the change of ground-strain and earthquake-occurrence have been published [Ref. 9]. In the case of the Yoshino Earthquake, as seen in Figure 6, the gradual exten-

sion of the ground had taken place nearly one year before and a rapid extension took place three months before the earthquake-occurrence. Nearly one month after the occurrence, the ground strain changed its behavior from extension to contraction and recovered the original state in nearly one year.

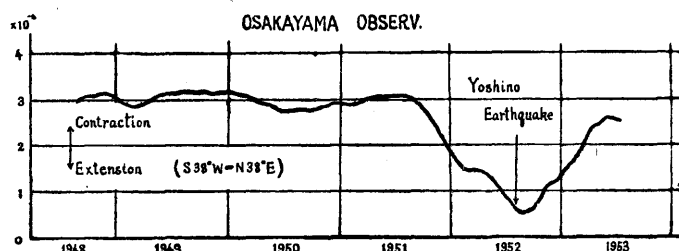


FIG. 6. — Secular variation of ground-strain (extension) observed at OSAKAYAMA OBSERV.

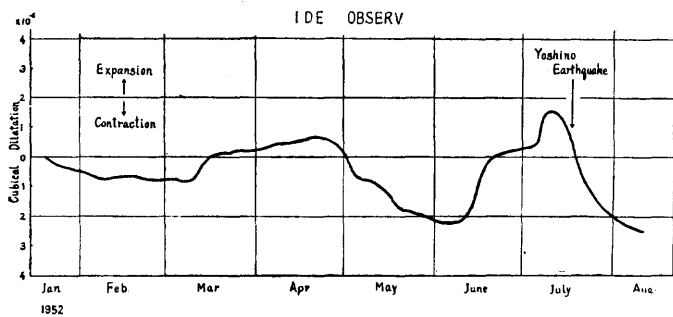


FIG. 7. — Secular variation of ground-strain (cubical dilatation) observed at IDE OBSERV.

Nearly the same remarkable ground-strain was also observed at the Ide Station. There the extensometric observation for the six directions had continued since 1951 and in the case of the Yoshino Earthquake, some anomalous ground-strains were observed nearly four months and the large ones nearly two months before the occurrence of the earthquake as seen in Fig. 7. In this Figure the anomalous cubical dilatation of ground-strain was shown by the composition of strain components.

In conclusion some anomalous changes of ground-tilt and ground-strain which are considered to precede and be intimately related with the occurrence of destructive earthquakes were reported. It is certainly dangerous to derive any hasty conclusions from such few examples on the phenomena forerunning earthquake-occurrence, but it is expected that these observed facts may throw some light upon

the future development of research in methods of forecasting the earthquake-occurrence and the essential nature of earthquakes.

Geophysical Institute.
Faculty of Science.
Kyoto University.
Kyoto, Japan.

REFERENCES.

1. NISHIMURA (Eiichi) : On some destructive earthquakes observed with the tiltmeter at a great distance. Bulletin No. 6, Disaster Prevention Research Institute, Kyoto Univ., Oct. 1953, 1-15.
2. SASSA (Kenzô) : Tilting motion of ground observed before and after the destructive Tottori Earthquake, Kagaku (Science), vol. 14, No. 6, pp. 220-221, 1944 (in Japanese).
3. SASSA (Kenzô) and NISHIMURA (Eiichi) : On phenomena forerunning earthquakes, Trans. Amer. Geophys. Union, vol. 32, No. 1, pp. 1-6, 1951.
4. HOSOYAMA (Kennosuke) : Characteristic tilt of the ground that preceded the occurrence of the strong earthquake of March 7, 1952. Journ. of Physics of the Earth, vol. 1, No. 2, pp. 75-81, 1952.
5. NISHIMURA (Eiichi) and HOSOYAMA (Kennosuke) : On tilting motion of ground observed before and after the occurrence of an earthquake. Trans. Amer. Geophys. Union, vol. 34, No. 4, pp. 597-599, 1953.
6. HOSOYAMA (Kennosuke) : On a mercury tiltmeter and its application. Bulletin No. 6, Disaster Prevention Research Institute, Kyoto Univ., Oct. 1953, pp. 17-25.
7. SASSA (Kenzô), OZAWA (Izuo) and YOSHIKAWA (Sôji) : Observation of tidal strain of the Earth (Part. I). Bull. No. 3, Disaster Prevention Research Institute, pp. 1-3, 1952.
8. OZAWA (Izuo) : Observation of tidal strain of the Earth by the extensometer (Part. II). Bull. No. 3, Disaster Prevention Research Institute, pp. 4-17, 1952.
9. OZAWA (Izuo) : Observation of ground-strain at Osakayama-Station, Rep. Disaster Prevention Research Institute, No. 2, Nov. 1949, pp. 115-121 (in Japanese).

LE TREMBLEMENT DE TERRE DE YENICE (18 MARS 1953)

par Hamit DILGAN et Takahiro HAGIWARA.
Institut séismologique, Université technique d'Istanbul.

I. ASPECT GÉNÉRAL.

Un tremblement de terre destructif s'est produit dans la partie NW de la Turquie (Vilâyet de Tchanakkalé) le 18 mars 1953. Les plus grands dégâts causés par ce séisme avaient été observés à Yenice, à Gönen et à Çan. Plus de 8.000 habitations ont été totalement détruites ou partiellement endommagées. Le nombre total des victimes s'élevait à 250. La secousse se faisant ressentir partout dans la partie NW de l'Anatolie (Asie Mineure), et même à Istanbul avec un degré de VI (Mercalli-Sieberg). La magnitude de ce violent séisme, selon l'échelle Gutenberg-Richter avait été estimée de 7 3/4 (Pasadena) ou de 8 (Berkeley). La valeur du temps (GCT) estimée pour le moment de l'origine du séisme du 18 mars 1953 est de 19 h. 06 m.13 s. pour (BCIS) et de 19 h. 06 m. 11 s. pour (USCGS).

II. DISTRIBUTION DES DOMMAGES.

L'Institut Séismologique de l'Université Technique d'Istanbul (créé par l'Unesco sous les directives de B. Gutenberg) dix jours après ce séisme a fait (durant 3 semaines) des études sur le terrain dévasté et a préparé un rapport détaillé sur la nature et les effets de ce tremblement de terre (Rapport du Dr. Roesli).

Les courbes isoséistes tracées se basent sur les observations personnelles de la mission de l'Institut et sur les informations de quelques Bureaux locaux. On voit nettement que ces courbes présentent des formes assez irrégulières et qu'elles sont beaucoup plus allongées vers la direction de la faille Yenice-Gönen. La plus grande intensité estimée X. (échelle Mercalli-Sieberg) se montre aux environs de Yenice, commune de Tchanakkalé, située sur des alluvions; c'est la région la plus éprouvée (*fig. 1*).

A Gönen les dégâts sont en moyenne un peu moins graves qu'à Yenice. Quant à Çan les dégâts sur les collines sont presque négligeables.

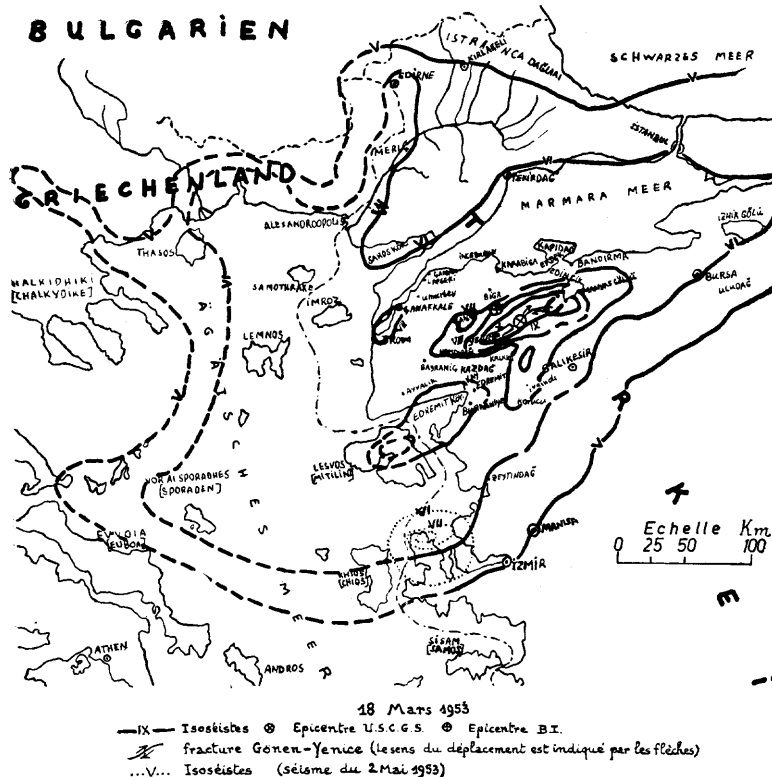


FIG. 1. — Carte des isoséistzes (d'après le Dr Roesli).
— Isoséistzes (échelle Mercalli-Sieberg) du 18 mars 1953.
(×) Epicentre d'après USCGS; (+) épicentre d'après BCIS.
..... Isoséistzes du séisme du 2 mai 1953 (Karaburun).

geables, tandis que dans la plaine alluviale les destructions sont très importantes (fig. 2, 3, 4).

L'existence d'accélérations anormalement grandes a attiré notre attention, pendant le tremblement de terre du 18 mars 1953 : camion arrêté, bouleversé à Gönen, colonnes tombées à Troie. (Isoséiste VII). A Trova (site de la ville homérique de Troie, située à 100 km. de la région épicentrale) une colonne en marbre de 180 cm. de hauteur et de 60 cm. de diamètre, se reposant par terre s'est renversée lors de ce tremblement de terre dans le sens de Yenice. Un calcul simple appliquée à la formule de West nous donne une accélération $\gamma = \frac{g}{3}$ ce qui correspond à peu près au No : X de Mercalli-Sieberg. Cependant le village situé à quelques kilomètres de Trova a eu des dégâts minimes. Il est intéressant de noter aussi, que

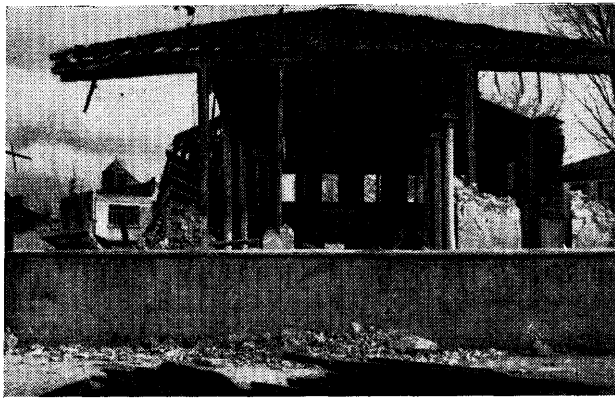


FIG. 2. — Murs complètement écroulés d'une mosquée (Tcharchi Djami) à Gönen.
Le toit autrefois supporté par des murs (pierre et de la boue) restait
après le tremblement de terre sur les colonnes ornementaux en bois.



FIG. 3. — Détail intéressant de l'Ecole primaire à Salur.
Les murs se sont enfoncés dans le sol, tandis que le plancher à l'intérieur est
poussé en haut.

deux jours avant le tremblement de terre à Tchanakkalé (selon le témoignage de la population et des fonctionnaires du Vilâyet) les eaux se sont retirées d'à peu près de 10 m. du quai de la ville, avec un



FIG. 4. — Constructions en brique (pièrres) avec quelques renforcements en béton armé. Effet d'une poussée latérale (Tchan).

abaissement de niveau de 20 à 25 cm. (le 16 mars 1953); puis le 18 mars 1953, après le tremblement de terre les eaux ont regagné le quai en état normal. C'est pour cette raison que le Professeur T. Hagiwara, nous recommande l'installation d'un marégraphe à la côte (Dardanelles) pour une étude systématique de ce phénomène (considéré comme rare par les habitants) de flux et de reflux.

III. FAILLE.

Une faille récente s'est ouverte (pendant le tremblement de terre du 18 mars 1953) entre Gönen et Yenice et est caractérisée par un déplacement horizontal et par des fissures qui s'arrangent plus ou moins diagonalement à sa direction générale. La faille de Gönen-Yenice est d'une longueur d'à peu près de 70 km. Cette faille marque la limite de deux blocs de la croûte terrestre qui se sont déplacés en direction opposée l'un à l'autre (*fig. 1*).

Dans la vallée de Yenice la route principale qui va de Balikesir à Tchanakkalé (au 105^e km de Balikesir) a été coupée en biseau et à l'Est de Yenice on a mesuré un déplacement de 3 m. (*fig. 8*).

Dans le cas de déplacement horizontal le sens est toujours le même, la partie SE a bougé relativement au bloc NW, vers le SW. C'est-à-dire l'observateur regardant d'un côté de la faille au côté opposé verrait déplacer ce côté vers sa droite. Ce phénomène de déplacement horizontal le long de la faille Gönen-Yenice, est exactement le même qui a été décrit par plusieurs auteurs, notamment par I. Ketin pour les différentes failles de la ligne Nord Anatolienne

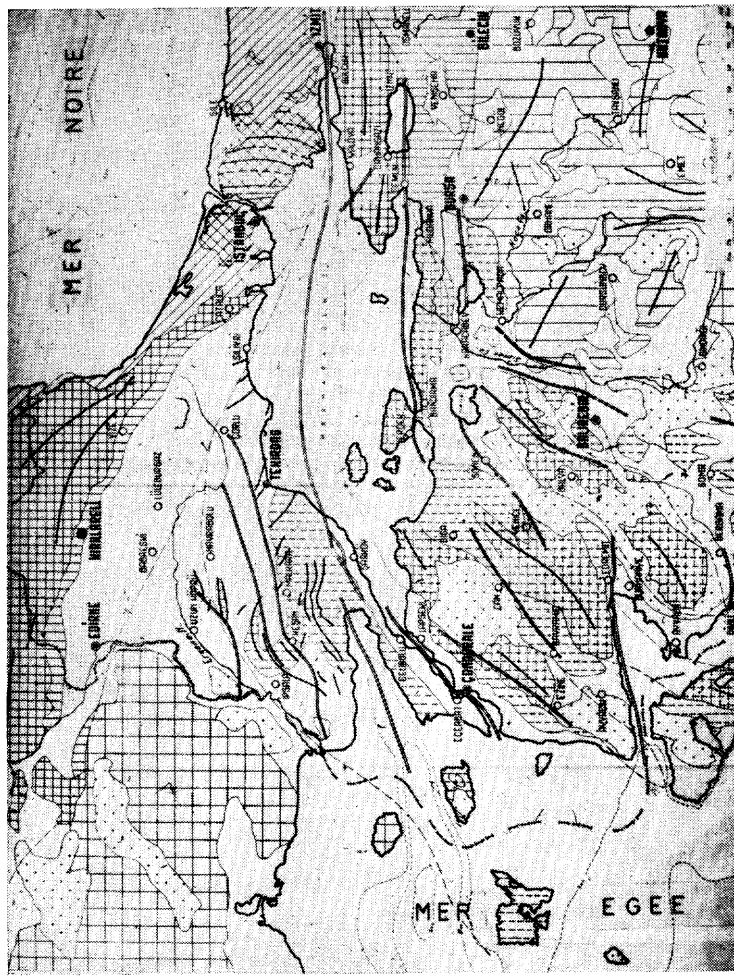


FIG. 5. — Carte tectonique de la région dévastée.

à l'occasion des tremblements de terre d'Erzincan (1939), Lâdik (1942), Tosya (1943), Bolu (1944).

Quelquefois dans la région affligée (dans la zone pléistoséiste) un déplacement vertical aussi a été constaté, mais son sens n'est pas fixe, parfois avec rejet vers le N, parfois vers le S. Dans certains cas on a pu observer que ce n'est pas un vrai déplacement vertical. Dr Roesli le considère comme l'effet d'un mouvement latéral dû à des accidents locaux du terrain.



FIG. 6. — Faille à fissures ouvertes dans la vallée de Gönen Tchay. SW de Gönen.



FIG. 7. — Faille à l'E de Yenice coupant à travers une colline.



FIG. 8. — Route principale qui va de Balikesir à Tchanakkalé coupée en biseau (Vallée de Yenidjé) déplacement de 3 m.

IV. CARACTÈRES COMMUNS.

Dans les dix dernières années la Turquie a eu plusieurs tremblements de terre destructifs possédant tous un caractère commun.

Premièrement, lors de ces tremblements de terre il naît toujours une faille coïncidant à peu près avec l'ancienne faille géologique dite la ligne tectonique. Deuxièmement, on a pu observer le long de ces failles naissantes des déplacements toujours horizontaux (sans aspect net d'une fissure verticale). Si on reporte sur une carte tectonique de la Turquie les déplacements maximums après les tremblements de terre cités plus hauts on voit nettement que l'activité séismique s'est déplacée de plus en plus vers l'Ouest : Erzincan (1939); Lâdik (1942); Tosya (1943); Bolu (1944); Yenice (1953). De ce point de vue nous trouvons qu'il est nécessaire de se mettre à la recherche des lignes de contrôle permettant un arpentage quantitatif indiquant les déplacements permanents dans ces régions séismiques. Récemment on a demandé au Service Géodésique du pays d'établir des lignes de nivelllements dans la zone de faille Yenice-Gönen pour y étudier les déformations de surface avant et après le tremblement de terre.

V. ÉTUDE SÉISMOLOGIQUE.

Actuellement en Turquie nous n'avons que l'Observatoire de Kandilli qui n'a pu obtenir que le mouvement initial du tremblement de terre de Yenice-Gönen. Les plumes des appareils mécaniques de Kandilli (et même d'Athènes) sautèrent après les premières ondes. Il est impossible, comme on le sait de déterminer l'épicentre à l'aide des données d'une station proche de l'épicentre. Notre Institut Séismologique par l'aide de l'Unesco a préparé un plan de prin-

cipe pour un réseau de 14 stations distribuées dans les différentes régions de notre pays. (Deux de ces stations à Kastamonu et à Tchiné entreront en service vers la fin de l'année 1954). D'après cela à l'avenir nous espérons participer d'une façon plus systématique aux travaux séismologiques internationaux.

Les coordonnées géographiques de l'épicentre selon les données de (USCGS) sont $40^{\circ},0$ N (lat) et $27^{\circ} 30'$ E (long). D'après cela l'épicentre se trouve sur la faille au milieu de la distance Gönen-Yenice. Sur la carte des isoséistes cet épicentre est désigné par le signe (\times). Selon (BCIS) les coordonnées de l'épicentre sont $40^{\circ} 1$ N (lat) et $27^{\circ} 20'$ E (long) (+) (à 20 km. NW de (\times)).

Vu la coïncidence de l'hodographe tracé pour ce tremblement de terre avec la courbe standard pour les séismes d'origine superficielle de Jeffreys et Bullen, nous pouvons conclure que l'hypocentre n'est pas très profond.

L'Institut possède les séismogrammes de plusieurs stations mondiales. Excepté Tokyo, dans tous les séismogrammes le mouvement initial marqué est une dilatation. Sur la carte (fig. 9) est indiquée

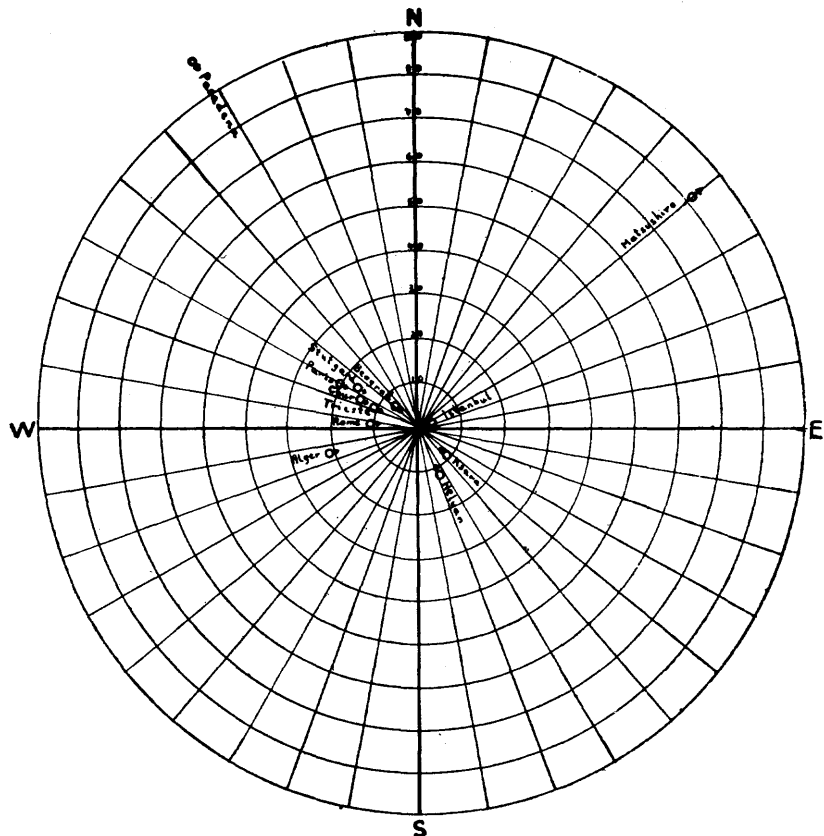


FIG. 9.

la distribution des sens des mouvements initiaux de 12 stations. Quoique la distribution des mouvements initiaux en quadrants est possible pour les tremblements de terre de peu de profondeur il nous a été impossible ici de faire cette division à cause de l'insuffisance du nombre des séismogrammes parvenus des diverses stations.

**LE SÉISME DU 18 MARS 1953 DE YENICE
GONEN (ANATOLIE NW) EN RELATION
AVEC LES ÉLÉMENTS TECTONIQUES**

par Dr Nuriye PINAR (T. B. M. M., Ankara).

Le grand tremblement de terre de Yenice-Gönen a une valeur tout à fait personnelle pour moi à cause de mon hypothèse de travail concernant les relations entre les séismes et les structures tectoniques dans la presqu'île de Çanakkale. Donc je me sens dans l'obligation de présenter les considérations suivantes.

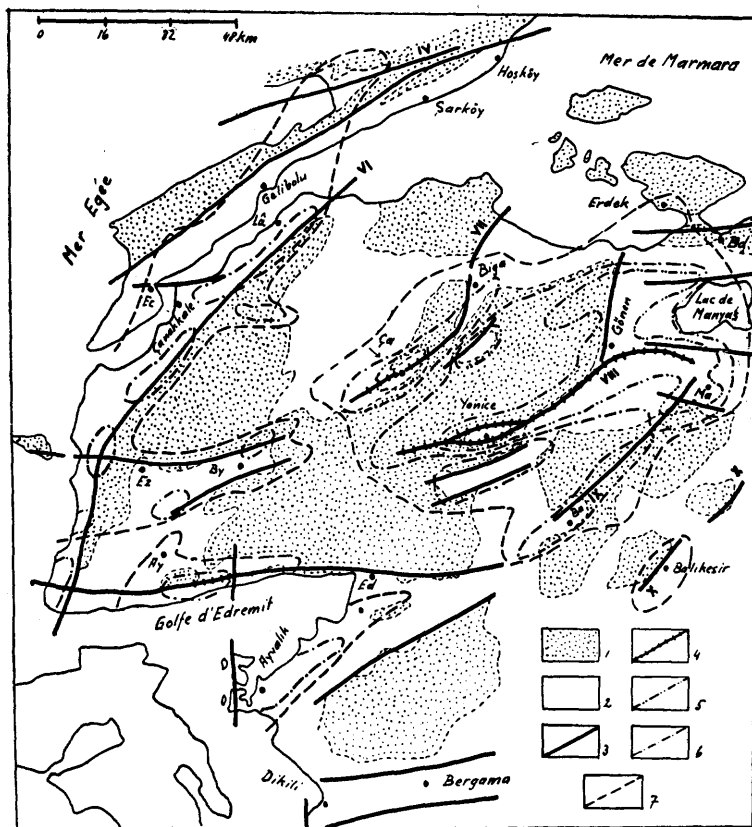
TECTONIQUE.

En 1943 et 1949, j'ai publié des études sur la tectonique et la géologie séismique des régions de la mer de Marmara et de la mer Egée; un résumé de ces études a été présenté à la Réunion de Bruxelles en 1951. Mes recherches complétées depuis ce temps, surtout mes investigations sur le terrain par suite du séisme du 18 mars 1953, me permettent maintenant de donner un abrégé plus complet de la géologie de la région éprouvée.

La presqu'île de Çanakkale (le promontoire NW de l'Anatolie, scène du séisme du 18 mars 1953) fait partie de la zone orogénique alpine anatolienne. Elle est dominée par des plis axés NE-SW (secteur N) et N-S (secteur central et S). Notre région occupe donc une place intermédiaire entre les deux ailes principales du bâti orogénique anatolien, entre l'aile nord-anatolienne et l'aile sud-anatolienne, axées toutes les deux approximativement W-E. La presqu'île de Çanakkale appartient aux « plis intermédiaires » de l'Egée accompagnant le littoral turc de la mer Egée (en englobant aussi les îles ouest-égéennes) et correspondant à une bande labile de terrains plissés enserrés entre les massifs rigides de Menderes à l'E, des Rhodopes au NW et des Cyclades au SW.

Ces plis égéens ne sont point des structures secondaires (par rapport aux ailes principales nord et sud-anatoliennes), mais ils possèdent, dans leur constitution stratigraphique, les traits typiques d'une zone orogénique, comme le prouve la présence de roches vertes et de radiolarites, de dépôts mésozoïques dynamométamorphisés, ainsi que par le développement des calcaires mésozoïques.

Comme partout ailleurs en Anatolie, aussi dans la région égéenne un réseau d'accidents épilogéniques très bien développé se superpose aux structures orogéniques qui ont formé le modèle de notre région comprenant un nombre de plis de fond limités et séparés, les uns



Croquis montrant la situation tectonique et les zones de dégâts du séisme de Yenice - Gönen du 18 mars 1953. (Presqu'île de Çanakkale, Anatolie NW).

1. — Formations anté-néogènes. 2. — Dépôts néogènes et roches volcaniques jeunes. 3. — Failles. 4. — Fissures séismiques. 5. — Zone épicentrale (50-100 % de dégâts). 6. — Zone de 15-50 % de dégâts. 7. — Zone à 1-15 % de dégâts. Contours géologiques : d'après la carte géologique de la Turquie au 1/800.000^e, corrigés selon les levés de l'auteur.

Ay : Ayvacik. — Bd : Bandırma. — Ba : Balya. — By : Bayramic. — Ça : Çan. — Ec : Eceabat. — Ed : Edremit. — Ez : Ezine. — Lâ : Lapseki — Ma : Manyas.

des autres, par des systèmes de failles et des fossés d'effondrement.

Les plis de fond sont constitués par des granites, des roches cristallines et des schistes ante-mésozoïques, des calcaires, des roches vertes et radiolarites mésozoïques, ainsi que des dépôts éocènes (secteurs N et SW de la région) et oligocènes (secteur NE). Quoique morcellés par des failles et recouverts en partie d'une nappe épaisse de dépôts néogènes lacustres, de tufs et de laves, ces plis de fond ont très bien conservé, en partie, leur allure anticlinale : les terrains

lités montrent un pendage très fort sur les flancs de ces structures.

Les accidents épirogéniques comprennent des systèmes de failles, des fossés d'effondrement et des bassins tectoniques occupés par des terrains néogènes pour la plupart lacustres, ainsi que par des dépôts quaternaires lacustres et fluviatiles. Je signale la présence de terrains marins du Miocène moyen jalonnant la côte égéenne de la presqu'île de Çanakkale et formant des boutonnières près de Çanakkale et de Hosköy (selon Arabu); cela montre que le sillon transégéen traversant au Miocène moyen le bassin égéen septentrional a emprunté, en partie, la dépression occupée actuellement par le Déroit des Dardanelles. Je dois signaler aussi la forte dislocation de tous les terrains le long de ces accidents épirogéniques; suivant les failles de Yenice et de Çan, le broyage devient tellement intensif qu'il est parfois difficile de reconnaître la nature des roches. Des sources minéralisées chaudes ou tièdes jaillissent le long de presque tous les accidents épirogéniques de la région. Dans mon étude sur la tectonique du bassin de la mer de Marmara publiée en 1943, j'avais déjà signalé un certain nombre de systèmes de cassures. La géologie de la région n'étant pas encore bien connue à ce moment, je m'étais basée sur l'alignement de sources chaudes et la répartition des roches volcaniques jeunes pour supposer les lignes de dislocation. J'ai réussi à vérifier l'existence de ces structures au cours de mes travaux sur le terrain en 1953.

Tandis que le plissement orogénique s'est terminé pendant l'Oligocène, le mouvement épirogénique continue jusqu'à des temps assez récents. C'est prouvé entre autres par la répartition verticale des dépôts pliocènes et quaternaires qui ne peut pas être attribuée simplement à des changements de niveau. Les dépôts tchaudiens de Gelibolu sont dispersés entre 0 et 80 m. d'altitude, tandis qu'à Hosköy, les mêmes dépôts s'élèvent jusqu'à 40 m. Les dépôts quaternaires marins, rencontrés à 12-15 m. au N de Çanakkale, à 13-17 m. près de Çardak (en face de Gelibolu), à 7 m. près de cette dernière ville, s'élèvent jusqu'à 130 m. près du phare de Hosköy (altitudes après Arabu).

En progressant du SE vers le NW nous pouvons distinguer dans notre région les unités suivantes :

- a) Série de bassins tectoniques de Susurluk-Balikesir (s'étendant, vers le S, jusqu'au golfe d'Izmir; ligne X).
- b) Plis de fond du Sularya Dagi (Balya) — Madra Dagi (Ayvalik).
- c) Zones de failles de Yenice-Gören; se prolongeant vers le NE dans le grand fossé tectonique de Manyas-Bursa (ligne VIII).

d) Plis de fond de l'Armutçuk Dagi — Kocakatran Dagi — Kaz Dagi.

e) Zone de failles de Biga-Çan; passant, vers le NE, aux dislocations accompagnant la côte S de la mer de Marmara (ligne VII).

f) Plis de fond de Karabiga-Kayalidag.

g) Zone de dislocations de Çanakkale (Dardanelles; ligne VI).

h) Zone anticlinale de la presqu'île de Gelibolu.

i) Zone de dislocations du golfe de Saros — fossés sous-marins de la mer de Marmara septentrionale se prolongeant vers l'E dans la grande zone séismique nord-anatolienne (ligne IV).

Toutes ces structures sont orientées du NE vers le SW, parallèles aux plis alpins; elles montrent la relation étroite existant entre mouvements orogénique et épilogénique. Les accidents suivants croisent les plis alpins perpendiculairement ou obliquement :

j) Le fossé E-W d'Ezine-Bayramiç constituant probablement le prolongement W (SW) des failles de Biga-Çan ou de Gönen-Yenice.

k) Dépression E-W du golfe d'Edremit.

l) Failles N-S de la région d'Ayvacik-Ayvalik faisant partie du système de failles N-S accompagnant la côte égéenne.

m) Fossé E-W du Bakırçayı (Dikili-Bergama) limitant le pli de fond du Madra Dagi.

Un nombre d'accidents épilogéniques secondaires se trouve entre les accidents principaux cités ci-dessus (p. ex. la dépression de Kalkim-Pazarköy à l'E de Yenice et celle de l'Inoba au SE de Biga).

Il est évident que par « ligne de faille » (mentionnée ici ou indiquée dans la carte annexée) je sous-entends un système de cassures plus ou moins en relation et plus ou moins continues entre elles.

Le Détrroit des Dardanelles se trouve compris entre les structures énumérées ci-dessus. Je ne discuterai pas ici le problème de la formation de ce détrroit survenue au Quaternaire. Je me contente de signaler deux faits prouvant la nature tectonique de ce détrroit : a) le détrroit est exactement parallèle aux failles de Çanakkale et de Gelibolu séparant le Néogène du Mésozoïque et de l'Eocène respectivement; b) de fortes dislocations existent dans les dépôts néogènes le long du rivage anatolien du détrroit. D'ailleurs, le détrroit est constitué, semble-t-il, de deux systèmes de dislocations, dont l'un orienté NE-SW forme la section du détrroit située entre la mer de Marmara et le cap de Nara, tandis que l'autre, oblique à la première et axé NNE-SSW, constitue la section de Çanakkale-Mer Egée.

ETUDE MACROSÉISMIQUE. — SÉISMES ANCIENS.

Les centres séismiques connus de notre région sont répartis le long des lignes tectoniques signalées ci-dessus. Des secousses déstructives sont survenues à Ayvalik (1940 et 1944, en relation avec les failles N-S du littoral), à Ayvacik (1944, faille du golfe d'Edremit), à Bursa (1855, partie E du fossé de Manyas-Bursa), à Tekirdag-Sarköy — Iles de Marmara (1912, dislocations du golfe de Saros — fossés sous-marins septentrionaux de la mer de Marmara), ainsi qu'à Erdek (1935, failles suivant la côte S de la Marmara). Des secousses légères ont été observées à Gönen et à Çanakkale. Mais un fait intéressant est que, aucune secousse séismique, légère ou forte, n'avait jamais été rapportée de Çan et de Yenice. En me basant sur des observations tectoniques, j'avais signalé en 1943 l'existence possible des lignes séismiques de Yenice-Gönen et de Biga-Çan. L'existence de ces lignes et l'exactitude de mes réflexions ont été prouvées par le séisme du 18 mars 1953.

LE SÉISME DU 18 MARS 1953.

Après quelques secousses légères senties à Balikesir et à Gönen dans les nuits du 6 au 7 et du 7 au 8 février 1953, un fort tremblement de terre ébranlait la presqu'île de Çanakkale le 18 mars 1953, à 19 h. 06 m. 13 s. (G. M.T.). Selon mes observations, ce séisme atteint le degré IX-X dans la zone pléistoséiste. Cela a été confirmé par la magnitude $7\frac{1}{2}$ calculée à Strasbourg, $7\frac{3}{4}$ à Pasadena et 8 à Berkeley.

Selon les rapports officiels du Ministère des Travaux Publics, 244 personnes ont été tuées, 9000 habitations, ainsi que 500 bâtiments publics, écoles et mosquées, ont été démolis ou sérieusement endommagés, 16.000 bâtiments légèrement touchés.

Les répliques, en partie assez fortes, étaient extrêmement fréquentes le premier temps après la secousse initiale; le bulletin préliminaire de Kandilli en compte 455 jusqu'à la fin du mois de mars. Ces secousses continuaient avec la fréquence de quelques-unes par semaine pendant les mois d'avril, mai et juin pour devenir plus rares à partir de juillet. Mais au temps de notre dernière visite à Çan et à Çanakkale, vers la fin de novembre 1953, on les sentait encore quelques fois par mois.

D'après les observations faites par moi, ainsi que par mes amis dans la région sinistrée, j'ai pu constater que beaucoup de ces répliques ont été senties dans un secteur limité seulement. Par exemple des répliques senties à Çan ou à Biga ne l'étaient pas à Yenice. Ces répliques ont été donc émises, en partie, par des centres

indépendants situés dans les régions de Çan, de Biga, de Yenice, de Gönen, de Manyas, de Balikesir, d'Ayvalik, au côté N du golfe d'Edremit et dans les Dardanelles. Beaucoup de ces répliques ont été senties sous forme de secousses verticales ce qui prouve déjà leur provenance de centres locaux

Pour l'analyse macroséismique de la région éprouvée par ce séisme je l'ai divisé en trois zones, à savoir : 1) une zone épicentrale où le pourcentage global des maisons écroulées ou sérieusement endommagées varie entre 50 et 100 %; 2) une zone à 15-50 % de dégâts et 3) une zone à 1-15 % de dégâts.

Je dois signaler toutefois que des facteurs locaux, tels que l'influence du terrain (dépôts meubles ou solides) et le type de construction troublent la délimitation exacte des zones de dégâts. On trouve, p. ex., dans la zone épicentrale des villages construits entièrement en bois ayant subi très peu de dégâts; il y a, par contre, dans la zone à 15-50 % de dégâts des villages complètement démolis parce que situés sur des alluvions meubles. En délimitant les zones de dégâts, ces cas exceptionnels dûs à des facteurs locaux ont été négligés.

L'épicentre du séisme du 18 mars 1953 : Selon mes observations l'épicentre est en relation avec la faille de Yenice-Gönen; il est situé aux environs de Yenice. En effet, le séisme a été senti, dans cette ville et aux alentours, comme une secousse verticale très courte; les constructions se sont écroulées sur place (verticalement); dans les secteurs éloignés de Yenice, par contre, la secousse a été de longue durée (40-50 secondes) et elle est venue du côté de Yenice (du SW); les dommages sont orientés dans ce sens (minarets, maisons et cheminées écroulées vers le SW). Cela cadre d'ailleurs avec les calculs faits par le B. C. I. S. et d'autres institutions : les coordonnées de Yenice sont $39^{\circ},9\text{ N}$, $27^{\circ},5\text{ E}$, tandis que les estimations portent sur $39^{\circ},8\text{-}40^{\circ},1\text{ N}$ et $27^{\circ},3\text{-}27^{\circ},5\text{ E}$.

La zone épicentrale (50-100 % de dégâts) : Elle constitue une bande large de 5-15 km. s'étendant de Yenice jusqu'à Gönen en direction SW-NE; d'ici jusqu'à Manyas en direction E-W; sa longueur totale est 80 km. Cette zone suit d'abord la faille de Yenice-Gönen; de Gönen jusqu'aux environs de Manyas elle accompagne la faille marginale S du fossé de Manyas-Bursa. Suivant ces dislocations, une fissure séismique typique a été ouverte sur une longueur de 80 km. Entre Yenice et Gönen, cette faille coupant routes, ruisseaux et haies a un rejet horizontal (véritable rejet tectonique, point dû à des glissements) de 3-4 m. et un rejet vertical (dépendant de la formation du sol) variant entre 0,50 et 1,50 m. A l'E de Gönen et à l'W de Yenice, cette faille prend l'allure d'une simple fissure comme

la trace d'une charrue. Sur le parcours de cette faille de l'eau chaude a jailli des crevasses dans la plaine de Manyas pendant quelques heures. La température et le débit des thermes de Hidirlir situées sur une faille locale parallèle à celle de Yenice-Gönen ont considérablement augmenté.

Dans la petite ville de Yenice, située sur la faille et sur un cône de déjection, 420 maisons sur un total de 450 ont été démolies et 192 personnes sur une population totale de 1.700 ont été tuées. Je note que, à part les constructions vieilles et peu résistantes, des bâtiments nouveaux construits sous le contrôle des Travaux Publics tels que la mairie et la sous-préfecture ont été démolis à Yenice.

Dans la ville de Gönen située à 40 km. au N de Yenice et à une distance d'un kilomètre seulement de la faille, 30 % des maisons ont été démolies ou sérieusement endommagées tandis que dans les quartiers bas de la ville situés sur des alluvions, le taux de dégâts était entre 50 et 80 %.

Cette zone épacentrale envoie une branche vers le N qui s'élargit, en direction E-W, dans le secteur situé au bord N de la plaine de Gönen : cette allure est due au jeu en relais des failles E-W du bord N du fossé de Manyas-Bursa (dont la plaine de Gönen fait partie). En relation avec le jeu de ces failles, une nouvelle source chaude a jailli à Ulukir et une source tiède à Bostanlı. Dans ce secteur des villages construits sur les marnes et calcaires solides du Néogène, montrent un taux de dégâts de 50 à 80 %.

Un nucléus épacentral se trouve autour de Çan (50-55 % de dégâts; de nombreuses maisons en briques à filets en béton armé se sont écroulées); il est dû au jeu en relais de la faille de Biga-Çan. Une série de crevasses et failles sans rejet vertical (car situées dans les alluvions) a été ouverte le long de cette dislocation dans la vallée du Biga-Çayı aux alentours de Çan. L'orientation uniforme (WSW-ENE) de ces failles et leur longueur totale de 20 km. prouve qu'il s'agit ici de l'effet de surface du jeu d'une ligne tectonique traversant le substratum. Les sources de Tepeköy et de Kirkgeçit situées sur cette faille ont tarri par suite du séisme, le débit de la source de Çan a considérablement diminué.

La zone à 15-50 % de dégâts : Elle entoure la zone épacentrale et est également axée approximativement SW-NE. Hors de cette zone, d'autres bandes et îlots de terrains à 15-50 % de dégâts sont dispersés dans la région secouée. Ils soulignent l'existence des failles ayant joué en relais au cours de ce séisme. Je cite ici les îlots accompagnant les failles de Çanakkale, ceux de Küçükkyuzu se trouvant en relation avec les failles du golfe d'Edremit (ici, une

fissure d'une longueur de 30 km. avait été ouverte au cours du séisme de 1944; une section longue de 12 km. a été réouverte le 18 mars 1953) et l'îlot d'Ayvalik soulignant les failles N-S du littoral égéen.

La zone à 1-15 % de dégâts entoure l'aire et les îlots à 15-50 % de dégâts; elle comprend presque la moitié de la presqu'île de Çanakkale.

Région à dégâts légers (Isoséiste V-VI) : Des murs ont été lézardés et des cheminées renversées dans une aire comprenant en territoire turc, une surface de 30.000 km²; elle englobe les provinces d'Istanbul, de Tekirdag, de Çanakkale, de Balikesir, de Bursa, de Manisa et d'Izmir. Les localités les plus éloignées de Yenice, d'où de tels dommages ont été rapportés sont Istanbul (distance de Yenice : 185 km.), Tekirdag (120 km.), Bursa (145 km.), Karacabey (95 km.), Bergama (100 km.) et Akhisar (au N de Manisa, 125 km.).

L'axe longitudinal de cette zone est orienté NE-SW parallèlement aux structures tectoniques de la région.

La zone, dans laquelle le séisme a été senti comprend toute la moitié W de la Turquie; à Ankara (distance de Yenice : 460 km.) des lampes ont oscillé dans quelques maisons (intensité : II-III).

Hors du territoire turc, le séisme du 18 mars 1953 a été senti dans les îles égéennes et même dans la partie E de la Grèce. Le bulletin préliminaire de Kandilli cite, entre autres, les localités suivantes : Lesbos (intensité : V-VIII), Samothraque (VI), Lemnos (VI), Thassos (V-VI), Chios (V-VI), Samos (V-VI), Icarie (IV), Kos (IV), Eubée (III-IV), Sporades N (IV-VI), Cyclades (III), Thrace Occidentale (IV-VI), Thessalie (III), Attique (III). La répartition de ces localités, ainsi que l'intensité des chocs font penser qu'un nombre de relais ont joué dans le bassin d'effondrement de l'Egée septentrionale.

PHÉNOMÈNES ACOUSTIQUES ET LUMINEUX.

De forts bruits souterrains accompagnaient le séisme dans la zone épicentrale; dans les localités plus éloignées (Çan, Gönen, Manyas), ils précédaient les secousses. Ces bruits ont été décrits comme ressemblant à des coups de canon ou au bruit d'un camion passant à grande vitesse.

Ces bruits se répétaient aussi au cours de nombreuses répliques; nous avons pu les observer pendant des répliques tardives vers la fin du mois de mai 1953. Ces secousses très faibles étaient précédées d'un bruit rappelant un camion venant de loin.

Signalons aussi que des bruits souterrains ressemblant à des coups de canon point accompagnés de secousses séismiques ont été rapportés de la région de Yenice pendant les mois suivant le grand séisme.

Des phénomènes lumineux ressemblant à des éclairs lointains ont été observés par un de mes collègues pendant les secousses principales à Bursa, à 145 km de distance de la zone épicentrale.

Selon les dires des habitants, les effets lumineux étaient très forts aussi dans le secteur situé au S de Gönen (sur la faille Gönen-Yenice) : la forte lumière rougeâtre faisait penser aux observateurs qu'un grand incendie avait éclaté dans cette ville.

Je me contente ici de signaler ces observations en laissant leur explication aux physiciens.

RÉSUMÉ ET CONCLUSIONS.

Le séisme du 18 mars 1953 est une des grandes catastrophes séismiques qui dévastent de temps en temps l'Anatolie. Il montre tous les traits d'un tremblement de terre de grande envergure : l'aire épicentrale étendue, des dégâts élevés, d'importantes fissures séismiques etc. Son épicentre est en relation étroite avec le système de failles épirogéniques recouvrant le pays.

Une particularité de ce séisme est sa relation avec une faille dont aucune activité séismique n'était connue jusqu'à présent. En effet, en 1943, j'avais conclu à la nature tectonique de la ligne de Yenice-Gönen (et de celle de Biga-Çan), ayant joué en relais le 18 mars 1953), en me basant surtout sur l'alignement des sources chaudes et j'avais signalé alors cette structure comme *une ligne séismique possible*, ce qui a été pleinement confirmé par le séisme du 18 mars. Cela nous montre que des structures épirogéniques, situées dans une région séismique, doivent toujours être considérées comme suspectes du point de vue séismique, même quand elles n'ont fourni jusqu'à présent aucun signe d'activité séismique. Toute entreprise de construction doit tenir compte de ce fait.

Quand j'avais essayé, en 1943, une analyse tectonique de la région de la mer de Marmara et de la presqu'île de Çanakkale, la géologie de ces régions était encore très peu connue (le levé géologique systématique du pays venait de commencer seulement) et j'avais essayé d'établir les accidents épirogéniques à l'aide des sources chaudes réparties le long de certaines lignes, en partant de la réflexion que des cassures tectoniques facilitant l'ascension des eaux thermales à la surface doivent exister à l'endroit où des sources thermales jaillissent. Cette hypothèse de travail a été fortement

critiquée par certains de mes collègues, mais je pense qu'elle a été pleinement vérifiée au cours des événements du 18 mars 1953. J'ai réussi, d'ailleurs à prouver par mes études sur le terrain, l'existence des failles qui ont été établies d'abord théoriquement.

Dans une région insuffisamment connue du point de vue tectonique, il est donc possible de conclure à la présence de failles (et, par conséquent, à l'existence possible de centres séismiques) en étudiant la répartition des sources thermales.

BIBLIOGRAPHIE.

- ARABU (N.) : Contribution à l'étude géol. aux environs de la Mer Marmara. — Inst. Géol. Roumanie, C. R., 1934/35, Bucarest, (et des publications plus anciennes apparues dans les C. R. Acad. Sc. Paris et dans le Bull. Soc. Géol. France).
- PINAR (N.) : Géologie et Météorologie sismiques du bassin de la Mer de Marmara. — R. Fac. Sc. Nat., Univ. Ist. t. VII, série A, fasc. 3-4, 1943.
- PINAR (N.) : Les lignes sismiques du bassin égéen de l'Anatolie et les sources thermales. — Ibid., t. XIV, fasc. 1, série A, 1949.
- PINAR (N.) : Etude géologique et sismologique du tremblement de terre de Karaburun du 23 juillet 1949. — Ibid., t. XV, série A, fasc. 4, 1950.
- PINAR (N.) : Les zones sismiques de l'Anatolie Occidentale. — Publ. Bur. C. Séism. Int., Série A, fasc. 18, 1951.
- PINAR (N.) : Preliminary note on the earthquake of Yenice-Gönen, Turkey, March 18, 1953. — Bull. Seism. Soc. Amer., Vol. 43, No 4, 1953.
- PINAR (N.) - LAHN (E.) : Türkiye Depremleri Izahli Katalogu (Catalogue expl. des Séismes de Turquie). — Bay. Bak., 1952, Ankara.
- CARTE GÉOLOGIQUE au 1/800.000^e de la Turquie. — 1942-1946, Ankara.

SUR QUELQUES ALIGNEMENTS SÉISMIQUES REMARQUABLES DU MAROC ESSAI D'INTERPRÉTATION TECTONIQUE

par Jean DEBRACH (Casablanca).

A l'occasion d'une révision des séismes survenus au Maroc depuis 1932, j'ai établi une carte de répartition des épicentres. Négligeant les plus faibles secousses tout à fait localisées, je n'ai retenu que les tremblements de terre enregistrés instrumentalement ou ceux dont l'intensité macroséismique a été égale ou supérieure au degré IV de l'échelle macroséismique internationale, pour les périodes au cours desquelles les sismographes de l'observatoire Averroes n'étaient pas en fonctionnement. Ces secousses n'ont pas dépassé le degré VIII. L'imprécision de la documentation antérieure à cette date (1932) m'a conduit à utiliser cette carte, malgré la durée évidemment trop faible de la période considérée, pour tenter d'exposer une vue d'ensemble et un essai peut-être prématûr d'interprétation tectonique de la séismicité du Maroc.

Un premier examen de cette carte montre que les épicentres sont localisés sur le relief, dans les zones de plissements récents (Tertiaires) comme on le constate en général (1952 a).

On peut ainsi distinguer deux domaines séismiques :

- a) le domaine rifain,
- b) le domaine atlasique plissé, proprement dit, c'est-à-dire : Moyen Atlas et Grand Atlas.

La meseta marocaine est peneséismique dans son ensemble (les rares séismes de cette zone paraissent localisés dans le Massif central ancien).

Le Maroc oriental (meseta) est aséismique. Il semble en être de même de l'Anti-Atlas où aucun séisme n'a été signalé.

Cependant, à regarder de plus près, ces épicentres paraissent s'aligner assez remarquablement sur des lignes droites. De tels alignements ont été signalés ailleurs.

Le tracé de telles lignes risque, il ne faut pas se le dissimuler, d'être quelque peu subjectif. Pourtant lorsque sept ou huit épicentres de tremblements de terre importants se rangent d'une telle manière, et que tous les épicentres d'une région se placent sur un petit nombre de tels alignements, il y a là une coïncidence qui vaut au moins d'être notée.

Pour les vingt années qui ont servi à l'établissement de la carte, on peut distinguer deux alignements principaux, et y rattacher des

alignements secondaires qui recoupent les premiers presque exactement à angle droit (voir figure).

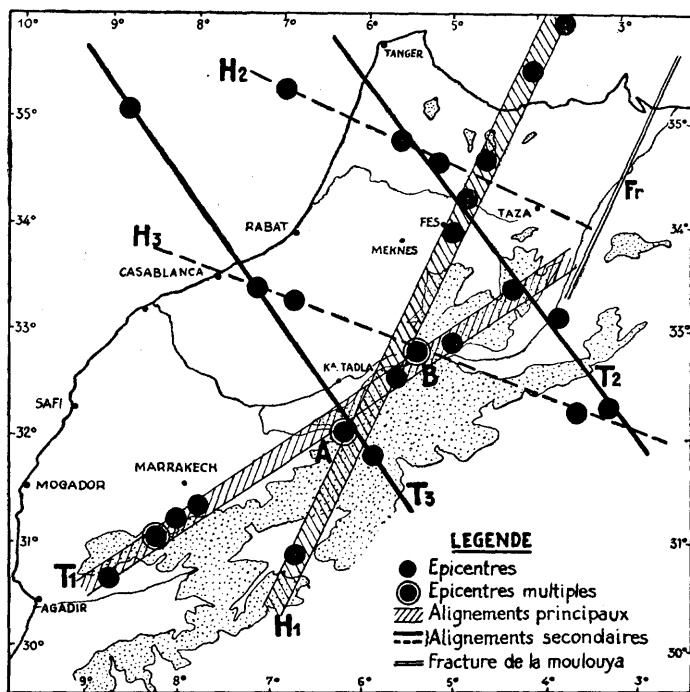


FIG. 1.

Décrivons-les brièvement :

A) Une première ligne groupant huit épicentres est orientée S.W.-N.E. (d'Agadir à Oujda) à peu près parallèlement aux plis-segments atlasiens (T₁).

Elle est recoupée par deux lignes secondaires orientées N.W.-S.E., l'une allant de Larache aux environs de Béni-Abbès (T₂), l'autre allant du Nord de Casablanca vers Tadla (T₃).

B) Un deuxième alignement important s'oriente du S.S.W. au N.N.E. (Ouarzazate-Fès) (H₁), (9 épicentres).

Celui-ci ne semble pas en rapport avec la tectonique récente ou du moins avec l'orographie actuelle du Maroc. Cet alignement est recoupé à l'angle droit par deux lignes W.N.W-E.S.E.; l'une vers Casablanca - Colomb-Béchar (H₃), l'autre plus problématique au Sud du Rif (H₂).

Les croisements de ces diverses lignes paraissent être des points particulièrement instables. En particulier au voisinage de la ren-

contre des deux lignes principales se situe l'origine des manifestations séismiques les plus importantes de la période considérée :

- a) Le tremblement de terre du 10 mai 1950 qui, avec une intensité macroséismique atteignant VII, a secoué une surface de plus de 80.000 km² (probablement classe *d*) (point B sur la figure);
- b) Un essaim de secousses centré vers Tillouguit qui, du 14 octobre 1936 à 1949, a groupé plus de cinquante secousses (A).

Si le premier de ces réseaux décrits plus haut semble en rapport avec la tectonique atlasique, il est loin d'en être de même du second dont la ligne principale s'oriente, rappelons-le, de S.S.W. à N.N.E. Nous n'examinerons ici avec quelque détail que les deux alignements principaux qui sont les plus caractéristiques.

Considérons d'abord *le premier de ces alignements principaux T 1*. Il s'oriente sensiblement (d'Agadir à Oujda) du S.W. au N.E., c'est-à-dire selon la direction tectonique générale des plissements du Grand Atlas. Les principaux épicentres se placent sur le front Nord de l'Atlas, et la signification d'ensemble de cet alignement apparaît ainsi liée au plissement de cette chaîne. Nous ne voulons pas dire évidemment qu'un seul accident est jalonné par une série de foyers. Il s'agit plus vraisemblablement d'une série d'accidents dont l'orientation générale est celle de la chaîne. De plus, comme nous le verrons par la suite, les séismes paraissent se localiser le plus fréquemment à la jonction de lignes structurales diverses. Voici ce que l'on peut ajouter sans vouloir rechercher des rapports trop étroits avec la géologie de surface : cette ligne T 1 représenterait pour le Haut Atlas Occidental l'accident Nord atlasique (Roch, Ambroggi, Neltner) puis au Nord du Haut Atlas Central, la ligne de contact du Haut Atlas et du Moyen Atlas (Atlas de Béni-Mellal à l'W., Atlas plissé plus à l'E.), marquée topographiquement par les vallées de l'Oued-el-Abid et de ses affluents sur le versant atlantique, par la cuvette de la haute vallée de la Moulouya sur le versant méditerranéen.

Massif ancien du Grand Atlas et Haut Atlas Central chevauchent en général les zones subatlasiques (Marçais); la surrection récente serait de la fin du Villafranchien, et l'on peut penser que les mouvements actuels résultent de la mise en place consécutive à la persistance de ces poussées.

D'autre part, vers Afourer, l'Atlas de Béni-Mellal subit un rebroussement net; orienté W.S.W.-E.N.E. après les Djebilet, il devient S.W.-N.E. vers le R'Nim. La structure de l'ensemble du massif apparaît comme fort complexe et paraît figurer la rencontre

de deux lignes orogéniques (de deux axes d'efforts si l'on préfère), soit que ces directions traduisent le sens d'efforts successifs de directions différentes, soit que l'une d'entre elles, celle du N., porte la marque de déformations antérieures du socle.

Quoi qu'il en soit, cette zone disloquée de structure complexe où s'affrontent les plis du Grand Atlas et ceux du Moyen Atlas (Atlas de Béni-Mellal) apparaît comme particulièrement séismique. (Secousses de la région de Tillouguït : point A.)

Le second des alignements principaux que nous avons décrits se présente de manière différente. De direction sub-méridienne, il est orienté S.S.W.-N.N.E., c'est-à-dire à peu près parallèlement aux axes tectoniques hercyniens du Maroc Occidental.

Pour juger de la généralité de cet alignement, j'ai reporté sur une carte les épicentres de la région retenus par MM. Gutenberg et Richter (1949) dans leur ouvrage « Seismicity of the Earth » (Région 31, Méditerranée occidentale). Bien que les coordonnées de ces épicentres ne soient le plus souvent données qu'à un degré près, six d'entre eux (sur dix) se groupent bien autour de la direction considérée.

De plus, et ceci est peut-être plus curieux, l'épicentre du tremblement de terre de profondeur exceptionnelle (650 km; magnitude : 7) survenu le 29 mars 1954 dans la Cordillère Bétique se place également sur cet alignement qui groupe ainsi quatorze épicentres, soit à peu près la moitié de ceux que nous avons notés.

Rappelons à ce sujet que Russo a signalé naguère (1933), dans son « Essai de coordination tectonique de la Méditerranée occidentale », une grande ligne de dislocation de la surface terrestre ayant la même direction S.S.W.-N.N.E. que cet alignement et passant à quelque 100 km à l'Est (fracture de la Moulouya).

« Si l'on examine, écrit Russo, la région qui va de Melilla au Figuig à travers le Maroc Oriental, on ne saurait manquer d'être frappé du fait que l'on y voit, sur une ligne sensiblement droite et orientée du N.N.W. au S.S.E., se produire un abaissement par ennoyage ou par fracture, de tous les plis atlasiens que l'on y rencontre. Cet abaissement est tel que, par exemple, M. Gauthier, qui avait déjà remarqué le phénomène (La structure de l'Algérie, Alger, 1921), dit qu'à l'Ouest du Figuig il n'y a plus d'Atlas mais de simples chicots; et d'ailleurs, ces chicots eux-mêmes font bientôt place à un régime tabulaire. Au Nord, c'est au contraire l'Est de la ligne ci-dessus indiquée qui ne laisse plus voir que des chicots.

« C'est au voisinage de cette ligne que s'ordonnent les volcans de Melilla, de la basse Moulouya (Ain-Aicha, Taourirt, etc...) et de la région d'Oujda, de Tiskennit, du Tigri, la dépression du Tamelet, « la Rue des Palmiers » avec le couloir de la Saoura. Au Nord, elle s'incurve et c'est encore sur elle ou à son voisinage que se montre l'île volcanique d'Alboran; les volcans de Carthagène et d'Almeria, ceux d'Olot et des Corbières, ceux du Massif Central français et de la vallée du Rhin. C'est cet alignement que Gauthier, sans en déterminer les conditions, avait remarqué, car sa disposition est extrêmement frappante morphologiquement. On voit que son rôle géologique apparaît aussi comme fort important. »

Remarquons ici que d'autres grandes zones rectilignes de dislocations ont été décrites à la surface de la terre, telle que la rainure érythréenne (Montessus de Ballore, Gutenberg et Richter). Rapelons encore la « grande ceinture d'argent » de Spurr sur les côtes occidentales de l'Amérique, dans laquelle Dauvillier (1947) voit la trace d'un relief lunaire primitif antérieur aux convulsions géologiques classiques.

J. Coulomb (1943-1945) envisage également pour les séismes profonds de gigantesques « failles » de profondeur considérable qui auraient souvent un pendage important (de l'ordre de 45°). Dans l'alignement décrit ci-dessus, si le séisme profond de 1954 se rattache au grand accident décrit par Russo, la cassure paraîtrait moins inclinée, ou quasi verticale, l'épicentre se situant bien sur l'alignement considéré.

Plus récemment, L. Glangeaud (1951) dans son « Interprétation tectonophysique de la Méditerranée occidentale », décrit également de grands accidents profonds et anciens (géosutures) qui ne représentent pas de simples failles. « Ce sont des structures profondes se traduisant dans la couverture par une zone de flexures, de failles parallèles, avec des accidents satellites, par des relais de plis et de nombreuses manifestations superficielles variées. »

« Les géosutures africaines délimitant les pièces de la mosaïque africaine que nous venons de définir ont joué à différentes époques des temps géologiques et notamment au moment du paroxysme oligocène. Elles sont accompagnées par un réseau de petites failles satellites du quatrième et cinquième ordre, dues aux mouvements relatifs des compartiments. »

Deux de ces structures intéressent la région étudiée ici; elles affectent la même direction que notre alignement H₁. Ce sont :

La transversale Tafna-Magoura et la transversale de la Moulouya. Cette dernière correspond plus précisément à la grande fracture de Gauthier-Russo. Zones de fractures ou géosutures, ces grands alignements apparaissent comme des traits fort anciens de la structure terrestre (Primaires? Précambriens?). Ce sont certainement des accidents de grande profondeur, et il nous paraît remarquable qu'ils apparaissent dans le groupement linéaire des épicentres. Ceci rejoint les vues de Glangeaud lorsqu'il écrit que « la bordure orientale nord-africaine a été découpée avant le paroxysme oligocène, « en différents panneaux, par de grands accidents profonds. « Certains d'entre eux peuvent avoir une origine plus ancienne « (Géosuture) et on déjà joué au secondaire ».

Cette transversale, vaste champ de fracture complexe, correspond à la zone de fracture du Nekor (Choubert et Marçais, 1952) et apparaît au reste sur une carte d'anomalies isostatiques. S'agit-il cependant d'un phénomène régional ou d'une « ligne de structure géonomique », suivant la nomenclature de Glangeaud, affectant l'ampleur que lui attribue Russo; il est difficile de le préciser. Il est aussi difficile d'affirmer que cette ligne se prolonge en profondeur vers le Sud et recoupe transversalement l'Atlas; mais la question vaut d'être posée.

En somme, il apparaît que les épicentres des principaux tremblements de terre marocains se groupent en deux réseaux de lignes droites, chacun d'eux étant constitué par un alignement principal recoupé à angle droit par des alignements secondaires.

Les alignements principaux sont orientés, l'un dans le sens des axes tectoniques Tertiaires, l'autre dans le sens des axes tectoniques hercyniens. Ce dernier paraît se poursuivre dans la Péninsule ibérique; il est à peu près parallèle et très voisin de la grande ligne de fracture décrite par Gauthier et Russo sous le nom de « fracture du bord oriental de l'Espagne » et correspond sans doute à l'accident du Nekor.

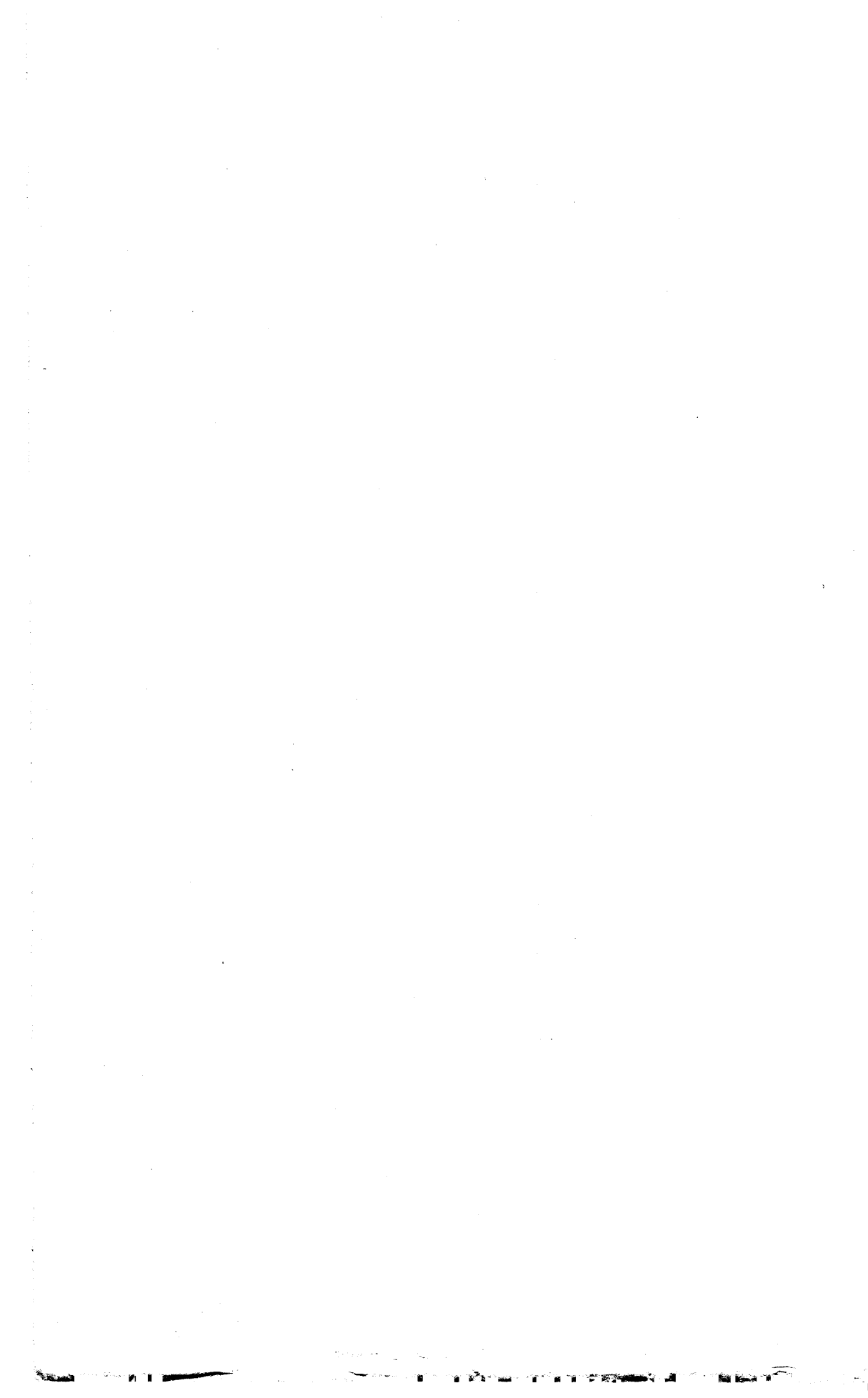
Remarquons encore :

a) que ces directions privilégiées jouent un rôle dans les répartitions des intensités de surface des séismes les plus importants. On le retrouve par exemple sur le tracé des isoséistes des tremblements de terre du 10 mai 1950 et du 29 mars 1954.

b) que les séismes du Maroc occidental ne sont à peu près jamais perçus au Maroc oriental, tandis que les tremblements de terre les plus importants d'Algérie sont sans répercussion à l'Ouest du méridien de Guercif, comme s'il existait entre ces deux régions une sorte de barrière, d'écran séismique.

BIBLIOGRAPHIE.

1924. — DE MONTESSUS DE BALLORE. — La géologie séismologique. — Paris .A. Colin.
1927. — REY PASTOR (A.). — Traits séismiques de la péninsule ibérique. — Madrid.
1933. — RUSSO (P.) & RUSSO (L.). — Essai d'une coordination tectonique de l'évolution de la Méditerranée. — Mem. Soc. Sc. nat. Maroc XXXIV.
1943. — COULOMB (J.). — Une interprétation simultanée des séismes profonds et des bandes d'anomalies de la pesanteur. — C. R. Ac. Sc. T. 217, p. 355.
1945. — COULOMB (J.). — Séismes profonds et grandes anomalies négatives de la pesanteur peuvent-elles être attribuées à une extension plastique? — Ann. de Géophysique. T. I — p. 244.
1947. — DAUVILLIER (A.). — Genèse et évolution des planètes. — Actualités Scientifiques. — Paris — Hermann.
1947. — ROTHÉ (J.-P.). — Hypothèse sur la formation de l'Océan Atlantique C. R. Ac. Sc. T. 224 — p. 1295.
1949. — GUTENBERG (B.) & RICHTER (C.-F.). — Seismicity of the Earth, Princeton. — New-Jersey.
- 1951 a. — GLANGEAUD (L.). — Interprétation tectono-physique des caractères structuraux et paléogéographiques de la Méditerranée occidentale. — Bull. Soc. géologique de France. — 1951, p. 735.
- 1951 b. — ROTHÉ (J.-P.). — La structure de l'Atlantique. — Annali di Geofisica, Vol. IV — N° I — p. 27. — Rome.
- 1952 a. — DEBRACH (J.). — Tremblements de terre marocains. Répartition géographique des épicentres. — Bull. Soc. Géogr. Maroc. N° I — p. II.
- 1952 b. — GOGUEL (J.). — Compte-rendu des séances du Comité pour la physique de l'intérieur de la terre. (U.G.G.I. Bruxelles 1951). — Ann. de Géophysique — T. 8, p. 121 — Exposé de L. Glangeaud.
- 1952 c. — CHOUBERT (G.) & MARÇAIS (J.). — Géologie du Maroc. — Notes et Mémoires du Service Géologique du Maroc — N° 100.
- 1952 d. — Congrès géologique international, XIX^e Session. — Alger — Livrets guides — cf. not. N° 7 — Maroc Septentrional — Rif — par P. Fallot — J. de Lizaur — J. Marçais et G. Suter — p. 34.
- 1954 a. — ROTHÉ (J.-P.), MARY (J.) & PETERSCHMITT (E.). — Le séisme « profond » du 29 mars 1954 en Espagne — C. R. Ac. Sc., T. 238, 5 avril 1954, pp. 1530-1531.
- 1954 b. — DEBRACH (J.). — Note préliminaire sur un séisme de profondeur exceptionnelle ressenti dans la péninsule ibérique et au Maroc (29 mars 1954). — C. R. Soc. Sc. Nat. Maroc, 1954, pp. 97-98.
- 1954 c. — DEBRACH (J.). — Deuxième note sur le séisme bético-rifain profond survenu le 29 mars 1954. Isoséistes au Maroc. — C. R. Soc. Sc. Nat. Maroc, 1954, pp. 115-117, une carte.



REMARKS ON THE FOUNDATION OF THE CONCEPTION OF ISOSTASY

by Karl JUNG, Bergakademie Clausthal (Germany).

The research of the geoid, as a purely mathematic problem, requires a reduction of gravity values that removes the topographic masses and transfers them into the interior of the geoid in any convenient way. But if we want to research strains and forces in the earth's crust, especially those which tend to equilibrium, the reduction must be well defined in a physical manner, and the masses to be removed must not be altered. The principle of isostasy suggests that the reductions should be founded on the conception of an exactly hydrostatic state of the subcrustal masses.

It is well known that the usual isostatic reductions correspond nearly, but not strictly, to this principle. This is the cause of some problematic secondary effects concerning the shift of equipotentials below the depth of compensation. In spite of Vening Meinesz' detailed investigation, their numerical treatment is rather complicated, and it would be desirable to avoid them.

Such a reduction — it may be called « perfectly isostatic reduction » — can be performed in such a way that the equilibrium state below the crust is unchanged, the potential on the level of compensation is only altered by a constant. It is possible to choose this constant in such a manner that the preservation of hydrostatic equilibrium is combined with the preservation of masses. But it is not possible to fix the removed masses strictly beneath their original place : a removed point mass spreads laterally with a considerable central condensation (fig. 1).

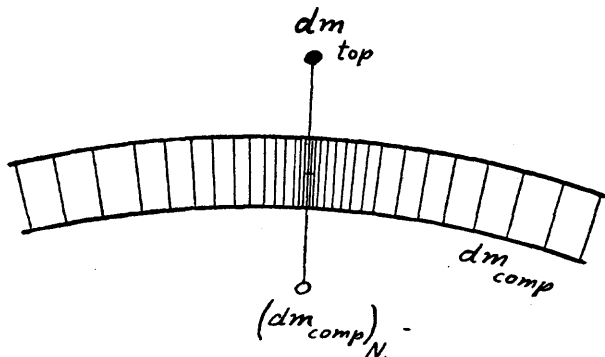


FIG. 1. — *Perfectly isostatic reduction*
 dm_{top} topographic mass element
 dm_{comp} its compensation
 $(dm_{comp})_N$ approximation of Niethammer

At first, the development of computation methods seems to be laborious. But, as Niethammer has pointed out, one gets a satisfying approximation by reducing in the usual way, replacing the removed mass by a concentrated mass, twice as deep as the real compensation.

Inversely, the usual isostatic anomalies may be interpreted as perfectly isostatic anomalies with real compensations half as deep as usually supposed. Instead of the usual density difference of 0.6 g/cm^3 , we have in this interpretation a real difference of 1.2 g/cm^3 which must be regarded as impossible. Thus this very interesting interpretation has little importance.

In flat areas, the difference of the perfectly isostatic reduction and the corresponding usual reduction is small. A rough estimation has proved that remarkable differences occur above striking features of the earth's crust, such as volcanic islands and deepsea trenches (*fig. 2*).

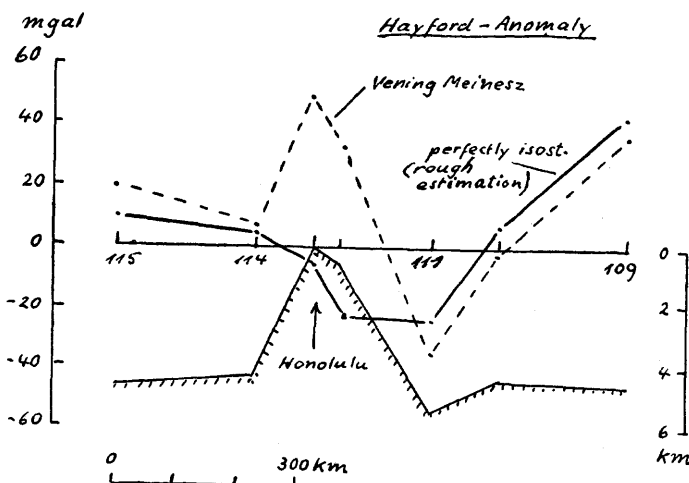


FIG. 2.

The perfectly isostatic reduction has some advantages :

It is founded on a physically well defined state of hydrostatic equilibrium below the earth's crust and leads to an estimation of the forces tending to reestablish this equilibrium if it is disturbed.

It may be adapted to the isostatic conceptions of Pratt, Airy, Heiskanen and others — for instance Daly and Mintrop — and at least approximately to the regional isostasy of Vening Meinesz.

There is no shift of equipotentials below the level of compensation. The layer between the geoid and the cogeoid may be regarded

as compensated, and then the effects of this layer and its compensation cancel each other.

There are no difficulties concerning a first order harmonic term of topography (fig. 3). Such a term may be in perfectly isostatic

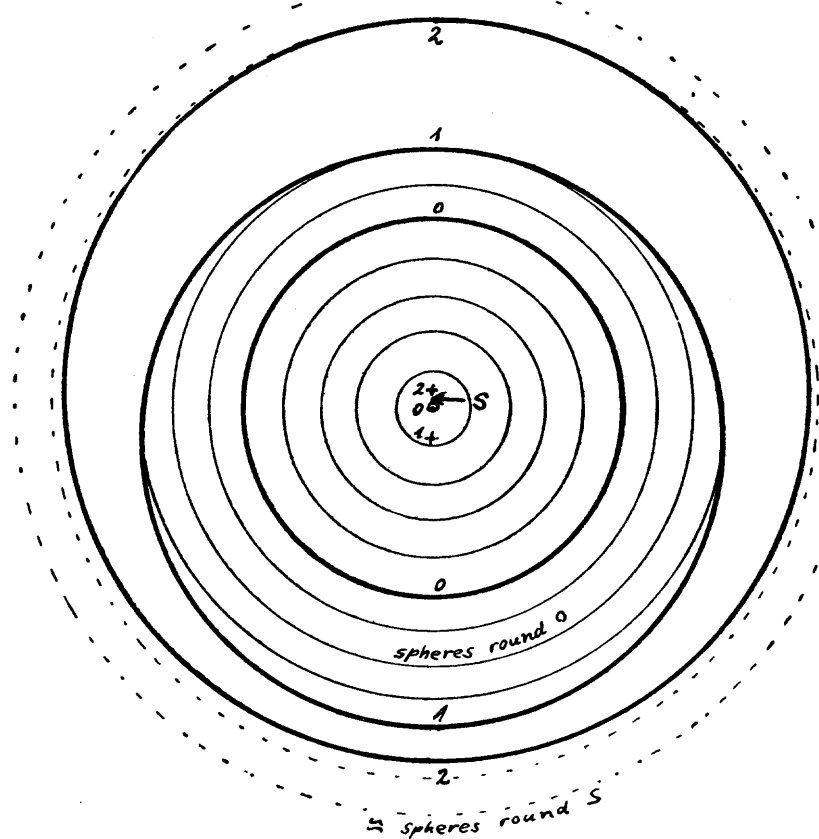


FIG. 3. — *First order harmonic term*

S = centre of gravity of the whole mass.

The concentric circles in the interior and the dashed circles outside the earth are equipotentials.

equilibrium. Before and after the reduction the development of the potential outside the earth contains no first order term.

Approximate computations prove that some ambiguities concerning the details of placing the removed topographic masses are not significant. It is a future task to investigate them more exactly.

I think, one should work out tables and contour maps for several kinds of perfectly isostatic reductions or for the differences of these reductions and the corresponding usual reductions. As there are

approximate relations with known computing methods, the numerical calculations are not too laborious.

It is not necessary to reduce all gravity values in the proposed manner. But in especially interesting regions some perfectly isostatic reductions should be computed, and the anomalies should be compared with the corresponding usual anomalies.

LITERATURE.

- JUNG (K.) : Über vollständig isostatische Reduktion. Zeitschrift für Geophysik 14, 27-44, 1938.
NIETHAMMER (Th.) : Bemerkungen zum Artikel von Karl Jung : « Über vollständig isostatische Reduktion ». Zeitschrift für Geophysik 14, 119-122, 1938.
VENING MEINESZ (F.-A.) : The indirect isostatic or Bowie reduction and the equilibrium figure of the earth. Bulletin géodésique N. S. No 1, 33-107, juillet 1946.
VENING MEINESZ (F.-A.) : The isostatic reduction and the indirect Bowie effect. Bulletin géodésique N. S. No 12, 170-179, juin 1949.
-

LES VITESSES DES ONDES SÉISMIQUES EXCITÉES PAR LES EXPLOSIONS INDUSTRIELLES EN BOHÈME

par VIT KARNIK

Institut Géophysique de l'Académie Tchécoslovaque des Sciences (Praha).

INTRODUCTION.

Sur le territoire de la République Tchécoslovaque un nombre d'explosions industrielles a été provoqué dans les carrières dès 1946. Dès 1950 la station séismologique de Praha inscrit les ondes séismiques excitées par ces explosions; souvent les stations de Collm, Jena et Stuttgart les inscrivent aussi. Le présent mémoire comporte l'étude de tout le matériel rassemblé : des séismogrammes de Praha (appareil Anderson-Wood), des séismogrammes ou leurs copies des stations Collm (appareil Benioff), Jena (pendule de 15 tonnes), Stuttgart (appareil courte-période, type Stuttgart), qui nous ont été communiquées par les Docteurs Hiller, Krumbach et Adlung.

Toutes les explosions étudiées ont été provoquées en présence d'un séismologue de l'Institut Géophysique qui a déterminé l'instant de l'explosion en se servant d'un chronomètre contrôlé; depuis cette année les explosions sont provoquées d'après les signaux horaires internationaux. Mais, en quelques cas, l'irrégularité du fonctionnement du chronomètre ou la correction non garantie ont causé une erreur inadmissible, plus grande que $\pm 0,1$ sec. Les explosions avec de telles heures d'origine ont servi seulement à l'analyse des phases.

Les observations sont étendues irrégulièrement quant à la distance épacentrale : la situation géologique en est la cause. Le plus grand nombre des observations se groupe aux distances de 12 km., 28 km., 63 km. et 110 km.; les observations individuelles se trouvent aux distances de 22 km., 58 km., 82 km., 120 km., 170 km., 330 km. et 443 km. A cause de la structure géologique compliquée de la Bohême les vitesses dérivées sont typiques seulement pour les rayons définis.

Toutes les inscriptions ont été dépouillées par l'auteur; les distances épacentrales ont été mesurées sur une carte géographique. Le nombre total des explosions utilisées pour la présente étude est 38.

Identification des phases.

Toutes les lectures des phases ont été reportées sur un graphique « temps-distances » après la réduction avec le quotient $\Delta/5,5$.

Les ondes longitudinales :

Les premiers impetus entre 10 et 80 km. sont bien représentés par la droite

$$t = \frac{\Delta}{5,62} + 0,2 \quad \dots \quad \bar{P}$$

Pour saisir la décroissance régulière et lente des temps d'arrivée, il semble qu'une courbe représenterait le mieux les premiers impetus entre 10 et 120 km. On peut aussi remplacer l'hodochrone \bar{P} par deux hodochrones

$$t = \frac{\Delta}{5,30} + 0,0 \quad \dots \quad \bar{P}_1$$

$$t = \frac{\Delta}{5,90} + 1,0 \quad \dots \quad \bar{P}_2$$

L'équation de la droite reliant sur l'hodochrone les premiers impetus à la distance 110 km. et les faibles secondes phases à

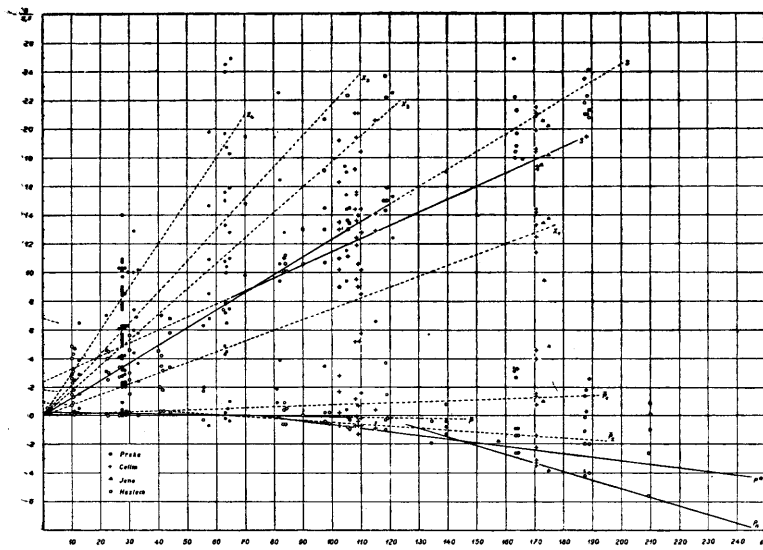


FIG. 1. — Courbes Hodochrones.

170, 330 et 443 km. s'écrit

$$t = \frac{\Delta}{6,35} + 1,8 \quad \dots \quad P^*$$

Les trois premiers impetus, très faibles, aux distances de 170, 330 à 443 km. définissent une nouvelle onde, P_n , à vitesse nota-

blement plus grande

$$t = \frac{\Delta}{8,15} + 6,8 \quad \dots \quad Pn$$

Les ondes transversales :

Dans ce groupe on peut déterminer avec garantie seulement deux phases \bar{S} et S^*

$$t = \frac{\Delta}{3,30} + 0,2 \quad \dots \quad \bar{S}$$

$$t = \frac{\Delta}{3,67} + 2,4 \quad \dots \quad S^*$$

La troisième onde, Sn , n'a pas été observée.

Les quotients des vitesses sont $v_{\bar{P}}/v_{\bar{S}} = 1,70$ et $v_{P^*}/v_{S^*} = 1,73$.

Les ondes X :

A la distance de 28 km. l'impetus défini apparaît sur les inscriptions entre les groupes P et S. Il s'agit ou d'une onde réfléchie — PP — sur le miroir de réflexion à la profondeur de 15,5 km. (en prenant $T = 7,0$ sec, $v = 6,0$ km./sec.) ou d'une onde directe

$$t_1 = \frac{\Delta}{4,03} + 0,0 \quad \dots \quad X_1$$

Sur les inscriptions de Praha les phases intensives avec les hodochrones suivants émergent derrière le groupe S :

$$t_2 = \frac{\Delta}{2,78} + 0,0 \quad \dots \quad X_2$$

$$t_3 = \frac{\Delta}{2,48} + 0,0 \quad \dots \quad X_3$$

$$t_4 = \frac{\Delta}{2,10} + 0,0 \quad \dots \quad X_4$$

$$t_5 = \frac{\Delta}{1,81} + 0,0 \quad \dots \quad X_5$$

L'épaisseur des couches et l'interprétation des phases.

L'application des formules habituelles fournit les résultats suivants :

L'épaisseur de la couche supérieure (granitique) $d_1 = 10,9$ km. (en utilisant les hodochrones des phases \bar{P} et P^*) ou $d_1 = 9,1$ km. (par les phases \bar{S} et S^*); l'épaisseur de la couche intermédiaire (gabbro-basalte) $d_2 = 19,9$ km. (par les phases \bar{P} , P^* et Pn). Avec la modification \bar{P}_1 , \bar{P}_2 les résultats sont : $d_{11} = 6,0$ km., $d_{12} = 4,5$ km.

Praha

Anderson-Wood EW

18.1.1954, H = 10 00 01,0 UT, $\Delta = 27,7$ km, C = 20, 3t

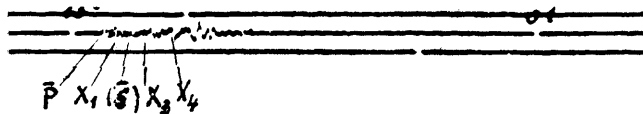


FIG. 2.

Praha

Anderson Wood EW

26. VI 1952, H = 11 59 59, 0 UT, $\Delta = 27,7$ km, C = 6,9 t



16. VII. 1952, H = 10 00 01, 0 UT, $\Delta = 57,5$ km, C = 15,0 t

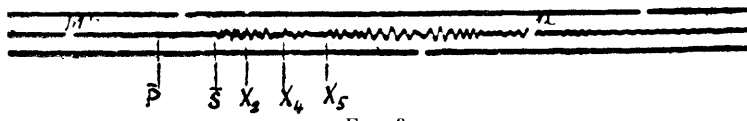


FIG. 3.

FIG. 2 et FIG. 3. — Enregistrements obtenus à Praha au séismographe Anderson-Wood ($T_0 = 3,2$ sec, $V_0 = 1350$, $\epsilon : 1 = 15,1$).

On a comparé les temps d'arrivée des explosions en Bohême avec ceux de l'explosion d'Haslach [1, 2] et on a trouvé une conformité très satisfaisante. Mais l'interprétation de l'auteur est un peu différente et les résultats s'accordent seulement dans la profondeur de la surface de Mohorovicic. On peut dire encore que, pour les deux régions, la vitesse des ondes sismiques augmente avec la profondeur dans les premiers dix kilomètres de la même manière.

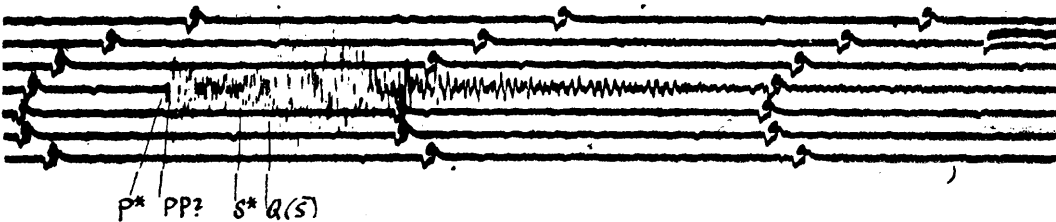
Aux distances de 12 et 28 km. les premiers impetus sont très brusques, de courte période, avec des amplitudes maximum; aux distances de 63 km., 82 km. et 110 km. ils deviennent déjà plus faibles. Au contraire, la phase S est peu marquée aux distances de 12 et 28 km. et il semble, qu'elle manque sur quelques séismogrammes; aux distances plus grandes elle devient intensive, mais elle se superpose avec l'onde superficielle Q.

Il faut faire remarquer un phénomène encore intéressant. Aux distances de 110 km. ca une phase intensive émerge derrière le premier impetus sur les séismogrammes de Collm. On peut la suivre des deux côtés avec l'intensité décroissante aux distances de 70 km. et 170 km. La différence entre les temps d'arrivée de cette phase

Collm

Benioff Z

7. V. 1952, H = 10 29 57,5 UT, $\Delta = 108,6$ km, C = 10,3 t



16. VII. 1952, H = 10 00 01,0 UT $\Delta = 115,2$ km C = 15,0 t

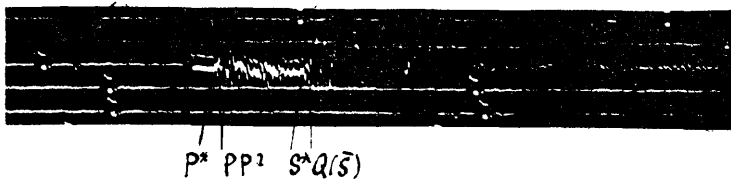


FIG. 4.

Enregistrements obtenus à Collm au séismographe Benioff Z (M : 100 kg., L = 1000 mm., To = 0,48 sec, Tg = 1,32 sec).

et du premier impetus est la plus petite à la distance de 110 km. (= 0,5 sec. ca). MM. J. P. Rothé, E. Peterschmitt [1] et MM. P. L. Willmore, A. L. Hales et P. G. Gane [3] ont observé la même phase avec les mêmes propriétés sur les inscriptions de l'explosion d'Haslach et sur les inscriptions des chocs locaux à Witwatersrand (Afrique du Sud). Les séismologues français expliquent cette phase par une onde passée dans la couche gabbro-basalte. Au contraire les séismologues Willmore et les autres attribuent cette phase aux réflexions sur la surface de Mohorovicic. J'adopte la deuxième interprétation, parce que les observations forment bien un « segment renversé » (angl. reversed segment) de l'hodochrone des premiers impetus.

Les phases désignées par le symbole X sont dues probablement aux ondes ayant traversé les sédiments. M. G. Krumbach signale des phases de même caractère sur les séismogrammes des explosions et des secousses de mine inscrites à Jena [4].

BIBLIOGRAPHIE.

- [1] ROTHÉ (J.-P.), PETERSCHMITT (E.) : Etude séismique des explosions d'Haslach, Annales de l'Institut de Physique du Globe, Nouvelle Série, T. V. Géophysique, 1950, 13-38.
- [2] REICH (H.), SCHULZE (G. A.), FÖRTSCH (O.) : Geophysik. Ergebnis der Sprengung bei Haslach im Schwarzwald, Geologische Rundschau, 36, 1948.
- [3] WILLMORE (P. L.), HALES (A. L.), GANE (P. G.) : A seismic investigation of crustal structure in the Western Transvaal, Bull. Seism. Soc. Am., Vol. 42, 1952, 53-80.
- [4] KRUMBACH (G.) : Charakteristische Seismogrammformen bei Aufzeichnungen in Herdgebieten, Bull. d'Inf. de l'U.G.G.I., Avril 1953, No 2, 243-244.

ENREGISTREMENT DES ONDES SÉISMIQUES PROVOQUÉES PAR DE GROSSES EXPLOSIONS

I. — CAMARGUE 1949.

par Y. BEAUFILS, P. BERNARD, J. COULOMB, F. DUCLAUX
Y. LABROUSTE, H. RICHARD, E. PETERSCHMITT, J.-P. ROTHÉ
et R. UTZMANN.

La Compagnie Générale de Géophysique et les Instituts de Physique du Globe de Strasbourg et de Paris ont réalisé, en 1949, des enregistrements d'explosions en Camargue. Une soixantaine d'enregistrements ont été obtenus à des distances variant de 1,7 à 26 km.
Séismographes.

L'appareillage comprenait : un laboratoire de la Compagnie générale de Géophysique (C.G.G.) qui a occupé quatre positions successives couvrant un intervalle de distances compris entre 1.735 et 9.475 mètres; deux séismographes Askania de l'Institut de Physique du Globe de Strasbourg (composante verticale et composante longitudinale) qui ont été installés successivement dans 5 stations à des distances des points d'explosion variant de 2.425 à 16.025 m.; un séismographe Mintrop, du même Institut, également à deux composantes, et deux appareils Mintrop à trois composantes de l'Institut de Physique du Globe de Paris qui ont occupé sept stations différentes (distances de 2.435 à 26.065 m.).

Enfin mentionnons que 4 des stations précédentes ont été équipées d'appareils électromagnétiques.

Enregistrement du temps.

Le laboratoire C.G.G. a utilisé son dispositif habituel de marques de temps à intervalle d'un centième de seconde. L'instant de l'explosion était donné par la déviation de l'un des galvanomètres enregistreurs.

Aux autres stations, l'enregistrement du temps était assuré par une pendule directrice donnant un signal par seconde. Ce signal, transmis par fil téléphonique, était inscrit sous forme d'une déviation aux stations Askania et Mintrop de Strasbourg et au moyen d'une lampe à argon dans celles de l'Institut de Physique du Globe de Paris. L'interpolation entre les signaux de seconde était obtenue, dans les appareils Askania, au moyen d'un petit pendule de période 0,178 que comportait l'enregistreur et par un diapason dans les stations de Mintrop. Des corrections de pendule et de relais ont été appliquées aux mesures de temps. La précision de ces dernières était de l'ordre du centième de seconde.

Enregistrements séismographiques.

Phase P. — Cinq arrivées d'ondes longitudinales ont été reconnues; leurs équations de propagation sont les suivantes :

$$t_1 = 0,23 + \frac{\Delta}{2,3}$$

$$t_2 = 0,45 + \frac{\Delta}{3,6}$$

$$t_3 = 0,70 + \frac{\Delta}{5,0}$$

$$t_4 = 0,80 + \frac{\Delta}{5,6}$$

$$t_5 = 0,87 + \frac{\Delta}{6,0}$$

(t : durée de propagation en secondes; Δ : distance en km.).

En outre, les prospections à faible profondeur indiquent la présence d'une couche superficielle à faible vitesse (de l'ordre de 1,0 km/s) dont l'épaisseur serait de quelques mètres seulement.

Le résultat le plus intéressant est l'existence, à une profondeur relativement faible (de l'ordre de 2.000 m.) de couches à grande vitesse; cette dernière est bien définie par les premières arrivées d'ondes aux stations comprises entre 4 et 16 km. de l'explosion. La carte gravimétrique mise à notre disposition par la S.N.P.L.M. montre que le profil séismique coupe l'axe d'un anticlinal, ce qui peut expliquer, par ailleurs, la disparition des phases P_4 et P_5 aux deux stations les plus éloignées.

La vitesse de 6,0 km/s pourrait se rapporter à un terrain du socle paléozoïque, lequel plongerait vers le sud, en bordure du delta où les couches sédimentaires secondaires et tertiaires seraient plus épaisses, ainsi, sans doute, que les formations alluviales du delta.

Phase S. — L'interprétation des débuts de phases comme arrivées d'ondes transversales est difficile en raison du petit nombre d'enregistrements comportant des composantes transversales. Quatre phases qui paraissent correspondre à des ondes S ont été interprétées, d'après leurs vitesses apparentes, comme S_1 , S_2 , S_3 et S_5 .

Ondes de surface. — Un train d'ondes de surface qui constitue la phase maxima est facilement identifié sur tous les enregistrements et a été interprété comme ondes de Rayleigh. Sa vitesse apparente est de 500 m/s.

II. — CHAMPAGNE 1952.

par Y. BEAUFILS, J. COULOMB, R. GENESLAY, G. JOBERT,
Y. LABROUSTE, E. PETERSCHMITT et J.-P. ROTHÉ.

Pour répondre au vœu émis par la Commission Séismologique Européenne, dans sa réunion de Stuttgart, en septembre 1952, les expériences qui devaient avoir lieu le mois suivant en Champagne ont été particulièrement orientées vers la recherche de réflexions sur des surfaces de discontinuité situées à grande profondeur. De Stuttgart même, M. Rothé avait demandé à la Compagnie Générale de Géophysique d'effectuer, à cet effet, des enregistrements des plus grosses explosions au moyen de séismographes disposés au voisinage des points d'explosion.

Par ailleurs, les stations des Instituts de Physique du Globe de Paris et de Strasbourg devaient jaloner un profil qui s'est étendu sur près de 100 km.

Onze explosions, dont neuf comportaient une charge d'une ou plusieurs tonnes, ont permis d'obtenir cinquante-deux enregistrements. Dans les trois premières, les stations étaient situées à l'Est du point d'explosion, entre 1,6 et 25 km. de ce dernier. Dans les suivantes, le point d'explosion avait été reporté de 15 km. vers l'Est et toutes les stations se sont échelonnées vers l'Ouest entre 1,3 et 70 km. Il a ainsi été possible de contrôler les valeurs des vitesses, par un tir inverse, jusqu'à une distance de 25 km.

Séismographes.

L'appareillage comportait, comme en Camargue, un laboratoire C.G.G., deux stations Askania et trois stations Mintrop.

Mais deux types d'appareils beaucoup plus sensibles ont permis d'équiper les stations les plus éloignées. De ces appareils, les uns, électromagnétiques, avaient été construits par P. Bernard. Ils comprenaient deux séismographes horizontaux, ayant une période propre de 0,7 s. et un vertical ayant une période de 0,4 s. Ces trois appareils étaient réglés à l'amortissement $\alpha = 0,5$ et reliés à des galvanomètres de courte période.

Leur courbe d'amplification en fonction de la période présente un palier entre 0,1 et 0,5 s. pour les séismographes horizontaux, entre 0,1 et 0,3 s. pour le vertical, avec des valeurs maxima de 51.000, 33.000 et 41.000.

Dans les séismographes électroniques construits par A. Godefroy, les pendules avaient une période de 0,4 s. Ces appareils ont très bien enregistré les débuts, jusqu'à 70 km. de l'origine, mais par

contre moins bien les ondes de surface.

Enregistrement du temps.

Les signaux de temps étaient émis par radiotélégraphie sous forme de 24 pulsations par seconde, lesquelles se succédaient à intervalle d'un vingt-cinquième de seconde, avec un intervalle double à chaque seconde.

Le signal d'explosion, d'une durée de quelques millièmes de seconde, était constitué par un train d'impulsions d'une fréquence de 1.500 c/s; il était émis entre deux signaux de la base de temps.

L'enregistrement était assuré au moyen de récepteurs alimentant soit un galvanomètre (stations C.G.G.), soit un tube à argon.

Grâce à ce dispositif, l'instant de l'explosion a pu être déterminé à un millième de seconde près.

Principales phases enregistrées.

Phase P. — Nous avons identifié six arrivées d'ondes longitudinales dont les équations sont les suivantes :

$$t_1 = \frac{\Delta}{1,8}$$

$$t_2 = 0,047 + \frac{\Delta}{2,92}$$

$$t_3 = 0,191 + \frac{\Delta}{3,80}$$

$$t_4 = 0,325 + \frac{\Delta}{4,50}$$

$$t_5 = 0,745 + \frac{\Delta}{5,20}$$

$$t_6 = 0,985 + \frac{\Delta}{6,00}$$

On retrouve, à une profondeur un peu plus grande qu'en Camargue, la vitesse de 6,00 km/s. qui paraît caractériser le socle paléozoïque.

Phase S. — Les phases S_3 , S_4 et S_5 ont été reconnues, en particulier sur la composante transversale des stations de l'Institut de Physique du Globe de Paris. Le rapport entre leurs durées de propagation et celles des ondes P correspondantes est voisin de 1,7.

Ondes de surface. — Des ondes de faible vitesse apparaissent, d'une part, sur certains films C.G.G. et, d'autre part, sur les enregistrements des stations éloignées dont elles constituent souvent la phase principale. L'identité des vitesses de propagation, soit 0,9 km/s, permet de supposer que, dans les deux cas, ce sont des ondes de Rayleigh.

Réflexions à grande profondeur.

Des ondes enregistrées 10 s. après l'explosion sur trois films C.G.G. pourraient être dues à une réflexion à grande profondeur. Cette interprétation conduirait à attribuer à l'écorce une profondeur de l'ordre de 30 km.

RÉFLEXIONS A GRANDE PROFONDEUR DANS LES GROSSES EXPLOSIONS (CHAMPAGNE, OCTOBRE 1952)

par R. GENESLAY, Y. LABROUSTE et J.-P. ROTHÉ

Cette note traite principalement de l'interprétation des enregistrements que la Compagnie Générale de Géophysique a effectués, sur notre demande, au voisinage des points d'explosion, spécialement en vue de rechercher l'existence d'ondes réfléchies à grande profondeur.

RÉSULTATS DES OBSERVATIONS.

Les principaux trains d'ondes réfléchies qui ont été relevés sur les films et dont la liste est donnée ci-contre (Tableau I) se répartissent en trois groupes.

a) Les premiers, observés dans le début de l'inscription (entre 0,6 et 1,4 s.), correspondent à des réflexions sur des surfaces de discontinuité situées à l'intérieur ou à la limite des formations sédimentaires.

b) Ceux du deuxième groupe peuvent être considérés comme des réflexions multiples dans les couches sédimentaires.

c) Enfin, les derniers pourraient être interprétés comme réflexions profondes; en particulier le train principal, observé 10 secondes après l'explosion, pourrait correspondre à la réflexion à la base de l'écorce.

ESSAI D'INTERPRÉTATION.

I. Le schéma suivant a été adopté pour représenter les couches sédimentaires compte tenu du profil de réfraction séismique et des données géologiques :

Couche	Epaisseur m.	Etage	Vitesse km/s
1	54	Sénonien supérieur	1,80
2	315	Sénonien inférieur	2,92
		Turonien	
		Cénomanien	
3	376	Albien	3,80
		Crétacé inférieur	
4	1690	Portlandien	4,50
		Jurassique supérieur	
		et moyen; Lias	
5	462	Trias et Permien	5,20
6		Socle paléozoïque	6,00

On en déduit les durées de propagation suivantes des ondes réfléchies, une, deux ou trois fois près de l'origine (Fig. 1) :

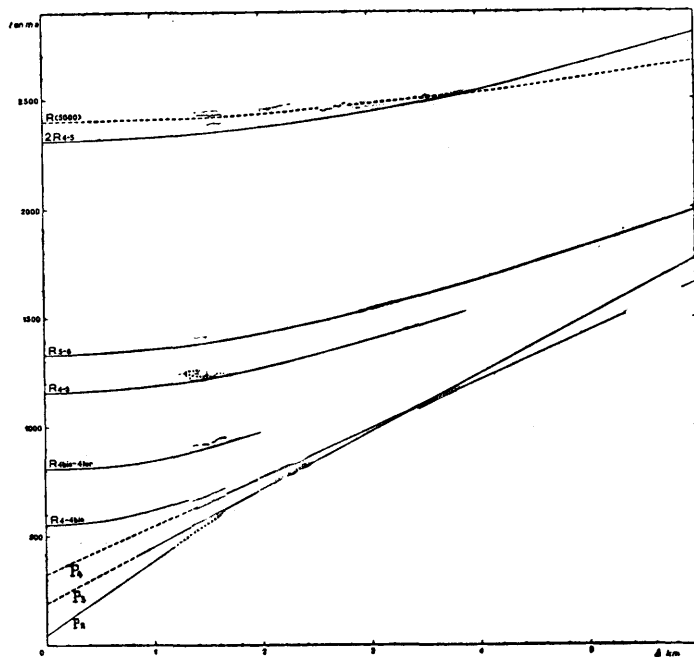


FIG. 1.

Nota : Cette figure a été établie en utilisant une hypothèse légèrement différente de celle qui a servi au calcul du tableau ci-dessous.

Surface de discontinuité	R s.	2R s.	3R s.
1-2	0,060	0,120	0,180
2-3	0,276	0,552	0,828
3-4	0,474	0,948	1,422
4-5	1,224	2,448	3,672
5-6	1,402	2,804	4,206

Remarquons que les valeurs numériques ci-dessus des vitesses et des épaisseurs sont celles que fournissent les équations de propagation des ondes P réfractées. Elles ne tiennent pas compte des alternances de fortes et de faibles vitesses fréquentes, en particulier, dans le Jurassique. Les vitesses moyennes dans les couches 4 et 5 sont donc certainement inférieures aux vitesses données.

II. Le tracé des graphiques $t^2 = f(\Delta^2)$ a permis de classer les réflexions et d'obtenir, dans certains cas, une estimation de la vitesse moyenne et de la profondeur de la surface de discontinuité. Ces données sont résumées dans le Tableau II.

TABLEAU I

Réflexion n°	Film	Δ en m.	t en s.
1	10	1340 - 1665	0,662 - 0,721
2	10	1340 - 1665	0,935 - 0,955
3	3	1235 - 1910	1,242 - 1,260
4	3	1170 - 1460	1,412 - 1,416
5	8	2525 - 2705	2,447 - 2,466
6	10	1430 - 1650	2,428 - 2,431
	9	1990 - 2290	2,471 - 2,478
7	10	1340 - 1620	3,419 - 3,422
8	9	1960 - 2290	3,684 - 3,691
9	10	1445 - 1665	3,912 - 4,000
10	10	1415 - 1620	4,209 - 4,221
	8	2435 - 2505	4,220 - 4,223
11	10	1360 - 1635	5,915 - 5,915
12	9	1960 - 2292	10,080 - 10,080
13	8	2305 - 2745	10,179 - 10,190

TABLEAU II

Réflexion n°	Phase	V _m	Profondeur	Profondeur d'après V _m ou t réfraction
1	R _{4 - 4bis}	3,25	830	850
2	R _{4bis - 4ter}	~ 3,5	~ 1300	~ 1300
3	R _{4 - 5}	3,5 - 4		~ 2200
4	R _{5 - 6}			~ 2700
5	2R _{4 - 5}			~ 2200
6		4,5	~ 5400	
13		~ 3,5		

CONCLUSIONS.

La discussion des différents résultats obtenus conduit aux conclusions suivantes :

1) Les réflexions 1, 2 et 3 paraissent bien se produire, les deux premières à l'intérieur de la couche 4, respectivement à la limite supérieure du Jurassique et dans le Jurassique moyen, la troisième sur la surface de discontinuité 4-5.

Les données relatives à la réflexion 4 sont insuffisantes pour qu'on puisse en déduire une estimation de la vitesse moyenne, mais la durée de propagation permet de penser qu'elle a lieu à la limite du socle paléozoïque.

2) D'après les vitesses moyennes, on est conduit à interpréter les réflexions 5 et 13 comme réflexions multiples à l'intérieur des formations sédimentaires, la réflexion 5 étant la réflexion double sur la surface 4-5.

3) Toutes les autres réflexions (6 à 12) indiquent de grandes valeurs de la vitesse moyenne et paraissent donc constituer des réflexions profondes.

La première d'entre elle permet seule de donner un ordre de grandeur de la vitesse moyenne (4,5 km/s) et de la profondeur (environ 5.000 km.).

Les suivantes (7-10) auraient lieu à des profondeurs que l'on peut estimer de 8 à 11 km si l'on suppose que la vitesse dans la couche 5 reste constante et égale à 6,00 km/s. On pourrait penser que l'une d'entre elles correspond à la limite du basalte, mais ces résultats demanderaient évidemment à être confirmés.

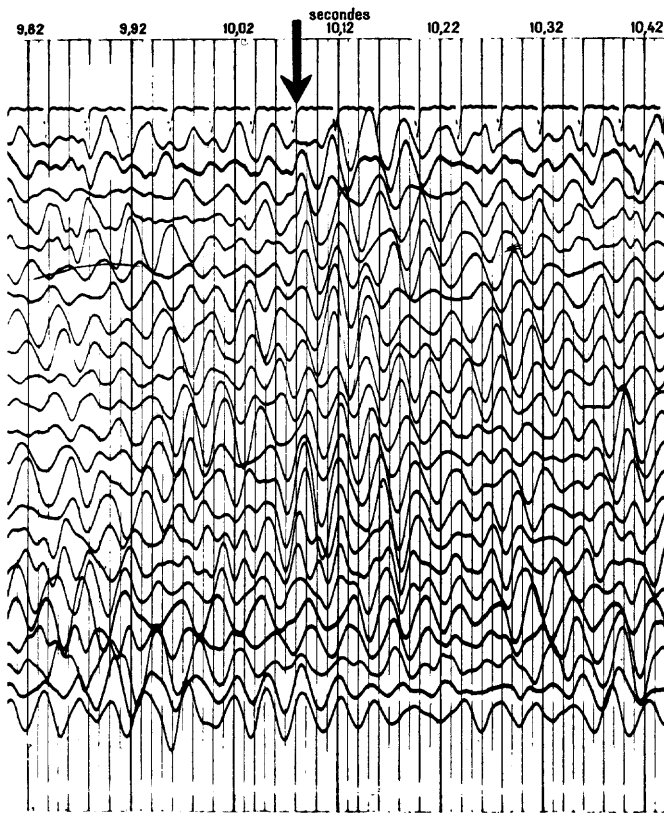


FIG. 2.

4) Enfin, en considérant également comme profonde la réflexion 12 (Fig. 2) et en admettant une vitesse moyenne de l'ordre de 7 km/s dans la partie inférieure de l'écorce, on en déduit pour l'épaisseur de cette dernière, une valeur de 30 km environ.

**RÉFRACTION MULTIPLES
DANS LES ENREGISTREMENTS SÉISMOGRAPHIQUES
DES EXPLOSIONS DE CHAMPAGNE**

Octobre 1952.

par Y. LABROUSTE et Y. BEAUFILS.

Les enregistrements obtenus par la Compagnie Générale de Géophysique (C.G.G.), à des distances des points d'explosion comprises entre 1340 et 5540 mètres, montrent de nombreux trains remarquables d'ondes réfractées. L'étude détaillée de ces ondes a permis de les classer, selon leur vitesse, en ondes P_4 , P_3 , P_2 et P_1 d'une part, S_4 , S_3 , S_2 et S_1 d'autre part. Beaucoup d'entre elles ont pu être reconnues sur les enregistrements séismographiques des stations situées à des distances de l'origine variant de 8 à 40 km.

Rappelons les équations de propagation des ondes directes et réfractées (Δ : distance en km; P : temps en secondes) :

$$P_1 = \frac{\Delta}{1,80}$$

$$P_2 = 0,047 + \frac{\Delta}{2,92}$$

$$P_3 = 0,191 + \frac{\Delta}{3,80}$$

$$P_4 = 0,325 + \frac{\Delta}{4,50}$$

$$P_5 = 0,745 + \frac{\Delta}{5,20}$$

$$P_6 = 0,985 + \frac{\Delta}{6,00}$$

La valeur 1,80 km/s indiquée dans la première équation est une vitesse moyenne dans une couche superficielle d'une soixantaine de mètres d'épaisseur; elle a été calculée à partir de déterminations faites à petite distance (de 60 à 1100 m.).

Les phases P_2 , P_3 et P_4 constituent le début de l'enregistrement, la première entre 1340 et 1820 m.; la deuxième de 1820 à 3340 m. et la troisième de 3340 à 3730 m.; les deux dernières n'ont pas été inscrites par le dispositif C.G.G. situé entre 5300 et 5550 m. de la source. A ces distances, les premières arrivées d'ondes, très faibles, pourraient correspondre à une phase P_5 qui serait également inscrite aux stations Askania installées entre 8100 et 10.840 m. de

l'origine. Enfin, la phase P_6 constitue le début de l'enregistrement aux distances comprises entre 13 et 40 km.

Les valeurs des vitesses vraies ont pu être déterminées directement grâce à un tir inverse entre 60 et 2000 m. ainsi qu'entre 11 et 25 km.; l'hypothèse de couches horizontales est donc justifiée entre ces limites.

Les profondeurs des surfaces de discontinuité, comptées en mètres à partir du niveau +130, les épaisseurs des couches et les distances minima de réception des ondes réfractées ont les valeurs respectives suivantes :

Couche	1	2	3	4	5	6
Surface	1-2	2-3	3-4	4-5	5-6	
Profondeur	54	369	745	2435	2897	
Épaisseur	54	315	376	1690	462	
Vitesse	1,80	2,92	3,80	4,50	(5,20)	6,00
Δ Minima	60	814	1778	7100		6440

Ces résultats ont d'ailleurs été confirmés par ceux de « forages » profonds, lesquels ont, en outre, montré l'existence de couches intercalaires à faible vitesse. La présence de ces dernières explique la disparition de la phase P_4 entre 5 et 10 km.

RÉFRACTION MULTIPLES.

Les équations de propagation $t = f(\Delta)$ des réfractions multiples se déduisent de celles des ondes directes par un changement du temps-origine (t pour $\Delta = 0$). Nous en donnerons seulement quelques exemples.

Phases PP_4 , SS_4 et SP_4 .

Nous désignons par PP_4 , SS_4 et SP_4 les phases bien reconnaissables sur les films C.G.G. et sur les autres enregistrements qui ont pour équations de propagation :

$$PP_4 = 2 \times 0,325 + \frac{\Delta}{4,50}$$

$$SS_4 = 2 \times 0,560 + \frac{\Delta}{2,64}$$

$$SP_4 = 0,790 + \frac{\Delta}{4,50}$$

Phases PP_3 , PPP_3, SS_3 , SSS_3, S_2P_3 .

Une série particulièrement remarquable (fig. 1) d'ondes réfractées est constituée par des ondes P_3 et S_3 et ($S_2P_3S_2$) qui satisfont aux équations :

$$PP_3 = 2 \times 0,191 + \frac{\Delta}{3,80}$$

$$P_3^3 = 3 \times 0,191 + \frac{\Delta}{3,80}$$

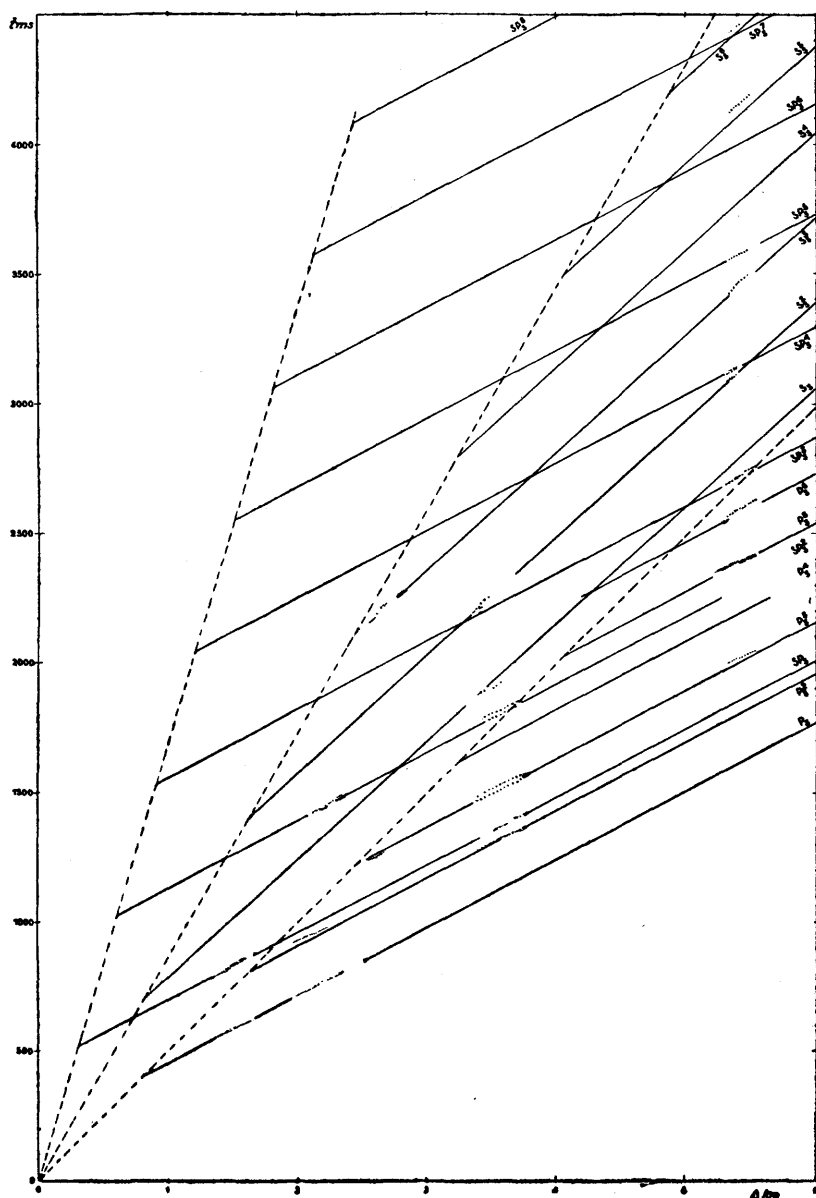


FIG. 1.

$$P_3^4 = 4 \times 0,191 + \frac{\Delta}{3,80}$$

$$P_3^9 = 9 \times 0,191 + \frac{\Delta}{3,80}$$

$$SS_3 = 2 \times 0,330 + \frac{\Delta}{2,20}$$

$$S_3^{10} = 10 \times 0,330 + \frac{\Delta}{2,20}$$

$$(S_2 P_3)^1 = 0,430 + \frac{\Delta}{3,80}$$

$$(S_2 P_3)^2 = 2 \times 0,430 + \frac{\Delta}{3,80}$$

$$(S_2 P_3)^5 = 5 \times 0,430 + \frac{\Delta}{3,80}$$

La phase PP_3 a pu être reconnue à partir de 1960 m., les suivantes (P_3^3 et P_3^4) à partir de 2500 m., S_3^3 à partir de 3390 m., P_3^5 et P_3^6 à partir de 2300 m., P_3^7 , P_3^8 et P_3^9 , à partir de 5345 m., ainsi que les ondes S_3^5 et S_3^9 , enfin P_3^{10} à partir de 8260 m. La phase $S_2 P_3$ a été observée à partir de 1300 m., $(S_2 P_3)^2$ à partir de 2000 m., $(S_2 P_3)^3$, $(S_2 P_3)^4$ et $(S_2 P_3)^5$ à partir de 5000 m. Ces limites sont conformes aux distances minimales de réception trouvées par le calcul.

Ces trois séries de réflexions multiples, qui présentent dans certains cas de grandes amplitudes, expliquent l'aspect extrêmement complexe des enregistrements en même temps que les périodicités qui y apparaissent de manière évidente.

**ÉTUDE DES ONDES SUPERFICIELLES
DANS LES ENREGISTREMENTS SÉISMOGRAPHIQUES
DES EXPLOSIONS DE CHAMPAGNE**

Octobre 1952.

par Y. BEAUFILS.

Données. — Les données utilisées dans cette étude comprennent :

1° Les enregistrements obtenus par la Compagnie Générale de Géophysique à des distances des points d'explosion qui ont varié de 1340 à 5540 mètres. Les vingt-quatre séismographes verticaux de la voiture-laboratoire étaient disposés suivant la ligne de tir, l'intervalle constant entre deux instruments successifs étant, selon les cas, de 32, 30, 20 ou 15 mètres.

2° Les stations, au nombre de seize, de l'Institut de Physique du Globe de Paris et de celui de Strasbourg se sont échelonnées entre 8 et 70 km de la source. Les enregistrements obtenus, entre 8 et 20 km, au moyen des appareils Askania, comportaient deux composantes, la verticale et la longitudinale.

Les documents obtenus avec les séismographes Mintrop se sont montrés les plus intéressants, à la fois parce qu'ils donnaient les trois composantes du mouvement et parce que les ondes de surface y étaient particulièrement bien enregistrées, les périodes de ces ondes se plaçant dans la bande de grande amplification des appareils. Les ondes de surface y sont aisément reconnaissables par leur grande période et leur grande amplitude.

Polarisation des ondes.

La comparaison des trois composantes enregistrées fait immédiatement apparaître quatre phases distinctes :

1° On observe d'abord des ondes L très régulières et de période sensiblement constante (environ 0,3 s. à 24 km) qui sont *polarisées dans le plan de propagation*. Les deux composantes du mouvement ont des amplitudes de même ordre au début de cette phase tandis qu'ensuite la composante verticale devient prépondérante.

2° Un peu avant la fin de la phase précédente apparaissent, *sur la seule composante transversale*, des ondes de Love (Q) bien caractérisées par leur période apparente qui est grande au début du train, puis rapidement décroissante.

3° On observe ensuite un train M, très bref, de grande amplitude *sur les trois composantes*.

4° Ce dernier est suivi immédiatement d'ondes (R) de grande période (0,5 à 0,9 s.) qui sont *polarisées dans le plan de propagation*.

tion et dont l'amplitude décroît progressivement jusqu'à la fin de l'enregistrement.

Si l'on construit les diagrammes représentatifs des trajectoires de particules (fig. 1) en portant, en abscisses, les déplacements

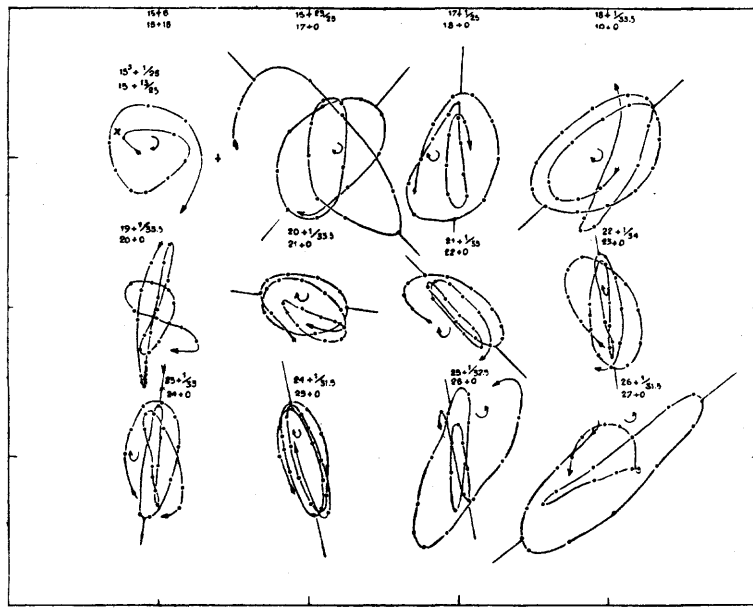


FIG. 1.

horizontaux comptés positivement dans le sens de propagation (c'est-à-dire de gauche à droite sur le graphique) et, en ordonnées, les déplacements verticaux, positifs vers le haut, on constate que ces trajectoires, de forme elliptique plus ou moins régulière, sont décrites dans le sens des aiguilles d'une montre dans la première partie des ondes de surface, tandis que, dans la deuxième partie, le mouvement des particules a généralement lieu dans le sens inverse, lequel caractérise les ondes de Rayleigh. On observe cependant, dans cette dernière partie, certains retournements qui indiquent une superposition des deux phases.

Durée de propagation.

1° Les débuts de la phase L s'alignent sur la droite :

$$t = \frac{\Delta}{1,68}$$

(t : durée de propagation en secondes

Δ : distance en km).

2° Les têtes de trains des ondes de Love observées entre 24 et 40 km sont sensiblement sur la droite :

$$t = \frac{\Delta}{1,06} .$$

3° Le début des ondes de Rayleigh étant défini par le changement du sens de rotation sur la trajectoire elliptique, les observations faites entre 8 et 40 km satisfont, en première approximation, à la droite :

$$t = \frac{\Delta}{0,96} .$$

4° L'arrivée du train maximum M se confond, vers 20 km, avec le début des ondes de Rayleigh, tandis qu'aux plus grandes distances on constate un retard par rapport à ce dernier.

Entre 22 et 52 km, les points d'observation s'alignent sur la droite :

$$t - 24,74 = \frac{\Delta - 24,40}{0,80}$$

Vitesses apparentes.

Les courbes de dispersion apparente obtenues en portant les quantités $\frac{\Delta}{t}$ en fonction de la période apparente T (fig. 2), comportent, dans la plupart des cas, trois branches :

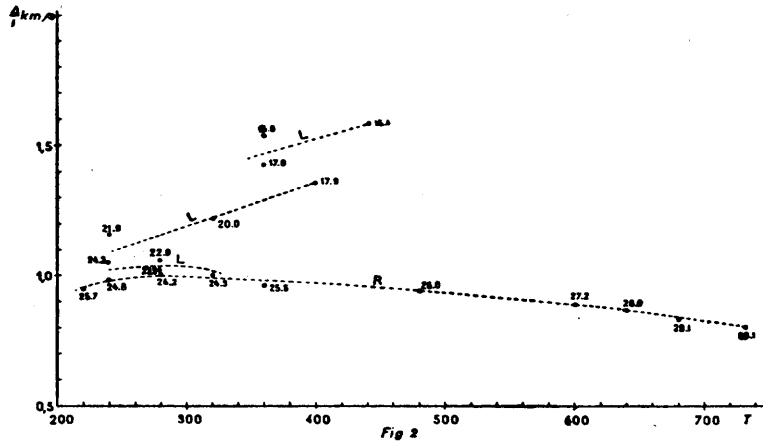


FIG. 2.

1° La première branche, relative à la phase L, représente une dispersion normale, la vitesse diminuant de 1,7 à 1,1 km/s en

même temps que la période apparente décroît de 0,40 à 0,30, à 25 km de la source.

2° La seconde branche, qui se rapporte aux ondes de Rayleigh, présente, à la même distance, un maximum voisin de 1 km/s pour la période 0,3 s., de sorte que la dispersion serait normale pour les courtes périodes (de 0,2 à 0,3 s.) et anomale pour les grandes périodes, la vitesse décroissant de 1,0 à 0,7 km/s, tandis que la période croît de 0,3 à 0,9 s.

3° On a pu mettre en évidence des ondes L de période comprise entre 0,2 et 0,4 s. qui se superposent aux ondes de Rayleigh; on constate que les courbes de dispersion des deux sortes d'ondes sont sensiblement confondues.

On pourrait essayer d'expliquer une dispersion anomale des ondes de Rayleigh par l'influence d'une couche sous-jacente à faible vitesse. Mais il apparaît plutôt que cette anomalie n'est qu'apparente car on ne la retrouve pas lorsqu'on détermine la vitesse de groupe.

Vitesse de groupe.

On constate en effet que les temps d'arrivée d'ondes de même période apparente s'alignent sensiblement sur une même droite et que les droites ainsi obtenues pour les différentes périodes sont sensiblement parallèles entre elles. L'imprécision des déterminations n'a pas permis de mettre en évidence une dispersion.

Vitesse de phase.

Deux enregistrements obtenus à des distances respectives de 25,345 et 24,405 km de la source et présentant entre eux une similitude presque parfaite ont permis de nombreuses déterminations de T et de $\frac{d\Delta}{dt}$. On peut résumer ainsi les résultats obtenus :

1° Les courbes $T = f(t)$ relatives aux deux stations sont superposées.

2° Les courbes $\frac{d\Delta}{dt} = \varphi(t)$ présentent les mêmes fluctuations que les précédentes; ces fluctuations sont particulièrement grandes dans la phase L.

3° Le graphique représentant $\frac{d\Delta}{dt}$ en fonction de T montre, dans la phase L, un étalement assez grand des points d'observation, sans qu'il soit possible de mettre en évidence l'existence d'une dispersion.

4° Le même graphique relatif aux ondes de Rayleigh montre que la vitesse de ces ondes croît avec la période.

On devrait donc conclure que les ondes de surface se sont formées à une certaine distance de l'origine et, par conséquent, avec quelque retard; mais de nouvelles expériences sont en préparation, en vue de préciser les résultats déjà obtenus.

TRIGGER CAUSES IN EARTH MOVEMENTS

by S. K. GUHA, Gurdas RAM and G. V. RAO.
(Central Water & Power Research Station, Poona, India.)

1. INTRODUCTION.

The region delineated by the Himalayan mountain systems and their extensions is well known for seismic activity. Historical evidences and instrumental investigations ranging over a period of half a century reveal that the tectonic movements in this region are acute in the entire Alpide belt (and those certainly fall below similar movements in circum-Pacific belt associated mostly with arcuate structures in the earth's crust). The Himalayas are along with mountain arcs of Burma and Baluchistan, with their convex side-faces towards the stable mass of Peninsular India. This structural juxtaposition of different geological units along with more or less younger thrusts along the Himalayan system are mainly responsible for the world-shaking earthquakes which occur along the sub-Himalayan belt known as the Himalayan boundary fault zones. It is thus seen that the region is sufficiently unstable from tectonic point of view as shown by tremendous concentrations and subsequent release of geological strains during earthquakes in earth's crust. Though instability associated with these large shocks was well known for this particular region no special study was so far taken in respect of this region regarding the nature and characteristics of geological strain associated with shocks of low and of even the very low magnitudes. The main hindrance, so far, in this direction was the absence of any seismological observatory equipped with high magnification seismographs of lower period, suitable for studies of near shocks of this type.

Recently, with the installation of a Vertical Benioff seismograph (T_0 = period of instrument = 0.8 sec., T_s = period of galvanometer = 0.45 sec. at critical damping, Time scale, 1 sec. = 1 mm.) at the Chatra Observatory (Lat. $26^{\circ} 50'$ N and long $87^{\circ} 10'$ E; height above M.S.L. = 527 ft.), it has been possible to study the nature and characteristics of the geological instability associated with smaller shocks which are in existence in this region. As expected, the records of the Benioff seismograph revealed the occurrence of a very large number of small shocks of local origin. The very minute nature of these shocks is seen from the fact that even moderately sensitive Wood-Anderson seismograph (T_0 = period of instrument = 1 sec., V_s = static magnifica-

tion = 1000, E = damping ratio = 70 : 1, Time scale, 1 sec. = 1 mm.) does fail to record most of them. These local shocks have been found to originate at distances even of the order of 500 km. from the Observatory. The nature of similar tectonic forces associated with small shocks has been studied by Conrad (1), Mead and Carder (2) in the United States of America. Though, the origin of larger shocks is attributed to the critical stress concentrations in the crust of the earth, the same for these smaller shocks has not been isolated clearly at present. However, the continued release of energy associated with after-shocks resulting from any major shocks has been most probably due to plastic adjustment following a prolonged stress deformation needed to produce a sudden fracture. This undulating readjustment in the stress field in any rock system due to alternate plastic and elastic deformations may be understood in case of after-shocks following a sufficiently big shock, but a similar hypothesis for these very large number of small shocks, common in this region, is not ordinarily feasible.

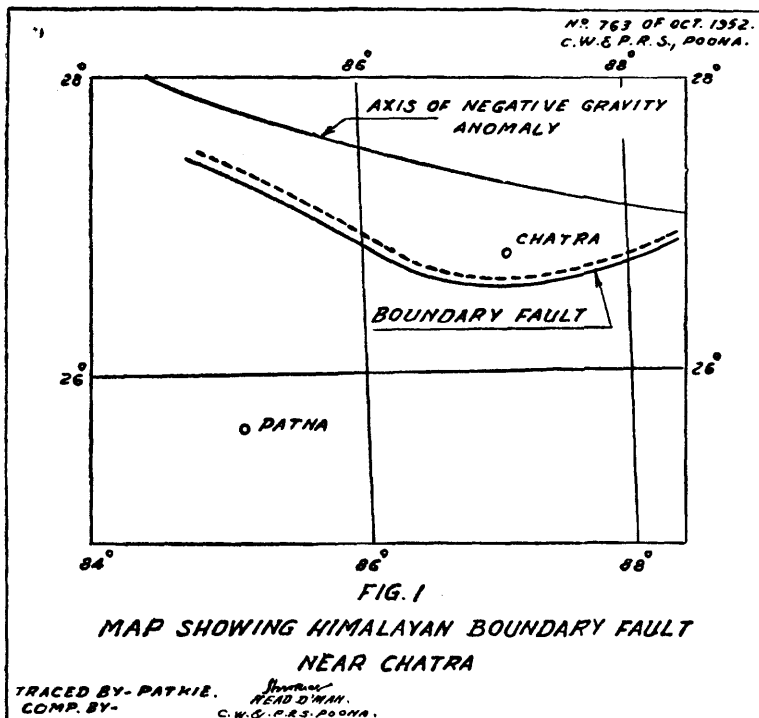
To understand the nature and characteristics of this large number of small shocks occurring in the Himalayan region a systematic analysis of these shocks (1951 to 1953) has been undertaken.

2. OBSERVATIONS.

Figure 1 shows the location of Chatra seismological Observatory, with respect to the axis of negative gravity anomaly and the Himalayan boundary fault. Due to absence of any other observatory in the region under study, the present investigation suffers from the fact that it has not been possible to trace the epicentres of the local shocks. Thus, this investigation will be restricted to frequency of occurrence and the respective epicentral distances of the earthquakes from the observatory irrespective of the direction of their occurrence.

The records of the Benioff seismograph were analysed, as usual, for assessment of epicentral distances of these local shocks. Further, it is seen that excepting the one on 28th May 1951 there was no shock of sufficient magnitude in this period (1951-53) in this region. The one shock of this type occurring in May, 1951 was followed by a swarm of after-shocks continuing for a period of three days.

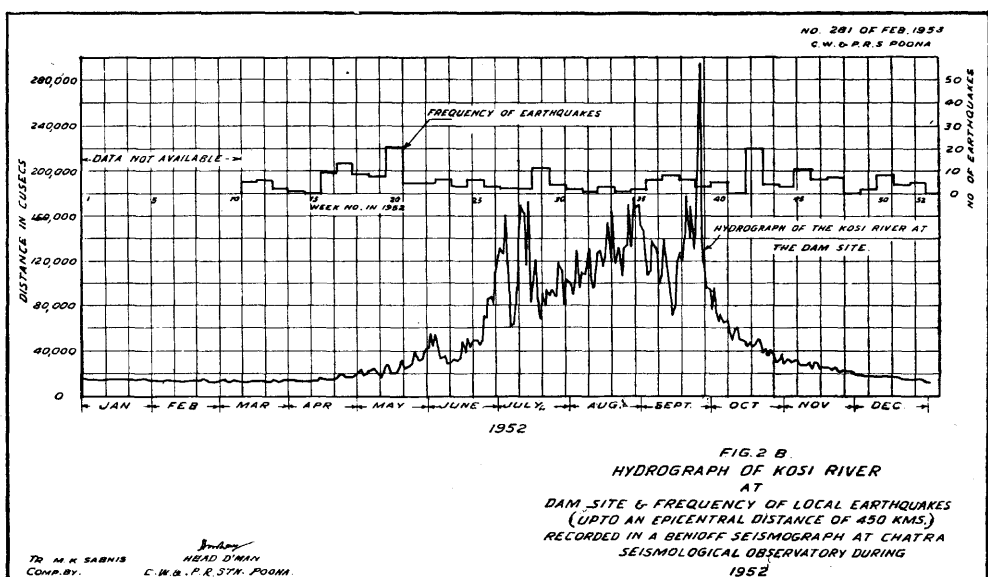
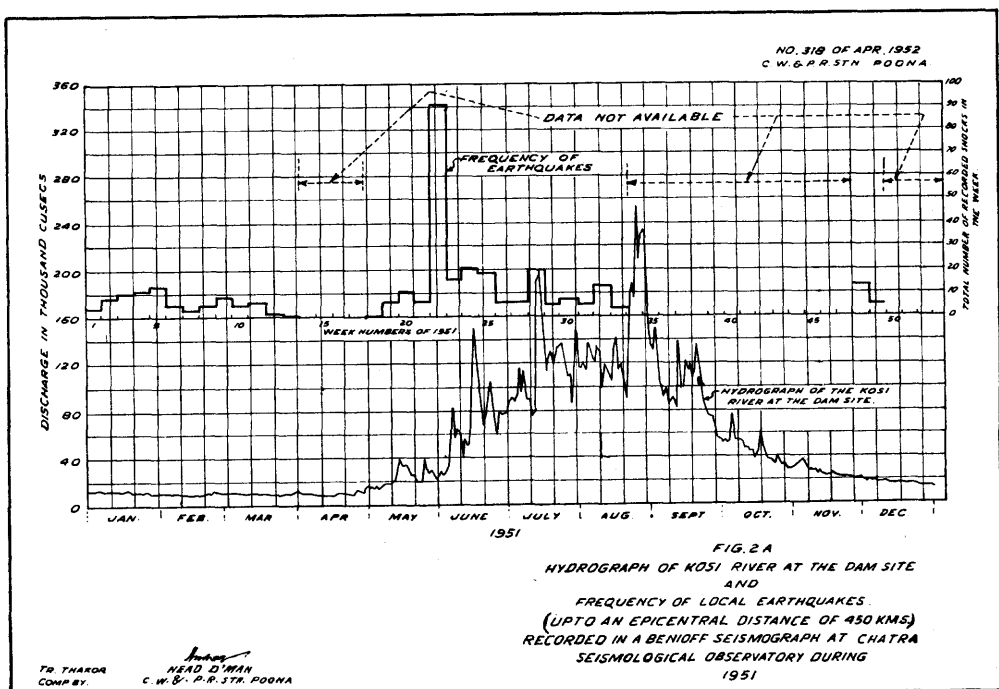
In order to show any possible correlation of difference of frequency of occurrence of these small shocks in different parts

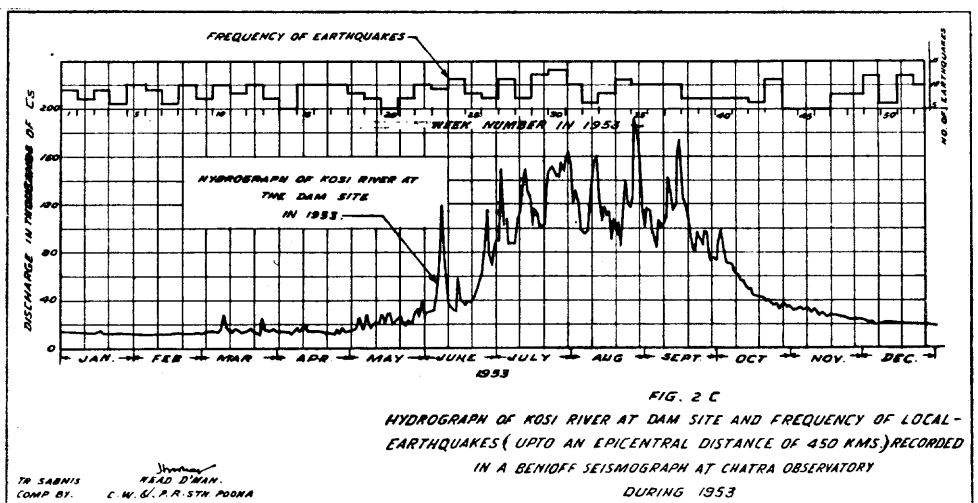


of the year, surface loading due to flood resulting from rainfall and snow melting on the Himalayan peaks was assumed to be directly correlated with flood discharge of the Kosi river, whose catchment extension includes sufficient area around the observatory. Thus the hydrographic data through the Kosi river were utilised for this purpose. Though there may be other causes behind these small shocks it was not possible to include them in this study.

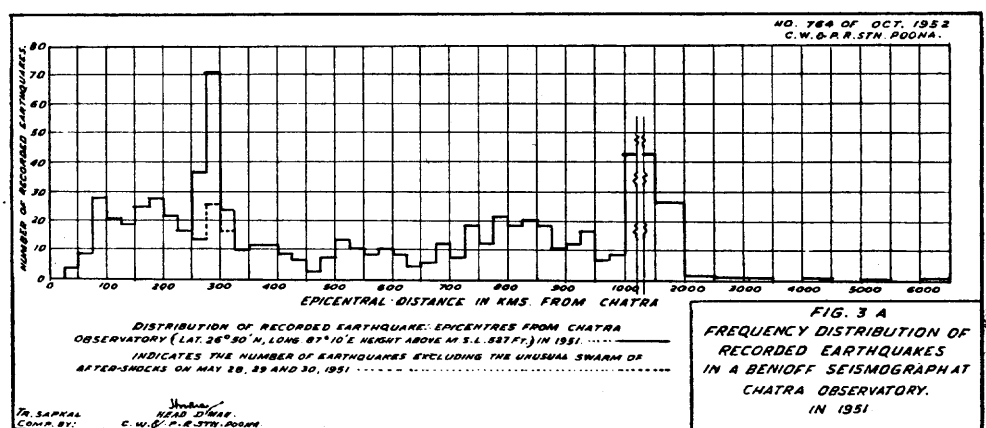
3. RESULTS.

All of the figures 2 A, 2 B and 2 C depict the annual hydrograph of the Kosi river near the observatory and the frequency of occurrence of the small local shocks within an epicentral distance of 450 km. taking weekly interval. The data for 1951 are, however, not complete for the post-floods period as the Benioff seismograph was out of order. It is felt that due to instrumental sensitivity





and to the nature of frequency distribution in figures 3 A, 3 B and 3 C, shocks occurring within an epicentral distance of 450 km. only conform to our classification of small local shocks intended to be investigated here.



A close visual scrutiny of the frequency of occurrence of these shocks from these figures reveals that there is an appreciable increase in this frequency just at the commencement and conclusion of flood period for every year. Statistical analysis also confirms the existence of significant enhancement of frequency of these shocks as mentioned above. Thus, it seems that change in loading due to the flood water can possibly help in increasing the frequency

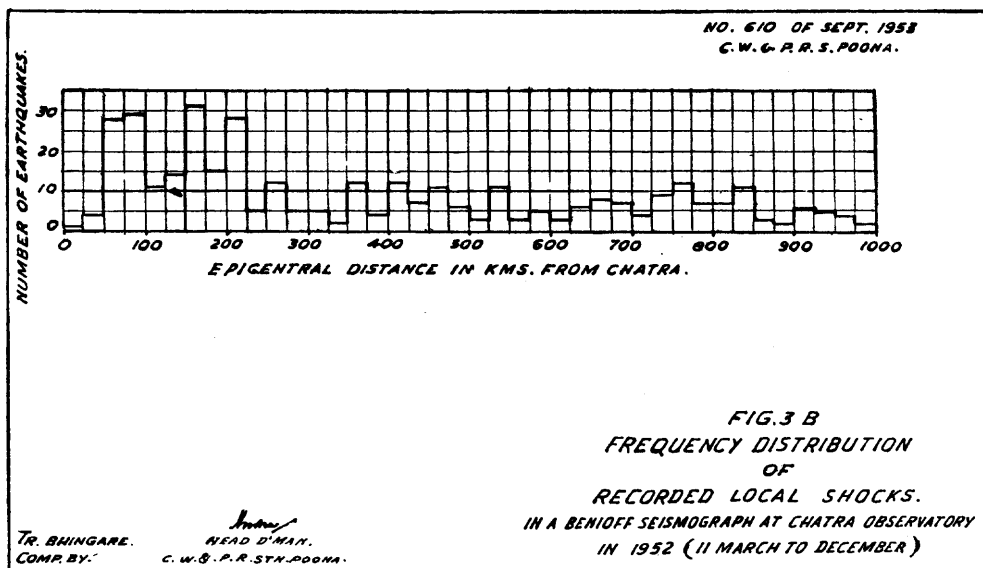
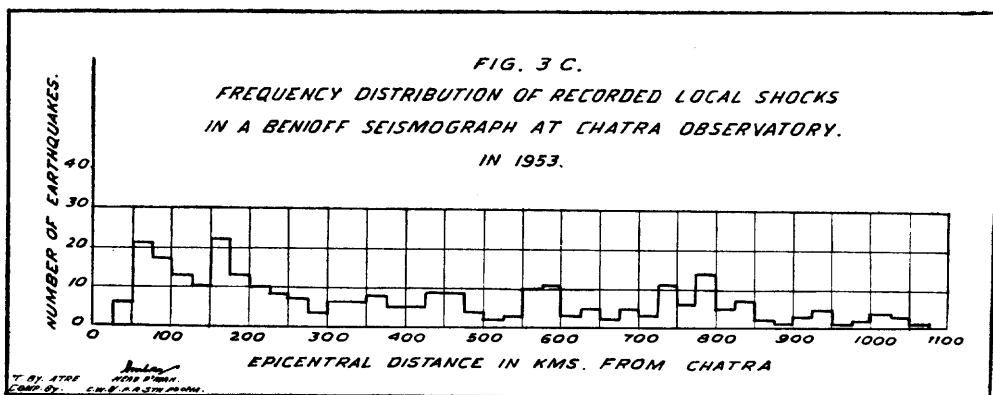


FIG. 3 B
FREQUENCY DISTRIBUTION
OF
RECORDED LOCAL SHOCKS.
IN A BENIOFF SEISMOGRAPH AT CHATRA OBSERVATORY
IN 1952 (11 MARCH TO DECEMBER)



of shocks, or in other words change in loading can « trigger-off » strain energy from geological formations in the form of these earth movements. Though, one of the immediate reasons of these triggering actions may be the rate of change of loading, yet other processes for similar trigger causes should not be ruled out. It is further seen that except during the period of change of loading due to flood intensity, there seems to be no significant variation in the frequency of occurrence of these small shocks. It is to be seen whether such a phenomenon indicates also one of the possible characteristics of underneath unstable formation. High frequency of occurrence of these small shocks further indicates

constant reorientation and adjustments in the stress patterns in the crust of the earth. Though a conspicuous increase in frequency is observed during rising and falling floods, yet a close scrutiny will also reveal similar increases, of course less prominent, associated with sharp and well defined peaks in the hydrographs. It can thus be concluded on reasonable facts that, in respect of occurrence of these small shocks, this region is, to a certain extent, susceptible to « trigger causes » due to change of flood intensity, though results in figure 2 C (1953), do not show the changes so conspicuously.

Figures 3 A, 3 B and 3 C show the frequency of occurrence of these shocks in respect of their epicentral distances from this Chatra Seismological Observatory. It is observed from these figures that the general trend of the overall frequency distribution in the three cases are more or less similar with a striking fact that the frequency of occurrence rises sharply to the maximum value after about 50 km. in each case. This striking behaviour may well point out to a region or regions situated beyond about 50 km. where the probability of occurrence of shock is more than the other parts. Or, in other words, prominent zone or zones of instability are situated beyond 50 km. from the Observatory. From figure 1, it is seen that the nearest distance of Himalayan boundary fault from the Chatra Observatory is of the order of 30 km. — a distance which is of similar magnitude as has been assessed from the striking behaviour of the frequency distribution curves in figures 3 A, 3 B and 3 C. It, thus, seems that the loci of the epicentres of the small shocks may well delineate more or less along the boundary fault region, though it would have been proper in this respect to locate the hypo-centres with the help of other nearby observatories. Due to the absence of any other observatory, this important point could not be checked properly. However, geological investigations carried out by Dr. Nickell (3) also confirm that thrusts and fault zones around the observatory have remained inactive during the last few centuries and zones of activity are probably further south under the alluvial region or south of the boundary fault zone. Though detailed seismological investigations are not yet available to confirm the ideas of Dr. Nickell, yet the critical distance of the order of 50 km. obtained from the figures 3 A, 3 B and 3 C conforms to the idea of Dr. Nickell that the zones of instability must be further south down the boundary fault region. There may be a further probability that the hypo-centres are situated along the region of boundary fault and in this

particular case, it is to be seen how surges of elastic energy emanate from the boundary fault zone and the mechanism behind this generation.

Broad peaks showing enhancements in frequencies of occurrence of earthquakes are found in figures 3 A, 3 B and 3 C within an epicentral distance of 700-900 km. from the observatory — a distance equal to that of the epicentre of the big Assam earthquake in 1950. This most probably suggests that this build up in frequency between 700 km. to 900 km. is due to after-shocks of this big earthquake. It may be noted here that this peak has become gradually insignificant in 1953 — a fact which is reasonable and expected. As these shocks do not strictly conform to the class of isolated local shocks, they are not of immediate interest in this investigation.

In figure 2 A, enhancement of frequency of shocks in the 22nd week (May 1951) includes the after-shocks of May 28, 1951 earthquake in this region and also some isolated small shocks which are not considered to be connected to any other major shock. If the number of after-shocks arising out of the above shock is excluded, as intended in this investigation, general trend of enhancement of frequency due to small shocks alone in May 1951 is even maintained. However, one important point regarding the maintenance of release of energy through after-shocks needs consideration when they occur during rising or falling part of the hydrograph because it is considered feasible that the high rate of change of load due to flood intensity in May 1951 may help, as a sort of catalytic agent, in the triggering process of after-shocks from the main earthquake. Of course it is realised that the main stress patterns involved in the geological formations are different in the two circumstances — (a) in case of isolated small shocks unrelated, in any way, to any big earthquake and (b) in case of after-shocks following a big earthquake. In the latter case, the stress-patterns have reached the critical breaking value of formation or if they occur along a fault zone, the same have attained the critical slipping value; on the other hand in the former case, the general value of the stress-field is probably low enough. In the case (b), further, some sort of oscillatory plastic and elastic deformations will exist during the period of after-shocks, as mentioned earlier. It is thus clear from the above description of the two kinds of stress-patterns that the resultant effect of the rate of change of load will not be same in the two cases. In the absence of further experimental data to distinguish the behaviour of rock system under the two

conditions, as mentioned above, it is felt not to pursue the matter further.

4. CONCLUSION.

Though a Benioff seismograph similar to the one installed at the Chatra Observatory was commissioned at Poona, situated on the stable Deccan Peninsula, the same did not record these large number of swarms of small shocks as the one at Chatra Observatory, near the Himalayas, has done. From this contrary behaviour of the instruments it can be concluded that the swarms of earthquakes recorded at Chatra are representative of the regional characteristics and in fact it reveals the constant changes taking place in the stress-field in the geological strata in that region. Similar swarms of shocks were also investigated and observed near Boulder Dam region in U.S.A., and it was shown there, with a close net of seismological stations, that most of them originated along some known fault zones. Similarly in this investigation a close correlation of the origin of swarm of shocks has been postulated with the Himalayan boundary fault — a fact which is in conformity with the known geological results. Another important characteristic which needs to be mentioned is the appearance of shocks in clusters. A true triggering phenomenon or process should conform to this type of clustering in which, events favourable for these shocks may release or multiply the number of shocks appearing in different successive swarms. Recent studies in United States (4) have confirmed that a better correlation is obtained between the slope of the hydrograph and the amount of the energy released in these swarms than between the hydrograph and the frequency of the shocks. But it was not possible up to this time to analyse the large number of shocks in such great detail to test these recent ideas found in the States. In this respect, it may be mentioned that magnitudes of most of these shocks are below 2.5 and the probable depth of occurrence for most of the swarms may be within 14 km. These estimates regarding the depth and magnitude of these shocks are very approximate. In Japan, at times, these local shocks are found to originate within a few kilometres from the surface of the earth. It is not known, however, how the depth of hypo-centres of these shocks are related to the vertical extension of the fault plane or in other words, whether it can be assumed that these shocks are limited within the vertical and horizontal extent of the fault plane and their origin is attributable to readjustments of geological blocks comprising the fault zone. This readjustment may result from the overall instability asso-

ciated with the region, namely, the instability due to proximity of the younger mountain system associated with a tremendous compression from the north as exists in this particular region. It is however realised that the nature of readjustments associated with compressional faults will be different from that associated with tensile faults as exist in the Boulder Dam region in Arizona. If the origin of these shocks associated with swarms is attributable to changes within fault zones due mainly to slipping, other modes of origin, such as, release of strain energy through simple fracture in geological strata is eliminated. The seismological and geophysical data available here are not sufficient to conclude in favour of one or other process of origin of these shocks associated with swarms.

It is seen from figures 2 A, 2 B and 2 C that apart from the increase and decrease of frequency in some periods, there is always a residual frequency of occurrence of these small shocks and this residual frequency seems to remain almost unaltered throughout the year. If the origin of the additional shocks triggered by the change in flood intensity is attributable to adjustments in fault planes, it does not necessarily follow that the small shocks associated with the residual frequency do also owe their origin to readjustments in the fault zone. Further, if it be even so, what are the extraneous processes or forces responsible for their origin? It is feasible from other evidences also that origin of these shocks included in residual frequency is attributable to the overall instability of the region as mentioned earlier. If so, whether it is a fact that all unstable regions of the world will under favourable circumstances trigger off additional number of shocks as in this investigation? Data collected up to this time confirm that such regions of instability may also exhibit triggering phenomena under favourable circumstances, like change of flood intensity, etc.

Associated with compression from the north, this region is situated very close to the axis of negative gravity anomaly, which runs parallel to the Himalayan boundary fault — see figure 1. Instances from other parts of the world show that such regions, in general, are highly active. But up to this time none of the geophysical elements, like gravity anomaly etc. have been correlated with triggering causes in earth movements. In conclusion, it may be said that, regions which are active in respect of shallow shocks of bigger magnitudes are also likely to be susceptible to exhibit trigger process in earth movements.

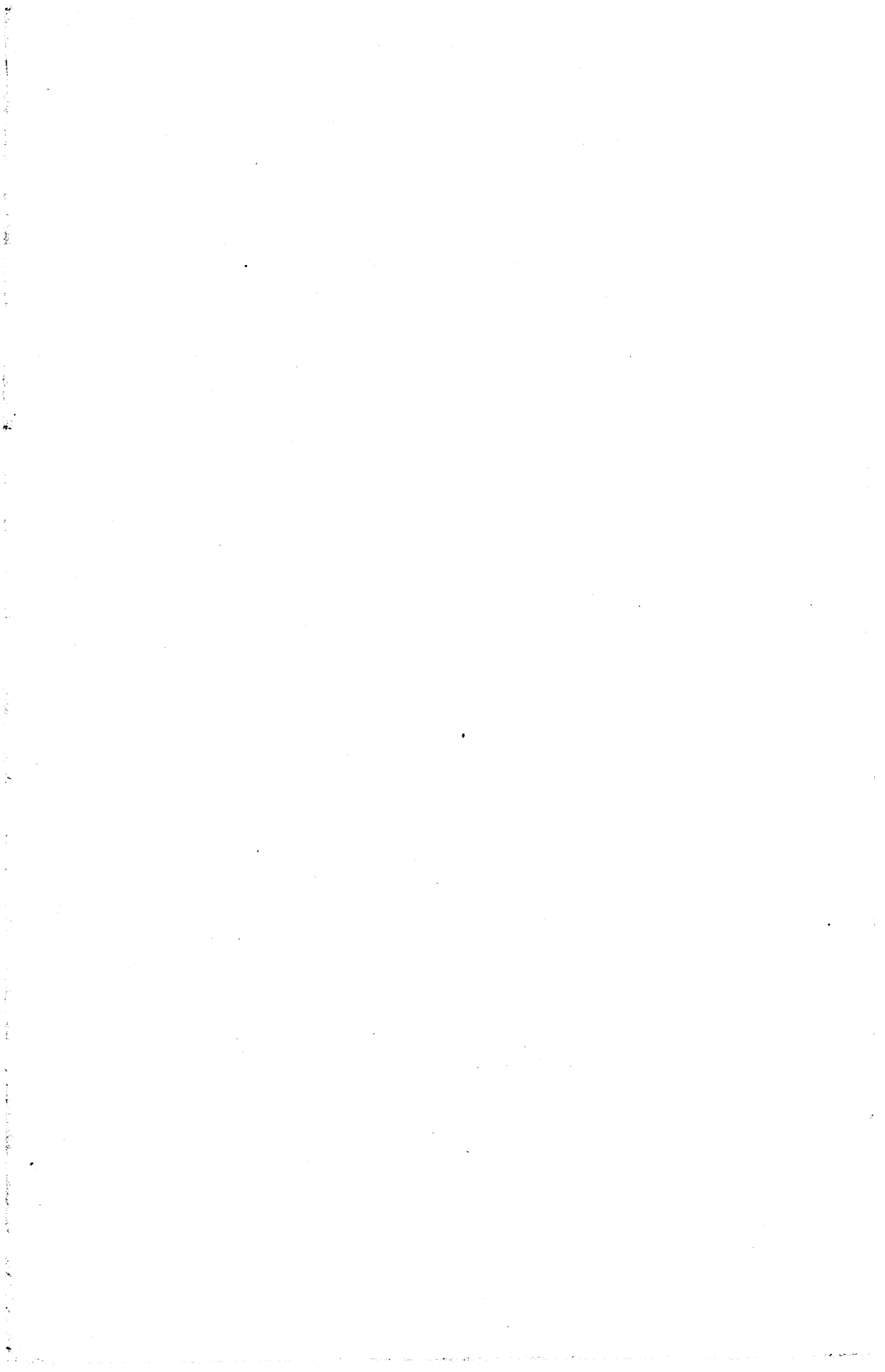
Though it has been possible here to show that there is some significant enhancement of local shocks due to triggering forces on account of rate of change of flood intensity, it has not been possible here to isolate other factors like temperatures, pressures etc. which may cause significant contribution towards triggering process. There are some instances when other physical factors have been reasonably correlated to increase or decrease of frequency of similar shocks. Probably, of all the triggering processes known so far, that due to rate of change of flood intensity in any region has been most conspicuously observed. It may be due to the magnitude of the triggering forces available here which is responsible for their conspicuous effects in releasing additional number of shocks or it may be the way in which it is imparted.

Acknowledgment.

The authors record with appreciation the keen interest shown by Mr. D. V. Joglekar, Director, Central Water and Power Research Station, Poona (India) in the preparation of this paper. Thanks are also due to Mr. P. D. Gosavi for help in the analysis of the data.

BIBLIOGRAPHY.

1. CONRAD (V.) — « Triggering causes of Earthquakes and Geological Structures (Part II) » Bull. Seis. Soc. Am., July 1947.
 2. MEAD (T. C.) & CARDER (D.-S.) — « Seismic investigation in the Boulder Dam area in 1940 » Bull. Seis. Soc. Am., October 1941.
 3. Dr. NICKELL (F. A.) — « Geology of the Barahakshetra Dam Site : Kosi river, Nepal »; Central Water and Power Commission, Government of India.
 4. ROBERTS (E. B.) and ULRICH (F. P.) — « Seismological Activities of the U. S. Coast and Geodetic Survey in 1950 » — Bull. of Seis. Soc. of Am., July 1952.
-



BASIC EQUIPMENT OF SEISMOLOGICAL STATIONS IN THE U.S.S.R.

by D. P. KIRNOS and D. A. KHARIN

Regular seismological observations in the U.S.S.R. are carried on now at 70 stations. These stations are divided according to their purpose and equipment on the whole into two types. The stations designed to register distant and near earthquakes and called stations of general type are equipped with seismographs of galvanometric registration, possessing constant magnification equal to 1000 in a wide range of periods of seismic waves (from 0.25 sec. to 10 sec.). The movements of ground during near earthquakes are reproduced by these instruments with insignificant distortion. Surface waves of long periods are also taken down clearly. At the stations of regional type, specially accommodated to registration of feeble local earthquakes, seismographs of galvanometric registration were installed which possess an acute peak of magnification (20,000-40,000) for the periods of vibration of earth of about 0.3-0.6 sec. Eight stations in the U.S.S.R. are equipped with widely known seismographs of academician B. B. Galitzin's system. The registration of earthquakes is carried on at the stations on photographic paper.

THEORY OF INSTRUMENTS.

The behaviour of a seismograph of galvanometric registration is characterized by a well-known system of two equations.

$$\begin{aligned}\ddot{\Theta} + 2 \varepsilon_1 \dot{\Theta} + n_1^2 \Theta &= -\frac{\ddot{X}}{l} + 2 \varepsilon_1 \sigma_1 \dot{\varphi} \\ \ddot{\varphi} + 2 \varepsilon_2 \dot{\varphi} + n_2^2 \varphi &= 2 \varepsilon_2 \sigma_2 \dot{\Theta}\end{aligned}\quad (1)$$

Here Θ is angular movement of the pendulum; φ — angular movement of the galvanometer coil; ε_1 and ε_2 — damping coefficients of the pendulum and galvanometer; n_1 and n_2 — circular frequencies of oscillations of the pendulum and galvanometer; σ_1 and σ_2 — mutual influence (coupling) coefficients of the pendulum and galvanometer; X — movement of ground; l — reduced length of the pendulum.

It should be noted that this system of equations of movement is common to all types of seismographs of galvanometric registration. This system and all conclusions following from it, fit both the instruments, offered first by academician B. B. Galitzin, with

transducer in which E.M.F. arises at the expense of a relative movement of the pendulum coil and the magnetic field, and the instruments (first applied by Benioff) in which E.M.F. arises at the expense of a variation of the resistance of the magnetic circuit of the instrument.

Periods of oscillations $T_1 = \frac{2\pi}{n_1}$ and $T_2 = \frac{2\pi}{n_2}$, damping constants $D_1 = \varepsilon_1 : n_1$ and $D_2 = \varepsilon_2 : n_2$ of the pendulum and galvanometer, and coupling coefficient $\sigma^2 = \sigma_1 \sigma_2$ are the basic parameters affecting properties of the instruments. Depending on correlations between these constants and the periods of movement of ground, the instruments of galvanometric registration can possess different properties. They can mark on the record movements of ground of definite periods, possess magnification invariable within a wide interval of frequencies of seismic waves, and last within a definite interval $\omega_1 — \omega_2$ of frequencies of ground movements their records can correspond to definite kinematic elements of movement of ground from the third derivative to the integral by time from the movements of ground.

The values of constants necessary to give the instrument predetermined properties are most conveniently determined by solving the system (1) according to the method of Fourier's integral. As it is known when using this method the movement of ground is translated into an indefinite sum of elementary sinusoidal movements according to the formula of Fourier's integral

$$X = \int_0^\infty S(\omega) \sin(\omega t + \Psi_i(\omega)) d\omega \quad (2)$$

where $S(\omega)$ is amplitude spectrum of the movement, $\Psi_i(\omega)$ — phase spectrum of the movement.

It is obvious that the solution of the system relative to φ will have the form analogous to (2) that is, it will consist of the same sum of harmonical oscillations but with amplitudes distorted and shifted by phase. Passing on to the movements on the tape $y = 2A\varphi$ where A is the length of the optical lever we see that

$$y = \bar{V} \int_0^\infty S(\omega) \bar{\mathcal{U}}(\omega) \sin(\omega t + \Psi_i(\omega) + \bar{\gamma}) d\omega \quad (3)$$

Here $\bar{\mathcal{U}} = \bar{\mathcal{U}}(\omega, n_1, n_2, D_1, D_2, \sigma^2)$ is a function characterising the amplitude distortions, $\bar{\gamma} = \bar{\gamma}(\omega, n_1, n_2, D_1, D_2, \sigma^2)$ is a function characterising the phase shifts, \bar{V} is a constant characterising the scale of magnification. The form of the functions $\bar{\mathcal{U}}$ and $\bar{\gamma}$

which are characteristics of the instruments is given by the following expressions.

$$\begin{aligned}\bar{U} &= U_1 \cdot \frac{1}{\sqrt{1 + \xi_2}} \cdot \frac{1}{\sqrt{1 + \zeta}} \\ U_1 &= \frac{1}{\sqrt{(1 - u_1^2)^2 + 4 D_1^2 u_1^2}}; \quad u_1 = \frac{n_1}{\omega} \\ \xi_2 &= \frac{1}{4 D_2^2} \left(\frac{1}{u_2} - u_2 \right)^2; \quad u_2 = \frac{n_2}{\omega} \\ \zeta &= \zeta (\omega, n_1, n_2, D_1, D_2, \sigma^2) \\ \operatorname{tg} \bar{\gamma} &= (1 + \delta) \operatorname{tg} \bar{\gamma}_0 \\ \delta &= \delta (\omega, n_1, n_2, D_1, D_2, \sigma^2) \\ \operatorname{tg} \gamma_1 &= \frac{2D_1 u_1}{1 - u_1^2}; \quad \operatorname{tg} \gamma_2 = \frac{u_2^2 - 1}{2D_2 u_2} \\ \gamma_0 &= \gamma_1 + \gamma_2\end{aligned}\tag{3a}$$

\bar{U} and $\bar{\gamma}$ are well-known functions of the independent variable quantity ω and of the parameters-constants of the instruments. It permits to select such parameters which would give the functions \bar{U} and $\bar{\gamma}$ the form with which the records of $y(t)$ of the instruments will possess predetermined properties, for example, will correspond within a predetermined interval $\omega_1 - \omega_2$ of frequencies to that or another kinematic element of the movement of ground.

For example, in order to make the record of the instrument correspond to the displacements of ground it is necessary to observe the following conditions.

$$\begin{cases} \bar{U} \approx 1 \\ \bar{\gamma} \approx 0 \end{cases}\tag{4}$$

with this we naturally have

$$y \approx \bar{V} \cdot X$$

The characteristics which would satisfy the conditions (4) can be obtained in the following cases.

a) The movement of the long-period ($n_1 \ll \omega$) and feebly damped pendulum ($D_1 < 1$) corresponds to the displacements of ground. The current coming into the galvanometer coil being corresponded to the velocity of the movement of ground, and the deflections of the over damped galvanometer ($D_2 \gg 1$) with its own frequency satisfying the condition

$$n_2 = \sqrt{\omega_1 \cdot \omega_2}\tag{5}$$

being corresponded to the integral by time from the strength of the current. In the formula (5) ω_2 is the maximum and ω_1 — the minimum frequency in a given interval $\omega_1 - \omega_2$.

The magnification \bar{V} under which the recording is carried on is determined by the following expression

$$\bar{V} = \frac{2A}{I} \sqrt{\sigma^2 \cdot \frac{\epsilon_1}{\epsilon_2} \cdot \frac{K_1}{K_2}} \quad (6)$$

Here K_1 is moment of inertia of the pendulum, K_2 is moment of inertia of the galvanometer coil.

This formula fits to all types of seismographs of galvanometric registration. In case of instruments in which the inert mass of the pendulum moves rectilinearly, this formula takes the following form.

$$\bar{V} = 2A \sqrt{\sigma^2 \cdot \frac{\epsilon_1}{\epsilon_2} \cdot \frac{M}{K_2}} \quad (6a)$$

where M is mass of the pendulum.

The expression (6) shows that it is possible to make magnification of the instruments of galvanometric registration be as great as one wants without any amplifier technique. Practically the limit of magnification is put by the mass of the instruments. For example, magnification \bar{V} equal to one million practically requires the mass M of the pendulum equal to one hundred kilograms.

b) As it is known the same characteristics of the instrument can be obtained by means of exchange the values of constants of the pendulum and galvanometer. It being done that the movement of the over damped pendulum ($D_1 \gg 1$) with its own frequencies of oscillations $n_1 = \sqrt{\omega_1 \cdot \omega_2}$ corresponds to the velocity \dot{X} of the movement of ground and the deflections of the long-period feebly damped galvanometer correspond to the double integral by time from the strength of the current in the galvanometer coil.

II. In case if

$$\begin{aligned} \bar{U} &\cong C_i \cdot \omega \\ \gamma &\cong \frac{\pi}{2} \end{aligned} \quad \left. \right\} \quad (7)$$

the record of the instrument corresponds to the velocity of the movement of ground

$$y = C_i \cdot \bar{V} \cdot \dot{X} \quad (7a)$$

The characteristics satisfying the correlations (7) can be obtained by the following ways.

a) The movement of the pendulum corresponds to the movements of ground and the deflections of the galvanometer of high frequency ($n_2 \gg \omega$) are proportionate to the strength of the current in its coil. In this case $C_1 = \frac{2\epsilon_2}{n_2^2}$

b) The movement of the pendulum corresponds to the velocity of the movement of ground and the deflections of the galvanometer correspond to the integral by time from the current in its coil.

In this case $C_1 = \frac{1}{2\epsilon_1}$

c) The movement of the pendulum corresponds to the acceleration of the movement of ground and the deflections of the long-period feebly damped galvanometer correspond to the double integral from the strength of the current. In this case $C_1 = \frac{2\epsilon_2}{n_1^2}$

III. In case if

$$\begin{cases} \bar{U} \approx C_2 \omega^2 \\ \gamma \approx \pi \end{cases} \quad (8)$$

the record of the instrument corresponds to the acceleration of the ground

$$y \approx C_3 \bar{V} \cdot \ddot{X} \quad (8a)$$

the characteristics satisfying (8) can be obtained by the following ways.:

a) The movement of the pendulum corresponds to the movement velocity of the ground and the deflections of the galvanometer — to the strength of the current in the coil. In this case

$$C_2 = \frac{1}{n_2^2} \cdot \frac{\epsilon_2}{\epsilon_1}$$

b) The movement of the pendulum corresponds to the acceleration of the ground and the deflections of the galvanometer correspond to the integral from the strength of the current that is to the movement of the pendulum. In this case $C_2 = \frac{1}{n_2^2}$. By analogous way we come to the instruments whose indications will correspond to the other kinematic elements of the movement of ground (\dot{X} and $\int_0^t X d\tau$) as well.

The dependence of magnification of a seismograph on the frequency of seismic waves is given by the formula

$$V = \bar{V} \cdot \bar{U} \quad (9)$$

The expression for \bar{U} permits, as it is known, to calculate whether the curves $V(\omega)$ of magnification or the constants within a wide interval ω or to the contrary the segregating oscillations in a narrow range of frequencies ω .

Proceeding from the theory and from the well-known spectra of frequencies of seismic waves for the new instruments of galvanometric registration which the network of stations in the U.S.S.R. has been equipped with the following values of the constants have been selected.

a) For seismographs of general type $T_1 = 12.5$ sec.; $D_1 = 0.45$; $T_2 = 1$ sec., $D_2 = 6$; $\sigma^2 \leq 0.05$; $\bar{V} = 1000$. In addition to this $\bar{U} \approx 1$ for the interval $0.25 \text{ sec.} \leq T\omega \leq 10 \text{ sec.}$ This characteristic is shown on Fig. 1 a. Within the limits $0.25 \text{ sec.} \leq T\omega \leq 5 \text{ sec.}$

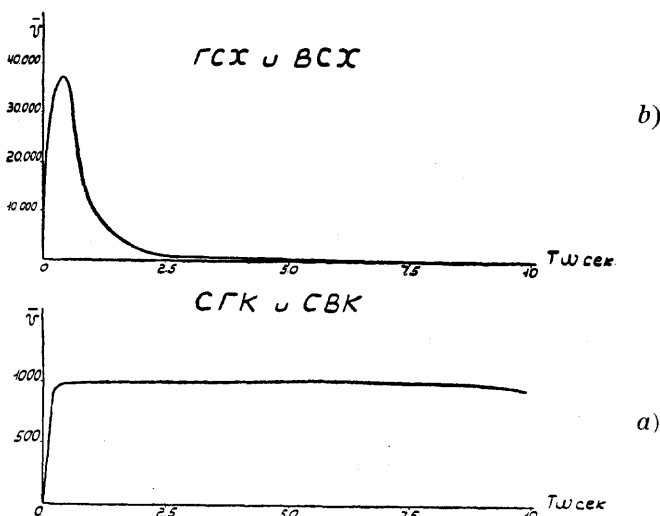


FIG. 1.

of the main part of the spectrum of near earthquakes, the record of the instrument corresponds to the displacements of ground. It is illustrated on Fig. 2 which shows the records of the movement of shaking table (5) resembling the movements of ground on near earthquakes, (4) is a corresponding record of a seismograph of general type, (3) and (2) are corresponding records of seismographs of Galitzin's and Nikiforov's type, (1) is marks of time in 1 sec.

b) For seismographs of regional type the constants are modified dependingly of the level and spectrum of microseisms in a given station and usually are within the limits $T_1 = 0.7 - 1$ sec.;

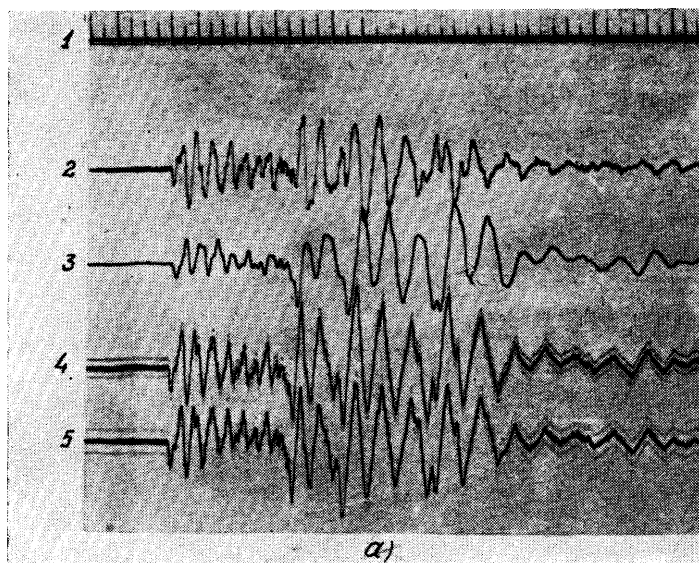


FIG. 2.

$D_1 = 0.6 - 0.9$; $T_2 = 0.3 - 0.5$ sec.; $D_2 = 1.5 - 3.0$; $\sigma^2 \leq 0.3$;
 $V_{\max} = 20.000 - 40.000$ with periods of waves $0.3 \text{ sec.} < T_\omega < 0.6 \text{ sec.}$

The form of the corresponding characteristic of \mathcal{U} is shown on Fig. 1 b.

DESCRIPTION OF THE INSTRUMENTS.

A) SEISMOGRAPHS FOR THE STATIONS OF GENERAL TYPE.

Horizontal seismograph « CTK ». — A general view of the pendulum is shown on Fig. 3. It is a horizontal pendulum hung up on two thin flat steel springs and on a steel string fixed in the foundation of the instrument. In the copper mounting at the end of the pendulum two induction coils joined with two pairs of terminals are fixed. One of the coils serves for registering the movements of the pendulum and with it the circuit of the galvanometer is connected. The second coil serves for regulating the damping of the pendulum and with it a special resistance R_b needed to obtain the necessary value of the constant D_1 is connected. The middle parts of the coils are situated in the air clearance of the permanent magnet. At the end of the pendulum in front of the coils a scale is fixed. Over the scale on the magnet, a thin pointer and a lens are fixed through which it is possible

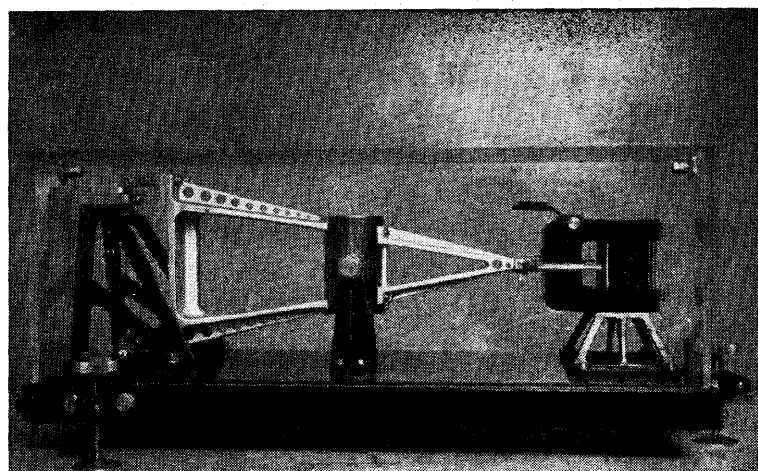


FIG. 3.

to read the position of the pointer with precision to 0.1 mm. These appliances serve for determining the constants of the instrument. The period T_1 of the pendulum is regulated within the limits from 5 sec. to 50 sec. by the front adjusting screw. The instrument is covered with a transparent protective case.

For registration of the movement of the pendulum the galvanometer TK-VI shown on Fig. 4 specially constructed for this purpose is used. The galvanometer consists of a magnet between the poles of which a copper tube is fixed. In the tube a special insert is fixed with a mobile system which consists of a flat coil with a mirror hung up on two tension wires which serve at the same time as conductors bringing the current to the coil. The length of the lower tension wire is easily varied. Thereby the value of the period T_2 is regulated. The limits of variation of T_2 are from 0.9 to 1.3 sec. The strength of the magnetic field in the air clearance and consequently the damping D_2 of the galvanometer can be regulated with the help of the magnetic shunt.

For regulation of magnification of the instrument into its electrical scheme compound shunts are introduced which practically do not affect the working regime of the instrument. These shunts are mounted on a special panel. Switching of magnifications is done with special plugs.

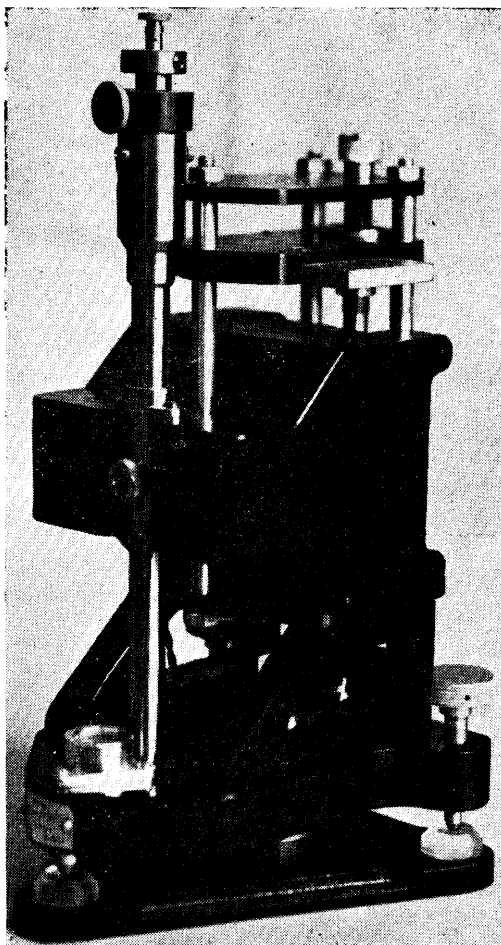


FIG. 4.

A general view of the pendulum of the vertical seismograph «CBK» is shown on Fig. 5. The pendulum consists of two masses, situated on different sides of the axis of rotation. The pendulum is hung up on two pairs of thin flat mutually perpendicular springs. In horizontal position the pendulum is kept by a spiral spring. The accepted disposition of the masses increases the reduced length of the pendulum and cuts the load on the supporting spring. It gave a possibility to create a stable long-period instrument.

The application of the supporting spring made of elinvar practically almost excludes temperature influence. Electrical schemes of the vertical and horizontal seismographs are practically identical.

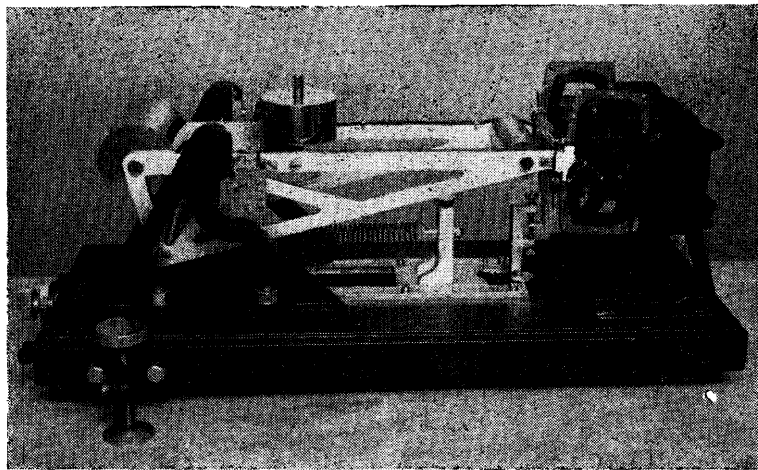


FIG. 5.

Registration of the movement of the pendulum is carried on with the help of the same galvanometer as in the horizontal seismograph. The instrument is also covered with a transparent protective case.

The period of own oscillations is regulated within the limits from 7 to 20 sec. by moving with the help of a micrometrical screw the point of attachment of the supporting spring to the foundation of the instrument. The position of equilibrium of the instrument is regulated with the help of the special screw whose head is led out to the front side of the foundation.

B) SEISMOGRAPHS FOR REGIONAL STATIONS.

Horizontal seismograph « Г CX ». A general view of the pendulum is shown on Fig. 6. The cylindrical mass of the pendulum is hung up to the post of the bed on flat springs and a string. The axis of the pendulum goes along a generatrix of the cylinder. The mass of the pendulum can be diminished twice by removing from the cylinder a special brass. The mass bears a truss with two cylindrical induction coils. The coils can move within the annular air clearance of the permanent magnet. One of the coils is connected with a galvanometer for recording movements of ground, the second coil serves for regulating the damping and the coupling coefficient. For determining the constants, a reading microscope is fixed in the transparent case, covering the instrument to observe the oscillations of the pendulum. A sharp change of the

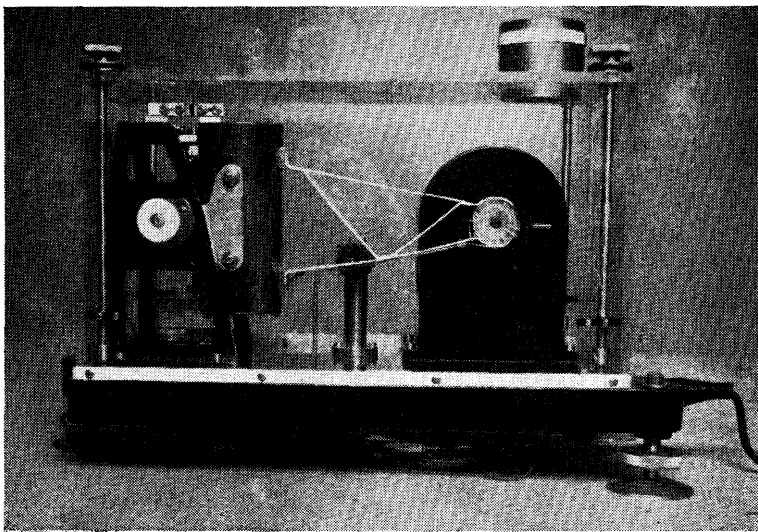


FIG. 6.

period of own oscillations is achieved by changing the mass and by replacing the suspended springs. A smooth regulation of the period is achieved by changing the angle of bank of the axis of rotation. The period of the pendulum can be changed within the limits from 0.3 to 4.0 sec.

For registration of the oscillations of the pendulum a galvanometer ГК-VI described above is used, but with another lighter suspended system, possessing shorter period of oscillation (0.2 — 0.5 sec.).

Vertical seismograph « BCX ». A general view is given on Fig. 7. The cylindrical mass of the pendulum rotates on the horizontal axis going along a generatrix of the cylinder. The axes is formed by two flat springs fixed in the posts to the bed. The mass is kept in equilibrium by a cylindrical spring, the upper end can move both in horizontal and vertical directions with the help of slides and screws. A second spring is envisaged for a fine regulation of the position of equilibrium.

The mass bears a truss with two induction coils. The induction coils, magnets and galvanometers of the instruments « BCX » and « ГСХ » are identical. A sharp change of the period of oscillations of the pendulum « BCX » is achieved by diminishing the mass and replacing the cylindrical spring.

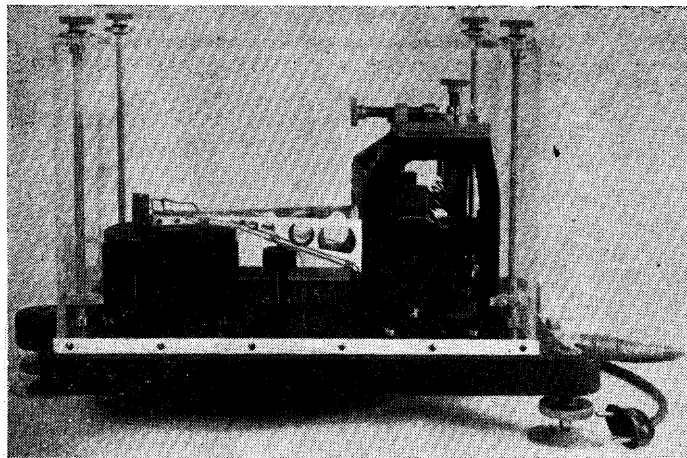


FIG. 7.

A smooth regulation of the period is realized by moving the upper point of attachment of the cylindrical spring. The period of the pendulum varies within the limits from 0.3 to 3.0 sec.

For determining the constants, a reading microscope is fixed in the transparent case covering the instrument.

Regulation of sensibility is realized by compound shunts included into the electrical scheme of the pendulum and galvanometer it being not affected their working regime.

At many stations photoelectrical automatic machines are installed which intensify the incandescence of the illuminators and reduce the sensibility of the instruments on long-amplitude vibration of ground.

DETERMINATION OF THE CONSTANTS AND REGULATION OF THE INSTRUMENTS.

The periods T_1 and T_2 of the seismographs of general type are determined visually, T_1 being determined on short amplitudes of the pendulum by observing the movement of the latter with the help of a galvanometer connected with the pendulum.

T_1 of the seismographs of regional type is determined visually through a microscope, T_2 is determined according to the record on photographic paper.

The constants of damping of the pendulum and the galvanometer have the following expressions.

$$D_1 = D_{10} + \frac{a_{11}}{R_{S_1} + R_D} + \frac{a_{12}}{R_{S_2} + R_{B_1}} = D_{10} + D_{11} + D_{12}$$
$$D_2 = D_{20} + \frac{a_2}{R_g + R_{B_2}} = D_{20} + D_{21}$$

where R_{s_1} , R_{s_2} , R_c , R_{b_1} , R_{b_2} are resistances of the induction coils of the pendulum, galvanometer and compound shunts, R_d — resistance regulating the damping of the pendulum, D_{10} and D_{20} — air dampings of the pendulum and galvanometer, a_{11} , a_{12} , a_2 — coefficients, depending on the constructive properties and the period of oscillations of the pendulum and galvanometer.

The coefficients are determined according to the record of own oscillations of the pendulum and galvanometer closed by different outside resistances. Having determined experimentally D_{10} , a_{11} and a_{12} it is possible to calculate the necessary value of the quantity R_d needed to obtain the predetermined value of D_1 .

Having determined D_{20} and a_2 it is possible to regulate the galvanometer in such a way that it will be in conformity with the necessary quantity D_2 .

All the schemes necessary to determine the constants are mounted in special panels and switched by commutators. The coupling coefficient σ^2 is calculated on the basis of the determinated values of damping.

The scale of magnification is given by the following correlation,

$$\bar{V} = \frac{2A}{l} \sqrt{\sigma^2 - \frac{T_1 D_1}{T_2 D_2}} \cdot \frac{K_1}{K_2}$$

where K_1 and K_2 are the moments of inertia of the pendulum and galvanometer, A — optical lever and l — reduced length of the pendulum.

It is not difficult to calculate the values of K_1 and K_2 if we determine the constants for the current (the static sensibilities) of the pendulum and galvanometric circuits. The reduced lengths and the moments of inertia of the pendula are determined by regulating the pendula with the help of special knives.

SEISMOGRAPHS FOR RECORDING STRONG EARTHQUAKES.

The stations situated in regions of intense earthquakes are also equipped with seismographs for recording earthquakes of average and destructive strength.

The seismograph «CMP-II» for recording earthquakes of average strength is shown on Fig. 8. It is a horizontal seismograph of mechanical registration and electromagnetic damping. Its indicator magnification is $V_0 = 7$, the period of own oscillations $T_1 = 5$ sec, $D_1 = 0.45$ sec. The construction of the instruments is understandable from Fig. 8.

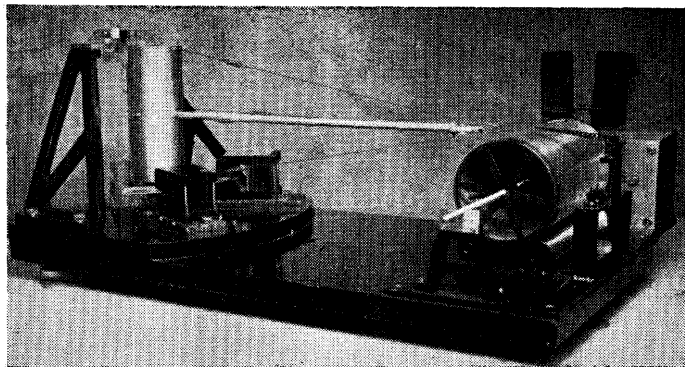


FIG. 8.

The seismograph « CP3 » designed to register earthquakes of destructive strength is constructed in such a way that in spite of a relatively great speed of registration (300 mm/min) necessary to record short-period vibrations in epicentral zone, it is possible to use it changing the tape of the instrument very seldom (once for a month and more seldom). The scheme of the instrument is shown on Fig. 9. The registering drum « 1 » continuously

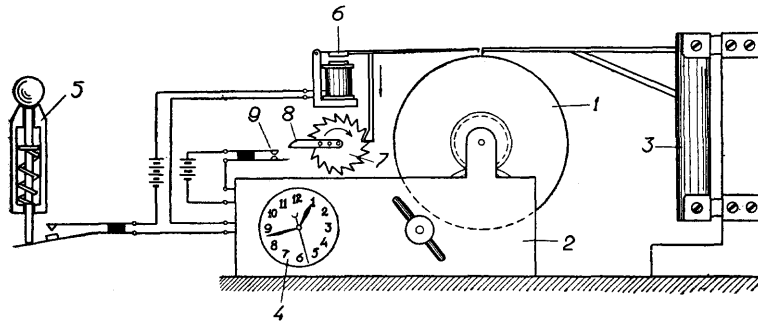


FIG. 9.

rotates with the help of a special clockwork « 2 » without translational movement along the axis, the speed of the movement of the paper being equal to 5 mm/sec. On the surface of the drum covered with soot continuous registration of the movement of two seismographs is carried on. The first seismograph possesses the period of about 2 sec, $D_1 = 0.3$ and indicator magnification $V_0 = 1/3$. The second seismograph possesses the period $T_1 = 0.2$ sec. $D_1 = 0.4$ and $V_0 = 5$. The first instrument marks on the record

oscillations of low frequency with long amplitudes, the second one — oscillations of high frequency with short amplitudes. When ground is quiet both instruments draw zero lines. On sufficiently strong earthquakes, a special seismoscope actuates the contacts of the clock and after one revolution of the drum both the drum and the clock stops.

Thus it is possible to record entirely, including the first shock, destructive earthquakes relatively seldom for every place, with great speed of registration, the service of the instrument being reduced to the minimum.

ON SOME NEW METHODS OF SEISMOLOGICAL RESEARCH

by G. A. GAMBURZEV.

During the past few years, in connection with the development of research in the field of earthquake forecasting, the Institute of Geophysics of the Academy of Science of the USSR, in collaboration with the Academies of Science of the Georgian, Tadzhik, Azerbaidjan, Turkmenien and others of the 16 constituent Union-republics, undertook a detailed study of the geological and geophysical conditions for origination of earthquakes in a number of seismically active areas of the Crimea, the Caucasus, Turkmenia and Central Asia.

In the present paper some new methods of seismological research, employed in these investigations, are reported.

1. AZIMUTH SEISMIC STATIONS.

Azimuth seismic stations are based on the idea of « azimuth » phase correlation of seismic waves. Phase correlation methods are, as known, extensively used in seismic prospecting. There phase correlation is an operation of tracing wave phases (or more

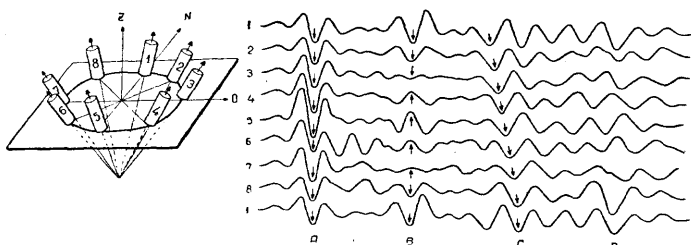


FIG. 1.

exactly, the maxima and minima of the vibrations) from one point to another, i.e. as a function of the position of the seismograph on the profile. This form of phase correlation we term « positional ». In distinction from positional, azimuth phase correlation is carried out as a function of the azimuth of the seismograph, with the observation point at a fixed position. Accordingly, an azimuth station consists of a group of differently orientated seismographs set up at one « point ». In the latest models of

azimuth stations « inclined » seismographs are used. The inclined seismograph differs from the vertical and horizontal ones in that it records the component of the ground movement along an inclined axis. The axes of the inclined seismographs are directed along the generatrices of a given cone at equal azimuth intervals. All the seismographs are identical in design and have the same inclines and exactly the same parameters.

An azimuth installation with inclined seismographs is illustrated diagrammatically to the left in Fig. 1 and part of the seismogram obtained to the right in the same figure. The numbers assigned to the records (channels) correspond to the numbers of the seismographs. In the given case azimuth correlation consists in tracing the maxima or minima of vibrations from one record to another as a function of the number of the inclined seismograph, i.e. of its azimuth.

To characterize the operation of an azimuth station with inclined seismographs let us construct a cone, whose generatrices form an angle $90^\circ - \varphi$ with the vertical, where φ is the angle between the vertical and each of the axes of the inclined seismographs.

Let us assume that a linearly polarized wave, for which the ground displacement vector lies within the given cone, approaches the azimuth set-up. This will be the case e.g., when a direct longitudinal wave from a sufficiently deep source strikes upon the observation surface. Corresponding to the given wave on the multichannel azimuth seismogram will be sector A, where the vibrations in the different channels will be exactly of the same shape. There will be a difference only in the amplitudes of the vibrations, which will be maximum at the azimuth of the seismic rays and evidently minimum at the opposite azimuth. By analogy with the correlation methods used in seismic prospecting, the cophasal axes, i.e. the lines linking the maxima or minima of the vibrations, can be drawn in this sector of the seismogram. And owing to the absence of phase shifts between the vibrations in different channels, the cophasal axes will be straight vertical lines.

Suppose now that the azimuth set-up is approached by a linearly polarized wave, for which, in distinction from the first case, the ground displacement vector lies outside the mentioned cone. This will be the case e.g. when a transverse wave from a deep source approaches the seismographs. Corresponding to this wave on the seismogram is sector B, which differs essentially from sector A. Whereas in the first case all the vibrations were in phase, here evidently in part of the channels the phase will be turned by 180° .

Accordingly, the cophasal axes, while remaining vertical, become discontinuous at two definite azimuths corresponding to zero amplitudes of the vibrations.

We consider now the third case of an elliptically (in particular, a circularly) polarized wave approaching the seismographs. This e.g. may be a Rayleigh surface wave, or a complex interference wave due to a superposition of two or more volume waves with differently directed displacement vectors. Here, depending on the orientation of the axes of the ellipse and on their ratio, a number of particular cases might be examined. Without going into detail, we point out that the cophasal axes will no longer be straight vertical lines. The phase shifts may run up to 360° . Corresponding to this case is sector C.

And finally, let us examine the fourth and last case. Suppose that the azimuth set-up is approached by a non-polarized wave, within whose limits the change in magnitude and direction of the ground displacement vector obeys no definite law. This may be the case of a diffuse vibration caused by the superposition of a large number of waves of different types and different directions of approach. Such waves ordinarily fill up the intervals on the seismograms between the arrivals of regular waves. Corresponding to this irregular diffuse wave on the seismogram is sector D of uncorrelatable vibrations, which do not permit to draw cophasal axes across the entire seismogram.

Summing up, we may conclude that due to the easily distinguishable singularities of the records, we are able to separate visually longitudinal, transverse and surface waves from the irregular background disturbance waves and also to distinguish simple waves from waves complicated by interference effects.

It should be noted that in principle the same could be accomplished by the use of the ordinary three-component records, but the treatment of results would be complicated and very laborious and there would be no simple visual criteria. Things would improve if the three-component set-up consisted of inclined seismographs.

In regard to the criteria for distinguishing regular seismic waves (e.g. longitudinal or transverse waves) from irregular (e.g. interference) ones, it is interesting to compare azimuth correlation with positional correlation, used in seismic prospecting. Both permit to distinguish between regular and irregular vibrations. In azimuth correlation this is done on the basis of the criterion of stability with time of the polarization of vibrations; in positional correlation — of the criterion of stability in space of the shape of

vibrations. However, whereas in positional correlation it is essential to obtain observations at a number of points, in azimuth correlation observations made at one point are sufficient.

The azimuth set-up not only helps to identify the types of waves, but also ensures higher accuracy in the determination of the direction of the ground displacement vector, which in turn increases the accuracy of determination of the earthquake foci coordinates. This is due to two circumstances. First, the ground displacement vector is determined not from three, as usual, but from 4 to 8 components and owing to the similar design of the seismographs, their identity can be easily checked up by setting up all the instruments at the same azimuth. Secondly, azimuth correlation permits to separate on the seismogram the vibrations phases least distorted by disturbances.

Azimuth installations with inclined seismographs are now used in seismic prospecting too.

2. EXTENSION ON THE FREQUENCY RANGE IN RECORDING EARTHQUAKES.

To make possible a more complete investigation of seismic phenomena, attempts were made to extend considerably the working range of the frequencies recorded. For the extension of the low frequency end, new instruments, called "seismotiltmeters" were devised. These differ from the usual tiltmeters only in that they measure not the inclines themselves, but the rates of inclines. Exclusion of the inclines remaining constant with time and the measurement only of the changes in inclines permits to increase considerably the sensitivity of the apparatus. In the region of the frequency characteristic maximum seismotiltmeters respond to inclines of the order of 10^{-3} — 10^{-4} arc sec. Exclusion of the constant components of inclines is accomplished by the introduction of electrical or mechanical differentiating cells. Seismotiltmeters permit recording of seismic waves in the period range from several to several dozen minutes.

The characteristics of the apparatus, used for the extension of the high-frequency end of the vibrations recorder, were very close to those of the apparatus used in seismic prospecting. In particular, ordinary prospecting seismographs equipped with amplifiers served as receivers of vibrations. Recording was done with special oscillographs permitting recording over a long period of time on a film moving at a relatively high rate (up to 1 m per min.). Observations were made in different parts of Central Asia (Kazakhstan, Turkmenia, Tajikistan). The following principal results were obtained.

The seismic wave spectra from earthquakes with epicentral distances exceeding 100 km contain high-frequency components but the low-frequency components prevail in intensity.

The weaker the shock and the closer its focus, the higher the frequency of the incoming waves. This can be explained by a decrease in volume of the focal region with the decrease in intensity of the earthquake and also by the selective (proportional to frequency) absorption of seismic waves. Weak shocks over focal distances of the order of dozens of kilometres (up to 100 km) are easily separated in the frequency range 15-30 Hertz.

It is interesting to note that in deep sounding of the earth's crust recording of explosions has to be done on somewhat lower frequencies. This indicates a sharp disturbing process taking place at the source of weak natural earthquakes.

Weak high-frequency seismic tremors give distinct phases of longitudinal and transverse waves, the latter being of higher intensity. This indicates for the weak seismic shocks a mechanism of origination similar to that for the stronger shocks, i.e. associated mainly with shearing in the focal region. It should be pointed out that on the records of artificial explosions from the same apparatus transverse waves are absent.

In the cases investigated the epicenters of weak high-frequency tremors were concentrated at the same place as those of the stronger shocks. The focal depths were also about the same. At the same time weak high-frequency tremors occur much more frequently than the stronger low-frequency shocks. In some sections of Tajikistan high-frequency tremors occur on the average every five minutes.

It should be pointed out that the high-frequency tremors, we are talking about, can be observed only under conditions of a state of complete rest at the recording point. The station should be located far away from inhabited points, public roads and other sources of industrial disturbances. The seismographs should be mounted of bed-rock at a spot protected from the wind. Under these conditions the microseisms do not hamper the increase in magnification of the apparatus in the indicated frequency range (15-30 Hertz) up to several or even tens of millions.

The results obtained give sufficient ground for a further development of methods of high-frequency seismometry. The effectiveness of these methods ensues from the following considerations.

1. Earthquakes and explosions can be recorded in the same frequency range. This provides a basis for a combined study of

the structure of the earth's crust and the seismic phenomena taking place in it from the records of both natural and artificial explosions.

2. The frequency range 10-30 Hertz is high enough to permit the use in recording earthquakes of some of the technical and methodical achievements of seismic prospecting.

3. Transition from frequencies of the order of one or some fraction of one Hertz to frequencies of the order of some dozens of Hertz should lead to an increase in the resolving power of the apparatus, thus facilitating the separation of seismic waves of different types. Moreover, this makes possible a more accurate determination of the foci coordinates.

4. The more frequent occurrence of weak tremors than of the stronger ones suggests the possibility of a quicker (and more exact) solution of some important problems of seismic district charting, such as e.g. the detection in the interior of the Earth's crust of deep seismically active faults.

3. DEEP SEISMIC SOUNDING OF THE EARTH'S CRUST.

A study of the conditions for origination of earthquakes should be evidently based on a detailed information on the singularities of the deep geological structure in the seismogenetic zones under investigation. The extent of details should be as high as possible and approach that attained in seismic prospecting. The depth reached in the investigation should be determined by the focal depth of most of the destructive earthquakes, i.e. should be no less than 30-50 km.

With a view to obtain such information, a method of deep sounding of the Earth's crust was developed in the USSR, at the base of which lies the correlation principles of recording artificially excited seismic waves.

The first experiments carried out in the USSR in this direction date back to 1939, when an attempt had been made to increase the depth reached in seismic prospecting by the reflection method. Due to the measures which had been developed at that time for increasing the effective sensitivity of the prospecting apparatus, recording of reflected waves over times up to one minute became possible. However, owing to the difficulties, associated with the separation of once-reflected waves from the multiple-reflected ones, no definite results could be obtained. All further work on deep sounding of the Earth's crust was conducted on the lines of correlation refraction shooting, the latter method having been developed

during the same years by the Institute of Geophysics of the Academy of Science of the USSR.

At the second stage of this work the chief task concerning the method consisted in increasing the distance over which refracted (head) waves could be recorded, since on the distance covered depended the depth reached in seismic prospecting. In 1949, in the course of experimental investigation in the region of the Northern Tyan-Shan mountains, this problem was brought to a quite satisfactory solution. The possibility was shown of systematically recording refracted waves over distances up to 400 km with comparatively small portions of explosives used (of the order of some hundred kgs of the explosives ordinarily used). Measures taken for increasing the effective sensitivity of the seismic receiving apparatus were the same as in 1939. They consisted in eliminating noise in the amplifiers and simultaneously increasing the amplification factor, in employing a group of seismographs in place of a single one to suppress microseisms, in selecting an optimal frequency of the vibrations recorded and in maintaining carefully the most favourable conditions of observations (recording mainly at night, far away from inhabited points, public roads etc.) Of no small significance of course were good conditions for explosion (blasts in water at a depth of 10-20 m).

From 1949 on work on deep seismic sounding was being carried out on a considerable scale in some regions of Balkhash (Kasakhstan), of the Zailii and Kirghiz ridges, in South-Western Turkmenia, in the Caucasus (by the personnel of the Georgian Academy of Science) and also on the Russian plain. The universality of the developed apparatus was proved as well as the possibility of using it for tracing the P^* — waves, corresponding to the surface of the basaltic layer and the P — waves, corresponding to the Mohorovicic discontinuity. Samples of records are shown in Fig. 2.

The method of observations was close to that used in seismic prospecting by correlation refraction shooting. But some deviations from it were allowed. In particular, when making observations on a long profile (300-400 km long) continuous « shooting » of the entire profile was replaced by continuous shooting of separate segments of this profile. The omitted intervals of the profile (up to 30 km long) did not ordinarily hamper the drawing up of the summary time-distance curves for the entire profile as a whole.

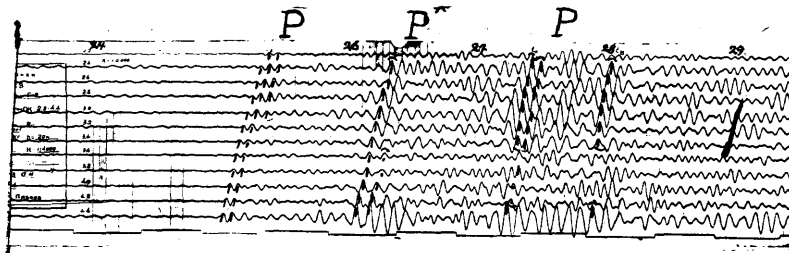
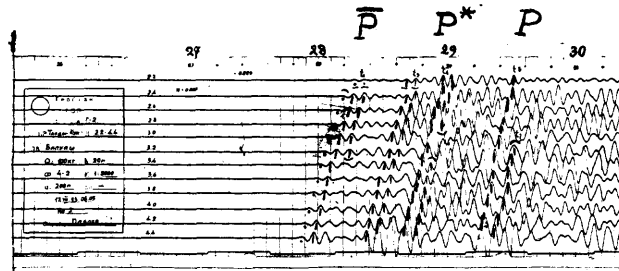
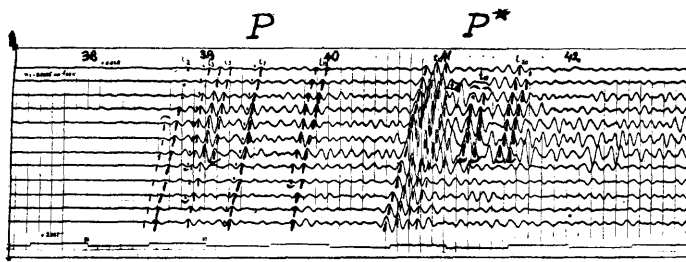


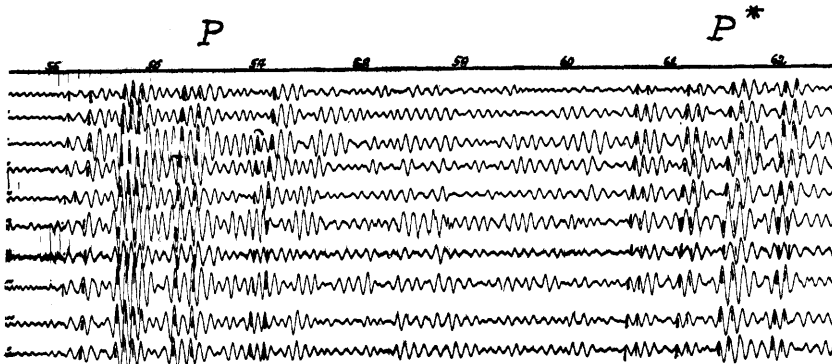
FIG. 2. — Seismograms obtained in deep seismic sounding :
a) distance from the shot point 150 km, intervals between seismographs
 $d = 200$ m, charge $Q = 200$ kg;



b) 166 km, $d = 200$ m, $Q = 100$ kg;



c) 237 km, $d = 200$ m, $Q = 200$ kg;



d) 366 km, $d = 100$ m, $Q = 300$ kg.

Correlation of isolated segments of the profile was accomplished by methods of wave correlation, based on a study of the kinematic and dynamic singularities of the waves recorded. Moreover, correlation (identification of waves) was controlled by observations made at other shot points.

In connection with some problems of deep seismic sounding in some regions a detailed system of longitudinal and transverse profiles was developed, thus giving a surface survey. This was done in particular to detect deep faults in the interior of the Earth's crust.

The work done has helped to throw light on the singularities of the deep geological structure of some mountain and foothill regions.

The most important of methodical conclusions arrived at was the possibility of increasing considerably the extent of details in investigating the deep layers of the Earth's crust. This was facilitated by the comparatively high frequency of the vibrations recorded and by the application of correlation principles of identifying and tracing seismic waves.

METHODS AND RESULTS OF THE INVESTIGATIONS OF EARTHQUAKE MECHANISM (A BRIEF INFORMATION)

by V. I. KEILIS-BOROK
Geophysical Inst. Acad. of Sci. USSR, Moscow.

1. Introduction.

A new method of determining dislocation (fault plane and motion direction) in the source of earthquakes has been worked out in the Geophysical Institute of the Academy of Science of the USSR. This method is based on the works by Academicians V. J. Smirnov and S. L. Sobolev and their successors on the elasticity theory and the classic theory of multipoles and plane waves.

In its main premises and general idea of interpretation this method has much in common with the well-known method of Byerly as it was improved by J. H. Hodgson (see the report at the same session) and especially by A. K. Ritsema (Ind. J. Meteorol. and Geophys., 1955, v. 6, No. 1) as well as with methods of Japanese seismologists.

We also consider « the straightened rays » (semitangents to the seismic rays at the hypocentre) and the « primary waves » (which would be observed in a homogeneous medium with the same source).

However the method described has some differences.

1. The greater part of the observations may be used :
 - a) The signs of the first or corresponding arrivals of P, SH, SV in any (direct, reflected, diffracted) wave.
 - b) The correlation of these signs in every point.

c) The ratio of amplitudes $\frac{SV}{SH}$ $\frac{P}{SH}$ or $\frac{P}{SV}$ of direct or reflected wave in every point.

2. The interpretation is unambiguous.
3. Various types of possible dislocations in the source have been considered.

Most essential proved to be the use of the signs of arrivals and correlation of these signs; the ratio of amplitudes yields satisfactory results only for some distant earthquakes.

The effectiveness of this method may be judged of by the fact that at present it made possible the unambiguous fault plane solutions for about 250 sources.

The problem is formulated as follows : to find a point source (approximate model of origin) which, being placed in the hypocentre, would produce the given displacements in the points of observation. Besides the origin is assumed as a point and the medium as ideally elastic with flat interfaces.

The investigation proves that the type of the source determines the type of rupture in the origin : a dipole with moment corresponds to fault displacements with sides moving in the fault-plane in opposed directions (shift, fault, thrust, etc.); a dipole without moment is equivalent to fracture openings; a double-dipole with moment corresponds to a dislocation of a narrow horst or graben type. Simple force corresponds to a simple shock without break or fault displacement at the contact of hard and soft rocks when intensive elastic deformations occurred only on one side of the shifting plane. The double centre of rotation corresponds to a fault displacement with sides rotating in the shifting plane. The centre of rotation differs from the double centre of rotation as a simple force differs from dipole with moment.

It may be noticed that dislocations in the source prove as a rule to be equivalent to the dipole with moment.

The direction of axes determines the orientation of the fault-plane ($Y = 0$) and the motion direction x in the origin; the intensity of the source determines the resultant or total moment of forces. Thus a mathematical model of an origin determines its geological and physical parameters.

2. Theoretical basis.

Theoretically the method is based upon the following equation, which may be deduced from the theory of waves in the semi-infinite medium (works of academicians V. I. Smirnov and S. L. Sobolev) and then generalized for layered medium [1] :

$$\mathbf{U}^{(p)} = \sum_{i=0}^k \left(\frac{1}{r}\right)^{i+1} \frac{\partial^{k-i}}{\partial t^{k-i}} K[t - f_p(r)] A_i^{(p)} + \int_0^{t-f_p(r)} K(t') A_{k+1}^{(p)} dt'.$$

Here $\mathbf{U}^{(p)}$ is one of the components of displacement (P, SV or SH); $K(t)$ — intensity-time relation; r — distance; $A_i^{(p)}$ — are determined by the properties of the medium, the type of waves and of the source; f_p depends on the path of the wave; k — is the order of multiplet.

The construction of the formula is the same as for homogeneous medium (Love's theory of multiplets), the terms for A_i being, however, much more complicated. With large r (or in vicinity

of wave front) (1) becomes greatly simplified because we may neglect all but the first items; that is equivalent to taking into account the influence of interfaces in accordance with the theory of plane, and not spherical, waves.

At given displacements (1) is the equation of the unknown parameters of the source. This equation is too complicated for direct computations.

It appears, however, possible to divide the problem into two stages :

a) Reduction to homogeneous medium eliminating the influence of all interfaces and of curvature of the rays; this can be done in accordance with the theory of plane waves [2].

b) Solution of a much simpler inverse problem for homogeneous medium; it is usually sufficient to take into account in formulae of the theory of multiplets only the main part of displacement and to consider only the signs of arrivals of seismic waves.

3. Procedure of interpretation.

In solving the approximate equations almost all computations can be carried out graphically with the help of special nomograms [3].

The method of interpretation of the data is unique for near and distant stations, all types of waves and deep or surface earthquakes.

Wolf's stereographic projection, whose centre coincides with hypocentre, and the pole with the vertical is used in graphical interpretation. Every point of this projection represents the direction of a straight line through the hypocentre.

The last scheme of analysis of observations [3] appears now simple enough and may be briefly described as follows :

1) *Determination of initial data.*

The signs and, if possible, the amplitudes of ground displacements are determined for all identified waves. Then the influence of the known interfaces (including the earth's surface) is eliminated and the relations of independent components are established.

2) *Plotting of initial data on Wolf's stereographic projection.*

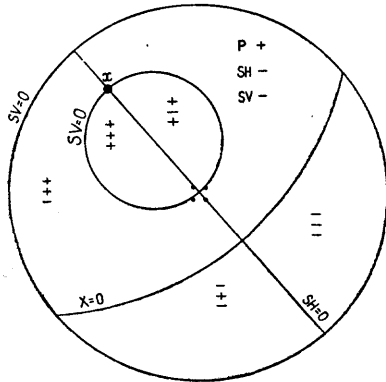
Conventional points of observations — the direction of tangents to the rays in hypocentre — are plotted on Wolf's stereographic projection. The observations of a single station can provide material for several such points; in each of them it is possible to measure up to 3 independent components of displacement. The signs (\pm) of these components are put beside each point.

3) *Determination of the point of emergence of the axis x* (direction of forces in the origin) if not only the signs but the amplitudes are known). Each of the relations of independent components of displacement — $\frac{P}{SH}, \frac{P}{SV}, \frac{SV}{SH}$ — forms on Wolf's stereographic projection an intersection line, containing the point sought for. These intersection lines are plotted with the help of a set of special nomograms [3] without additional computation.

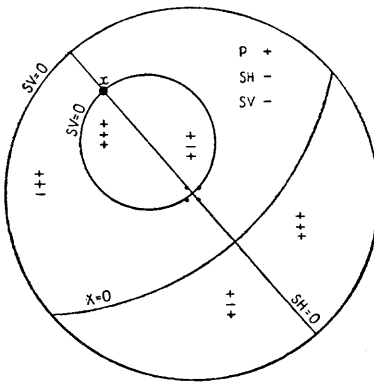
4) *Interpretation of the signs of displacements* constitutes the principal and the most reliable stage of analysis.

To every type of sources corresponds its own system of nodal lines for longitudinal ($P = 0$) and for both components of transverse waves ($SV = 0, SH = 0$) (fig. 1). The fact that the combination of signs of P, SH, SV , in each point are not arbitrary is of the greatest importance; for example, only two different ways of distri-

a)



b)



c)

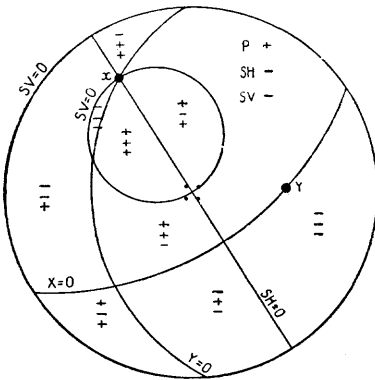
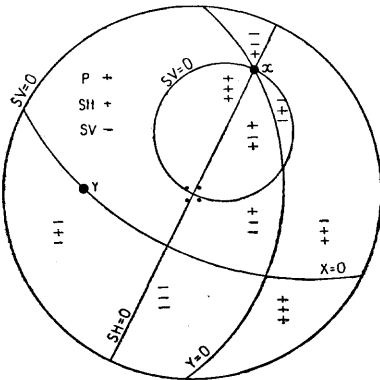


FIG. 1. Nodal lines and reference distributions of signs for various sources :
a) simple force ; b) dipole without moment ; c) dipole with moment ($Y=0$ — a fault plane and nodal line for P, SV, SH).

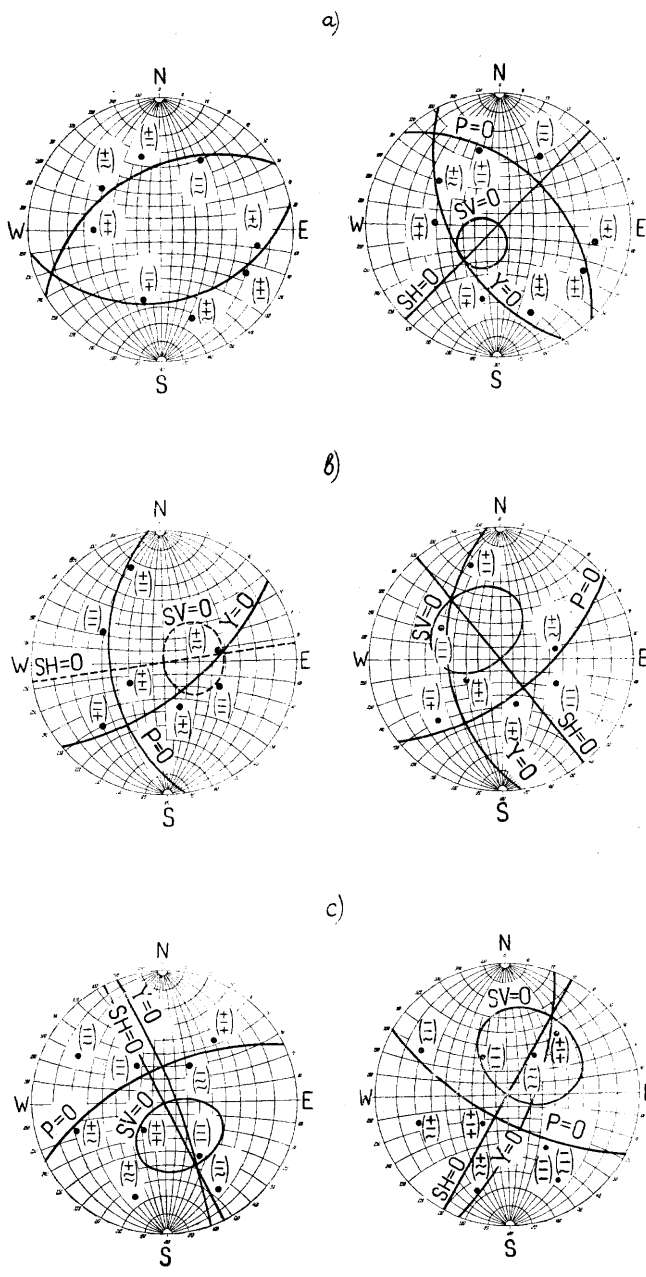


FIG. 2. — Examples of interpretation using signs of P, SH, SV and their correlation in each point.

All the points (direction of seismic rays in the hypocentre) are plotted in a stereographic projection of Wolf.

The signs of P, SH, SV are given for each point from top to bottom. The correct solutions are shown to the right.

bution of displacement signs are possible for a dipole with moment (*fig. 1*). This enables us to determine from the minimum of observations the exact position of nodal lines (and from them the type and direction of the axes of the source).

Figs 2 a-2 c show some examples of the unambiguous interpretation of signs, *fig. 1 c* being used.

On *fig. 2 a* the signs can be divided in two ways. But the signs of SV and SH render the interpretation unambiguous. On *fig. 2 b* one can draw two variants of nodal lines for all the signs of P, SV, and SH. But the comparison with the possible combination of the signs (*fig. 1 c*) assures that only the variant on the right is correct.

On *fig. 2 c* both variants of the system of nodal lines are consistent with *fig. 1 c*, however the interpretation will be rendered unambiguous by determining (even most roughly) the motion direction from the amplitude ratios $(\frac{P}{SH}, \frac{P}{SV}, \frac{SV}{SH})$. In all cases the signs of SH, SV permit to recognize which of the nodal lines corresponds to the fault plane ($Y = 0$).

5) *Computation of intensity.*

The intensity must be computed with respect to the amount and not relation, of displacements, and that, as might be expected, considerably worsens the precision of obtained data.

The interpretations of a single earthquake take an average from 2 — 3 to 5 — 6 hours, provided that the investigator has already acquired experience in studying the origins of the given region. A detailed instruction is published in [3].

4. Results of interpretation and comparison with geology.

4. I shall illustrate the effects of the application of the method described to the deep-focus shocks in Pacific Ocean and Central Asia and to shallow-focus earthquakes in Pamir and Kopet-Dagh.

a. The first attempt of a large-scale interpretation was carried out by a seismic expedition to the Garm district (N. Pamir). The region is one of the world's regions of greatest seismic activity. Continuous weak shocks are uninterruptedly recorded, and many strong and even destructive earthquakes occur there. The results obtained are shown on *fig. 4*.

The direction of faults and of motion in the origins is determined with an error of 15-20°.

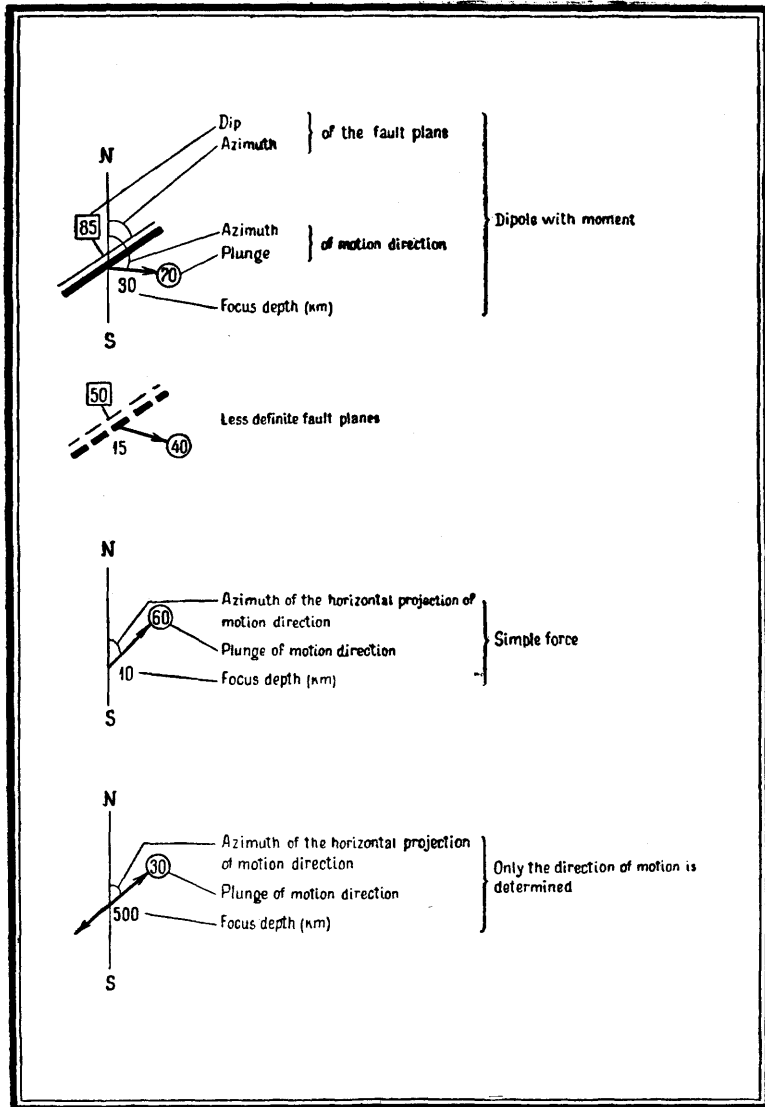


FIG. 3. The representation of seismic faults on figs 4-7. The heavy line corresponds to the side of a fault which moves upward.

The main source of errors is the inexact geometrical computation — the result of inexact determination of hypocentre and of the direction of rays emerging from it. This error is to some extent compensated by the fact that the initial formulae include only the angular coordinates of origin which change slightly with the displacement of the hypocentre. The reliability of interpretation is confirmed by the data from stations situated in different geological conditions.

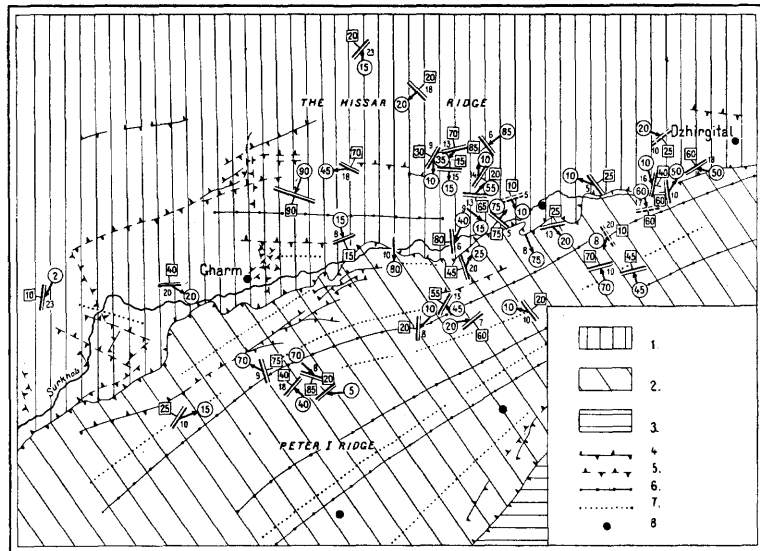


FIG. 4. Scheme of dislocations in the origins of Garm district.

1) The Hissar Ridge. 2) Peter I Ridge. 3) The Darvaz Ridge. 4) Lines of tectonic faults. 5) Supposed lines of tectonic faults. 6) Anticline axes. 7) Syncline axes. 8) Seismological stations. The representation of seismic faults see on fig. 3.

The tectonic activity of the region is related to the rapid and irregular uplift of the Guissar and Darvaz Ridges with respect to the Peter I Ridge. In the crystalline rocks of the Guissar Ridge prevail the two systems of faults shown on the map; in the Peter I Ridge crest-shaped folds are parallel to a large fault along the boundary of the ridges.

For comparison it is necessary (in view of tectonic complexity) to distinguish the general principal features of the system of faults in origins.

Almost all origins are equivalent to a dipole with moment. The faults in the origins strike in two predominant directions roughly perpendicular to one another and coinciding with the orientation of geological faults. The first is parallel to the fault separating the mountain ridges. A large number of minor shocks (and the two destructive earthquakes of the surveyed region) belong to the second (transverse) direction.

Correlation with geological data may be traced also in smaller features but it is better to neglect than to overestimate it.

b. The deep-focus earthquakes. They are of great interest as the direct manifestation of movements occurring at a great depth. The relation of these movements to the movements at the earth's surface is one of the fundamental problems of geotectonics.

The analysis of these earthquakes is also of interest from the point of view of method because of successful application of the principles of phase correlation to the interpretation of the records from distant stations. Thanks to this method weak and indistinct arrivals could be taken into account and the interpretation became better grounded [2].

The origins investigated in the Pacific stretch along the western coast of the Ocean from the Aleutian to the Marian Islands. The origins explored in Hindukush are located in a sharp narrowing of the Alpine geosyncline at the junction of the greatest mountain systems in Central Asia. The accuracy of interpretation is estimated to be about 20° . The use of reflected sP and ScS waves proved especially effective. All the origins proved to be equivalent to a dipole with moment, which does not contradict the idea of plastic state of matter in the earth's shell for elastic deformation and breaks may occur in plastic rocks, when the strains change rapidly enough.

The obtained results are shown on fig. 5 and 6.

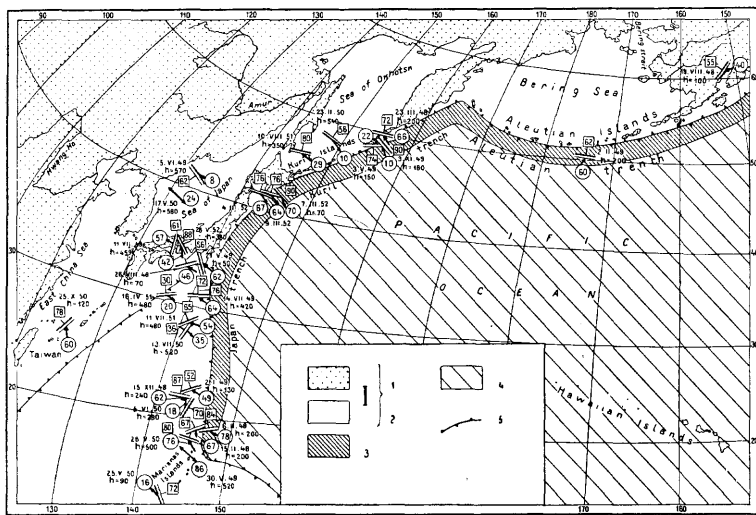


FIG. 5. Scheme of dislocations in the origins of the Island arcs of the Pacific.

1) Alpine geosynclines. 2) Parts of land. 3) Alpine foredeeps. 4) The Pacific Ocean bottom. 5) Large tectonic faults. The representation of seismic faults see on fig. 3.

The general features of the fault systems in the origins of the Pacific Ocean are as follows :

1. Everywhere except the Aleutian Islands the predominant strike is approximately perpendicular to the arcs of the islands.

2. In the majority of cases the motion direction has a great horizontal component almost perpendicular to the borderline of the continent.

3. The majority of faults have an abrupt dip roughly to the north.

In Hindukush almost all the explored origins are connected with

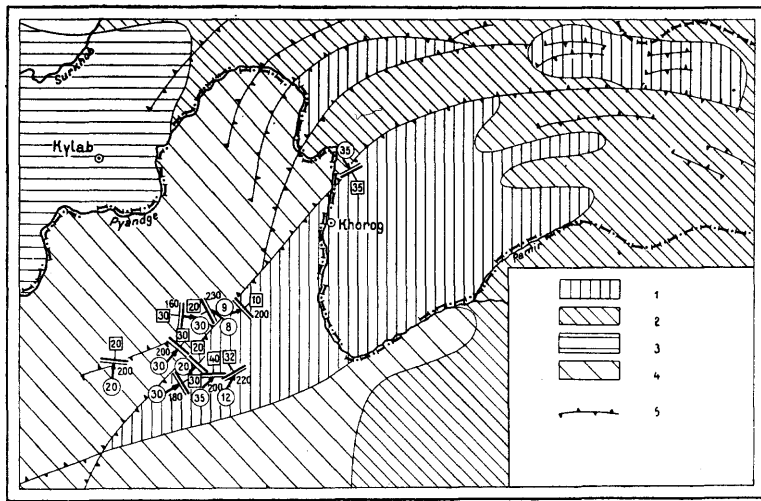


FIG. 6. Scheme of dislocations in the origins of deep-focus earthquakes of Central Asia.

1) Paleozoic structural complex. 2) Mesozoic structural complex. 3) Fore-deeps. 4) Alpine folding without subdivision. 5) Lines of tectonic faults. The representation of seismic faults see on fig. 3.

gentle thrusts (10-35° dip), more seldom with shift-faults oriented in 7 cases out of 10 across the main strike of the folding system and the fault related to the epicentres. The horizontal component of the shift in 6 origins is directed along and in 4 origins across the strike.

As a working hypothesis which seems to agree with the obtained results (particularly with the direction of faults and shearing displacements from geosynclines to platforms) may serve the suggestion that the investigated earthquakes are due to irregular flows of subcrustal material.

It seems to be worth to mention one more result, which is less important for the present paper but may have its own value. The use in this interpretation of waves, reflected from the earth's core, gives a limited but as yet the only one possible opportunity of studying the boundary conditions of the core.

c. It remains to discuss the earthquakes registered by the seismic expedition in Western Turkmenia, at the border of Kopet-Dagh and the Kara-Kum Desert. It is possible to distinguish there sections sharply differing in tectonics (fig. 7) : the spurs of the

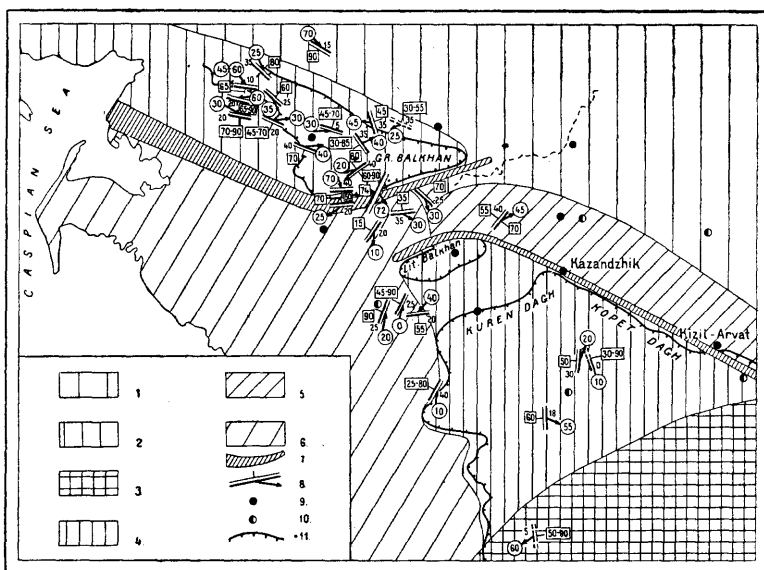


FIG. 7. Scheme of dislocations in the origins of the S. W. Turkmenistan.

- 1) Post-Hercynian platform.
- 2) Great Balkhan-Kubadagh meganticline-part of the post Hercynian platform.
- 3) The Kopet-Dagh meganticlinorium.
- 4) The folded region of the Western Kopet-Dagh.
- 5) The deepest part of the foredeep.
- 6) Trans-Caspian depression-zone of Neogen and Quarternary subsidence.
- 7) Boundary-line between big tectonic complexes where sharply different vertical movements of the earth's crust occur.
- 8) Kazandzhik earthquake of 1946.
- 9) Seismological stations of 1951.
- 10) Seismological stations of 1952.
- 11) Outcrops of country rocks. The representation of seismic faults see on fig. 3.

Kopet-Dagh; the Great Balkhan uplift; intermediary zone bordering the platform from the Caspian depression; meganticline adjoining the Great Balkhan from S-W.

When analysing the results it becomes immediately evident that different fault systems correspond to different tectonic regions; the strikes of faults : are parallel to the meganticline axis; reflect the curvature of the margin of the platform (it is, for instance, parallel to the break in the origin of the destructive Kasanjik earthquake); are parallel to the general direction of the border of the uplift near the Kopet-Dagh (although almost perpendicular to more local structures).

It is interesting to note that in the zone of meganticline the south-western sides of the faults are sharply thrust upon the north-eastern ones although there is a depression from south-west.

A similar phenomenon is noted for some sources in the Caucasus and the Tien Shan. This indicates that the mechanism of forming uplifts is complex.

The uniformity of faults in some sections justifies the attempt to take into account the influence of the asymmetry of forces in the origins upon the isoseismal pattern. The real isoseismals depend in the first place on the inhomogeneity of the medium (especially of the upper layers). Nevertheless, the theoretical isoseismals of Kasanjik earthquake (computed for homogeneous medium) proved to be stretching roughly in the same direction as the real ones.

5. In attempting to generalize the obtained results we established a considerable uniformity in the observed fault systems in regions most complicated tectonically.

That proves that an earthquake cannot be related to the development of separate local structures; these structures as well as the earthquakes seem to be the parallel results of general seismotectonic strains acting in vast regions.

Arises a second reverse problem : when the fault-system in origins is known, to characterize the field of these strains and to trace its change with time (in particular, before strong earthquakes).

In carrying out this investigation it is necessary to study earthquakes in as various regions as possible, in order to classify the observed fault system and to study their relationship with geological structures and their change with time.

BIBLIOGRAPHIE.

- [1] KEILIS - BOROK (V. I.), Dokladi Akademii Nauk SSSR, No. 6, 1951.
 - [2] KOGAN (S.D.), Trudi Geofisitcheskogo Instituta Ak. Nauk SSSR, No. 30, 1956.
 - [3] MALINOVSKAYA (L.N.), Trudi Geofisitcheskogo Instituta Ak. Nauk SSSR, No. 22, 1954.
-

HEAT FLOW THROUGH THE PACIFIC OCEAN BASIN

by A. E. MAXWELL and Roger REVELLE,
Scripps Institution of Oceanography of the University of California.*

ABSTRACT.

Fifteen measurements of the heat flow through the Pacific Ocean floor give an average value similar to that found for the continents. Neglecting three extremely high values the average of the remaining twelve measurements is 1.25×10^{-6} cal cm^{-2} sec $^{-1}$. The measurements have been made in widely separated areas in the Pacific and it is thought that they are representative of true oceanic values. Considerable variations exist, suggesting that anomalies of heat flow are present under the ocean and may represent previously undetected geophysical phenomena. Heat flow values were determined by measuring separately the thermal gradient and the thermal conductivity in the bottom sediments. The sum of the errors of measurement is found from experiment and theoretical analysis to be about 10 %. Investigation of the origin of the heat indicates that past fluctuations of bottom water temperature and processes occurring in the sediments are probably negligible, and that virtually all the heat must originate beneath the Mohorovicic discontinuity. Comparison of the oceanic with the continental heat flow suggests inconsistencies in the usually assumed distribution of radioactive materials in the earth's crust and mantle if heat transfer is taking place by molecular conduction. If the earth was initially hot, the present temperature at depths of a few hundred kilometers would be markedly higher under the oceans than under the continents, and this is difficult to reconcile with other geophysical data. It is possible that convective processes of outward heat transport dominate in the oceanic area.

* Contribution from the Scripps Institution of Oceanography New Series No. 820. This work was supported by the Office of Naval Research and the Bureau of Ships of the Navy Department and by the Institute of Geophysics of the University of California.

Introduction.

The continental heat flow is usually attributed to the decay of radioactive elements in the crust. Indeed, the heat flow is thought to vary directly with the thickness of the crust and in particular with the thickness of the granitic layer, in which it is believed the radioactivity is highly concentrated. Beneath the oceans, a granitic layer is thin or absent and one might anticipate a comparatively low heat flow. The oceanic measurements do not bear out this expectation; the heat flow is found to be about the same as in the continental areas. This result is of importance in considering the earth's thermal state, because the oceanic areas cover some 70 % of the earth's surface.

Measurements.

The flux of heat through the ocean floor may be determined from measurements of the thermal gradient and conductivity within the sediments, the relation being

$$\Sigma Q = - k \frac{dt}{dx}$$

where ΣQ is the heat flux, k the thermal conductivity and $\frac{dt}{dx}$ the thermal gradient.

TABLE 1
MID-PACIFIC (1950) AND CAPRICORN (1952-53) HEAT FLOW RESULTS.

Station	Water Depth (m)	Gradient (°Cm ⁻¹)	Conductivity (10 ⁻³ cal cm ⁻¹ sec ⁻¹ °C ⁻¹)	Heat Flow (micro cal cm ⁻² sec ⁻¹)
M. P. 1	4000	.0671	1.9*	1.27
M. P. 21	4500	.0650	1.8*	1.17
M. P. 32	3900	.0350	2.1*	0.74
M. P. 35-2	4900	.0623	2.0*	1.24
M. P. 36	5040	.0661	1.8*	1.19
M. P. 38	4750	.0692	1.6*	1.11
CAP. 2-B	4310	.0760	2.48	1.88
CAP. 5-B	5000	.0723	1.87	1.35
CAP. 9-B	2700	.0630	2.40	1.51
CAP. 10-B	3900	.1250	2.07	2.58**
CAP. 31-B	4880	.0862	1.83	1.58
CAP. 33-B	4300	.0210	1.71	0.36
CAP. 40-B	3020	.2150	2.44	5.25**
CAP. 48-B	4100	.0730	2.26	1.65
CAP. 50-B	4350	.1240	1.96	2.43**
Average				1.69
Average without values marked by**				1.25
Conductivities measured by the National Physical Laboratory, Teddington, England.				

Table 1 shows the results of six measurements of heat flow made on the Scripps Institution — U. S. Navy Electronics Laboratory Mid-Pacific Expedition of 1950 (Revelle and Maxwell, 1952) and nine measurements made on the Scripps Institution's Capricorn Expedition of 1952-53. The observed thermal gradients are three or four times larger than most continental gradients and the conductivities correspondingly smaller; so that the oceanic heat flows are similar to the continental values. The average of all 15 values is $1.69 \mu \text{ cal cm}^{-2} \text{ sec}^{-1}$. Omitting three extraordinarily high values, the remaining 12 give an average of $1.25 \mu \text{ cal cm}^{-2} \text{ sec}^{-1}$ with a standard deviation of $0.395 \mu \text{ cal cm}^{-2} \text{ sec}^{-1}$ or 31.5 %. The individual variation is markedly higher for the Capricorn results, which represent a much larger area of investigation, than for the Mid-Pacific values. One very low value obtained on the Capricorn Expedition is retained, although some unknown large source of error may be involved.

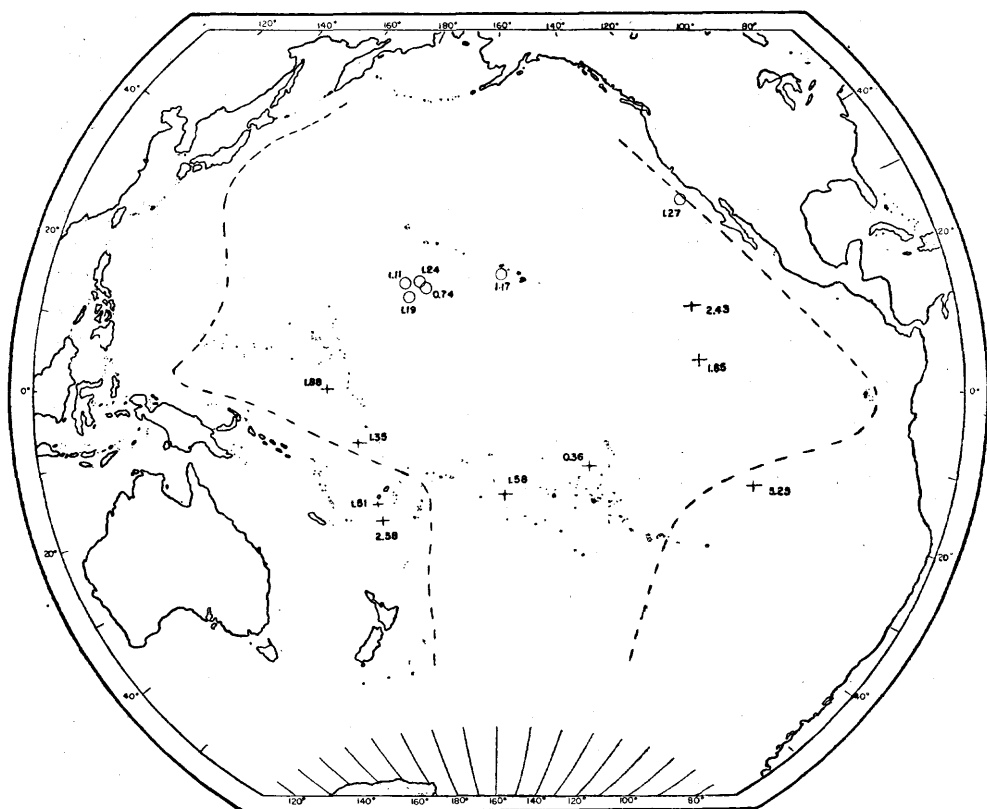


FIG. 1. Geographic distribution of oceanic heat flow measurements.

The geographic distribution of the results is presented in Fig. 1. Mid-Pacific values are shown as circles and the Capricorn results are represented by crosses. The heavy dashed curve gives the approximate location of the « andesite line », which at least in the South Pacific may be the boundary of the true Pacific basin. Two of the extremely high values lie on the continental side of the andesite line while the third appears to be well within the Pacific basin. For the present, we shall consider these three values as anomalous. Whether this is justified can not be determined without many more measurements. (In any case, the following interpretation will be little affected whether or not these high values are included in the average.) Obviously, the data are too meager to conclude whether a major pattern exists in the heat flow or the high values represent isolated local effects. On the other hand, the average value may be fairly representative of the entire Pacific basin.

Additional evidence on the similarity of the oceanic and continental heat flow has been obtained by Sir Edward Bullard (1954) with five measurements in the Atlantic Ocean. The Atlantic values obtained by him average somewhat less than our Pacific ones.

Sources of the heat.

All or part of the heat flow might be the result of temperature changes in the water immediately above the bottom. If the water was warmer in the past than at present a fraction of the heat introduced into the sediments would still remain and would contribute to the observed heat flow. We have satisfied ourselves that the magnitude of the temperature changes over time of one year or more necessary to account for a significant part of the heat flow would have to be much larger than available evidence permits. Consequently, the heat must originate either in the sediments or in the rocks underlying the sediments.

For convenience in discussion we may divide ΣQ , the observed heat flow, into components :

$$\Sigma Q = Q_s + Q_c + Q_m + Q_i$$

where the subscripts s , c , m and i refer to those portions of the observed heat flow arising from the heat generated in the sediments, the crust and the mantle, and from cooling of an « initially » hot earth, respectively. Computations show that various exothermal processes occurring within the sediments, including biological activity, compaction, diagenetic processes and radioactive decay, produce less than one per cent of the observed heat flow. This leaves the deeper layers of the earth as the primary source.

Raitt's (1951) seismic refraction measurements show that the Mohorovicic discontinuity lies about 7 kilometers beneath the Pacific Ocean floor. If we consider that this discontinuity marks the boundary between the earth's crust and mantle, and assume that all the material above the Mohorovicic discontinuity in the Pacific has a radioactivity similar to basalt, we find that Q_c can be only 10 % of the observed heat flow. Therefore, 90 % must have its origin in the mantle. This is in marked contrast to conditions under the continents, where it is generally believed that at least 70 % of the heat flow originates in the crust. The estimates of relatively high heat production in the continental crust are based on evidence that the Mohorovicic discontinuity is about 35 km below the surface, and that the rocks above the discontinuity are relatively high in radioactive materials. This is partly confirmed by the higher heat flows found in some mountain areas where the crust is presumably thickened (Birch 1950).

To make an estimate of the heat arising from the initial distribution of temperature, Q_i , we may assume that cooling has been taking place by conduction alone; then Q_i should be the same under both continents and oceans. In the continental case Q_c is predominant. As an upper limit for Q_c (continental), the heat generated in the continental crust might account for all the observed heat flow. As a lower limit, if the entire 35 km of the continental crust had an average radioactivity similar to basalt, Q_c (continental) would be about $0.7 \mu \text{ cal cm}^{-2} \text{ sec}^{-1}$. The heat flow resulting from radioactive decay in the mantle, Q_m (continental), must be at least $0.1 \mu \text{ cal cm}^{-2} \text{ sec}^{-1}$. Consequently Q_i must lie between 0 and $0.6 \mu \text{ cal cm}^{-2} \text{ sec}^{-1}$. The probable upper limit of Q_i , utilizing the available evidence on the distribution of radioactivity in the continental crust, is $0.3 \mu \text{ cal cm}^{-2} \text{ sec}^{-1}$. This value is represented by the dashed line in Fig. 2.

We have considered a sphere that has been cooling for 3×10^9 years with an initial temperature distribution, $a + b x$, and a thermal conductivity, k (constant with depth), where a is the temperature at the earth's surface and b is the increase with depth, x . As an upper limit for the initial temperature we may assume the earth to have been molten throughout, whence $a = 1300^\circ \text{ C}$ (the melting point of basalt at atmospheric pressure). Following Jeffreys (1952), we may estimate the melting point gradient from the Clausius-Clapeyron equation to be $3^\circ \text{ C km}^{-1}$. This probably gives an upper limit for the change of melting point with depth. For the lower limit of the initial temperature we have assumed

$a = 650^\circ$ and b to be the adiabatic increase in temperature with depth. Verhoogen, (1954), estimates that the adiabatic gradient is $0.5^\circ \text{ C km}^{-1}$. These two cases will be referred to as the « hot » and « cool » earth.

Figure 2 shows calculated values of Q_i plotted against thermal conductivity, k . For a hot earth, the estimated upper limit of Q_i , $0.3 \mu \text{ cal cm}^{-2} \text{ sec}^{-1}$, will be obtained if the average value of k is $0.006 \text{ cal cm}^{-1} \text{ sec}^{-1} {}^\circ\text{C}^{-1}$. For a cool earth, k must be $0.035 \text{ cal cm}^{-1} \text{ sec}^{-1} {}^\circ\text{C}^{-1}$.

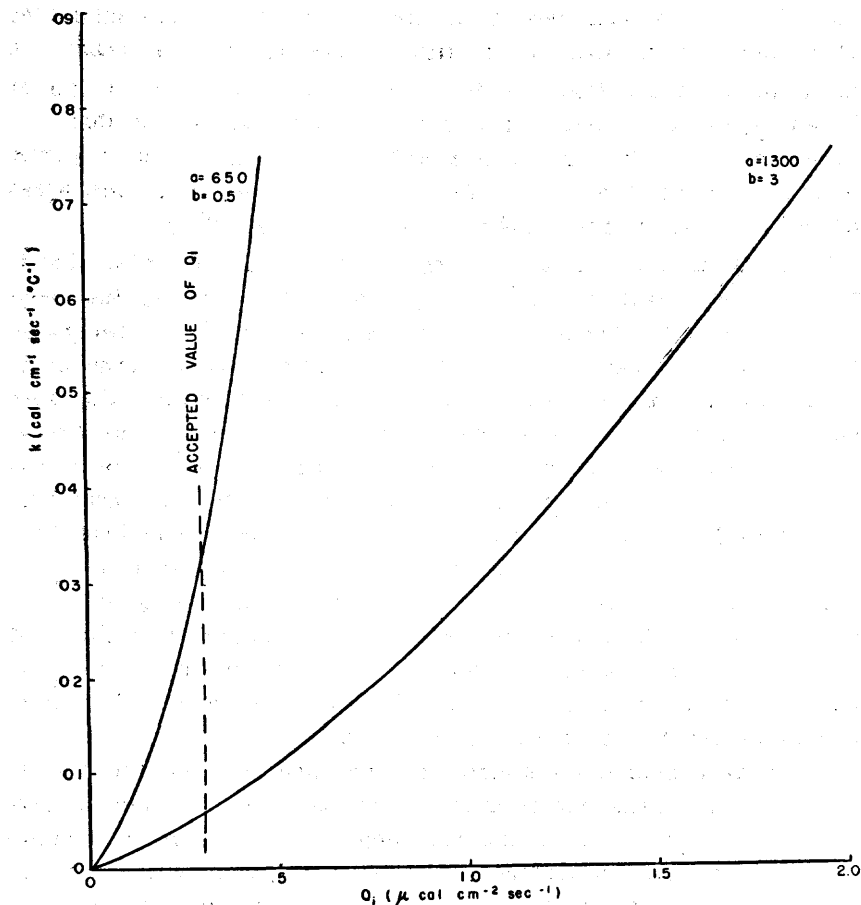


FIG. 2.

Values of Q_i as a function of the thermal conductivity for an initially « hot » and « cool » earth.

With the preceding values of Q_e and Q_i , Q_m beneath the oceans must be at least $0.8 \mu \text{ cal cm}^{-2} \text{ sec}^{-1}$. We have assumed, for simplicity, that the total radioactive heat production per unit area is just

sufficient to prevent either heating or cooling of the mantle as a whole, and that this radioactivity is uniformly distributed down to a depth L , beneath which the radioactivity is negligible. The

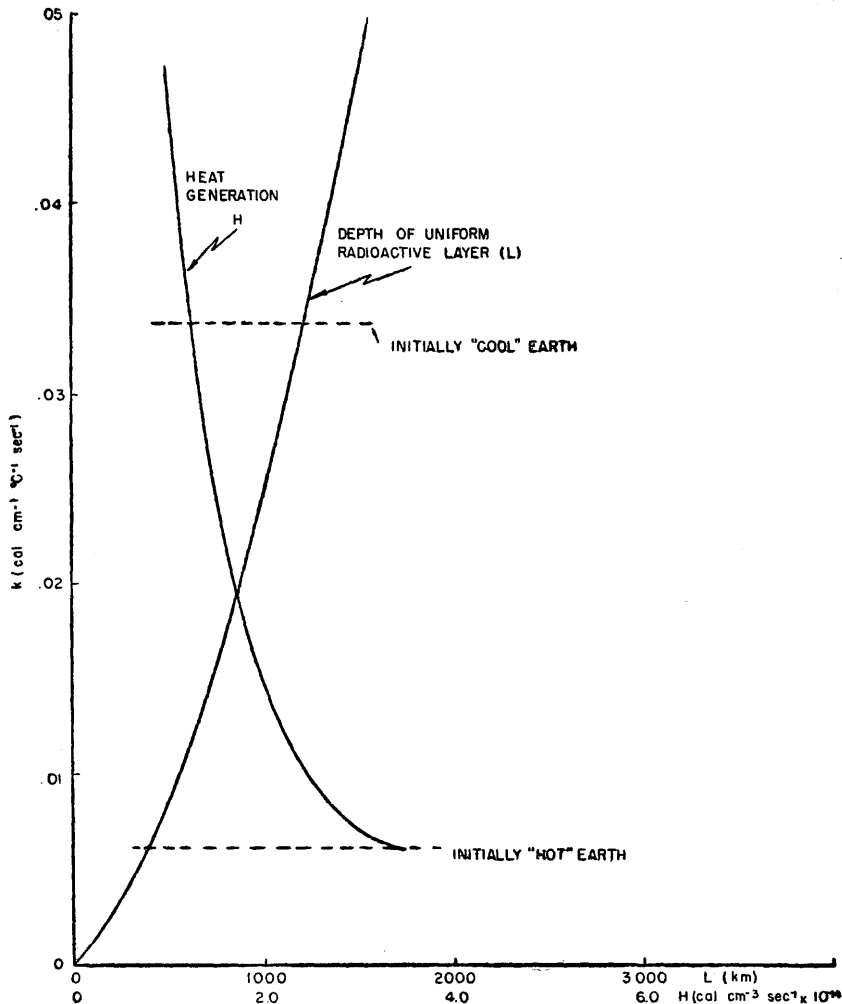


FIG. 3. Depth of uniformly distributed radioactive layer L and corresponding heat generation H as a function of the thermal conductivity.

maximum depth L over which the radioactivity can be distributed to give the observed heat flow is plotted in Fig. 3 as a function of the thermal conductivity. The corresponding amounts of radioactivity per unit volume (expressed in terms of heat production H , $\text{cal cm}^{-3} \text{ sec}^{-1}$) are also shown. If the mantle was initially at the assumed melting point at all depths, the previous considerations concerning Q_i indicate that k must approximate $0.006 \text{ cal cm}^{-1}$

$\text{sec}^{-1} \text{ }^{\circ}\text{C}^{-1}$. We see from Fig. 3 that L can not then be more than 400 km and H not less than 3.7×10^{14} cal $\text{cm}^{-3} \text{ sec}^{-1}$. This value of H appears improbably high in the light of the usual suppositions about the composition of the mantle. On the other hand, for an initially cool earth (initial surface temperature 650° , increasing adiabatically with depth $H = 1.2 \times 10^{14}$ and $L = 1200$ km. But in this case the thermal conductivity must be quite high, although possibly not beyond the limits of Uffen's (1954) recent theoretical considerations.

It is of interest to examine the case of a hot earth in somewhat more detail. In order to prevent rapid cooling, k must be small and there must therefore be an upward concentration of the radioactivity. The limit of such an upward concentration would be a distribution of radioactivity under the oceans similar to that under the continents. This is difficult to reconcile with the depths to the Mohorovicic discontinuity, 5 to 10 km beneath the oceans and 30 to 40 km under the continents. It would appear more likely that most of the continental radioactivity is above the Mohorovicic discontinuity while the oceanic radioactivity is distributed over a greater range of depth.

Fig. 4 shows the temperature that would result from different distributions of radioactivity under the continents and oceans. For simplicity we have assumed, as before, that the radioactivity is uniformly distributed down to a given depth and zero at greater depths, and that the total radioactivity is sufficient to maintain the observed heat flow. The depths of the radioactive layers have been taken as 35, 165 and 200 km, representing a typical continental and two possible oceanic distributions, respectively. Two salient features are noted. First we see that if the radioactive layer extends to depths greater than 165 km, heating, and presumably melting, of the mantle will occur. Second, the temperatures beneath the oceans will be several hundred degrees higher than beneath the continents over a considerable range of depth. The magnitude of this difference will be somewhat smaller if exponential distributions of radioactivity are considered instead of a two-layer model. A large temperature difference in the mantle between the oceans and continents is difficult to reconcile with the data on gravity, as has been pointed out by Griggs (1954). We consider it more likely that the radioactivity is distributed over considerable depths and that high conductivities and comparatively low mantle temperatures are required.

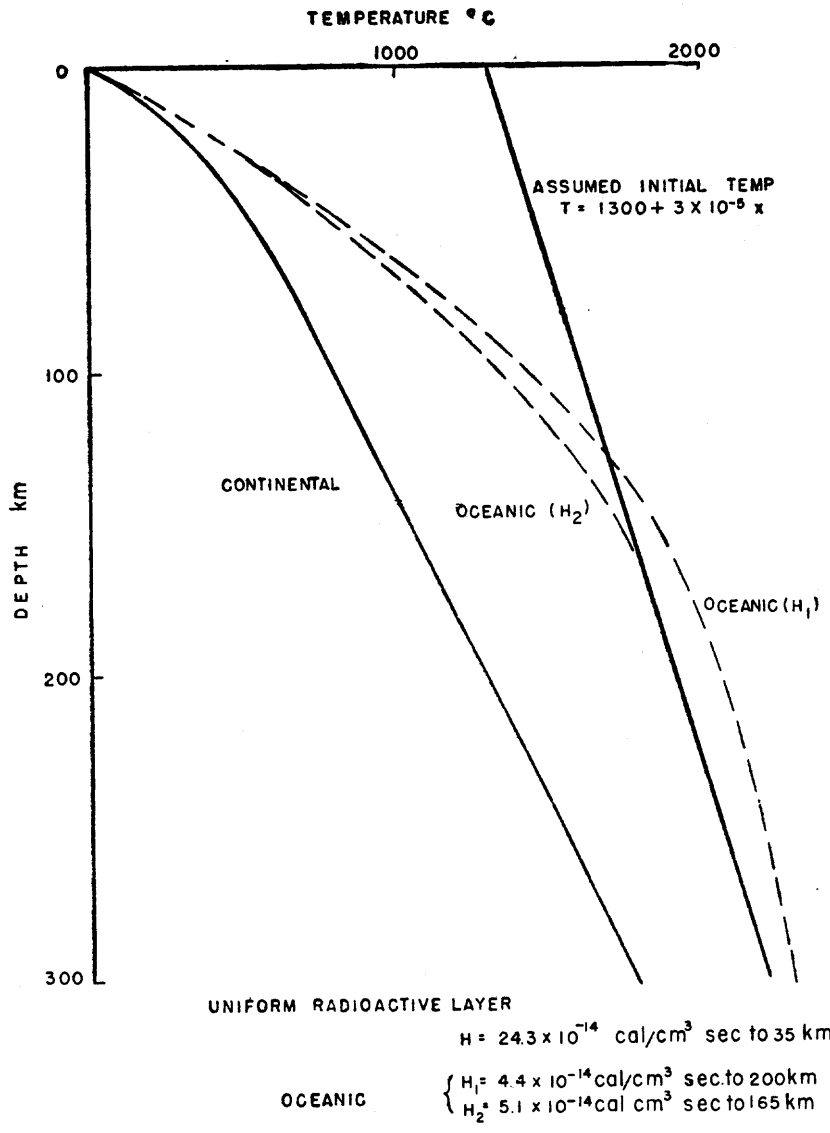


FIG. 4.

Possible temperature — depth distributions under continents and oceans.

Provided the temperature gradient within the earth is nearly adiabatic, the existence of radioactive substances at depth in the oceanic mantle might cause continuous convection there and consequently a relatively rapid upward transport of heat generated by radioactivity, while convection might be absent in a continental mantle that had been largely drained of its radioactive elements. The average heat flow originating in the continental crust and in

the oceanic mantle would then be nearly the same, but if convection cells of moderate size exist under the oceans there should be a detectable pattern of variations from place to place in the heat flow through the sea floor.

If convection were not continuous but intermittent, as Griggs (1939) and others have suggested, there would be no restrictions on initial conditions and the oceanic heat flow could be a relic of a past overturn. In this case it would be coincidental that the oceanic and continental heat flows are similar.

SUMMARY.

Measurements of oceanic heat flow give an average value similar to but somewhat higher than the average for the continents. Over 90 % of the observed oceanic heat flow must come from beneath the Mohorovicic discontinuity. This is in marked contrast to the continental situation, where it is usually estimated that not more than 30 % of the heat flow originates within the continental mantle. Consequently the oceanic mantle must differ from the continental mantle either in its properties or its behavior. The oceanic heat flow and the total radioactivity per unit area under the oceans could both be the same as the continental values, provided that under the oceans one of the following three situations hold :

1. The radioactivity is concentrated near the earth's surface. Improbably high values of radioactivity are then necessary for the rocks in the outer part of the mantle.
2. The radioactivity is distributed more or less uniformly throughout a considerable thickness of the mantle. This requires a « cool » earth and relatively high thermal conductivity at all depths.
3. The heat is transported from the earth's interior by convection as well as conduction. This also requires a cool earth.

A detailed mathematical presentation of the above arguments is given by Revelle and Maxwell (1956).

REFERENCES.

1. BIRCH (F), 1950, Flow of Heat in the Front Range, Colorado, Geo. Soc. Amer. Bull., vol. 61, pp. 567-630, 16 fig.
2. BULLARD, Sir EDWARD, 1954, The Flow of Heat Through the Floor of the Atlantic Ocean, Proc. Roy. Soc. A vol. 222, pp. 408-429 17 fig.

3. GRIGGS (D.), 1939, Discussion on A Theory of Mountain Building, Amer. Jour. Sci., vol. 237, pp. 611-650.
4. GRIGGS (D.), 1954, Symposium on Earth's Mantle, Amer. Geophys. Union, Trans., vol. 35-1, pp. 93-96.
5. JEFFREYS (H.), 1952, *The Earth*, 3rd edition, Cambridge Univ., 392 p.
6. RAITT (R. W.), 1951, Seismic Refraction Studies of the Pacific Ocean Basin, Paper presented at Seismol. Soc. Amer., Annual meeting March 23 and 24.
7. REVELLE (R.) and MAXWELL (A. E.), 1952, Heat Flow Through the Floor of the Eastern North Pacific Ocean, Nature, vol. 170, pp. 199-200.
8. REVELLE (R.) and MAXWELL (A. E.), 1956, Heat Flow Through the Ocean Floor IV. Bull. Geol. Soc. Amer. (in press).
9. UFFEN (R. J.), 1954, A Method of Estimating the Thermal Conductivity of the Earth's Mantle (abstract), Amer. Geophys. Union, Trans., vol. 35, p. 380.
10. VERHOOGEN (J.), 1954, Petrological Evidence on Temperature Distribution in the Mantle of the Earth, Amer. Geophys. Union, Trans., vol. 35, p. 380.

TABLE DES MATIÈRES

	Pages
AVERTISSEMENT	III
INDEX ALPHABÉTIQUE DES MATIÈRES	1
The Problem of Earthquake Magnitude Determination, by MARKUS BATH (Uppsala)	5
On Frequency Distribution of Seismic Magnitude, by Toshi ASADA, Ziro SUZUKI and Yoshibumi TOMODA	95
Intensity and Magnitude of Shallow Earthquakes, by Hirosi KAWASUMI (Tokyo)	99
The Velocity of P and S Waves in the Upper Part of the Earth's Mantle, by I. LEHMANN	115
On the Stress-Strain Relation in a not perfectly Elastic Solid Body, by H. MENZEL (Hamburg)	125
La structure interne et l'évolution de la Terre à la lumière des données géotectoniques, par V. V. BELOUSOV (Moscou)	129
Transfer of Radioactive Matter through Rocks by Diffusion by U. ASWATHANARAYANA (Inde)	137
Some Statistical Aspects of the Distribution of Radioactivity in the Salem Gneisses of Madras State, by U. ASWATHANARAYANA	151
The Thermal History of the Earth with Particular Reference to a Number of Radioactive Earth Models, by J. A. JACOBS (Toronto, Canada)	155
Le mécanisme des explosions phréatiques, par J. GOGUEL (Paris)	165
The Great Lakes — A Source of Two-Second Frontal Microseisms, by Rev. J. Joseph LYNCH, S. J. (Fordham University)	177
Sur les microséismes de Praha, par A. ZATOPEK (Université Charles, Praha)	183
Microseisms at Cochin, by H. M. IYER and J. N. NANDA	193
Microséismes d'origine tyrrhénienne, par M. GIORGI et E. ROSINI (Roma)	197
Microseisms used in Hurricane Forecasting, prepared by Marion H. GILMORE, U. S. Navy Microseismic Research Project, U. S. Fleet Weather Central, Miami, Florida	203
Elastic Tides and Irregularities of the Earth's Rotation in Connection with its Structure, by M. S. MOLODENSKY and N. N. PARIJSKY	217
Dispersion of Seismic Surface Waves and the Structure of Continents and Oceans, by T. S. AKIMA (Tokyo) and T. NAGAMUNE (Matusiro Observatory)	223
Crustal Structure in North-East Japan, by Explosion-Seismic Observations by Research Group for Explosion Seismology	229
Earthquake Epicentres, Volcanoes and Gravity Anomalies in and near Japan, by Ch. TSUBOI (Tokyo)	243
Development of Seismic Research and Analysis of Seismic Observations in the USSR, by E. F. SAVARENsky	249
General Survey of Seismicity of the Territory of the USSR (in addition to the Report, by E. F. SAVARENsky), by G. P. GORSHKOV	257
The Minute Investigation of Seismicity in Japan (2nd paper), by K. WADATI and Y. IWAI (Tokyo)	261
Seismicity and Erythrean Disturbances in the Levant, by N. SHALEM (Jerusalem)	267
On Phenomena Forerunning Earthquakes, by Kenzô SASSA and Eiichi NISHIMURA	277

	Pages
Le Tremblement de Terre de Yenice (18 mars 1953), par Hamit DILGAN et Takahiro HAGIWARA (Istanbul)	287
Le séisme du 18 mars 1953 de Yenice-Gönen (Anatolie NW) en relation avec les éléments tectoniques, par Dr. Nuriye PINAR (T. B. M. M., Ankara)	297
Sur quelques alignements séismiques remarquables du Maroc. Essai d'interprétation tectonique, par Jean DEBRACH (Casablanca)	307
Remarks on the Foundation of the Conception of Isostasy, by Karl JUNG, Bergakademie Clausthal (Germany)	315
Les vitesses des ondes séismiques excitées par les explosions industrielles en Bohême, par Vít KARNIK (Institut Géophysique de l'Académie Tchécoslovaque des Sciences)	319
Enregistrement des ondes séismiques provoqués par de grosses explosions. I. — Camargue 1949, par Y. BEAUFILS, P. BERNARD, J. COULOMB, F. DUCLAUX, Y. LABROUSTE, H. RICHARD, E. PETERSCHMITT, J.-P. ROTHÉ et R. UTZMANN. II. — Champagne, octobre 1952, par Y. BEAUFILS, J. COULOMB, R. GENESLAY, G. JOBERT, Y. LABROUSTE, E. PETERSCHMITT et J.-P. ROTHÉ	325
Réflexions à grande profondeur dans les grosses explosions (Champagne, octobre 1952), par R. GENESLAY, Y. LABROUSTE et J.-P. ROTHÉ	331
Réfractions multiples dans les enregistrements séismographiques des explosions de Champagne, octobre 1952, par Y. LABROUSTE et Y. BEAUFILS.	335
Etude des ondes superficielles dans les enregistrements séismographiques des explosions de Champagne, octobre 1952, par Y. BEAUFILS.	339
Trigger causes in Earth Movements, by S. K. GUHA, Gurdas RAM and G. V. RAO (Central Water and Power Research Station, Poona, India)	345
Basic Equipment of Seismological Stations in the U.S.S.R., by D. P. KIRNOS and D. A. KHARIN	357
On some new Methods of Seismological Research, by G. A. GAM-BURZEY	373
Methods and Results of the Investigations of Earthquake Mechanism (a brief information), by V. I. KEILIS-BOROK	383
Heat flow through the Pacific Ocean Basin, by A. E. MAXWELL and Roger REVELLE (Scripps Institution of Oceanography of the University of California)	395

TOULOUSE — IMPRIMERIE EDOUARD PRIVAT. — 983-10-56
PRINTED IN FRANCE.
